Integrated Powertrain Control

for

Twin Clutch Transmissions

Manuel Goetz

Submitted in accordance with the requirements for the degree of

Doctor of Philosophy

University of Leeds

School of Mechanical Engineering

February 2005

Abstract

In this thesis an integrated powertrain control for gearshifts on twin clutch transmissions is developed.

First, a detailed model of an automotive powertrain featuring a twin clutch transmission is developed in Matlab/Simulink®. This model includes detailed friction models for the twin clutch that enable an investigation into the effects of different friction materials on the performance of the gearshift controller. The transmission model also includes detailed models of the synchronisers and thus allows a simulation of synchroniser-to-synchroniser shifts. A simplified phenomenological model, derived from a more complex non-linear model, is employed to model the hydraulic actuation of clutches and synchroniser. The thesis finds that the dependency of the friction coefficient on the sliding speed has an important influence on the gearshift quality and the performance of gearshift controller, while the absolute level of the friction coefficient is less important.

Based on this powertrain model the key problems of gearshifts on twin clutch transmissions were identified and a control that overcomes these problems was developed. The first stage was to devise a gearshift control algorithm that handles single clutch-to-clutch shifts without a one-way (freewheeler-, overrunning-) clutch. This basic gearshift control algorithm featured a control of clutch slip for the engine torque transfer and a control of engine speed through engine torque manipulation (plus clutch pressure manipulation for downshifts). In a second stage, an optional transmission output torque control was developed that could be integrated in the basic control. The thesis shows that these control strategies are superior, in terms of shift quality, to conventional gearshift controls as used on planetary-type transmissions and are also robust against variations in the powertrain parameters (including friction coefficient) and sensor noise. The control strategies developed for single clutch-to-clutch shifts were extended to handle double and other multiple gearshifts that take place in the same transmission half.

The thesis also investigates the other main part of gearshifts on twin clutch transmissions, the gear pre-selection. The thesis shows that, on power-on gearshifts, the torque reactions at the transmission output due to the gear pre-selection with conventional hydraulically actuated synchronisers can be effectively compensated for by a simple manipulation of engine torque.

Acknowledgements

I am very grateful to Prof. Dave Crolla and Dr. Martin Levesley for their excellent supervision, their continuous support and encouragement over the past years. The many inspiring comments that they have provided have been an enormous help in the creation of this thesis.

I would also like to thank all the people in the school of mechanical engineering and in particular, my colleagues at the control and dynamics laboratory for their valuable support and help over the last years.

Finally, I would like to thank the School of Mechanical Engineering and the EPSRC for providing the funding for this PhD studentship.

I would like to dedicate this thesis to my father.

Table of Contents

List of Illustrations

List of Tables

Notation

$a_{vehicle}$...Vehicle acceleration in the longitudinal direction [m/s^2]

A_{air}...Cross sectional area in air gap at armature of solenoid valve [m^2]

$A_{exhaust}$...Orifice area at exhaust port of solenoid valve [m^2]

A_{front}...Frontal area of the vehicle [m^2]

$A_{maxsupply}$...Maximum orifice area at supply port of solenoid valve [m^2]

$A_{maxexhaust}$...Maximum orifice area at exhaust port of solenoid valve [m^2]

A_p...Hydraulic actuator piston area [m^2]

A_{supply}... Orifice area at supply port of solenoid valve [m^2]

A_v...Frontal area of spool of solenoid valve [m^2]

A,B,C,D,E,F...Coefficients of polynomial description of kinetic friction coefficient [-]

A/F...Air-to-fuel ratio in engine cylinder [-]

B...Magnetic flux density in solenoid of the solenoid valve [T]

$c_{C1,2,in}$... Damping of inertia at input of clutch 1,2 [Nms/rad]

$c_{C1,2,out}$...Damping of inertia at output of clutch 1,2 [Nms/rad]

c_D...Aerodynamic drag coefficient [-]

c_{Diff}...Damping of inertia of differential [Nms/rad]

c_{drive}...Sum of damping rates of left and right hand side drive shaft [Nms/rad]

$c_{In1,2}$... Damping rate of input shaft 1,2 [Nms/rad]

$c_{out1,2}$... Damping rate of layshaft 1,2 [Nms/rad]

c_p...Damping of hydraulic actuator piston [Ns/m]

$c_{S1,in}$...Damping of inertia at input of synchroniser of 1st, 3rd and 5th gear [Nms/rad]

$c_{S1,out}$...Damping of inertia at output of synchroniser of 1st, 3rd and 5th gear [Nms/rad]

$c_{S2,in}$... Damping of inertia at input of synchroniser of 2nd, 4th and 6th gear [Nms/rad]

$c_{S2,out}$... Damping of inertia at output synchroniser of 2nd, 4th and 6th gear [Nms/rad]

c_{TD}... Damping rate of torsional damper [Nms/rad]

c_{tyre}...Sum of damping rates of left and right hand side tyre [Nms/rad]

c_v...Damping rate of armature and spool of solenoid valve [Ns/m]

c_{12}... Damping rate of shaft connecting clutch 1 and 2 [Nms/rad]

C_D...Orifice discharge coefficient (solenoid valve) [-]

C_1,C_2,C_3...Constants used in gear pre-selection compensating control of upshift [m^3],[Nm],[s^2]

d_{spool}...Diameter of spool of solenoid valve [m]

e_{Tout}...Transmission output torque error (torque control) [Nm]

$e_{\Delta\omega}$...Clutch slip error (clutch slip control) [rad/s]

c_{we}...Engine speed error (engine speed control) [rad/s]

f_R...Rolling resistance coefficient at tyres of the vehicle [-]

F_A...Aerodynamic drag force [N]

$F_{brake,f}$...Braking force at front wheels [N]

$F_{brake,r}$ ...Braking force at rear wheels [N]

F_f...Tangential force at clutch [N]

F_{lift}...Aerodynamic lift force at vehicle [N]

F_N...Clamp force at clutch [N]

$F_{N1,2}$...Clamp force at clutch 1,2 [N]

$F_{N,S1,3,5}$...Clamp force at synchroniser of 1st,3rd and 5th gear [N]

$F_{N,S2,4,6}$...Clamp force at synchroniser of 2nd,4th, and 6th gear [N]

F_R...Total rolling resistance force at vehicle [N]

F_{Rf}...Rolling resistance force at front wheels [N]

F_{Rr}...Rolling resistance force at rear wheels [N]

F_{Sol}...Solenoid force [N]

F_{Spring}...Force of synchroniser actuator return spring at end of idle stroke of the actuator piston [Nm]

$F_{tractive}$...Tractive force at drive wheels [N]

F_{Xf}...Tractive forces at front wheels [N]

F_{Xr}...Tractive forces at rear wheels [N]

F_{Zf}...Axle Load at front wheels [N]

F_{Zr}...Axle load at rear wheels [N]

g... Gravitational constant [m/s^2]

$G_1(s)$, $G_2(s)$ and $G_3(s)$ ... Linear transfer functions according equations (36) to (38)

H...Magnetic field intensity (solenoid valve) [H]

i...Electric current (solenoid valve)[A]

i_{Acc} ...Gear ratio of accessory load drive [-]

i_f...Final drive gear ratio [-]

i_g...gear ratio of gear currently engaged on the torque transmitting path [-]

$i_{high/low}$...Ratio of gear ratios of high gear (target gear) and low gear (initial gear) of gearshift [-]

$i_{1,3,5}$... Gear ratio 1st, 3rd or 5th gear [-]

$i_{2,4,6}$... Gear ratio 2nd, 4th or 6th gear [-]

J_{Acc}... Inertia of accessory loads [kgm^2]

$J_{C1,2,in}$... Inertia at input side of clutch 1,2 [kgm^2]

$J_{C1,2,out}$... Inertia at output side of clutch 1,2 [kgm^2]

J_e... Inertia of engine parts [kgm^2]

$J_{eff,In1,2}$... Inertia of gearwheels reduced to input shaft 1,2 [kgm^2]

J_{Diff}... Inertia of differential [kgm^2]

$J_{gear1,2,3,4,5,6}$... Inertia of gearwheels 1 to 6 according Figure 3.15 [kgm^2]

$J_{gear7,8,9,10,11,12}$... Inertia of gearwheels 7 to 12 according Figure A.1 [kgm^2]

$J_{rot,non\text{-}driven}$... Inertia of all non-driven rotating part [kgm^2]

$J_{S1,in}$... Inertia (effective) at input of synchroniser of 1st, 3rd and 5th gear [kgm^2]

$J_{S1,out}$... Inertia at output of synchroniser of 1st, 3rd and 5th gear [kgm^2]

$J_{S2,in}$... Inertia (effective) at input of synchroniser of 2nd, 4th and 6th gear [kgm^2]

$J_{S2,out}$... Inertia at output of synchroniser of 2nd, 4th and 6th gear [kgm^2]

J_{Wheel}... Inertia of both driven wheels and drive shafts [kgm^2]

k_{drive}...Sum of stiffness of left and right hand side drive shaft [Nm/rad]

k_{CP}...Axial stiffness (compressibility) of clutch pack [N/m]

$k_{In1,2}$...Stiffness of input shaft 1,2 [Nm/rad]

$k_{out1,2}$...Stiffness of layshaft 1,2 [Nm/rad]

k_R...Spring rate of actuator return spring [N/m]

k_{R+CP}...Combined spring rate of actuator return spring and clutch pack [N/m]

$k_{TD1,2,3,4}$...Spring rates of stages 1,2,3,4 of torsional damper [Nm/rad]

k_{tyre}...Sum of rotational stiffness of left and right hand side tyre [Nm/rad]

k_v...Spring rate of armature return spring (solenoid valve) [N/m]

k_{12}...Stiffness of shaft connecting clutch 1 and 2 [Nm/rad]

K_d...Derivative Gain of PID controller [-]

K_i...Integral Gain of PID controller [-]

K_p...Proportional Gain of PID controller [-]

K_1,K_2...Gains of linear solenoid model [Pa/V]

L_{gap}...Length of air gap at armature (solenoid valve) [m]

L_{steel} ...Length of magnetic circuit in steel (solenoid valve) [m]

m_a...Mass of air inside the engine cylinder for combustion [10^{-3} kg]

m_p...Mass of hydraulic actuator piston [kg]

m_v...Mass of armature and spool of solenoid valve [kg]

$m_{vehicle}$...Vehicle mass [kg]

$\dot{m}_{ai}$ ...Mass flow rate of air into intake manifold of engine [10^{-3} kg/s]

$\dot{m}_{ao}$ ...Mass flow rate of air out of the intake manifold of engine [10^{-3} kg/s]

$M_{vehicle,total}$...Total vehicle mass (including inertia of non-driven wheels) [kg]

MMF...Magnetomotive force (solenoid valve) [A]

N...Number of turns (solenoid valve) [-]

p... Road gradient in percent [%]

p_C...Hydraulic pressure at clutch actuator (and at control port of solenoid valve) [Pa]

p_m...Engine manifold pressure[10^5Pa]

p_S...Hydraulic pressure at synchroniser actuator [Pa]

p_{supply}...Hydraulic pressure at supply port (line pressure) [Pa]

p_0...Atmospheric pressure [10^5 Pa]

$Q_{control}$...Net oil flow out of control port of solenoid valve [m^3/s]

$Q_{exhaust}$...Oil flow out of exhaust port of solenoid valve [m^3/s]

$Q_{feedback}$...Oil flow through feedback path of solenoid valve [m^3/s]

Q_{supply}...Oil flow into valve at supply port of solenoid valve [m^3/s]

r_{tyre}...Tyre radius [m]

R...Specific gas constant [kJ/(g K)]

R_i...Inner radius of friction contact area of clutch/synchroniser [m]

R_m...Mean friction radius of friction contact area of clutch/synchroniser [m]

R_o...Outer radius of friction contact area of clutch/synchroniser [m]

R_{wind}...Winding resistance (solenoid valve) [Ω]

s... Laplace variable [-]

t...Variable of running time [s]

$t_{inertia}$...Parameter determining the length of time of the inertia phase [s]

$t_{0,inertia}$...Value of t at the beginning of the inertia phase [s]

$t_{0,torque}$...Value of t at the beginning of the torque phase [s]

T...Temperature [K]

T_{Acc}...Torque from accessory loads [Nm]

T_C...Friction torque at clutch [Nm]

$T_{C1,2}$...Friction torque at clutch 1,2 [Nm]

$T_{C1,2,enagaged}$...Torque at clutch 1,2 in "engaged" state [Nm]

T_{drive}...Torque at drive shaft [Nm]

Tgrad...Parameter defining the gradient of the reference torque trajectory [Nm]

T_{ind}...Indicated engine torque [Nm]

T_{k12}...Torque at shaft connecting clutch 1 and 2 [Nm]

$T_{kIn1,2}$...Torque at input shaft 1,2 [Nm]

$T_{kOut1,2}$...Torque at layshaft 1,2 [Nm]

T_{Loss}...Loss torque at the input side of the synchroniser (clutch disengaged) [Nm]

T_{out}...Transmission output torque [Nm]

$T_{out,ref}$...Reference trajectory for transmission output torque control [Nm]

T_{Syn}...Friction torque at synchroniser [Nm]

$T_{Syn1,2}$...Friction torque at synchroniser 1,2 [Nm]

$T_{Syn1,2,enagaged}$...Torque at synchroniser 1,2 in "engaged" state [Nm]

$T_{tractive}$...Drive torque that produces a tractive force at the wheels [Nm]

T_{TD}...Torque at torsional damper [Nm]

T_0... (Mean-) Value of T_{out} sampled at the beginning of the gearshift [Nm]

$T_{0,torque}$... Value of T_{out} sampled at the beginning of the torque phase [Nm]

$T_{0,inertia}$...Value of T_{out} sampled at the beginning of the inertia phase [Nm]

ΔT_e...Necessary reduction in engine torque to compensate for ΔT_{out} (gear pre-selection) [Nm]

ΔT_{out}...Change in T_{out} due gear pre-selection [Nm]

v_{Sol}...Solenoid Input Voltage [V]

$v_{Sol,SlipCtrl}$...Output of clutch slip controller [V]

$v_{Sol,SpeedCtrl}$...Output of engine speed controller [V]

$v_{Sol,TorqueCtrl}$...Output of torque controller [V]

$v_{vehicle}$...Longitudinal velocity of vehicle [m/s]

Δv...Differential velocity across clutch [m/s]

V_m... Volume of engine manifold [m^3]

V_{offset}...Constant voltage offset depicted in Figure 3.25 (solenoid valve) [V]

$V_{v,0}$...Initial volume of feedback chamber (solenoid valve) [m^3]

$x_{exhaust}$... Maximum orifice width at exhaust port of solenoid valve [m]

x_{max}...Maximum displacement of spool of solenoid valve [m]

x_p... Piston travel of hydraulic actuator [m]

$x_{pstroke}$...Position travel where actuator piston is in contact with clutch pack [m]

x_s...Displacement of synchroniser actuator rod [m]

$x_{s,max}$...Displacement of synchroniser actuator rod where mechanical locking starts [m]

x_{supply}...Maximum orifice width at supply port of solenoid valve [m]

x_v...Displacement of armature/spool of solenoid valve [m]

x_1...Position of solenoid valve spool where supply port opens/closes [m]

x_2...Position of solenoid valve spool where exhaust port closes/opens [m]

z...Number of frictional contacts of clutch/synchroniser [-]

α...Cone angle of friction surface at synchroniser [deg]

α_{road}...Angle of road gradient [deg]

β...Bulk modulus (solenoid valve) [Pa]

ζ_1 and ζ_3 ...Damping parameters of linear transfer functions of the solenoid valve [-]

η_{Acc}...Efficiency of accessory load drive [-]

η_{Diff}... Efficiency of the differential [-]

$\eta_{gearbox1}$...Efficiency of gear box 1 [-]

$\eta_{gearbox2}$...Efficiency of gearbox 2 [-]

θ...Throttle Angle (denoted as "alpha" in figures) [deg]

$\theta_{SpeedCtrl}$...Output of engine speed controller manipulating throttle angle [deg]

μ...Friction coefficient (static or kinetic) [-]

μ_k...Kinetic friction coefficient at Clutch/Synchroniser [-]

μ_s...Static friction coefficient at Clutch/Synchroniser [-]

μ_0...Permeability of air [H/m]

ρ_{air}...Density of surrounding air [kg/m^3]

ρ_{oil}...Density of oil (hydraulic actuator) [kg/m^3]

σ...Spark advance in engine (denoted as "SA" in figures) [deg BTDC]

$\sigma_{SpeedCtrl}$...Output of engine speed controller manipulating spark advance [deg BTDC]

φ_c...Angular displacement at input side clutch1 [rad]

φ_{c2}...Angular displacement at input side clutch 2 [rad]

φ_{co}...Angular displacement at output side of clutch 1[rad]

φ_{c2o}...Angular displacement at output side of clutch 2 [rad]

φ_{Diff}...Angular displacement at input side of the differential [rad]

φ_{Drive}...Angular displacement at the drive shaft [rad]

φ_e...Angular displacement at engine side (crankshaft) [rad]

$\varphi_{In1,2}$...Angular displacement at input shaft 1,2 [rad]

$\varphi_{Out1,2}$...Angular displacement at output side of synchroniser 1,2 [rad]

$\varphi_{vehicle}$...Angular displacement of wheel (tyre surface) [rad]

φ_{Wheel}...Angular displacement at the wheels (rims) [rad]

$\Delta\varphi_{1,2}$...Boundaries for torsional clutch damper stages [rad]

ϕ... Magnetic flux (solenoid valve) [Wb]

ω...Joint speed of both clutch/synchroniser halves when clutch/synchroniser is engaged [rad/s]

ω_c...Speed at input side of clutch1 [rad/s]

ω_{co}...Speed at output side of clutch1 [rad/s]

ω_{c2}...Speed at input side of clutch 2 [rad/s]

ω_{c2o}...Speed at output side of clutch 2 [rad/s]

ω_{Diff}...Speed at input side of differential [rad/s]

ω_{Drive}...Speed at drive shaft [rad/s]

ω_e...Engine speed [rad/s]

$\omega_{e,ref}$...Reference engine speed trajectory (engine speed control) [rad/s]

$\omega_{e,0}$...value of engine speed at t_{shift} [rad/s]

$\omega_{gear2,4,6}$ ... Speed of gearwheel 2,4,6 according to Figure 3.15 [rad/s]

$\omega_{gear8,10,12}$ ...Speed of gearwheel 8,10,12 according to Figure A.1 [rad/s]

$\omega_{In1,2}$...Speed at input shaft 1,2 [rad/s]

$\omega_{Out1,2}$...Speed at output shaft 1,2 [rad/s]

$\omega_{vehicle}$...Equivalent vehicle speed [rad/s]

ω_{wheel}...speed at the wheels [rad/s]

$\Delta\omega$...Differential angular speed across the clutch (clutch slip) [rad/s]

$\Delta\omega_{ref}$ ...Reference value for clutch slip controller [rad/s]

ω_1, ω_3 and α_2... Frequency parameters of the linear transfer functions of the solenoid valve [-]

List of Abbreviations

AT...Automatic (planetary type) transmission

AMT...Automated manual transmission

AMT-2...Automated manual transmission with 2nd clutch

CVT...Continuously variable transmission

DCT...Dual (Twin-) clutch transmission

MT...Manual transmission

SI...Spark ignition (engine)

LQR...Linear quadratic regulator

ATF...Automatic transmission fluid

MVEM...Mean value engine model

BTDC...Before top dead centre

WOT...Wide-open throttle

Chapter 1
Introduction

In times where people become more aware of problematic issues connected to the automobile such as environmental pollution, shortages of resources and traffic congestions, the need for new technologies to escape these problems increases. In particular for an automobile the exhaust emissions, the fuel consumption and driveability are major concerns of the automotive development. Since restrictions on exhaust emissions through legislation will get stricter and the requirements concerning fuel economy will rise, there is an increasing need to improve the design and the operation of a variety of components in an automobile. The automotive component that offers the greatest potential for improvements with regard to fuel consumption and exhaust emissions is the automotive powertrain containing engine and transmission.

To ensure proper operation of the driveline in terms of low exhaust emissions and fuel economy whilst guaranteeing fast response to the driver commands, the driving environment and its interaction with the driver and the vehicle has to be taken into account. New electronic powertrain management devices can help to coordinate the operation of engine and transmission in an intelligent way to ensure optimum driveability, efficiency and environmentally friendliness of the automobile, taking into account a varying driving environment. However, this powertrain management approach requires the installation of an automatic transmission in the powertrain, which enables the controller to manipulate engine power, select the gear ratio and the point of the gear change independently of the driver. Manual transmissions, although still superior with regard to their mechanical efficiency, suffer from the intrinsic disadvantage of leaving the choice of gear and shift point to the driver who, on average, cannot achieve the same performance (fuel consumption and driving performance) as provided by an automatic transmission. One current aim of the automotive industry is to find new automatic transmission concepts that offer the above-mentioned advantages, however, with increased mechanical efficiency, thus closing the efficiency gap to the manual transmission.

1.1 Transmission Concepts - An Overview and Discussion of Characteristics

The following summary will give an overview of the most important transmission concepts that are currently in production or under investigation. The main characteristics are distinguished and advantages are compared. Due to the importance for the work, the question of how gearshifts are executed and its effects on drivability is given special emphasis in the comparison. Table1.1 gives an overview of the transmission family and compares the following characteristics: gear ratios, capability for powershifts, mechanical layout, common start devices, gearshift principle and provides a chart showing qualitatively the tractive effort during an upshift.

The transmission family depicted in Table1.1 compares the following transmission layouts: the continuously variable transmission (CVT), the planetary type automatic transmissions (AT), the twin clutch transmission, which is also known as dual clutch transmission (DCT), the automated manual transmission with a second assisting clutch (AMT-2), the normal automated manual transmission (AMT) and the manual transmission (MT). Apart from the CVT where the gear ratio can be varied continuously by changing the radius of a push belt or roller running on the variator, all other transmissions have fixed gear ratios that are engaged discretely. As can be seen from the tractive force (or effort) chart for an upshift, the CVT offers a smooth gearshift, which maintains traction throughout the change of gear ratios and that can be barely noticed by the driver. This also allows an optimal matching of engine and transmission operation and provides in theory a very good fuel economy. However, in practice due to the requirement for high hydraulic pressures at the actuator of the variator, the overall efficiency is greatly reduced cancelling the theoretical advantages. The conventional planetary type automatic transmission (AT) also offers gearshifts without an interruption in traction (i.e. powershift) but it achieves this in a different way as compared to the CVT. The gearbox itself contains planetary gearsets, where the single elements such as sun gear, planetary carrier and ring gear have to be coupled to each other (or have to be retained against the gearbox housing) through friction or one-way (i.e. freewheeler-, or overrunning-) clutches to realise different gear ratios. A gearshift can be accomplished by changing between friction clutches or one-way clutches in a so-called clutch-to-clutch shift. How many friction clutches or one-way clutches are involved in the gearshift depends on the mechanical layout of the geartrain. Since this kind of transmission often contains several clutches usually of wet type, hydraulic energy has to be provided and clutch drag is created due to the oily environment.

Table 1.1 Overview of transmission concepts and their characteristics

Transmission Family						
Transmission Type	Continuously Variable (CVT)	Automatic (AT)	Dual/Twin Clutch (DCT)	Automated Manual+2nd Clutch (AMT-2)	Automated Manual (AMT)	Manual (MT)
Gear Ratios	Variable	Fixed	Fixed	Fixed	Fixed	Fixed
Powershifts	Yes	Yes	Yes	Yes (Lower Traction)	No	No
Mechanical Layout	Pushbelt or Toroid Variator	Planetary Gearsets, Friction and One-Way Clutches	Simple Gearsets, 2 Friction Clutches and Synchroniser	Simple Gearsets, 2 Friction Clutches and Synchroniser	Simple Gearsets, 1 Friction Clutch and Synchroniser	Simple Gearsets, 1 Friction Clutch and Synchroniser
Start Device	Hydraulic Torque Converter or Friction Clutch (Automated)	Hydraulic Torque Converter	Friction Clutch (Automated)	Friction Clutch (Automated)	Friction Clutch (Automated)	Friction Clutch (Manual)
Gearshift	Automated (Variation of contact-radius between variator and belt/roller)	Automated (Clutch-to-clutch shift and/or clutch-to-one-way clutch shift)	Automated (Clutch-to-clutch shift and pre-selection of gear)	Automated (Clutch disengaged during change of gear, 2nd Clutch for torque fill-in)	Automated (Clutch disengaged during change of gear)	Manual (Clutch disengaged during change of gear)
Tractive Effort vs. Time (Upshift)		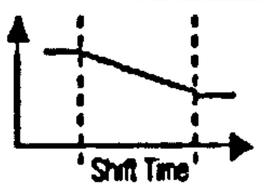	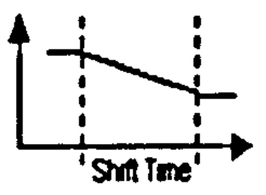	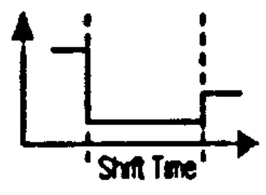	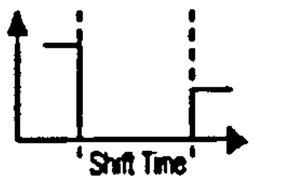	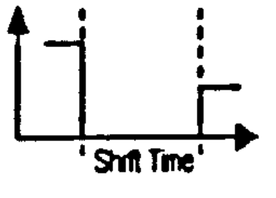

This circumstance, together with the hydraulic torque converter that is commonly used as a start device, is responsible for the low mechanical efficiency of a planetary-type transmission. The problem of the low mechanical efficiency has led to the investigation of a couple of alternatives, which are all in a way related to the layout of a manual transmission. The manual transmission (MT) comprises simply gear sets, synchronisers to engage the gears and a friction clutch for launching the vehicle. This simple mechanical layout results in superior mechanical efficiency compared to the two previously described transmissions.

In a first approach it was attempted to simply take the layout of the manual transmission and convert it to an automatic transmission by robotizing the actuation of synchroniser and start clutch. This resulted to the concept of the automated manual transmission (AMT), which comes with either a hydraulic or an electric actuation of dry clutch and synchronisers. In particular the electric actuation offers good efficiency, on the other hand, it lacks the response speed and actuator forces of the hydraulic actuation of similar size. By combining the mechanical simplicity of the manual transmission with the automatic gear selection and gear change, the overall fuel consumption could be drastically reduced to a level even below that of the manual transmission. However, as can be seen from the chart showing the tractive force during an upshift in Table1.1, both the manual transmission and the automated manual transmission show an interruption in traction at the wheels during the gearshift. This is a result of the necessary disengagement of the friction clutch during the gear change, thus making the transmission torque-free and enabling a change of synchronisers. This circumstance restricted the application of the automated manual transmission to heavy-duty vehicles, performance cars and to some extent to small cars, where the driver might accept an interruption in traction.

A step in developing the concept of the AMT further and thus eradicating the one principle disadvantage, the lack of powershifting capability, was to add a 2nd clutch to the AMT thus, creating the interruption-free AMT (i.e.AMT-2). The second clutch can be engaged whilst the main clutch is disengaged to provide some fill-in torque. In detail, the second clutch is also connected to the engine and is coupled to the output of the transmission via a fixed gear stage (lowest gear ratio in the transmission) or is simply connected to the output via the highest gear. The fact that only the lowest gear ratio is used explains that only little torque is transferred during the gearshift as can be seen from the traction chart in Table1.1. Thus, by offering some traction throughout the shift, the gearshift can be smoothed making the change in gear ratio less noticeable to the driver. This provides an improvement over the normal AMT but still does not offer the true powershift capability of the planetary type automatic transmission. Also, the shifts on the AMT-2 require two clutch changes, one at the beginning from the main clutch to the 2nd

clutch and one at the end of the gearshift that changes back to the main clutch. Hence, the principle of the gearshift is different from that of a clutch-to-clutch shift.

The concept that seems to be most promising in solving all the shortcomings of the other transmission types introduced so far, by combining good mechanical efficiency with true clutch-to-clutch powershift capability, is likely to be the twin clutch transmission. The discussion of the principle and characteristics of this transmission type forms the content of the next section.

1.2 The Twin Clutch Transmission

As already mentioned in the previous section the twin clutch transmission attempts to combine advantages of an automated manual or manual transmission (high efficiency, simplicity and small rotational inertias) with the advantage of planetary type automatic transmissions (power shifts). The principle of the twin clutch transmission originates in a patent by Kégresse back in 1939 [Kégresse 1939 (Patent DE 894 204)] and is depicted in Figure1.1. The idea behind this transmission concept is to split a manual gearbox into two separate sub-gearboxes. One sub-gearbox, or half of the transmission, carries the odd gear ratios (gearbox 1 in Figure .1) whilst the other one carries the even gear ratios. Each of the two halves of the twin clutch transmission is connected to the engine through a separate friction clutch (clutch 1 and 2 in Figure1.1).

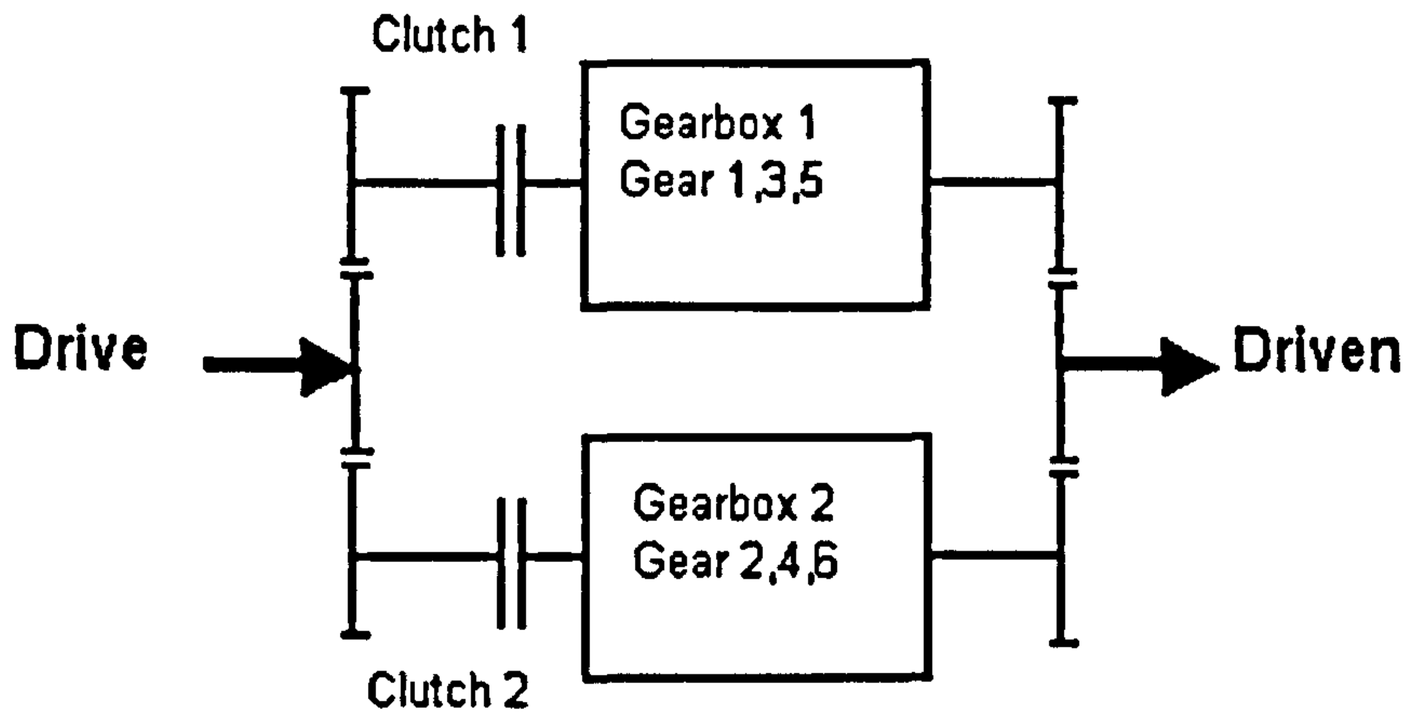

Figure 1.1 Principle of the twin clutch transmission

The torque of both transmission halves is gathered at the output of the transmission by a gear stage meshing with output gears located in the two halves. Gearshifts can be accomplished as clutch-to-clutch shifts by changing from one sub-gearbox to the other, thereby retaining full

traction at the wheels. Comparing the tractive effort charts in Table1.1 for the twin clutch transmission and the conventional automatic transmission (AT) reveals that the tractive force profiles of both clutch-to-clutch shifts are in principle similar thus, full powershift capability is provided by the twin clutch design. The sub-gearboxes of the twin clutch transmission comprise simple gear sets and synchronisers such as found on conventional manual gearboxes. This mechanical design offers superior mechanical efficiency compared to that of planetary-type automatic transmissions equipped with a hydraulic torque converter. This difference in the mechanical layout explains why the twin clutch transmission is so interesting from an economical and driving performance point of view. Similar to the AMT, the actuation of clutches and synchronisers can be accomplished by a hydraulic or electric system. Especially, the combination of dry friction clutch and electric actuation would be beneficial in terms of overall efficiency. However the currently preferred approach still seems to be wet friction clutches in combination with a hydraulic actuation, offering better controllability and smoother engagements.

The automatic control of the two friction clutches during gearshifts has to be performed with great care and is a difficult task to achieve. In the early development phases, the twin clutch was operated manually through foot pedals. In the mid eighties, the concept of the twin clutch transmission was picked up again but the electronic control of the two clutches remained difficult thus, preventing commercial production of the transmission. Also, the inherent disadvantage of skipping one gear (i.e. multiple gearshifts such as from 4^{th} to 2^{nd} gear) without disengaging the torque-transmitting clutch was considered a major shortcoming. The advent of faster and more capable electronics at the end of the nineties led to new interest in the twin clutch design from all major car and transmission manufacturers. In the year 2003, the twin clutch transmission was finally put into production for the first time. This gearbox was presented in [Rudolph et al 2003] and featured a combined twin clutch at the input of the transmission and conventional cone-type synchronisers. The twin clutch was of wet type and the actuation of both twin clutch and synchronisers was hydraulic.

1.3 Powertrain Controls and the Integrated Powertrain Control Approach

Table 1.2 gives an overview of the different control tasks evolving during the operation of a vehicle powertrain. In the past, engine and automatic transmission were controlled separately. Thus, for example, on the engine side control tasks such as control of fuel injection, throttle angle and/or control of spark advance on a spark ignition (SI) engine, were designed with the single aim of providing a certain torque at the crankshaft, based on the driver input via accelerator pedal. Other classic control tasks in the engine environment are, for example, control of engine speed during idle running or, on SI engines, the control of knocking in the combustion and the control of the air/fuel ratio λ. The classic task of the transmission controller was to select the appropriate gear to provide the propulsion power requested by the driver. Other tasks of the transmission controller were the control of the gearshift (i.e. the actual gear engagement process and change of gears) and if equipped with a start clutch instead of a hydraulic torque converter, the control of the vehicle launch. These control tasks are listed in the first row of Table1.2 and are described briefly in the following paragraphs.

Transmission/Powertrain Control Tasks
(fixed gear ratio transmissions)

Control Tasks:	Shift schedule/ Powertrain management	Gearshift	Start
Description:	Selection of gear/ Engine power	Change of Gears	Vehicle Launch
Objectives:	Optimal driving performance, Low fuel consumption, Low exhaust emissions, etc.	High shift quality, Minimum loss in traction, Low clutch wear, etc.	Smooth vehicle launch, Good hill start/hold, Low heat production,etc.
Controls:	Gear ratio/ Engine torque/speed	Clutch torque and Engine torque/speed	Clutch torque and Engine torque/speed

Table 1.2 Transmission and powertrain control tasks

Shift Schedule/Powertrain Management

The powertrain is controlled to optimise control objectives such as minimum fuel consumption, low exhaust emissions etc. If the control strategy involves only local transmission control tasks

(i.e. gear selection), then the control scheme is often denoted by the term "shift schedule". However, if the powertrain control strategy also actively manipulates engine torque and speed in addition to the selection of a gear ratio, then this is denoted here as powertrain management.

Control of the Gearshift

The control of the gearshift is necessary when a change in gear ratio on the transmission is required. There are various objectives in achieving a good gearshift (e.g. low vehicle jerk, minimum loss in traction at the wheels etc.). Again, this can be achieved through a local transmission control strategy alone. This involves the control of shift elements on the transmission (e.g. clutches, synchroniser etc.). However, to improve the gearshift control strategy, the engine can be included in the control strategy, involving either a manipulation of engine torque or a control of engine speed or a combination of both, depending on the degree of sophistication of the control strategy.

Start Control strategy

If a device other than a hydraulic torque converter is used for the vehicle launch (e.g. start clutch), then this device requires a controller as well. Again, one can distinguish between a "local control strategy", restricted to the control of the start device only, and a control scheme where the engine is controlled as well. Various control objectives such as good launch characteristics and low energy dissipation, often require the active control of engine torque and speed.

At the end of the eighties and beginning of the nineties, car manufacturer started to realise the potential of an integrated powertrain control concept, where both engine and automatic transmission are controlled in a combined way. This step helped to improve vehicle driveability and fuel consumption in order to satisfy the growing request for a smooth drive feel and increased economy by the customer. Some early steps in that direction are described in [Lorenz et al. 1988] where the authors showed that an engine torque control (torque reduction by retardation of spark advance) during gearshifts of an automatic transmission could improve the shift quality. In [Schwab 1990] transmission control strategies were reviewed and some of the benefits of employing electronic control to local transmission control tasks, including the benefits of an integration of engine control, are listed. The author emphasises again that an engine torque control has to be included in the control of gearshifts in order to improve the shift quality. Also, some new transmission concepts were reviewed and various requirements concerning the controller were given. Among these transmission concepts, the twin clutch transmission and its advantages (greater efficiency, less complexity etc.) was listed, but it was stated that an automation and therefore control turned out to be difficult and "can only be

reasonably achieved with an electronic control scheme" [Schwab 1990] (compared to a conventional fully hydraulic control scheme). [Narumi et al 1990] stated that "modern control theories", which make use of an integrated control approach are necessary to improve shift quality. The authors also demand "intelligent" control techniques for gear selection (shift schedule) in order to predict the road conditions and driver intentions – fuzzy control is proposed by the authors as a solution to this problem.

1.4 Map of the Thesis

Chapter 1 has started with a brief introduction on twin clutch transmissions and powertrain control concepts.

This first introductory chapter is followed by a review of literature on gearshift control and powertrain modelling in Chapter 2. Chapter 2 concludes with a summary of findings of the literature review and with the aims and objectives of this thesis.

In Chapter 3 the powertrain model is developed in detail. At the beginning of the chapter the engine model is described. This is followed by a detailed development of the model of the twin clutch transmission including hydraulic actuation. After that, the remainder of the powertrain model is explained and a first simulation result is presented at the end of the chapter.

A basic control algorithm for single gearshifts on twin clutch transmissions is developed in Chapter 4. The chapter starts with an analysis of the problems associated with conventional gearshift control as used on planetary-type transmissions. The gearshift control is then developed for upshifts and downshifts and its operation and advantages are demonstrated based on simulation results. The chapter ends with an explanation of the detailed layout of the proposed controller and an investigation into its robustness.

The controller developed in Chapter 4 is then extended in Chapter 5 to incorporate torque control. At the beginning of this chapter the motivation for torque control is explained, followed by a detailed description of how the torque control can be integrated in the basic gearshift control strategy. The advantages of the torque control are demonstrated based on simulation results. At the end of the chapter, again, the layout of the controller is explained and its robustness is investigated.

In Chapter 6 the control of single gearshifts developed in Chapters 4 and 5 is extended to cope with double/multiple gearshifts. This is demonstrated based on simulation results for a couple of multiple downshift and upshift cases.

Chapter 7 treats the topic of gear pre-selection on twin clutch transmissions. The problems associated with employing hydraulically actuated synchronisers for gear pre-selection, are lined out at the beginning of this chapter and a control strategy that compensates for these problems is developed subsequently for upshifts and downshifts. At the end of this chapter the robustness of the proposed compensating control strategy is investigated.

Finally, the findings of this work are summarised in Chapter 8.

Chapter 2
Review of Literature

This chapter reviews the literature of mainly two key areas, the control of gearshifts and the dynamic modelling of powertrains. The first section (Section 2.1) reviews gearshift control concepts as found on fixed gear powershift transmissions (i.e. planetary-type and twin clutch transmissions). This section is split into three subsections, the first one gives an introduction to powershifts, the second one reviews "local" gearshift control concepts and the third subsection reviews "integrated powertrain control" concepts applied to gearshifts.

The following main sections review control issues specific to twin clutch transmissions (Section 2.2), the control of gearshifts on automated manual transmissions (Section 2.3) and shift quality metrics in Section 2.4. Section 2.5 discusses the issue of torque measurements versus mathematical observation and Section 2.6 reviews the literature on powertrain modelling. This section reviews literature firstly, on powertrain modelling issues in general and then secondly, on engine and transmission modelling (including hydraulic actuation) specifically.

The chapter ends with a section of conclusions from the literature review (Section 2.7) and finally, a section stating the aims and objectives of this thesis (Section 2.8).

2.1 Control of Gearshifts on Powershift-Transmissions

This section reviews gearshift control concepts for powershift transmissions (AT, DCT), found in the literature. The first subsection reviews the principle of powershifts and points out the key differences between powershifts on planetary-type automatic transmissions and twin clutch transmissions. The first of the two following subsections reviews "local" gearshift controls and the subsequent section reviews gearshift controls that make use of the "integrated powertrain control" approach. What distinguishes the two approaches will now be explained briefly: Since nearly all of today's production automatic transmission controllers integrate the engine to some degree in their gearshift control strategies, mainly in the form of a simple reduction of engine torque, the distinction between local and integrated control strategy is made here in a wider sense. If the gearshift control strategy involves an active manipulation of engine controls such

as throttle angle (SI-engine) or fuel injection (Diesel engine) in a closed-loop control, then it will be referred to as an "integrated powertrain control". On the contrary, control schemes that only make use of simple open-loop engine torque reduction techniques, in conjunction with a manipulation of the actuation pressure at the shift elements on the transmission, will be treated as "local" gearshift control strategies.

2.1.1 Brief Introduction to Clutch-to-Clutch Powershifts

The key feature of conventional planetary-type automatic transmissions and twin clutch transmissions is the powershift capability, which means that there is no interruption in the tractive forces at the wheels during the gearshift. On conventional planetary-type transmissions and twin clutch transmissions a gearshift can, in principle, be carried out as a "clutch-to-clutch" shift, i.e. shifting from a clutch carrying the original gear to a clutch carrying the target gear, without disconnecting the engine from the wheels.

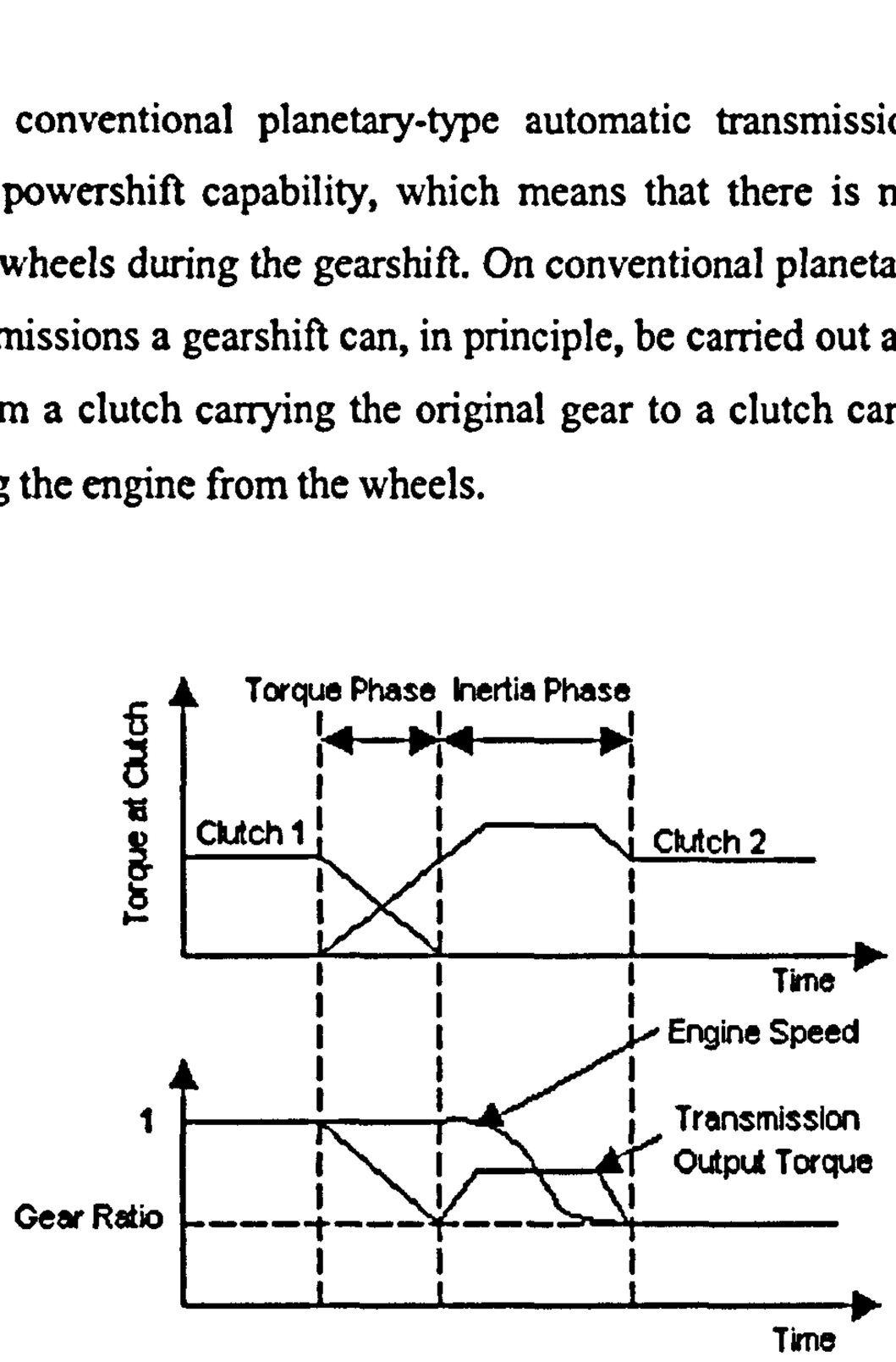

Figure 2.1 Principle of a conventionally controlled clutch-to-clutch power-on upshift

To make the concept of a clutch-to-clutch powershift clear, the example of a power-on (i.e. throttle on) upshift is briefly explained based on a conventionally controlled power-on upshift, which makes use of simple pressure ramps and does not involve a manipulation of the engine (see Figure2.1). The power-on upshift is also often used in the literature as a gearshift example to demonstrate the operation of the proposed control strategy. For a more detailed explanation of powershifts please refer to Chapter 4.

The power-on upshift starts with a "torque phase", where engine torque is transferred from the offgoing (clutch 1 in Figure2.1) to the oncoming clutch (clutch 2 in Figure2.1) carrying the target gear (i.e. a gear higher than the original one). This transfer of engine torque between the two clutches results to a drop in the transmission output torque according to the change in gear ratio. In the following inertia phase the engine is synchronised (i.e. decelerated) to the speed level of the new gear. The deceleration of the engine can be accomplished through an increase in torque at the oncoming clutch (clutch 2) beyond the level necessary for transmitting the engine torque. The deceleration of the engine inertia transfers torque to the transmission output and results to a "hump" in the transmission output torque profile and increased vehicle jerk at the transition between torque and inertia phase.

The dynamics of clutch-to-clutch shifts and the influence of application timing of the two clutches were investigated in principle in [Förster 1991]. In this treatise, also the improvement of shift quality through engine torque reduction was discussed. Furthermore, differences in the dynamics of clutch-to-clutch shifts between layshaft transmissions, such as the twin clutch transmission and planetary-type transmissions were discussed. One finding was, that the inertia of planetary gears can have a considerable influence on the dynamics of the clutch-to-clutch shift leading to a smoother transmission output torque profile and longer shift times (upshifts) compared to a layshaft design. The torque converter was also found to be beneficial to the shift quality when the lock-up clutch (device that enables a mechanical locking of the two halves of the torque converter) was disengaged during the inertia phase, leading to decreased inertia at the transmission input. The use of two or more planetary gearsets can also mean differences in the gearshift dynamics. Shifting between different planetary gearsets ("group change") requires control of several clutches/brakes and can produces a severe decrease in transmission output torque. To avoid this problem, certain requirements concerning the mechanical layout and procedure of the gearshift have to be considered. If these requirements are fulfilled, the shift between planetary gearsets can then be executed as a "pseudo-group change", which can be handled like a clutch-to-clutch shift.

A key difference in the practical aspects of the control of clutch-to-clutch shifts between planetary-type and twin clutch transmissions is given by the lack of a one-way or overrunning clutch on twin clutch transmissions. These devices can help to a smooth transfer of engine torque in the torque phase by disengaging precisely at the time where the oncoming shift element (i.e. clutch) is able to carry the full engine torque. Any further engagement of the offgoing clutch beyond this point would lead to the creation of a negative torque contribution by this clutch and thus, would result in a larger drop in transmission output torque.

The above listed differences make it necessary to modify some of the clutch-to-clutch techniques applied to planetary-type gearboxes. Also, on twin clutch transmissions a pre-selection of the target gear on the torque-free half of the transmissions needs to be accomplished in addition to the clutch-to-clutch shift.

2.1.2 Gearshift Control – Local Transmission Control Strategies

As mentioned before the "local" gearshift control approach contains all control strategies that do not involve an active manipulation of throttle angle or fuel injection by the controller. However, simple engine torque reduction can be part of the local gearshift control.

The techniques for local gearshift control can be divided into two sections:

- Open-loop control (majority of production transmissions), where the gearshift is controlled based on clutch pressure profiles as functions of transmission and engine variables.
- Closed loop control methods, where transmission (or engine variables) are controlled to track specified reference trajectories.

Open-Loop Control Concepts

Open-loop control methods for gearshifts on automatic transmissions are basically simple concepts that involve application of look-up tables. In these look-up tables the hydraulic clutch pressure profiles and values for engine torque reduction are stored as functions of various engine and transmission variables such as throttle angle, engine speed, engine torque, transmission input/output speed, selected gear etc. (Figure2.2).

The clutch pressure profiles can also be functions of the transmission oil temperature to account for changes in the friction coefficients at the clutches. These pressure profiles normally have the shape of ramp functions and the parameters of those ramp function i.e. slope and time span need to be adjusted manually during time-consuming calibration tests. These methods still prevail with production transmissions. Although sometimes relatively good results can be achieved in terms of shift quality, such open-loop gearshift control cannot per se account for parameter variations and changes in the driving situation that have not been considered at the time of the calibration.

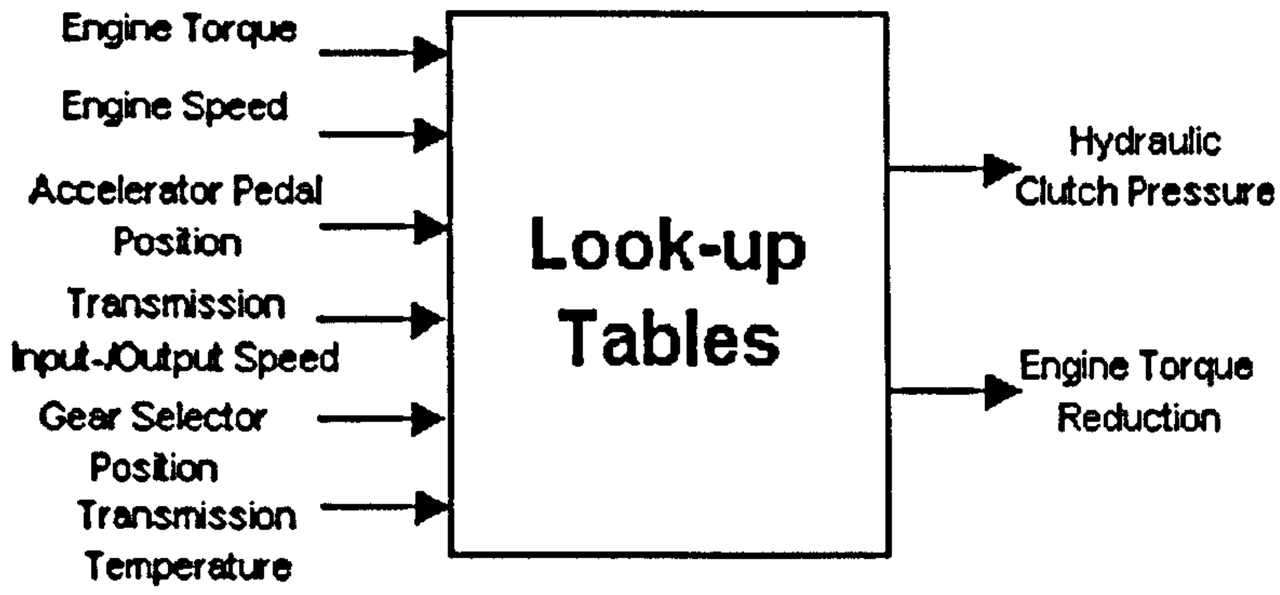

Figure 2.2 Example of an open-loop control concept in an automatic transmission

Open-loop control strategies for twin clutch transmission were described in [Webster 1981, Flegl et al. 1982, Flegl et al 1987, Op de Beck et al. 1983]. In [Webster 1981] each upshift and downshift was controlled by its own open-loop timing circuit and the time delay in releasing the offgoing clutch was a function of the throttle position. This was found to be vital to a smooth gear change. Furthermore to overcome poor rollout shifts (when coming to rest the gearbox would change down through all the gears and then disengage the clutch) and bad shift performance under heavy braking (not enough time to complete the full gearshift sequence and thus danger of stalling the engine exists), speed sensitive clutch disengagement was employed. The controller of the twin clutch transmission presented in [Flegl et al. 1982] processed engine speed, engine load, accelerator pedal position, program selection, engaged gear, transmission speed as input variables to determine clutch pressure, timing of clutch and shift rail (synchronisers) application. The average time of the total gear change including disengagement of the previous gear after the clutch-to-clutch shift was about 0.4 to 0.7 seconds, whereas the actual clutch-to-clutch shift took about 0.3 to 0.5 seconds. In order to avoid longitudinal shocks, the clutch pressure profile was modified to be a function of the engine load. The same transmission has been described in [Flegl et al 1987], where the authors emphasised the strong influence of the pressure profiles at both clutches during the gear change on shift quality. Therefore the pressure profiles were made to be dependent on the engine speed and throttle position. In [Op de Beck et al. 1983.] the synchronisation during the inertia phase was executed by manipulating the clutch pressure depending on the engine torque and on the nature of the shift (up- or down shift).

To overcome the deficits of open-loop control strategies in terms of a lack of adaptability to disturbances, methods of parameter adaptation and optimisation have been developed that allow considerable reduction in the calibration time and improve the shift quality. The following control techniques were applied to planetary-type automatic transmission.

For a conventional automatic transmission an off-line optimisation of the parameters "engine torque reduction" and "clutch pressure" during a gearshift was described in [Haj-Fraj, Pfeiffer 2000]. The optimisation was based on a multi-criteria approach, with the goal to minimise dissipated energy and maximise shift quality (defined through vehicle jerk – i.e. the first time derivative of the vehicle acceleration). A powertrain model for simulation of the gearshift from the 1st to the 2nd gear was developed. In this particular shift a one-way clutch was used as an offgoing "clutch". To minimise dissipated energy a cost function that minimised the shift time was employed. For the maximisation of the shift quality a cost function containing the integral over the square of the vehicle jerk was minimised. The optimisation parameters contained the clutch pressure as a function of turbine torque and speed and the engine torque reduction factor as a function of engine torque and speed and were stored as sampling points in a look-up table and were represented by a parameter vector. The aim of the optimisation process was to find a parameter vector that solved the equations of motion (constraint to the optimisation problem) and optimised the cost functions. The vector problem was reduced to a scalar problem by using the method of objective weighting, where also the relative importance of the two objectives could be influenced. This non-linear optimisation problem was solved by a sequential quadratic programming algorithm. The simulation result showed an improvement in both the shift time and the level of vehicle jerk during an upshift from 1st to 2nd gear. However, the optimisation procedure was only applied to that specific gearshift and since the control principle was still open-loop control, parameter variations could, of course, not be compensated for.

The optimisation criteria used in the previously discussed paper were extended in [Haj-Fraj, Pfeiffer 2002], with the result that three different criteria for shift quality and two for energy dissipation could be used alternatively. The three cost functions for the shift quality were defined as a quadratic form of the vehicle jerk, a quadratic form of the deviation of the longitudinal vehicle acceleration from the target value and peak-to-peak values of the acceleration and the vehicle jerk. The last cost function was defined according to [Gebert, Kücükay 1997] by evaluating peak-to-peak values and slopes of flanks in the vehicle acceleration and jerk. As cost functions for the evaluation of the clutch wear, either the dissipated energy during the gearshift or alternatively the shift time was used. The results show that for a wide-open throttle condition the optimisation procedure produced gearshifts with improved shift quality for all three shift comfort criteria (all having the same criterion for clutch wear). In particular the third criterion (Peak-to-peak values) provided a low jerk level at the beginning of the gearshift but showed a higher level of vehicle jerk at the end of the shift. The optimisation of clutch wear produced a similar result for both alternative criteria. With both criteria a reduction in the dissipated energy at the clutch could be achieved.

In [Gebert, Kücükay 1997] a detailed characterisation of the longitudinal vehicle acceleration profile of a gearshift was undertaken and a shift metric was developed. The shift metric is discussed in detail in Section 2.4. After the shift metric had been developed, a sensitivity analysis by means of a parameter variation was carried out to identify those parameters (e.g. clutch fill pressure, fill time), which influence the gearshift metric most. Based on this parameter identification, a control algorithm that automatically determined the parameter settings for optimum shift quality was developed. Although, the parameter variation and adaptation could be, in principle, executed on board, the control algorithm was not able to recognise which parameter had to be varied, which limited the application of the presented control technique to calibration procedures only.

The optimisation of the pressure trajectories for open loop control of torque and inertia phase was the aim of [Yoon et al.1999]. Optimisation criteria such as the drop of transmission output torque during the torque phase and the increase of transmission output torque during the inertia phase were introduced in the optimisation procedure. The optimal pressure trajectories were then determined by three different random search algorithms. For this aim the pressure profiles of oncoming and offgoing clutch were parameterised (basically a series of pressure ramps, characterised by slope and time span). Then, appropriate cost functions were chosen to characterize the shift quality. In particular, the five cost functions penalized the torque drop during the torque phase, the torque increase during inertia phase, the total shift time and the period of time the pressure at the off-going clutch takes to reach zero. The overall cost function was formulated as a sum of these single costs, which could be weighted to specify the relative importance. The optimum solution was determined by three different techniques, which were all modifications of a random search algorithm and showed only slight differences in the solution. However, as with every open loop technique, the control algorithm is not robust against changes in, for example, friction coefficient and delays in the hydraulic actuation. This fact was also recognised in the paper and it was admitted that closed-loop control is necessary to make the gearshift control robust against these parameter variations.

A completely different approach was chosen in [Jacobsen 2000], where a clutch-to-clutch control concept was proposed that made use of a third clutch. The pressure gains for the oncoming clutch and the additional clutch were derived in that paper based on an optimisation procedure. This optimisation procedure attempted to minimise "discomfort" (first derivative of the output torque) and "wear" (energy dissipation during gear shift). To find the pressure gains that minimise "wear" and "discomfort" an iterative optimisation algorithm was developed. The best results were achieved if the gear ratio corresponding to the additional clutch was chosen to be larger than those of the other clutches. The additional clutch was only applied in the inertia

phase and hence, the torque phase was not improved. The simulation results showed that the proposed control algorithm was able to reduce the size of the transmission output torque "hump" in the inertia phase. Also, energy dissipation was slightly reduced in the inertia phase. However, the gradient of the increase in transmission output torque at the beginning of the inertia phase, responsible for the high vehicle jerk at this point, was not reduced.

An approach to the control of the engine torque transfer in the torque phase from a design point of view was suggested in [Bai et al. 2002]. Instead of using two independently operating proportional pressure control solenoid valves for the two clutches involved in a clutch-to-clutch shift, the actuation pressure (outlet port of control valve) of the higher gear was used as a "washout" pressure at the solenoid valve of the lower gear. Essentially, the pressure of the oncoming clutch was used to "push down" the pressure of the offgoing clutch. This technique made the coordination of the two clutches independent of the oncoming clutch fill time. However, the correct "overlapping" of the two clutch pressure ramps still needed to be calibrated by choosing the correct pressure control and washout gain for the low gear clutch. The pressure ramp at the offgoing clutch was a function of engine torque and gear. Simulation results for upshifts and downshifts between the 2nd and the 3rd gear show the effectiveness of the proposed hydraulic design in the torque phase. A robustness study was carried out for different oil temperatures and thus different filling times and showed that the proposed design could cope with these variations. However, since the control strategy relies on choice of control valve gains, it still seems to be sensitive to variations in the hydraulic system. The inertia phase was controlled in a conventional way by pressure manipulation with its problematic creation of output torque "hump" and resulting high levels of vehicle jerk.

Closed-Loop Control Concepts

The discussion of the closed-loop control concepts in this section starts with the most sophisticated control concept, the optimal control, next leads to torque-based gearshift control strategies and ends with the simplest approach the, speed based control of gearshifts. Controlling transmission variables in a closed-loop way during the gearshift can help to decrease or even cancel the influence of disturbances and, to some extent, parameter variations. It also allows a gearshift performance that is unaffected by the driving situation. Furthermore the closed-loop control approach enables a direct influence of the gearshift character (shift feel) by specifying appropriate reference trajectories for engine and transmission variables.

Optimal Control of a Gearshift

The objective of optimal control theories is to generate "optimal" control laws or controller gains that minimise a given performance index. State variables of the transmission (e.g. rotational speeds) or of the whole powertrain are fed back in a state variable feedback loop. The state variables are then controlled to some initial or fixed reference value (optimal regulator) or to track specific reference trajectories (optimal tracker). The performance index specifies the objectives of the control strategy that should be optimised. Common contents of performance indices are the control signal expenditure, the amount of time to reach end state, the tracking errors etc. If applied to gearshift control, additional optimisation criteria might be included in the performance index. Figure 2.3 shows the main criteria of an optimal gearshift control.

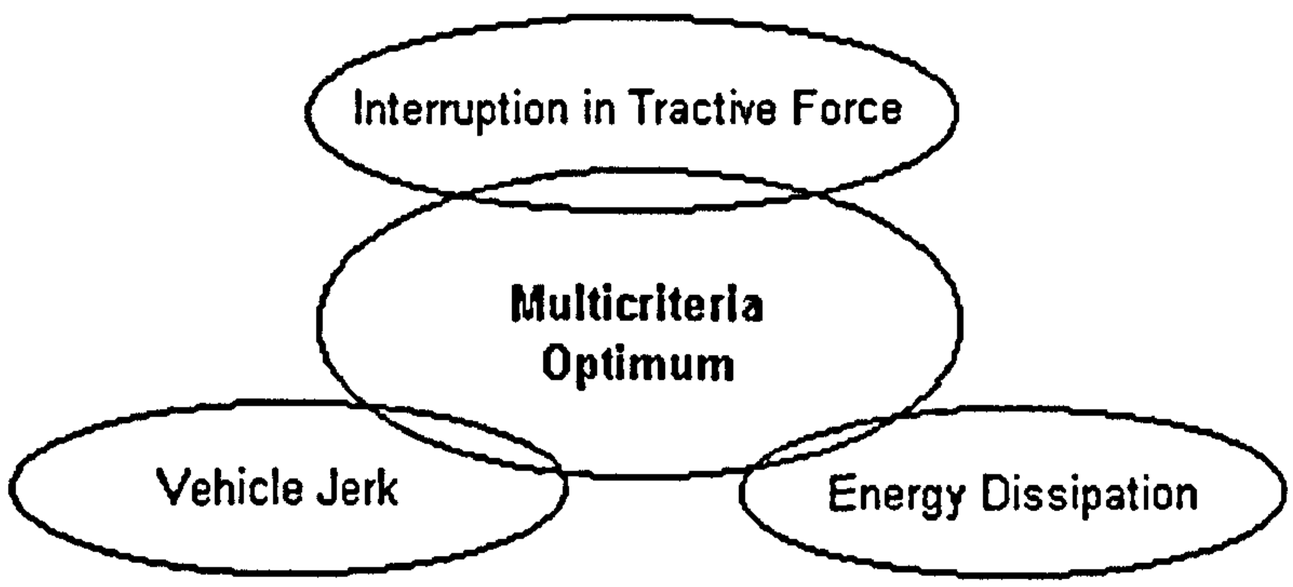

Figure 2.3 Optimisation targets of an optimal control of gearshifts

The equations of motion are usually also included in the performance index as a constraint to the optimisation problem. This, together with other constraints, can be used to ensure that no interruption in traction occurs during the gearshift. The two other optimisation criteria attempt to minimise vehicle jerk while at the same time minimising energy dissipation. By introducing weights in the performance index, the optimisation of these two conflicting aims can be adjusted towards the more important objective. In the most common form of optimal control these objectives are specified as quadratic forms, which leads to the concept of linear quadratic regulators (LQR) or trackers. For such quadratic optimisation problems, solutions exist, in the form of a so-called Riccati equation. From this Riccati equation the gains of the controller or the control law can be derived. Techniques to obtain the Riccati equation include for example, Pontryagin's minimum principle, dynamic programming, minimisation via Lagrange multipliers, calculus of variation etc.

For a planetary-type automatic transmission [Haj-Fraj, Pfeiffer 2001] have derived an optimal control law that minimised vehicle jerk. The powertrain was described by using a state space model containing five state variables (engine speed, turbine speed, output speed, input speed at

the differential, difference in angular displacement at the input and output of the propeller shaft and the vehicle acceleration). The control vector contained the amount of engine torque reduction and the clutch pressure as control variables. Only the upshift from first to second gear was considered (one-way clutch-to-clutch shift). The problem of the transition of the state of the oncoming clutch at the end of an upshift from slipping to being locked was given specific consideration. Thus, the performance index contained two cost functions, a quadratic form of the vehicle jerk in the inertia phase and at the end of the gearshift and a quadratic form evaluating the control signal expenditure. The optimal control law, which was derived through use of dynamic programming, has only been applied to the inertia phase, thus leaving the problematic transfer of engine torque in the torque phase apparently to conventional open-loop clutch pressure control. Simulation results were presented which demonstrated that the level of vehicle jerk could be drastically reduced at the end of the gearshift. The vehicle jerk in the torque phase was naturally unaffected by the control algorithm.

In [Hojo et al. 1992], a gearshift controller for gearshifts between the 2nd and the 3rd gear was developed. This was necessary because, on the considered automatic transmission, a gearshift between these two gears required changing the gear ratios on two planetary gear sets simultaneously (see "group change" explained in Section 2.1). In particular, on one planetary gear set the gear ratio had to be changed to a higher value and on the other gear set to a lower value. This circumstance, as also explained in Section 2.1, caused considerable shift quality problems. To solve the troublesome shift from 2nd to 3rd gear a new so-called "two-clutches cooperative controller" was developed. The idea behind this control strategy was, to specify speed reference trajectories for the two brakes taking part in the gearshift and to devise a controller that enables the tracking of the reference speed trajectories by manipulation of brake pressure. A discrete state space model of the transmission was constructed using a state vector that contained as state variables, the speed errors at both brakes, the speed errors for the next sampling step k+1 (discrete equivalent to derivative) and variables to compensate for a delay in the hydraulic actuation. A normal linear state variable feedback loop was introduced (as a servo system) and the controller gain matrix was obtained by solving a discrete Riccati equation that minimised a quadratic performance index (has not been stated in detail in the paper). For various different weightings the gain matrices were calculated and the optimum gain was determined through simulation of shift transients. The presented simulation and vehicle results showed that the proposed controller could reduce torque vibrations at the end of the gearshift from 2nd to 3rd gear. Since the proposed controller was applied to a special gearshift case involving a "group shift" it is not quite clear, whether this controller can also be used in a beneficial way for normal clutch-to-clutch shifts.

Torque-based Control of a Gearshift

The problem with controlling the pressure at the clutches involved in a clutch-to-clutch gearshift is, that because it is not possible to accurately determine the torque transmitted by the clutches from the clutch pressure signal, the influence of the application timing and parameter changes (e.g. change in friction coefficient) on the transmission output torque and therefore on the shift quality is not exactly known. Other advantages of torque control are added robustness and a direct influence on the shift character because the clutch torque or transmission output torque trajectories are directly related to the vehicle acceleration. Ideally, a direct control of clutch torque would have to be employed. However, information about the torque at the clutches is difficult to obtain. Thus, the more easily obtainable transmission output torque is controlled directly to improve shift quality. The problem of obtaining the torque signal is reviewed in detail in Section 2.5. All the control strategies reviewed here were applied to planetary-type automatic transmissions and made use of torque observation techniques.

The problem with conventional automatic transmissions is, that because of the existence of a torque converter and its non-linear dynamic behaviour when mechanically unlocked, the turbine torque is difficult to determine. A torque estimator and controller applied to an upshift were described in [Ibamoto et al. 1997]. The torque estimator calculated the turbine speed and turbine torque from throttle opening, engine speed and transmission output speed by using engine and torque converter characteristics. With the gear ratio the output torque could then be calculated in the inertia phase from the turbine torque.

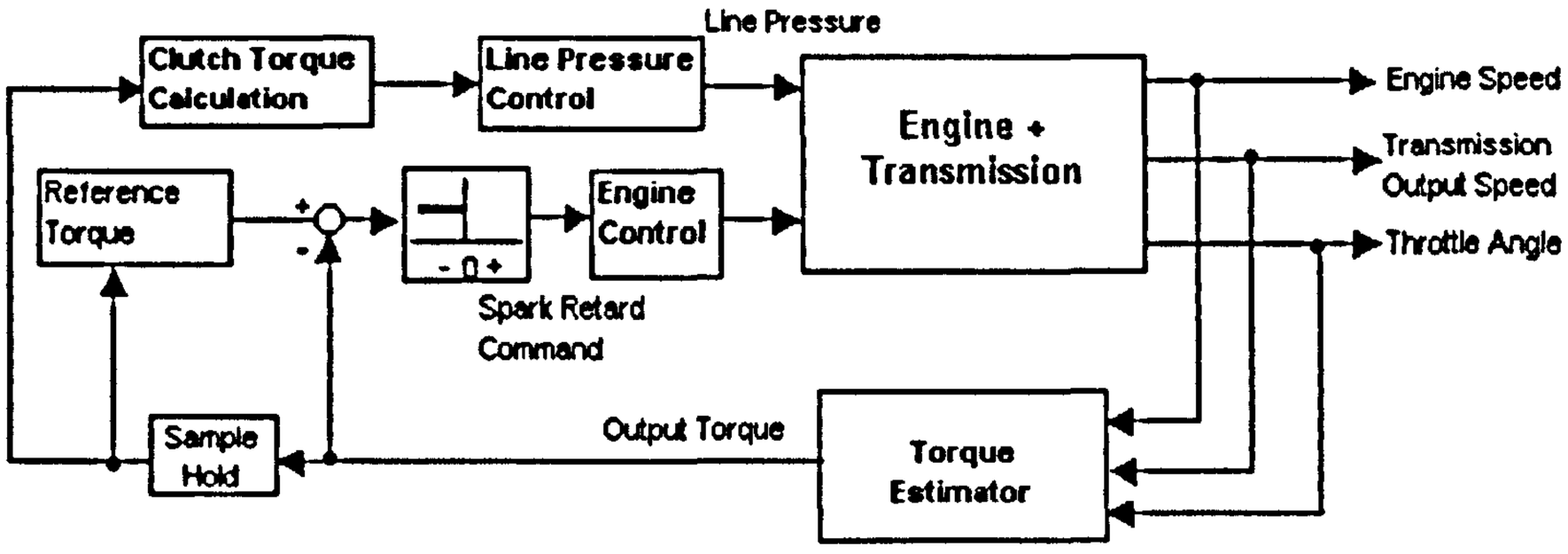

Figure 2.4 Closed-loop control by torque observation [Ibamoto et al 1997]

The torque control is depicted in Figure2.4 and was only activated in the inertia phase. The estimated output torque was sampled at the beginning of the gearshift. From this sampled output torque, an optimum line pressure and a reference torque was calculated. The output torque was compared with the reference torque during the inertia phase and a spark retard request was sent to the engine controller if the error in torque was negative. The accuracy of this estimation

method was evaluated against measurements for steady state and was reported to be +/- 10% of the measured value. The time delay between the measured and the estimated signal was about 50ms. The output torque peak at the end of the gearshift (upshift) could be reduced by the proposed control method. How the torque estimator coped with uncertainties in the model (engine and torque converter characteristics) and sensor noise has not been investigated. Also, how the synchronisation of the engine speed was managed in the inertia phase and how the torque phase was controlled has not been explained in the paper.

Another form of "torque" control for downshifts was described in [Minowa et al. 1996]. However, in this paper the first time derivative of the rotational speed at the output shaft was controlled instead of an estimated value of the output torque. The aim of the proposed control strategy was to reduce the vibrations at the end of the torque phase of a downshift. From comparison of measured shaft acceleration and shaft torque signals it was concluded, that the beginning of the torque vibrations at the output shaft could be effectively detected in the differential value of transmission output speed (acceleration). At the point where the start of the vibrations was detected, the torque control was activated. In this torque control the shaft acceleration, calculated from the rotational speed of the shaft, was fed back with a proportional gain to manipulate the spark advance. The feedback gain was determined by calibration. Further investigations on road gradients had shown that for a 2-1 kick-down shift on a 9% gradient the acceleration characteristic was different, which made it necessary to add a detection of the road slope and to suppress the proposed torque control on a steep road slope. Although the experimental results show that the torque fluctuations could be reduced on downshifts changing to the first gear, the sensitivity of this method to changes in the driving situations and the operating point of the engine is obvious. In the considered downshifts, the torque transfer in the torque phase was managed by a one-way clutch and the proposed control strategy was only used to suppress vibrations coming from the engagement of this device. Hence a control of the transmission output torque, leading to a smoother increase in torque in the torque phase, was not achieved.

The results obtained in both of the above described approaches had been combined by the same authors in [Minowa et al 1999] to detect both the beginning of the torque phase and the beginning of the inertia phase more accurately and to be able to control the estimated transmission output torque in the inertia phase of upshift and downshift. The proposed gearshift control system was developed for a conventional automatic transmission without a one-way clutch and made use of a feedback clutch pressure control, designed by H∞ control theory. Since the proposed torque control relied on clutch pressure manipulation in the inertia phase, it is not quite clear how the engine synchronisation was controlled. Use of engine control for this

task was not mentioned. However, the pressure profiles depicted in that paper, hint that clutch pressure manipulation was still used for engine synchronisation and that the torque control was only activated once the engine has already started to change its speed. Experimental results were given for a 2-3 upshift and 3-2 downshift and showed that the torque control was able to compensate for changes in the oil temperature (i.e. friction coefficient). However the large change of the output torque (vehicle jerk) at the point of transition between torque and inertia phase could not be reduced and hence it is questionable whether this control strategy really improves shift quality as proposed in the paper.

A further step towards precision of torque estimation was accomplished in [Shin et al. 2000], where the torque at the turbine shaft of the hydraulic torque converter was estimated using a neural network, which proved to be more accurate than a static model. The data for training the neural network had been acquired from experiments. The estimation error of the neural network method was less than 10%. Again the torque control was only active in the inertia phase where the aim was to control the acceleration of the turbine shaft along a specified reference trajectory. The tracking error was fed into an inverse model of the powertrain and solenoid valve located in the feed forward path of the controller to calculate the necessary clutch pressure (i.e. controller gain). The friction coefficient in this inverse plant model was estimated and adapted based on measurements of turbine shaft speed and transmission output speed. Thus, the control algorithm could compensate for variations in the friction coefficient. The presented experimental results showed that the control algorithm was indeed robust against changes in the oil temperature and thus friction coefficient. The change of the friction coefficients with increasing temperature lead to a spike in the transmission output torque at the end of the inertia phase of an upshift. This torque peak was successfully reduced by the control. However, since the control had only been applied to the inertia phase (of an upshift) and engine speed synchronisation was apparently accomplished in a conventional way by manipulation of clutch pressure, no substantial improvements in the overall shift quality could be observed.

Speed-based Control of a Gearshift

Most of the control strategies described in this section, have as their main objective, the tracking of a reference engine speed profile (turbine shaft speed if transmission is equipped with a torque converter) in the inertia phase, by a modulation of clutch pressure. The reference speed trajectories are usually obtained from vehicle tests. The closed loop tracking of an engine reference speed profile provides a means for a direct, if limited, influence on the gearshift characteristic and some consistency in the gearshift performance when the operating point of the engine changes. In Figure2.5 an example of such a speed based control circuit of a multi disc

brake (conventional automatic transmission) is depicted. The pressure at the brake (clutch) is manipulated via a proportional solenoid valve. The advantage of an inexpensive control method (speed measurement) is opposed by the disadvantage of not being able to directly influence the shift quality through due to the lack of a control of transmission output torque. At the end of this section a speed-based control strategy is described for application to the control of the transfer of engine torque in the torque phase.

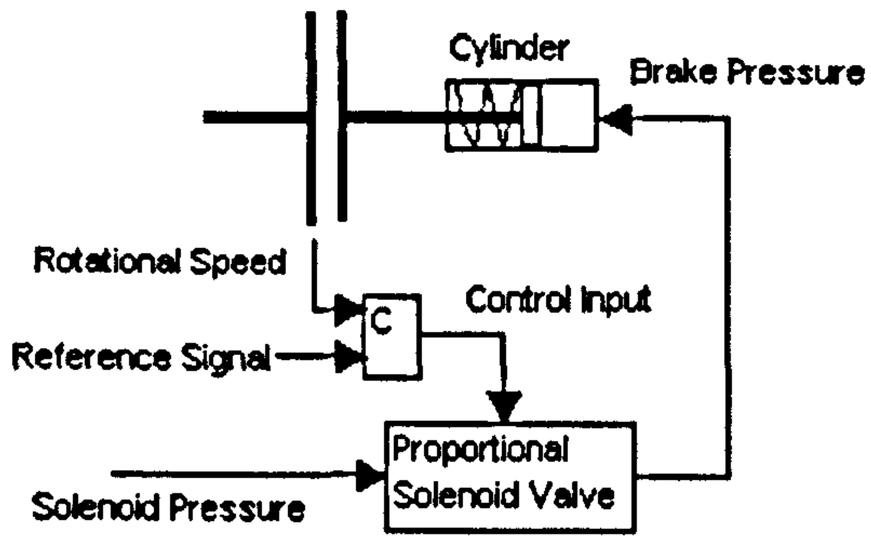

Figure 2.5 Speed control through manipulation of clutch pressure [Sanada, Kitagawa 1998]

For a conventional automatic transmission such speed-based controllers have been described in [Zheng et al. 1998 and 1999]. In the earlier paper a powertrain model, which included engine, torque converter, transmission and clutch hydraulics was developed. The dynamic model of the turbine speed response to accumulator backpressure was non-linear and had to be linearised. Due to pole cancellation it was possible to reduce the seventh order model to a fourth order model. The solenoid valve that manipulated the accumulator backpressure was modelled as a linear second order transfer function. In the latter paper, a 1-2 upshift controller was developed that manipulated the accumulator backpressure in order to let the turbine speed track a specified trajectory (simply a linear decrease of engine speed) during the inertia phase. By varying the slope of the reference trajectory, the time and smoothness of the shift could be influenced. The controller basically consisted of a lead compensator together with a free integrator for tracking and was designed in the frequency-domain. The simulation results showed clutch speed and output shaft torque profiles for various slopes of the reference trajectory and demonstrated the effect of these different slopes on the output shaft torque and hence shift quality.

In [Sanada, Kitagawa 1998], a robust control system consisting of a feed forward and a feedback loop (two-degrees-of-freedom control system) was developed, where the feedback controller ensured stability and the feed forward loop enabled the system to follow the specified speed trajectory (ramp signal). The design of the feed forward controller required the development of a reference model, in order to let the rotational speed follow the desired signal without any steady state error and within a specified shift time. The feedback controller was

designed using μ-synthesis. The uncertainties introduced in the model contained, an error in the model of the proportional valve and a variation in the coefficient of friction. The specifications of the robust controller contained norms of weighted sensitivity and complementary sensitivity. The controller gain was obtained by using the Matlab® μ–toolbox. Experimental results showed the effectiveness of the proposed controller in tracking the reference speed signal. The robustness against variations in the friction coefficient was demonstrated for two values (0.16 and 0.1). However, the friction coefficients have been assumed to be constant values, i.e. not functions of the sliding speed. This simplification may allow robust tracking of the speed signal, however, does not eliminate the effects of the friction coefficient on the transmission output torque, hence shift quality.

A robust speed controller for an automatic transmission of layshaft type was developed in [Furukawa et al. 1994], using H∞ control theory. The plant (transmission) was treated as a time-varying system, which was linearised around five sampling points. The controller, which manipulated clutch pressure in the inertia phase, was designed using the worst-case design approach. The uncertainties considered in the model, contained variations in engine torque, in the friction coefficient and in the measured speed variable. Simulation results have been presented that show the difference in the speed profiles between a case where no disturbances (friction coefficient, engine torque) occurred and one with disturbances. It was argued that the robust controller can cope with these disturbances and thus the shift quality improves. However, judging from the vehicle acceleration profiles depicted in that paper, it was not apparent that the shift quality actually improved when using the proposed controller.

A speed-based control applied to the torque phase of a clutch-to-clutch shift on a twin clutch transmission was proposed, in principle, in [Volkswagen AG 1998 (Patent DE 196 31 983 C1)]. The relative speed across the offgoing clutch (i.e. clutch slip) was controlled to a fixed constant value of about 50 rpm during the torque phase of upshifts and downshifts. The control of clutch slip was accomplished by manipulating hydraulic pressure at the offgoing clutch. Ramping the pressure up at the oncoming clutch, forces the clutch slip controller to reduce the pressure at the offgoing clutch, in order to maintain the clutch slip reference value. At the time the pressure at the offgoing clutch has been reduced to zero by the controller, all engine torque has been transferred to the oncoming clutch, without a negative torque contribution from the offgoing clutch. The slip controller effectively mimics the behaviour of a one-way clutch disengaging the original gear, once the oncoming clutch carries the full engine torque. This is a very powerful technique of controlling the torque transfer between the two clutches without creating too much vehicle jerk and without actually employing a one-way clutch.

In [Meinhard and Berger 2003] the application of clutch slip control for vibration damping during vehicle launch was described. An interesting observation was made, namely, that if the clutch is controlled to operate in part-slip (alternating transitions between the states of slipping and of stiction), then the mean value of the transmitted torque would increase with increasing clutch slip. This behaviour effectively reflects a positive gradient of friction with sliding speed and thus avoids the problem of self-excited vibrations (negative gradient) leading to instability in the control system.

2.1.3 Gearshift Control – Integrated Powertrain Control Approach

This section reviews techniques that tackle the control of gearshifts by an integrated powertrain control approach. Common to all the concepts reviewed in this section is the attempt to produce certain specified rotational speed and torque profiles at the input and/or output shaft of the transmission. By controlling the powertrain along those trajectories (closed-loop control), the gearshift can be executed more precisely and robustly in terms of engine torque transfer and engine speed synchronisation.

Optimal Control of a Gearshift

The principles of optimal control have already been explained in the section on local transmission control concepts. Here the concept of optimal control is applied to an integrated powertrain control, also featuring closed-loop engine torque control.

An optimal control for clutch-to-clutch shifts with clutch torque and engine torque as control variables was developed in [Geering, Schmid 1995, Schmid 1994] where the control problem was treated as a linear quadratic regulator. The optimal control law was derived on a theoretical basis (analytic optimisation based on calculus of variation) and the problems of torque observation and the dynamics of the hydraulic clutch actuation were not considered. The idea was to use the LQR to govern the state of the powertrain to an end state corresponding to the target gear, which functioned as a reference point for the regulator. The optimal control law governed the actual state to the target state along state trajectories that minimised the performance index. The performance index included two main terms. The first main term was a final state penalty, which included a weighted quadratic function of the error in achieving the desired terminal state values (solutions to the differential equations of the target gear) and an

extension that included a function of the torque at the offgoing clutch (upshift), which ensured continuity at the state transition from stick to slip. The second main term consisted of two integral terms, each containing a product of a Lagrange multiplier and a term that included the implicit form of the dynamic equations of motion in the phase of transition from the original gear to the target gear (this ensures that the equations of motion are fulfilled while the performance index is minimised). The first integral term contained the equations of motion before the change in structure and the second one after the transition. The performance index of the regulator was then extended by a weighted quadratic function to account for the energy dissipation at the clutches during the gearshift. This, however, caused a discontinuity in the clutch torque trajectories. To avoid this problem, the state vector had to be extended by including the engine torque and the torque at both clutches as additional state variables. This modification made it necessary to introduce the rate of change of clutch and engine torque as control variables. Although a smooth transition of the control and state variables without a discontinuity at the time of the structural change was accomplished, no explicit performance index for the vehicle acceleration or the vehicle jerk was introduced. This explains that, although, the proposed controller was able to reduce the amount of dissipated energy, vehicle jerk was not decreased effectively during the gearshift. The presented simulation results of an upshift and downshift between the 3rd and the 4th gear confirm this theory by showing an improvement in the energy dissipation, however, not in the amount of longitudinal vehicle jerk.

Torque-based Control of a Gearshift

The aim of closed-loop torque-based gearshift controllers is to manipulate powertrain control variables (e.g. throttle angle, spark advance, clutch pressure etc.) thus tracking certain pre-specified or optimised trajectories for clutch torque, engine torque or transmission output shaft torque (drive shaft torque) in order to achieve robustness of the gearshift control and offering a way to directly influence the character of the gearshift.

In [Wheals et al 2001, O'Neil and Harrison 2000] an integrated control applied to a twin clutch transmission was developed for improved shift quality. A sensor was applied to the transmission output for measurement of the torque at the output shaft. The supervisory control used for powertrain management provided as one parameter a direct request for transmission output shaft torque, which was used as a target for the gearshift controller. By selecting a smooth output torque trajectory as reference trajectory for the torque-based gearshift controller it could be ensured that the vehicle jerk stays at a minimum. The torque based controller consisted of three core control loops, one for each clutch and one to execute an increase (downshift)/decrease

(upshift) in the engine torque. In the torque phase the off-going clutch was disengaged by an open loop control (pre-calibrated pressure profile), whilst the oncoming clutch was manipulated to let the transmission output torque track a specified reference trajectory. The engine control loop incorporated a speed control system, which was used to prevent the offgoing clutch from generating a negative torque contribution due to a late disengagement (tie-up). Unfortunately it was not explained how this speed control worked. During the inertia phase the oncoming clutch was used to control the output shaft torque to follow the reference torque trajectory. The engine speed controller was then switched to a new reference speed trajectory in order to achieve synchronisation with the target gear. Simulation results (upshifts) of the shift controller for different objectives from a smooth to a sporty shift were presented in the form of vehicle acceleration profiles. However, since reference profiles and clutch pressure profiles have not been included in the figures it was difficult to see how the control algorithm actually worked. This made it difficult to assess the performance of the gearshift control in detail. In particular, the successfulness in controlling the engine torque transfer in the torque phase could not be evaluated. However, the benefits in controlling the transmission output torque during an upshift in terms of influence on the gearshift character have been clearly pointed out in the paper. It was also established that the torque-based approach is superior to open loop or speed-based techniques for the control of gearshifts.

In [Minowa et al. 1994] the estimation of transmission output shaft torque was managed by a mathematical observer using steady state characteristics of the torque converter. It was found that the start of the inertia phase could be detected through the occurrence of a sharp rise in the estimated output shaft torque signal. This had been verified in experiments where the actual torque was measured by a torque sensor on a test vehicle. A torque controller was then developed for the tracking of a reference torque profile during the inertia phase of an upshift by manipulation of the throttle angle. In this torque control system, a target value for the drive torque (transmission output shaft torque) was calculated from the accelerator pedal angle and the vehicle speed, which was then inputted to an inverse model of the torque converter to get the target engine torque. The error between the target drive torque and the estimated drive torque was fed into a PID controller, which determined the change in engine torque necessary to follow the reference drive torque trajectory. The target of the engine torque was then corrected based on the contribution from the PID controller. Finally, the corrected engine torque value was inputted into an inverse model of the engine to produce the necessary change in the throttle angle. The estimated output shaft torque was also used to determine a target value for the hydraulic clutch pressure (oncoming clutch). The results for a power upshift from 1st to 2nd gear at 25% acceleration pedal angle showed a reduction of 35% in the peak-to-peak value of the longitudinal vehicle acceleration. An accurate tracking of the reference torque, however, has not

been accomplished and a shift shock still existed at the end of the inertia phase with the proposed controller. This has to do with the slow response of the engine to changes in the throttle angle, which makes a throttle manipulation in general less suited for torque control.

A simple integrated engine/transmission (conventional automatic transmission) control concept to reduce the "shift shock" (defined as half the value of the product of the time span of the torque phase times the drop in torque during the torque phase) was described in [Sawamura et al. 1998] where both throttle angle and spark advance were controlled to reduce torque fluctuations during the inertia phase of up and downshifts. Based on information from various sensors about accelerator pedal position, vehicle velocity etc. the target drive shaft torque was calculated. From this torque value the target torque at the torque converter turbine shaft was calculated, which was compared to the actual turbine torque (lock-up clutch torque) calculated from vehicle velocity and actual throttle opening. This provided the necessary change in engine torque, which was then used to calculate the necessary change in throttle angle. Two simulation results were presented, one for a power-on upshift from 1st to 2nd gear and the other one for a power-off downshift from 4th to 2nd gear. The proposed control strategy was compared to a strategy without throttle manipulation. For the upshift a small improvement in terms of vehicle jerk at the point of transition to the inertia phase could be seen. However due to a poor coordination between engine control and the control of pressure at the oncoming clutch, the effect of the throttle manipulation was only limited. A more pronounced improvement could be seen for the power-off downshift, where the engine torque increase could help to avoid a large decrease in brake torque.

Speed-based Control of a Gearshift

As already explained, the advantage of speed-based gearshift control is that no complicated torque estimation or cost intensive torque sensor measurement is required. Only easy-to-measure speed signals are required. However, as with local gearshift control concepts, simple engine speed control in the inertia phase cannot achieve the same performance as torque-based gearshift controllers.

In [Moskwa 1993, Moskwa, Hedrick 1990] a method of controlling the engine torque by modulation of the two engine controls spark advance and throttle opening was proposed to obtain a smooth shift. The jerk at the planetary carrier (situated at the output shaft) of a conventional automatic transmission was related to engine and torque converter speed. Those speeds were then controlled by a sliding mode control law to obtain zero vehicle jerk in the

inertia phase of the gearshift (upshift from 1st to 2nd gear). To obtain a smooth upshift, the engine torque was decreased during the inertia phase to bring the differential speed at the second clutch smoothly to zero. At the synchronous point the engine torque was brought back to its original value to ensure proper acceleration. To use the strength of both spark advance control (fast response) and throttle control (which enables both large increases and decreases in the engine torque but is relatively slow in the response), a multivariable control was developed by the authors, where the throttle was used as much as possible and the control of spark advance was only added when a fast response of the controller was required. The engine speed was controlled in the inertia phase to follow a linear trajectory to the speed level of the target gear. Sliding mode control laws for spark advance and throttle angle were derived, which led the speed error trajectory (error between engine speed and desired engine speed) along a sliding surface to zero. Both engine controls had weighted feedback gains to adjust dominance in the speed control. From simulation results it was found that equal weighting gave a poor tracking performance, whereas if less feedback gain was put on the throttle, the test trajectory (sinusoidal speed profile) was tracked well. Since the control laws contained a simple model of the engine, an investigation of the robustness of the control algorithm against modelling errors would have been interesting. Although it was stated that the sliding mode control provides robustness against modelling errors, a detailed demonstration of this claim has not been carried out.

A control method that minimised the vehicle jerk during the gearshift of a conventional automatic transmission was described in [Hong et al.1999]. By manipulating the torque at the offgoing clutch, clutch slip was controlled during the torque phase. This clutch slip control was employed to avoid increased vehicle jerk at the transition to the inertia phase. During the inertia phase the speed at the reaction carrier and turbine shaft were controlled along a sliding surface, which represented the error between the actual and the desired speed trajectory. The sliding mode controller manipulated spark advance, throttle angle to follow a specified speed trajectory. The sliding mode controller looked similar to that of the above reviewed paper. However, the focus of this paper was on aspects of powertrain modelling and the description of the controller was only schematic. Simulation results show vehicle acceleration and jerk for an upshift from 1st to 2nd gear. An improvement in the shift quality by the proposed controller over a conventional controller was definitively achieved. However, the problem of how the, essentially model-based, sliding mode controller can cope with the influence of modelling errors and a variation in the clutch friction on the operation of the controller and the shift quality has not been investigated. Also the problem of acquiring the torque values at the clutches (an information required in the control law) was also not been touched upon.

A description of an integrated control strategy of a gearshift applied to a powertrain equipped with a twin clutch transmission was found in [Daimler Chrysler AG 2001 (Patent DE 199 39 334 A1)]. In that patent, the engine speed was controlled along a specified trajectory during inertia phase by manipulation of engine torque (throttle manipulation). It was further explained that in a case where it is not possible to control the engine speed during synchronisation through engine torque modulation, the synchronisation had to be accomplished by controlling the clutch pressure (conventional way). Such a case may, for example, occur during an upshift under coasting, when the engine torque has reached its minimum (i.e. drag torque) or during a power-on downshift, where the engine torque has reached its maximum. In addition to a closed-loop control of engine speed, clutch slip was controlled for an optimum transfer of engine torque in the torque phase. Due to the nature of a patent, a detailed evaluation of the control strategy through simulation or experimental results was missing.

2.2 Control Issues specific to Gearshifts on Twin Clutch Transmissions

In the previous sections control strategies for clutch-to-clutch powershifts have been reviewed. However, as already mentioned in the introduction to the section on gearshift control, gearshifts on twin clutch transmission consist of two parts: a clutch-to-clutch shift and a gear pre-selection on the torque-free half of the transmission. Furthermore, multiple gearshifts in particular gearshifts within the same half of the twin clutch transmission (gearshift from 4^{th} to 2^{nd} gear) cannot be accomplished as simple clutch-to-clutch shifts. These two problems are special to the twin clutch transmission design and will be treated in the following two sub-sections.

2.2.1 Multiple Gearshifts

The unique layout of a twin clutch transmission makes it impossible to shift between gears located in the same half of the transmission by simple clutch-to-clutch shifts. Such gearshifts are henceforth denoted as multiple gearshifts (within the same half of the transmission) or in case only one gear is skipped (e.g. direct shift from 4^{th} to 2^{nd} gear) "doubleshifts". Since both, the original and target gear are located in the same half of the transmission and the disengagement of the original gear and the engagement and synchronisation of the target gear requires this transmission half to be torque-free, either the clutch has to be disengaged for the duration of the

change of gears (torque interruption), or an alternative way for controlling such multiple gearshifts needs to be employed.

To overcome this limitation without any interruption in traction [Wagner 1994] has investigated how in principle the pressure at the two clutches has to be modulated, in order to accomplish so called "doubleshifts" within a minimum time. The author first discusses the two obvious strategies:

1) A shift with an interruption in traction, where the power-transmitting clutch is disengaged to make the relevant transmission half torque-free and to enable the engine to accelerate. Such a shift has the character of gearshifts found on manual and automated manual transmissions. Although such a shift is very fast and therefore spontaneous, the disadvantage of the loss in drive power still prevails.
2) Two consecutive shifts. The consecutive shifts are clearly distinguishable by the driver as two single gearshift events. However, the advantage is that traction is maintained at the wheels throughout the multiple gearshift.

[Wagner 1994] then proposes an alternative to these two methods that maintains powershifting capability whilst at the same time enabling the engine to constantly accelerate to the level of the target gear and hence not be detectable as two gearshifts. This was achieved by integrating the two gearshifts into one single gearshift and by using the second clutch to transmit part of the engine torque whilst changing the gear.

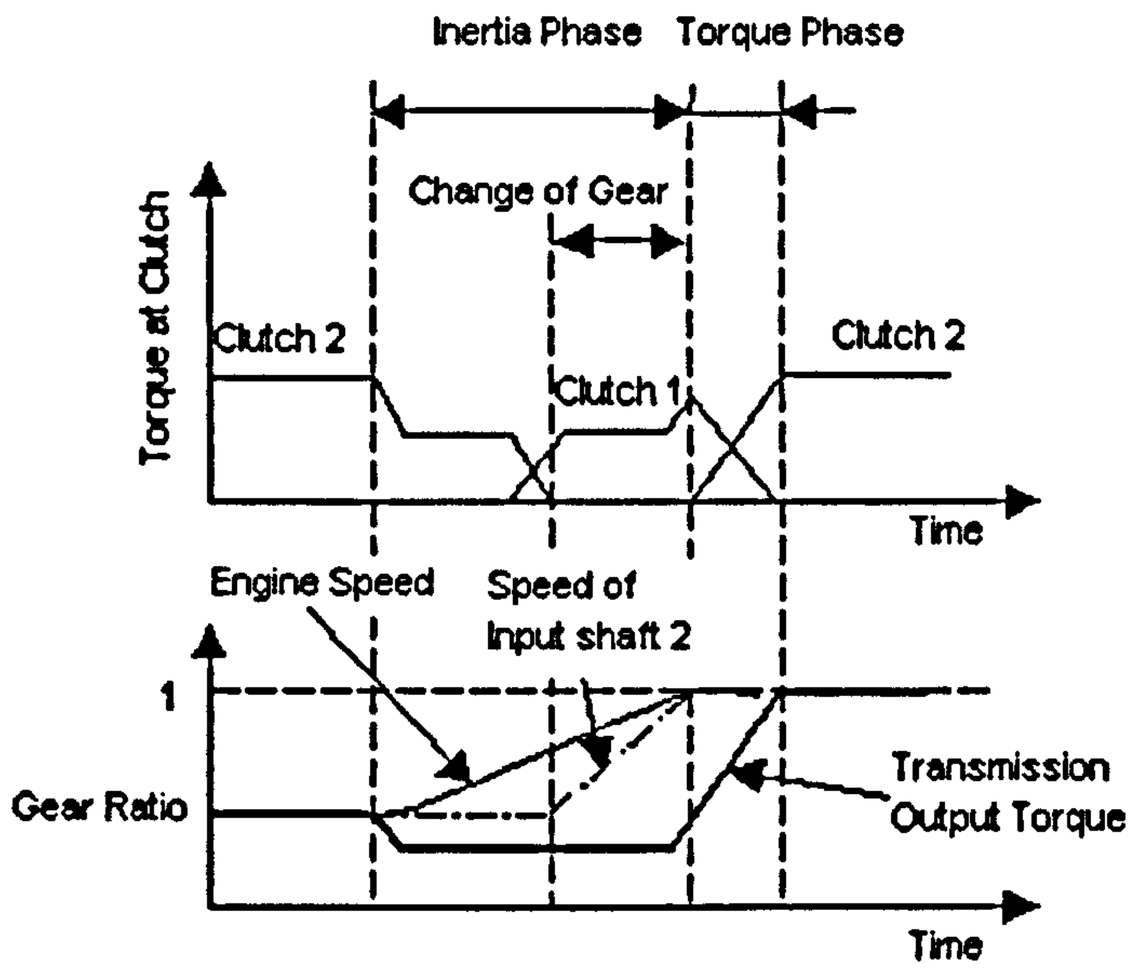

Figure 2.6 "Double-downshift" realised as two integrated downshifts [Wagner 1994]

During the first part of the shift (Figure2.6) the engine (denoted as transmission input speed in Figure2.6) speeds up due to pressure decrease at the offgoing clutch (clutch 2 in Figure2.6).

Shortly before reaching the synchronous speed of the intermediate gear, engine torque is partially transferred to the clutch of the intermediate gear (clutch 1in Figure2.6) through an increase in pressure at this clutch. Thus, the engine can continue its acceleration and the output torque can be kept at around the same level as for the original gear. After this first part of the shift the relevant half of the transmission is now torque-free, enabling the change of synchronisers to engage the target gear. To end the acceleration of the engine, the pressure at the "intermediate clutch" is raised again for a short time, followed by the second and final torque phase where engine torque is fully transferred to the clutch carrying the target gear. The quality of the shift can be compared to that of a single shift; the disadvantage of a long shift time still exists (about 0.3 to 0.4 s longer than doubleshifts on conventional automatic gearboxes). The described procedure can, in principle, also be applied to double upshifts. Experimental results were presented which showed a total time for such integrated doubleshifts of about 1 to 1.1 seconds.

A strategy, which also had the aim of using the second clutch to provide fill-in torque, has been described in [Volkswagen AG 1998 (Patent DE 197 11 820)]. In this patent, the highest gear ratio that is available on the half of the transmission in which the doubleshift occurs is selected (usually either 5^{th} or 6^{th} gear). This is in contrast to the strategy discussed above where the intermediate gear was selected on the second clutch and the doubleshift consisted effectively of two integrated upshifts or downshifts. The strategy, which is proposed in the above-mentioned patent, requires a slightly different approach in the control of the gearshift, more closely resembling that of an automated manual transmission with a second clutch (AMT-2). First the torque-transmitting clutch is disengaged, whilst at the same time the second clutch, carrying the highest gear of that transmission half, is engaged (effectively an upshift). The first half of the transmission is then torque-free enabling a change of synchronisers. Once the engine has been synchronised to the speed level of the target gear and the target gear has been engaged the second clutch is again disengaged and the original clutch engaged (effectively a downshift). Thus, the second clutch transmits engine torque to the transmission output during the doubleshift. Since the second clutch carries a gear ratio that is lower than both the original and the target gear, the output torque must naturally also be lower compared to the torque level before and after the gearshift. Hence, this approach does not represent a "true" powershift as compared to the strategy of [Wagner 1994], however, it is easier in its application.

2.2.2 Gear Pre-Selection

As already mentioned, gearshifts on twin clutch transmissions consist of a clutch-to-clutch shift and a gear change or gear pre-selection on the torque-free half of the transmission. Two main problems do appear with gear pre-selection. Firstly, the question of which gear to select and secondly, the problem of how to control the actual gear engagement. The change of gear always takes considerable time. Hence, it is desired to keep this procedure as short as possible in order not to increase the overall shift time. One way would be, to simply not engage a gear in the torque-free half of the transmission at all, unless a request for a gearshift occurs [Volkswagen AG 1998 (Patent DE 196 31 983 C1)]. This saves the trouble of a time consuming change of gears, if a discrepancy between the requested gear and the actually engaged gear occurs. However, this strategy has the disadvantage of requiring the input shafts in the transmission to be synchronised from standstill, which again increases time. An alternative strategy was proposed in [Wagner 1994], where always a gear lower than the actually engaged one is pre-selected. This has the big advantage, that for a downshift where a quick response of the transmission is important, no change of gear is necessary prior to the gearshift. However, subsequent to the downshift the gear needs to be changed on the half of the transmission from which the gearshift started. Consequently, on upshifts the gear needs to be changed beforehand. A strategy for an "intelligent" gear pre-selection was proposed in [Daimler Chrysler AG 2000 (Patent DE 199 37 716 C1)]. The proposed strategy aims to predict a likely target gear, so this predicted gear could be engaged before an actual request for a gearshift takes place. Unfortunately, the patent is not very specific about the nature or structure of the predictor, however, the prediction is based on information about variables such as engine speed, vehicle speed, actual gear, accelerator pedal position and brake pedal position. This predictor probably works similar to shift schedule techniques applied to planetary type automatic transmission, often using fuzzy logic with rule tables obtained from test data. Since such a strategy works satisfactorily only if the driving situation is quite clear and non-changing, it is doubted whether such an approach really is successful over a range of, often highly transitory, driving situations.

As for the second problem, the engagement and synchronisation of the pre-selected gear, a number of techniques are available. The problem arises, when conventional cone-type synchronisers with hydraulic actuation are employed. In particular, in the lower gear range, the required short synchronisation times can lead to either destruction of the synchroniser mechanism or to large reactions at the transmission output torque. This is due to the energy, necessary for synchronising the input shafts to the selected gear, which is transferred to or from the transmission output and leads to increased vehicle jerk. Apart from using the engine for gear

synchronisation, which is only applicable to automated manual transmissions, the only other well-known alternative is to use central synchronisation. In a central synchronisation scheme, external devices provide the power for synchronisation (e.g. an electric motor for accelerating the input shaft and an external brake for decelerating the input shaft). Thus, the problem of torque reaction can be avoided at the cost of additional apparatus and complexity.

Another solution for twin clutch transmissions was proposed in [Volkswagen AG 1998 (Patent DE 196 31 983 C1)], which, as already explained, makes use of the fact that the target gear is not engaged until the gearshift commences. This has the disadvantage of increased synchronisation energy and duration, but offers additional flexibility in the gear engagement. The approach described in that patent makes use of the clutch that is currently not transmitting torque. By partially engaging this clutch shortly before the torque phase of the upshift and downshift the input shaft carrying the target gear is accelerated from standstill. Since the input shaft is decoupled from the transmission output (gear is not yet engaged) during the synchronisation, the torque reactions at the transmission output are much smaller and theoretically only simple dog clutches need to be employed for the final engagement of the gears. In this strategy the energy for gear synchronisation is provided by the engine, which requires an accurate control of the clutches during the gear synchronisation.

The paper of [Franke 1999] proposes a new central synchronisation for a twin clutch transmissions that also works without conventional synchronisers. The input shaft of the torque transmitting half of the transmission can be coupled to the other idle running input shaft through a gear stage (gear ratio of a single gear step between geometrically stepped gear ratios) by means of a small synchronisation clutch. The employment of two small clutches, ensures that the idle running input shaft can be either accelerated or decelerated to a lower or a higher gear ratio. The gears can then be engaged through simple dog clutches. The actual gearshift is not accomplished as a clutch-to-clutch shift in that paper, however, the disengagement of the offgoing clutch and the engagement of the oncoming clutch is separated by a small time span, where the engine is synchronised to the level of the target gear via manipulation of throttle angle or fuel amount. This results to a short interruption in the traction at the wheels, which is considered by the author as not critical to the shift feel. In the described synchronisation method the input shaft that is synchronised is not connected to the output shaft, hence, the problematic transfer of synchronisation torque to the output is avoided here as well. However, the proposed central synchronisation seems to allow only synchronisations to the next higher or lower gear, thus making multiple gearshift and hence also synchronisations over more gear ratios impossible. The author has not discussed this problem.

An interesting approach, that tackles the problem of gear synchronisation from a design point of view, was presented in [Albers et al 2003], where switch-able one-way clutches (overrunning clutches) are used instead of cone-type synchronisers. These so-called "Gear Coupler" automatically handled the synchronisation and engagement of the target gear when the oncoming clutch was applied. The gear coupler of the original gear automatically disengaged the gear and thus disconnected the offgoing clutch from the engine. The engine synchronisation was carried out conventionally by increasing (decreasing on downshifts) the torque at the oncoming clutch (offgoing clutch on downshifts). This approach is very interesting due to the fact that it theoretically allows a smooth acceleration of the vehicle. However, the test rig results still show transmission output torque reaction due to the abrupt engagement of the one-way clutches, which under high engine torque produce oscillations in a compliant driveline. The proposed design certainly needs validation through real vehicle tests but the idea shows promise, because it provides a way of substituting conventional synchronisers by shift elements that "automatically" engage the gear when the oncoming clutch is engaged and thus avoid the problematic transmission output torque reactions.

2.3 Control of Gearshifts on Automated Manual Transmissions

Gearshifts on manual- and therefore also on automated manual transmissions are different in nature from clutch-to-clutch shifts on planetary-type automatic transmissions or twin clutch transmission. The main difference is, that during the gearshift the main clutch has to be disengaged in order to enable an engagement and synchronisation of the new gear on the transmission. The engine is disconnected from the transmission and therefore also from the wheels during this period of time, which results to an interruption in the traction at the wheels. During the gearshift the engine also needs to be synchronised to the speed level of the new gear. This engine synchronisation can be achieved through clutch control alone, or through a more sophisticated control strategy that incorporates a manipulation of engine controls. The latter approach requires employment of integrated powertrain control techniques and often involves tracking of engine speed and/or torque trajectories during the gearshift.

An integrated powertrain control strategy for gearshifts on automated manual transmissions was developed in [Löffler 2000] where the control objectives included minimisation of vehicle jerk and energy dissipation and maximisation of "drive power" at the wheels. Maximising "drive

power" ensures that the interruption in tractive force during the gearshift is kept at a minimum. The three objectives were stated in the form of an error function for drive power (deviation of actual drive power from desired drive power), certain parameters that characterise the longitudinal vehicle acceleration profile such as peak-to-peak value, slope etc. and the energy that is dissipated at the clutch during the gear change. For these three objectives a cost function was developed that also included a parameter accounting for the type of driver and the operating conditions. The aim of the optimisation was to determine trajectories for engine torque engine, speed and clutch torque (control variables) that govern the system from the beginning of the gearshift to the end, whilst minimising the cost function. To solve this optimisation problem, the system state trajectories (state vector contained engine speed, engine torque and clutch torque) were approximated by means of a sum of B-spline functions during the gearshift. As a second step in the so called "collocation method", which is a direct numerical optimisation method, the optimal trajectory that minimised the cost function was selected from the set of all possible system trajectories. In this way, the reference trajectories for clutch torque engine torque and engine speed were produced. Once the reference trajectories were determined, engine and clutch variables were controlled to track these optimum reference trajectories during the gearshift. The optimisation procedure was executed onboard. A few results from simulation and vehicle experiments were presented that showed the effects of changes in the optimisation criteria. For example, a sporty shift was compared to a smooth shift. Apart from a difference in the slopes of engine torque reduction and re-application no major difference could be observed. A sporty shift did not show any torque vibrations as a result of the fast increase of engine torque. Since the proposed control strategy has not been compared to a conventional control strategy, it is difficult to say whether the lack of any torque vibrations is actually a result of the superior control strategy or whether this is due to an overly simplified dynamic model of the powertrain.

The gear change on an automated manual transmission without use of a dry clutch [Petterson, Nielsen 2000] or without use of synchronisers [Fredrikson, Egardt 2000] was accomplished in those two papers by controlling the engine torque to zero and by controlling the engine speed during the synchronisation phase. Furthermore a suppression of torque oscillations was accomplished by controlling the "twist" in the driveline to zero.

In [Fredrikson, Egardt 2000] the gearshift was split into five distinctive phases. In the first phase engine torque is governed to zero, which means that the transmission becomes torque-free and the dog clutch can be disengaged. In the second phase the dog clutch is disengaged and the transmission is put into neutral gear. This is followed by the synchronisation of engine speed to level of target gear in the third phase. In the forth and fifth phase the dog clutch is engaged again and engine torque is re-applied to the transmission. A state vector containing five state

variables including engine speed, pressure in the turbo charger, compressor power, torsional displacement in drive shaft and speed of wheels was introduced to describe the operating state of the powertrain. The control variables included the fuel amount and the inlet valve position of the turbine of the turbo charger. The engine torque was approximated by a function of fuel amount and pressure in the turbocharger. The control objectives of the transmission torque control and synchronisation speed control were to minimise shift time, exhaust emissions and driveline oscillations. During the torque control phases the driveline torque and the pressure in the turbo charger were controlled in a closed-loop system. During the speed synchronisation the engine speed was controlled along the desired trajectory by a closed loop system, while keeping the air-to-fuel ratio at a steady level to avoid exhaust problems. From the simulation result for an upshift the single control steps of making the transmission torque-free, synchronising the engine and increasing the engine torque at the end of the shift could be clearly discerned. The simulation result has demonstrated that a gearshift without use of conventional synchronisers (only dog clutches required) is possible. However, the simulation result shows strong torque reactions during the gearshift, which means poor shift quality

The paper by [Petterson, Nielsen 2000] described, in principle, the same procedure of a reduction of engine torque to zero and a subsequent engine speed synchronisation. However, with the difference that, synchronisers were exclusively used for the speed synchronisation without employing a dry clutch at all. Also the problem of torque measurement was paid more attention, which was managed by torque estimation employing a Kalman filter. A state space representation using the following state variables: drive shaft torsion (estimated), engine speed and wheel speed (measured) was used to describe the powertrain dynamics. The aim of the control strategy was to control driveline torque oscillations resulting from the fast reduction of engine torque to zero. A PID controller was employed as a torque controller. The performance of the PID controller was evaluated against a PI controller. The PI-controller could not handle a robust and fast control and showed oscillations. However due to the simplicity of the engine torque production model (steady state engine map) it is difficult to say whether the controller works properly even if the dynamics in the engine torque production (i.e. delay in engine torque production from a change in the fuel amount as control variable) are taken into account.

In [Ercole et al 1999] a fuzzy logic supervisory controller managed the coordination of engine and transmission controls during vehicle launch and gearshifts. First a detailed analysis was carried out that showed which engine or transmission controls influenced the smoothness of gearshifts and wear of the clutch. It was found that throttle opening during the gearshift and the timing of the re-engagement of the clutch was crucial for a smooth shift. To coordinate engine and transmission operation, a supervisory controller that contained fuzzy rule tables was

developed. Input variables to this fuzzy controller included engine torque, engine speed derivative, clutch slip speed and its derivative and clutch speed. The output variables included the derivatives of throttle angle and clutch lever position. The performance was demonstrated based on a simulation result for a vehicle launch. Unfortunately no result was given for a gearshift. It was also concluded that due to the high computing power necessary for the fuzzy controller, an onboard execution of the control algorithm was not possible.

2.4 Gearshift Quality Metrics

As has been noticed in the last three sections on gearshift control one of the main objectives, if not the most important, was the improvement of the shift quality. How can "shift quality" be measured? Certainly, the shift feel is subjective and something that different passengers experience differently. Various attempts have aimed at finding a metric to quantify shift quality.

In the section on local open-loop control concepts of powershifts an adaptive open-loop gearshift control [Gebert and Kücükay 1997] had been discussed. In that work a detailed characterisation of the acceleration profile during a gearshift was undertaken and a shift metric based on those results was developed. The main ideas of this work will be briefly restated here. By analysing the profile of the longitudinal acceleration during a gearshift (signal was filtered and only the range from 4 to 10 Hz was recorded), it was found that, signal flanks in the acceleration profile that oppose the general acceleration tendency, were considered worst by passengers. For example on an upshift the general acceleration tendency is falling that means that only rising signal flanks have to be considered to characterise the shift quality. To characterise these signal flanks a number of parameters have been used such as amplitude of the flank, maximum slope of the flank, amplitude of vehicle jerk (i.e. the first time derivative of the vehicle acceleration). In this way a general description for the shift feel based on the vehicle acceleration profile was found.

[Naruse et al 1993] attempted to derive a shift metric for powershifts that reflects the human shift feel. From experiments with subjective ratings it was found that the human body responded more sensitively to fore and aft vibrations in low frequency ranges and to vertical vibrations in high frequency ranges. Considering this finding, data from vibration measurements have been filtered accordingly. It was distinguished between for fore-aft acceleration and vertical accelerations. The shift shocks were evaluated differently according to the type of shift (down-, upshift). A correlation between measurements of vehicle vibrations and torque fluctuations at

the drive shaft had been derived. The results showed that about 90% of the fore and aft vibrations were in the low frequency range (0 to 7 Hz) and could be attributed to torque fluctuations coming directly from the automatic transmission.

From signal analysis [Schwab 1994] found that a discrepancy between vehicle acceleration and wheel torque after the initial shift shock of a powershift occurred. This was attributed to the fact that backlash in the driveline filters out frequencies above 5Hz. For this reason the fore/aft acceleration was used to describe the shift feel. A shift quality metric was developed that was made up of four acceleration components, which could be extracted from a raw acceleration signal. These components included the peak-to-peak acceleration, the peak-to-peak jerk, the maximum average power (power level of the shift) and the 10-14 Hz contribution (to capture body and suspension resonance). A neural network was created and trained based on data from vehicle measurements and subjective gearshift ratings. Inputs to this model were the four components of the shift quality metric. The aim was to obtain a subjective rating based on new acceleration data. The results agreed very well, also at the extreme ends of the subjective scale.

In [Wheals et al 2001] it was stated that conventional approaches of shift quality characterisation, which derive their measures from experimental data and try to correlate the values of parameters such as longitudinal acceleration, jerk etc. to subjective driver ratings, show an error of up to 2 points in the ATZ (Automobil Technische Zeitschrift) 1-10 scale. Therefore, an alternative approach was proposed (still under development) that derived a shift metric from a range of variables such as pressure profiles acting on the driver's body, time derivatives of head pitch, vehicle pitch, visual effect of rpm-meter, acoustic effect of engine revolution, and the muscular effort to maintain the seat position. A neural network was applied to determine a shift metric out of vehicle measurements of these variables.

In [Wheals et al 2002] an investigation of different shift quality metrics applicable to automated manual transmissions was conducted. It was found that the shift time alone (i.e. time of torque interruption) is not sufficient to characterise the shift quality on an AMT. Two techniques for improved shift quality metrics were proposed. In the first approach, a cost function that assesses the acceleration time profile of the actual AMT gearshift relative to an ideal shift was introduced. The second approach, builds upon the technique described in [Wheals et al 2001] and made use of an "android" model (model of a human body) to model the response of the driver to the gearshift event (variables such body pressure distribution, head pitch are included). A neural network is then applied to establish a correlation between vehicle data and driver model responses to predict an ATZ gearshift rating. Real vehicle measurement data and real subjective ratings are taken for comparison to the model.

Three investigations into shift quality that head in a slightly different direction can be found in the papers by [Szadkowski 1991, Szadkowski and McNerney 1993], where objective measures to describe the shift feel on a transmission equipped with cone-type synchronisers were developed. In these papers the manual engagement of a gear by a shift lever and hence the control of the synchronisation process by the shift lever force (applied by the driver) was investigated. Although not of direct relevance to the gearshift quality metric for a planetary-type automatic transmission, they give an interesting insight in the shift quality aspects of synchronisation processes, which are, for example, part of the gear change on a twin clutch transmission.

In the earliest paper [Szadkowski 1991] the main objective was to develop a mathematical model for the synchroniser engagement to describe "shiftability" and shift quality for the gear engagement. Furthermore design recommendations for clutch and transmission and quality measures for clutches and transmissions were derived. Three synchronisation phases were distinguished. In the first phase, the synchroniser torque forces the speed of the gear to match that of the shaft (synchronising function). In the second, phase the synchroniser torque forces the blocker to index (synchroniser indexing function) and in the third phase, the synchroniser torque forces the clutching teeth to engage the index gear (gear indexing function). The linkage between shift lever and synchroniser was assumed to be rigid (i.e. shift time was assumed to be equal to synchronisation time). To rate the shift quality, a variable called "shift effort" (shift impulse) was defined as the product of handball load and shift time. A parameter variation study was carried out using the mathematical model of the synchroniser engagement to investigate the influence on the "shift effort". From this study two main recommendations were drawn. Firstly, shift quality improvements can be achieved by a decrease in the driven disc inertia, a decrease in drag torque generated by the clutch, an increase in the synchronising torque, a decrease in the inertia within the transmission and a decrease in the viscous drag torque (downshift). Secondly, shift quality is more sensitive to clutch parameters than parameters of the transmission.

In [Szadkowski and McNerney 1993] the studies of the earlier paper had been extended. The synchroniser linkage was now considered to produces losses and a coefficient for the efficiency of the linkage was derived from experimental data. The shift quality was rated by use of the synchronising time only, assuming a constant maximum handball load. Vehicle experiments were carried out to verify the shift quality rating and to determine the efficiency of the linkage. One of the conclusions was that less than 65% of the handball force was effectively transmitted to the synchroniser cone.

In this brief review of literature on gearshift quality metrics, one variable has crystallised to be a main predictor for shift quality, namely the longitudinal vehicle acceleration profile (or the wheel torque, which is related to it). Although, only the torque at the wheels is actually of interest, because vibration contributions from the powertrain as a whole affect the shift feel, it is nevertheless also possible to use the torque at the output shaft of the transmission to assess shift quality. This is possible since the contributions of both, engine and transmission in creating vibrations in the drivetrain are actually contained in the value of the transmission output torque and these forced vibrations only excite the rest of the drivetrain downstream from the transmission. In the acceleration profile various parameters characterise the shift quality, one of the most important is the steepness of the gradients. This first time derivative of the acceleration is called vehicle jerk.

2.5 Sensor Measurements and Observation of Transmission Torque

As already discussed in the sections on torque-based gearshift controls, the gearshift control can improve from the knowledge of the transmission output torque. Either, for use in a control algorithm that directly controls the transmission output torque, or a control strategy where the output torque value is used to get information about the torque transmitted through the clutches participating in the gearshift. The application of a torque sensor has long not been possible because of various reasons such as cost, reliability and a complicated application and calibration process. Nowadays, the torque sensor technology has improved; the costs have dropped so it is providing an interesting alternative to obtain the torque signal. The great advantage is the accuracy, once it has been calibrated properly.

The estimation of torque through a mathematical observation is an inexpensive alternative, which basically determines the torque value from, easy-to-measure signals like angular speeds at various points in the transmission. The problem of observer techniques is, that they rely on the accuracy of a dynamic model of the transmission/powertrain. Although the value of the estimated torque is constantly monitored and corrected based on measurable variables used in the observer model (usually rotational speeds), neglected dependencies of variables or neglected nonlinear effects are difficult to compensate. Also the adaptability of the observer to parameter changes and the robustness against noise-polluted sensor signals needs to be taken in account.

In [Yi et al. 2000], estimation of the output torque of a conventional automatic transmission, equipped with a hydraulic torque converter, was achieved by use of a non-linear so-called "adaptive sliding observer". The basic idea was to use a "Luenberger" observer, which reconstructs the state of a linear system from measurements of its input and output. With this type of observer the system parameters (system model contained in observer) have to be known beforehand. If they are not known (initial values have to be known), the observer can be extended to adapt the system parameters during operation such that the state observation error asymptotically approaches zero (along a sliding surface). In the paper a non-linear adaptive sliding observer to estimate the turbine torque (at the turbine shaft of the hydraulic torque converter) from engine and turbine speed measurements was developed. This enabled observation of the turbine torque throughout the gearshift despite the change in the system structure at the point of transition from torque to inertia phase. The sliding surface was defined as the error between the measurement and the estimation of the turbine speed from which then the turbine torque and the transmission output torque could be determined. Experimental studies were carried out, using a transmission set-up on a test rig. A variation of 8-25% in the turbine torque was observed for a temperature range from 29-85 degrees Celsius (oil temperature in torque converter). This effect was due to the increase of the turbine torque with an increase in the oil temperature (i.e.fluid viscosity). It was demonstrated that a simple "steady state" observer could not cope with the changes in operating conditions of the torque converter (change in temperature and thus oil viscosity). However, the adaptive observer handled the variation in the system well.

[Moskwa and Pan 1995] also applied a sliding mode observer to estimate the turbine torque in a planetary type automatic transmission. Two possible designs of the sliding mode observer, one with and one without integrators were compared. The proposed observers required measurement of four speed values (engine, turbine, planetary carrier and ring gear) to produce an estimate of the turbine torque. A gaussian random noise with an intensity of 100 rpm was added to these speed signals to test the robustness of the observer. It was found that the observer design with integrators allowed use of smaller gains in the observer model and thus showed smaller estimation errors when subjected to sensor noise.

The non-linear observer presented in [Hahn et al 2001] was applied in a different form to estimate the hydraulic pressure in a torque converter lock-up clutch. The value of the actuation pressure was reconstructed based on measurement of the clutch slip velocity and information about the input to the solenoid valve (i.e. duty ratio). The observer included models for the hydraulic actuation (2^{nd} order linear transfer function derived by system identification theory) and the friction clutch. The observer was designed to be robust against uncertainties in friction

coefficient and system damping; however, uncertainties in the hydraulic model have not been accounted for. The simulation results show that the estimation error is generally bounded within a range of around 0.5 bar. It was argued that the performance could be further improved by using a better model of the hydraulic system.

The application of a torque sensor has been suggested in [Wheals et al 2001] for use in a twin clutch transmission. Possible torque sensor designs, which are both rugged and inexpensive have been described in [Turner 1988], [Beckley et al 2002] and [Ruser et al 2002]. The prime problems of torque sensors so far had been their costs, ruggedness and size. For prototype vehicles an application has not posed any problems since costs and size do not matter there.

In [Turner 1988] a torque sensor, for measurements on rotating shafts in automotive applications, was proposed. The sensor made use of the fact that a torque applied to the sensor part in the driveshaft changes the resonance frequency of this sensor system. The change in the resonance frequency could be then detected by a change in the impedance of the exciting coil (non-rotating part of the sensor). The coils are connected to a capacitor, where the change in the impedance and hence torque could be detected as a change in the electric current. It was found that the repeatability of the senor measurements was very good. This is of more importance to, for example, the control of transmission output torque, than the absolute accuracy of the measurements. It was further found that the linearity of the sensor deteriorated when the temperature was raised, the repeatability, however, was unaffected by the increase in temperature.

The torque sensor presented in [Beckley et al 2002] made use of the SAW (Surface Acoustic Wave) principle, which offers the advantages of being able to withstand heat, dirt and mechanical vibrations. Also the nature of the principle (i.e. using radio frequencies) makes it ideal for a non-contact coupling. Usually two SAW devices are located on the rotating shaft and a differential measurement is used to compensate for changes in the temperature or bending of the shaft. When torque is applied to the shaft either the phase of a reflected sound wave is delayed or the natural frequency of a resonator is changed. Either of the two effects can be used to infer the applied torque. In the paper a dynamic model of the presented SAW resonator is developed and simulation results are discussed. The results show that the accuracy of the torque measurement stays within +/-2.5% in the temperature band between –40 and +125°C. Measurement of the temperature could improve accuracy of the torque measurement further (+/-0.15%)

In the paper of [Ruser et al 2002], a torque sensor is discussed that makes use of the magneto-elastic effects of ferromagnetic materials (i.e. rotating shaft). A torque applied to the shaft leads to a change in the magnetic properties (permeability) of the shaft material, which result in a magnetic flow that induces a voltage in the non-rotating detector coil. These sensors offer high robustness and good repeatability of the measurement results. However, these sensors suffer from a reduced accuracy and are dependent on the material properties as well as the gap between shaft and coil. The paper proposes a technique to overcome these limitations by a cyclic magnetisation and re-magnetisation to obtain defined operation points.

2.6 Powertrain Dynamics and Modelling

In this section, the literature in the field of powertrain modelling and dynamics will be reviewed, the problems or peculiarities associated with the actual modelling of a powertrain equipped with a twin clutch transmission will be treated in Chapter 3 in more detail.

2.6.1 Automotive Powertrain: Dynamics, Modelling Techniques and Simulation

This section reviews literature that is aimed at the fundamental principles of powertrain modelling for controller development.

In [Ciesla and Jennings 1995] the development of a powertrain model using a modular approach has been described. These modules contained a model of a diesel engine, a torque converter, a clutch, shafts etc. and were programmed using EASY 5 simulation language. A similar approach to powertrain modelling was described in the paper of [Moskwa et. al. 1997], where the authors also made use of the modular approach, however, MATLAB/SIMULINK® was employed as simulation software. Both papers emphasise the importance of the causality (cause and effect relationship between input and output variables) in modular modelling, in order to avoid the existence of algebraic loops, which slow down the simulation. Such a causality can be achieved if for example modules, which contain purely inertial components, are linked with compliant parts (spring-damper elements) in an alternating series. The paper of [Schreiber Schindler 2001], which also makes use of the modular approach for powertrain modelling,

stressed the importance of considerations on the necessary accuracy level and hence complexity, at an early stage in the modelling of a powertrain model.

Although the paper of [Powell et. al. 1998] dealt with dynamic modelling of hybrid electric powertrain systems, all major "common" drivetrain modelling issues were tackled. Equations of motion were given for all powertrain components including those for an automated manual transmission; also a simple mathematical model for a gasoline engine was described in that paper. The paper of [Quinn, Lyons 1998] dealt with the features SIMULINK® and STATEFLOW® provide for the dynamic modelling powertrains. A simple model of an automotive powertrain including an automated layshaft transmission with torque converter and simple hydraulic actuation was developed in SIMULINK®. The STATEFLOW® toolbox was introduced and the advantage of this toolbox for the development of a sequentially operating gearshift controller, in particular its easy implementation, were demonstrated.

An important factor, when modelling the dynamics of a powetrain in the low frequency range, is the dynamics of the tyre. The dynamic properties of the tyre determine the effect that torsional vibrations in the driveline have on the vehicle longitudinal acceleration. To capture and analyse these effects properly it is of importance to model the tyre dynamics correctly. The modelling of a tyre by means of spring-damper elements and mass inertias was described in [Zegelaar and Pacejka 1997]. The tyre tread-band behaves like a rigid body in the frequency range of 0-100 Hz, hence the tread band can be modelled as ring with mass inertia and the whole tyre model is called "rigid ring model". In order to capture the compliance of the tyre in all three dimensions, spring damper elements were introduced that connected the tread-ring to the rim (second mass inertia) and reflected the stiffness and damping properties of the tyre sidewalls. A "brush" model was employed to model the stationary slip of the tyre and hence to reflect the stick-slip behaviour of the tyre in the road contact patch. The equations of motion were developed and the results were compared to experimental data obtained from a test rig where the tyre was driven by a big drum to reflect the road surface. Frequency response functions of brake torque and wheel slip variations, obtained by experiments, were compared to simulation data and showed a satisfactory agreement. The same model was used in [Bruni et al 1997], where the focus was on an identification of the stiffness and damping parameters. The parameter values were obtained by minimising the difference between the natural frequencies that were obtained through calculation of a dynamic model and the damped natural frequencies acquired from experimental data (mean square approach). The model was then used to calculate certain dynamic responses and was verified against experimental data.

2.6.2 Engine Dynamics and Modelling

All of the engine models reviewed here, are basically four stroke spark ignition (SI) engines. It is thought that these engines incorporate all the interesting engine control issues and represent a more general case for controller development then diesel engines where only the amount (and timing) of fuel injected into the cylinder is manipulated. Each of the following five papers made use of a so-called mean value engine model, which simply described the overall dynamic behaviour of the engine in the low frequency range by producing a mean torque value at the output and neglecting high frequency fluctuations in the torque production. The restriction to the low frequency range (5-15Hz) is sufficient from the standpoint of gearshift controller development and analysis because here only the engine behaviour in this low frequency range is of relevance. This restriction allows use of simpler engine models (i.e. mean value engine models).

[Crossley Cook 1991] described a four-cylinder engine model where the functions for mass rate of air flowing through throttle and intake manifold and the regression function for the combustion process, were derived by regression analysis from experimental test rig data. This engine model was created in MATLAB/SIMULINK® in [The Math Works 1998] with the only difference that the exhaust gas re-circulation had been neglected for reasons of simplicity.

A model of a SI-engine based on theoretical considerations was developed in [Moskwa, Hedrick 1992]. This model offered the advantage of having a more general applicability, but required detailed parameter identification. A MATLAB/SIMULINK® description for that model was obtained in [Weeks Moskwa 1995]. In this paper only the structure of the main modules was depicted, however, a detailed analysis of the behaviour of internal variables of the engine to transient throttle inputs was carried out based on simulation results.

A general overview and investigation on engine modelling was carried out in [Hendricks 1997], where the author first compared various mean value engine modelling approaches, including the above listed, and then developed a relatively simple engine model suited to a wide range of applications. However, explanations were kept short in that paper and the model was still more complex than the one of Crossley and Cook.

In [Song and Byun 1999] a throttle actuator control system based on the reference model following approach was developed. A second order state space model captured the dynamics of an electric motor used as a throttle actuator. The open loop response time of a variation in

throttle angle from wide open to zero degrees at the maximum duty ratio (pulse-width modulated input signal to the electric motor) was about 30ms. The controller was able to improve response times of the throttle angle, in particular, in the range of smaller variations in reference input. Thus, response delays in the throttle actuation could be minimised to values that are considerably lower compared to the response times of the engine to throttle inputs.

2.6.3 Transmission Dynamics and Modelling

Transmission Dynamics – General Modelling Issues

A mathematical description of the transmission and the rest of the drivetrain can be obtained in various ways. First, the equation of motion can be represented in different forms: In a state space description, which includes the equation of motion in one set of equations (which can be put into matrix form) or as a loose set of equations for each single powertrain component from which linear transfer functions may be generated. The latter representation is often used when the model is built up in a modular way. The former approach is more compact and can provide advantages in the simulation time (can be of interest if used as an inverse model in an observer or as a reference model) but can get very complicated and inflexible if the size of the model and increases. The advantage of a modular structure is that it can be easily modified and is therefore much more flexible when changing the configuration of the drivetrain.

The equations of motion can be derived in several different ways; by applying Newton's second law, the Lagrange equations or principles of classical mechanics such as d'Alembert's or Hamilton's principle. Newton's second law can be applied to each of the powertrain components separately to produce equations of motion in the longitudinal and rotational direction. This approach is often selected if the model is built up in a modular way. The other approaches basically produce the equations of motion from energy functions that need to be derived beforehand and are often applied if a closed linear set of equations for the powertrain/drivetrain model as a whole is desired. Another important element that needs to be considered in the process of deriving the equations of motion for the powertrain, is the existence of nonlinear elements and the problem of how to linearise them.

The equations of motion for a drivetrain can also be derived with the help of graphical methods of system design. This was demonstrated in [Cho, Hedrick 1989] where a mathematical model of a conventional automatic transmission was created from a bond-graph description. The bond graph technique basically depicts the power flow through the transmission from which the equations of motion can be easily deduced. The bond graph method was also applied in [Kwon,

Kim 2000], where a detailed model of a planetary-type automatic transmission including hydraulic actuation of the shift elements, was developed to obtain a more accurate simulation model for gearshift quality analysis.

To study transient characteristics of an automatic transmission including torque converter, especially during a gearshift, [Kim et al 1994] developed a transmission model using the approach via Newton's second law. The same method for an automatic transmission of the same type but different mechanical structure was employed by [Pan, Moskwa 1995], to simulate the dynamic behaviour of the transmission during a gearshift. The Newtonian approach was also used in [Zheng et al. 1998] to derive equations of motion for a planetary type transmission. In addition to the transmission model also the dynamics of the hydraulic clutch actuation system were modeled. From these nonlinear equations, a linearised seventh order model was derived for aim of an easy application of linear control principles.

A different approach was chosen by [Zhong et al 1999], who developed a transmission model based on the "Lever analogy", which is another graphical method that depicts the kinematical relationship between the single transmission components (planetary gear sets). Based on that graph the authors were able to derive the equations of motion by application of the Lagrange equations including a Lagrange multiplier to account for the dynamic constraints.

The only evidence of a twin clutch transmission model was found in [Veehof 1996]. The author mainly restricted himself to the discussion of simulation results for gearshifts and only briefly described the structure of the transmission model, which was kept very simple. The model was constructed using ACSL-modeling language.

One of the main complications in modelling a transmission arises from the occurrence of non-linear effects such as backlash, friction and other phenomena, which contain hysteresis, switching or saturation properties. Another complication results from the time varying structure of the equation of motion. When modelling a transmission that contains a friction clutch, two sets of equation of motion have to be derived, one for the state where the clutch is engaged and the other one for the state when the clutch slips. In other words the structure of the system and the degree of freedom change at the time of transition from one state to the other (stiction to friction). This makes it necessary to determine the conditions for the transition in terms of a switching logic, which in turn enables the decision which set of equation is active and has to be solved.

The construction of equations of motion of multibody systems with unilateral contacts has been treated in [Pfeiffer,Glocker 2000]. Unilateral contacts involve contact problems where a multi body system is constrained by a contact surface (e.g. ball suspended by a spring is restricted in its motion by a wall). This can also be applied to a clutch where the tangential movement (rotation) at the friction interface is limited by the friction coefficient and the applied load. The book contained various papers devoted to that topic and treated several unilateral contact problems including the switching character of a clutch engagement, at a theoretical level. A similar endeavour was pursued in [Pankiewicz, Schuller 2002], where the theoretical basis for the development of a modular simulation tool that copes with time varying systems such as those containing a friction clutch, was constructed. Equations of motion were derived and limits for the torque transmitted by the clutch (set by the friction coefficient) were included as inequality constraints. Based on these equations a tool library for powertrain simulation had been developed in MATLAB/SIMULINK®.

In [Klages et al 1997] a model of a conventional automatic transmission that could be used for a real-time Hardware-in-the-loop simulation was constructed. The dynamic behaviour of a clutch was modelled in a peculiar way, by making use of a "control loop" that included a proportional part to model static friction for small differential speeds and a limiter, which restricted the torque to the clutch capacity while the clutch was slipping. The model was implemented in MATLAB/SIMULINK®. Gearshift simulation results were given, however, were not compared to results achieved by conventional modelling or experimental measurements.

Although common-type synchronisers ("synchromesh") can be in principle treated like clutches, some special features remain to be considered when modelling. One of the main differences, apart from the conical friction contact is, that after the two friction halves of the synchroniser run at the same speed, the dog clutch-like part of the synchroniser engages, thus mechanically locking the synchroniser. In order to increase the torque capacity of the synchroniser, more friction contacts can be employed. An investigation of such multicone synchronisers was carried out in [Abdel-Halim et al. 2000], where dynamic models for two different triple-cone synchronisers were derived. The authors showed mathematically that there is a difference in the dynamic performance between the independent triple-cone (each of the friction cones can rotate independently) and the coupled triple-cone type. This was then also demonstrated on a test rig, where the distinctive behaviour of each of the two types of synchroniser was investigated for various temperature levels. These results have been compared to those of a single cone synchroniser and showed that the overall performance of the multicone synchroniser had improved. Only, at low temperatures the single cone type synchroniser was found to perform better (high oil viscosity).

Friction Dynamics and Clutch Model

An overview of different friction models to capture the stick- slip phenomenon and therefore to describe the friction behaviour at low speed levels in the vicinity of zero sliding speed was given in [Haessig and Friedland 1991]. The standard model to capture the behaviour of dry friction is depicted in Figure 2.7a. It assumes that the static friction coefficient is larger than the dynamic friction coefficient at zero differential speed. The kinetic friction coefficient can be a function of the sliding speed, but is assumed to have a constant value in the classic Coulomb friction model. Since the discontinuity at zero sliding speed does not reflect the physical reality in which the two contacting bodies are allowed to assume a small relative velocity before changing from stiction (static friction) to sliding, the standard model has been be modified. An approximation (Figure2.7b) through "stiffness" in the vicinity of zero sliding speed can help to capture this low speed behaviour. The disadvantage of this approximation is that it allows the body to accelerate even though the applied forces are less than the static friction force. To avoid this problem [Haessig and Friedland 1991] have presented three alternative friction models.

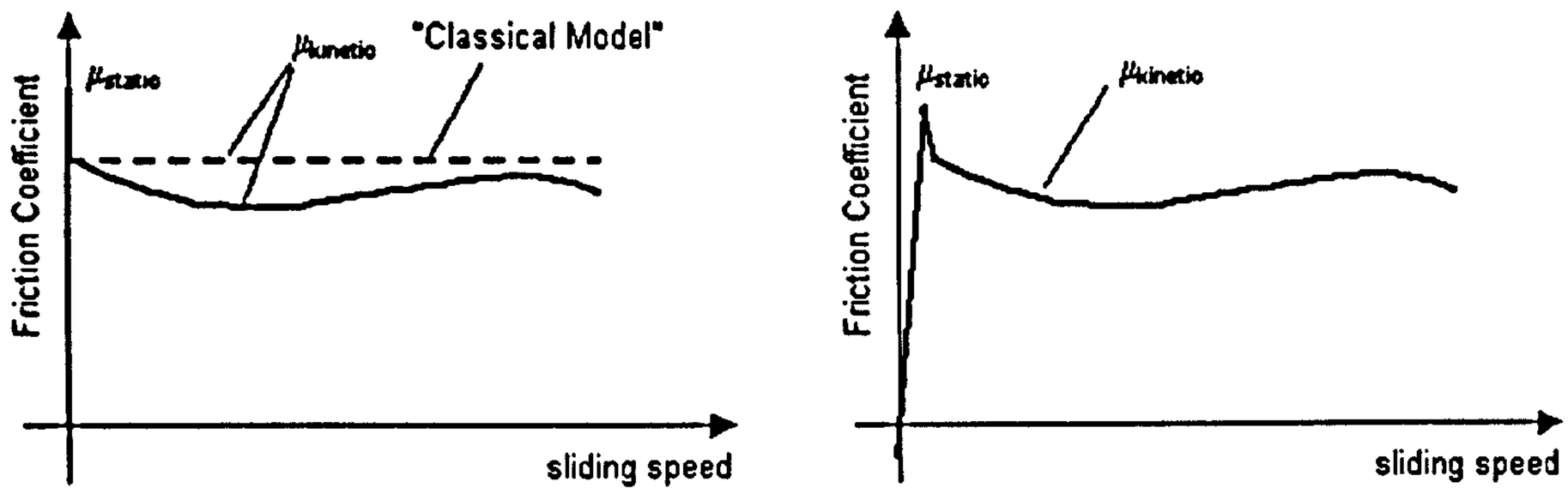

Figure 2.7 Friction coefficient versus sliding speed a) standard and classical model b) Approximation

One of the models presented there was "Karnopp's model"(denoted after the author who first published this model as described in [Haessig and Friedland 1991]), in which the order of the system is reduced at every instant the relative velocity vanishes. This can also be extended to incorporate the fact that the relative velocity can vary within a small band while the system still remains in the stiction state. Another model presented was the so-called "Reset Integrator Model", which includes a mechanism for zero velocity stiction. The input to this model is the relative velocity that is integrated to yield the relative displacement of the two friction parts. If the relative displacement goes beyond a certain initial position (boundaries must be defined), the model computes the slipping model otherwise the position is multiplied by a spring rate to simulate the behaviour in the vicinity of zero relative velocity. A further alternative is the "Bristle Model" where the facing surfaces have bristles extending from them, which models the

asperity contacts in dry friction. When the strain of any bristle exceeds a certain level the bond is broken and a new bond having smaller strain is established.

The "Karnopp Model" showed the fastest computation time but gets more complicated as the complexity of the system rises, whereas the other two remain fairly simple. All models incorporated the fact that there can be a small difference in the relative velocity of the two friction partners before sliding occurs and therefore the kinetic friction coefficient can be applied. However, the simulated contact loads and relative velocities were very small, which might be appropriate for a high accuracy positioning controller, but do not occur in an automotive clutch engagement. For that reason, it is doubted that the small deviation from zero relative velocity in the stiction phase, plays an important role under the fast, high energy engagements of automotive clutches. A version similar to "Karnop's model", however, without the "stiction band" around zero slipping speed, was generated in MATLAB/SIMULINK® in [The Math Works 1998]. The clutch model described in that paper made use of two main blocks, each containing the equations of motion for either the slipping or the stiction case and a block containing the switching logic to determine the point of transition between the two states. In many problems it might make sense to assume a constant kinetic friction coefficient (classic model). This might be justified from an accuracy point of view if it reflects the behaviour of the system in the area of interest properly enough. However, in the analysis of an automotive clutch engagement, the dependency of the friction coefficient on the differential speed across the clutch is of great importance and thus can not be neglected.

Friction Type and Friction Coefficient

In general two different friction types can be found on automotive clutches; dry friction, where the clutch plates are in contact without having a fluid between them and wet friction, where an automatic transmission fluid is present in the contact zone, which influences the friction behaviour of the clutch. The paper of [Großpietsch, Sudau 2000] compares dry and wet-type clutch concepts for application to a twin clutch transmission. As main advantages of the dry clutch design, good efficiency and small drag torque were listed. The wet clutch, however, was said to provide the advantage of having a small mass and size (therefore small mass inertia), good controllability, high power density and torque capacity. The conclusion of the authors was that the wet clutch possesses the greatest potential for employment in a twin clutch transmission, mainly because of the torque capacity, the mass inertia and the size.

Dry friction

The classic model for dry friction assumes a constant kinetic friction coefficient once sliding between the friction partners occurs. However, upon introspection of the characteristics of a typical dry friction material from a well-known clutch facing material manufacturer [www.raybestos.de] one can see that the friction coefficient is dependent on the slipping speed and on the temperature across the clutch. These dependencies, of course, vary with different friction materials. In general, the friction coefficient for the listed friction materials was observed to increase with increasing slipping speed, probably to achieve a positive gradient in order to avoid clutch judder. Furthermore, from the charts of the manufacturer it was observed, that the gradient of the fiction coefficient with sliding speed seemed to have changed slightly over the period of the complete test program, which included several thousands of engagement cycles. The mean values for the friction coefficient ranged between 0.37-0.44 in that test and are thus, considerably larger compared to those found for wet friction, which lie in the range of around 0.12-0.16. The influence of an increase in clutch temperature on the friction coefficient could also be observed in the test charts. In those charts a decrease in the friction coefficient could be seen to be starting at a temperature of around 380°C (more temperature resilient material). At this point the friction coefficient almost instantly dropped from a value of around 0.4 to 0.1. Below that critical temperature, the friction coefficient was quite stable and remained almost constant with increasing temperature. For another obviously less temperature resilient material the critical temperature lay at around 250 °C, but the friction coefficient decreased more gradually from around 0.45 at 250°C to around 0.35 at 350 °C. Temperatures above 250 °C should not be reached under normal engagement conditions. However, under hill start/hill hold conditions such high temperatures might be easily reached due to elongated engagement times resulting to intense heat production.

For the analysis of the clutch judder phenomenon in automotive dry clutches [Rabeih and Crolla 1996], applied a linear function for the friction coefficient with sliding speed in the form of: $\mu = A_0 + A_1\Delta v$. The gradient (A_1) was varied from +0.05 to –0.45. It was found that apart from the system damping and stiffness parameters a large negative gradient of the friction coefficient with sliding velocity leads to system instability and clutch judder. A similar study was carried out by [Centea et al 1999 and 2001], which also investigated the influence of the system damping and gradient of the friction coefficient on clutch judder. In the earlier paper they employed a similar function for the friction coefficient where they chose the coefficient A_0 to be 0.43 and varied A_1 from –0.016 to +0.016. In the more recent paper the authors employed a polynomial function of 3rd order ($\mu = A_0 + A_1\Delta v + A_2 (\Delta v)^2 + A_3 (\Delta v)^3$). They compared four dry friction materials with coefficients values shown in Table2.1.

Friction Material	A_0	A_1	A_2	A_3
1	0.3663	-0.031	0.0051	-0.00020
2	0.3961	-0.024	0.0034	-0.00010
3	0.3850	-0.0229	0.0036	-0.00010
4	0.6032	-0.0146	0.0009	-0.00001

Table 2.1. Coefficients of dry friction polynomial shown for different materials used in [Centea et al 2001]

The authors found that material 2 showed the worst judder behaviour and put this down to the negative slope of the friction gradient. Although material 2 and 3 have very similar friction polynomial the same severe effect was not observed with material 3. The polynomial friction coefficient functions given here have to be applied with care, because some of them only produce correct results in a limited range of relative velocity, typically between 0 m/s and 30 m/s. Outside this range some of the functions produce strongly negative values which certainly do not represent the reality appropriately.

The problem of finding a function to describe the friction coefficient at high speed sliding conditions (sliding speeds in the range between 30 to 300 m/s) was tackled by [Jiang and Ulbrich 2001]. The work was not directed at an investigation of a clutch engagement but treated the problem of dry friction at high sliding speeds on a more general basis. It was shown, that the applied load only had a strong influence on the friction coefficient at very high relative velocities of around 60 m/s and greater. For steel-to-steel contacts a decrease in the value of the friction coefficient between 30 and 300 m/s from about 0.1 to 0.06 was given. Clearly the value of the friction coefficient at automotive dry clutches is much larger and the sliding velocities much lower. This leads to the conclusion that the influence of the clamp load on the friction coefficient at the clutch can be neglected when analysing the effects that a variation in clutch friction has on the dynamics of an engagement of an automotive clutch.

Wet Friction

In contrast to dry friction clutches, which most commonly consist of two or sometimes three clutch plates, wet friction clutches usually feature several clutch plates or disks. The clutch pack of wet friction clutches consists of an alternating series of separator plates made of steel and friction plates. The friction plates consist of a core plate made of steel and a friction lining bonded to the core plate. As a material for the friction lining either sinter materials or paper (cellulose fibres) may be used. The sinter material is normally only employed for heavy-duty

applications. The vast majority of clutches installed on automatic transmissions incorporate paper based wet clutches which offer friction characteristics that lead to smoother engagements. On wet clutches, an automatic transmission fluid (ATF) occupies the space between the friction plates and the separator plates. The presence of this fluid and its properties greatly influences the shape of the friction coefficient and therefore the torque transmitted by the clutch. The clutch engagement process can be roughly broken down into three phases [Scott and Suntiwattana 1995], with the influence of the ATF varying from phase to phase:

- Squeeze film phase where the friction material and the separator plates are separated by the hydrodynamic ATF film (hydrodynamic lubrication)
- Squash film phase where the asperities (surface roughness) of the friction material come into contact with the separator plates to create some adhesive friction (mixed lubrication).
- Adhesive contact phase where the surface of the friction lining comes into contact with the separator plates

How the oil (ATF) influences the friction characteristics, strongly depends on the type of the base oil and the additives. This can be seen from a comparison between the friction coefficient of a normal ATF and that of an ATF with friction improvers. Two basic friction characteristics are distinguished in [Förster 1991]:

- Wet friction with friction improvers (GM specification) where the kinetic friction coefficient increases with increasing sliding velocity (positive gradient) and where the static friction coefficient is smaller than the kinetic one.
- Wet friction without friction improvers (FORD specification) where the kinetic friction coefficient decreases with increasing sliding velocity (negative gradient) and where the static friction coefficient is greater than the kinetic one.

Both types of ATF and their influence on the friction characteristics are shown in Figure2.8.

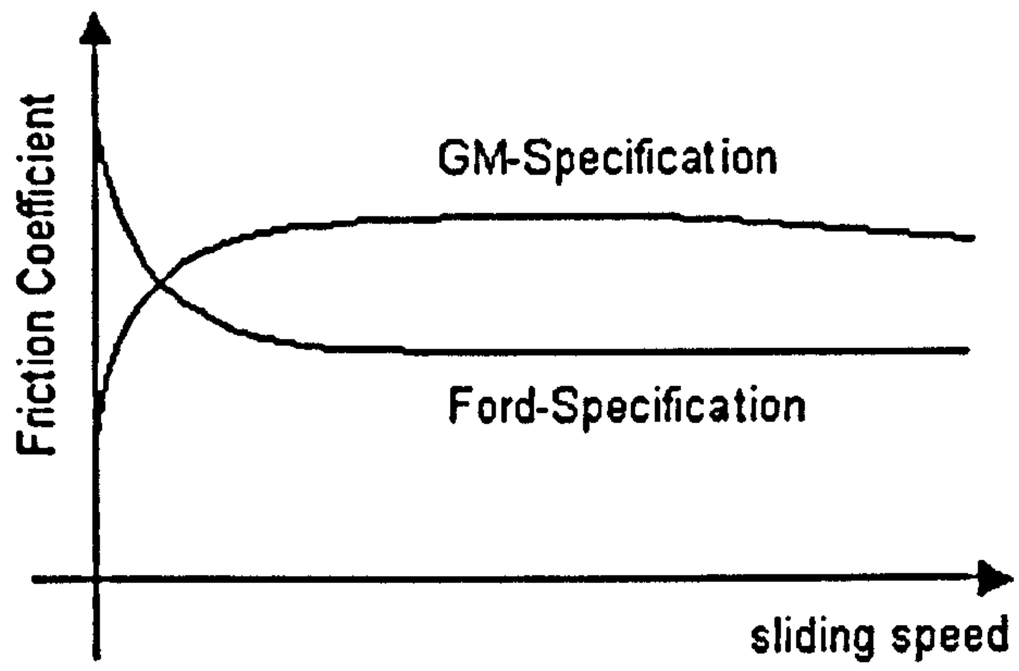

Figure 2.8 Friction coefficient versus sliding speed for GM and Ford Specification of ATF

The ATF plays a significant role in the engagement of a wet clutch especially in the first two phases where mainly hydrodynamic and mixed lubrication takes place. Since the properties of the hydrodynamic film and therefore the friction characteristics in those two phases are strongly affected by the viscosity of the fluid and the pressure distribution in the hydrodynamic film, the temperature (instant and start temperature) and the clamp load cause additional influences to the friction coefficient.

The influence of the temperature on the engagement of a wet clutch was investigated in [Holgerson and Lundberg 1999 Part 2] based on clutch engagement test rig results. The authors found that the static friction coefficient (here defined as the friction coefficient shortly before the clutch engages) decreased for an engagement at high energy levels (high initial sliding velocity) because of the higher temperature at the clutch facing (0.18 for 20 m/s initial relative speed and 0.17 for 30 m/s). However the energy level did not seem to have the same effect on the dynamic friction coefficient, which remained unaffected. Furthermore, the static friction coefficient decreased much stronger than the dynamic friction coefficient with increasing initial temperature (static dropped from 0.18 at 50 °C to 0.15 at 150 °C and the dynamic friction coefficient remained around 0.12). This means that the quotient between static and dynamic friction decreased with increasing initial temperature, which reduced the inclination to stick-slip vibrations (i.e. tendency towards a smaller negative or even positive gradient with sliding speed).

The influence of the presence of drive torque on wet clutch engagements was studied by the same authors [Holgerson and Lundberg 1999 Part 1], but was found to have negligible effect on the friction coefficient, however, engagement times increased compared to a case were only inertial torque was present (same amounts of dissipated energy assumed in both cases). Similar findings were reported in [Höhn et al 2003], which also found that the negative gradient of the friction coefficient (i.e. negative damping) with sliding speed, in addition to low values of the existing damping (i.e. the overall system damping becomes negative) forms a necessary condition for self-excited vibrations. Whether these friction-induced vibrations occur, also depends on the contact pressure in the friction contact, which was identified to be of lower importance compared to the gradient. In particular the gradient between 5 and 20 percent of the maximum relative velocity was found to be a reliable indicator for the occurrence of friction-induced vibrations.

To model the engagement of a wet clutch and capture the effects of temperature and clamp load on the hydrodynamic ATF film and therefore on the transmitted torque, [Yang, Lam and Fujii 1998] split the amount of torque transmitted by the clutch in two components. The first part

accounted for the asperity contacts between the friction material and the separator plate and the second part considered the hydrodynamic shear forces in the ATF film. The amount of the second component could be obtained by solving the Reynolds equations for the hydrodynamic film. It was found that this effect decreased as the two contact surfaces approached each other, the film thickness decreased to zero and more and more asperity contacts were developed. The hydrodynamic component of the transmitted torque was found to depend on the viscosity of the ATF (and thus temperature), the surface roughness, the film thickness, shear stress in the film and the relative velocity. However, the asperity component depended mainly on the kinetic friction coefficient as a function of the sliding speed. The simulation model was then validated against measured data and showed good agreement. The complexity (solution to Reynolds equations required) of the dynamic model makes it better suited for detailed clutch engagement investigations and less suited for the applications in powertrain models for controller design. The same authors developed a mathematical model to predict the temperature and thermal degradation in a wet clutch [Yang and Lam 1998]. It was found that the degradation mechanism of a paper based friction material consists of two parts, a thermal degradation (carbonisation of friction lining) and a mechanical degradation (wear). However, for a paper-based friction material the thermal degradation was found to be the major component.

A simple method to calculate the temperature across the clutch was developed in [Wouters 1991]. In that paper a control volume was laid over the clutch pack (included separator plate friction material and core plate) and divided into several small blocks. A heat balance was then applied to each block in order to derive a temperature distribution in one dimension (longitudinal axis of clutch pack). The heat balances were approximated by a forward-difference method and then solved by a matrix-solving algorithm. The method is simple but certainly not very accurate because the temperature distribution is calculated only in one dimension and any cooling effects of the oil between the clutch facings are neglected.

Hydraulic Actuation of the Transmission

The hydraulic circuit on a planetary-type automatic transmission can be very complex, consisting of several hydraulic elements for each of the friction clutches. In [Watechagit and Sirinivasan 2003] a dynamic model of such a hydraulic actuation system was developed for one shift element. The model consisted of several blocks, each containing a detailed model of the dynamics of a pulse-width-modulated (PWM) solenoid valve, a pressure control valve, an accumulator (for a stable oil flow to the clutch) and finally the dynamics of the clutch piston. With this detailed model, the authors were able to accurately simulate the dynamics of a clutch engagement and thus a gearshift. The simulation results have clearly shown that at the end of

the clutch-filling stroke, when the clutch piston comes in contact with the clutch pack, the clutch pressure rises sharply.

Often on automated manual transmissions and twin clutch transmissions, a single valve, a so-called proportional solenoid valve, substitutes the pressure control and PWM-solenoid valve. In [Rinderknecht et. al. 2002] a hydraulic circuit of an automated manual transmission was presented where a 3 way proportional valve was employed to actuate the main clutch and a 3-way pressure reducing valve was used for the control of the shift rails to engage the gears.

Hydraulic clutch actuation systems for twin clutch transmissions were depicted in [Wheals et.al. 2001] and [Flegel et. al. 1987]. In the first paper the hydraulic layout featured pressure-reducing valves for clutch actuation in combination with on/off valves for the actuation of the shift rails. Unfortunately the authors did not specify the exact type of pressure reducing valve and hence it is not clear whether the valves were proportional type valves or pulse width modulated valves. The hydraulic circuit presented in the second paper comprises proportional pressure reducing valves for clutch actuation and simple on/off valves for the operation of the shift rails.

In [Cho et.al. 1999], equations of motion for each part (electromagnetic, mechanical and hydraulics) of a proportional pressure-reducing valve were derived. From these equations of motion a simple linear model, consisting of three linear transfer functions and a feedback loop, was developed. The parameters of the model were determined by applying system identification theory. A proportional non-linear solenoid valve was also modelled in [Vaughan and Gamble 1996]. This non-linear model was used to predict the displacement of the valve spool. It included models of the magnetic saturation and hysteresis in the solenoid, which were based on regression functions derived from experiments. The non-linear model of the proportional solenoid valve model was developed with the aim of having a more accurate model for the development of spool/armature position controllers. It is, thus, too comprehensive to be employed as part of the hydraulic clutch actuation in a transmission model exclusively used for the development of a gearshift controller.

In [Kwon and Kim 2000], [Zheng et al 1999] and [Wang et al 2001] a simple linear second order transfer function was employed to model the dynamics of a solenoid valve. The input of this model was a voltage signal and the output was a control pressure at the outlet port of the valve (Wang et al.) or the accumulator backpressure for the system of a planetary type automatic transmission (Kwon and Kim, Zheng et al). Although the parameter values of the solenoid models were similar in all three papers (undamped natural frequency around 10 Hz, damping ratio 0.707 to 0.93), the types of valves were not specified exactly. The paper of

[Zheng et al 1999] further found that the dynamics of the solenoid valve significantly contribute to the overall response behaviour of the clutch actuation system. Thus for an application to controller development it is sufficient to consider the solenoid valve dynamics without having to account for the dynamics of the rest of the hydraulic system.

2.7 Conclusions of the Literature Review

The only twin clutch transmission that is currently on the market [Rudolph et al 2003] is yet not very well documented in the literature in terms of either the design of the controller or specifically the algorithms used to control the gearshift. Whether, the gearshift control is of open-loop type, like those of the twin clutch transmissions of the 80's [Webster 1981, Flegl et al. 1982, Flegl et al 1987, Op de Beck et al. 1983], or involves closed-loop concepts could not be discovered from the literature. For that reason, much of the information about state-of the-art control concepts for twin clutch transmissions was retrieved from patents.

On the modelling and simulation basis the only evidence of a model of a twin clutch transmission has been found in [Veehof 1996]. However, the author has developed only a crude model (without an engine model) to study the effects that the application timing of clutches has on shift quality. Most detailed dynamic models used for controller development found in the literature were derived for planetary-type transmissions. The reviewing of these models has shown that certain key points of special importance to the modelling of twin clutch transmissions have not been addressed at all or where addressed, not in the necessary detail.

Following simulation issues remain to be addressed:

- The dynamic models of clutches in the existing transmission models for controller development have only contained a simple friction model of the clutch incorporating a constant dynamic friction coefficient.
- The study of the effects of different friction characteristics (different wet friction characteristics or even dry friction) on the dynamic behaviour of a gearshift controller.
- In the existing transmission models for controller development/analysis the internals of the transmission (e.g. shafts inside the transmission, synchronisers) were not modelled in sufficient detail. Thus, for example, synchroniser-to-synchroniser shifts could not been analysed and simulated in the necessary detail.
- Only few transmission models (mostly of planetary-type) featured a model of the (hydraulic) actuation of clutches. No general model of a complete hydraulic actuation

suitable for a twin clutch transmission (i.e featuring a proportional solenoid valve and hydraulic actuator) that was also sufficiently simple for a controller development and modelled the critical clutch filling process could be found in the literature.

- Another shortcoming of the powertrain models found in the literature on controller development was that these models either included a simple engine model and a detailed transmission model or vice versa. Hence, actuation delays and dynamics were only accounted for in part.

Most of the gearshift control concepts found in the literature were applied to planetary-type transmissions. These concepts included highly sophisticated control strategies such as optimal control for gearshifts, which although superior in theory, seems hardly suited for a practical gearshift control on fixed-gear automatic transmissions. This is because these strategies rely on an internal model of the transmission, which is highly simplistic, furthermore, they require the measurement (observation) of lot of different state variables, which are often difficult to obtain. The literature also contained simpler approaches to gearshift control, which were still of closed-loop nature and mainly involved the control of engine speed through clutch pressure modulation. Other closed-loop strategies found in the literature attempted to achieve a control of the gearshifts on planetary transmissions based on information about transmission output torque. Finally, some concepts found in the literature attempted to integrate the engine in the gearshift control mainly to achieve a synchronisation of the engine to the speed level of the target gear in the inertia phase. Gearshift issues specific to twin clutch transmissions such as multiple gearshifts and gear pre-selection have been treated scarcely in the literature and were mainly covered in patents, which only provided descriptions of principles, without supporting the ideas in the form of simulation results or measurement data.

From the point of controlling the gearshift on a twin clutch transmission following problems remain to be solved:

- The control of the transfer of engine torque in the torque phase without a one-way (i.e. freewheeler- or overrunning-) clutch is discussed in a patent [Volkswagen AG 1998 (Patent DE 196 31 983 C1)]. The effectiveness of this solution remains to be investigated based on measurement or simulation results, in particular, its suitability to gearshifts on twin clutch transmissions remains to be demonstrated.
- A gearshift control for clutch-to-clutch shifts without a one-way clutch and with engine torque manipulation in the inertia phase was described in principle in [Daimler Chrysler AG 2001 (Patent DE 199 39 334 A1)]. Such an integrated powertrain control concept has not been developed in detail in the literature. Also, its superiority over simpler gearshift control strategies without engine involvement has to be investigated and demonstrated.

- It remains to be demonstrated if and in what form a torque-based control can be beneficial to the control of gearshifts on twin clutch transmissions. A step in this direction was made in [Wheals et al 2001], however, the treatment only sketched the idea for a power-on upshift and did not go into any details about the layout of the controller nor were downshifts treated at all.
- Although a few attempts have been made in the literature to make the gearshift control (mainly speed control in the inertia phase) robust against changes in the friction coefficient, the friction coefficient was assumed constant in these treatments, which is a crude simplification. Also, only the robustness in terms of stability of the controller has been investigated and not how shift quality is affected by a change in the friction coefficient. The robustness of the gearshift control to changes in other powertrain parameters and sensor noise has not been investigated either in the literature.
- Double gearshifts and their control have been investigated in principle in [Wagner 1994]. The control concepts applied there, however, involved only simple open-loop clutch pressure manipulation. It remains to be investigated whether closed-loop concepts can also be applied beneficially to double gearshifts.
- The problems involved with gear pre-selection on a twin clutch transmissions have not yet been treated in the literature at all. This problem specific to twin clutch transmission remains to be investigated in full and if found to be of negative influence to shift quality, a remedy for this problem, if possible, remains to be found.

2.8 Aim and Objectives of the Research

Following from the conclusions drawn from the literature review the aim and objectives can be identified as following for this thesis:

The aim of this thesis is to develop a robust integrated powertrain controller for gearshifts on twin clutch transmissions that improves shift quality over conventional powershift control strategies used on planetary-type transmissions.

The objectives of this thesis are:

- To develop a dynamic powertrain model that features a detailed model of engine and twin clutch transmission (has to include detailed models of internal parts such as synchronisers and clutches with a sufficiently sophisticated description of the friction coefficient).

- To develop a simple yet sufficiently accurate model of the dynamics of the hydraulic actuation of clutches and synchroniser.
- To devise a basic gearshift controller for single clutch-to-clutch shifts without a one-way clutch that utilises the engine as part of the control strategy (integrated powertrain control strategy). To demonstrate the effectiveness of this controller based on simulation results.
- To integrate the control of transmission output torque into the basic gearshift controller and show how the torque control can improve the basic gearshift controller.
- To extend the basic gearshift controller with or without torque control to cope with double and multiple gearshifts.
- To investigate the problem of the gear pre-selection and, if required, to devise a control strategy to compensate for these problems.
- To make the gearshift controller robust, in terms of stability of the controller and shift quality, against disturbances and changes in the powertrain parameters (e.g. friction characteristics and sensor noise).

Chapter 3

Dynamic Model of the Powertrain

Chapter 1 and 2 have provided an introduction and an extensive review of literature of state-of-the-art gearshift controllers and powertrain modelling. Chapter 2 has concluded with a summary of findings of the literature review and with the aims and objectives of this thesis.

In the current chapter the powertrain model is developed in detail. Section 3.1 explains the general structure (i.e. layout) of the powertrain to be modelled. First, the engine model is described in Section 3.2.

This is followed by the development of a model of the twin clutch transmission in Section 3.3. The dynamics of the transmission model (Section 3.3.1) are treated first, for the basic model for simulation of single gearshifts and then for the extended model for simulation of gearshifts with gear pre-selection and double/multiple gearshifts. Section 3.3 ends with the development of a model of the hydraulic clutch/synchroniser actuation (Section 3.3.2).

Section 3.4 explains the remainder of the powertrain model and the longitudinal vehicle dynamics. Chapter 3 ends with the presentation of a first simulation result in Section 3.5 and the conclusions in Section 3.6.

3.1 General Structure of the Powertrain Model

In order to develop, validate and simulate the gearshift controller it is necessary to develop a mathematical model of a vehicle powertrain. The mathematical model serves the purpose of showing how a real powertrain will respond to inputs by the gearshift controller, the driver and the driving environment. For this end it is only necessary to model the dynamic behaviour of the vehicle powertrain in the low frequency range (usually in the range of 5-15 Hz). This enables capture of vibration phenomena coming from, for example, transient changes in engine torque (variation of throttle angle, spark advance etc.) or rapid clutch engagement/disengagement as a product of the gearshift controller or a driver intervention. Driveline oscillations can also result from self-excited vibrations as a product of certain dynamic properties of system parameters

(e.g. friction coefficient of clutch). High frequency vibrations, which are not considered in the model, can have various sources such as, for example, gear rattle or fluctuations in engine torque due to the periodic combustion. These high frequency vibrations mainly influence the noise behaviour of the powertrain and are thus of no interest in this work.

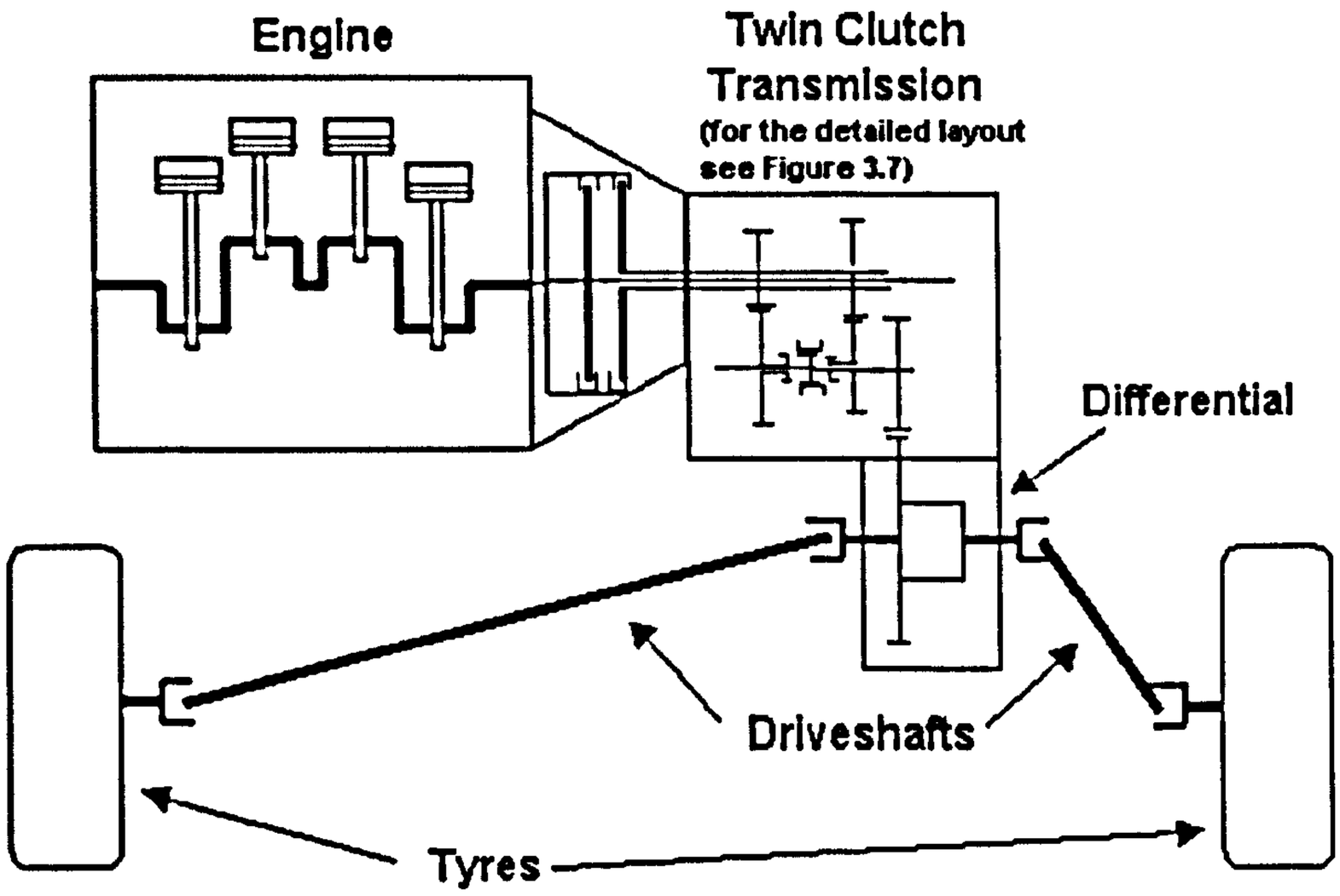

Figure 3.1 Layout of powertrain modelled in this thesis

The configuration of the powertrain modelled here, is depicted in Figure 3.1 and shows a front wheel drive configuration. The engine and transmission are shown in a transverse installation. This has no influence on the structure of the powertrain model and does not restrict the general validity of the simulation results. As a consequence of the front wheel drive configuration, there is no propeller shaft between the transmission output and the final drive and the output gears of the transmission mesh directly with the ring gear of the differential. The two output shafts of the differential are connected to each of the two driveshafts (axleshafts), which drive the front wheels.

In this work, a symmetric layout of the powertrain is assumed, i.e. the properties of driveshafts and wheels (tyres) are assumed to be equal for the left and for the right side and can thus be lumped into one driveshaft/tyre assembly. Furthermore, it is assumed that the differential distributes the drive torque equally to both sides and that no cornering of the vehicle takes place. It is assumed that no tyre slip takes place and therefore the full drive torque is transmitted equally through both drive wheels onto the road. These assumptions are justified from a gearshift controller development point of view, where any difference in the torque profile between the left and the right wheel is of no interest.

Figure 3.2 shows the overall structure of the dynamic powertrain model. Torque and speed values are passed between the single components of the powertrain. Dash-dotted lines represent torque signals and dashed lines represent speed signals. Inputs to the engine model are the throttle angle, the spark advance and a load torque from the driveline. From these inputs the engine block generates the engine speed signal at its output. Connected to the engine model is a model of the twin clutch transmission. Engine speed and speed of the differential are inputs to the transmission model. Further inputs to the transmission block are, the input voltages at the hydraulic solenoid valves of clutch and synchroniser actuators. From these inputs the transmission block calculates an output torque to the differential and a load torque to the engine.

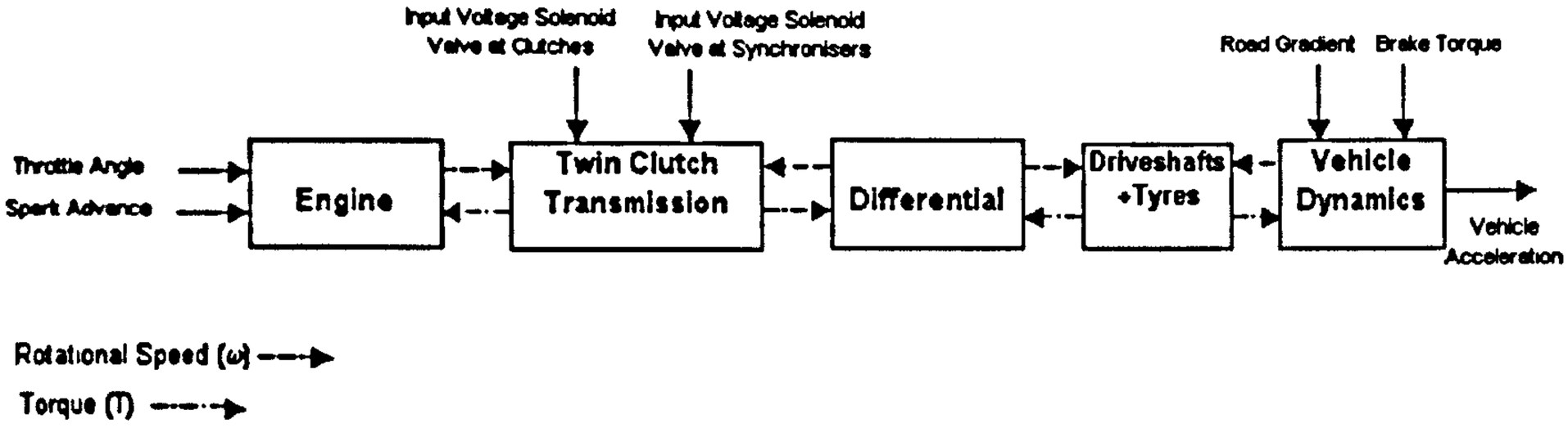

Figure 3.2 Simplified block diagram of the powertrain model

Located after the block of the twin clutch transmission is a block containing the rotational dynamics of the differential, a block containing the compliances of driveshafts and tyres and a block containing the longitudinal vehicle dynamics. This vehicle dynamics block accepts as input variable the tractive torque at the wheels, a brake torque and a load torque coming from the road loads acting on the vehicle. The net torque of these torque contributions can be used to accelerate the vehicle mass and hence determine the vehicle velocity and its derivatives (acceleration and jerk).

In general, the model is structured in such a way as to produce an alternating series of inertial and compliant components. Inertial elements (e.g. mass inertia of layshafts, gear wheels etc.) accept torque as input variable and produce angular speed as output variable, whereas compliant elements (e.g. stiffness of driveshafts, tyres, etc.) accept speed as input variable and produce torque as output variable. This modular structure provides flexibility in altering the structure of the powertrain model. In addition, the modular structure of the powertrain model also ensures an integral causality of the system (cause and effect relationship between input and output variables), because connections between components of the same type (e.g. connection between two inertial components) are avoided. The advantage of this model structure is that one can avoid the occurrence of differential algebraic equations in the model. These differential

algebraic equations can produce algebraic loops that involve iterative solutions of algebraic equations and therefore slow the simulation process. Further considerations to this problem can be found in [Moskwa et al 1997; Ciesla, Jennings 1995].

All equations of motion of the powertrain model were derived by applying Newton's Second Law. The powertrain model was created in Matlab®/Simulink®, which was also used for the numerical solution of the equations of motion and the production of the simulation results. The parameter values used in the powertrain model are listed in the Appendix A.4 and were chosen to represent a typical c-segment car with matching engine power and transmission size. Section A.4 in the appendix also explains how the parameters were derived.

3.2 Dynamic Engine Model

In Figure 3.3 the engine block from Figure 3.2 is depicted in detail. The functional structure of the engine model can be broken down into two main parts (see Figure 3.3):

- The torque production part that accounts for the production of an indicated engine torque, due to combustion of an air/fuel mixture in the engine cylinders.
- The rotational dynamics part that determines the acceleration of the crankshaft as a result of the indicated engine torque and applied load torques.

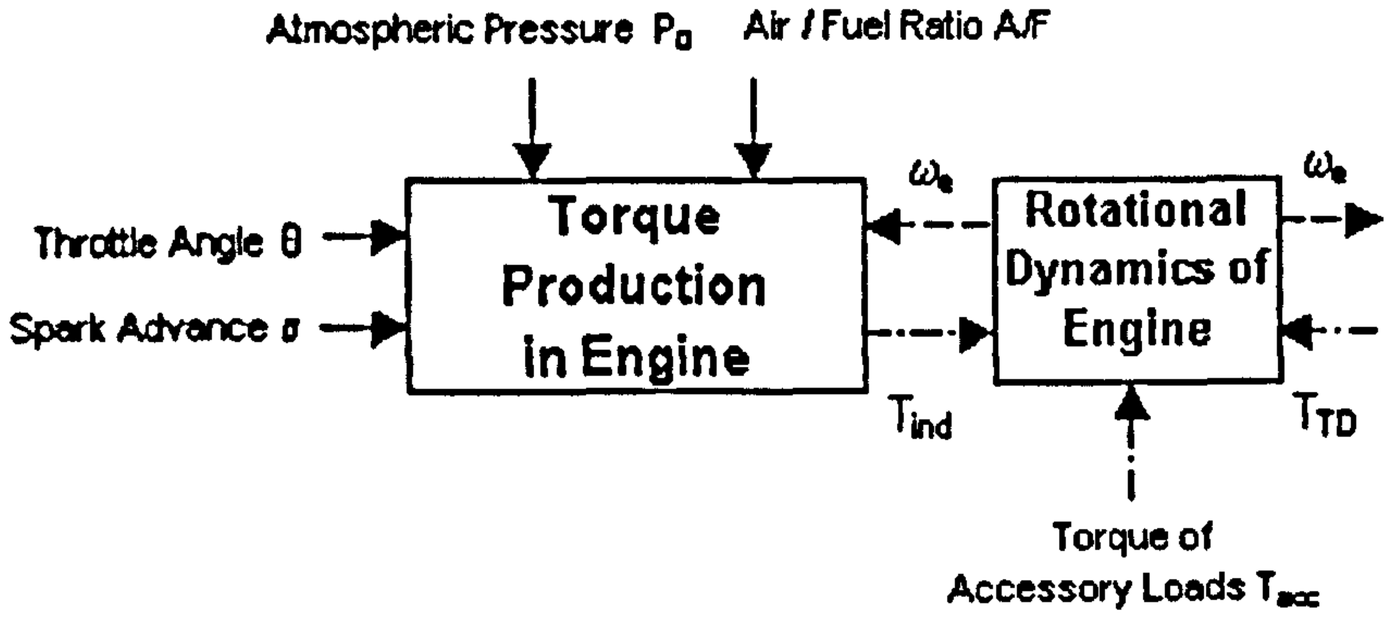

Figure 3.3 Detail of the engine model block in Figure 3.2

3.2.1 Engine Model - Torque Production

The torque production model consists of a so-called mean value engine model (MVEM), which means that the model captures only the overall dynamic behaviour and hence neglects any

torque fluctuations resulting from an unsteady (but cyclic) combustion. This is justified for an application to the development of a powertrain controller, where only the low frequency behaviour has to be considered. There are several MVEM for SI-engines existing in the literature; for example [Moskwa,Hedrick 1992; Weeks, Moskwa 1995 and Hendricks1997]. The main difference between these models is the degree of complexity and in the degree of general applicability.

For this study the MVEM engine model of [Crossley and Cook 1991] was selected, which although lacking generality, since it was designed for a particular engine, has the advantage of being very simple and therefore especially suited for the development of an integrated powertrain controller. The model is a low frequency phenomenological representation of a four-cylinder spark ignition (SI) engine. It includes models of the throttle body, the airflow through the intake manifold, the intake and compression strokes and the torque generation. These models are non-linear algebraic relations, which are based on experimental data from an engine dynamometer. The original engine model by Crossley and Cook also included the dynamics of an exhaust gas re-circulation. [The Math Works 1998] has created a Matlab®/Simulink® representation of this engine model, which does not include exhaust gas re-circulation. It is this latter model that is adopted here with some modifications, mainly in the rotational dynamics block. The equations of motion of the torque production model are taken from [The Math Works 1998] and are listed in the Appendix A.1.

3.2.2 Engine Model – Rotational Dynamics

The rotational dynamics part of the engine block in Figure 3.2 determines the acceleration of the engine crankshaft and all mass inertias connected to it from the sum of the applied torques. The free-body diagram of the engine is depicted in Figure 3.4.

The disk in Figure 3.4 represents the mass inertia of all moving engine parts like piston, connecting rod and crankshaft, which are lumped into a single effective inertia about the crankshaft axis. The mass of the flywheel, which has the function of "damping" any torque oscillations produced by the engine, is lumped together with the crankshaft inertia. The crankshaft is assumed to be rigid (i.e. no torsional compliance). The efficiency of the engine in producing an indicated torque is considered in the torque production equations. Here only losses in the accessory load drive are accounted for by a coefficient of efficiency.

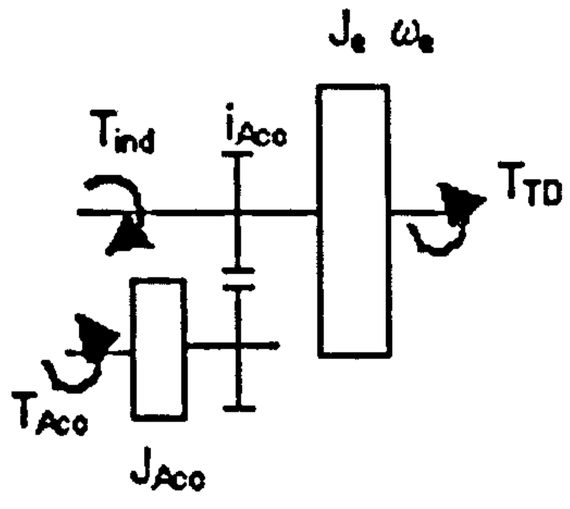

Figure 3.4 Free-body diagram of engine

The engine accessory loads like electric power generator, water pump, air conditioning etc., produce a load torque at the crankshaft. In addition, to this load torque the engine has to accelerate the inertia of each accessory device. These inertias are lumped together in a single mass inertia, which is coupled to the crankshaft through a gear stage. The torque balance at the crankshaft is given in equation (1).

$$J_{e+Acc}\dot{\omega}_e = T_{ind} - T_{Acc}\frac{1}{i_{Acc}\eta_{Acc}} - T_{TD} \tag{1}$$

$$J_{e+Acc} = J_e + J_{Acc}\left(\frac{1}{i_{Acc}}\right)^2 \tag{2}$$

Solving equation (1) and (2) for ω_e produces the engine speed, which is the output of the rotational dynamics block of the engine.

3.2.3 Engine Model – Characteristics and Map

To obtain the engine map (engine torque versus speed) a simulation engine test bed was constructed in Matlab®/Simulink®. This test bed model simply consisted of a PID controller that applied a certain load torque (brake torque) to the engine model in order to keep the engine to a specified engine speed. By selecting various settings for throttle angle (and spark advance) and engine speeds, points in the steady state engine map (torque and speed values) could be obtained. As already mentioned, the engine maps are steady state maps, where the engine has settled to the target speed and all transients have vanished.

The engine map in Figure 3.5 shows a standard map where engine torque is depicted versus engine speed for various throttle angles. To achieve more engine power, the pressure at the opening of the intake manifold was slightly raised above the atmospheric. This did not change the dynamic behaviour of the engine model or the shape of the curves in the engine map, but essentially shifted the torque curves to higher torque values in the engine map. The large

difference in engine torque in the lower throttle angle range (10 to 40 degrees) and the comparably little change in engine torque in the upper throttle angle range (40 to 90 degrees) is a fact that can often be observed in engine maps of SI- engines.

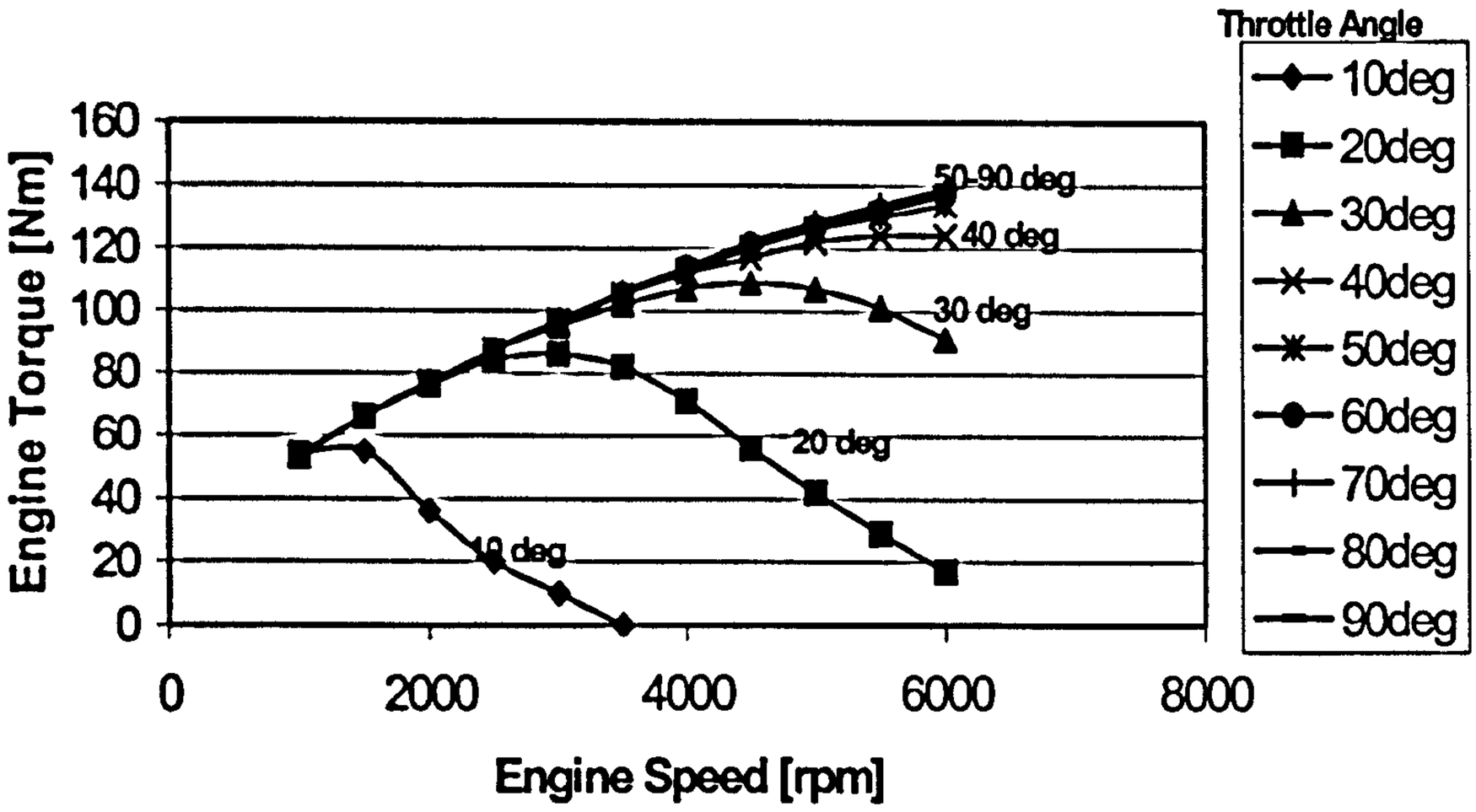

Figure 3.5 Characteristics of engine model

Although, the engine speed would steadily increase beyond the maximum speed shown in the chart when accelerated, the torque curves are only depicted up to 6000 rpm, which is a realistic maximum for such an engine. As can be seen from Figure 3.5, the maximum torque (140 Nm) and the maximum power (90 kW) are both reached at 6000 rpm.

Figure 3.6 also shows an engine map. However, this engine map shows how the spark advance affects the engine torque. This created a three dimensional map plotting the spark advance (measured in degrees BTDC), the engine torque and the reduction in engine torque. The term spark advance is used here to denote the spark timing and hence a change in spark advance to a negative value means that the spark is retarded from the nominal value of 15 degrees BTDC. The map can be read as follows: The x-axis shows the level of engine torque at which a change in the spark advance took place. The z-axis shows the amount of change in spark advance from the original value and the y-axis shows the decrease in engine torque (torque reduction) resulting from the change in the spark advance. The special engine map presented in Figure 3.6 is used as part of a control algorithm that is presented in Chapter 7.

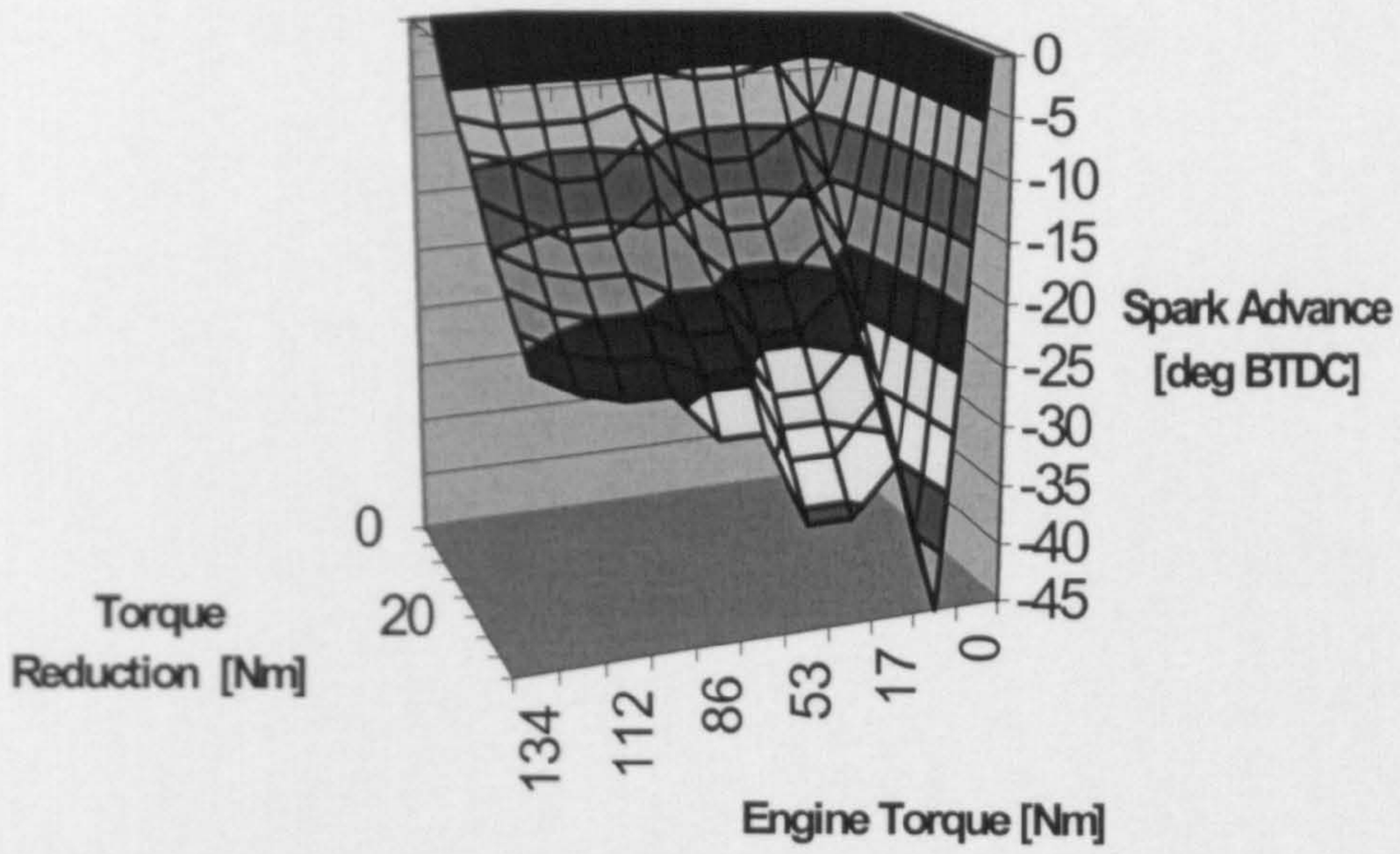

Figure 3.6 Engine map showing the reduction in engine torque with change in spark advance

3.3 Dynamic Model of the Twin Clutch Transmission

The mechanical layout of the twin clutch transmission modelled in this thesis is depicted in Figure 3.7. It comprises two layshafts (layshaft 1and 2) and offers 6 speeds. The two clutches of the twin clutch (clutch 1 and 2) take separate locations in the gearbox housing and their input sides are connected by a shaft (connecting shaft). The output sides of the clutches are connected to the input shafts (Input shaft 1 and 2), which are constructed as quill (hollow) shafts. The input gear wheels are fixed to these two input shafts and mesh with the output gear wheels running on the layshafts. In this transmission model, the pairs of gearwheels that belong to the odd gears (1^{st}, 3^{rd} and 5^{th} gear) are running on input shaft 1 and layshaft 1 and the pairs of gearwheels that belong to the even gears (2^{nd}, 4^{th} and 6^{th} gear) are running on input shaft 2 and layshaft 2. The output gearwheels can be connected to the output shafts by means of synchronisers, thus engaging the gear. The two gearwheels each located at the end of the output shafts belong to the final drive unit and mesh with the ring gear of the differential.

From Figure 3.7 the structure of the twin clutch transmission model can be derived. A block representation of this transmission model is depicted in Figure 3.8. Values of angular speed and torque are passed between the blocks. The torsional damper at the transmission input, the connecting shaft, the input shafts and the layshafts are compliant components and produce torque values at their output and accept angular speed values at their input. On the other hand, the two clutch blocks and the synchroniser blocks contain friction models and inertial

components and thus produce speed values at their output and accept torque values at their inputs.

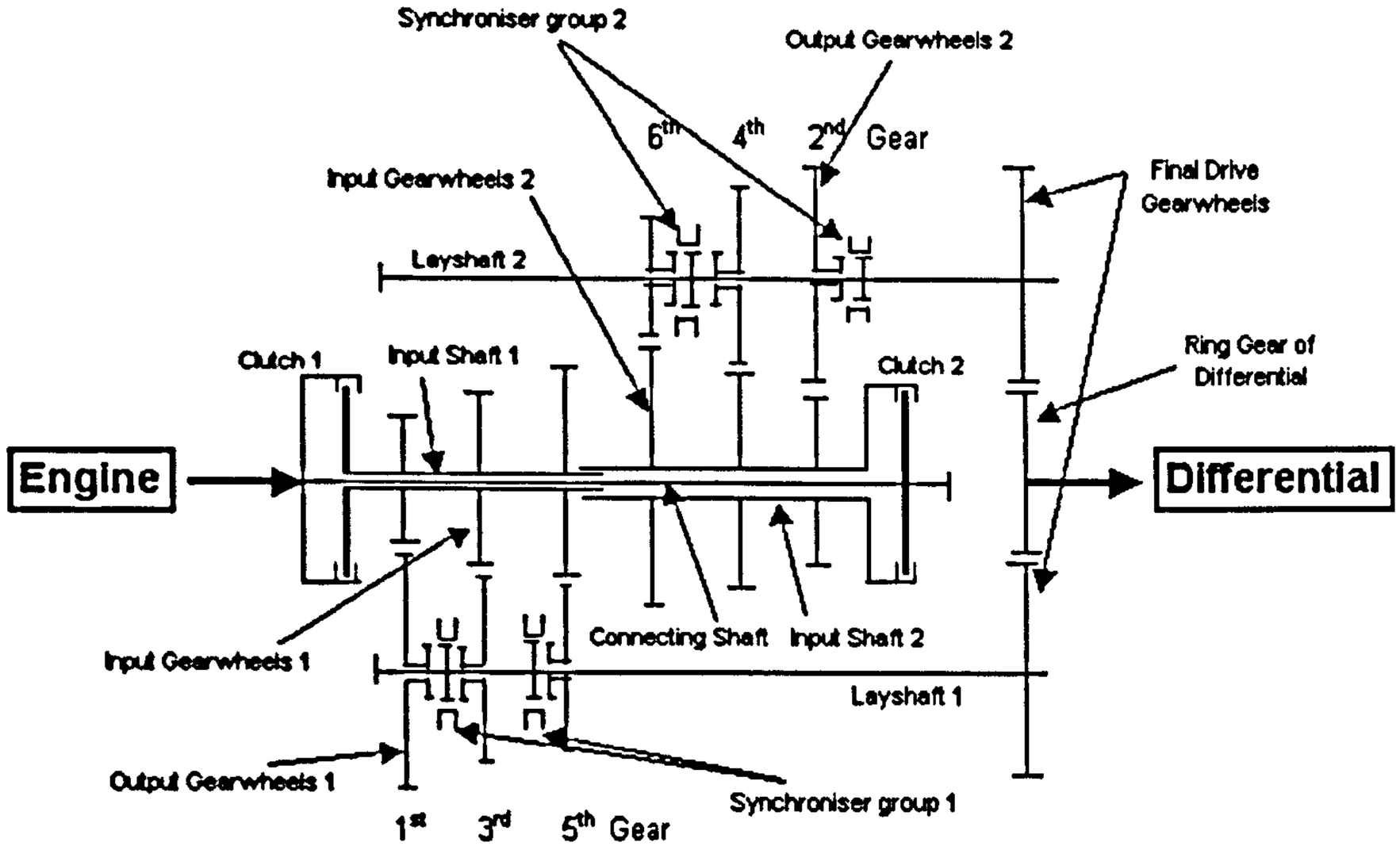

Figure 3.7 Mechanical layout of the modelled twin clutch transmission

The hydraulic valve/actuator blocks contain the dynamic models of clutch and synchroniser actuators including solenoid valves. A clamp force at the clutch/synchroniser is outputted from the hydraulic actuator blocks as a result of an input voltage to the solenoid valve. In general the transmission model consists of two parts: the rotational dynamics of the transmission and the dynamics of the hydraulic actuator system.

For the simulation of gearshifts two versions of the transmission model were used. A basic model as shown in Figure 3.8, where the synchroniser (and thus the gears) were selected at the beginning of the simulation and the synchronisers were kept engaged throughout the simulation. In this basic version of the transmission model the parameters of synchroniser, input shaft and layshaft models varied with the gear (e.g. different shaft stiffness due to different locations of gearwheels on the shafts, different inertia of the gearwheels etc.). However, the basic model did not enable a change of gear (synchroniser) within the same half of the transmission without discontinuities in the simulation results and was only used for single gearshifts.

To simulate double/multiple gearshifts and gearshifts with gear pre-selection a second, more detailed model (see Figure 3.19) had to be developed as an extended version of the basic model. On this extended transmission model, one input shaft/synchroniser/layshaft assembly was added

to be able to model a synchroniser-to-synchroniser shift within the same half of the transmission.

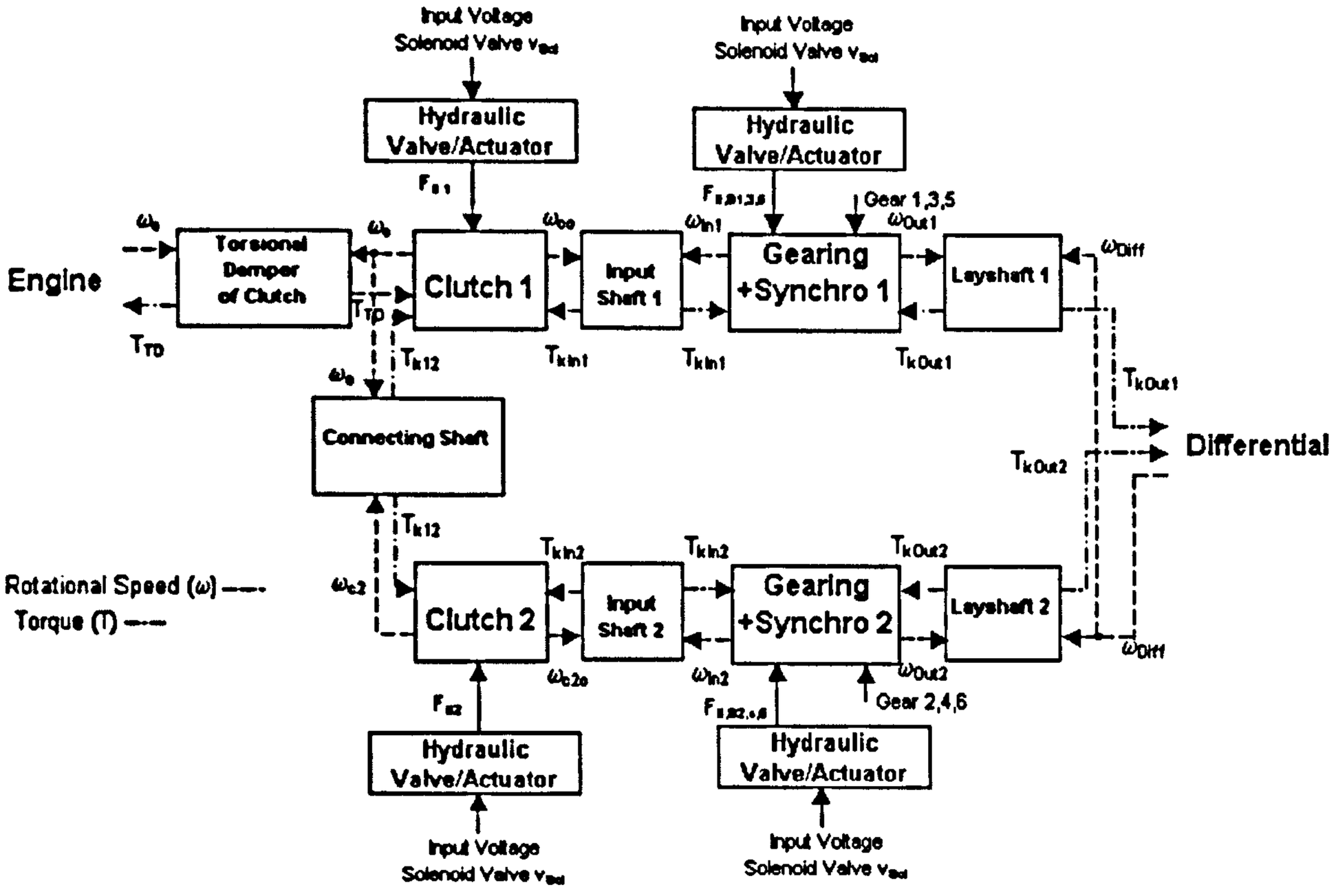

Figure 3.8 Detailed block diagram of the twin clutch transmission block from Figure 3.7

The variables used in the equations of motion of the transmission model are indicated in the block diagram of Figure 3.8. These equations of motion will be derived in the following section for transmission half 1. The equations of motion of the transmission half 2 (comprises clutch2, input shaft 2, synchroniser 2 and layshaft 2) are similar to those of transmission half 1 and are thus not given in the text but listed in the Appendix A.2.

3.3.1 Dynamics of the Transmission

Basic Transmission Model (for simple Gearshifts)

As already explained in the previous section, for the simulation of simple clutch-to-clutch shifts a basic model of the twin clutch transmission was used that comprised only two synchroniser models. The basic structure of this model is depicted in Figure 3.8. The equations of motion for the transmission model are derived for four main groups of components. The first group of components contains the torsional damper and twin clutch assembly. The second group contains

the models of the two inputs shafts. The third group comprises gearing and synchroniser models and the fourth group of components contains the two layshafts.

Torsional Damper and Twin Clutch Assembly

Figure 3.9 shows the free-body diagram of the torsional damper and twin clutch assembly. The torsional damper at the transmission input is modelled as a four-stage damper with varying stiffness and damping rates, depending on the relative displacement. The number of stages (four) was chosen arbitrarily, however, represent a compromise between including enough detail in the damper model to model the multistage behaviour on one hand and producing a model that is not too complex. Clutch 1 and 2 contain friction models that determine the acceleration and thus speed of inertias at input and output from the frictional torque generated from the clamp force at the friction contact. The connecting shaft is modelled as a simple spring damper element.

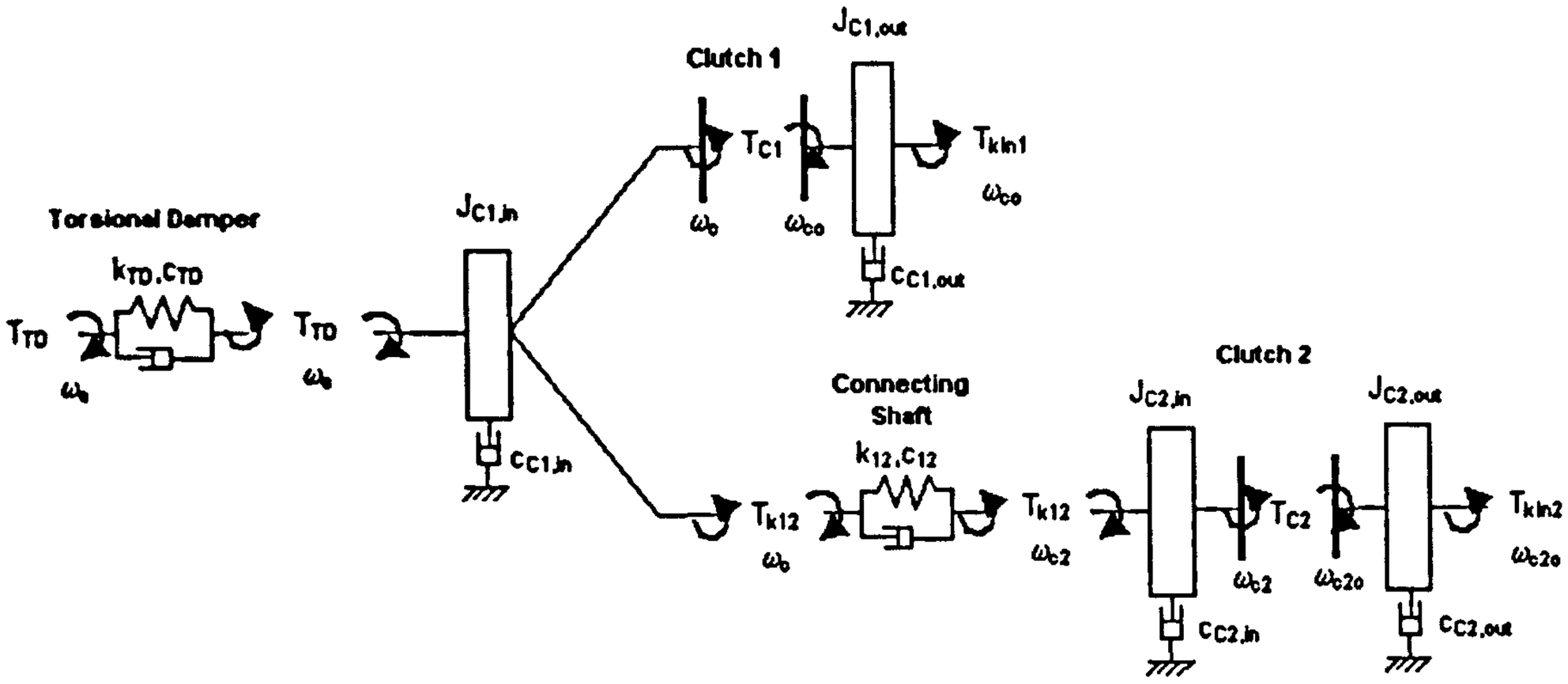

Figure 3.9 Free-body diagrams of torsional damper and twin clutch assembly

The mass inertias at the input and output of the clutches (clutch mass, mass of shafts etc.) are represented by non-compliant mass carrying discs. These discs are connected to the "ground" via damper elements to model the drag (viscous drag) that is created in transmission.

Torsional Damper:

The torsional damper serves as a decoupling device, which insulates the powertrain from any torsional vibrations produced by the engine. It usually consists of two plates that are connected by two or more springs of variable stiffness and is part of the clutch assembly. By changing the springs (stiffness) the characteristics of the torsional damper can be adjusted. The amount of stages indicates the number of stiffness values used in the characteristics of the damper. The

characteristic of the multistage (four stages) torsional clutch damper chosen in this work is depicted in Figure 3.10.

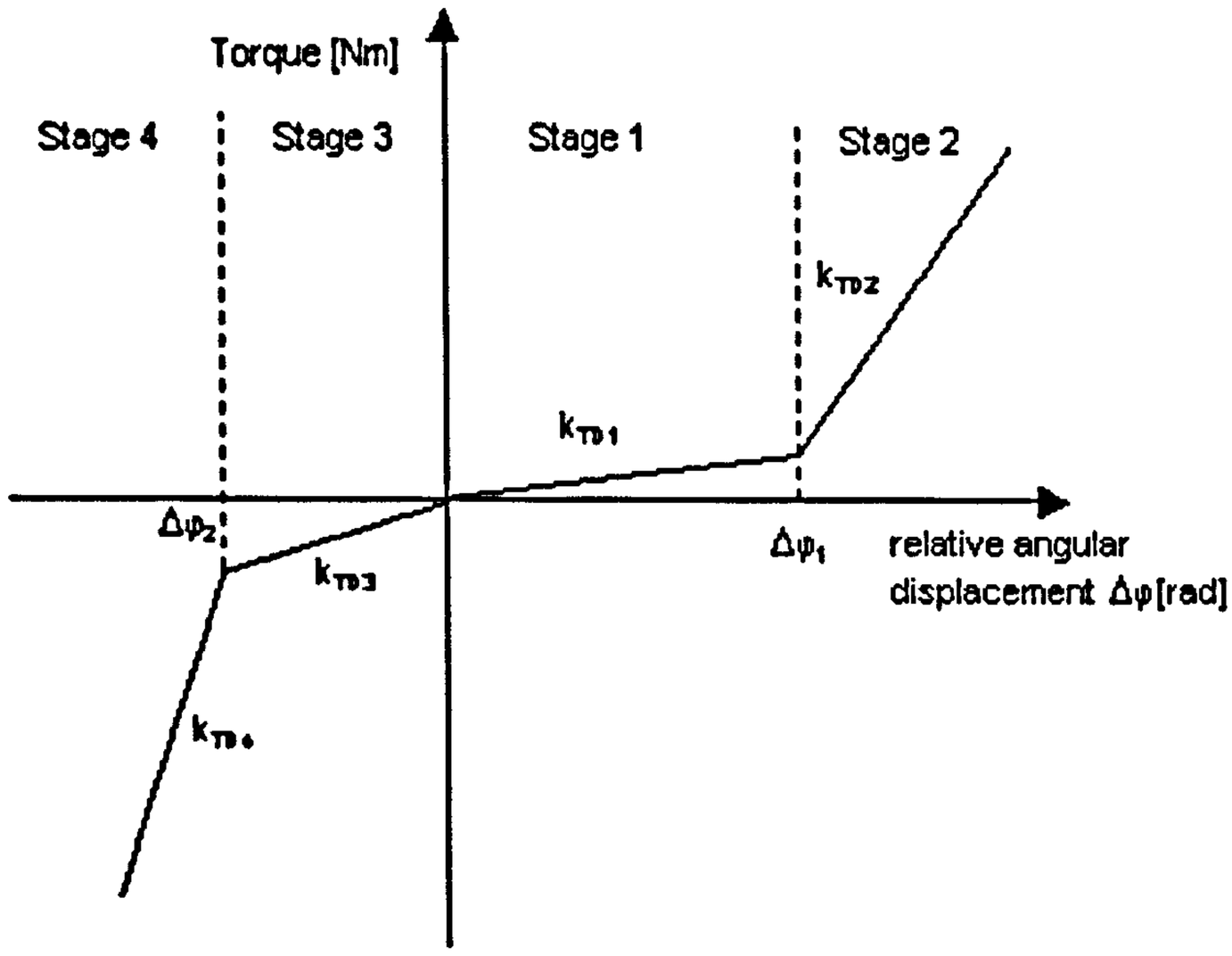

Figure 3.10 Characteristics of the four-stage torsional damper model

Damping in the torsional damper can come from both, a frictional portion that occurs when the two halves of the torsional damper rotate relative to each other and the springs rub against the plates, and from a viscous (or speed dependent) damping portion. In the four-stage torsional damper modelled here only a speed dependent damping part was considered. From the free-body diagram of the torsional damper depicted in Figure 3.9 and the damper characteristic shown in Figure 3.10 the equations of motion can be derived (Equation (3).

$$
\begin{aligned}
T_{TD} &= k_{TD2}(\varphi_e - \varphi_c - \Delta\varphi_1) + k_{TD1}\Delta\varphi_1 + c_{TD}(\omega_e - \omega_c) && (\varphi_e - \varphi_c) \geq \Delta\varphi_1 \\
T_{TD} &= k_{TD1}(\varphi_e - \varphi_c) + c_{TD}(\omega_e - \omega_c) && 0 \leq (\varphi_e - \varphi_c) < \Delta\varphi_1 \\
T_{TD} &= k_{TD3}(\varphi_e - \varphi_c) + c_{TD}(\omega_e - \omega_c) && \Delta\varphi_2 < (\varphi_e - \varphi_c) < 0 \\
T_{TD} &= k_{TD4}(\varphi_e - \varphi_c - \Delta\varphi_2) + k_{TD3}\Delta\varphi_2 + c_{TD}(\omega_e - \omega_c) && (\varphi_e - \varphi_c) \leq \Delta\varphi_2
\end{aligned}
\tag{3}
$$

<u>Clutch 1</u>

The friction contact of a clutch can be modelled by two separate states and a set of conditions for the transition between the two states. The two states of the friction model are:

- The clutch is engaged (stiction): The differential speed across the clutch is zero and the static friction coefficient (positive and negative value) limits the torque at the clutch.

- **The clutch is slipping: The differential speed across the clutch is non-zero and the torque at the clutch is determined by the (kinetic-) friction coefficient.**

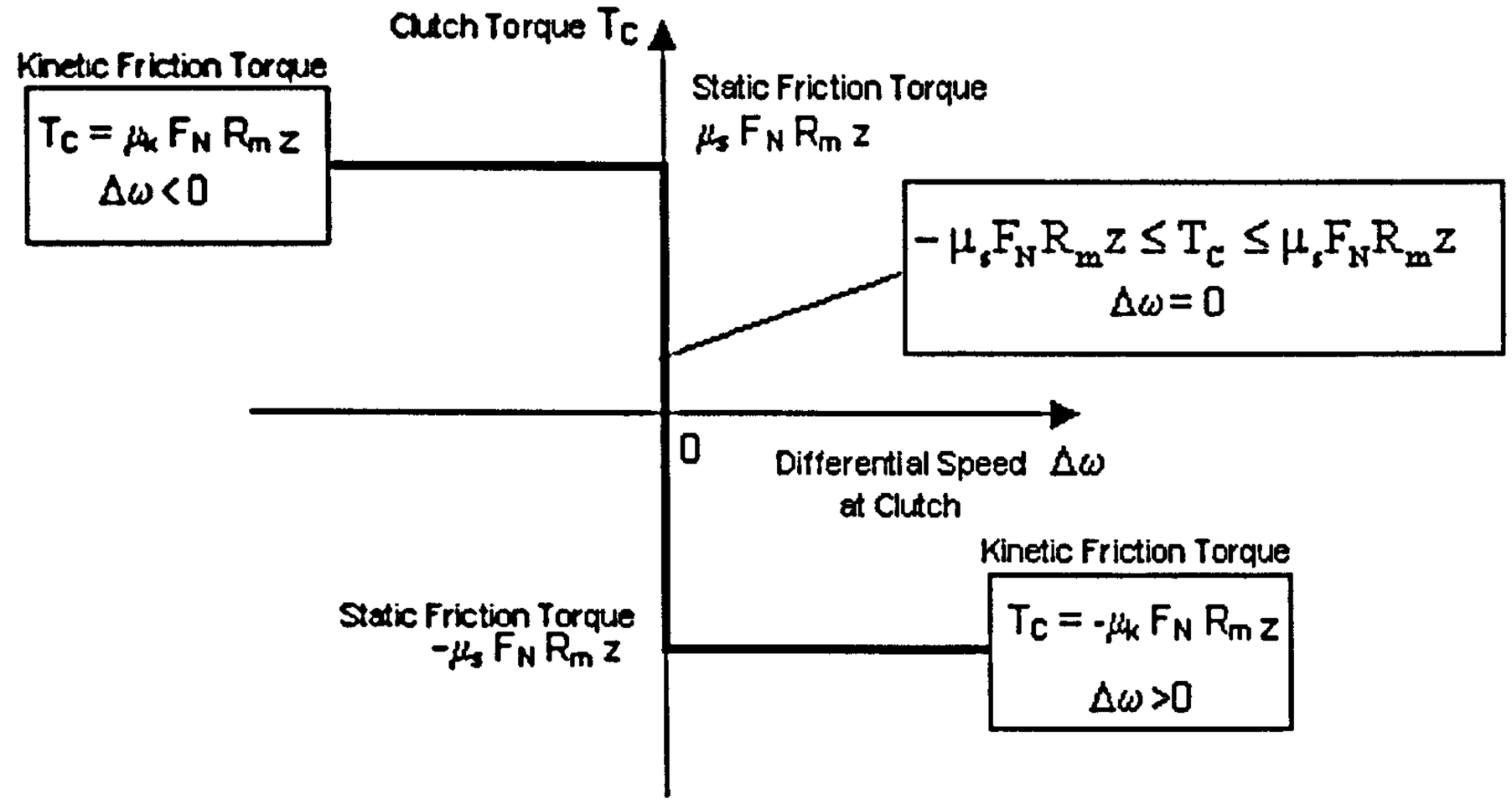

Figure 3.11 Friction torque at clutch versus differential speed across clutch

This contact law is depicted in Figure 3.11. The graph shows the torque at the clutch versus the differential speed at the clutch. The friction contact (unilateral contact) is active if the differential speed ($\Delta\omega$) across the clutch is zero and the value of torque transmitted through the clutch T_C (depends on inertial and load torques) is less than the static friction torque at the clutch. If the differential speed across the clutch is zero, the friction contact is active and the clutch is in the state of stiction. However, if the differential speed across the clutch is non-zero, the friction contact is passive and the clutch is in the state of slipping. In this state the kinetic friction coefficient (usually different from the static friction coefficient), the applied clamp force, the mean friction radius and the sign of the differential speed (tangential friction forces opposes direction of motion) determine the value and direction of the transmitted clutch torque.

Concerning the time varying structure of the clutch model, the following observations can be made: In case the clutch is engaged, the whole system (inertia at input side and output side of clutch) rotates with one single rotational speed (1 degree of freedom). In case the clutch is slipping, the system has 2 degrees of freedom, and both sides are rotating with different speeds depending on the applied load and inertial torques. If the clutch is completely disengaged, the torque at the clutch becomes zero and the equation of motion for the two halves become totally independent and the rotational speeds can be determined by the applied load torques, inertial

torques. This case can be treated by the same set of equations of motion as the slipping state. The only difference is that the normal constraint force at the contact vanishes.

The applied load torque and the static friction torque at the clutch determine the instant of time where a transition from "slipping" to "engaged" occurs. The switching logic for the transition between the two states is depicted in Figure 3.12. If, the value of the torque at the clutch lies between the limits set by the static friction torque and if, the differential speed across the clutch is zero then the clutch stays engaged. If, otherwise the value of the torque at the clutch is greater then the static friction torque, then the clutch starts to slip. The equations of motion at the clutch can now be derived by applying the friction laws from above together with Newton's Second Law to the free-body diagram of clutch 1 depicted in Figure 3.9.

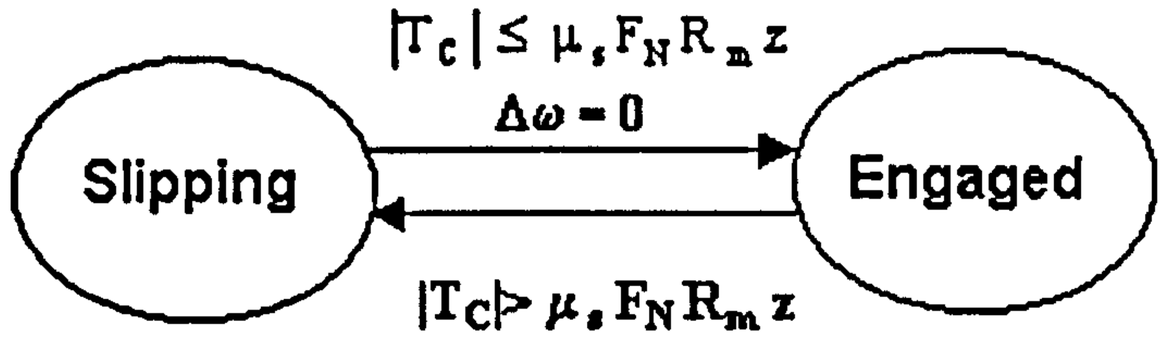

Figure 3.12 Switching logic of state transition at the clutch

Clutch 1 in a state of slipping:

Torque balance at mass inertia $J_{C1,in}$

$$J_{C1,in}\dot{\omega}_c = T_{TD} - T_{C1} - T_{k12} - c_{C1,in}\omega_c \tag{4}$$

Torque balance at mass inertia $J_{C1,out}$

$$J_{C1,out}\dot{\omega}_{co} = T_{C1} - T_{kIn1} - c_{C1,out}\omega_{co} \tag{5}$$

Integrating the friction torque at an infinitely small ring element of the frictional contact surface over the complete friction area of the clutch yields the torque transmitted by the clutch when slipping:

$$T_{C1} = \mathrm{sgn}(\omega_c - \omega_{co}) R_m F_{N1} \mu_k z \tag{6}$$

where:

$$R_m = \frac{2}{3}\frac{R_o^3 - R_i^3}{R_o^2 - R_i^2} \tag{7}$$

$$\mu_k = A + B\Delta v + C\Delta v^2 + D\Delta v^3 + E\Delta v^4 + F\Delta v^5 \tag{8}$$

$$\Delta v = (\omega_c - \omega_{co}) R_m \tag{9}$$

A five degree polynomial was chosen for the kinetic friction coefficient to have more degrees of freedom in adapting the friction coefficient to given profiles.

Clutch 1 in the "engaged" state:

In the "engaged" state, the two halves of the clutch are locked together and rotate with the same speed (Equation (10)).

$$\omega_c = \omega_{co} = \omega \tag{10}$$

Combining equation (4) and (5), using equation (10), yields equation (11), which describes the rotational dynamics of the engaged clutch system.

$$(J_{C1,in} + J_{C1,out})\dot{\omega} = T_{TD} - T_{k12} - T_{kIn1} - (c_{C1,in} + c_{C1,out})\omega \tag{11}$$

Solving equation (4) or (5) for $\dot{\omega}$, entering the result in equation (11) and solving for T_{C1}, yields the torque at the clutch in the "engaged" state (Equation (12)).

$$T_{C1,engaged} = \frac{J_{C1,out}(T_{TD} - T_{k12} - c_{C1,in}\omega) + J_{C1,in}(T_{kIn1} + c_{C1,out}\omega)}{J_{C1,in} + J_{C1,out}} \tag{12}$$

The dynamic behaviour of the clutch is determined by equation (4) and (5) in the state of slipping and by equation (12) in the "engaged" state.

From the switching logic depicted in Figure 3.12 the following conditions for the transition between the state "engaged" and "slipping" can be formulated:

- *Clutch 1engaged:* As long as (as soon as) the value of the torque transmitted by the clutch in the engaged state (Equation (12)) stays within the boundaries set by the static friction coefficient (Equation (13) and as long as (as soon as) the differential speed across the clutch is zero, the clutch is in the engaged state.

IF $\{-\mu_s R_m F_{N1} z \le T_{C1,engaged} \le \mu_s R_m F_{N1} z\}$ AND $\{\omega_c = \omega_{co}\}$ THEN {Clutch Engaged} (13)

(Or stated differently:

IF $\{|T_{C1,engaged}| \le \mu_s R_m F_{N1} z\}$ AND $\{\omega_c = \omega_{co}\}$ THEN {Clutch Engaged})

- *Clutch 1 slipping:* As long as (as soon as) the value of $T_{C1,engaged}$ (Equation (12) is greater then the static friction torque the clutch is in the slipping state

$$\text{IF } \{|T_{C1,engaged}| > \mu_s R_m F_{N1} z\} \text{ THEN } \{\text{Clutch Slipping}\} \quad (14)$$

Connecting Shaft

Applying Newton's second law to the free-body diagram (spring damper element) of the connecting shaft in Figure 3.9 yields the torque in that shaft (Equation 15).

$$T_{k12} = k_{12}(\varphi_c - \varphi_{c2}) + c_{12}(\omega_c - \omega_{c2}) \quad (15)$$

Clutch 2

The friction laws at clutch including the switching logic have already been explained for clutch 1 and apply similarly to clutch 2. The structure of the equation of motion is the same as for clutch 1. The equations of motion for clutch 2 are listed in the Appendix A.2.

Friction Materials and Friction Coefficients

The main difference between dry friction and wet friction exists in the level of the friction coefficient (both static and kinetic) and the shape of the function of the friction coefficient. Also, in the vicinity of zero sliding speed the difference between static and kinetic friction is much larger for the dry friction than for the wet friction.

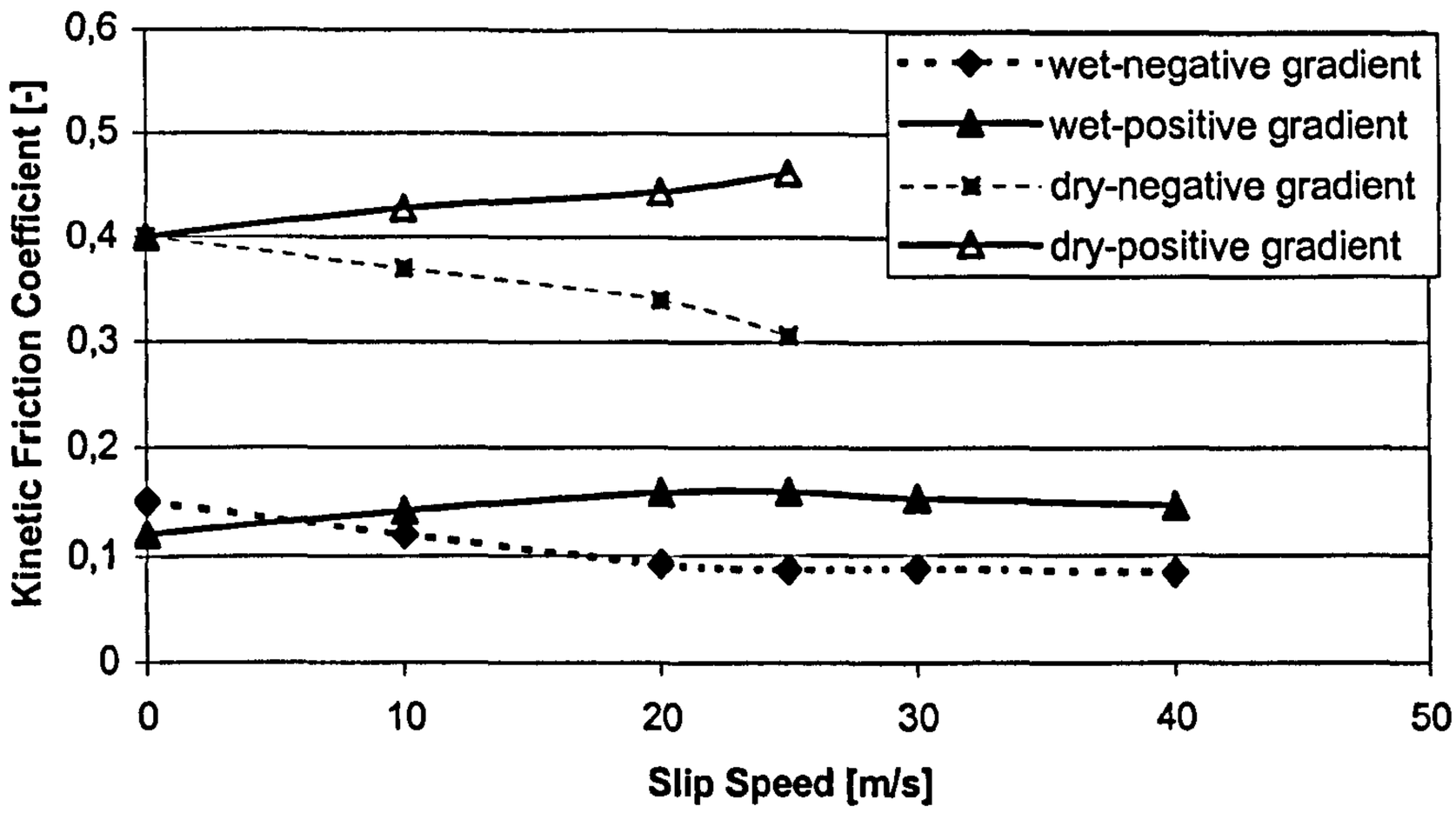

Figure 3.13 Kinetic Friction coefficients of wet and dry friction materials

Both wet and dry friction show a strong dependency on the sliding speed. This dependency is influenced by the pairing of friction material and, in case of wet friction, on the ATF (Automatic Transmission Fluid). Furthermore, the dependency of wet friction on the temperature is stronger due to the active role of the oil in the friction contact and the influence of the temperature on the viscosity of that fluid. However, at severe clutch engagement conditions like hill-hold and

vehicle launch at maximum engine revolution, the influence of the clutch temperature on the dry friction characteristics has to be taken into account too. There is also a poorer cooling capability due to the lack of any oil (ATF), which further worsens the situation for dry friction clutches under severe engagement conditions. For the control of gearshifts (short slipping times, no high temperature) it suffices to describe the friction behaviour of a clutch, be it of wet-type or dry-type, by specifying a static and a kinetic friction coefficient and by assuming that the kinetic friction coefficient is a function of the differential speed across the clutch.

Four different friction coefficient profiles have been chosen in this work to account for differences in the clutch type (wet or dry type) and differences in the characteristics (function relationship between friction coefficient and differential speed). Two for wet friction and two for dry friction. In each of those two pairs, one friction coefficient has a positive gradient with slip speed and the other one a negative gradient with slip speed. Third order polynomials (only coefficients A- D are used in Equation (8)) were selected to model dry friction, whereas fifth order polynomials were chosen for wet friction. These polynomials for the kinetic friction coefficient are depicted in Figure 3.13. The coefficients of these kinetic friction coefficient polynomials are listed, together with, the values for the static friction coefficient in the Appendix A.4

Input Shafts

The free-body diagrams of the input shafts 1 and 2 are depicted in Figure 3.14. The equations of motion are in principle similar to those of the connecting shaft, with one exemption.

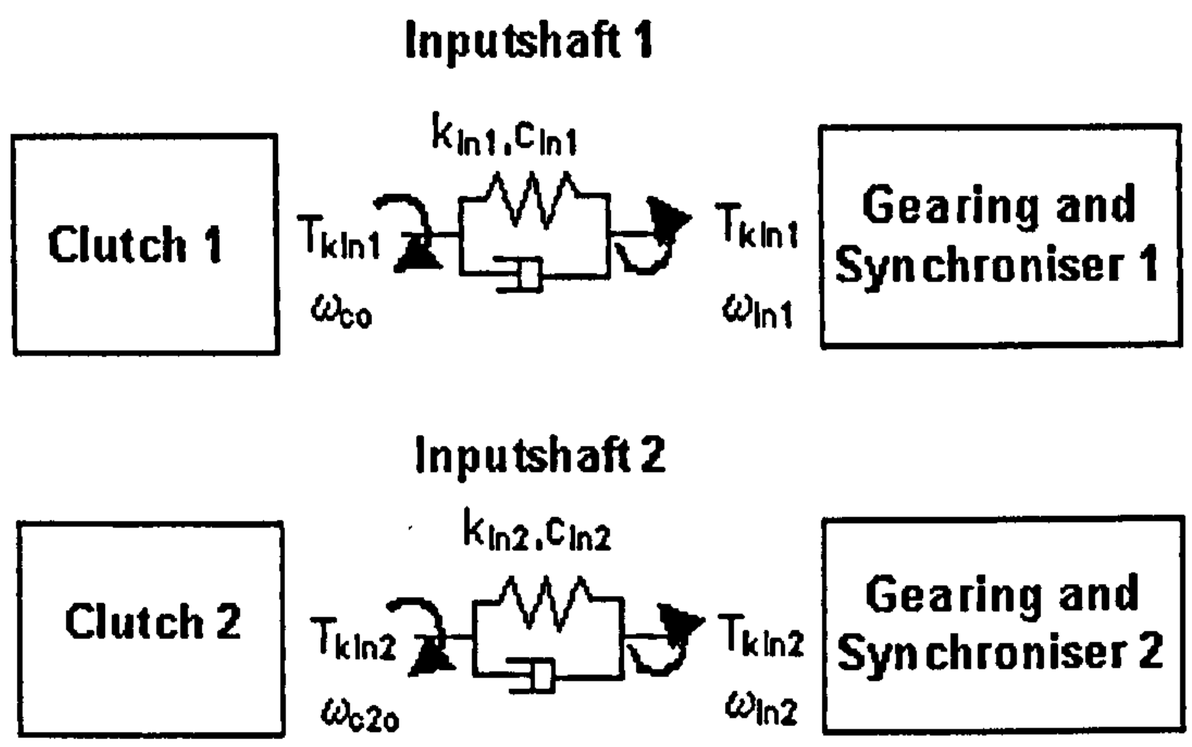

Figure 3.14 Free-body diagrams of the two input shafts

As can be seen from the mechanical layout of the twin clutch transmission depicted in Figure 3.7, the gearwheels are located at different positions on the input shaft, hence, also the stiffness and damping properties of the shafts vary with the location of the gearwheels and thus the gear. Consequently, the spring and damper rates in Equation (16) are functions of the gear (-ratio). For example, for the input shaft 1 there are three pairs of spring and damper rates, for the 1st, 3rd and the 5th gear.

Inputshaft 1

Referring to the free-body diagram depicted in Figure 3.14, the torque at the inputshaft 1 can be determined by applying Newton's second law.

$$T_{kIn1} = k_{In1}(\varphi_{co} - \varphi_{In1}) + c_{In1}(\omega_{co} - \omega_{In1}) \tag{16}$$

$$k_{In1} = f(gear=1,3,5),\ c_{In1} = f(gear=1,3,5)$$

Inputshaft 2

The inputshaft 2 is modelled in the same way as inputshaft 1. The equation of motion is listed in the Appendix A.2.

Gearing and Synchronisers

Transmission half 1 contains the gearing and synchronisers of the 1st, 3rd and 5th gear and transmission half 2 the gearing and synchronisers of the 2nd, 4th and 6th gear.

Transmission Half 1: Gearing and Synchroniser of 1st, 3rd and 5th Gear

The efficiency of the gearing in each transmission half is accounted for by multiplying an efficiency coefficient to the input torque of the gearing. This efficiency coefficient accounts for all frictional losses that are not speed depended (no viscous damping). This includes for example: frictional losses in the gear mesh (sliding of teeth), in sealing and in bearings. The efficiency of a single gear mesh is around η=0.98-0.99. Furthermore, this efficiency roughly stays constant for all gear ratios, since in every gear the same number of gear wheels, bearings and sealing contribute to the losses.

As a first step it is necessary to determine the effective inertia seen by the synchroniser (i.e. effective inertia at the synchroniser input). This effective inertia can be determined using Figure 3.15, which depicts half 1 of the twin clutch transmission shown in Figure 3.7.

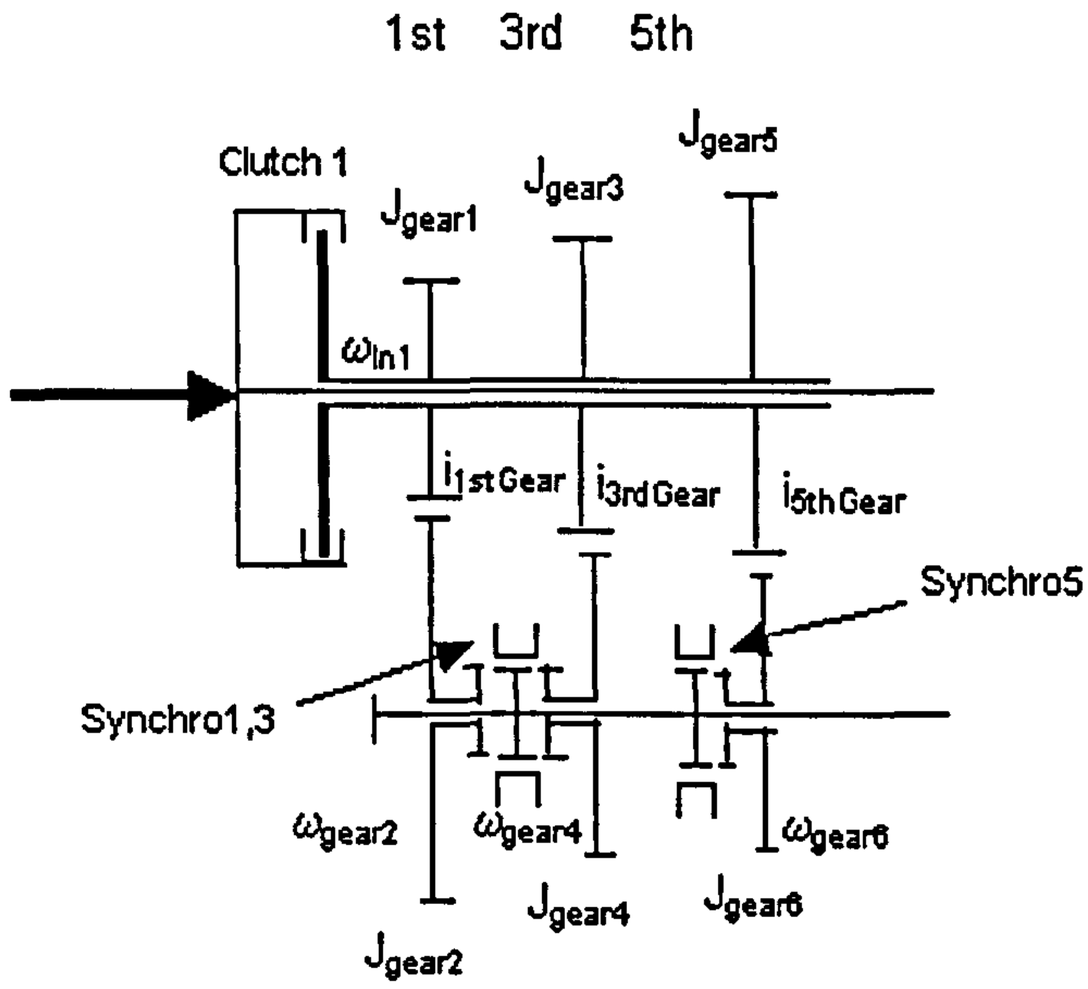

Figure 3.15 Half 1of the twin clutch transmission depicted in Figure 3.7

First, applying the law of energy conservation (Equation (17)) to the gearwheels in transmission half 1 (see Figure 3.15) yields the total inertia reduced to the input shaft 1 (Equation (19)):

$$J_{eff,In1}\frac{\omega_{In1}^2}{2}=(J_{gear1}+J_{gear3}+J_{gear5})\frac{\omega_{In1}^2}{2}+J_{gear2}\frac{\omega_{gear2}^2}{2}+J_{gear4}\frac{\omega_{gear4}^2}{2}+J_{gear6}\frac{\omega_{gear6}^2}{2} \qquad (17)$$

With the definition of the gear ratio for the 1st,3rd and 5th gear,

$$i_{1,3,5}=\frac{\omega_{In1}}{\omega_{gear2,4,6}} \qquad (18)$$

The inertia of the gearwheels in half 1 reduced to the input shaft is given by equation (19)

$$J_{eff,In1}=J_{gear1}+J_{gear3}+J_{gear5}+J_{gear2}\left(\frac{1}{i_1}\right)^2+J_{gear4}\left(\frac{1}{i_3}\right)^2+J_{gear6}\left(\frac{1}{i_5}\right)^2 \qquad (19)$$

The inertia reduced to the input shaft can be further reduced to the input of each synchroniser by again applying the law of energy conservation. The effective inertia at the input of each synchroniser is given by equation (20):

$$J_{S1,in}=J_{eff,In1}\cdot i_{1,3,5}^2 \qquad (20)$$

Having determined the effective inertia at the synchroniser input, the equations of motion for each synchroniser can be derived. As already explained, in the basic transmission model the synchronisers in transmission half 1 (and 2) are modelled by a single synchroniser model only.

For the friction contact in the synchroniser, the kinetic friction coefficient was assumed to be constant (i.e. not depending on the sliding speed). This simplification is justified because sliding times are very short and the relative velocities at the friction surface are small compared to those at the friction surface of the clutch. Different friction materials are not considered here for the synchronisers.

The two-state switching logic of the clutch model had to be extended for the synchroniser model to incorporate a third state. This was necessary to account for the engagement of the dog clutch-like part of the synchroniser once the differential speed across synchroniser has vanished. This third state has the effect of mechanically locking the synchroniser. The three-state switching logic is depicted in Figure 3.16.

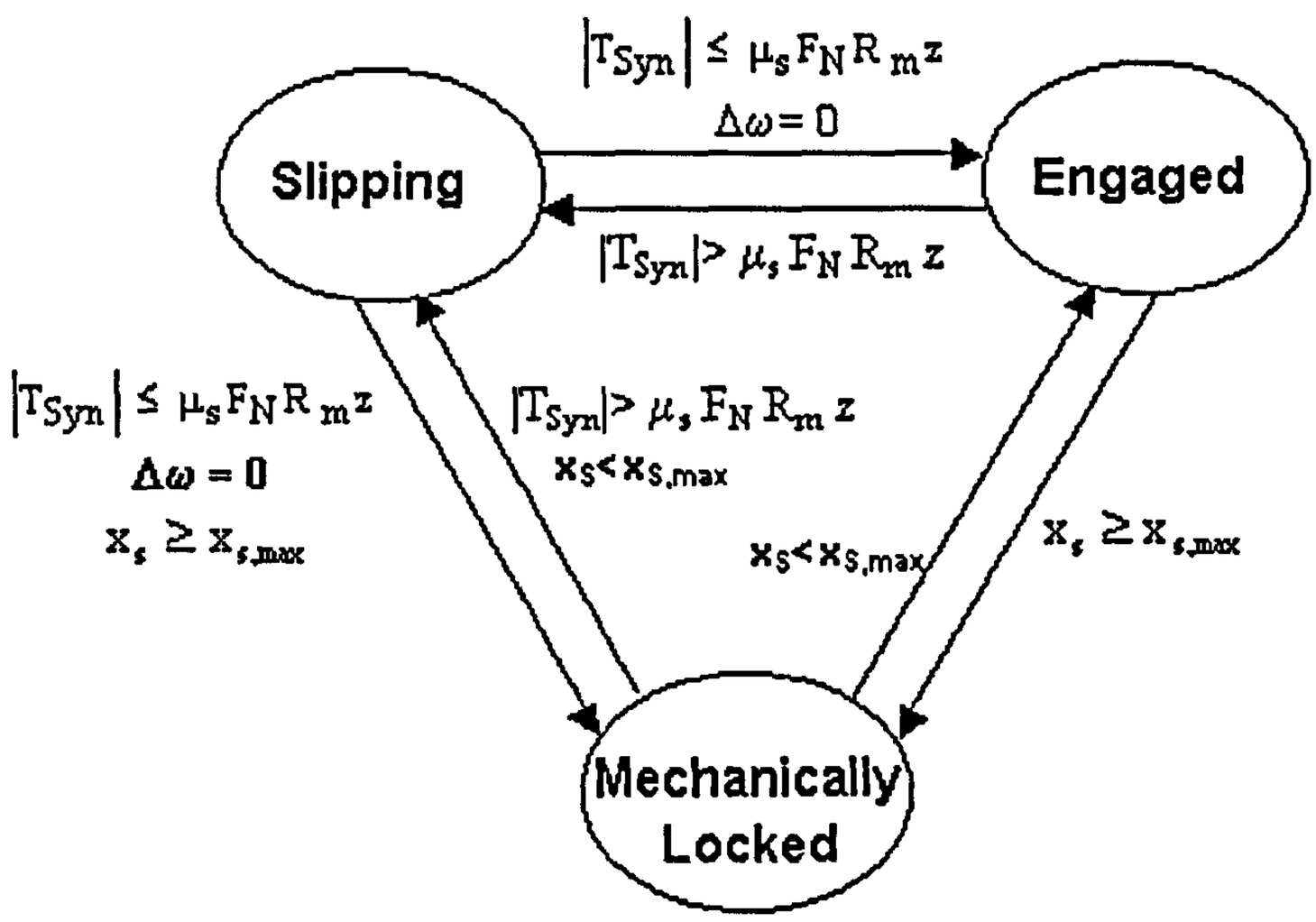

Figure 3.16 Three-state switching logic of the synchroniser model

The two upper states "slipping" and "engaged" are the same as for the clutch model. Also the conditions for a transition between those two states remain the same. What is new for the synchroniser is the third state "mechanically locked", which represents the state where the dog clutch-like part of the synchroniser engages. The dog clutch can be engaged if the conditions for the "engaged" state are met and the position of the synchroniser actuator (or shift rail) has reached its maximum displacement where the mechanical locking starts. The dynamics of the

indexing process (torque reactions and time delay) have not been accounted for since they do not significantly influence the dynamics of the fast engagement of hydraulically actuated synchronisers due to the large indexing forces. The information about the actuator position comes from the actuator model developed in the section on the hydraulic actuation. If the actuator position becomes smaller than this critical displacement, the mechanical locking is cancelled an the synchroniser either transits to the "engaged" state, if the conditions for a frictional locking are still valid, or if these conditions are not met the state of the synchroniser transits to the "slipping state". The conditions for a transition are listed below (Equation (28) to (33)).

The equation of motion of the synchroniser model for the stages "slipping" and "engaged" can be derived using the free-body diagram of synchroniser 1, which is depicted in Figure 3.17. The equations of motion are basically the same as for the clutch model apart from the constant kinetic friction coefficient and the different geometry of the friction surface (conical friction interface). The equations of motion in the state "mechanically locked" are the same as for the "engaged" state, since no change in the structure of the equations (no change in degree of freedom) occurs. Only the conditions of transition between the states are different. The mechanical locking was assumed to be rigid without any compliance.

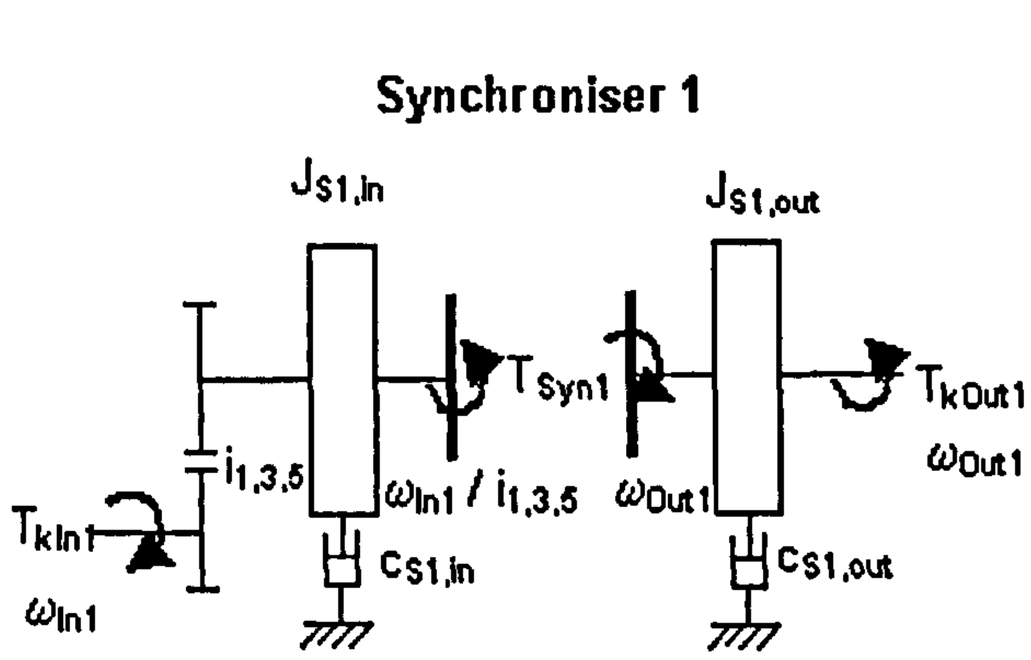

Figure 3.17 Free-body diagram of the synchroniser 1 in the "slipping state"

Synchroniser in state of slipping:

Referring to Figure 3.17, the equations of motion can now be derived.

Torque balance at mass inertia $J_{S1,in}$

$$J_{S1,in}\frac{\dot{\omega}_{In1}}{i_{1,3,5}} = T_{kIn1}i_{1,3,5}\eta_{gearbox1} - T_{Syn1} - c_{S1,in}\frac{\omega_{In1}}{i_{1,3,5}} \tag{21}$$

Torque balance at mass inertia $J_{S1,out}$

$$J_{S1,out}\dot{\omega}_{Out1} = T_{Syn1} - T_{kOut1} - c_{S1,out}\omega_{Out1} \tag{22}$$

Friction Torque at Synchroniser 1:

$$T_{Syn1} = \mathrm{sgn}(\omega_{In1} - \omega_{Out1})\frac{R_m}{\sin\alpha}F_{N,S1,3,5}\mu_k z \tag{23}$$

$$\mu_k = \text{const.} \tag{24}$$

Although only single cone synchronisers (i.e. z = 1) are considered in the transmission model, equation (23) could also be used for multiple cone type (z > 1) synchronisers if it is assumed that, the mean friction radii and the cone angles are equal for all friction interfaces. Furthermore for the multiple cone type synchronisers it has to be assumed that the single interfaces are coupled (i.e. the single parts can not rotate independently) in order to use equation (23). Multiple cone type synchronisers are employed to increase the capacity of the synchronisers. Further details on the performance of multiple cone synchroniser can be found in [Abdel-Halim et al 2000].

Synchroniser in the "engaged" state

In the "engaged" state, the two sides of the synchroniser are locked together (either through friction due to the applied normal force or mechanically through the engagement of the dog clutch) and rotate with the same speed (Equation (25)).

$$\frac{\omega_{In1}}{i_{1,3,5}} = \omega_{Out1} = \omega \tag{25}$$

Combining equation (21) and (22) and using the relation in equation (25), results to equation (26), which describes the rotational dynamics of gearing and synchroniser in the "engaged" state.

$$(J_{S1,in} + J_{S1,out})\dot{\omega} = T_{kIn1}i_{1,3,5}\eta_{gearbox1} - T_{kOut1} - (c_{S1,in} + c_{S1,out})\omega \tag{26}$$

Solving equation (21) or (22) for $\dot{\omega}$, entering the result in equation (26) and solving for T_{Syn1}, produces the torque at the synchroniser in the "engaged" state (Equation (27)).

$$T_{S1,engaged} = \frac{J_{S1,out}(T_{kIn1}i_{1,3,5}\eta_{gearbox1} - c_{S1,in}\omega) + J_{S1,in}(T_{kOut1} + c_{S1,out}\omega)}{J_{S1,in} + J_{S1,out}} \tag{27}$$

The conditions for the transition between different states of the synchroniser are depicted in Figure 3.16 are listed here again (Equations (28) to (33)).

- *Engaged:*

  Transition from the state "Slipping":

$$\text{IF } \{\left|T_{S1,engaged}\right| \le \mu_s \frac{R_m}{\sin\alpha} F_{N,S1,3,5} z\} \text{ AND } \{\frac{\omega_{In1}}{i_{1,3,5}} = \omega_{Out1}\}$$

$$\text{THEN } \{\text{Synchroniser Engaged}\} \tag{28}$$

  Transition from the state "Mechanically Locked":

$$\text{IF } \{x_s < x_{s,\max}\} \text{ THEN } \{\text{Synchroniser Engaged}\} \tag{29}$$

- *Slipping:*

  Transition from state "Engaged":

$$\text{IF } \{\left|T_{S1,engaged}\right| > \mu_s \frac{R_m}{\sin\alpha} F_{N,S1,3,5} z\} \text{ THEN } \{\text{Synchroniser Slipping}\} \tag{30}$$

  Transition from state "Mechanically Locked":

$$\text{IF } \{\left|T_{S1,engaged}\right| > \mu_s \frac{R_m}{\sin\alpha} F_{N,S1,3,5} z\} \text{ AND } \{x_s < x_{s,\max}\}$$

$$\text{THEN } \{\text{Synchroniser Slipping}\} \tag{31}$$

- *Mechanically Locked*:

  Transition from state "Engaged":

$$\text{IF } \{x_s \ge x_{s,\max}\} \text{ THEN } \{\text{Synchroniser Mechanically Locked}\} \tag{32}$$

  Transition from state "Slipping":

$$\text{IF } \{\left|T_{S1,engaged}\right| \le \mu_s \frac{R_m}{\sin\alpha} F_{N,S1,3,5} z\} \text{ AND } \{\frac{\omega_{In1}}{i_{1,3,5}} = \omega_{Out1}\}$$

$$\text{AND } \{x_s \ge x_{s,\max}\} \text{ THEN } \{\text{Synchroniser Engaged}\} \tag{33}$$

<u>Transmission Half 2: Gearing and Synchroniser of 2nd, 4th and 6th Gear</u>

The equations of motion for the gearing and the synchronisers of transmission half 2 are similar to those for transmission half 1 and are thus listed in the Appendix A.2.

Layshafts

The free-body diagram of both layshafts is depicted in Figure 3.18. The modelling of the layshafts is similar to that of the inputshafts. The stiffness and damping properties of layshaft

also vary with the location of the gearwheels (Gearwheels 2,4,6 in Figure 3.15) and hence the selected gear. Therefore, the spring and damper rates in Equation (34) are functions of the gear. In case of layshaft 1, there are three pairs of spring and damper rates for the 1st,3rd and the 5th gear.

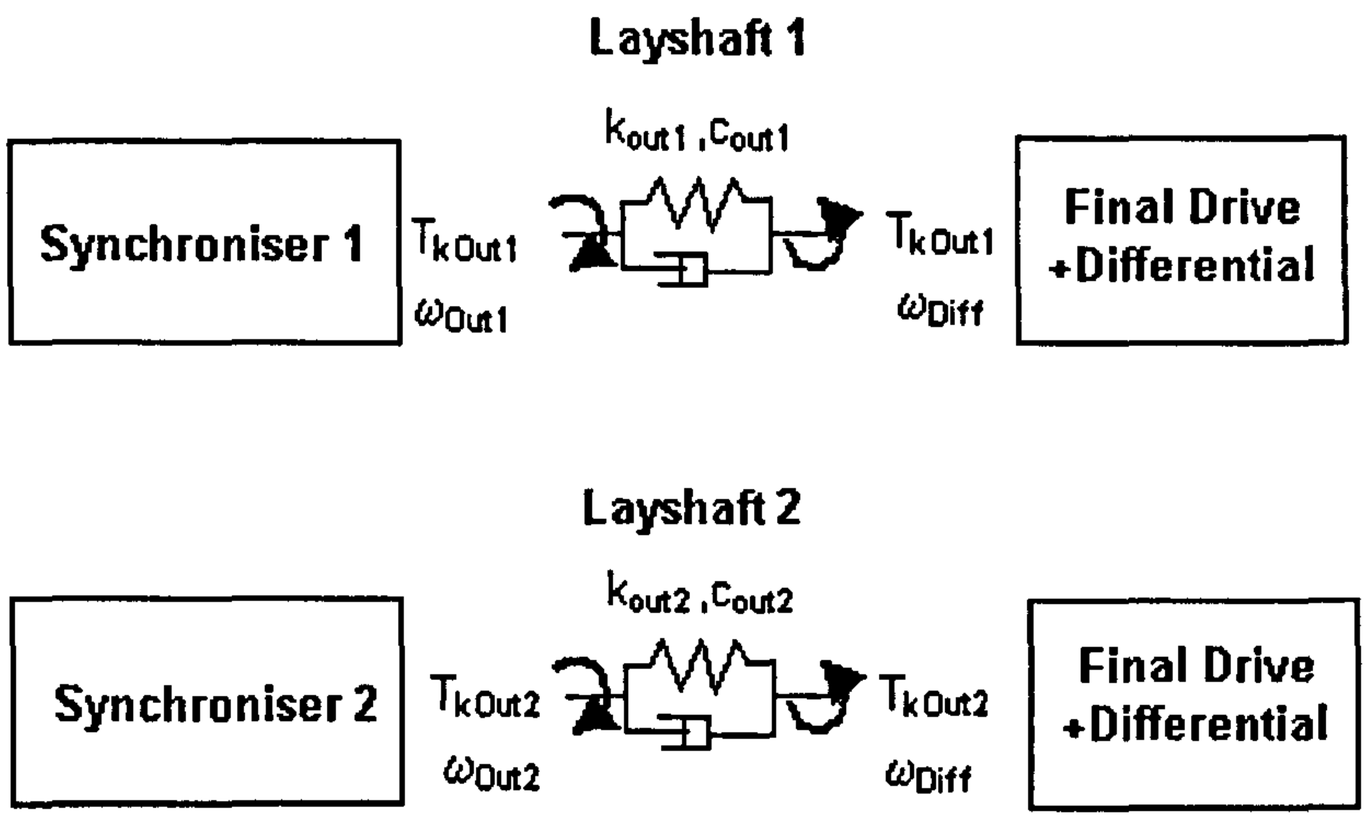

Figure 3.18 Free-body diagrams of layshafts 1and 2

Layshaft 1

By applying Newton's Second law to the free-body diagram depicted in Figure 3.18, the torque at the layshaft 1 can be derived to yield:

$$T_{kOut1} = k_{Out1}(\varphi_{Out1} - \varphi_{Diff}) + c_{Out1}(\omega_{Out1} - \omega_{Diff}) \tag{34}$$

$$k_{Out1} = f(gear=1,3,5),\ c_{Out1} = f(gear=1,3,5)$$

Layshaft 2

Layshaft 2 is modelled in the same way as layshaft1. The equations of motion are listed in the Appendix A.2.

Extended Transmission Model (for Doubleshifts and Gearshifts with Gear Pre-Selection)

The extended transmission model used for simulation of synchroniser-to-synchroniser shifts as part of a double/multiple gearshift or a gearshift with gear pre-selection is depicted in Figure 3.19. Figure 3.19 depicts the extended transmission model for a configuration where the synchroniser of the 1st and 3rd gear in half 1 and the synchroniser of the 2nd gear in half 2 take

part in the simulated gearshift. If gearshifts or synchroniser-to-synchroniser shifts between other gears have to be simulated, the extension can be placed in the other transmission half accordingly.

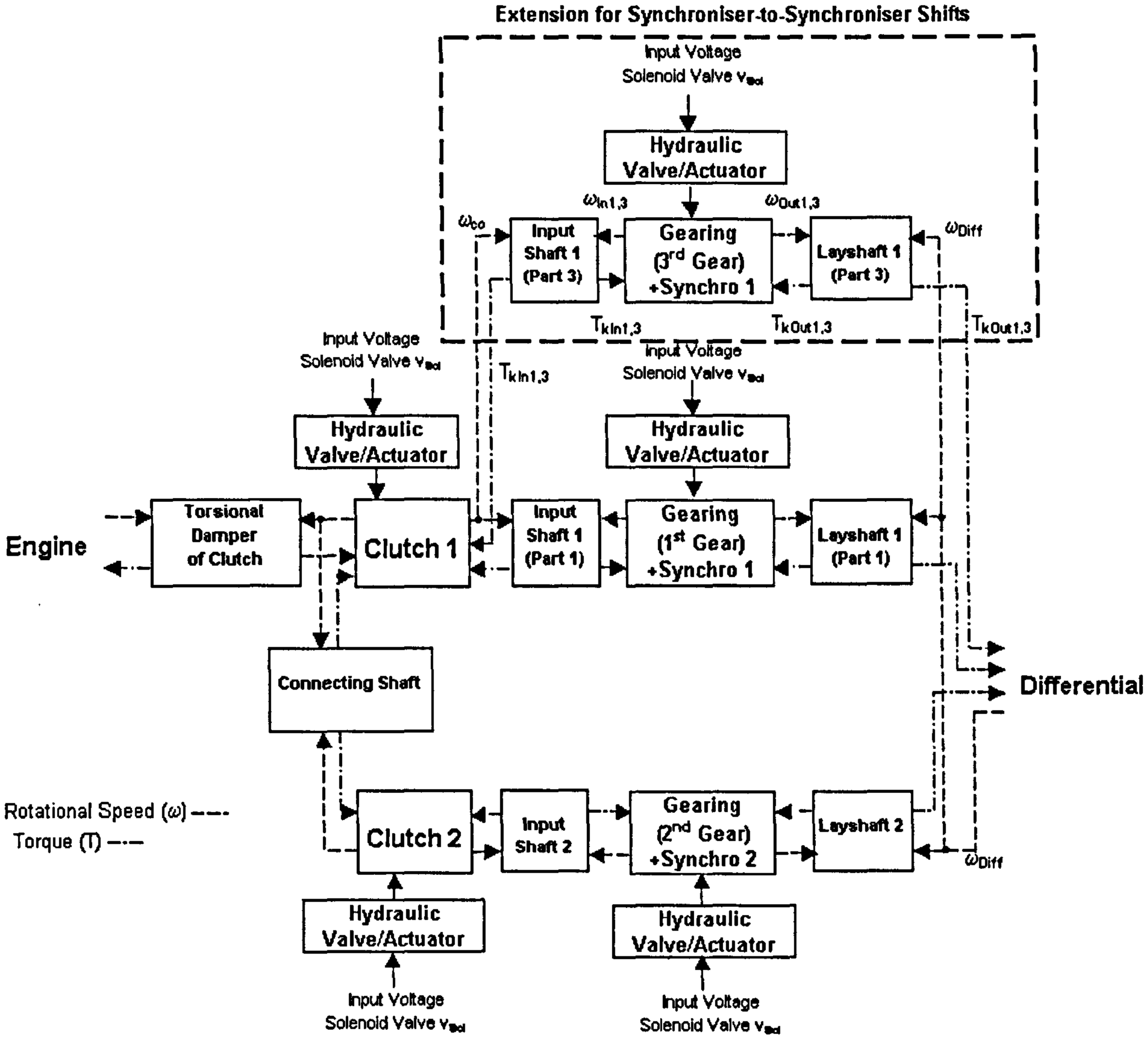

Figure 3.19 Extended model for synchroniser-to-synchroniser shifts depicted for configuration: 1st and 3rd gear in transmission half 1 and 2nd gear in transmission half 2.

The lower half of Figure 3.19 is similar to the one of the basic model. The upper half of Figure 3.19 can be interpreted as follows: The two blocks of input shaft 1 (part 1 and 3) represent those parts of the input shaft (stiffness) reaching from the output of clutch 1 to the input gearwheel of either the 1st gear or the 3rd gear (see also Figure 3.7 for the mechanical layout of the transmission). The same applies to the layshaft where the two parts again represent the part of the layshaft from either the synchroniser of the 1st gear or the synchroniser of the 3rd gear to the gearwheel of the final drive unit at the output of the transmission (see Figure 3.7). Both

synchroniser blocks contain the models of the synchronisers of the 1st and the 3rd gear respectively, together with the gearings of the two gears.

The upper half of Figure 3.19 essentially models the transmission half containing the odd gear numbers, when either the 1st gear or the 3rd gear is engaged. This model is valid as long as no overlapping of the synchronisers takes place and either, the synchroniser of the 1st gear or the synchroniser of the 3rd gear is engaged. This simplification is justified, because in reality one of the two synchronisers must be disengaged before the other one can be engaged. If this were not the case, tie up of the transmission or elongated slipping of the oncoming synchroniser (in case offgoing synchroniser still mechanically locked) would be the result, which would immediately lead to a destruction of the synchronisers. The controller has to take care of this problem, by starting a pressurisation of the oncoming synchroniser, only if the offgoing synchroniser has been fully disengaged. This allows decoupling the two branches in the upper transmission half in Figure 3.19 and requires a "switching" between the two branches by engaging/disengaging the two synchronisers. Similar considerations apply, of course, also if the extension is added to the lower half (even gear numbers) of the transmission model in Figure 3.19. The extended model will be used extensively in the chapters where multiple gearshifts and gear pre-selection are discussed.

3.3.2 Dynamics of Hydraulic System

In the block diagram of the twin clutch transmission model depicted in Figure 3.8, the hydraulic actuators of the twin clutch and synchronisers were represented by blocks accepting an input voltage (to the solenoid valve) and producing a clamp force at the friction contacts of clutches and synchronisers.

A possible layout of a hydraulic actuation system of a twin clutch transmission is depicted in Figure 3.20. This hydraulic scheme is roughly based on two hydraulic actuation systems found in the literature [Flegl et al. 1987] and [Wheals et al. 2001] for twin clutch transmissions. The hydraulic actuation scheme depicted in Figure 3.20 basically consists of two 3-way proportional solenoid valves for each of the two clutches in the twin clutch assembly. Furthermore the actuation scheme in Figure 3.20 includes 3-way proportional solenoid valves and on/off valves (3 way, 2 position valves) to operate the shift rails for an engagement of gears by means of synchronisers. The rest of the hydraulic system comprises the hydraulic actuation cylinders, a pressure-regulating valve to control the main (or supply, or line) pressure in the whole system

and a variable displacement pump. The accumulator is employed to keep the pressure in the system constant during transient valve and actuator operations and therefore minimise pressure pulses and pressure vibrations. Further supplementary elements are: a one-way valve, a filter, oil cooler and a tank that stores the hydraulic medium (oil). The proportional solenoid valves enable a continuous modulation of the actuation pressure through a proportional change in the solenoid voltage or current. This characteristic makes the proportional valve especially suited for a closed-loop clutch control. The function of the on/off valves is simply to activate the appropriate synchroniser actuator and to enable a quick filling (engagement) or empting (disengagement) of the actuator.

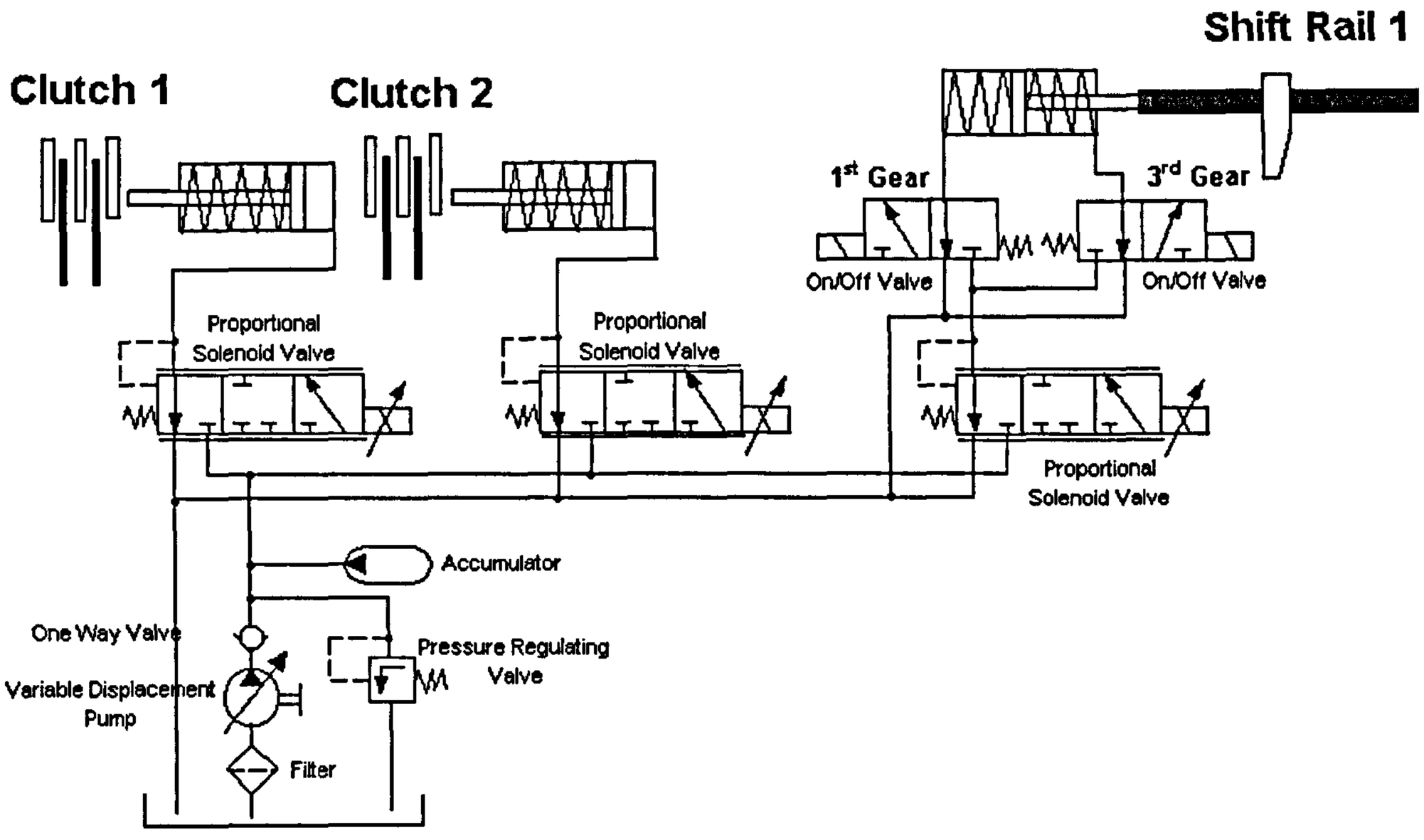

Figure 3.20 Hydraulic system of a twin clutch transmission (depicted with shift rail for 1st and 3rd gear only)

To simplify the model of the hydraulic actuation and to include only the essential parts and their dynamic behaviour, only important parts of the hydraulic actuation of clutches and synchronisers were considered. The essential parts of the hydraulic actuation of clutches and synchronisers are depicted in Figure 3.21 and include a dynamic model of a proportional solenoid valve of a hydraulic actuator and a model of the clutch pack. The supply pressure at the inlet port of the solenoid valve is assumed to be constant to reflect the function of the accumulator in smoothing pressure variations.

For the actuation of synchronisers, the same hydraulic actuator model as for the clutches was used. A model for the on/off valves was not included since these valves do not contribute to the

dynamics of the hydraulic actuation significantly. Instead it was assumed that the on/off valves are already in an open or closed state when the solenoid valve is operated.

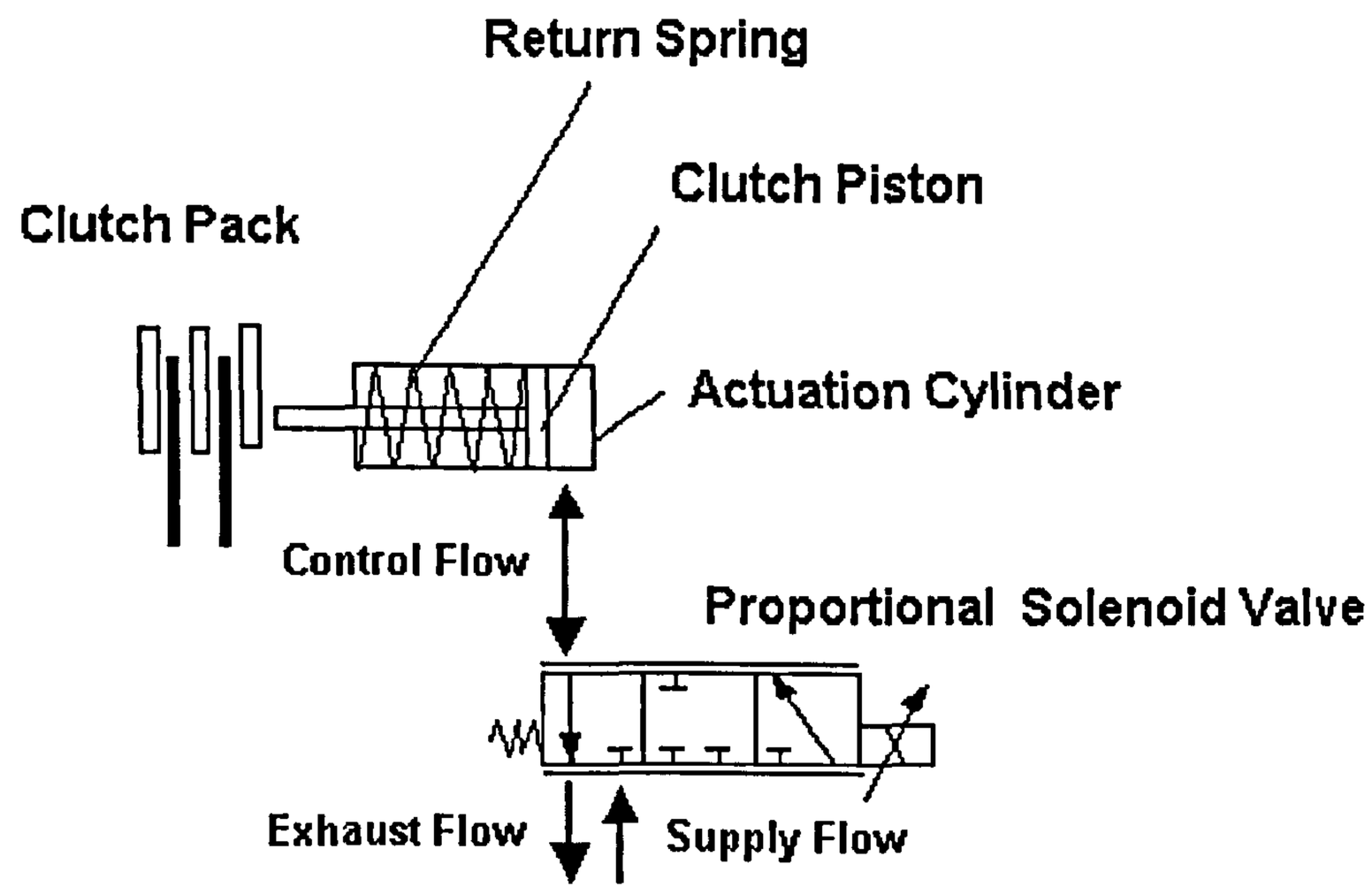

Figure 3.21 Essential parts of hydraulic system

In the following two sections, first a full non-linear model of the proportional solenoid valve including flow dynamics in the actuator is developed. From step responses (time domain) of this non-linear model, a simplified model with linear transfer functions was generated. The simplified model was less complex and thus better suited for controller development. Subsequent to the treatment of the solenoid valve dynamics, a dynamic model that describes the process of the generation of a clamp force at the friction contact due to a change in the hydraulic pressure at the actuator piston is developed (clutch pack model).

Model of the Proportional Solenoid Valve and Flow Dynamics in the Actuator

Full Non-linear Model

Figure 3.22 depicts a block diagram of the model of the hydraulic system shown in Figure 3.21. The block diagram of Figure 3.22 contains two main groups of blocks. The first group contains the parts belonging to the proportional solenoid valve and the flow dynamics in the hydraulic actuator, whilst the other group contains the blocks modelling the dynamics of the actuator piston and the compliance of the clutch pack. The solenoid valve and flow dynamics group accepts as input variable a voltage signal and produces as output variable the pressure in the

clutch (synchroniser) actuator. This pressure signal functions as input to the clutch piston dynamics and clutch pack block, which produce a clamp force at the output. This clamp force is the input variable to the friction models of clutch and synchroniser.

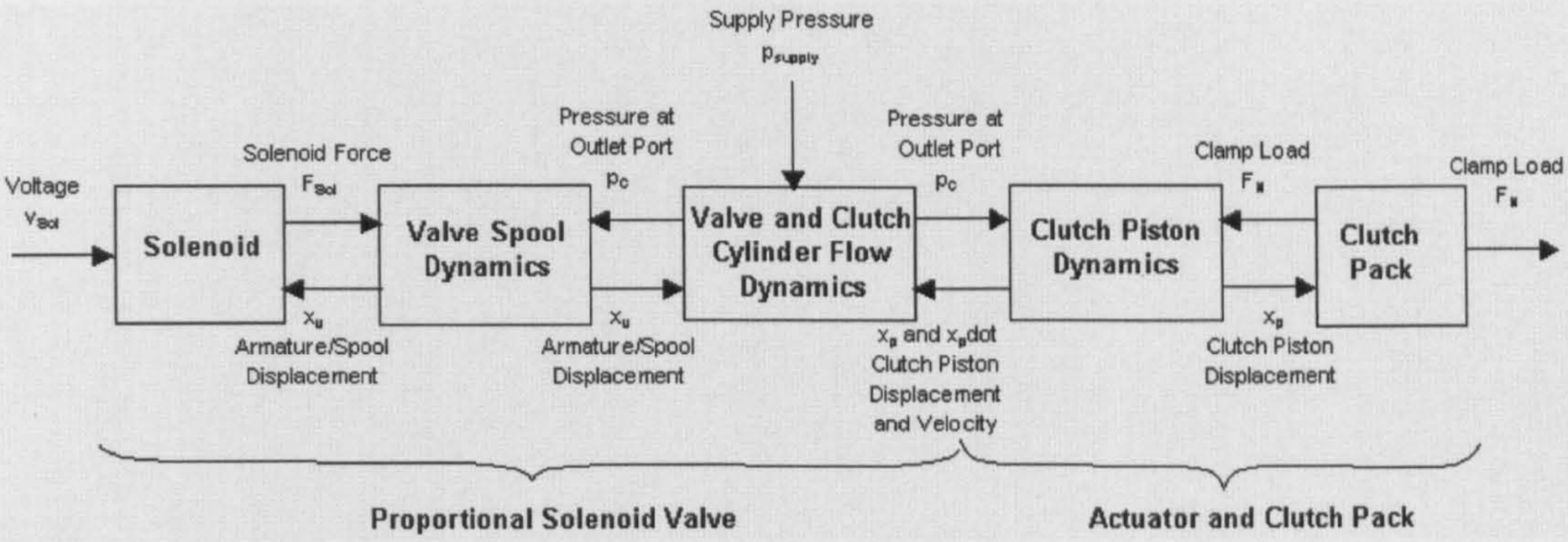

Figure 3.22 Block diagram of the full non-linear model of the hydraulic system depicted in Figure 3.21

A schematic picture of a 3 way proportional solenoid valve is shown in Figure 3.23. The valve in Figure 3.23 operates as follows: At the solenoid an analog electric signal (voltage or current) is converted into a proportional magnetic force, which generates a movement of the armature. A displacement of the armature moves the spool of the proportional valve. Through a displacement of the spool, exhaust or supply ports are covered and uncovered respectively, which determines the oil flow at each of the ports. The line or supply pressure of the hydraulic system acts at the supply port. The exhaust port is connected to the ambient pressure. By controlling the oil flow through both the supply and the exhaust port, the net oil flow at the control port and therefore to the clutch can be controlled.

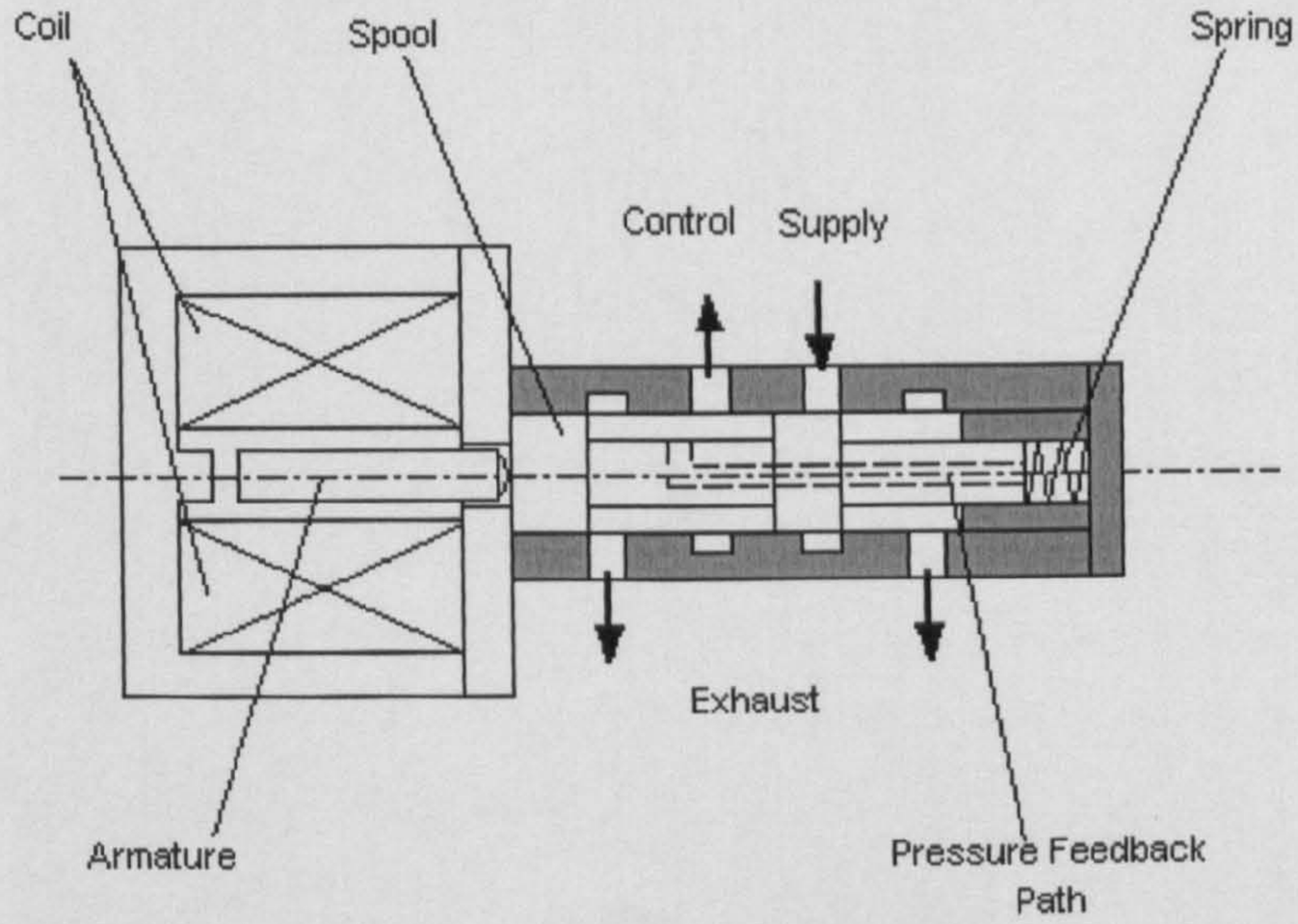

Figure 3.23 Schematic picture of a 3 way proportional pressure-reducing valve

The net oil flow through the control port determines the pressure in the hydraulic actuation cylinder of the clutch and therefore also at the control port of the valve (hydraulic flow resistances and compliances of the connecting lines are not considered). The oil flow out of the control port of the proportional solenoid valve (control flow in Figure 3.21) is fed into the hydraulic actuator of the clutch, which takes the form of a hydraulic cylinder. The oil flow expands the oil volume in the cylinder and hence creates a movement of the piston. The actual pressure rise depends not only on the net oil flow into the cylinder but also on the expansion volume of the cylinder together with the velocity of the expansion and the bulk modulus of the oil. The considered proportional solenoid valve is of normally open type, which means that when the input voltage is zero, a return spring holds the spool in the end position where the exhaust port is opened.

The equations of motions for the full non-linear model of the proportional solenoid valve and actuator flow dynamics (proportional solenoid valve part in Figure 3.21), are taken in principle from [The Math Works 1998] and were modified in this work to reflect the behaviour of a linear proportional solenoid valve. These equations of motion are listed in the Appendix A.3.

The full non-linear model of the solenoid valve and flow dynamics is very complex and not very well suited for controller development. Therefore a simpler model that can be implemented in the whole powertrain model more easily will be developed in the next section.

Simplified, Phenomenological Model

The models of the proportional solenoid valve and the actuator flow dynamics contained non-linear mathematical relationships. The advantage of this non-linear model was that it allowed monitoring the trajectories of every single variable in detail. However, for controller development this model is not very well suited because of its complexity and size. These attributes considerably slow the simulation of the powertrain model and add a potential source of instability to the simulation. For application in this thesis the only output variables of the hydraulic system model that are of interest are the pressure and clamp force at the clutch or synchroniser. Thus, a phenomenological model that describes the input/output behaviour of the hydraulic actuation in a qualitative way without sacrificing accuracy too much is sufficient for the purpose of controller development.

This simplified model is depicted in Figure 3.24. It consists of three main blocks. The first block (containing K_1 and $G_1(s)$) in Figure 3.24 contains a second order transfer function in the

denominator ($G_1(s)$) that basically reflects the dynamics of the solenoid, which were found to dominate those of the overall hydraulic system. The dominant nature of the electro-magnetic part of the solenoid valve over the dynamics of the armature and spool was also found in [Cho et al 1999]. For this reason, the dynamics of the solenoid valve were modelled in this work by a second order transfer function with a gain in the numerator that relates the solenoid input voltage to a clutch pressure value. A second order transfer function to model the dynamics of a solenoid valve had also been employed in [Wang et al 2001] [Kwon and Kim 2000] and [Zheng et al 1999].

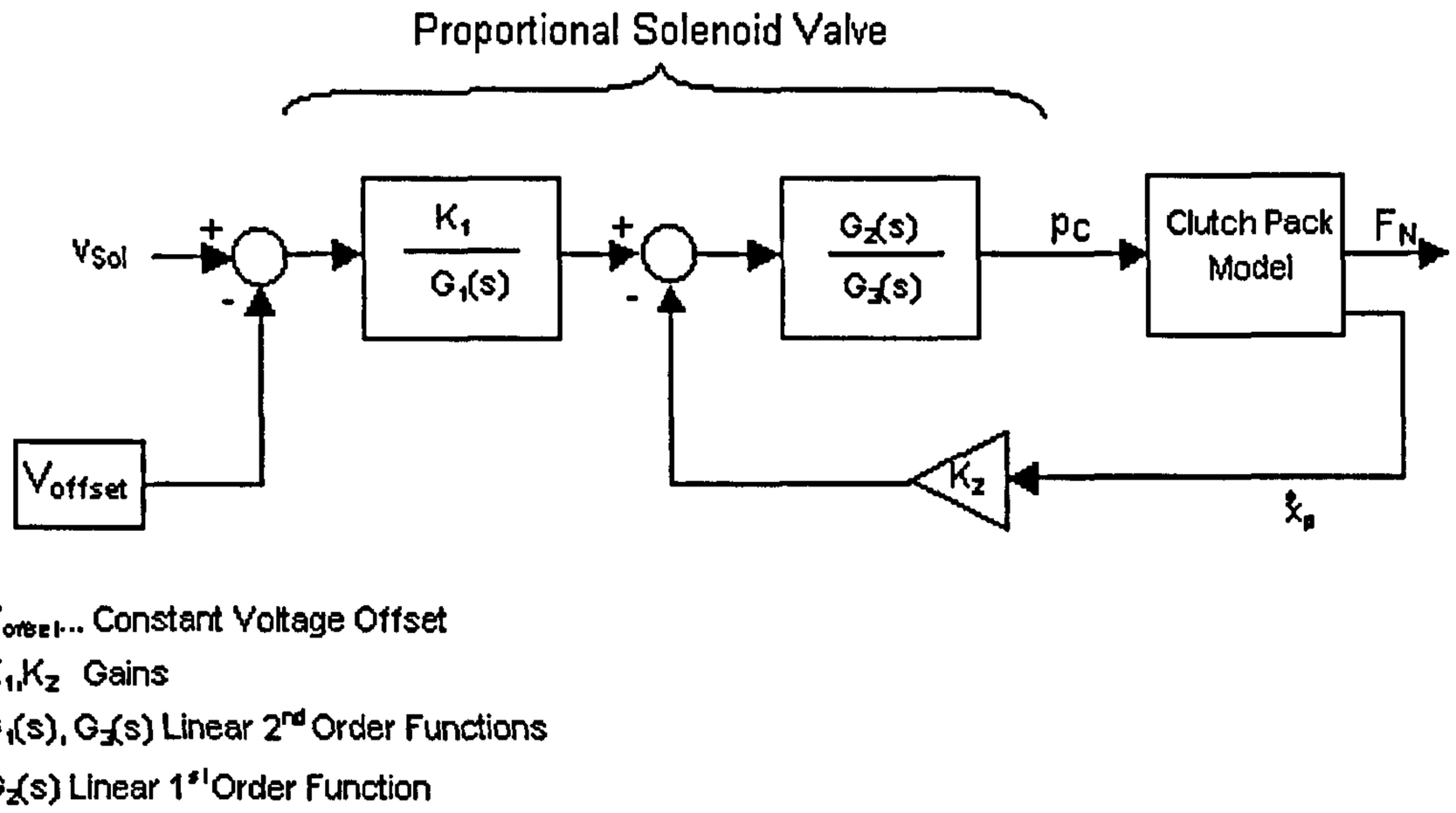

Figure 3.24 Simplified, phenomenological model of the hydraulic actuation

The parameters of this second order transfer function (undamped natural frequency and damping ratio) were identified from step responses of the full non-linear model. Such pressure trajectories as a response to voltage step inputs are depicted in Figure 3.26. The pressure gain was found from steady state responses of the non-linear model to voltage step inputs. The steady state pressure values for the full non-linear and the phenomenological model are depicted in Figure 3.25. Although, Figure 3.25 shows a difference between the steady state pressure curves of the non-linear and the linear model, the literature indicates that there should be a slightly stronger correlation between the two. This slight disagreement can be probably brought down to the choice of parameter values for the non-linear model. The "dead-zone" behaviour between 0 and 4 volts (voltage offset V_{offset} in Figure 3.25), where an increase in voltage produces no proportional increase in the clutch pressure was also observed, for a different type of proportional solenoid valve, in [Maiti et al 2002]. In that paper the "dead zone" stretched from 0

to 2 volts. The "dead zone" behaviour was incorporated in the model by offsetting the input voltage by the "dead zone" (in this work by 4.2 volts).

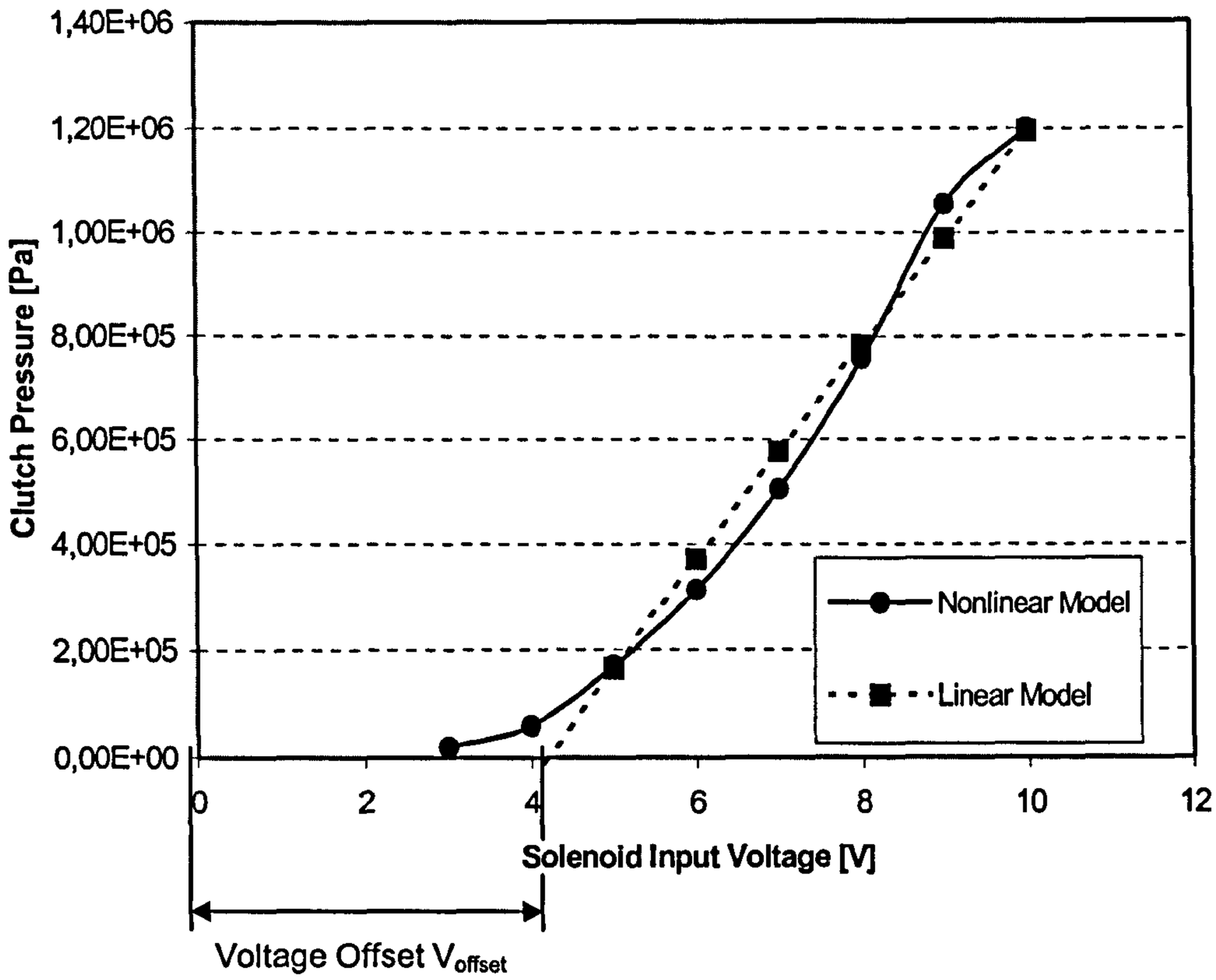

Figure 3.25 Steady-state values of clutch pressure versus solenoid input voltage for the non-linear and linear model

Simply putting the linear second order transfer function of the solenoid valve together with the clutch pack model and running simulations showed a good general agreement between the linear and the non-linear model if the piston was in contact with the clutch pack. However, in the phase where the piston was stroking and the actuator cylinder was filled (or emptied), as well as in the subsequent short phase where the piston compresses the clutch pack, the behaviour of the linear second order model strongly disagreed with that of the non-linear model. The linear model simply did not reflect the behaviour of the non-linear model in the phase where the piston-return spring is compressed and the actuation cylinder is filled with oil and where the pressure rises very slowly. Also, in the following phase where the piston gets in contact with the clutch plates and compresses the clutch pack, the simulation results of the linear model did not show the sharp rise in pressure observed for the non-linear model. Since the literature review has shown that most papers that described models of hydraulic clutch actuation (see e.g. [Wang et al 2001]) also found that this peculiar dynamic behaviour of the hydraulic

system poses an important influence to clutch control, the model needed to be modified to incorporate this non-linear response.

To account for this non-linear behaviour a simple way has been adopted here in this work. The linear second order model of the solenoid valve dynamics and the non-linear clutch pack model were both kept unchanged (including parameter values) and an additional block (containing $G_2(s)$ and $G_3(s)$ in Figure 3.24) with feedback loop (velocity of actuator piston multiplied by gain K_2 in Figure 3.24) was introduced to account for the filling (flow dynamics) of the actuator cylinder. This additional block was placed after the block of the solenoid (i.e. the block containing gain K_1 and $G_1(s)$ in Figure 3.24) and before the clutch pack block (see Figure 3.24). In [Cho et al 1999] this part of the hydraulic valve was modelled by a transfer function with one zero and one pole. Here a similar transfer function with a first order function in the numerator ($G_2(s)$ in Equation (35)) was chosen to model the filling of the clutch actuator. However, in the denominator a second order function ($G_3(s)$ in Equation (35)) was employed. The reason for this was, that due to the velocity feedback and the non-linear stiffness of the clutch pack the clutch pressure showed substantial ripples in the simulation. Those ripples could be removed by introducing a second order function instead of a first order function in the denominator of the transfer function.

The transfer function for the phenomenological model of the proportional solenoid valve can be derived from Figure 3.24 and is given by equation (35):

$$p_C = \left(\frac{K_1}{G_1(s)} \left(v_{sol} - V_{offset} \right) - K_2 \dot{x}_p \right) \frac{G_2(s)}{G_3(s)} \tag{35}$$

With:

$$G_1(s) = (s/\omega_1)^2 + (2\zeta_1 s/\omega_1) + 1 \tag{36}$$

$$G_2(s) = (s/\alpha_2) + 1 \tag{37}$$

$$G_3(s) = (s/\omega_3)^2 + (2\zeta_3 s/\omega_3) + 1 \tag{38}$$

Figure 3.26 compares the pressure trajectories of the full non-linear model of Figure 3.22 and the phenomenological model of Figure 3.24. The voltage step inputs to produce the pressure trajectories included an initial rise to 8 volts, then further up to 9 volts and at the end a reduction to 2 volts. Simulation of a variety of other step inputs was carried out to identify the parameters of the phenomenological model and to ensure a close matching to the full non-linear model.

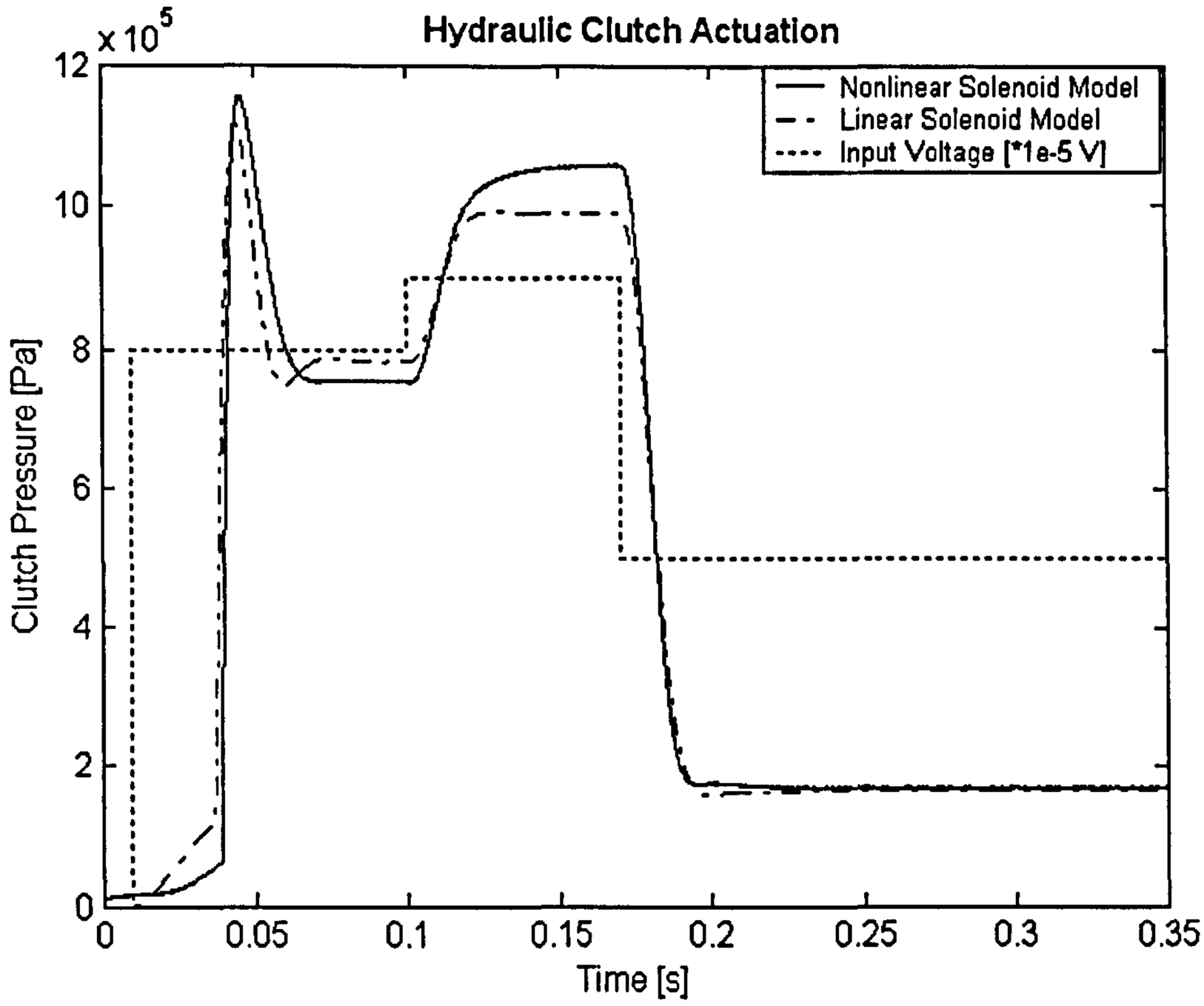

Figure 3.26 Comparison of step responses of the phenomenological model of Figure 3.24 and full non-linear model of Figure 3.22

From Figure 3.26 it can be seen that the phenomenological model (denoted as linear solenoid model in Figure 3.26) and the non-linear model (denoted as nonlinear solenoid model) display a similar behaviour by responding with a sharp rise in the pressure due to the initial step in the input voltage and associated impact of the clutch piston upon the clutch pack. The simplified model also agreed well with the non-linear model when the input voltage was decreased instantly in that both produced a sharp drop in pressure until the piston was moved away from the clutch pack (step from 9 to 2 volts). The differences in the steady state pressure levels that can be observed in Figure 3.26 come from the difference in linearity depicted in Figure 3.25.

Model of Clutch Piston Dynamics and Clutch Pack

At the piston of the hydraulic cylinder (actuator) the hydraulic pressure to actuate and control the clutch/synchroniser is converted to a mechanical force. The stroke of the piston consists of two phases. During the first phase the return spring is compressed until the piston comes in contact with the clutch pack. In this phase the force developed by the hydraulic pressure acts against the force of the return spring, a damping force and the inertial force at the piston. The second phase is entered when the piston has come in contact with the clutch pack and starts to

build up a clamp force by compressing the clutch pack. The piston is in an equilibrium position when the hydraulic pressure holds balance with the combined forces of the stiffnesses of the clutch pack and the return spring. This second phase of the piston motion can be modelled by introducing a second stiffness that accounts for the compliance of the clutch pack. Only in this second phase a clamp force is generated at the clutch plates.

The equation of motion for the piston reads as follows:

$$m_p \ddot{x}_p + c_p \dot{x}_p + k_{R+CP} x_p = p_C A_p \tag{39}$$

$$\begin{aligned} k_{R+CP} &= k_R x_p & 0 \le x_p < x_{pstroke} \\ k_{R+CP} &= k_{CP}(x_p - x_{pstroke}) + k_R x_p & x_{pstroke} \le x_p \end{aligned} \tag{40}$$

The function of this combined stiffness at the clutch is depicted in Figure 3.27.

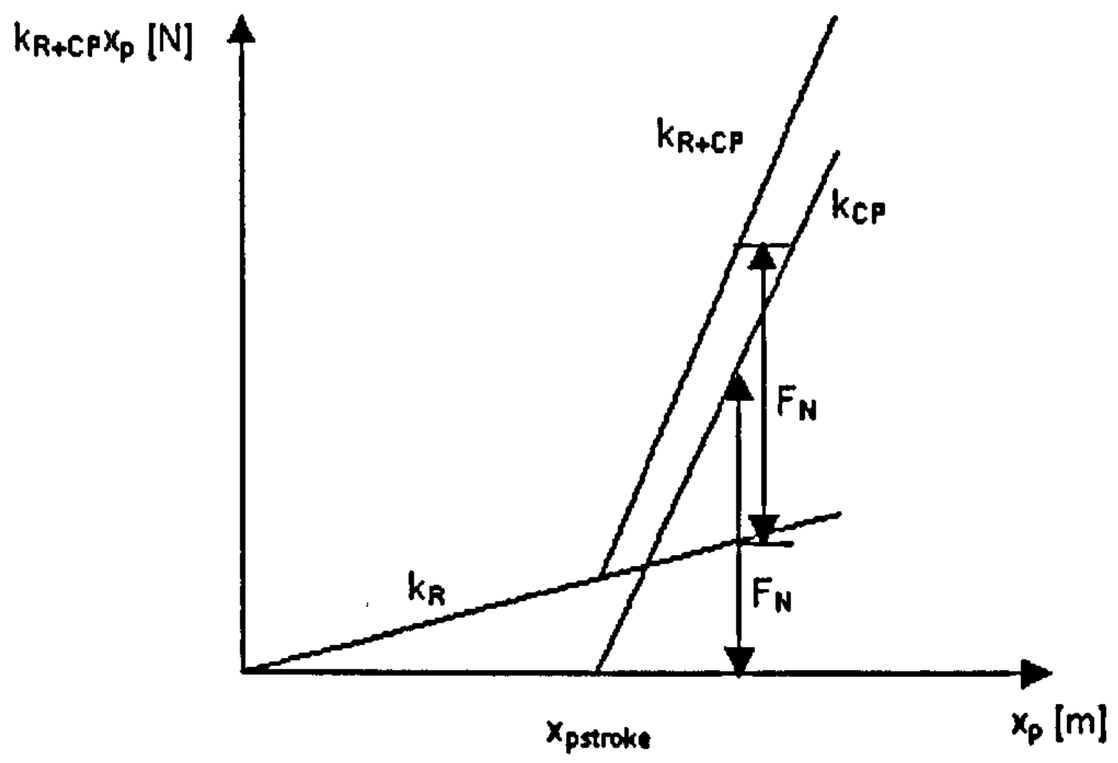

Figure 3.27 Function of combined stiffness of return spring and clutch pack

As can also be seen from Figure 3.27 the clamp force builds up as soon as the piston has come in contact with the clutch plates and starts to compress the clutch pack.

The clamp force at the clutch can be obtained from following relationship:

$$\begin{aligned} F_N &= 0 & 0 \le x_p < x_{pstroke} \\ F_N &= k_{CP}(x_p - x_{pstroke}) & x_{pstroke} \le x_p \end{aligned} \tag{41}$$

3.4 Model of Differential, Driveshafts, Tyres and Vehicle Dynamics

The remainder of the drivetrain is responsible for transmitting the transmission output torque to the wheels, which in turn deliver a drive torque through the tyres to the ground.

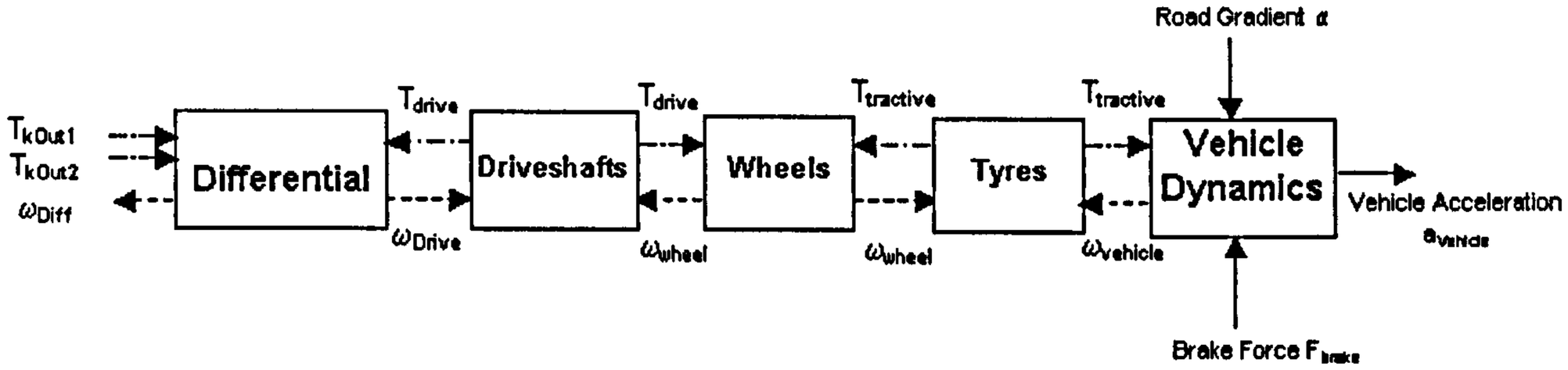

Figure 3.28 Powertrain model modules from differential to tyres

At the road the drive torque at the wheels is converted to a tractive force at the tyres, which has to be in balance with the road loads and vehicle inertial forces. Each block in Figure 3.28 contains the equations of motion of each of the drivetrain components from the transmission output downwards to the tyres. Figure 3.29 depicts the torque balance at these drivetrain components.

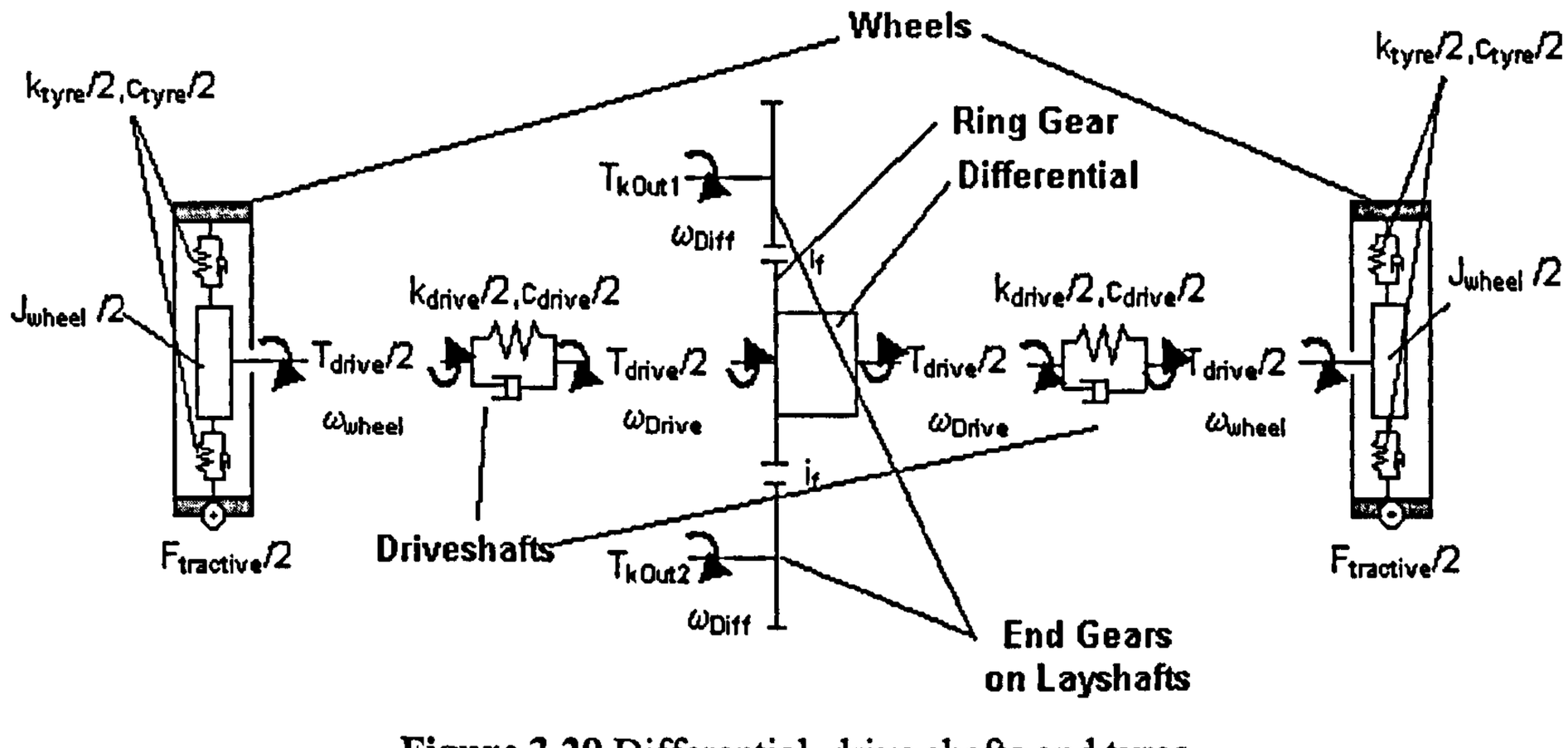

Figure 3.29 Differential, drive shafts and tyres

Because of the fact that the differential is located at the output of the transmission (front wheel drive), the two gear wheels at the end of each of the two layshafts in the transmission (denoted as "end gears on layshafts" in Figure 3.29) belong to the final drive unit and mesh with the ring

gear (see Figure 3.29) of the differential. At the ring gear the torque of both layshafts (transmission halves) is gathered and inputted to the differential. As can be seen in Figure 3.29, the torque at the ring gear of the differential is distributed to the left and to the right drive shaft (axle or halfshafts) by means of the differential. The torque at the driveshafts is transmitted further to the wheels and to the tyres. The driveshafts and the tyres are considered as compliances in the drive train model.

In this work, a symmetric layout of the drivetrain is assumed, i.e. the properties of the drive shafts and wheels (tyres) are assumed to be similar at both the left and the right hand side. Furthermore, it is assumed that the differential distributes the drive torque equally to both sides and that no cornering takes place. Tyre slip is also not considered (pure rolling assumed); therefore the whole drive torque can be delivered equally through both drive wheels to the road. These assumptions are justified from a powertrain controller development point of view, where a difference in wheel torque between the left and the right side is of no interest.

3.4.1 Differential, Driveshafts and Tyres

<u>Differential</u>

Examining Figure 3.29, it can be seen that the gear wheels at the end of the two layshafts (end gears at layshaft 1 and 2 in Figure 3.29) mesh with the ring gear of the differential, both with the same gear ratio (final drive gear ratio i_f in Figure 3.29). The total torque at the input of the differential is therefore the sum of the torque values from layshaft 1 and 2, multiplied by the final gear ratio.

The torque at the two outputs (left and right driveshaft) of the differential amounts to half the value of the torque at the input of the differential (see also Figure 3.29), since an equal torque distribution to either side is assumed (no self locking or other asymmetric torque distribution is allowed). Due to the symmetric layout (symmetric torque distribution and angular speeds) assumed for the drivetrain, the components on both sides can be lumped together. As a consequence the differential has only one output in the model, which produces the torque sum of both sides (T_{drive} in Figure 3.30). It is assumed that all internal components of the differential (ring gear, side gears and shafts, pinions and differential housing) rotate with the same angular speed (no cornering and no tyre slip); therefore the inertia of the differential is simply the sum of all the inertia of these internal components.

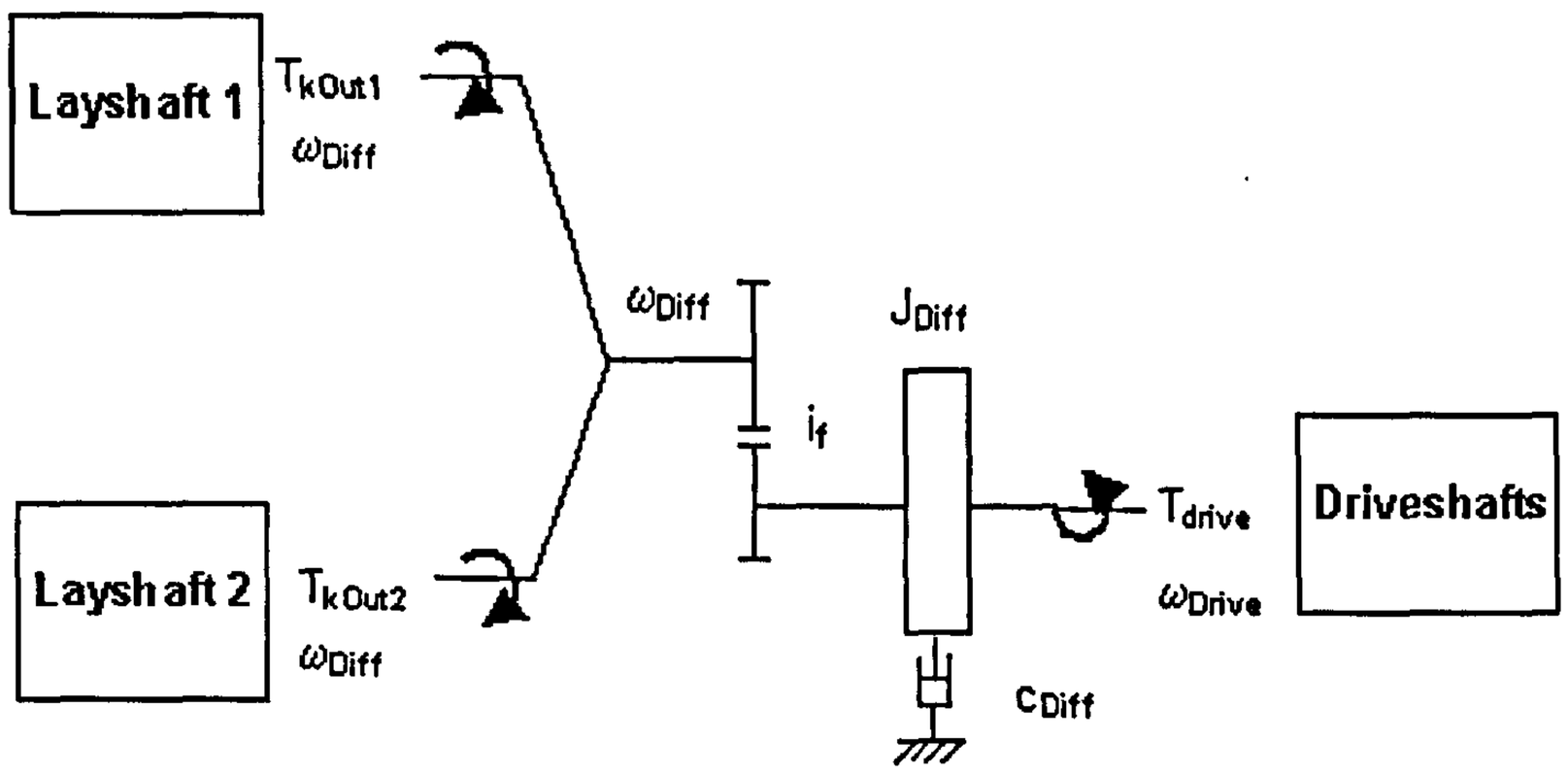

Figure 3.30 Torque balance and angular speeds at the differential

With these observations and together with Figure 3.29, a free-body diagram of the differential assembly can be derived. This free-body diagram is depicted in Figure 3.30 and application of Newton's Second Law yields the equation of motion for the differential:

$$J_{Diff}\dot{\omega}_{Drive} = (T_{kOut1} + T_{kOut2})i_f\eta_{Diff} - T_{drive} - c_{Diff}\omega_{Drive} \tag{42}$$

with:

$$i_f = \frac{\omega_{Diff}}{\omega_{Drive}} \tag{43}$$

Drive Shafts and Tyres

Because of the assumption of a symmetric drivetrain, the two drive shafts can be lumped together into a single drive shaft block, which comprises the sum of the stiffness and damping values of both sides. This can be viewed as two spring-damper elements (for each side) in parallel, having the same boundary. This simplification is valid as long as the wheels at the left and right hand side have equal inertias and rotate with equal angular speeds. Again, the mass of both wheels is lumped into one inertia disk, containing the mass contribution of wheels and tyres.

A spring-damper representation was selected to model the torsional compliance of the tyre. The tyre model basically has the characteristic of a so called "rigid ring model" [Zegelaar and Pacejka 1997 and Bruni et al 1997] where the tyre tread band is modelled as a rigid ring and the compliances of the tyre sidewalls are represented by spring-damper elements that are coupled to the rims.

The tyre stiffness and damping rate are assumed to be linear functions of the relative angular displacement (relative angular speed) between rim and tyre tread band.

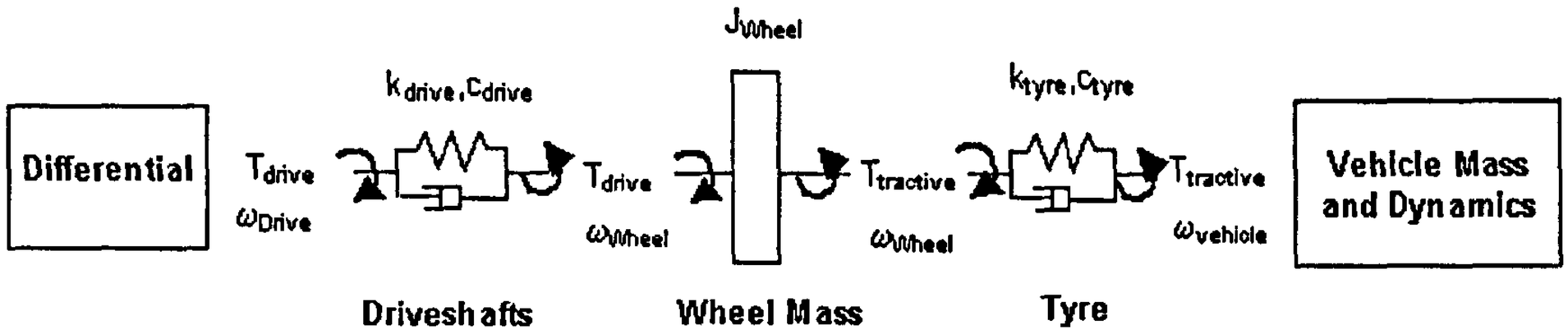

Figure 3.31 Free-body diagram of the lumped driveshaft/wheel/tyre assembly

Equipped with these considerations and Figure 3.29, a free-body diagram of the lumped driveshaft/wheel/tyre assembly can be derived, which is depicted in Figure 3.31. Applying Newton's Second law to this free-body diagram yields the equations of motion for the lumped driveshaft/wheel/tyre assembly (Equation (44) to (48)).

$$T_{drive} = k_{drive}(\varphi_{Drive} - \varphi_{Wheel}) + c_{drive}(\omega_{Drive} - \omega_{Wheel}) \tag{44}$$

$$J_{Wheel}\dot{\omega}_{Wheel} = T_{drive} - T_{tractive} \tag{45}$$

$$T_{tractive} = k_{tyre}(\varphi_{Wheel} - \varphi_{vehicle}) + c_{tyre}(\omega_{Wheel} - \omega_{vehice}) \tag{46}$$

with:

$$T_{tractive} = F_{tractive} r_{tyre} \tag{47}$$

$$\omega_{vehicle} = \frac{v_{vehicle}}{r_{tyre}} \tag{48}$$

3.4.2 Vehicle Dynamics

The vehicle dynamics block depicted in Figure 3.28 is shown again in Figure 3.32. It accepts as input variables the tractive torque (force) that is developed at the drive wheels, a brake force and the angle of the road gradient. At the output, the vehicle dynamics block produces the vehicle acceleration and vehicle speed.

A more detailed analysis of all the forces acting on the vehicle shows that not only the road gradient creates a load force but also the aerodynamic drag and the rolling resistance at the

wheels contribute to the load forces. All these load forces are summed up under the term "road loads" and are depicted in Figure 3.33, which shows a free-body diagram of a vehicle.

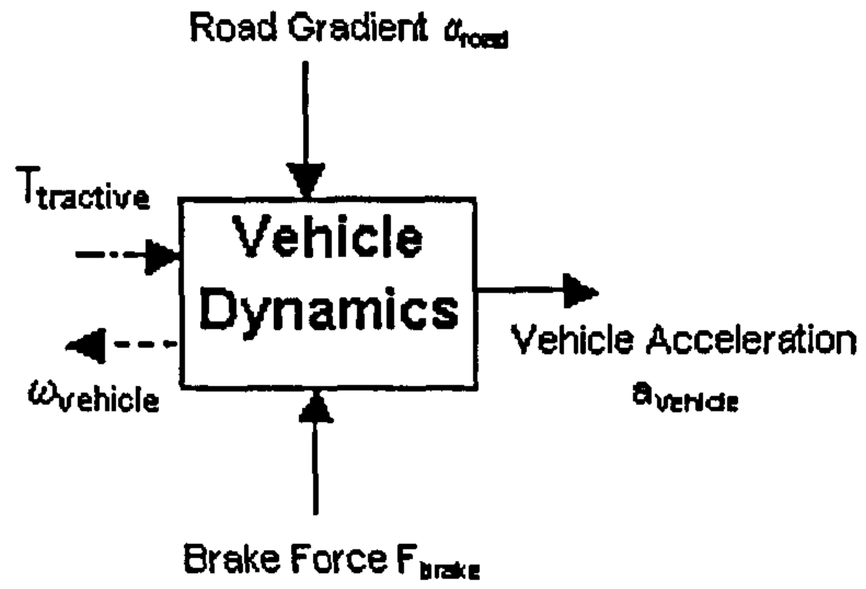

Figure 3.32 Vehicle dynamics block from Figure 3.28

Applying Newton's Law to the free-body diagram of the vehicle from Figure 3.33 provides the equation of motion of the vehicle in the longitudinal direction (see also for example [Gillespie 1992 and Mitschke 1972]).

$$M_{vehicle,total}\, a_{vehicle} = F_{Xf} + F_{Xr} - F_{Rf} - F_{Rr} - m_{vehicle}\, g \sin\alpha_{road} - F_A \tag{49}$$

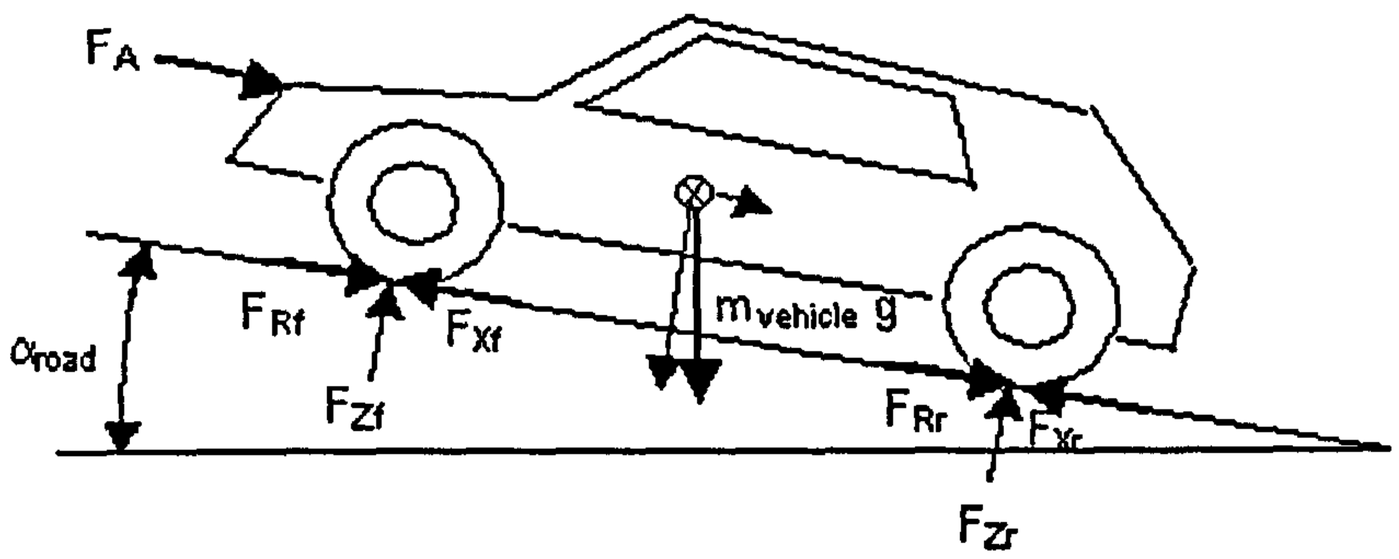

Figure 3.33 Forces acting on the vehicle

The total vehicle mass consists of the vehicle mass and the equivalent mass of all rotating parts that are not considered in the drivetrain dynamics and hence are not included in the tractive force generated at the wheels by the powertrain:

$$M_{vehicle,total} = m_{vehicle} + \frac{J_{rot,non-driven}}{r_{tyre}^2} \tag{50}$$

The sum of the tractive forces at the front and at the rear wheel can be stated immediately, considering that the vehicle is a front wheel drive:

$$F_{Xf} = F_{tractive} - F_{brake,f} \tag{51}$$

$$F_{Xr} = -F_{brake,r} \tag{52}$$

The rolling resistance at the front and at the rear wheels can be summed up into a total rolling resistance depending on the normal component of the vehicle weight, on the aerodynamic lift force (neglected here) and on the rolling resistance coefficient.

$$F_R = F_{Rf} + F_{Rr} = f_R(m_{vehicle} g \cos\alpha_{road} - F_{lift}) \approx f_R m_{vehicle} g \tag{53}$$

The Aerodynamic drag force acting on the vehicle depends on the shape of the vehicle body, its frontal area and the relative velocity between the vehicle and the surrounding air.

$$F_A = \frac{\rho_{air}}{2} c_D A_{front} v_{vehicle}^2 \tag{54}$$

From the standpoint of gearshift analysis, a common simplification when modelling the dynamics of the powertrain is that variations in the dynamic axle loads (F_{Zf} and F_{Zr}) due to an acceleration or deceleration of the vehicle can be neglected. A further simplification, justified from the standpoint of analysing the dynamics of gearshifts, is to assume that the tractive forces produced at the wheels can be transmitted to the road without tyre slip.

Entering equations (50) to (54) into the equation (49) yields the final equation of motion for the vehicle:

$$\left(m_{vehicle} + \frac{J_{rot,non-driven}}{r_{tire}^2}\right) a_{vehicle} = F_{tractive} - F_{brake,f} - F_{brake,r} - f_R m_{vehicle} g - m_{vehicle} g \sin\alpha_{road} - \frac{\rho_{air}}{2} c_D A_{front} v_{vehicle}^2 \tag{55}$$

From this equation the vehicle acceleration and velocity can be determined. The vehicle jerk can be determined directly from the vehicle acceleration by taking the first time derivative.

3.5 The Powertrain Model – A first Simulation Result and Discussion

3.5.1 Simulation of a Clutch-to-Clutch Upshift and Model Validation

As a first simulation result, a power-on upshift from 1st to 2nd gear will be presented. This gearshift is depicted in Figure 3.34 and was executed by a simple clutch-to-clutch gearshift control. The principle of a clutch-to-clutch gearshift was already explained for a power-on upshift in Chapter 2. In Figure 3.34 the two distinctive phases of a clutch-to-clutch shift are indicated: a torque phase, where engine torque is transferred from the offgoing to the oncoming clutch and an inertia phase where the engine is synchronised to the speed level of the target gear.

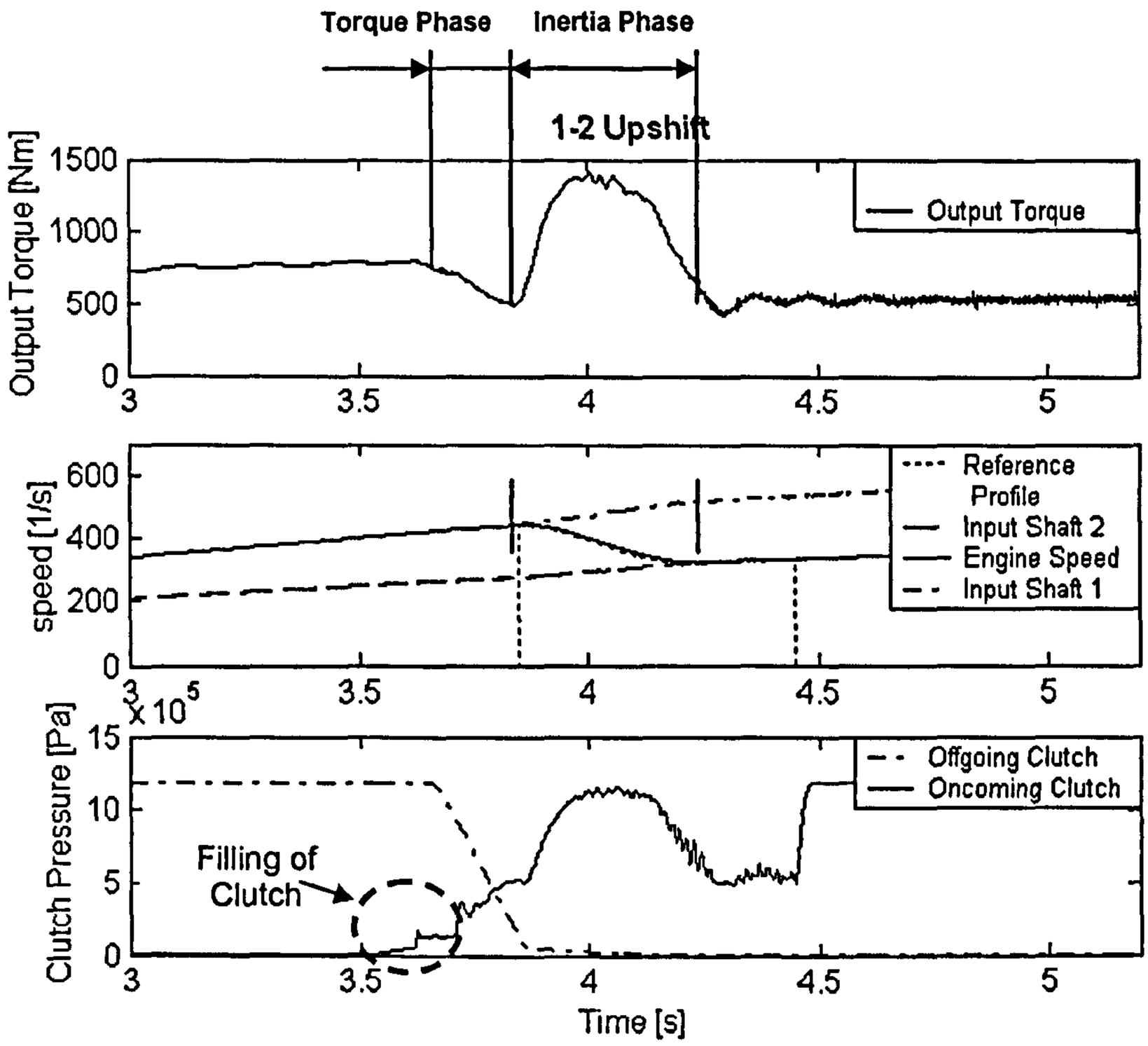

Figure 3.34 Simple clutch-to-clutch upshift from 1st to 2nd gear at 27 km/h (wet-type friction, positive gradient)

To control the gearshift depicted in Figure 3.34 a simple clutch pressure modulation scheme has been adopted, incorporating closed-loop torque control in the torque phase and closed-loop control of the engine speed in the inertia phase. Although closed-loop control was employed, the transmission output torque, clutch and engine speed and pressure trajectories (first second and third graph in Figure 3.34) look in principle similar for an open-loop controlled gearshift. The drop in transmission output torque in the torque phase comes from the change to a higher gear (smaller gear ratio and thus lower torque) and the characteristic "hump" in the torque profile results from inertial torque being transferred to the output during engine deceleration. The filling of the actuator of the oncoming clutch with associated actuation delay and sharp rise in pressure is indicated in Figure 3.34 by a dashed circle.

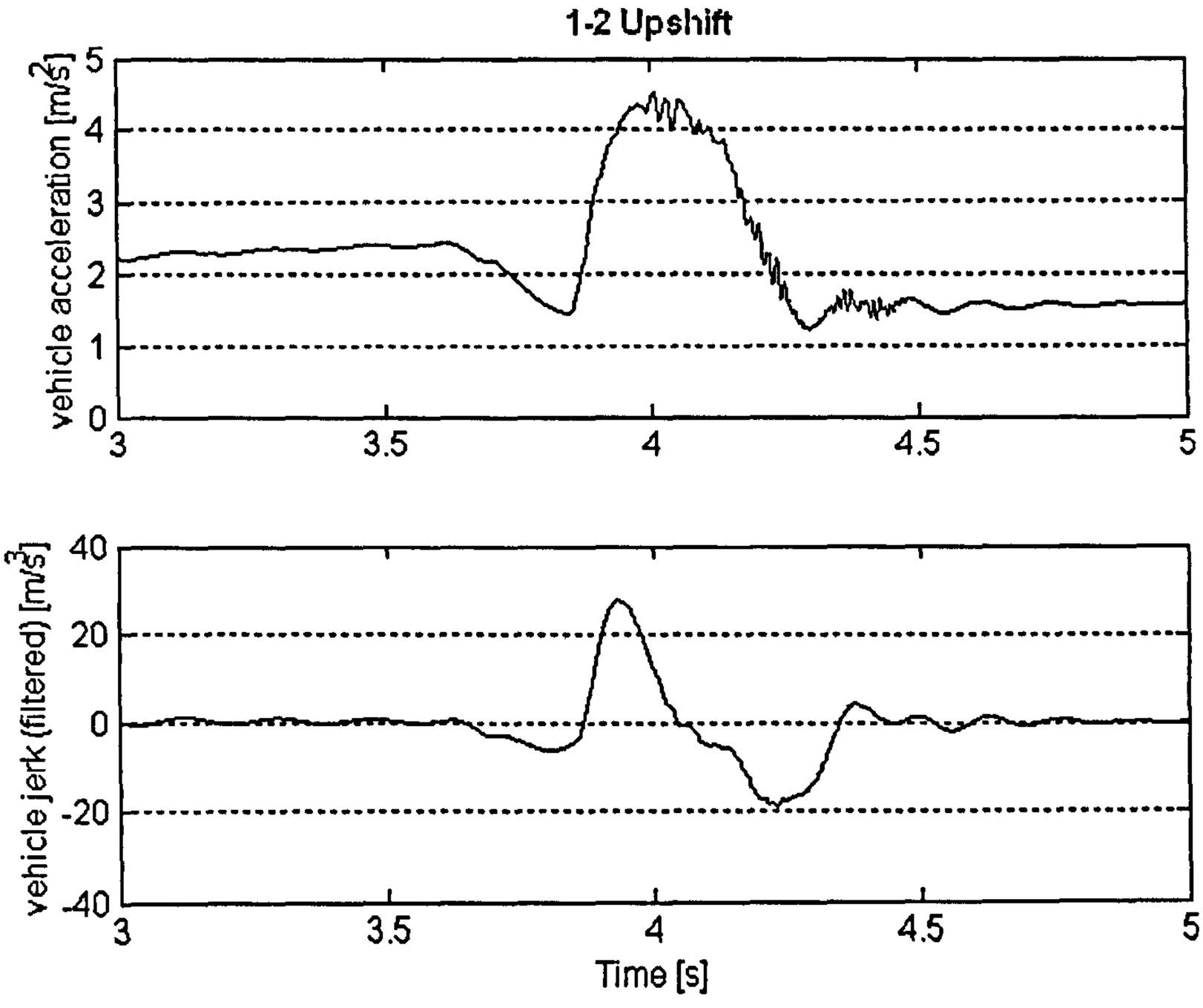

Figure 3.35 Longitudinal vehicle acceleration and jerk of the gearshift depicted in Figure 3.34

As was explained in Chapter 2 for any investigation of gearshift quality, the shape of the vehicle acceleration profile is one of the most important shift quality metrics. In this work the longitudinal vehicle acceleration was filtered by a 2nd order lowpass filter of Butterworth type with a corner frequency of 5Hz and the vehicle jerk (defined as the first time derivative of the vehicle acceleration) was determined from this filtered acceleration signal. Figure 3.35 shows the unfiltered longitudinal acceleration and the filtered vehicle jerk for the gearshift from Figure 3.34. Filtering the acceleration signal is a common technique to extract only those signal parts,

which the driver can actually sense and has also been applied in [Schwab 1994 and Naruse et al 1993]. In the latter paper a range from 0-7 Hz was given for the for-aft vibrations. The longitudinal vehicle acceleration in Figure 3.35 clearly has the same shape as the transmission output torque trajectory depicted in Figure 3.34. This observation demonstrates that the transmission output torque trajectory is directly related to the longitudinal vehicle acceleration and can be thus used for analysing shift quality. The vehicle jerk profile indicates that high jerk levels occur at the beginning and end of the inertia phase and are closely connected to the torque "hump". This problem will be discussed in more detail in Chapter 4.

To validate the powertrain model experimental data for a twin clutch transmission would be required. Since the twin clutch design is still a novelty, such data could not be found in the literature and could also not be obtained from industry. However, since a clutch-to-clutch gearshift on a twin clutch transmission is qualitatively similar to that on a planetary-type transmission, the simulation result depicted in Figure 3.35 can be compared in a qualitative way to experimental data of a clutch-to-clutch upshift on a planetary-type automatic transmission.

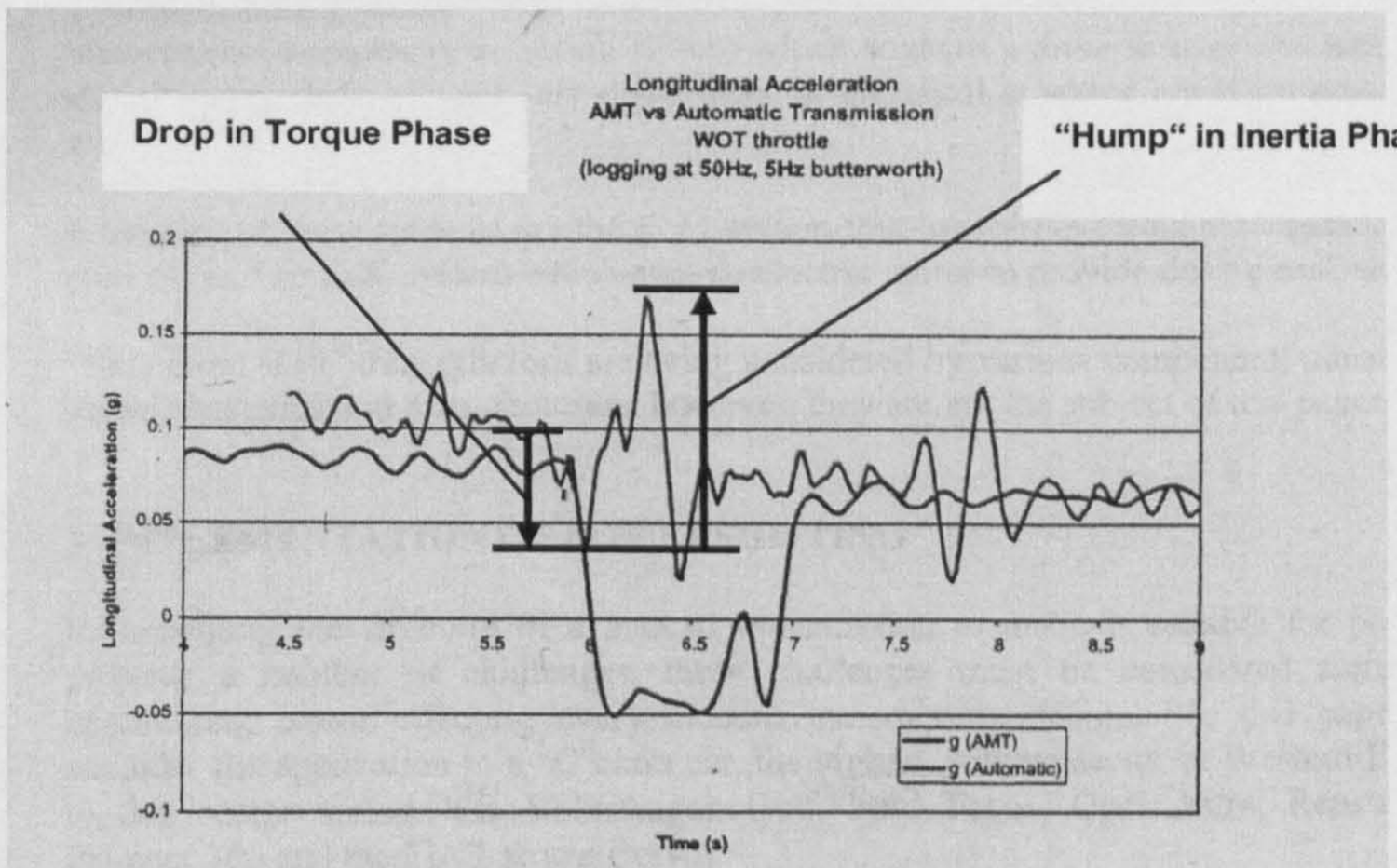

Figure 2 Longitudinal acceleration during upshifts – AMT and automatic

Figure 3.36 Measurement result: longitudinal vehicle acceleration during an upshift compared for a planetary-type automatic transmission (Automatic) and an automated manual transmission (AMT) taken from [O'Neill and Harrison 2000]

Such measurement data is depicted in Figure 3.36 and was taken from [O'Neill and Harrison 2000]. In Figure 3.36, the longitudinal vehicle acceleration profiles (filtered by a 5 Hz Butterworth filter) for upshifts on a planetary-type automatic transmission and on an automated manual transmission are compared. The comparison is of less interest here, but the acceleration

profile of the planetary-type automatic transmission is important. Comparing the simulation result depicted in Figure 3.35 and the measurement result in Figure 3.36, it can be observed that the two graphs look very similar (apart from different time scales). Both results show the typical drop in torque in the torque phase and the torque "hump" in the inertia phase. This was to be expected since the gearshift in Figure 3.36 was produced by a simple clutch-to-clutch shift control that is also common on planetary-type automatic transmissions.

3.5.2 Discussion of Clutch Friction

In this section the problem of clutch friction will be briefly discussed, in particular the differences between wet-type and dry-type friction materials will be explained. The gearshift in Figure 3.34 was simulated using wet-type friction with a positive gradient of the friction coefficient with slip speed (see Figure 3.13 for characteristics of friction materials used here). For a comparison the gearshift illustrated in Figure 3.34 was repeated with a dry-friction material with a negative gradient of the friction coefficient with slip speed (see Figure 3.13 for friction characteristic). The simulation result of this gearshift is depicted in Figure 3.37. Although the number of clutch plates (friction contacts) was reduced for the dry-friction case, in order to account for the different clutch designs in reality, the clutch torque was still considerably greater with dry friction than with wet friction. This lead to a decreased clutch pressure level during the gearshift as indicated by the arrow in Figure 3.37.

It can be observed from the two different simulation results, that the size of the torque-drop in the torque phase and the size of the torque "hump" in the inertia phase did not change when the friction type was varied. This indicates that the type of friction (wet or dry-type friction) does not influence the dynamics of the gearshift but only affects the clutch pressure level. This means that the friction type does not, in principle, influence the gearshift control. The only exemption is given in cases where the clutch temperature rises considerably causing the friction coefficient of dry friction materials to drop significantly. These conditions do not normally occur during gearshifts and only take place during extensive slipping of the clutch (during hill-hold, vehicle launch).

However, what did influence the dynamics of the gearshift was the gradient of the friction coefficient with slip speed (positive versus negative). The effect of the negative gradient on the gearshift can be seen at the end of the shift in Figure 3.37. Comparing Figure 3.34 and Figure 3.37, shows that the friction material with a negative gradient produced strong torque vibrations

(dashed circle in Figure 3.37) at the end of the inertia phase. The reason for this is, that the friction torque increases due to a decrease in the relative speed across the clutch in the inertia phase. This effect is due to the negative gradient of the friction material and is to some extent concealed underneath the torque "hump". This problem will be analysed in detail in Chapter 4 for wet type friction.

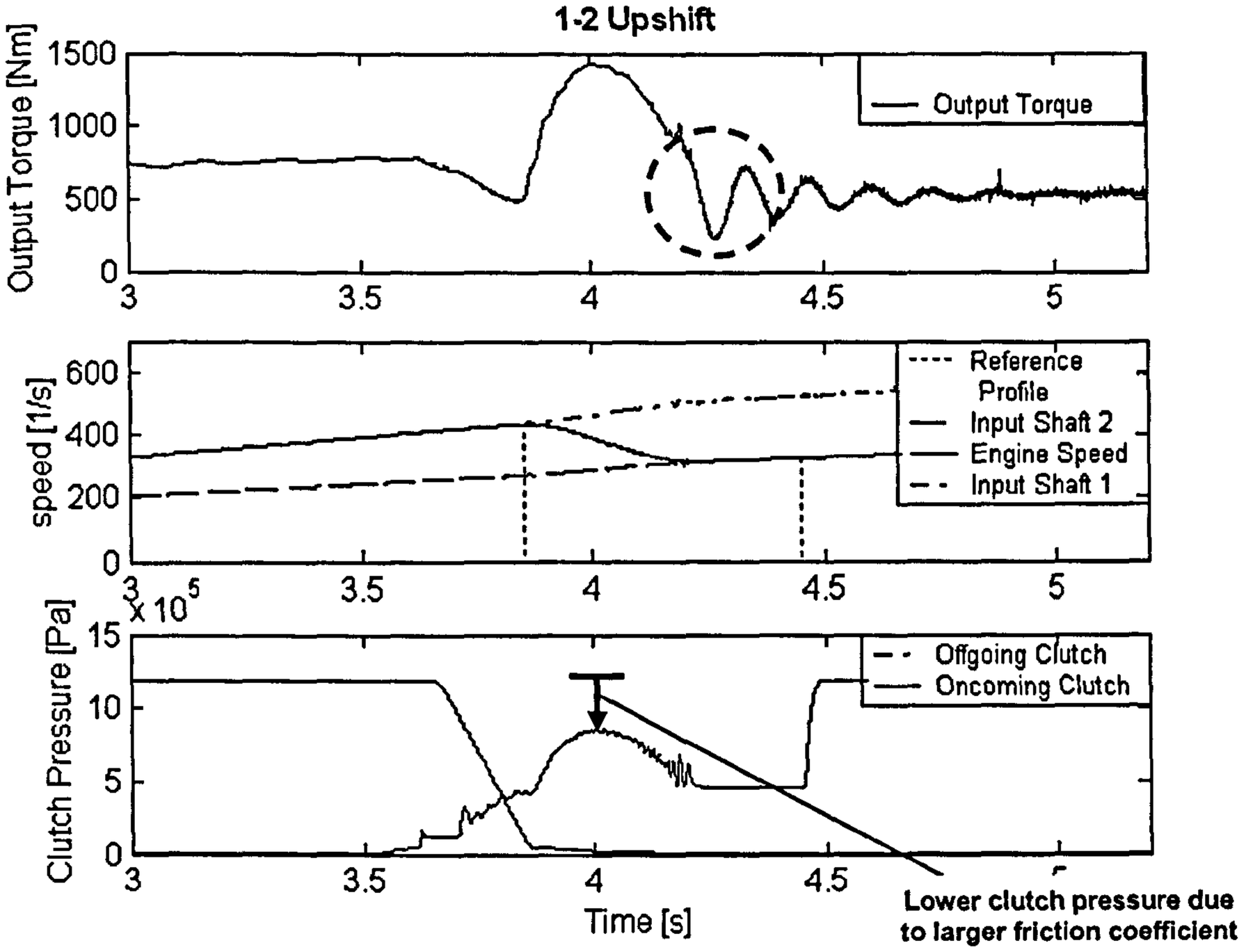

Figure 3.37 Gearshift from Figure 3.34 for dry-type friction with negative gradient

3.6 Conclusions

The engine model explained in this chapter was taken from the literature. For this model engine maps were derived by means of a simple "virtual" engine test bed specially developed for this application.

The model of the twin clutch transmission allowed, as a novelty, modelling of different friction characteristics by including a friction coefficient as a function of the differential speed across the clutch. The internals of the twin clutch transmission were modelled in more detail (stiffness, damping, friction models etc.) than existing models used for controller development.

An extended model of the twin clutch transmission included an additional synchroniser model and thus allowed for the first time simulation of synchroniser-to-synchroniser shifts.

The hydraulic actuation of clutches and synchroniser was first modelled as a comprehensive non-linear model. In a second step a novel simplified; phenomenological model of the hydraulic actuation was derived from the full non-linear model.

At the end of the chapter an important result on friction materials was discovered:

- The type of friction material (wet versus dry-type) at the clutch did not influence the dynamics of the gearshift and only affected the level of clutch pressure. Hence, the type of friction does not have to be taken into account when designing the gearshift controller.
- However, the gradient of the friction coefficient with slip speed did influence the dynamics of the gearshift (different clutch torque trajectory). Thus, the gradient of the friction coefficient has to be taken into account when designing a gearshift controller.

Chapter 4

Gearshift Controller for Twin Clutch Transmissions

Chapter 3 has given an extensive description of the powertrain model and ended with a first simulation result for a conventional gearshift control strategy as used on planetary-type transmissions.

This chapter starts with a brief introduction to the control of powershifts (Section 4.1), which explains how upshifts and downshifts are controlled conventionally on planetary-type transmissions.

In the two subsequent sections the basic version of a new gearshift control strategy for twin clutch transmissions is developed in detail firstly, for power-on shifts (Section 4.2) as the more important case and then secondly, for power-off shifts (Section 4.3).

The sections on power-on and power off shifts are each split into two subsections describing the new control strategies first for upshifts (Sections 4.2.1 and 4.3.1) and then for downshifts (Sections 4.2.2 and 4.3.2). The two subsections on power-on upshifts and downshifts (Sections 4.2.1 and 4.2.2), both start with a discussion of the shortcomings of conventional gearshift control strategies used on planetary-type transmissions. This is then followed by an explanation of the proposed novel control strategy and a demonstration of how it can deal with the shortcomings of the conventional control strategy.

Section 4.4 describes in detail the layout of the gearshift controller and the control loops used by that controller. This is followed by an investigation into the robustness of the proposed control strategy of in Section 4.5. Section 4.6 summarises the findings of this chapter

4.1 Introduction to Powershifts and Conventional Clutch-to-Clutch Control Strategy

The key feature of a twin clutch transmission (and also of a conventional planetary-type automatic transmission) is the "powershift". The essence of a powershift is the uninterrupted transfer of power from the engine to the wheels during a gearshift. In comparison, on manual and automated manual transmissions the dry clutch has to be disengaged during a gearshift (engagement of synchronisers requires the transmission to be torque-free) and therefore torque is no longer transmitted to the wheels.

On conventional planetary-type transmissions and twin clutch transmissions, a powershift can, in principle, be carried out as a clutch-to-clutch shift, i.e. shifting from a clutch carrying the currently engaged gear to a clutch carrying the target gear, without disconnecting the engine from the wheels. However, differences in the mechanical layout of the two transmission types, as pointed out in Chapter 2, require slightly different approaches to the control of clutch-to-clutch shifts. Also, on twin clutch transmissions a pre-selection of the target gear on the torque-free half of the transmissions needs to be accomplished in addition to the clutch-to-clutch shift.

To summarise, a gearshift on a twin clutch transmission consists of two major tasks:

- The pre-selection of a new target gear on the torque-free half of the transmission
- The clutch-to-clutch shift, where the clutch carrying the initial gear is disengaged and the clutch carrying the target gear is engaged.

As reviewed in Chapter 2, it is common to separate these two tasks. The order of execution of these two tasks depends on the gear pre-selection strategy. The procedure of pre-selecting the target gear, its consequences and possible control concepts are discussed separately in Chapter 7. The current chapter only deals with the dynamics and control of clutch-to-clutch shifts on twin clutch transmissions.

Before explaining the fundamentals of clutch-to-clutch shifts it is important to note that it has to be distinguished between power-on and power-off clutch-to-clutch shifts.

- Power-on gearshift: Gearshift takes place whilst the engine drives the wheels (engine produces positive torque)
- Power-off gearshift: Gearshift takes place whilst the wheels drive the engine (engine produces brake torque when vehicle is coasting)

In the following explanation of powershifts, the principle of the power-on upshift is discussed prior to that of the power-on downshift. In these explanations it is assumed that the clutch-to-clutch shift is controlled through clutch torque manipulation alone, as would be the case in a conventional control strategy commonly found on production planetary-type automatic transmissions, which is also applicable, in principle, to twin clutch transmissions.

Conventional Clutch-to-Clutch Power-On Upshift (Figure 4.1):

At the beginning of a power-on clutch-to-clutch upshift, a transfer of engine torque from the offgoing (clutch 1 in Figure 4.1) to the oncoming clutch (clutch 2 in Figure 4.1) carrying the target gear (i.e. a gear higher than the original one) takes place in a so called "torque phase".

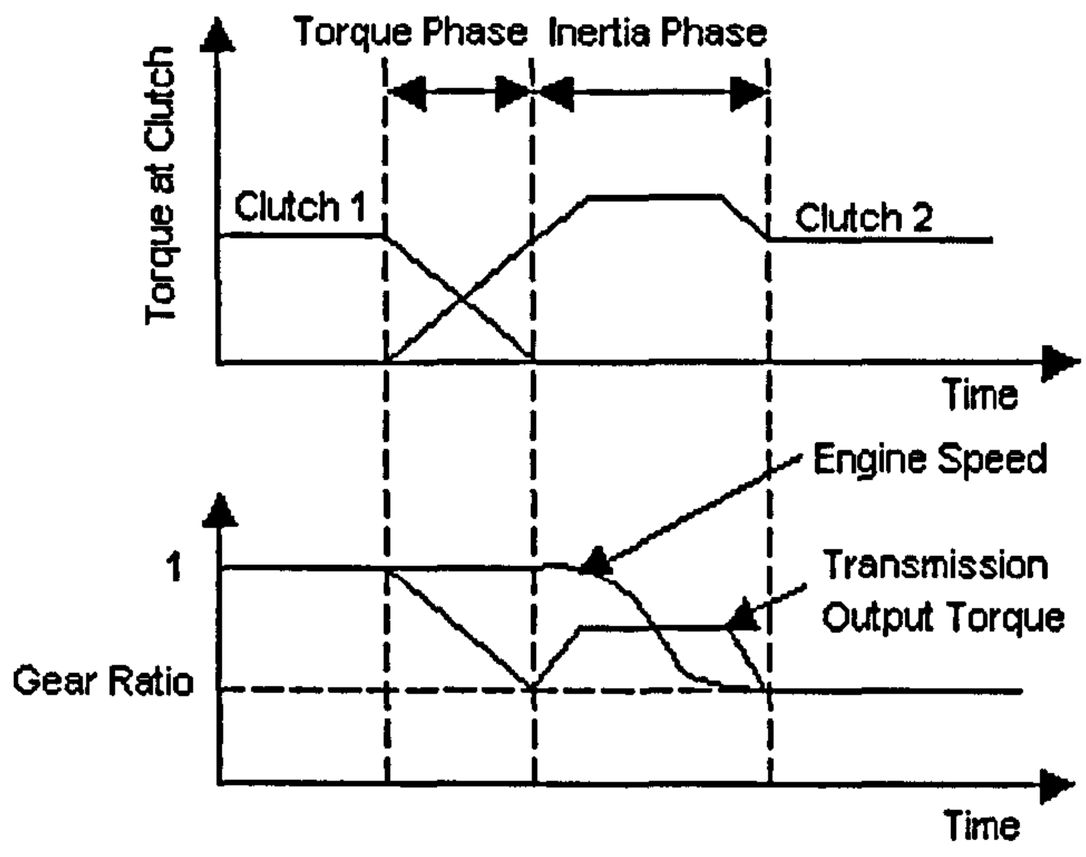

Figure 4.1 Principle of a conventional clutch-to-clutch power-on upshift

This transfer of engine torque between the two clutches results in a drop in the transmission output torque according to the change in gear ratio (transmission output torque profile in lower graph in Figure 4.1). In the following "inertia phase" the engine is synchronised (i.e. decelerated) to the speed level of the new target gear. The deceleration of the engine (engine speed in lower graph of Figure 4.1) can be accomplished through an increase in torque at the oncoming clutch (clutch 2 in Figure 4.1) beyond the level necessary for transmitting the engine torque. The deceleration of the engine inertia transfers torque to the transmission output and results to a "hump" in the transmission output torque profile. This torque "hump" is also responsible for increased vehicle jerk at the transition between torque and inertia phase.

Conventional Clutch-to-Clutch Power-On Downshift (Figure 4.2):

On a power on downshift the order of torque and inertia phase is reversed. Starting with the inertia phase where the engine (engine speed in lower graph of Figure 4.2) is allowed to speed up in order to match that of the target gear. The acceleration of the engine can be accomplished

by decreasing the transmitted torque at the offgoing clutch (clutch 2 in Figure 4.2) in the inertia phase. By decreasing the amount of transmitted engine torque at the (slipping) offgoing clutch, the engine is released and can use the amount of engine torque that is not transmitted through the clutch to accelerate itself. However, the decrease in transmitted engine torque at the offgoing clutch also means a decrease in transmission output torque (see lower graph in Figure 4.2). To end the inertia phase and to stop the engine from continuing its acceleration, the torque at the offgoing clutch has to be increased to its original level again. Now, the torque phase can begin where engine torque is transferred from the offgoing clutch to the oncoming clutch (clutch 1 in Figure 4.2). Due to the larger gear ratio of the lower target gear the output torque has to rise to a level above the level at the beginning of the clutch-to-clutch downshift.

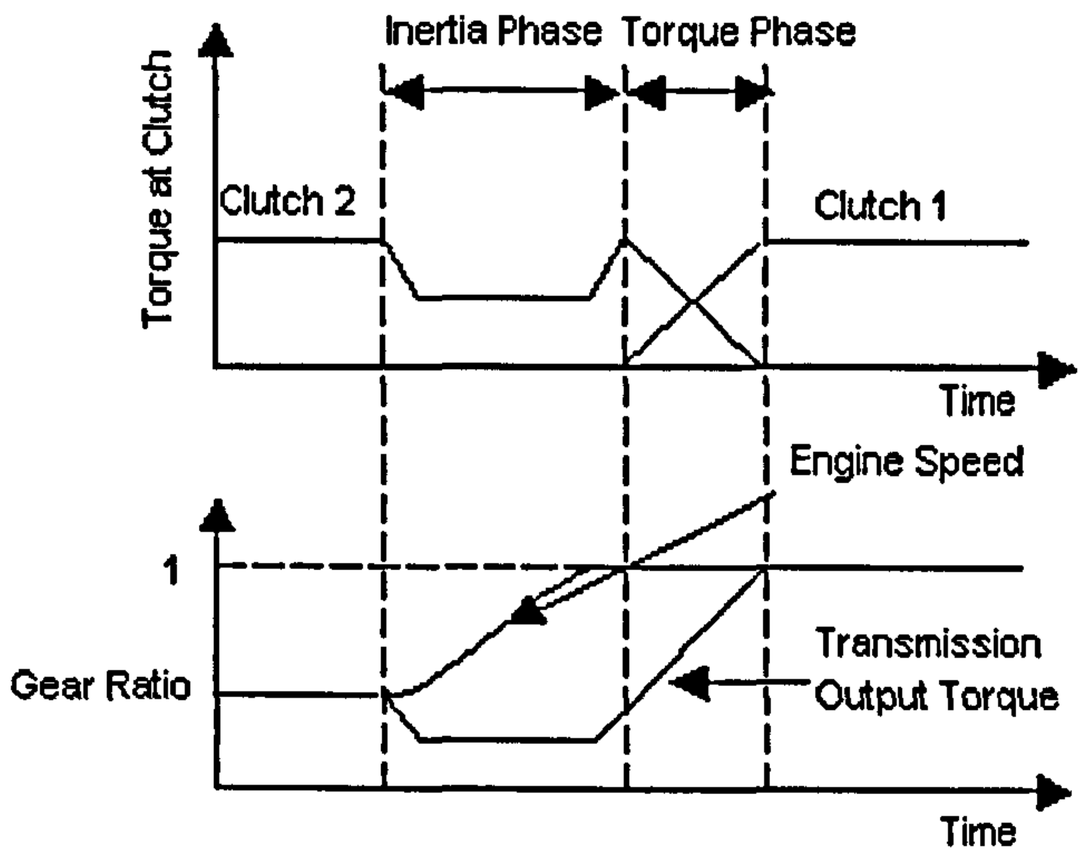

Figure 4.2 Principle of a conventional clutch-to-clutch power-on downshift

Clutch-to-Clutch Power-Off Shifts (Table 4.1):

Table 4.1 gives an overview of clutch-to-clutch shift possibilities and indicates the order of torque and inertia phase. As could be seen in the previous discussion of power-on clutch-to-clutch shifts, the inertia phase involves either a decrease in torque at the offgoing clutch or an increase in the torque at the oncoming clutch. For the simple case of a clutch-to-clutch shift involving only a manipulation of clutch torque (i.e. clutch actuation pressure), the information whether the inertia phase involves a decrease or increase in clutch torque is also included in parentheses in Table 4.1.

From Table 4.1 it can be seen that a clutch-to-clutch power-off upshift can be controlled in a similar way as a power-on downshift. The same applies to a clutch-to-clutch power-off downshift, which can be executed similar to a power-on upshift [Förster 1991, Wagner 1994]. Due to the small clutch torque (engine brake torque) involved and because of the fact that

length of time of the shift is not critical in the power-off case, the control of clutch-to-clutch power-off upshifts is not as crucial to shift quality as is that of power-on upshifts [Förster 1994].

	Upshift	**Downshift**
Power-On	1. Torque Phase 2. Inertia Phase (increase in clutch torque)	1. Inertia Phase (decrease in clutch torque 2. Torque Phase
Power-Off	1. Inertia Phase (decrease in clutch torque) 2. Torque Phase	1. Torque Phase 2. Inertia Phase (increase in clutch torque)

Table 4.1 Order of torque and inertia phase for power-on and power-off clutch-to-clutch shifts

Clutch-to-clutch power-off downshifts, often occur under braking or coasting to standstill of a vehicle and thus take place at low vehicle speeds and are hence also seldom problematic. However, the time for power-off downshifts under heavy braking can be very short, which can result in increased vehicle deceleration in the inertia phase. Since the driver deliberately executes a braking of the vehicle, the power-off downshift does not affect the shift feel as much as a power-on downshift, where the driver often does not expect a shift. Furthermore, in case of heavy vehicle braking, a power-off downshift does not need to be executed at all as long as the oncoming clutch is always ready to start a downshift once the vehicle is accelerated again. This last comment shows that the discussion of power-off downshifts is also strongly connected to the shift strategy selected for such special shift case.

Due to the greater importance with regard to shift quality, the main part of this chapter is devoted to the control of clutch-to-clutch power-on shifts on twin clutch transmissions. However, Chapter 4 ends with a brief discussion of power-off shifts. All simulation results shown in Chapter 4 and 5 make use of the basic model of the twin clutch transmission developed in Chapter 3.

4.2 Control of Power-On Shifts on Twin Clutch Transmissions

4.2.1 Control of Power-On Upshifts

Problems of Conventional Clutch-to-Clutch Upshift Control Strategies

Conventional clutch-to-clutch upshift control strategies through manipulation of clutch torque (i.e. actuation pressure) as described in the previous section (Figure 4.1) show two key control problems, which are detrimental to shift quality.

Control problems:

1. "Torque Hump": The increase in torque (pressure) at the oncoming clutch in the inertia phase required to decelerate and thus synchronise the engine, leads to a "hump" in the output torque. This "torque hump" produces increased vehicle jerk at the point of transition between torque and inertia phase and at the end of the inertia phase (see Figure 4.4). The hump in the output torque results from inertial torque being released during the deceleration of the engine and being then transferred to the transmission output. The "torque hump" also results in increased energy dissipation and hence clutch wear at the oncoming clutch.
2. "Negative Torque": An incorrect (early) application of the oncoming clutch in the torque phase can create a negative torque at the offgoing clutch which, when released at the beginning of the inertia phase results to a sharp rise in transmission output torque and thus vehicle jerk. A late application of the oncoming clutch has to be avoided at all cost as it would result into a sharp drop in output torque that could, in the worst case lead to a momentarily loss in traction.

The second problem is directly connected to clutch-to-clutch shifts on twin clutch transmissions, whilst the first problem also applies to clutch-to-clutch shifts on planetary-type transmissions. To demonstrate the two control problems, a power-on upshift from 1^{st} to 2^{nd} gear was simulated using a conventional clutch-to-clutch control similar to that discussed in Figure 4.1, where the control of the engine synchronisation in the inertia phase was managed by a closed-loop control manipulating hydraulic pressure at the oncoming clutch (the reference trajectory and the controller-type are described in Section 4.4). A simulation result of this upshift is depicted in Figure 4.3 (torque and inertia phase are indicated in the graph). The uppermost graph in Figure 4.3 depicts the transmission output torque profile, the second graph shows the engine speed (input speed in Figure 4.3) and the speeds of the input shafts connected to the outputs of

oncoming and offgoing clutch, whilst the third graph depicts the actuation pressure profiles at oncoming and offgoing clutch. The graph at the bottom of Figure 4.3 shows throttle angle and spark advance, which were both kept at a constant level during the gearshift.

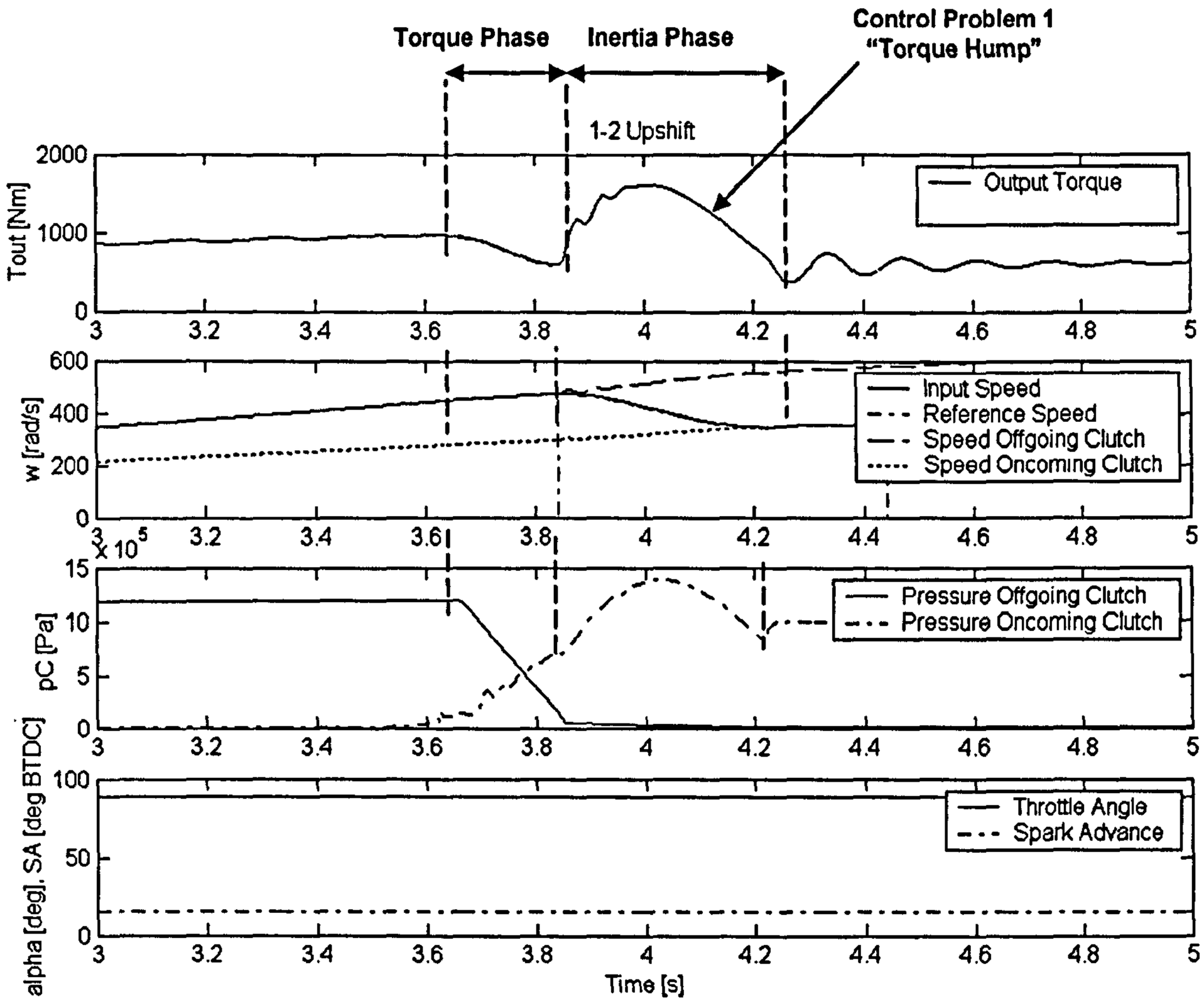

Figure 4.3 Simulation result: Upshift from 1st to 2nd gear with conventional clutch-to-clutch control strategy showing control problem 1,"torque hump"

Control Problem 1: As discussed above, controlling the engine synchronisation by manipulation of clutch torque leads to a "hump" in the transmission output torque profile as indicated in Figure 4.3. The effect of the torque "hump" on the longitudinal vehicle jerk can be seen in Figure 4.4, which reveals that the vehicle jerk (lower graph) reaches values of around 30 m/s^3 at the beginning of the inertia phase (at around 3.9 seconds) and around -20 m/s^3 at the end of the inertia phase (at around 4.25 seconds).

Decreasing the rate of engine deceleration in the inertia phase reduces the level of both vehicle jerk peaks but, increases the slipping time at the offgoing clutch and thus leads to higher energy dissipation. However, an increase in slipping time and thus total shift time might not be acceptable. This dilemma remains a huge disadvantage of conventional clutch-to-clutch control

strategies for power-on upshifts. In particular, the additional change in the sign of the vehicle jerk poses a serious problem for shift quality.

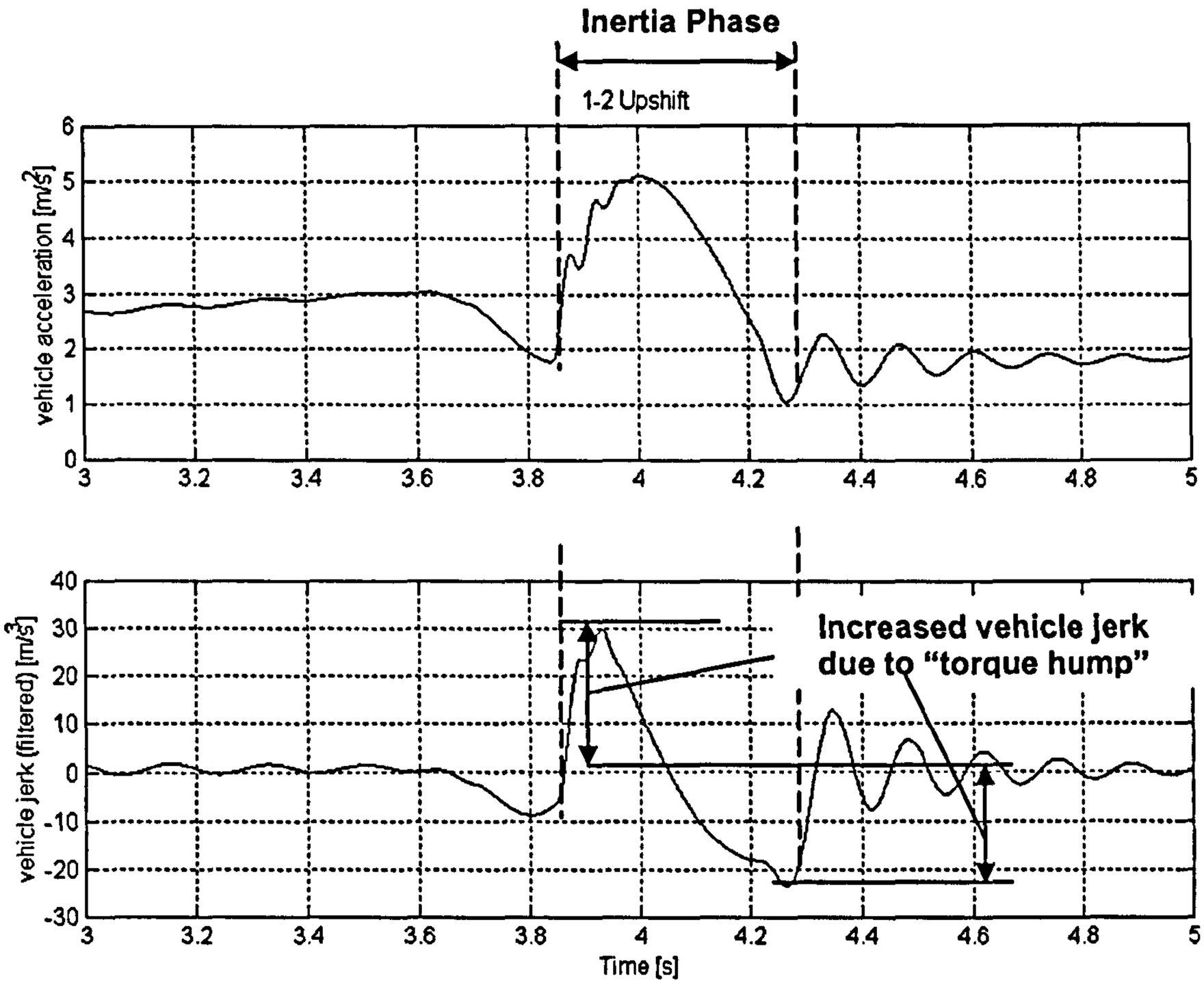

Figure 4.4 Vehicle acceleration and jerk for the upshift from Figure 4.3 (Control Problem 1).

The control problem 1 could be easily solved if an involvement of the engine is allowed in the gearshift control strategy. This requires the manipulation of engine variables like throttle angle and/or spark advance to control engine synchronisation. The use of open-loop reduction of spark advance (reduction of engine torque) in the inertia phase of a conventionally controlled upshift (such as depicted in Figure 4.3) to assist engine synchronisation is state-of-the-art. Such an approach essentially attempts to smooth the transmission output torque profile but does not offer the potential of a closed-loop engine speed control, which involves a full manipulation of engine controls. In the latter case the clutch pressure does not need to change at all throughout the inertia phase, thus, completely eliminating the problematic "torque hump".

Control Problem 2: The second problem is more difficult to solve and will thus be explained more thoroughly. The effect of the second problem on the output torque profile and thus vehicle jerk, is somewhat concealed by the "torque hump" of problem 1. To make the effect of problem 2 visible, the upshift from Figure 4.3 is repeated in Figure 4.5 only with the engine synchronisation in the inertia phase being controlled exclusively by manipulation of engine variables (closed-loop tracking of reference speed profile). The pressure at the oncoming clutch

was kept at a constant value throughout the inertia phase. The details of this closed-loop speed control are explained in the next section. The control of the torque phase remained unchanged.

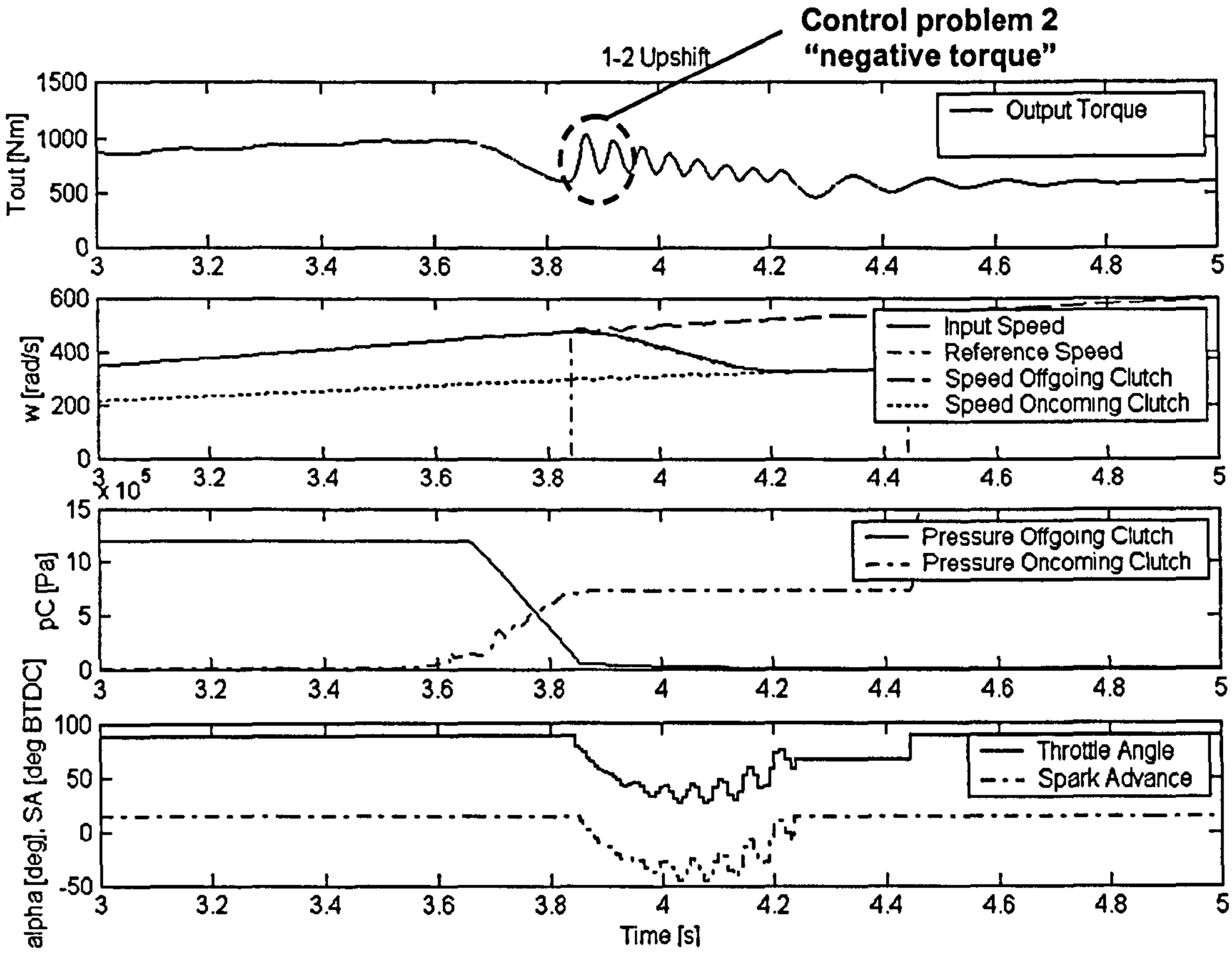

Figure 4.5 Simulation result: Upshift from Figure 4.3 with engine manipulation in the inertia phase, showing control problem 2 "negative torque"

Control problem 2 leads to a sharp rise in transmission output torque as can be seen in Figure 4.5 (dashed circle), although no such abrupt change can be observed for the clutch pressure or engine controls (third and bottom graph of Figure 4.5). Analysing the torques at the layshafts of oncoming and offgoing clutch (Figure 4.6) shows that the shaft torque at the offgoing clutch assumes a negative value of around -70 Nm (dashed circle in Figure 4.6). It then jumps at around 3.8seconds and settles after brief oscillations at a value of about –25 Nm (= transmission drag in Figure 4.6). The drop in negative torque occurs because the offgoing clutch is pressurised beyond the point where the oncoming clutch already carries the full engine torque. Since the pressure (i.e. torque) at the oncoming clutch is increased further, the offgoing clutch must produce a negative torque in order for the torque balance to be correct (both clutch torques need to be equal to input torque plus inertial torques involved). Once the offgoing clutch disengages fully, the torque suddenly jumps to its "stationary" value, which is given by the transmission drag. The consequence of this jump in layshaft torque can also be detected when looking at the vehicle jerk that shows increased values at this point in time (Figure 4.7).

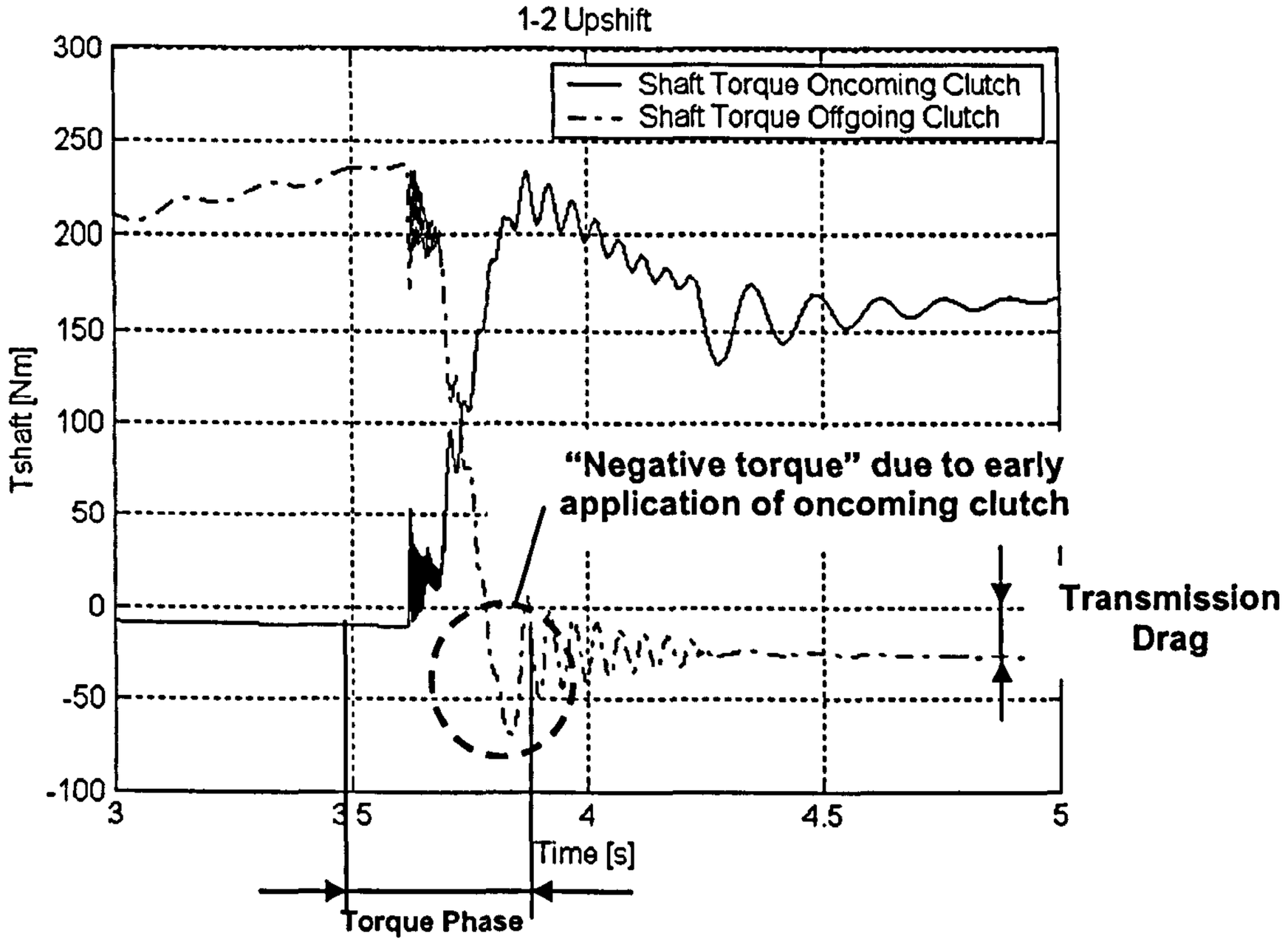

Figure 4.6 Torque profiles at the layshafts of offgoing and oncoming clutch for the gearshift from Figure 4.5 (Control Problem 2)

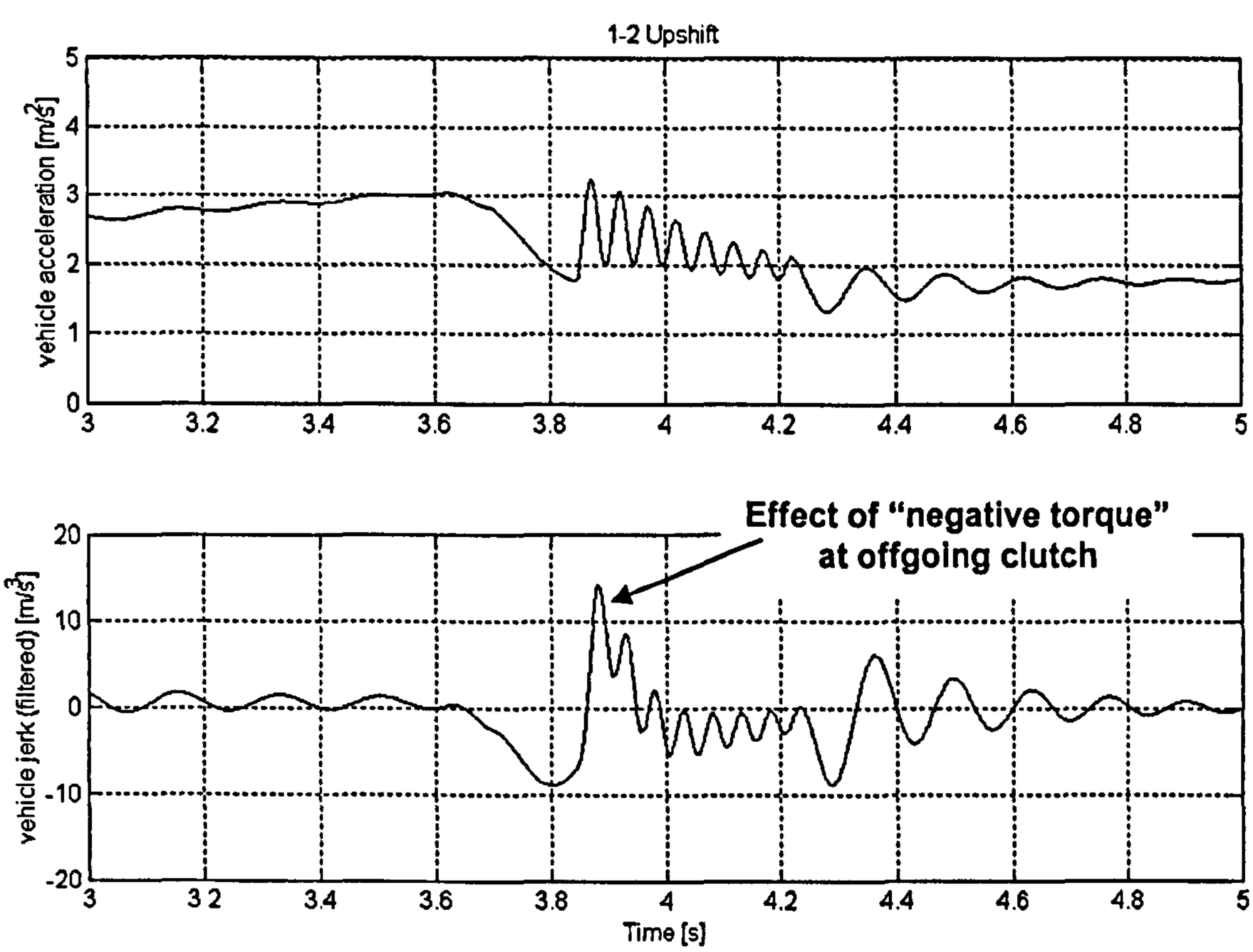

Figure 4.7 Vehicle acceleration and jerk for upshift from Figure 4.5 (Control Problem 2)

To solve the two fundamental problems: the "torque hump" in the inertia phase and the negative torque at offgoing clutch, a new control strategy incorporating engine control was developed in

this work. This integrated powertrain control strategy for power-on upshift on twin clutch transmissions is described in the next section.

Proposed Integrated Powertrain Control Strategy for Power-on Upshifts on Twin Clutch Transmission

As already mentioned in the previous section, control problem 1 ("torque hump") can be solved if the engine is employed to control the synchronisation in the inertia phase. This leads to the concept of an integrated powertrain control strategy.

Control problem 2 ("negative" torque at the offgoing clutch) is more difficult to solve and requires a unique approach. In conventional automatic transmissions creation of negative torque at the offgoing clutch is avoided by employing a one-way clutch (i.e. free-wheeler, overrunning clutches) instead of a friction clutch as oncoming shift element. The one-way clutch can only transmit positive torque hence engages when positive torque is inputted and disengages when the input torque becomes negative. However, one-way clutches are commonly employed on planetary-type automatic transmissions only for gear changes in the lower gear range. The reason for this is, that gearshifts between low gears produce, due to the larger difference in gear ratio, the largest and hence most noticeable changes in transmission output torque in the torque phase. The disadvantage of one-way clutches is the poor packaging, since they require additional shift elements (friction clutches and brakes) to keep them from disengaging on power-off shifts. For twin clutch transmissions the problem of the packaging seems to be one reason why employment of one-way clutches appears to be unsuitable. Another reason is that there is no real neutral position available, making it necessary to have an additional clutch for starting or decoupling the transmission from the engine.

On the other hand, there is a way of controlling friction clutches in such a way as to mimic the operation of one-way clutches i.e. to disengage if the input torque becomes negative. Such a control mechanism requires the control of clutch slip at the offgoing clutch and is described, in principle, in [Volkswagen AG 1998 (Patent DE 196 31 983 C1) and Daimler Chrysler AG 2001 (Patent DE 199 39 334 A1)]. The principle of this clutch slip control and the development of the rest of the integrated powertrain controller will now be described in more detail.

Figure 4.8 depicts the principle of the integrated powertrain control strategy for upshifts on twin clutch transmissions, featuring clutch slip control in the torque phase and engine control in the inertia phase. At the beginning of the torque phase the offgoing clutch (clutch 1 in Figure 4.8) is

brought to a state where it slips. The clutch slip is then controlled to stay at a small but constant reference value. This is achieved by a closed-loop controller, which manipulates clutch pressure at the offgoing clutch. Whilst clutch slip is controlled at the offgoing clutch, the pressure at the oncoming clutch (clutch 2 in Figure 4.8) is ramped up in an open loop way to transfer engine torque from the offgoing to the oncoming clutch. As a consequence of the increase in pressure at the oncoming clutch, the clutch slip controller decreases the pressure at the offgoing clutch in order to maintain the reference slip value.

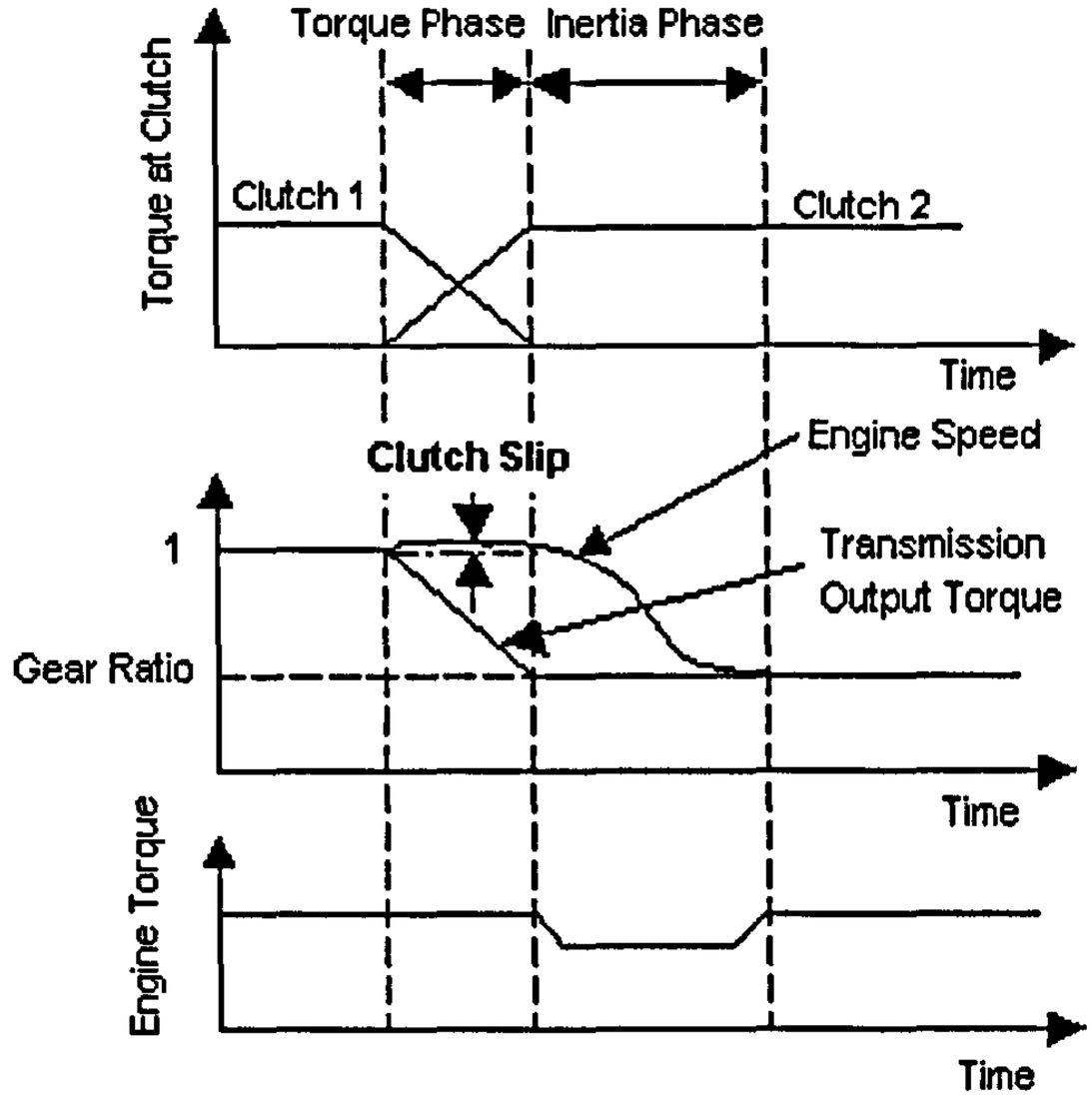

Figure 4.8 Control principle of integrated powertrain controller for power-on upshifts with clutch slip and engine control

At the point where the full engine torque has been transferred to the oncoming clutch, the pressure at the offgoing clutch becomes zero and the offgoing clutch disengages automatically without creating a negative torque. The transmission output torque has dropped according to the gear ratio (engine torque assumed constant in Figure 4.8) and a transition to the inertia phase can take place. In Figure 4.8 an engine-assisted control of the inertia phase is indicated where engine torque is reduced by a closed-loop control manipulating engine controls to follow a specified engine speed reference trajectory to achieve synchronisation. The layout and structure of the proposed integrated powertrain controller for gearshifts and its control loops is discussed in Section 4.4.

The control algorithm that determines when a control loop is active is depicted, for a clutch-to-clutch upshift, in Figure 4.9 and consists of a mixture of open-loop and closed-loop control. The steps of the control algorithm are also indicated in the clutch pressure profiles of the simulation

result of an upshift from 1st to 2nd gear presented in Figure 4.10. In step 1 of the control algorithm (Figure 4.9), hydraulic pressure is reduced at the offgoing clutch ("C1" in Figure 4.9). The closer the pressure is decreased to the value where the clutch starts to slip, the smaller are the resulting torque vibrations coming from the stick-slip transition when the clutch starts to slip. This behaviour made it necessary to create a look-up table for the release pressure depending on transmission output torque and the currently engaged gear (these two variables provide information about the clutch torque). Alternatively, if the information about transmission output torque is not available, information about engine torque can be used instead (only crude information about the torque is necessary in both cases).

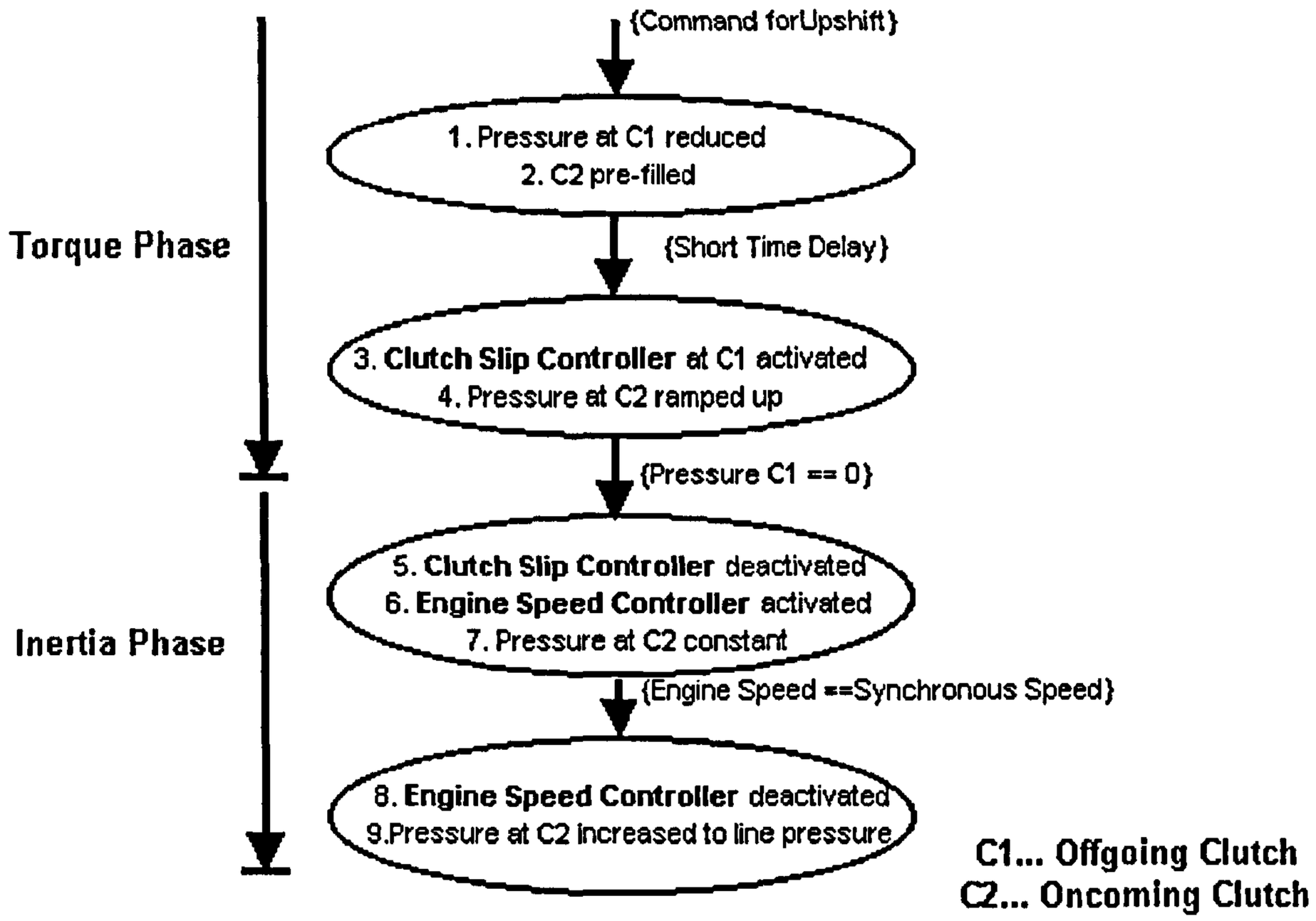

Figure 4.9 Control algorithm for the proposed integrated powertrain controller for power-on upshifts on twin clutch transmissions

The transition from stick to slip at offgoing clutch is accomplished by the clutch slip control, which is activated in step 3. Prior to activation of the clutch slip controller, the oncoming clutch ("C2" in Figure 4.9) is pre-filled in step 2. This pressure needs to be selected on the basis of a compromise between fast filling on one hand and little effect on driveline torque on the other. The filling of the clutch has a second positive effect: when the slip controller brings the offgoing clutch to a state where it slips, the transmission output torque would drop for a brief moment. This torque drop can be "smoothed" if the oncoming clutch can already carry some torque. The

function of the time delay in Figure 4.9 (denoted as "short time delay") was to allow the pressure to settle to a stationary value and was chosen arbitrarily at 0.05 seconds.

The closed-loop control of clutch slip maintains a small clutch slip reference value (5 rad/s) by manipulating the pressure at the offgoing clutch. By ramping up the pressure at the oncoming clutch (step 4), the slip controller automatically reduces the pressure at the offgoing clutch, thus transferring engine torque without creating negative torque at this clutch. At the point where the pressure at the offgoing clutch has become zero, the slip controller is deactivated and the control algorithm can proceed to the inertia phase. However, the detection of this point would require information about the clutch pressure. As a more practical, however less accurate method, the start of the inertia phase can also be inferred from the clutch slip signal, where a change in sign of the clutch slip indicates the end of the torque phase.

In the inertia phase, the engine speed is synchronised to that of the target gear by tracking a reference speed profile. For the engine reference speed trajectory a (semi-) cosine profile was selected here (Equation (63), Section 4.4.3). The closed-loop speed controller, which is activated in step 6, manipulates both throttle angle and spark advance, thus uniting the advantages of large engine torque variations and fast engine response. The pressure at the oncoming clutch is kept constant during the inertia phase (step 7). At the end of the inertia phase the clutch pressure is raised to the line pressure (step 9). It was observed, that the torque vibrations created at the end of the gearshift where the clutch locks up, could be reduced by abruptly raising the spark advance to its original value at this point.

Figure 4.10 depicts a simulation results for the above described uspshift control algorithm applied to the powertrain model developed in Chapter 3. The simulated shift was an upshift from 1^{st} to 2^{nd} gear at wide-open throttle (90 degrees throttle angle). The upshift took place at a vehicle velocity of around 30 km/h. The clutch friction characteristic chosen for all simulation results in this section is wet friction with a positive gradient of the friction coefficient with slipping speed.

The graphs included in Figure 4.10 are the same as in the previous simulation result (Figure 4.3 and 4.5) and show the transmission output torque in the uppermost graph, the rotational speeds at both clutches an the reference speed profile in the graph below, the hydraulic pressure at both clutches in the third graph and the throttle angle and spark advance (degrees before top dead centre) in the graph at the bottom. From Figure 4.10 the various stages of the control algorithm can be seen: Starting with a reduction in the hydraulic pressure at the offgoing clutch at around 3.5s (step 1) proceeding to the filling of the oncoming clutch (dashed circle and step 2). After

these two steps the actual torque phase begins where the clutch slip controller (step 3) decreases the pressure at the offgoing clutch due to a linear increase in pressure at the oncoming clutch (step 4).

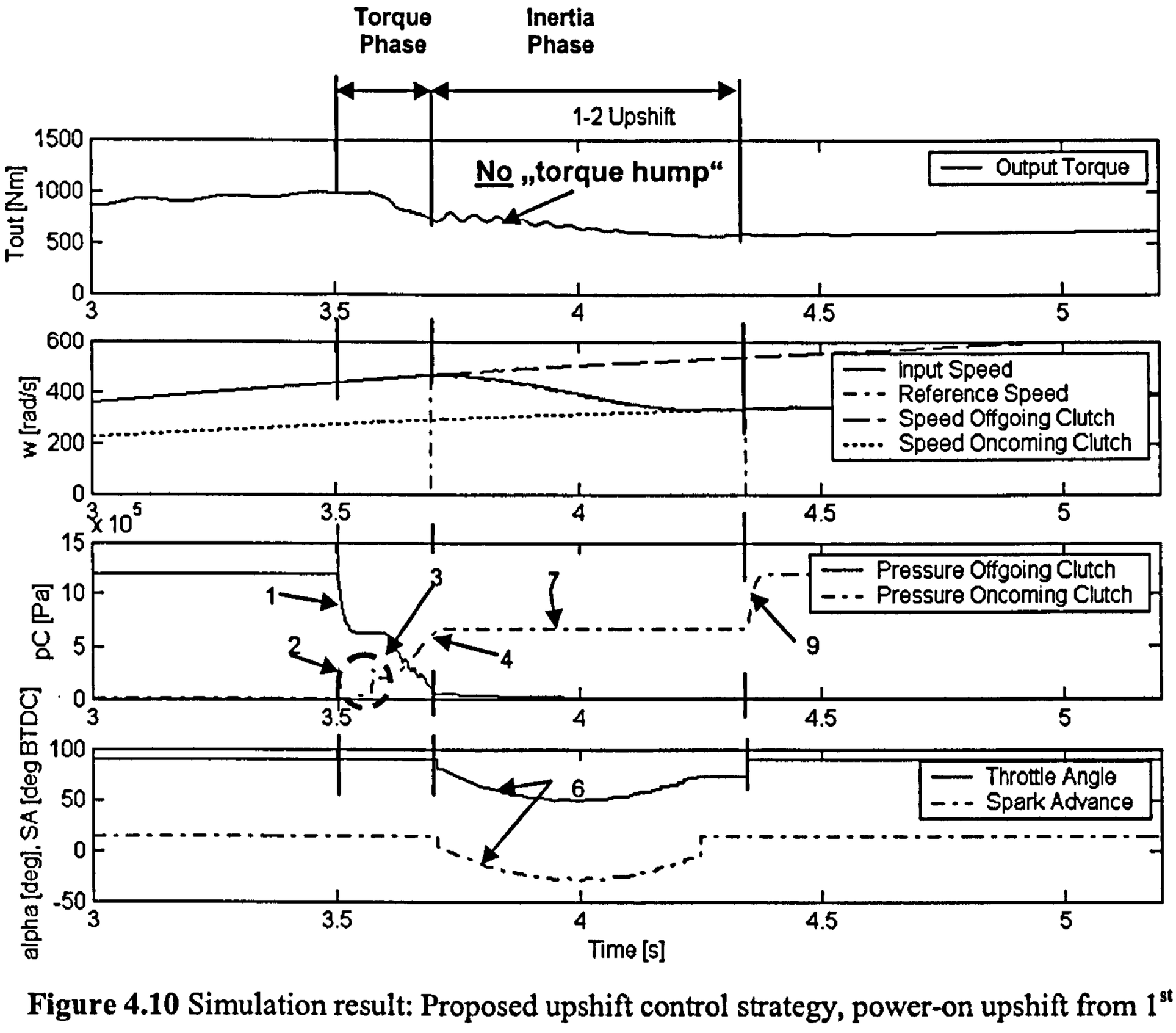

Figure 4.10 Simulation result: Proposed upshift control strategy, power-on upshift from 1st to 2nd gear, wide open throttle (WOT), at around 30 km/h, included are steps of the control algorithm depicted in Figure 4.9

During the torque phase, the output torque decreases gradually. At the point where the pressure at the offgoing clutch has gone to zero the inertia phase starts where the transmission input speed (i.e. engine speed) is synchronised along a reference profile by the engine speed control to the level of the target gear. In the bottom graph of Figure 4.10 the modulation of engine controls by the engine speed control (step 6) can be clearly seen (late spark has been allowed here). The tracking of the reference speed profile is very good (second graph in Figure 4.10). Slight vibrations can be observed at the beginning of the inertia phase, which result from the offgoing clutch changing its state from stick to slip at the end of the torque phase. However, it is believed that these small vibrations do not affect the gearshift quality greatly. Overall the output torque profile looks very smooth without showing any abrupt changes and steep gradients, thus indicating that the two key problems, mentioned at the beginning of this section, are effectively

solved. To back this assumption, the torque at the layshafts and the longitudinal vehicle jerk for the upshift depicted in Figure 4.10 are presented in Figure 4.11 and Figure 4.12.

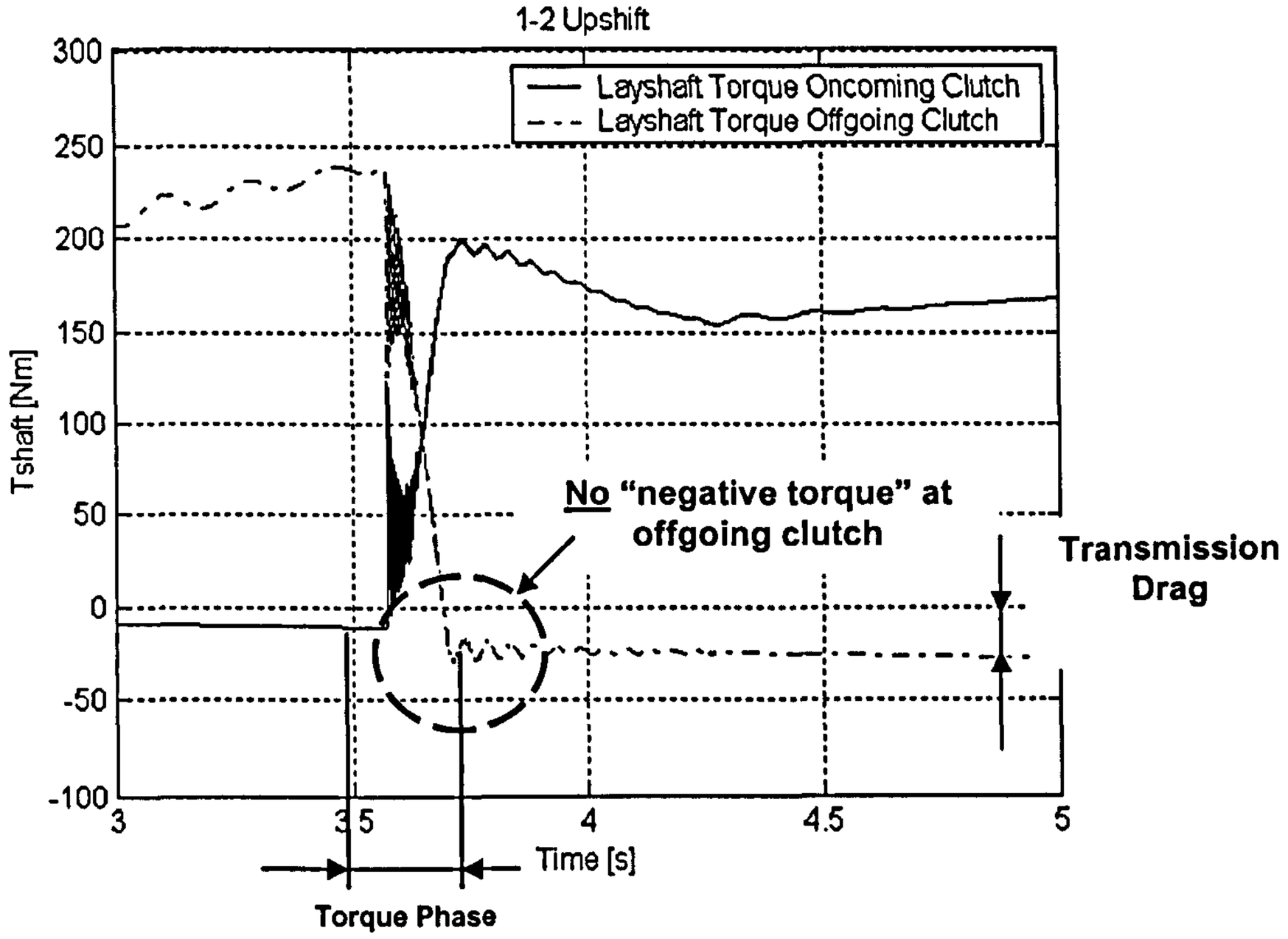

Figure 4.11 Torque profiles at the layshafts of offgoing and oncoming clutch for the gearshift from Figure 4.10 (proposed upshift control strategy)

Comparing the torque profiles at both layshafts for the shift with a conventional clutch-to-clutch control strategy (Figure 4.6) to those for the proposed control strategy (Figure 4.11) clearly shows that the clutch slip control can effectively solve the problems resulting from a negative torque contribution of the offgoing clutch due to an early application of the oncoming clutch. Where Figure 4.6 shows a strong negative torque value (torque drop) with subsequent jump in layshaft torque, Figure 4.11 shows no such behaviour and the torque trajectory at the offgoing clutch continues at the level of the drag torque after the torque phase has been completed.

The elimination of the negative torque contribution also leads to reduced vehicle jerk at the point of transition from torque to inertia phase. The profile of the longitudinal vehicle jerk for the shift from Figure 4.10 is depicted in Figure 4.12 and shows that the peaks in vehicle jerk occurring for conventionally controlled upshifts can be almost completely removed. Whereas the conventionally controlled upshifts showed vehicle jerk values of around 30 m/s^3 (Figure 4.4) and 15 m/s^3 (Figure 4.7) at the point of transition from torque to inertia phase, the proposed integrated powertrain control strategy for upshifts can reduce these jerk values to almost zero (Figure 4.12). Also at the end of the inertia phase the vehicle jerk strongly reduced compared to

that of conventionally controlled upshifts (from -25 m/s^3 in Figure 4.4 compared to almost 0 m/s^3 in Figure 4.12). These reductions in vehicle jerk indicate a vast improvement in shift quality of the proposed upshift control strategy over conventionally controlled upshifts.

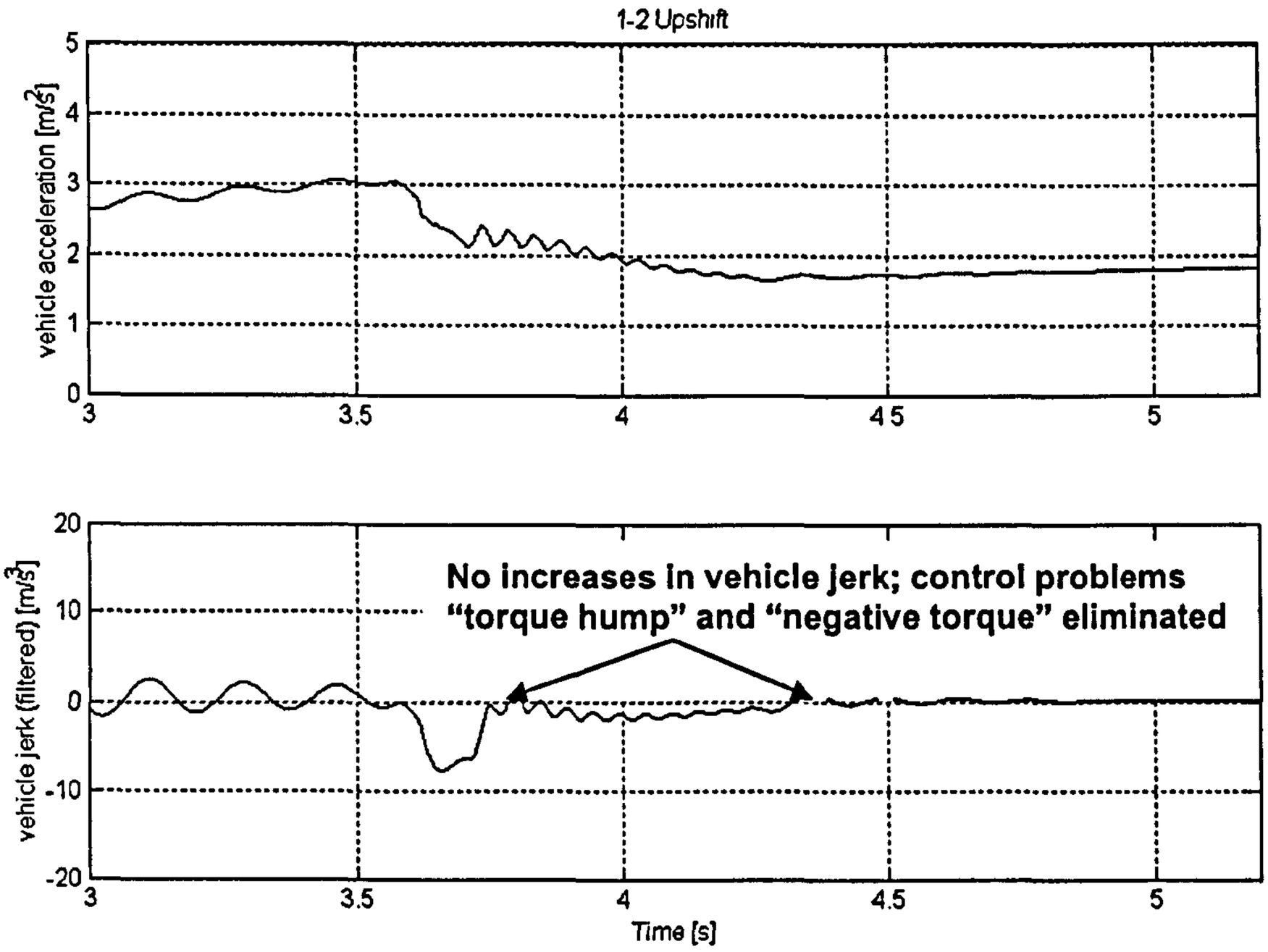

Figure 4.12 Vehicle acceleration and jerk for upshift from Figure 4.10 (proposed upshift control strategy)

Figure 4.13 shows the same shift as in Figure 4.10, though with a steeper gradient of the reference speed profile for engine synchronisation. This leads to decreased shift time (inertia phase was reduced by 0.2 seconds compared to the upshift in Figure 4.10) and shorter slipping at the clutch, which, due to decreased energy dissipation (torque transmitted through clutch stays the same), positively affects clutch durability. Figure 4.14 depicts the vehicle jerk profile of the shift from Figure 4.13 and shows that the vehicle jerk profile remains almost unchanged, despite the shorter shift time. This means that with the proposed engine–assisted upshift control strategy (integrated powertrain control strategy) a decrease in shift time is possible without sacrificing shift quality. Also, the good tracking performance of the speed controller is maintained for the steeper engine speed reference profile.

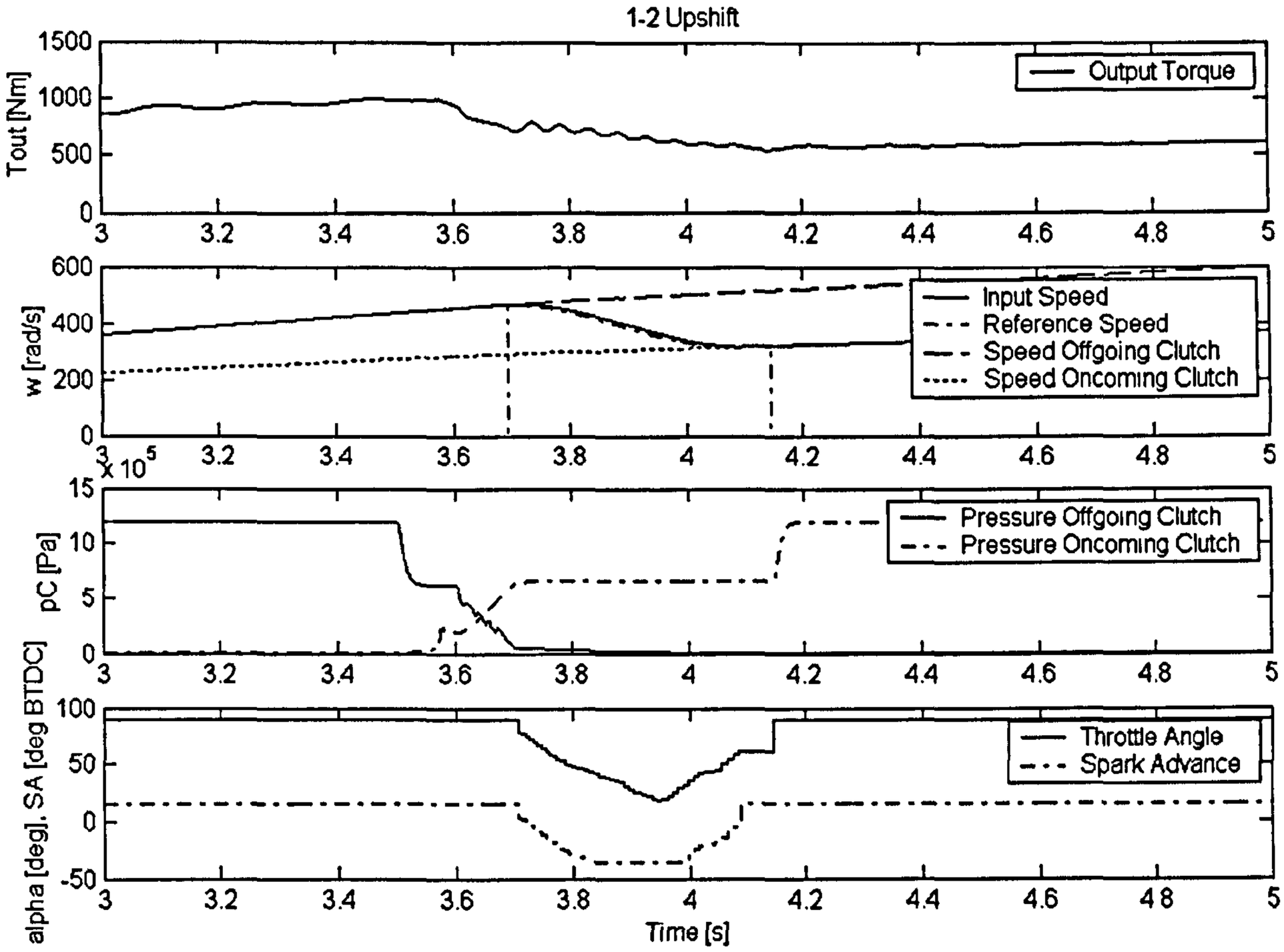

Figure 4.13 Simulation result: Proposed upshift control strategy, power-on upshift from Figure 4.10 with inertia phase reduced by 0.2 seconds

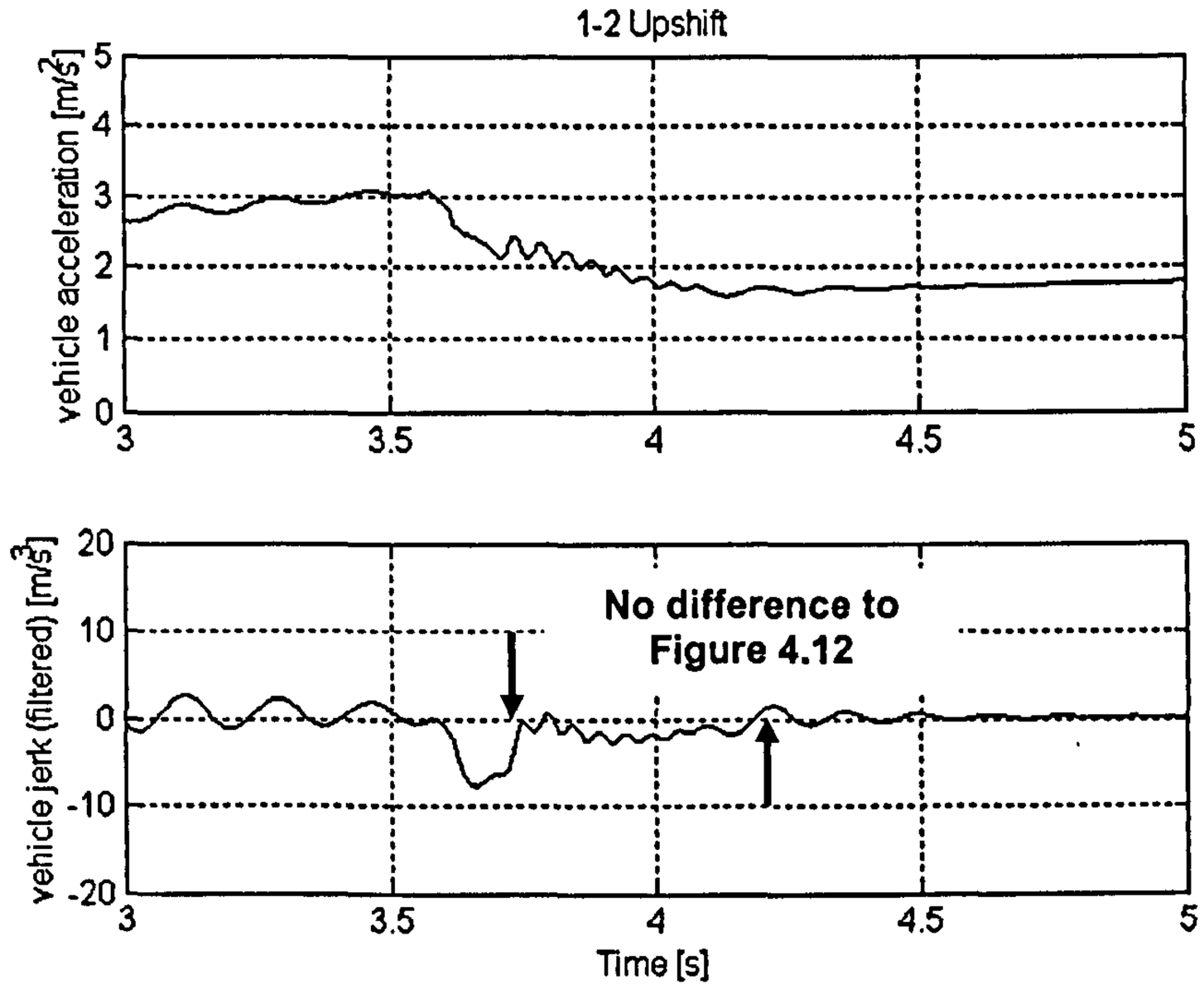

Figure 4.14 Vehicle acceleration and jerk for upshift from Figure 4.13

Figure 4.15 depicts an upshift from 2nd to 3rd gear and Figure 4.16 an upshift from 3rd to 4th gear respectively. In general the torque profiles of the two shifts look smooth, indicating low vehicle jerk values and thus good shift quality. The tracking performance of the speed controller in the inertia phase remains good, keeping the engine speed close to the cosine reference trajectory. The drop of transmission output torque at the end of the inertia phase is due to the oncoming clutch locking up (i.e. transition from a state where it slips to a state of sticking). This slip-stick transition can result in a change in clutch torque since the torques in both states can be different. As already explained abruptly rising the spark advance at this point to its original value can slightly compensate for this change in output torque at the end of the inertia phase. However, if the spark advance is already close to its original value, or if the increase does not take place at the exact moment, then this strategy will not improve the problem. But, it shall be noted that the change in transmission output torque due to clutch lock-up can be noticed less strongly in the higher gear ranges (due to the smaller gear ratios involved).

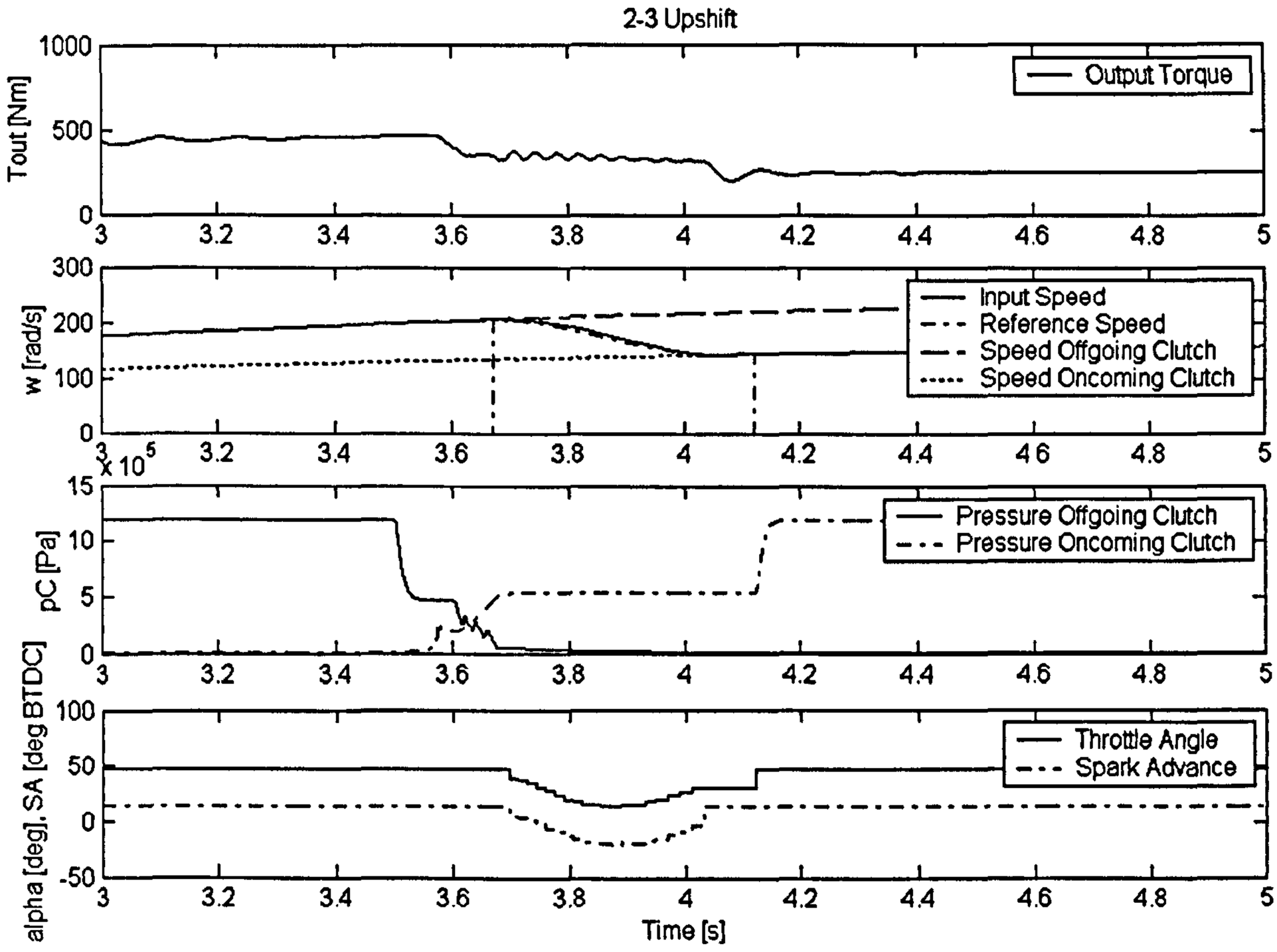

Figure 4.15 Simulation Result: Proposed upshift control strategy, power-on upshift from 2nd to 3rd gear, medium throttle, at around 25 km/h

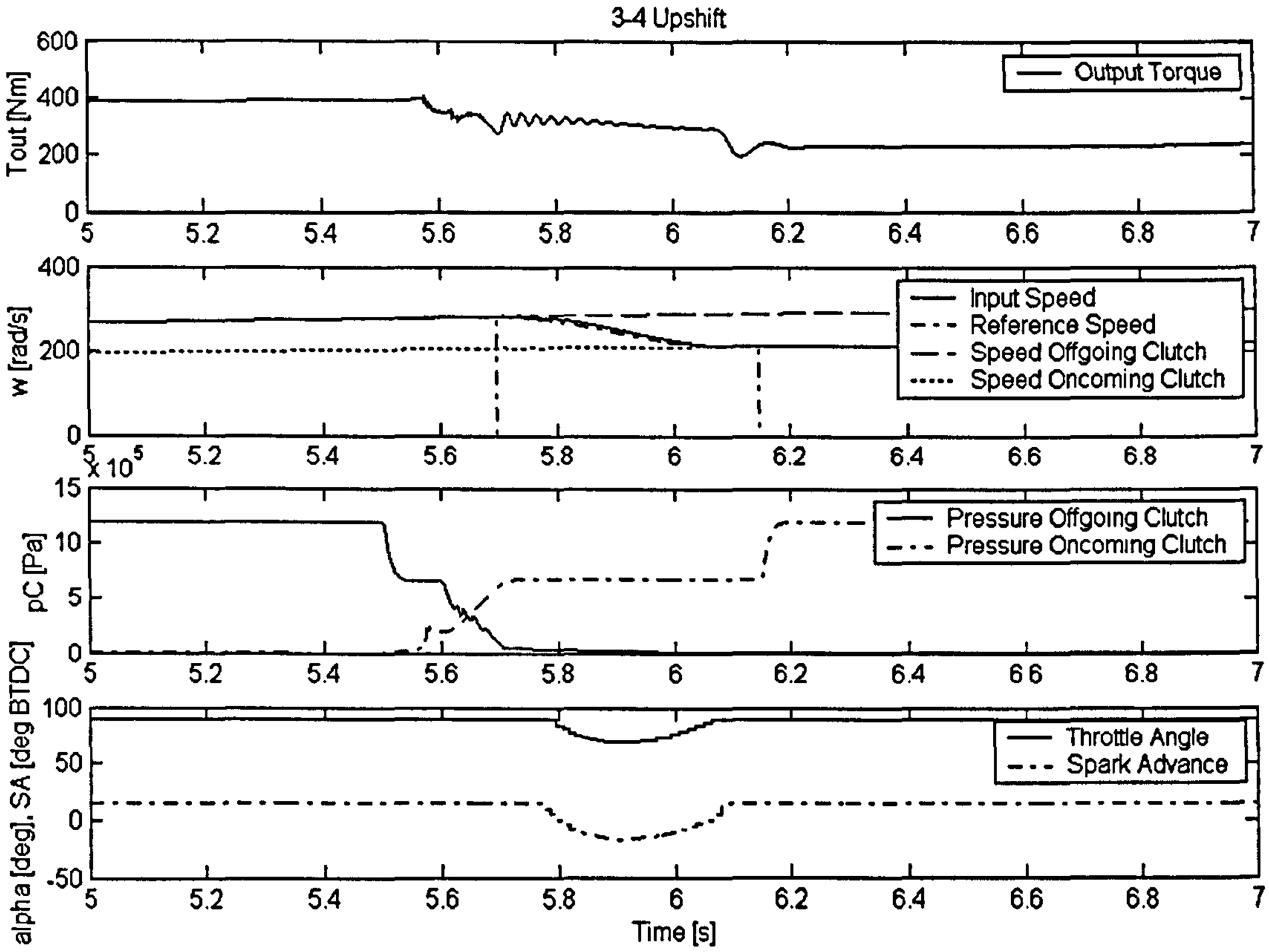

Figure 4.16 Simulation result: Proposed upshift control strategy, power-on upshift from 3rd to 4th gear, WOT, at around 50 km/h

4.2.2 Control of Power-On Downshifts

Problems of Conventional Clutch-to-Clutch Downshift Control Strategies

Conventional clutch-to-clutch downshift control strategies that make exclusively use of a manipulation of clutch torque (i.e. actuation pressure) as described in Section 4.1 (see downshift principle in Figure 4.2) shows two key control problems detrimental to shift quality.

Control problems:

1. "Loss of traction": With conventional cutch-to-clutch downshift control strategy, engine acceleration in the inertia phase is achieved by decreasing the hydraulic pressure at the offgoing clutch (open or closed-loop control) thus bringing the clutch to a state where it slips and allowing the engine to accelerate. However, a partial disengagement of the offgoing clutch causes the transmission output torque to drop severely and thus traction is

diminished or even lost at the wheels. Hence, it is desirable to reduce the pressure at the offgoing clutch as little as possible.

2. "Negative torque": Again, similar to upshifts, a correct application timing of the oncoming clutch in the torque phase of a downshift is crucial if increased vehicle jerk is to be avoided.

Control Problem 1: The problem of loosing traction at the wheels if the time for engine synchronisation becomes very short and the downshift is solely controlled by clutch pressure manipulation is illustrated in Figure 4.17, which shows a simulation result for a downshift from 2^{nd} to 1^{st} gear at low throttle. The time for synchronising the engine to the target gear (inertia phase) was chosen to be around 0.6 seconds. The problem of decreased power transfer to the wheels can be clearly recognised when inspecting the profiles of transmission output torque (uppermost graph in Figure 4.17) and clutch pressure (third graph in Figure 4.17).

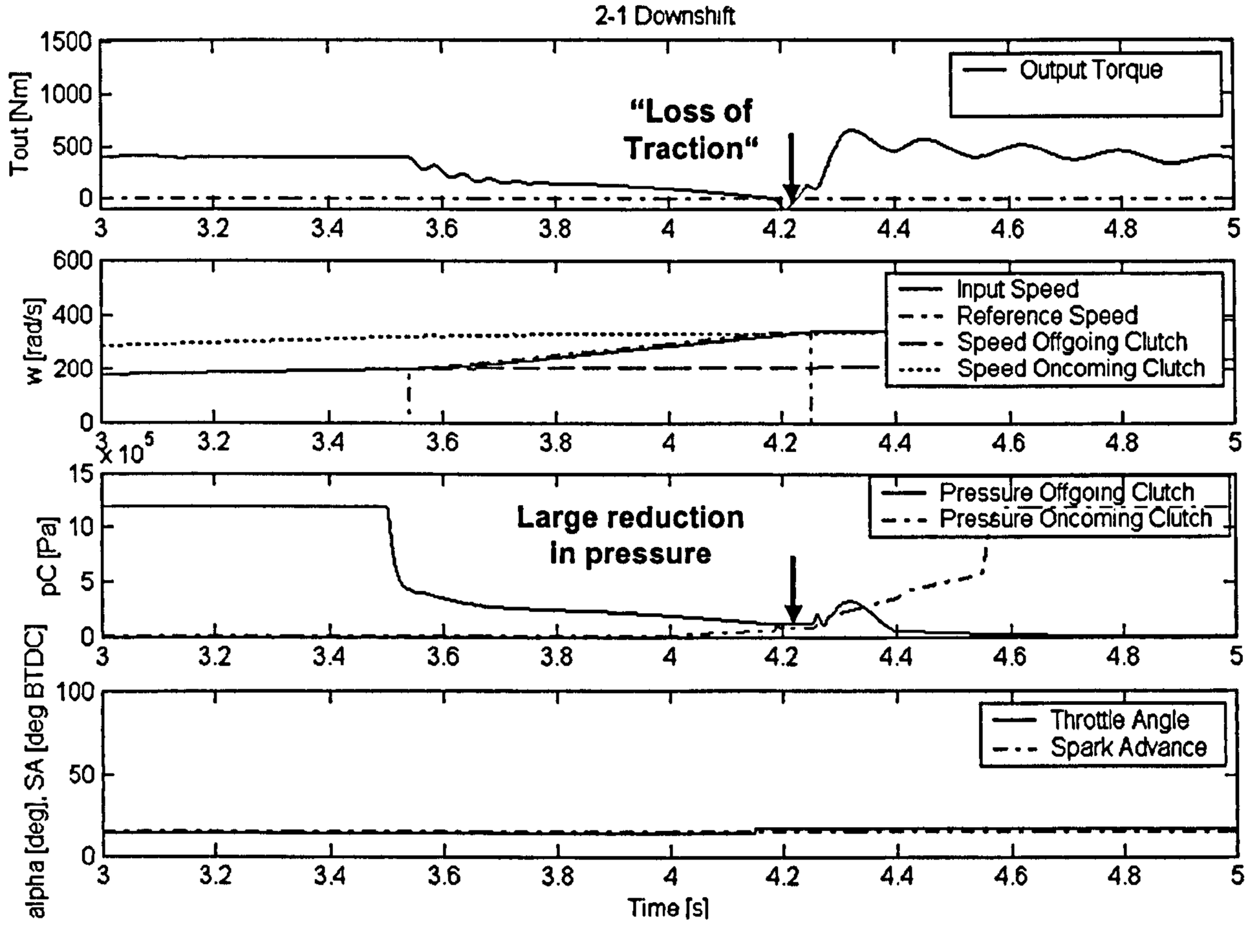

Figure 4.17 Simulation result: downshift from 2^{nd} to 1^{st} gear, at low throttle, controlled with a conventional clutch-to-clutch control strategy, exclusively using clutch pressure manipulation (Control problem 1).

Due to the short time available for engine synchronisation, the closed-loop speed control has to reduce the pressure at the offgoing clutch severely, causing the transmission output torque to drop to zero at the end of the inertia phase. This drop in transmission output torque means a momentary loss in traction (arrow in Figure 4.17), which has to be avoided.

The solution to this problem would be to increase engine torque to accelerate the engine in the inertia phase instead of reducing clutch pressure. To rely on engine control alone, would require a very powerful engine and would not work in the case where the engine torque is already at its maximum. However, a combination of clutch pressure manipulation and increase in engine torque can help to improve the problem of loosing traction when the time for engine synchronisation becomes very short.

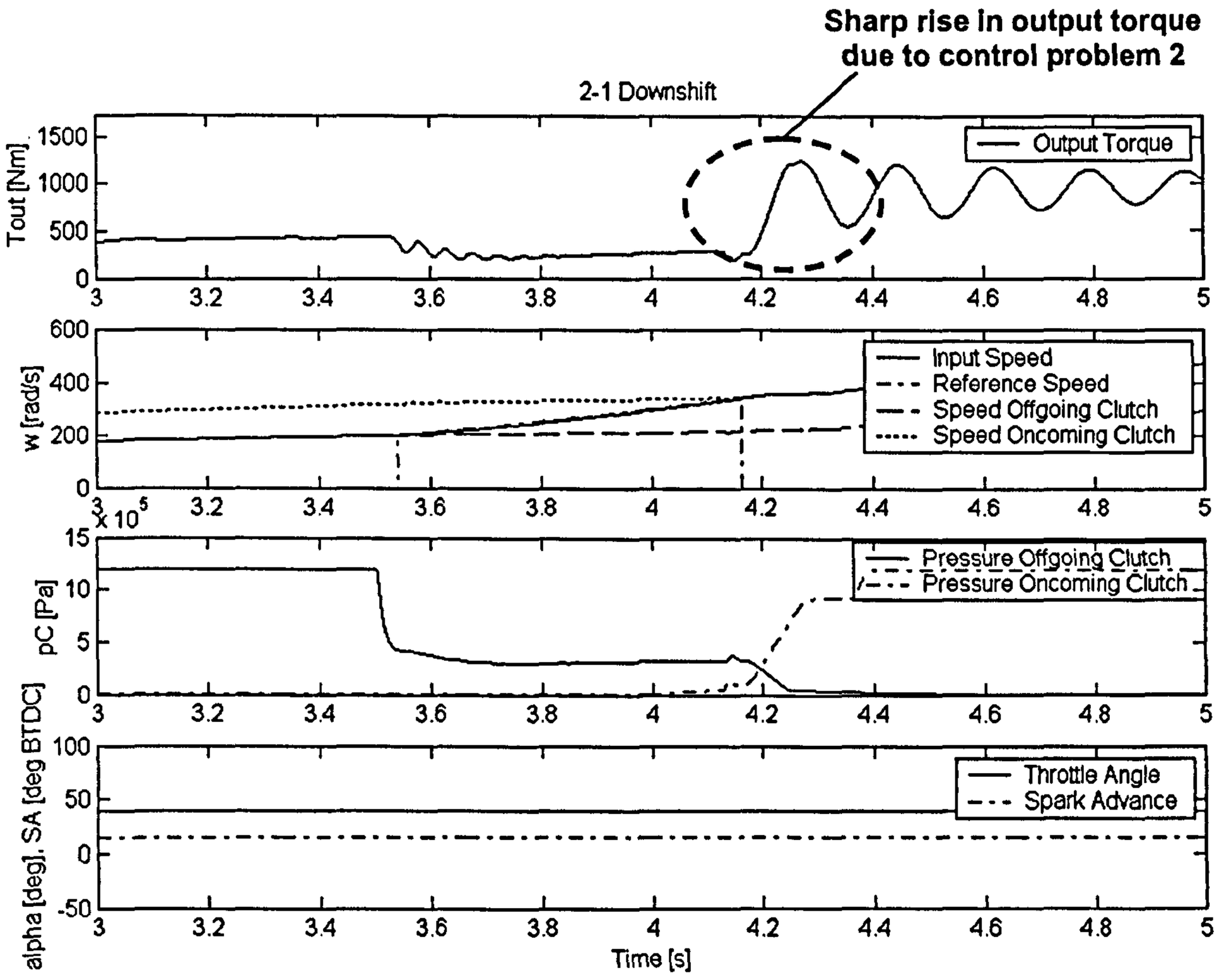

Figure 4.18 Simulation result: downshift from 2nd to 1st gear, at low throttle, controlled with a conventional clutch-to-clutch control strategy using pressure ramps in the torque phase (control problem 2).

Control Problem 2: The torque phase of a clutch-to-clutch downshift can be controlled by simply ramping down the hydraulic pressure at the offgoing clutch to zero whilst ramping up the pressure at the oncoming clutch (e.g. open-loop control in Figure 4.2), thus transferring engine torque between the two clutches. Again, a correct timing of the clutch application and

release is crucial, however, not easily calculable due to the delay in the hydraulic actuation. If the pressure at the oncoming clutch is increased too late (after the engine has reached synchronous speed of the target gear), transmission output torque drops and thus traction at the wheel is lost. Furthermore, the engine accelerates beyond the synchronous point and any increase in pressure at the oncoming clutch decelerates the engine to the synchronous speed again, resulting in inertial torque being transferred to the transmission output. To avoid these problems, the oncoming clutch could be applied early. However, if the pressure increase at the oncoming clutch takes place too early, the offgoing clutch creates a large negative torque and once released, results in a sharp rise in output torque. This steep rise in transmission output torque severely increases vehicle jerk and causes heavy torque vibrations in the driveline. Thus an early application of the oncoming clutch has to be avoided as well. This demonstrates that application of open-loop control in the torque phase does not provide satisfactory results in terms of shift quality. The control problem described here is similar to the one encountered with upshifts.

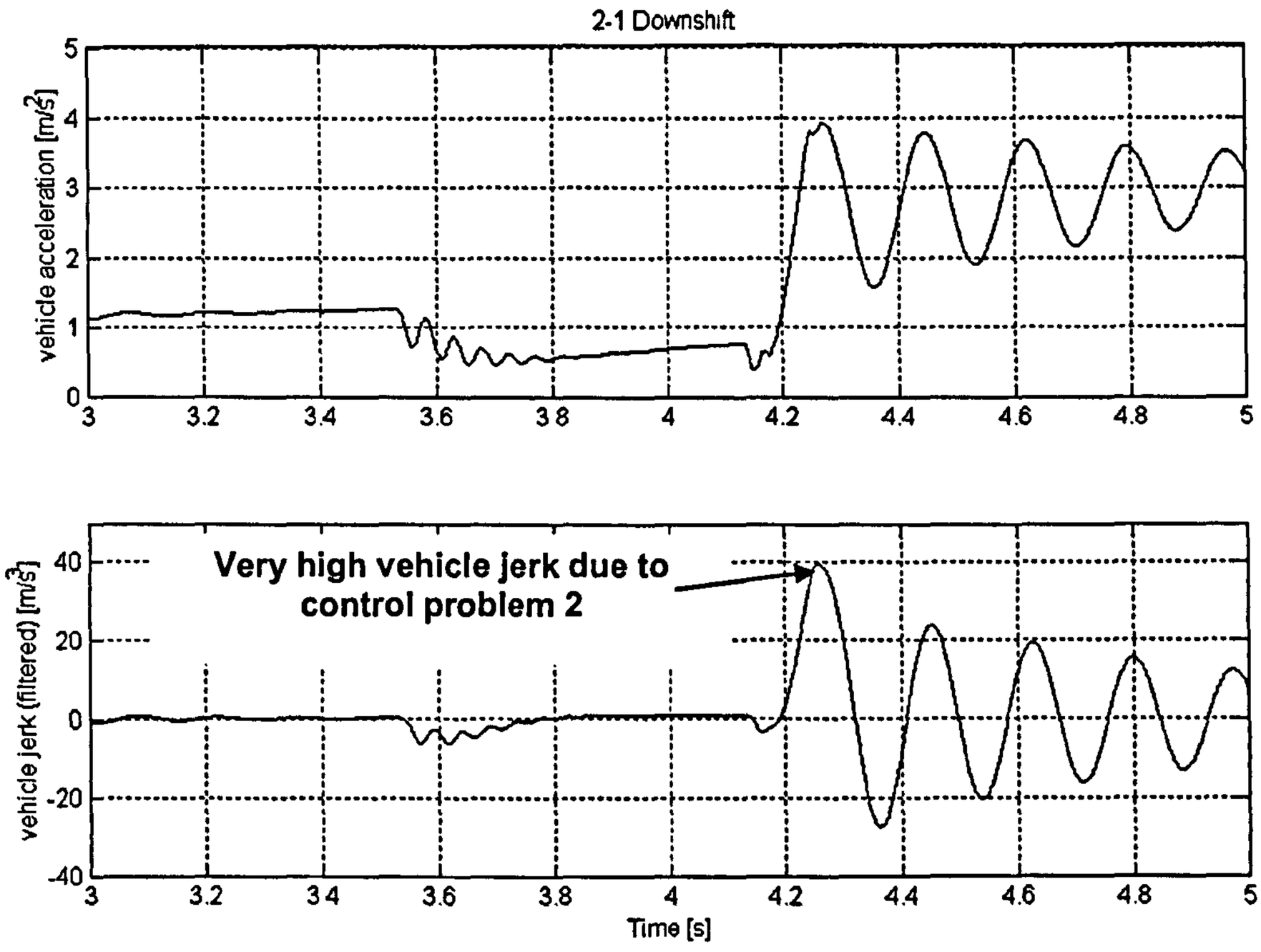

Figure 4.19 Vehicle acceleration and jerk for downshift from Figure 4.18, conventional clutch-to-clutch control strategy, control problem 2

To illustrate control problem 2, a simulation result is presented in Figure 4.18 that depicts a downshift from 2nd to 1st gear where the torque phase is simply controlled by use of pressure ramps. The dashed circle in Figure 4.18 marks the sharp increase in transmission output torque

with subsequent heavy driveline oscillations; both a result of a wrong application timing of the oncoming clutch due to use of pressure ramps. The negative effect of control problem 2 on shift quality can also be observed in the vehicle jerk profile depicted, together with the vehicle acceleration, in Figure 4.19. The sharp rise in torque due to a wrong application timing of the oncoming clutch leads to a peak in vehicle jerk values of around 40 m/s^3 (Figure 4.19). This high level of vehicle jerk and the subsequent torque vibrations are an indicator for very poor shift quality.

Proposed Integrated Powertrain Control Strategy for Power-on Downshifts on Twin Clutch Transmission

Control problem 1 (reduced torque at the transmission output in the inertia phase due to conventional control strategy) can be improved if the loss in traction is compensated by an increase in engine torque, thus integrating the engine in the downshift control strategy (integrated powertrain approach).

Control problem 2 (application timing of oncoming clutch in the torque phase) is in principle similar to the problem discussed for the upshift. Again, because twin clutch transmissions usually do not feature one-way clutches, a control of clutch slip at the offgoing clutch can be employed as remedy.

The principle of the proposed clutch-to-clutch downshift control strategy is illustrated in Figure 4.20. In the inertia phase, engine synchronisation is controlled by a closed-loop speed control manipulating clutch pressure, which is assisted by increasing engine torque via throttle operation. This has the advantage that the engine can be accelerated in the inertia phase with as little as possible modulation (decrease) in clutch pressure, thus ensuring maximum tractive force at the wheels and a smoother transmission output torque profile. In case the downshift takes place at maximum engine torque, the engine synchronisation has to be controlled by manipulation of clutch pressure alone. The combined engine/clutch control strategy is indicated in Figure 4.20 by showing a decrease in clutch torque at clutch 1 (offgoing clutch) together with an increase in engine torque during the inertia phase.

Further indicated in Figure 4.20, is the use of clutch slip control for controlling the transfer of engine torque in the torque phase. This requires a switch in control tasks at the offgoing clutch from tracking a reference speed profile in the inertia phase to maintaining a certain amount of clutch slip in the torque phase. Whilst the pressure at the offgoing clutch is manipulated by the

clutch slip control, the pressure at the oncoming clutch (clutch 2 in Figure 4.20) has to be ramped up. The transfer of engine torque results to an increase in transmission output torque in the torque phase according to the change in gear ratio.

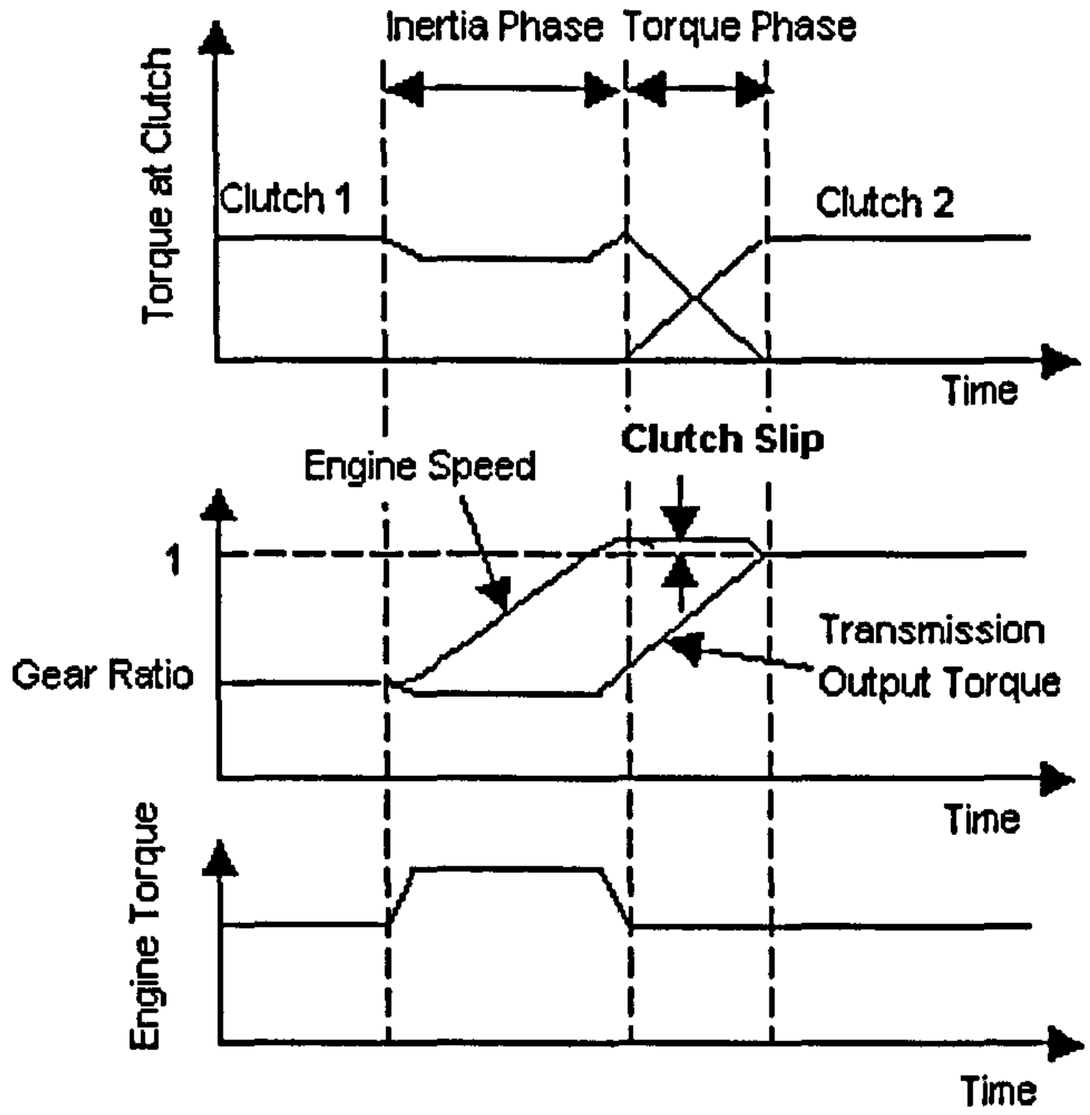

Figure 4.20 Control principle of integrated powertrain control strategy for power-on downshifts incorporating control of clutch slip and engine torque

The detailed control algorithm of the proposed integrated powertrain control strategy for clutch-to-clutch downshifts is depicted in Figure 4.21. Again the explanation of the control algorithm can be followed in the simulation result of a downshift from 2nd to 1st gear depicted in Figure 4.22 (control steps are indicated and marked with small arrows). At the beginning of the inertia phase (step 1 in Figure 4.21), the pressure at the offgoing clutch ("C1" in Figure 4.21) is reduced to a level close to the point where the clutch starts to slip (similar to the beginning of the torque phase on the upshift). This is necessary because it is difficult to exactly hit the point where clutch slip starts. However, decreasing the pressure too far results to a harsh drop in output torque when the clutch starts to slip. As a consequence, this "release" pressure has to be made dependent on the transmission output torque and gear ratio (reflects torque transmitted through), or alternatively, the transmitted engine torque. Again, the time delay after step 2 (denoted as "short time delay" in Figure 4.21) serves the purpose of helping the clutch pressure to settle to a stationary value. The value of the time delay was chosen to be 0.05 seconds similar to power-on usphifts.

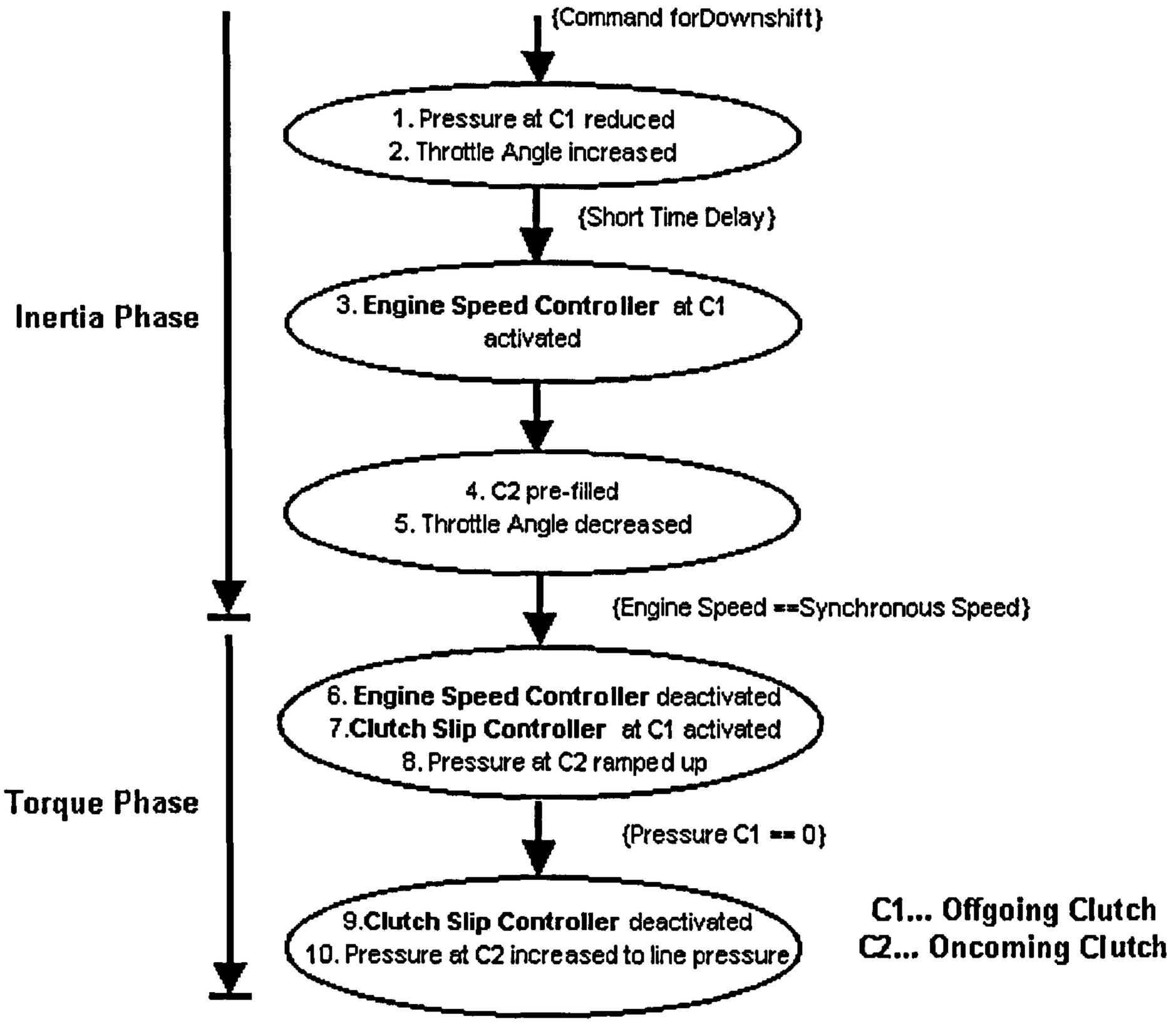

Figure 4.21 Control algorithm of proposed integrated powertrain control strategy for power-on downshifts on twin clutch transmissions

Throughout the inertia phase of the downshift the engine needs to be accelerated in order to reach the synchronous speed of the target gear. A combination of an increase in throttle angle (step 2) and clutch pressure modulation by the engine speed controller (step 3), allows tracking of a reference speed profile (linear increase in engine speed) without having to decrease the clutch pressure too much. Prior to the end of the inertia phase, the oncoming clutch is pre-filled in step 4 (low pressure to suppress torque vibrations) and the throttle angle is decreased again (step 5) to a level slightly above that at the beginning of the inertia phase. This compensates for an increase in engine torque due to engine acceleration. The throttle angle was decreased here to a level that lay 10 degrees (this is an arbitrary value that was used in all downshift cases) above the level at the beginning of the inertia phase as a safety margin. However, a more accurate value of the throttle angle at the end of the inertia phase could be obtained based on information about the change in engine speed, the original throttle angle and an engine map.

Contrary to the upshift control strategy, where a cosine trajectory was chosen as engine speed reference profile during the inertia phase, the closed-loop engine speed control of the downshift makes use of a linear engine speed reference trajectory. For the downshift, a cosine reference trajectory would, at end of the inertia phase, aid the subsequently activated clutch slip control in smoothly "catching" the engine at the synchronous speed. The disadvantage, however, is that at the beginning of the inertia phase where the clutch has to be brought to slip, a cosine trajectory would not lead to a clean stick-slip transition. The reason for this is that the speed controller reduces clutch pressure only slowly at the beginning (due to initial gentle gradient of the cosine trajectory and the therefore closeness of engine speed and reference trajectory), yet, the clutch has not started to slip and thus the engine speed cannot follow the reference trajectory. As a consequence as the reference trajectory progresses and the gradient of the cosine trajectory becomes steeper the speed controller suddenly produces a large decrease in clutch pressure in order to compensate the large tracking error. This behaviour is not desired as it produces a sudden drop in transmission output torque and thus deteriorates shift quality. Using a linear increase in engine speed as reference trajectory was observed to result to a smoother and faster stick-slip transition. Obviously, a combination of cosine part at the end and linear increase at the beginning of the inertia phase would offer the best of both worlds. As a simplification a full linear reference profile is used in this work (Equation 60, Section 4.4.2).

In a similar way as previously explained for the upshift, clutch slip control is employed in the torque phase for a smooth transfer of engine torque (step 7). At the offgoing clutch the control task has to be switched from a speed control in the inertia phase to control of clutch slip in the torque phase. The reference value for the closed-loop clutch slip control is again 5 rad/s. In step 8, the pressure at the oncoming clutch ("C2" in Figure 4.21) is ramped up, forcing the clutch slip control to decrease the pressure at the offgoing clutch accordingly. After the engine torque has been transferred to the oncoming clutch in full (pressure at the offgoing clutch has become zero, or alternatively the clutch slip has changed sign), the pressure at the oncoming clutch can be increased to the line pressure again (step 10). However, before the pressure at the oncoming clutch is raised to the line pressure it is held constant for a brief time before in order to ensure a smooth slip-stick transition.

Figure 4.22 shows a downshift from 2nd to 1st gear at a throttle angle of 15 degrees and a vehicle speed of around 20 km/h. Again, the uppermost graph shows the transmission output torque profile and the second graph from above the input and output speed trajectories at both clutches. The third graph depicts the hydraulic pressure profiles at both clutches and the graph at the bottom shows throttle angle and spark advance.

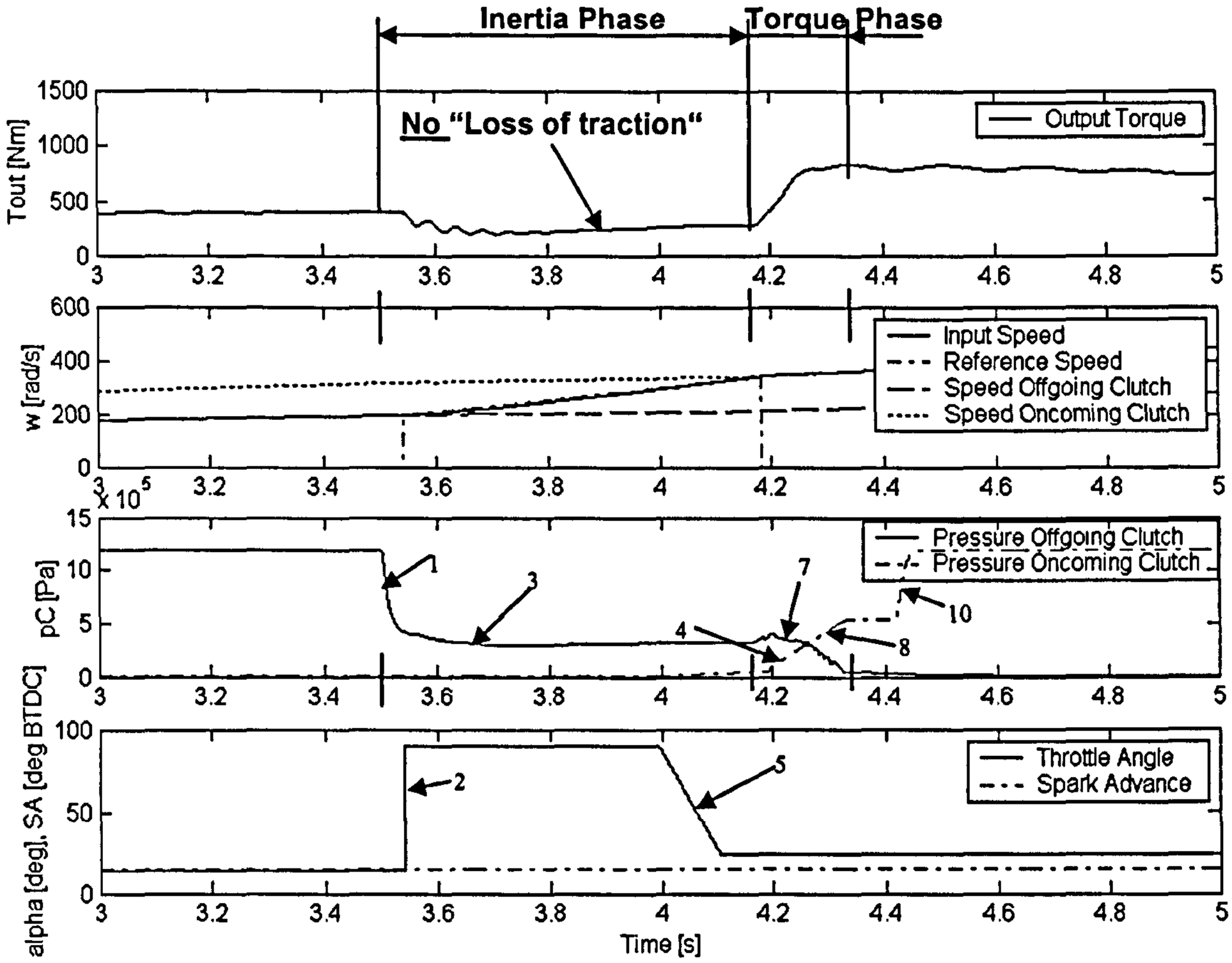

Figure 4.22 Simulation result: Proposed downshift control strategy, power-on downshift from 2nd to 1st gear, low throttle, at around 20 km/h, included are the steps of the control algorithm depicted in Figure 4.21

Both inertia phase and torque phase are indicated in the output torque profile. The friction coefficient used for the simulation results shown in this section, again, is of wet type and has a positive gradient with slipping speed. Comparing the simulation result of the proposed downshift control strategy (Figure 4.22) to that of the downshift with a conventionally controlled inertia phase (Figure 4.17), it can be seen that indeed the traction can be maintained. The drop in transmission output torque ("loss of traction") is avoided in the gearshift in Figure 4.22 despite the same gradient of the engine speed trajectory. The tracking of the reference engine speed profile is also satisfactory.

Comparing the profile of longitudinal vehicle acceleration and jerk of the downshift executed with the proposed controller (from Figure 4.22) depicted in Figure 4.23, to that of the conventional clutch-to-clutch control strategy (Figure 4.19), it can be clearly seen that firstly, the jerk level in the torque phase is reduced from around 40m/s^3 (conventional control strategy) to around 18 m/s^3 (proposed control strategy) and secondly, the acceleration and jerk profiles do

not show any kind of torque vibrations at the end of the downshift. Also, the vehicle acceleration remains positive throughout the whole downshift indicating that engine power is transmitted to the wheels without interruption. However, compared to the vehicle jerk values observed for upshifts (and proposed control strategy), the level of vehicle jerk in Figure 4.23 (proposed downshift control strategy) is still quite high. In order to reduce this jerk level further a remedy will be proposed in the Chapter 5.

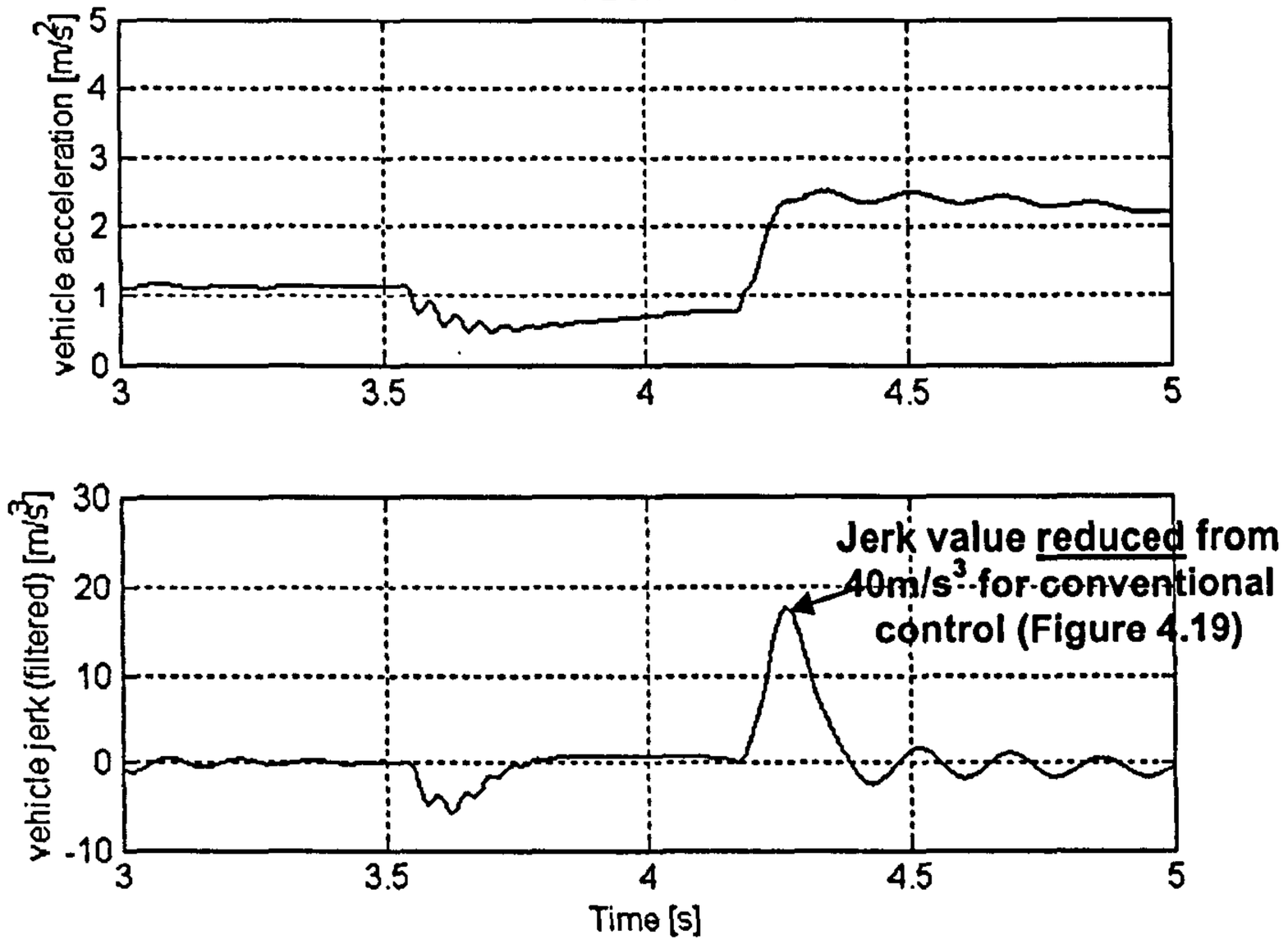

Figure 4.23 Vehicle acceleration and jerk for the downshift from Figure 4.22

Figure 4.24 depicts the downshift from Figure 4.22, however, with the inertia phase reduced by 0.25 seconds. This can be achieved if a steeper engine speed reference trajectory is selected in the inertia phase. Of course, since the throttle angle is already at its maximum value in the inertia phase, this means that the speed controller has to decrease the pressure at the offgoing clutch to a larger extent than in the downshift shown in Figure 4.22. This leads, of course, also to a larger drop in transmission output torque as can be seen from the transmission output torque profile in Figure 4.24. As a consequence of the steeper reference speed trajectory, the level of the vehicle acceleration is lower in the inertia phase and the vehicle jerk is increased both in the inertia phase and the torque phase.

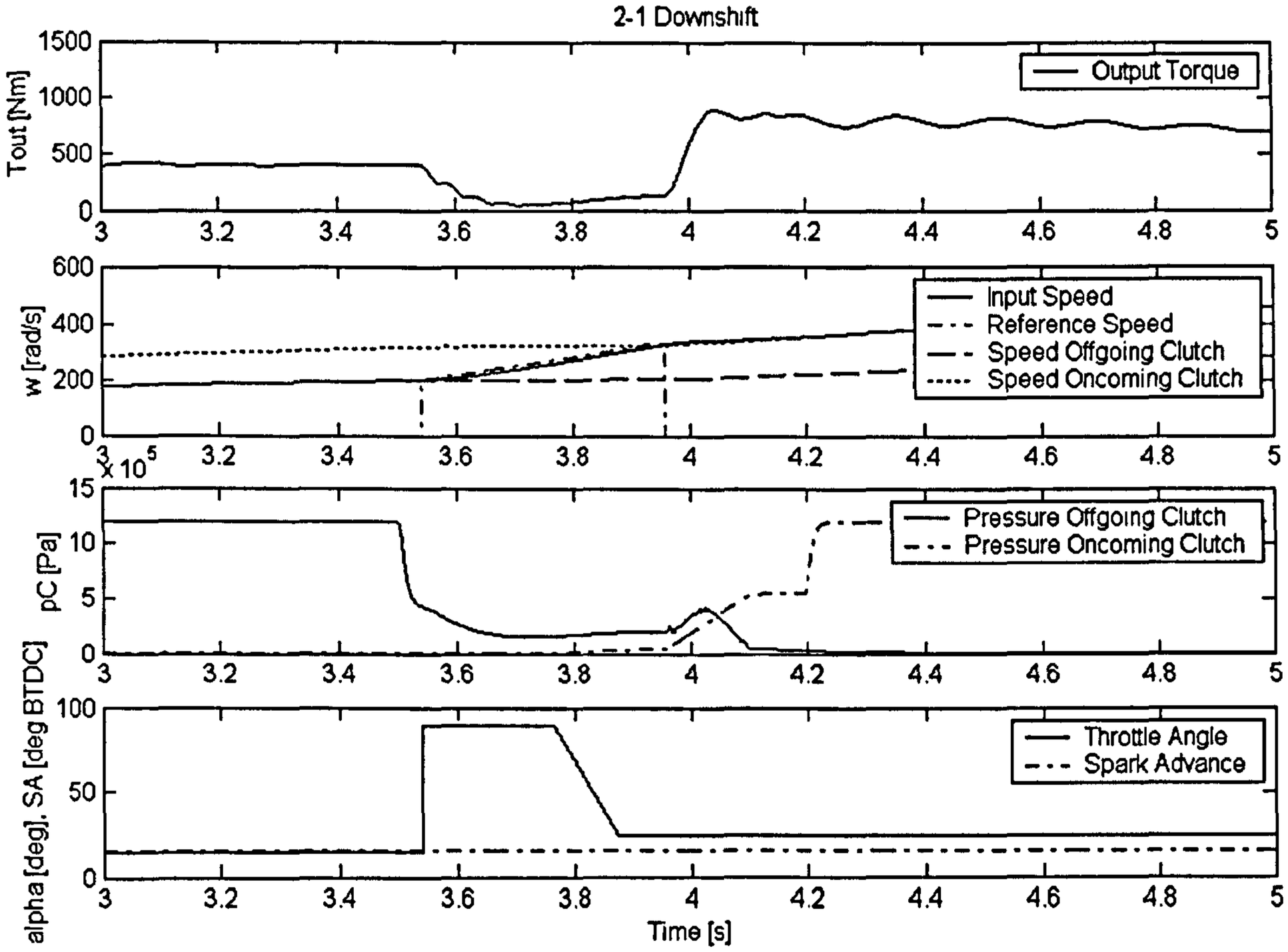

Figure 4.24 Simulation result: Proposed downshift control strategy, power-on downshift from Figure 4.22 with inertia phase reduced by 0.25 seconds

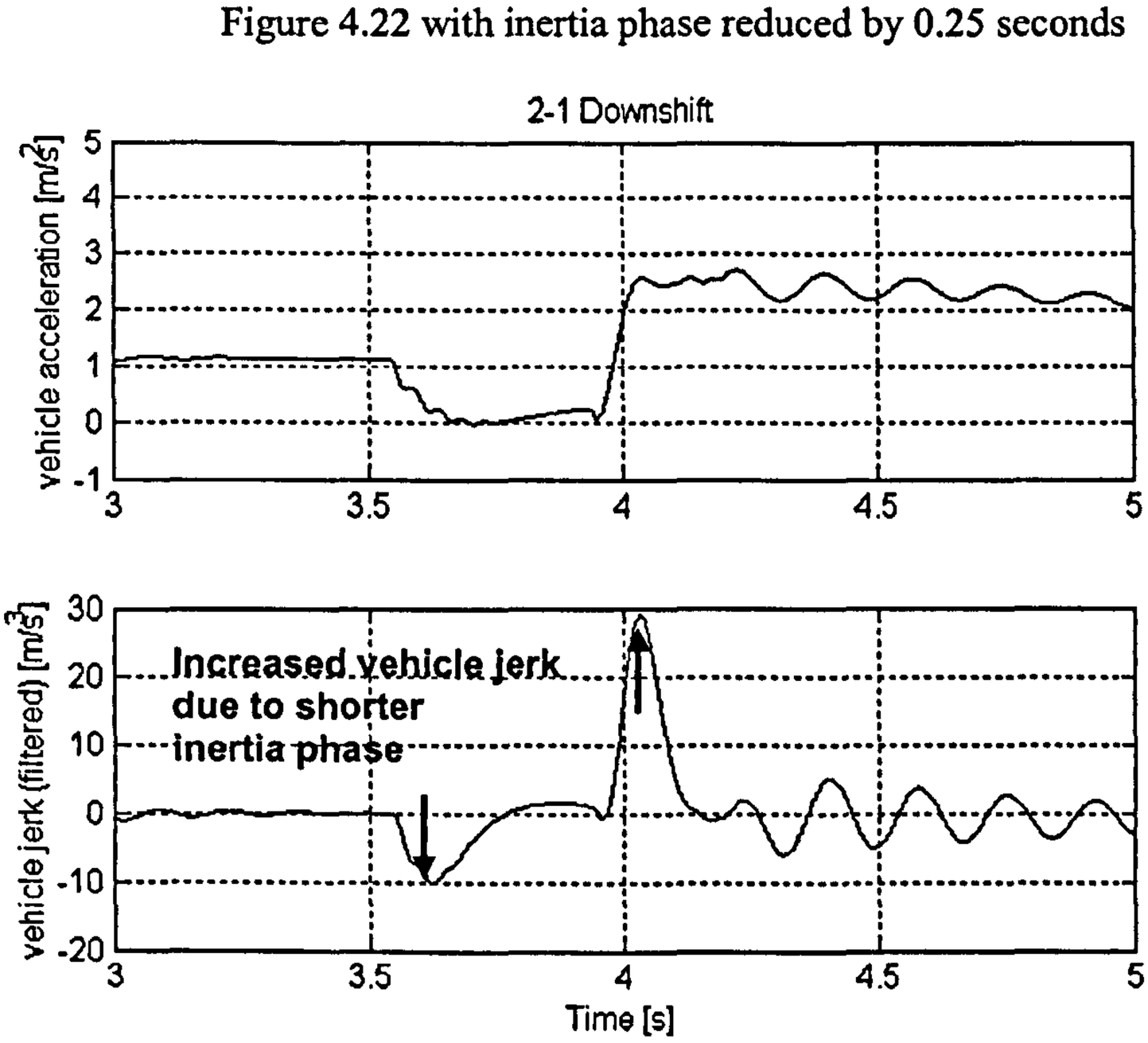

Figure 4.25 Vehicle acceleration and jerk for the downshift from Figure 4.24

This situation is illustrated in Figure 4.25, which shows vehicle acceleration and jerk for the downshift in Figure 4.24. In particular, the level of vehicle jerk in the torque phase is high (around 30 m/s^3) which is detrimental to shift quality. Again, Chapter 5 discusses a possible way to improve this problem.

Figure 4.26 depicts a downshift from 3rd to 2nd gear at medium throttle (40 degrees throttle angle) and a vehicle speed of around 20km/h. A good tracking performance can be observed in the inertia phase. The torque profile reveals small vibrations at the end of the gearshift when the oncoming clutch locks up. However, since the damping in the powertrain (-model) is one of the parameters of the model that are difficult to know exactly and since the damping in the powertrain model used in this work are chosen to be rather on the conservative side, it is believed that small vibrations in the simulation results cannot be taken as indicator for poor shift quality.

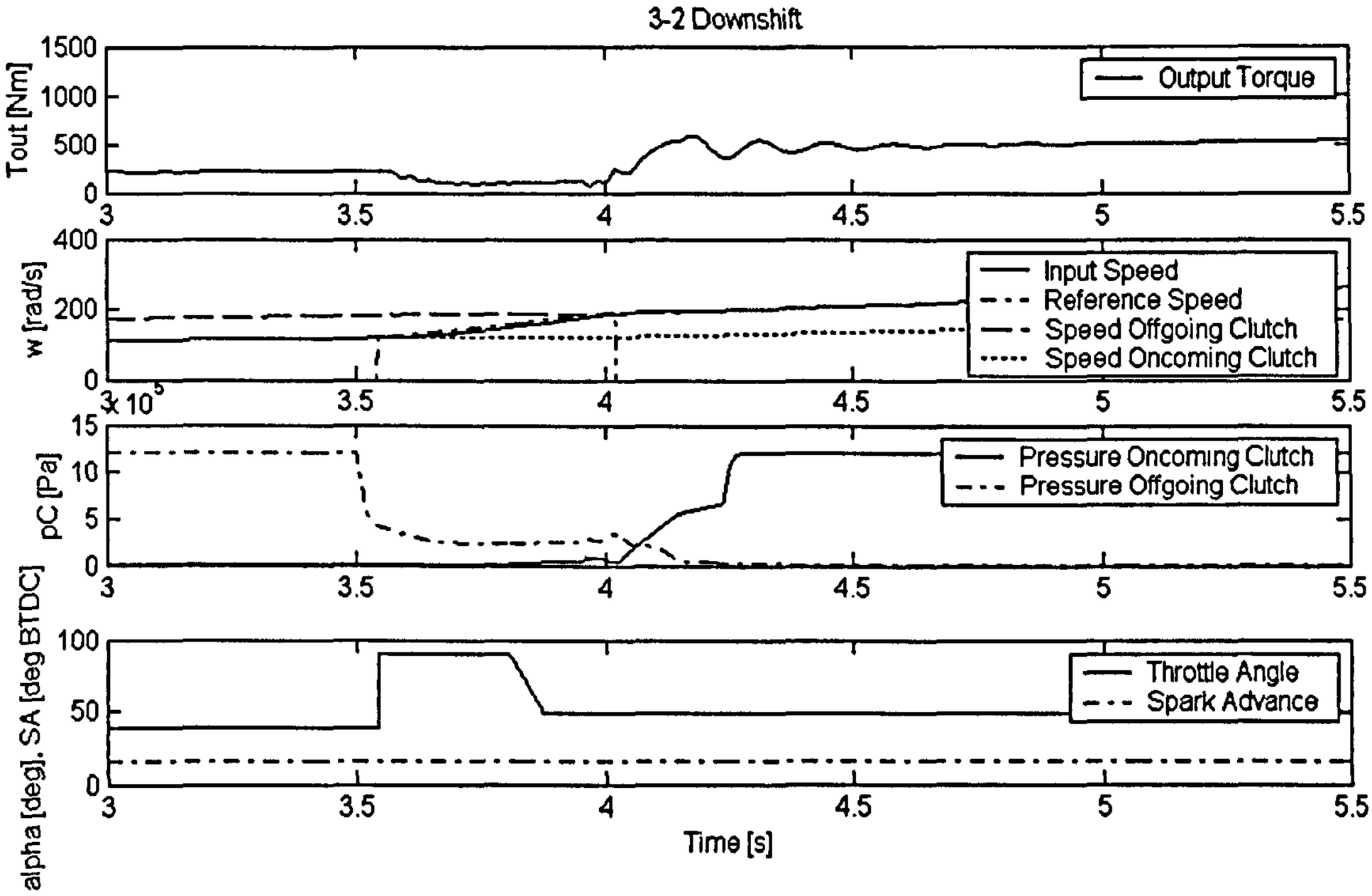

Figure 4.26 Simulation result: Proposed downshift control strategy, power-on downshift from 3rd to 2nd gear, medium throttle, at around 20 km/h

Figure 4.27 depicts a downshift from 4th to 3rd gear at a throttle angle of 40 degrees and a vehicle speed of around 40 km/h. Again, tracking of the engine speed reference profile is good. The output torque profile of Figure 4.27, however, reveals a sharp but small rise at the beginning of the torque phase, which then becomes smoother as the torque phase proceeds. Almost no torque vibration can be discerned. How the shift quality and shape of the

transmission output torque profile can be improved in the torque phase of the power-on downshift is part of Chapter 5.

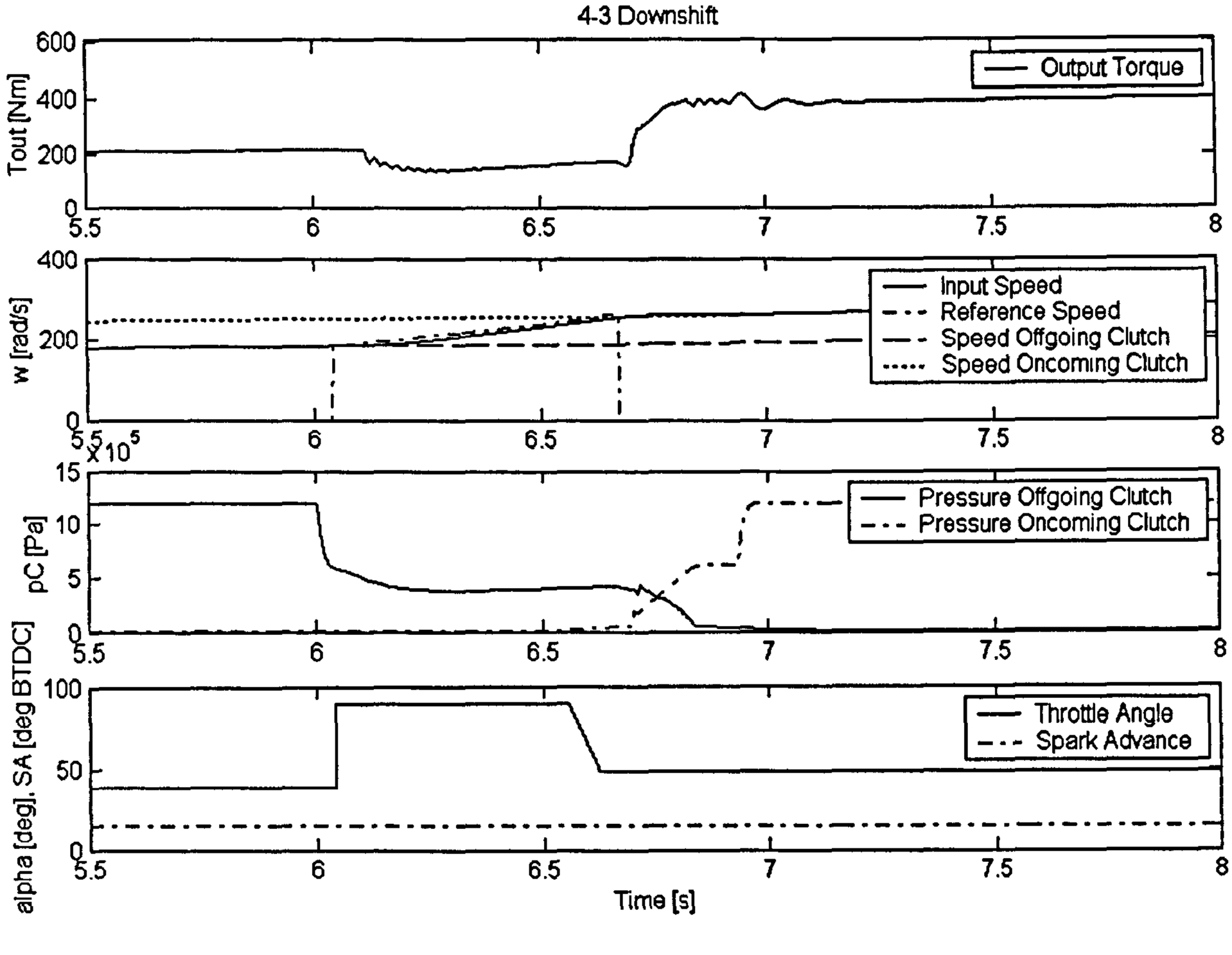

Figure 4.27 Simulation result: Proposed downshift control strategy, power-on downshift from 4th to 3rd gear, medium throttle, at around 40 km/h

4.3 Control of Power-Off Shifts on Twin Clutch Transmissions

As already discussed, power-off clutch-to-clutch gearshifts are less critical in terms of shift quality compared to power-on shifts. Nevertheless, a brief discussion of how the control elements developed in the last section for power-on gearshifts can be applied to the control of power-off gearshifts is presented in this section. The power-off shift control explained in this section is also of clutch-to-clutch shift type. A similar control strategy is treated, in principle, in [Patent DE 196 31 983 C1 1998 and Patent DE 19939334 A1 2001]. This section demonstrates the detailed development and the successful implementation of such a power-off gearshift control.

4.3.1 Control of Power-off Upshifts

As mentioned before, power-off upshifts can, in principle, be controlled as power-on downshifts. On power-off gearshifts power is transferred from the wheels to the engine. The engine provides a brake torque to decelerate the vehicle. This circumstance is often desired, in particular, in cases where a deceleration of a vehicle is required without application of the vehicle brakes (long descents, braking on motorway exits, etc.).

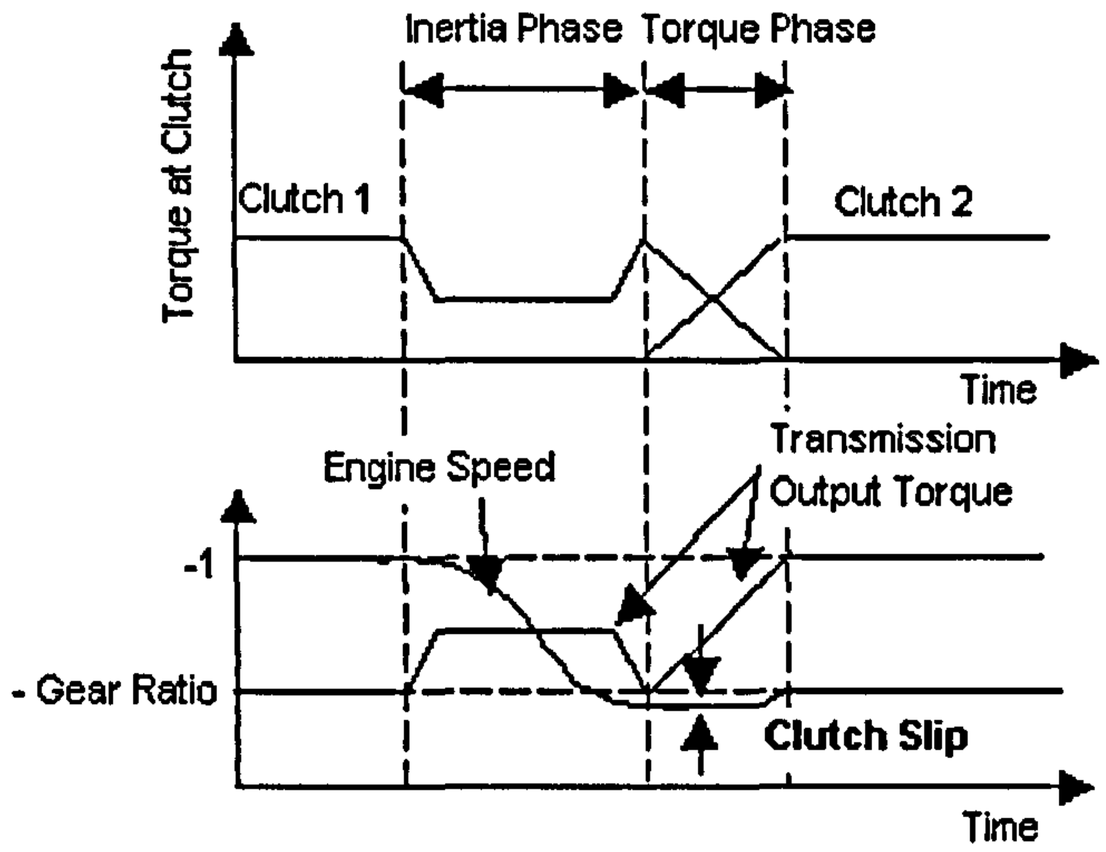

Figure 4.28 Principle of power-off upshift control strategy

Therefore it is important that the braking capability of the vehicle is maintained throughout the gearshift. This also ensures that the transmission output trajectory is in general smooth (no abrupt disconnection of the engine from the wheels), providing good shift quality. The principle of the power-off upshift control strategy is depicted in Figure 4.28. It works without engine involvement in the inertia phase since the engine torque is already at its minimum and hence engine torque cannot be reduced further to assist a deceleration of the engine to the speed level of the target gear. However, to assist the torque transfer in the torque phase, closed-loop clutch slip control is employed again.

As can be seen from Figure 4.28, the power-off upshift starts with the inertia phase, where similar to the power-on downshift, the offgoing clutch (clutch 1 in Figure 4.28) is brought to slip and a closed-loop speed controller controls the engine speed along a reference speed trajectory (linear decrease in speed to level of target gear). To allow a deceleration of the engine, the speed controller has to decrease the torque (i.e. pressure) at the offgoing clutch. This reduces the amount of power transferred from the wheels to the engine. As a consequence the (negative-) transmission output torque decreases and the vehicle braking is reduced (see Figure 4.28). At the synchronous speed of the target gear the clutch slip control is activated at the

offgoing clutch (similar to the power-on downshift control strategy). However, here the engine speed is controlled to stay slightly below (by the amount of clutch slip) the speed level of the target gear. After the engine torque has been transferred to the oncoming clutch (clutch 2 in Figure 4.28), the (negative-) transmission output torque falls to the level of the target gear (lower gear ratio means smaller negative torque) and the power-off upshift ends.

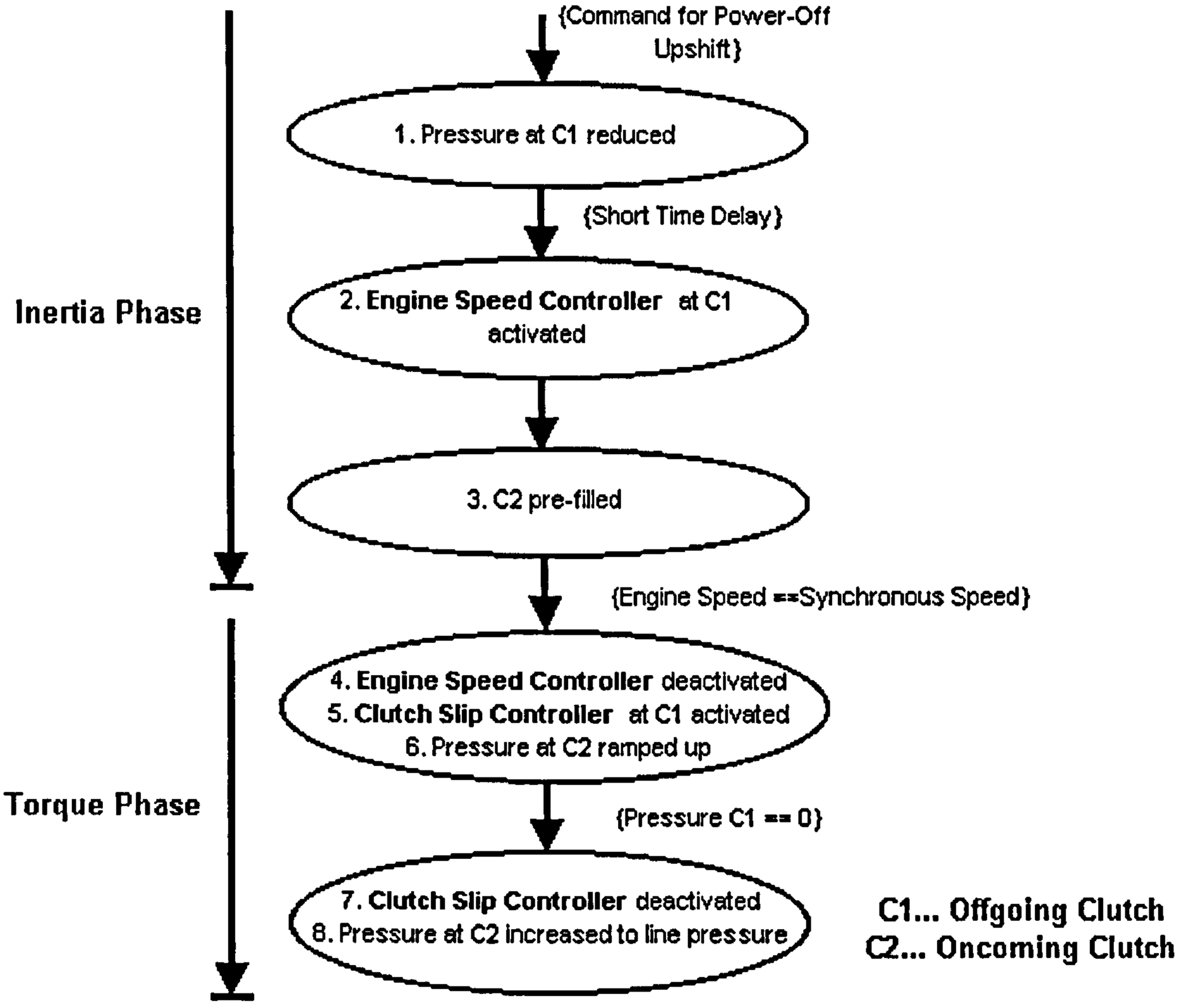

Figure 4.29 Control algorithm of clutch-to-clutch control strategy for power-off upshifts on twin clutch transmissions

Although the control algorithm for power-off upshifts is similar to that of the power-on downshift (excluding the increase in throttle angle), it is depicted in Figure 4.29 for the sake of completeness. Since the control algorithm of power-off upshifts depicted in Figure 4.29 is essentially the same in operation as that of power-on downshifts (excluding the throttle manipulation), the explanations apply similarly and will not be given again here.

Figure 4.30 shows a power-off upshift from 2nd to 3rd gear at around 20 km/h. The necessary decrease in pressure at the offgoing clutch, at the beginning of the inertia phase, to start a

deceleration of the engine, results to a slight decrease in the (negative-) transmission output torque (as also illustrated in Figure 4.28). Although this means reduced engine braking, the power transfer between wheels and engine is not interrupted. Tracking of the reference speed profile is acceptable, only at the end of the inertia phase the engine speed deviates from the reference profile. This is due to the fact that the output of the speed controller was limited to (to avoid a large decrease in pressure and thus engine braking). A gentler gradient of the reference speed trajectory would have avoided this problem, however, at the cost of increased shift time. The torque fluctuation at the end of the gearshift comes from lock-up of the oncoming clutch and is due to a difference in the clutch torque between the state of slipping and the state of sticking and is difficult to eliminate.

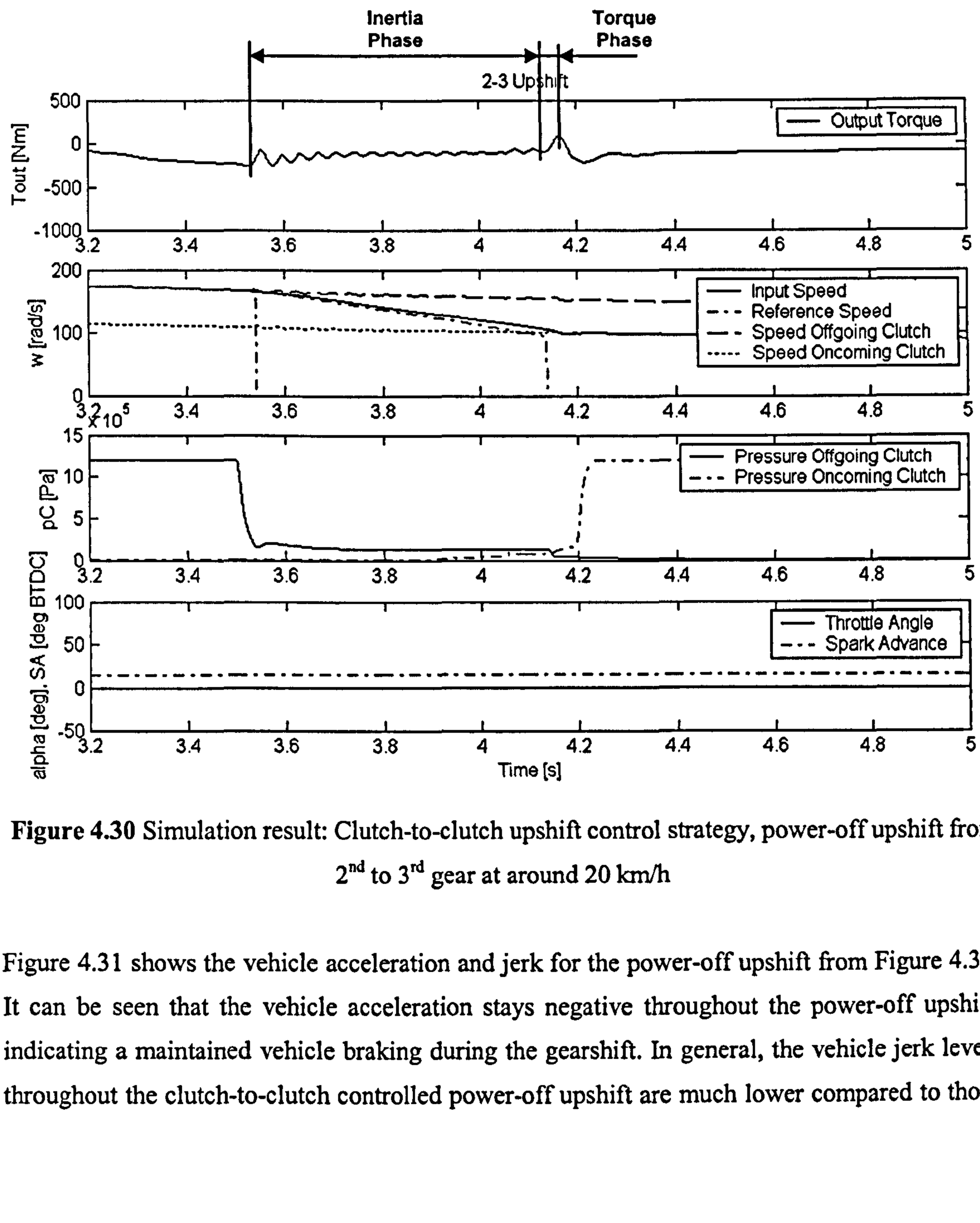

Figure 4.30 Simulation result: Clutch-to-clutch upshift control strategy, power-off upshift from 2^{nd} to 3^{rd} gear at around 20 km/h

Figure 4.31 shows the vehicle acceleration and jerk for the power-off upshift from Figure 4.30. It can be seen that the vehicle acceleration stays negative throughout the power-off upshift, indicating a maintained vehicle braking during the gearshift. In general, the vehicle jerk levels throughout the clutch-to-clutch controlled power-off upshift are much lower compared to those

of the clutch-to-clutch controlled power-on upshift. The only area of increased vehicle jerk is at the end of the upshift when the oncoming clutch locks up.

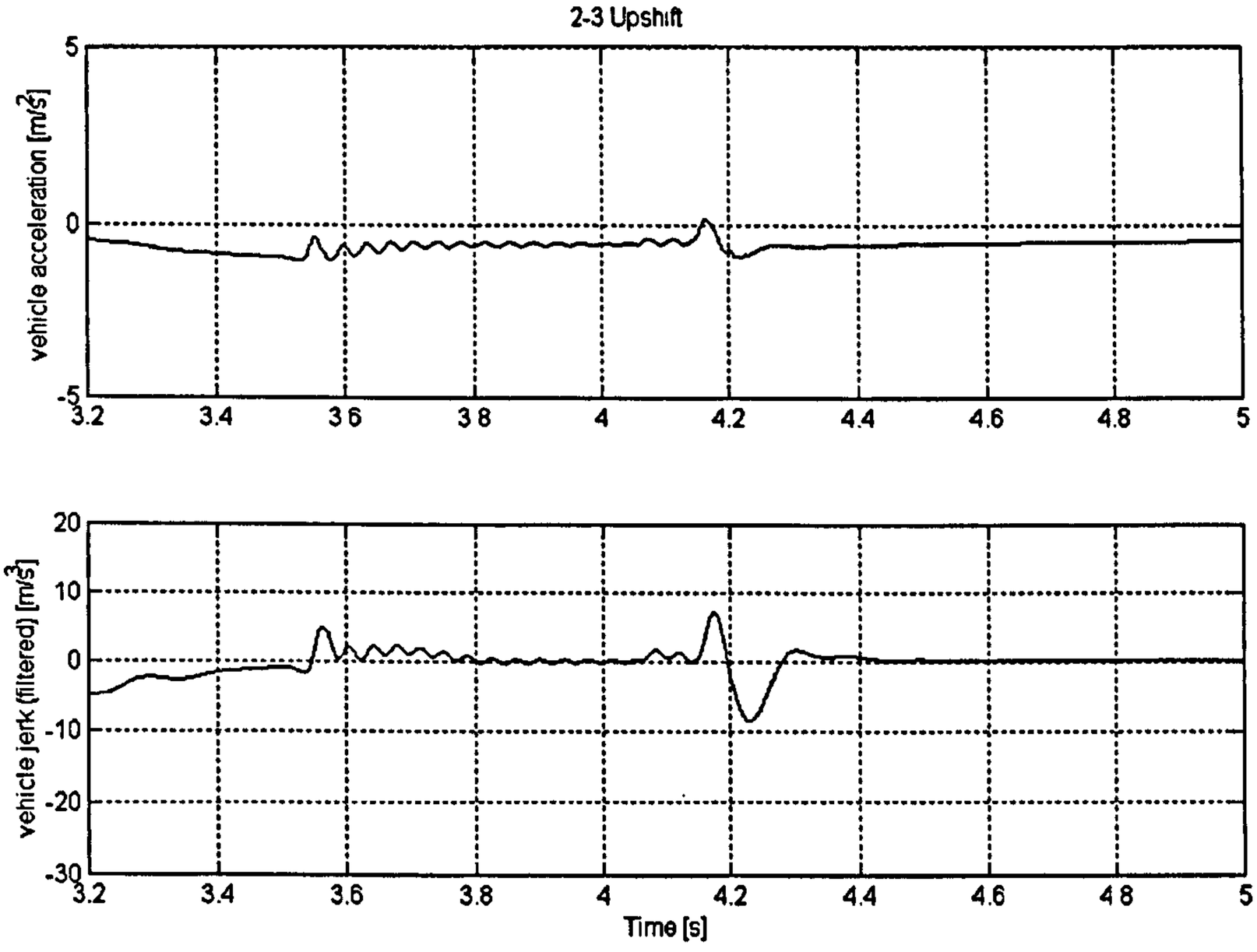

Figure 4.31 Vehicle acceleration and jerk for power-off upshift from Figure 4.30

However, this phenomenon is difficult to control and is governed by the profile of the friction coefficient in the vicinity of zero slipping speed and the difference between static and kinetic friction coefficient at that point.

4.3.2 Control of Power-off Downshifts

Power-off downshifts can, in principle, be controlled in the same way as power-on upshifts. Again, it is desirably to keep the transmission output torque profile as smooth as possibly thus providing good shift quality and undisturbed engine braking at the wheels (wheels drive engine when the vehicle is coasting).

The principle of the power-off downshift control strategy is depicted in Figure 4.32. The transfer of engine torque in the torque phase is again managed by a closed-loop control of clutch slip at the offgoing clutch (clutch 1in Figure 4.32). The engine speed is controlled to a value (clutch slip reference value) slightly below the speed level of the presently engaged gear. The transfer of engine torque to the oncoming clutch (clutch 2 in Figure 4.32) causes the (negative-) transmission output torque to increase due to the change to a larger gear ratio.

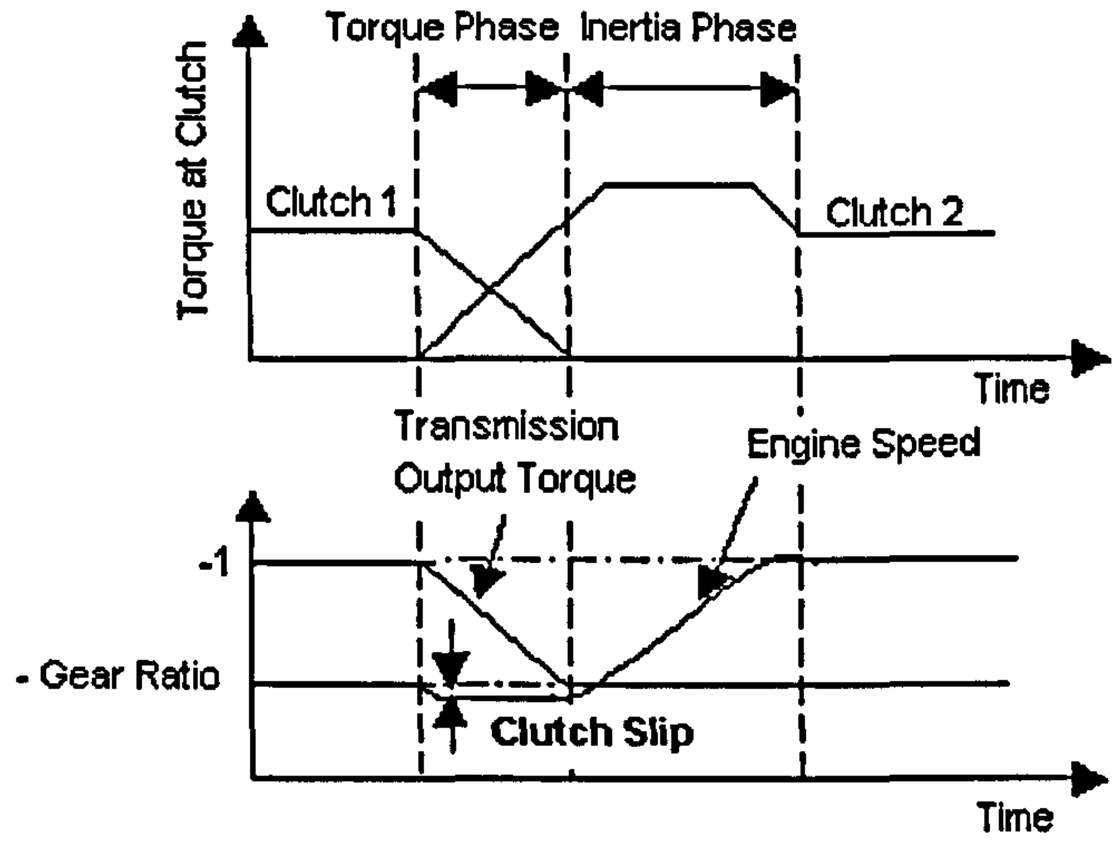

Figure 4.32 Principle of power-off downshift control strategy

A control of the inertia phase through modulation of engine variables (as used in the power-on upshift control strategy presented earlier) is possible, because in the inertia phase of a downshift the engine needs to be accelerated. This requires an increase in engine torque, which is possible when the vehicle is coasting.

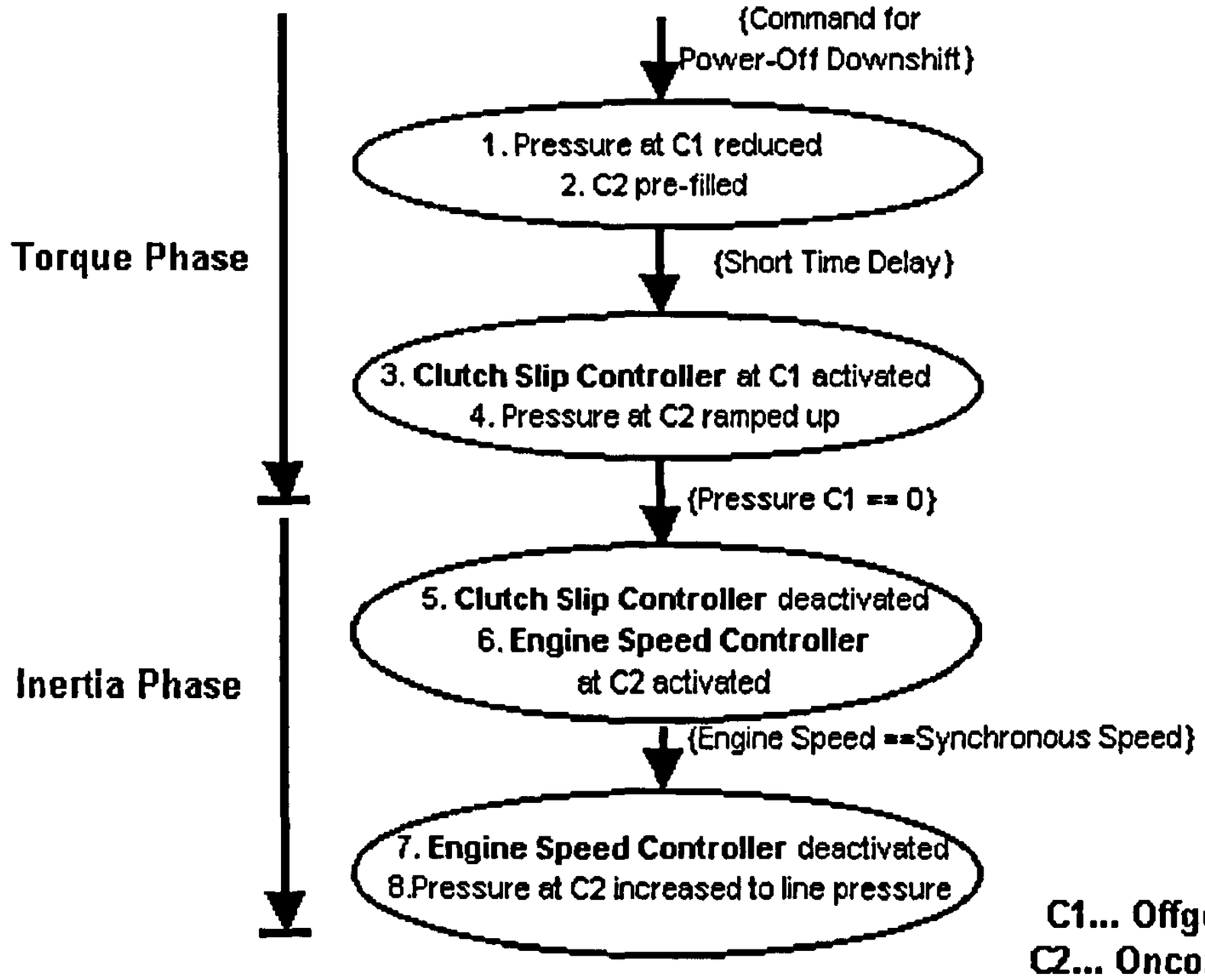

Figure 4.33 Control algorithm of clutch-to-clutch control strategy for power-off downshifts on twin clutch transmissions

However, the tracking performance with such an engine-based speed control is poor due to the slow response of the engine to changes in the throttle angle. For this reason the inertia phase of the power-off downshift was controlled through manipulation of clutch pressure only.

The control algorithm for power-off downshifts is depicted in Figure 4.33 and will not be explained in detail because of its similarity to that of power-on upshifts. The only difference is that the closed-loop speed control through manipulation of engine variables is substituted by a closed-loop speed control through manipulation of clutch pressure. As will be seen this does not have the same drastic negative effect as for power-on upshifts.

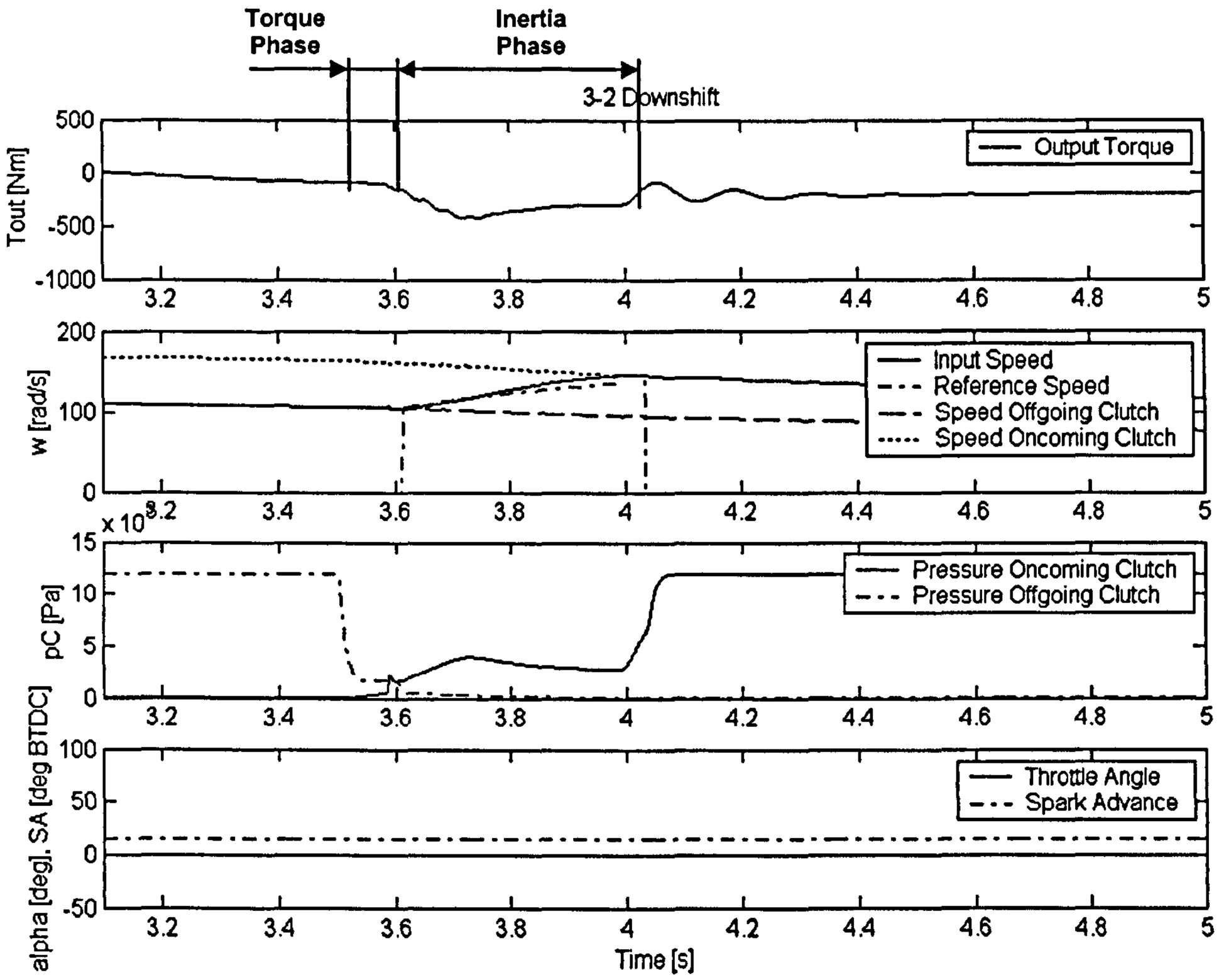

Figure 4.34 Simulation result: Clutch-to-clutch downshift control strategy, power-off downshift from 3rd to 2nd gear at around 18 km/h

A simulation result of the power-off downshift control strategy is depicted in Figure 4.34 showing a power-off downshift from 3rd to 2nd gear. The pressure at the offgoing clutch is reduced to a very low level at the beginning of the torque phase in order to aid the subsequently activated slip controller. The actual torque phase is very short and the pressure at the oncoming clutch has to be raised barely above the filling pressure. In the first half of the inertia phase the speed controller raises the pressure at the oncoming clutch to allow acceleration of the engine (more torque is transferred from the wheels to the engine). This causes the transmission output

torque to become more negative. In the second half of the inertia phase, the speed controller decreases the pressure again to slow acceleration of the engine and to keep the engine to the reference speed profile, hence, the negative transmission output torque decreases again. The tracking performance is acceptable, only at the end of the inertia phase a small tracking error can be observed. A better tuning of the speed controller could improve this situation.

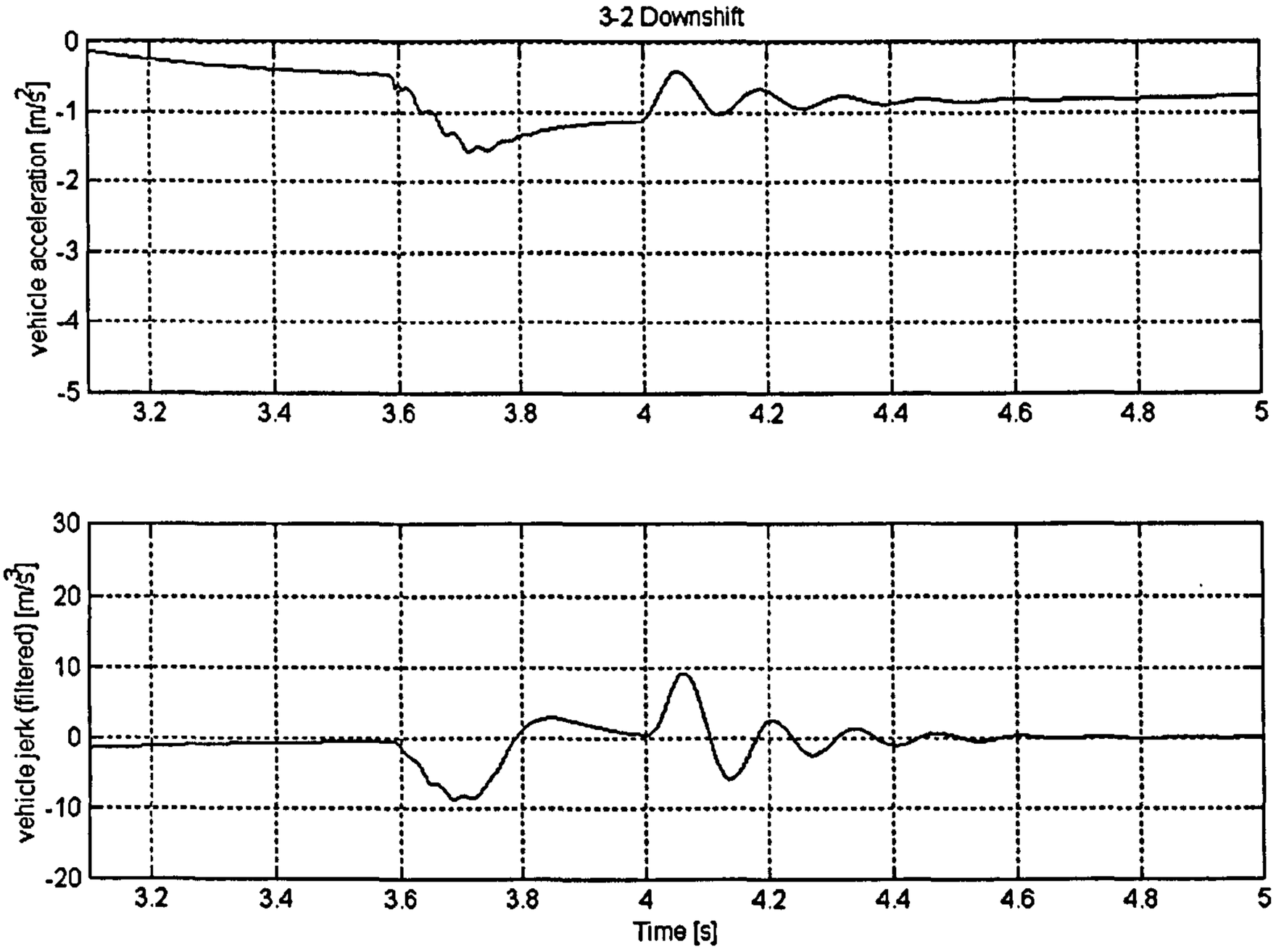

Figure 4.35 Vehicle acceleration and jerk for the power-off downshift from Figure 4.34

The whole power-off downshift only takes around 0.4 seconds, yet still the vehicle jerk (Figure 4.35) is relatively low compared to power-on downshifts. Again, as was observed with the power-off upshift, the increased vehicle jerk at the end of the power-off downshift is a result of the oncoming clutch locking up and is closely connected to friction characteristics of the clutch.

4.4 Structure of the Proposed Integrated Powertrain Controller for Gearshifts

So far, only the operational principles and the according control algorithms (for upshifts and downshifts) of the integrated powertrain controller have been discussed. The control algorithms explained in Section 4.2 for power-on shifts and in Section 4.3 for power-off shifts, basically

determine the sequence of control actions that need to be accomplished throughout the gearshifts. This includes open-loop actions like decrease in clutch pressure (to bring the clutch to a point where it starts to slip), increase in throttle angle to aid engine synchronisation, etc. However, apart from open-loop control actions, the control algorithms also determine the point in time during the gearshift when a closed-loop control action has to be performed. The discussion of the layout of these control loops, the type of controller used in those control loops and the overall structure of the integrated powertrain controller for gearshifts is part of this section.

Figure 4.36 gives an overview of the structure of the integrated powertrain controller for gearshifts. The dash-dotted rectangle in Figure 4.36 contains all the elements of the gearshift controller. Small lines represent signal paths carrying a single signal whereas wide lines represent signal paths carrying more than one signal. A dotted line represents an optional signal.

The supervisory controller at the top of the figure contains the control algorithms for power-on/off upshift (Figure 4.9 and 4.29) and downshift (Figure 4.21 and 4.33). This supervisory controller determines when a closed-loop control should be active (On/Off signal in Figure 4.36). It furthermore produces the necessary reference values and trajectories for the speed and clutch slip controllers. The inputs to this unit are: engine speed, angular speeds at both input shafts (i.e. at outputs of both clutches) and, optional, the measurement values of the hydraulic pressure at both clutches. From information about these variables the timing and switching points of the single phases of the gearshifts (torque- and inertia phase) can be determined.

Although, the end of the torque phase was detected in the control algorithms from the signal of the actual (measured) pressure at the offgoing clutch, it was mentioned that this information could also be obtained from the clutch slip (change in sign). For this reason the feed back of the measurement signal of the hydraulic pressure at the clutch actuator to the input of the supervisory controller is optional and has, thus, been included in the figure as a dotted line. However, it was observed that the feedback of the measured clutch pressure produced better results in terms of detecting the end of the engine torque transfer correctly.

Apart from on/off signals and reference values for the controllers, the control algorithms also produce some open-loop outputs (reduction in pressure, increase in throttle angle, etc.). These outputs are shown at the left end of the supervisory controller block and the signals are added to the contributions of the closed-loop controls and to the values at normal operation. The values of throttle angle, spark advance and clutch pressure for normal operation are generated outside

the gearshift controller based on driver inputs, engine torque and speed etc., and are governing engine and transmission in all non-gearshift operation modes of the powertrain.

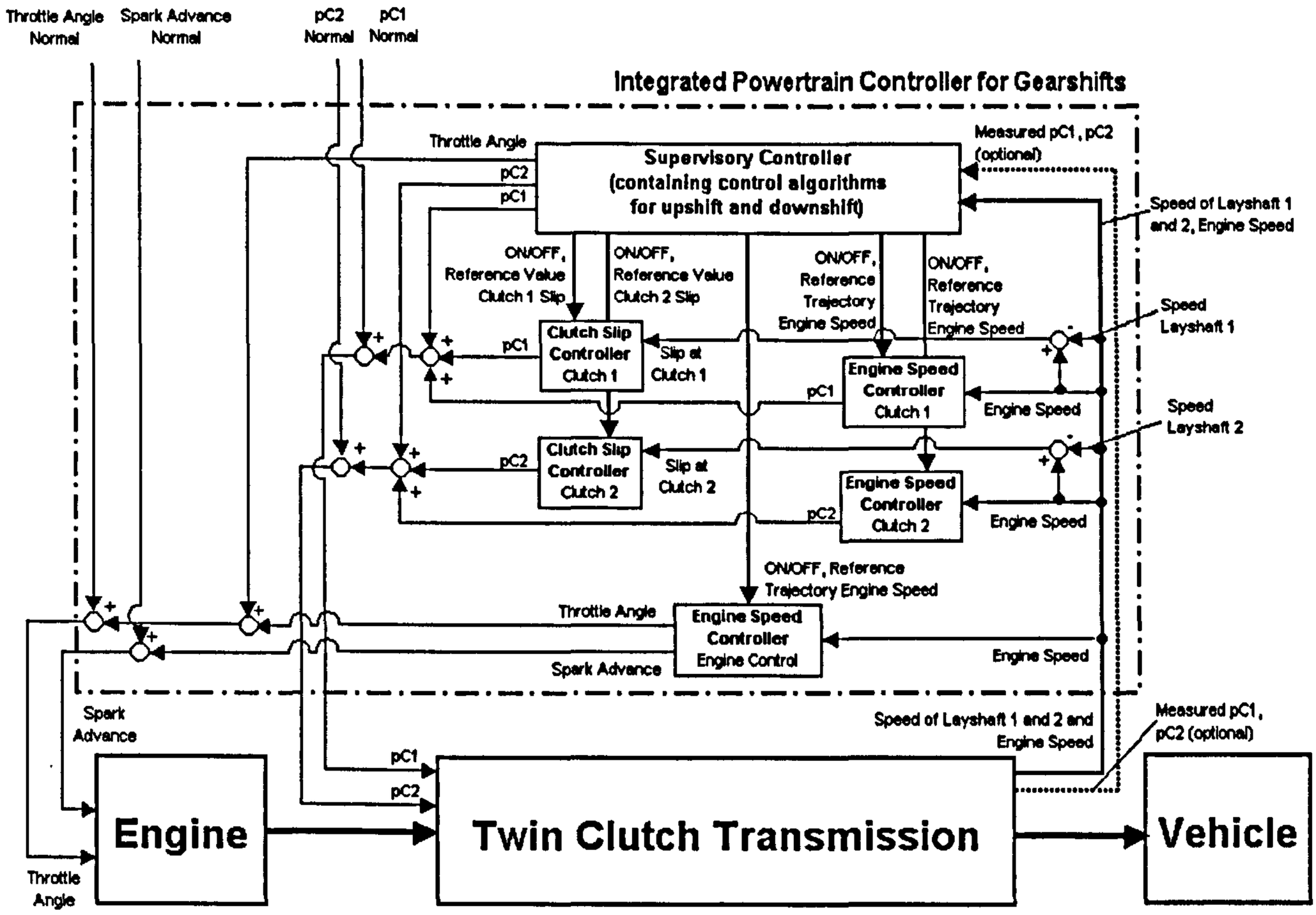

Figure 4.36 Structure of proposed integrated powertrain controller for gearshifts

The integrated powertrain controller for gearshifts includes five control loops: two clutch slip control-loops (one for each of the two clutches), two engine speed control loops manipulating clutch pressure (again one for each of the two clutches) and one engine speed control loop that manipulates engine controls (throttle angle and spark advance). The signals produced by the closed-loop controllers and the supervisory controller pictured in Figure 4.36, of course, only represent inputs to the actuators at the engine and transmission. The clutch pressure signals (pC1 and pC2 in Figure 4.36) are actually input voltages (v_{Sol} in Equation (35) in Chapter 3) to the solenoid valves of the hydraulic clutch actuators. Inputs to the clutch slip controllers are the clutch slip, calculated as difference between speed at the input (engine speed) and the output (speed of input shaft 1 or 2) of the clutch. Input to the engine speed controller is the engine speed, which is compared to the engine speed reference trajectory. Based on the control error an output (pressure, throttle angle spark advance) is generated by the controller, which is then added to the signal for normal operation.

The controllers were designed as digital controllers (digitised analog controllers) and are discussed in the following sections in more detail. The sampling rate used in the gearshift controller (including supervisory controller) was $T_S=5\cdot10^{-4}$ seconds, for an accurate signal reconstruction. Although usually part of a practical digital controller, anti-aliasing filter at the input of the closed-loop controllers were not considered here. The controllers were exclusively of Proportional-Integral-Derivative (PID) type and featured anti-wind up devices to avoid a wind-up of the integral part of the controller when the controller output saturates at the actuator input. PID controllers were selected in this work, because they are still the most widely applied type of controller in industry. Their control algorithm is easy to implement in an electronic powertrain control unit and furthermore offers some robustness to disturbances and small parameter variations. The tuning of the PID controllers was achieved by applying a mixture of a trial and error method and Ziegler-Nichols tuning rules (tuning rules that aim at 25% maximum overshoot in a step response, see e.g. [Ogata 1997]). The parameter values for the controller gains of the PID controllers described in the following sections can be found in the Appendix A.4.

4.4.1 Closed-Loop Clutch Slip Control

The clutch slip controller at clutch 1 and 2 is shown in more detail in Figure 4.37. The slip at the clutch is calculated as the difference between engine speed and angular speed at the output of the clutch (ω_{co} for clutch 1 and ω_{c2o} for clutch 2; see powertrain model Chapter 3). In practice, the difference between the signals ω_e or ω_c or ω_{c2} are insignificant, therefore the speed sensor can be positioned at any of these locations (see powertrain model Chapter 3).

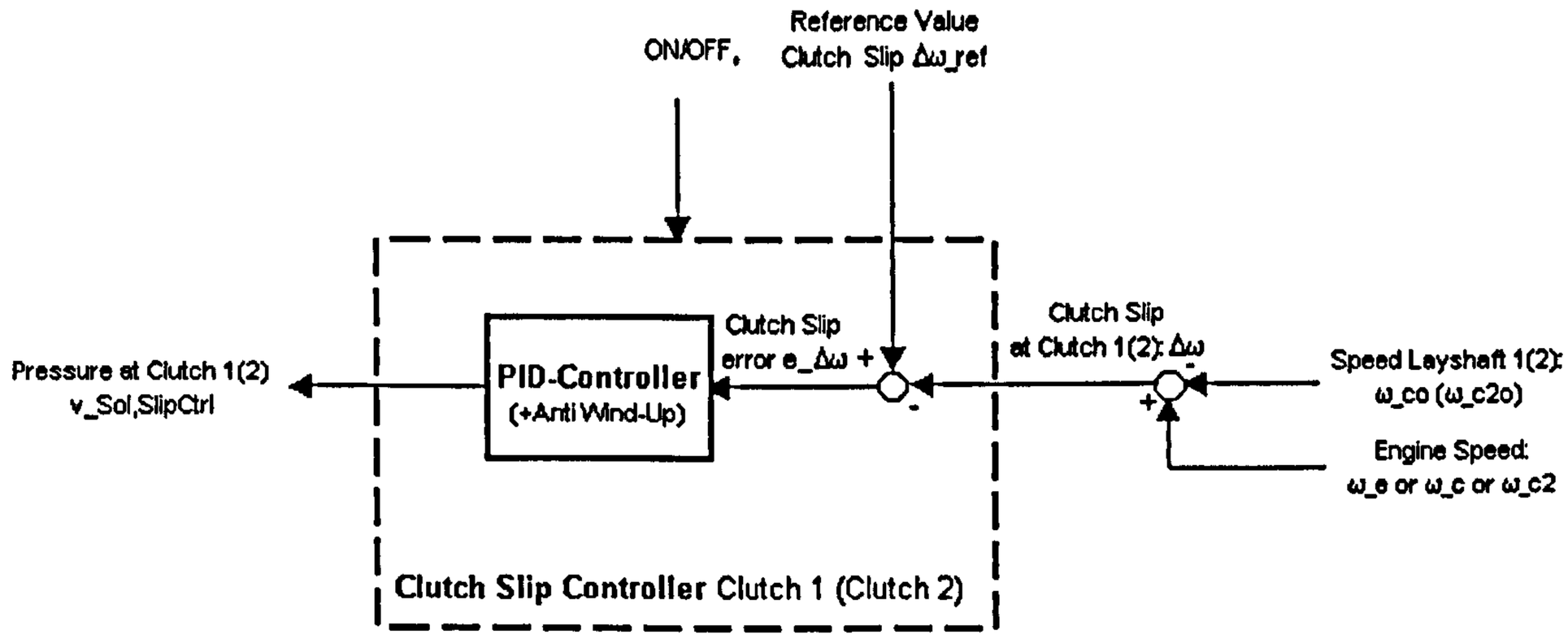

Figure 4.37 Detail of the clutch slip controller from Figure 4.36

Input to the PID controller inside the clutch slip controller is the clutch slip error $e_{\Delta\omega}$ (Equation (57)), which is calculated as the difference between the reference value for the clutch slip ($\Delta\omega_{ref}$) and the actual clutch slip $\Delta\omega$. The reference value for the clutch slip controllers was selected to be 5 rad/s. This reference value was found by experimenting with different values and was found to produce the best response and control behaviour of the clutch slip controller in the simulations (a similar value is also used in the literature see Chapter 2, Section 2.1.2, [Volkswagen AG 1998 Patent DE 196 31 983 C1]). The PID controller outputs a voltage signal to the according solenoid valve at the clutch ($v_{Sol,SlipCtrl}$). This controller output is processed according to equation (56) as a function of the clutch slip error. Equation (56) gives the equation of the PID controller in the s-domain without sample and hold units and with an idealised derivative term (the derivative was approximated in the simulation model).

$$v_{Sol,SlipCtrl}(s) = (K_p + \frac{K_i}{s} + sK_d)e_{\Delta\omega}(s) \tag{56}$$

where:

$$e_{\Delta\omega} = \Delta\omega_{ref} - \Delta\omega \tag{57}$$

4.4.2 Closed-Loop Engine Speed Control through Clutch Pressure Manipulation

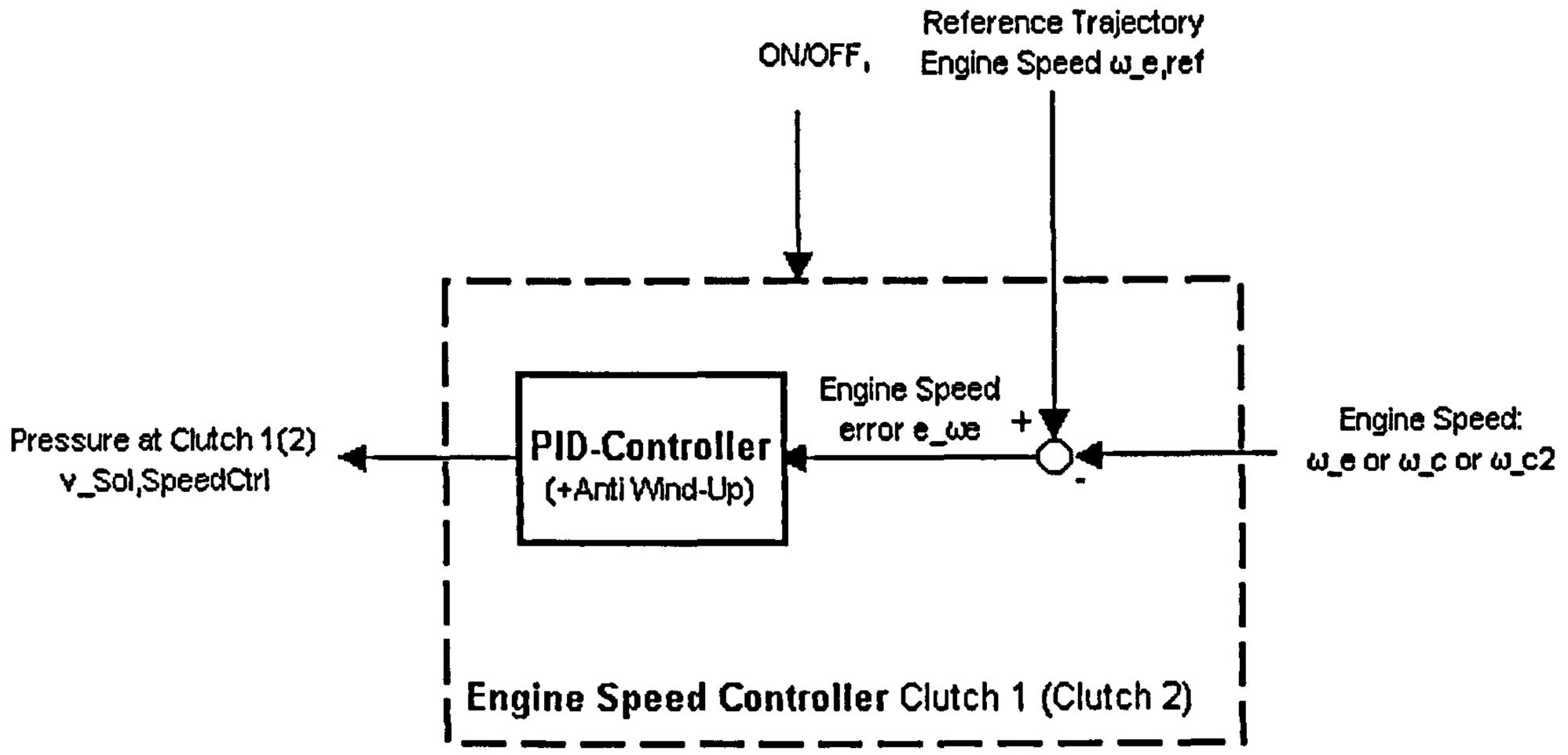

Figure 4.38 Detail of the engine speed controller (manipulation of clutch pressure) from Figure 4.36

The engine speed controller that operates with manipulation of clutch pressure at clutch 1 and 2 is depicted in more detail in Figure 4.38. The error in engine speed ($e_{\omega e}$) is calculated from the difference between engine speed (again any of the signals ω_e or ω_c or ω_{c2} may be used) and the reference trajectory for the engine speed $\omega_{e,ref}$.

The speed error (Equation (59) is inputted to the PID controller inside the engine speed controller. The output of the PID controller of the engine speed controller is a voltage signal to the solenoid valve at the according clutch ($v_{Sol,SpeedCtrl}$) and is processed according to equation (58) as a function of the engine speed error. Equation (58) gives the equation of the PID controller (engine speed controller) in the s-domain without sample and hold units.

$$v_{Sol,SpeedCtrl}(s) = (K_p + \frac{K_i}{s} + sK_d)e_{\omega e}(s) \tag{58}$$

$$e_{\omega e} = \omega_{e,ref} - \omega_e \tag{59}$$

For engine speed controller manipulating clutch pressure (all gearshift cases except power-on upshift) the engine speed reference trajectory was given by equation (60):

$$\omega_{e,ref} = \omega_{e,0} + (\omega_{co} + \Delta\omega_{ref} - \omega_{e,0})\frac{(t - t_{0,inertia})}{t_{inertia}} \tag{60}$$

This represents a linear increase (or with a change of signs in equation (60) a linear decrease for power-off upshifts) of engine speed during the inertia phase. This simple trajectory worked better for the power-on downshift (and power-off shifts) than the more complicated reference profile chosen for the power-on upshift. The reason for this is that, with a linear reference profile, the engine speed controller is able to bring the clutch to a state where its slips (necessary for fast engine synchronisation) more quickly. As already discussed the ideal profile for a power-on downshift would have been a linear lower part and a cosine-like upper part. The gentle gradient of the upper cosine-like part of the reference trajectory would have produced a

- smoother transition to the speed of the target gear (power-on downshift).

4.4.3 Closed-Loop Engine Speed Control through Manipulation of Engine Controls

The engine speed controller that manipulates engine controls (power-on upshift) is shown in more detail in Figure 4.39. The error in engine speed ($e_{\omega e}$) is again, in the same way as before, calculated from the difference between engine speed (again any of the signals ω_e or ω_c or ω_{c2} may be used) and the reference trajectory for the engine speed $\omega_{e,ref}$.

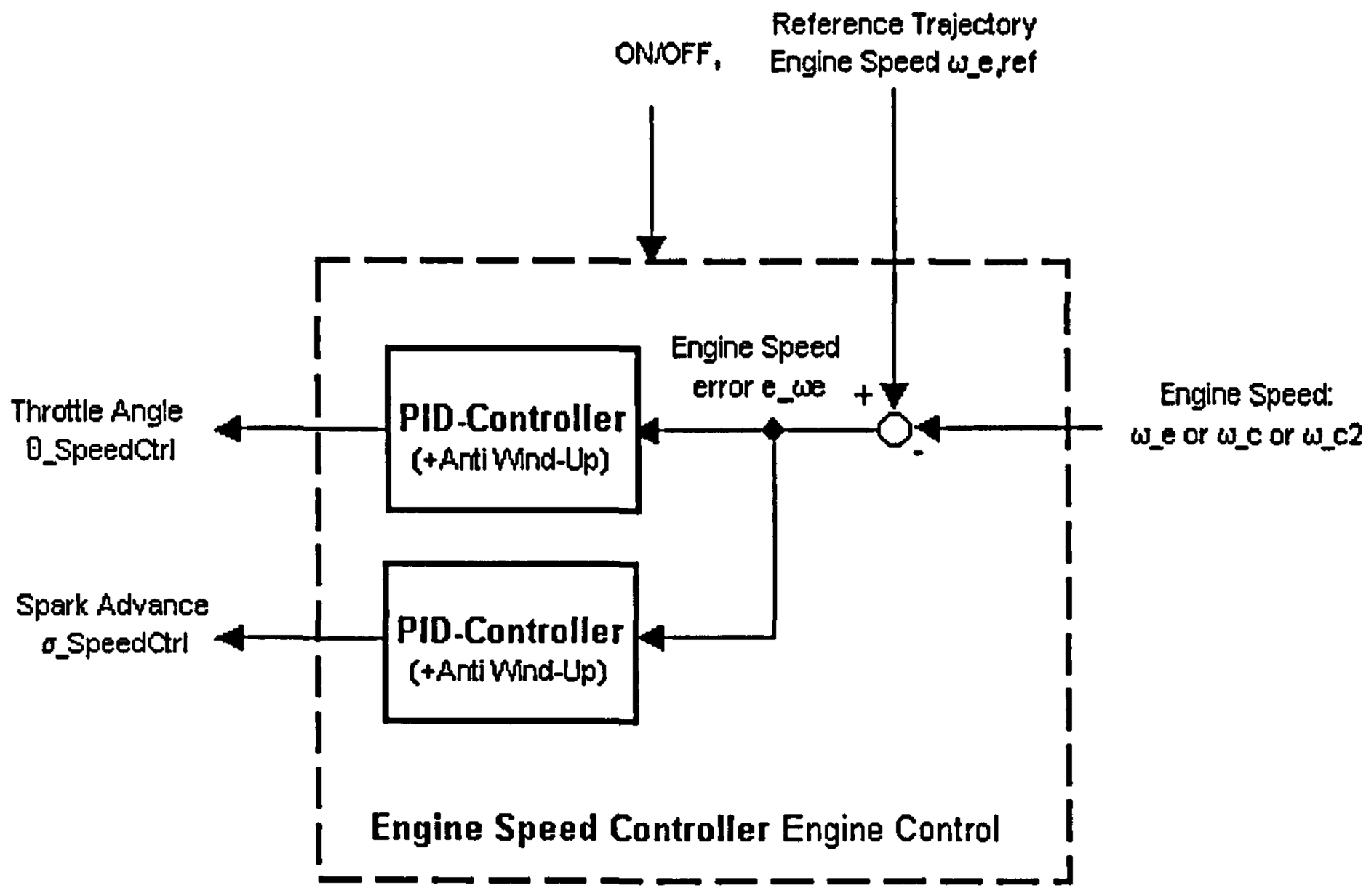

Figure 4.39 Detail of the engine speed controller (manipulation of engine controls) from Figure 4.36

Again, the speed error (Equation (59) serves as input to the PID controllers inside the engine speed controller. However, this time two PID controllers are employed; the first PID controller manipulates the throttle angle ($\theta_{SpeedCtrl}$) according to equation (61) and the second PID controller manipulates spark adavance ($\sigma_{SpeedCtrl}$) according equation (62) (both controller equations are given for the s-domain without sample and hold units).

$$\theta_{SpeedCtrl}(s) = (K_p + \frac{K_i}{s} + sK_d)e_{\omega e}(s) \tag{61}$$

$$\sigma_{SpeedCtrl}(s) = (K_p + \frac{K_i}{s} + sK_d)e_{\omega e}(s) \tag{62}$$

For the engine speed controller with manipulation of engine controls (power-on upshift) the engine speed reference trajectory was given by equation (63):

$$\omega_{e,ref} = \omega_{e,0} - \frac{(\omega_{e,0} - \omega_{co})}{2}\left(1 - \cos\left(\frac{\pi(t - t_{0,inertia})}{t_{inertia}}\right)\right) \tag{63}$$

The cosine function in the reference trajectory was employed to obtain a gentler gradient in the engine speed trajectory at the points where the engine deceleration starts and ends. Thus, no abrupt change of deceleration of the engine takes place at these points, which helps to avoid increased vehicle jerk values at the transition between torque and inertia phase and at the end of the shift when the oncoming clutch locks up.

4.5 Investigation into Robustness of the Proposed Integrated Powertrain Controller for Gearshifts

Three main sources influence the robustness of the developed integrated powertrain control for gearshifts:

- **A change in the parameters of the powertrain (-model)**

  A variation of powertrain parameters needs to be investigated because of two reasons: Some of the powertrain parameters may change due to the selection of components (engine, transmission, etc.) having different performance and design specifications (different engine inertia, different dimensions of parts in the transmission, different vehicle mass, etc.). The other reason is that modelling errors can occur in the powertrain model (assumption of damping rates etc.)

- **A change in the friction coefficient**

  This is very important since a change in the friction coefficient (in particular the gradient with slipping speed) can occur, during operation of the clutches on a gearshift. This might happen due to a change in the clutch temperature, due to clutch wear etc. Strictly speaking, this can be also considered as a change in a powertrain parameter. However, due to the importance to the performance of the gearshift controller it will be treated separately.

- **Disturbance due to sensor noise**

  This is an important source of disturbance to the measured variables that are inputted to the controller(s).

The following three subsections will investigate the robustness of the proposed gearshift controller to these three main sources of disturbances.

4.5.1 Robustness to Parameter Changes

As a first step, the parameters that influence the dynamic behaviour of the powertrain most (during a gearshifts), need to be identified. Table 4.2 lists the parameters of the powertrain model that were varied and includes the range of variation.

Varied Parameter - Powertrain Model	**Lower Value**	**Upper Value**
Engine Inertia J_e [kgm^2]	0.08	0.25
Reduced Inertia of Transmission Half 1(2) $J_{eff,In1(2)}$ / $J_{out1(2)}$ [kgm^2]	0.0001/0.0005	0.002/0.0025
Inertia of Differential J_{Diff} [kgm^2]	0.012	0.25
Inertia of Wheels (pair) J_{wheels}[kgm^2] / Vehicle Mass $m_{vehicle}$ [kg]	0.5/500	1.8/2000
Damping due to Transmission Drag $c_{C1(2)in,out}$,$c_{S1(2)in,out}$,c_{Diff} [Nms/rad]	0.0001	0.04
Relative Damping in Shafts of Transmission c_{12},$c_{in1(2)}$,$c_{out1(2)}$ [Nms/rad]	0.05	10
Relative Damping in Driveshafts c_{drive} [Nms/rad]	0.5	100
Relative Damping of Tyres c_{tyres} [Nms/rad]	5	500
Stiffness of Shafts in the Transmission k_{12},$k_{In1(2)}$,$k_{Out1(2)}$ [Nm/rad]	50000	500000
Stiffness of Driveshafts k_{drive} [Nm/rad]	35000	150000
Stiffness of Tyres k_{tyres} [Nm/rad]	100000	400000

Table 4.2 List of varied powertrain model parameters and range of variation

The range of variation (upper and lower bounds) was chosen arbitrarily. However, both end values were selected to still represent reasonable and realistic values. The parameter values used as normal values in the powertrain model are listed in the Appendix A.4.

From Table 4.2 it can be seen, that most of the parameters were varied over a broad range of values. However, only some of these parameter variations did seem to have a major influence on the dynamic behaviour of the powertrain model. A variation in the following model parameters (or combined variation of more parameters) did seem to have a significant influence on the dynamics of a gearshift:

- Engine inertia
- Damping of shafts in the transmission, driveshafts and tyres and drag
- Stiffness of driveshafts

Of course, a variation in the vehicle mass (and inertia of wheels) and the transmission drag did change the gradient of the vehicle acceleration trajectory, but did not significantly influence the dynamics of the gearshift.

The first parameter, the engine inertia, did influence the tracking performance of the engine speed controller in the inertia phase on both, upshifts and downshifts. However, this effect was only observed when the engine inertia was increased (A decrease in the engine inertia did not have a significant effect). The larger engine inertia caused the engine speed controllers to saturate at their lower limits and any decrease in the manipulated variables (engine controls or clutch pressure) beyond that limit could not be accomplished. However, the problem of increased engine inertia can be simply accounted for by selecting a gentler engine speed reference trajectory, thus increasing the length in time of the inertia phase and hence requiring a less severe change in the manipulated variables. The performance of the clutch slip controller did not seem to be affected at all by the change in engine inertia.

The second parameter variation that was identified to influence the performance of the gearshift controller most was found to be a decrease in the values of the damping rates in the transmission, driveshafts and tyres (An increase was not found to have a major influence). In particular, a combined decrease in every damping rate value (transmission drag, relative damping in transmission, damping of driveshafts and tyres) to the lower limits listed in Table 4.2 was identified to have the strongest effect on controller performance. This combined reduction in damping values will be investigated now for upshifts and downshifts.

Figure 4.40 shows a simulation results for an upshift from 1st to 2nd gear with the damping rates in the powertrain model reduced to their lower limits according to Table 4.2. The performance of the clutch slip controller seems fine. On first sight, the tracking performance of the engine speed controller also looks acceptable. However, at the end of the upshift strong torque vibrations can be observed (dashed circle in uppermost graph in Figure 4.40). These torque

vibrations are of course even more increased due to the low damping in the powertrain model. As source of those vibrations, oscillations in the manipulated variables (throttle angle and spark advance) can be identified (dotted circle in bottom graph of Figure 4.40). These control variable oscillations indicate that the speed controller reaches its stability limit. As a result, the tracking of the engine speed reference trajectory at the end of the inertia phase becomes poor, causing a harsh transition of the engine speed to the speed of the target gear (To force a lock-up of the oncoming clutch at the end of the gearshift despite the torque vibrations, the pressure was raised slightly before fully increasing it to the line pressure).

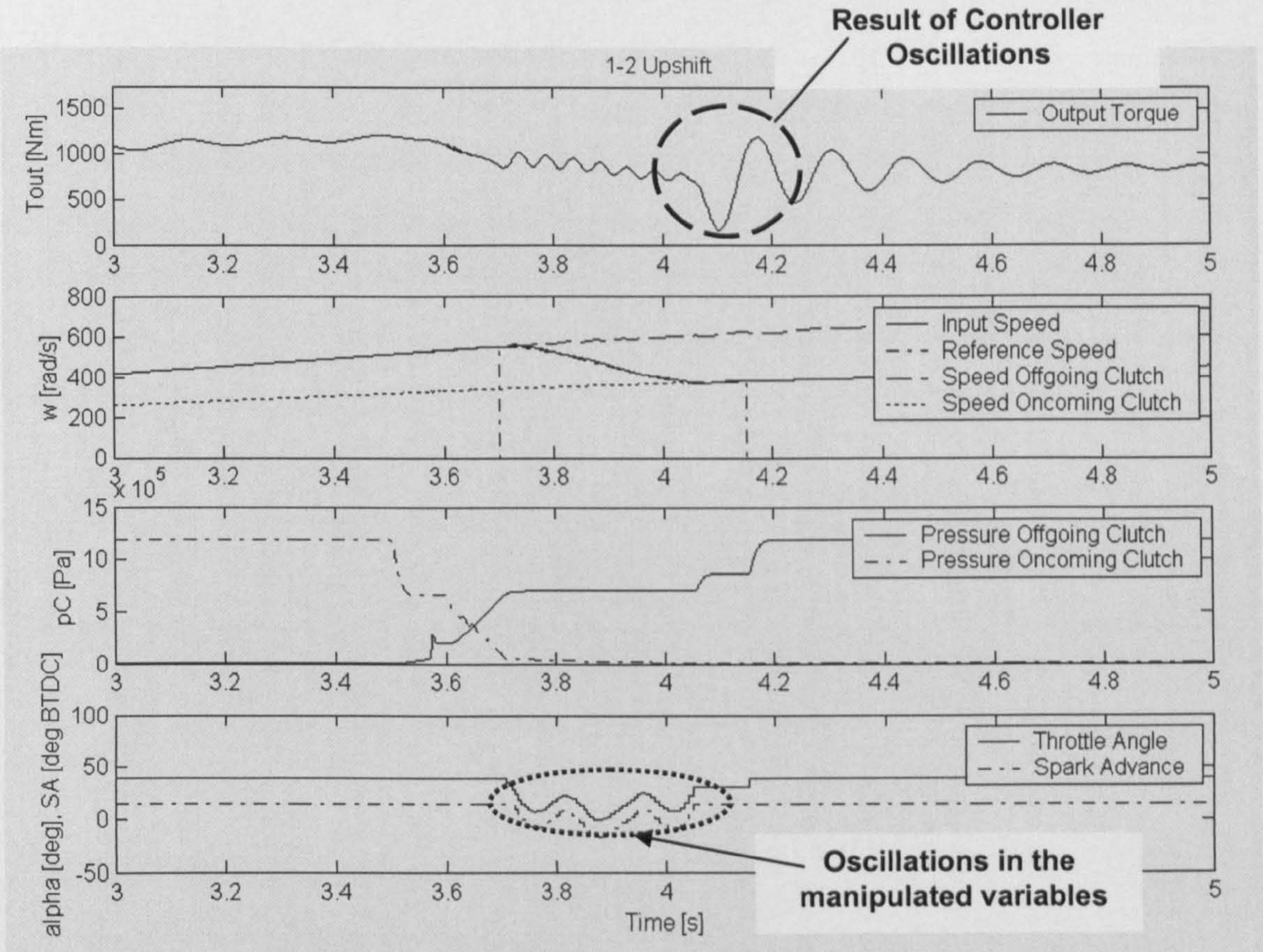

Figure 4.40 Simulation result: Upshift from 1st to 2nd gear, combined reduction of damping rates in the powertrain model

The example in Figure 4.40 shows that the settings of the gains of the PID controllers of throttle angle and spark advance need to be selected carefully for a robust operation. To show that the engine speed controller can work even with low damping, the gearshift from Figure 4.40 was repeated in Figure 4.41, this time with modified gain settings in both PID controllers. The proportional gains of both controllers were changed from a value of $K_p = 4$ to a value of $K_p = 2$ (throttle angle and spark advance). The integral gains were changed from a value of $K_I = 8$ to a value of $K_I = 4$ (PID of throttle) and from $K_I = 9$ to $K_I = 5$ (PID of spark advance).

Figure 4.41 shows that the engine speed controller is still able to track the engine speed reference trajectory despite the modifications of proportional and integral gain in the two PID engine speed controllers. The oscillations can be eliminated from the manipulated variables (dotted circle in Figure 4.41) by the modifications in the gain settings of the PID controllers. Also, the torque vibrations are much reduced (dashed circle in the uppermost graph of Figure 4.41).

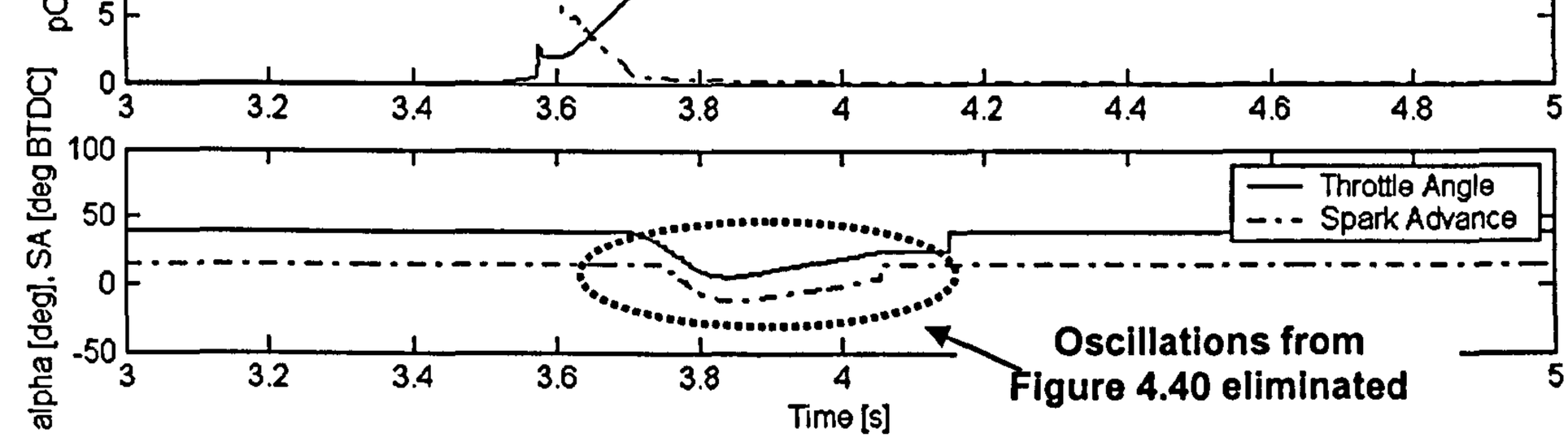

Figure 4.41 Simulation result: Upshift from Figure 4.40, however, with modified settings of the PID engine speed controller

Figure 4.42 shows a downshift from 2nd to 1st gear with decreased drivetrain damping similar to the above upshift cases (Figure 4.40 and 4.41). Again, all damping rates in the powertrain model were reduced to their lower limits (Table 4.2). Apart from small high frequency transmission output torque vibrations (uppermost graph in Figure 4.42) during the inertia phase, the reduced damping did not affect the performance of either the clutch slip controller or the engine speed controller. The high frequency vibrations are small in amplitude and hence do not affect shift quality. The tracking performance of the engine speed controller is not affected by the reduced damping. The manipulated variable (pressure at offgoing clutch) of the engine speed controller does not show any stability problems, thus indicating a robust operation despite the low driveline damping.

The third parameter, the stiffness of the driveshafts, had a similar influence on the gearshift controller as the variation in damping. Again, reduced driveshaft stiffness did present the more critical case as compared to increased driveshaft stiffness. The downshift controller was again completely unaffected by the reduction in driveshaft stiffness to the lower limit listed in Table 4.2. However, the upshift controller showed the same oscillatory behaviour in the manipulated variables (throttle angle, spark advance) also leading to increased torque vibrations at the end of the gearshift. Again, the remedy was to reduce the values of proportional and integral gain in both engine speed PID controllers in a similar way as demonstrated for the case of reduced damping. Because, the simulation results and remedies are similar to those for the case of reduced damping, they will not be presented here again, instead they can be found in the Appendix B.1 (Figure B.1 and Figure B.2).

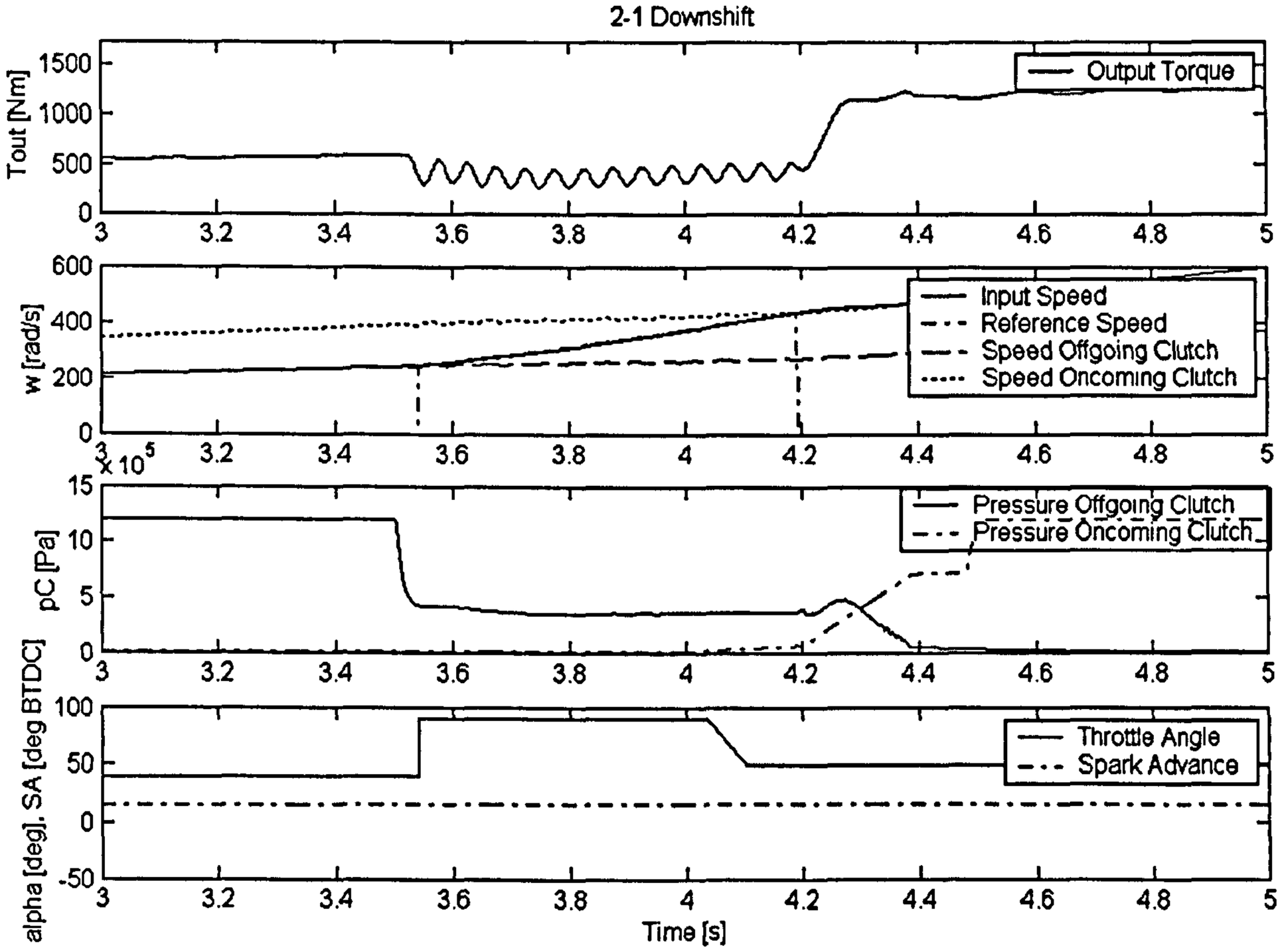

Figure 4.42 Simulation result: Downshift from 2nd to 1st gear, combined reduction of damping rates in the powertrain model

As a conclusion, it can be noticed that the clutch slip controller on both upshift and downshift showed robustness against all cases of parameter variation. The engine speed controller using manipulation of clutch pressure (downshift) also showed a robust operation in all parameter variations. Only the engine speed controller using manipulation of engine controls (upshift) did

show critical stability when driveline damping or driveshaft stiffness was reduced. The stability problem could be resolved by a change in the gain settings of the PID controllers manipulating throttle angle and spark advance. The tracking performance was not influenced too much by the change in the controller gains. This indicates that the engine speed controller in the upshift requires careful tuning of the PID controllers.

4.5.2 Robustness to Changes in the Friction Coefficient

The robustness to changes in the friction coefficient is one of the most important aspects in the analysis of gearshift controllers. It is not important that the gearshift controller can cope with every friction material possible without any modification of the gain settings, since normally the controllers will be specially adjusted to a specific friction material anyway. However, changes in the friction coefficient that occur during the operation of the gearshift controller are an important source of disturbance to the controller.

Severe changes in the friction coefficient, such as a large temporary drop of the friction coefficient due to extreme clutch temperatures, are not considered here. Such conditions can occur due to elongated slipping of a friction clutch at high slipping speeds across the clutch. These condition are more of a problem when designing the clutch control for a vehicle launch (on uphill climbs) or for a hill-hold facility. On gearshifts clutch slipping-times are, in general, much shorter and hence also the change in clutch temperature during the gearshift is less severe. However, repeated shifting can gradually lead to higher oil temperatures (or clutch surface temperatures), which can then lead to a change in the friction coefficient, often affecting the gradient of the friction coefficient with slip speed. If the oil temperature exceeds a certain limit for an extended time, it can happen that the oil changes its characteristic. In particular, for wet friction this can mean a change from a positive gradient with slip speed to a negative gradient with slip speed due to a permanent damage of the friction modifiers (oil additives) in the transmission oil.

On all gearshift simulations presented so far in Chapter 4, a wet-type friction coefficient with a positive gradient with slip speed (according to Figure 3.13) was selected. At the end of Chapter 3 it was found that the level of the friction coefficient (wet versus dry friction coefficients in Figure 3.13) did not influence the gearshift in the same way as the sign of the gradient of the friction coefficient with slip speed (positive versus negative gradient in Figure 3.13). Hence, the investigation into robustness to changes in the friction coefficient focuses on the change from a

positive to a negative gradient of the friction coefficient and how this affects the performance of the gearshift controller. Nevertheless, for the sake of completeness, the simulation results of an upshift and downshift with dry friction with positive gradient of the friction coefficient are presented in the Appendix B.1 (Figures B.3 and Figure B.4).

For this aim the upshift from 1st to 2nd gear of Figure 4.13 and the downshift from 2nd to 1st gear of Figure 4.22 are repeated here but this time with a wet friction coefficient with negative gradient (according to Figure 3.13). Figure 4.43 shows the upshift from Figure 4.13, with a wet friction coefficient with negative gradient with slip speed. The performance of the slip controller is not affected by the change in the friction gradient. Also the tracking performance of the engine speed controller is not affected. However, the pressure level at the oncoming clutch is higher in the inertia phase as compared to the shift case with a positive gradient of the friction coefficient (Figure 4.13). This is due to the fact that the friction coefficient with negative gradient has a lower value at higher slip speeds, hence when the inertia phase starts the pressure has to be higher to compensate for the lower friction.

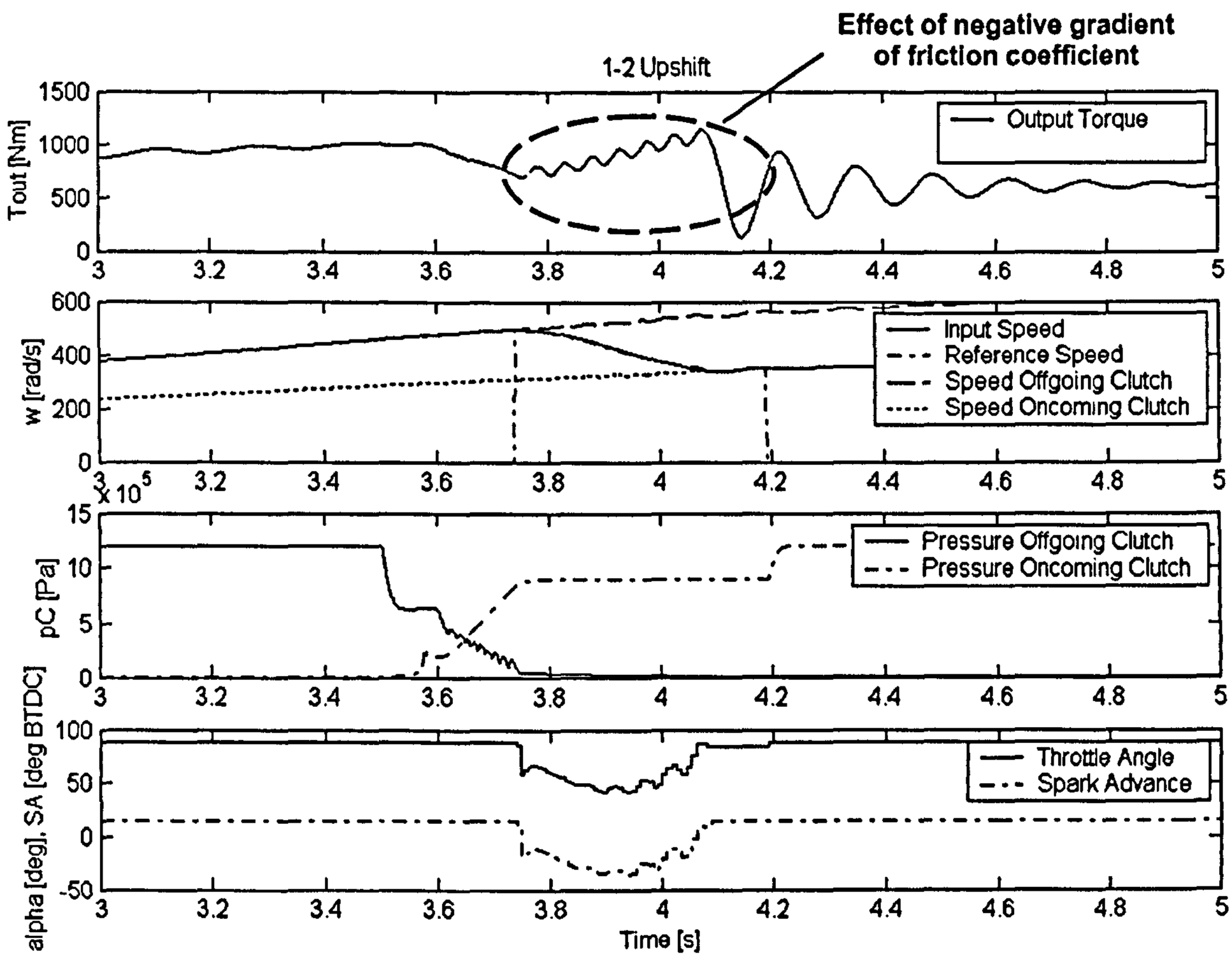

Figure 4.43 Simulation result: Upshift from 1st to 2nd gear from Figure 4.13, with wet-type friction with a negative gradient

Another important difference, which can also be attributed to the negative gradient, can be observed, namely, that the clutch torque and hence the transmission output torque rises (dashed circle in Figure 4.43) as the relative speed at the oncoming clutch is decreased to zero during the inertia phase. This happens because the pressure at the oncoming clutch remains unchanged throughout the inertia phase. As a result of this rise in transmission output torque in the inertia phase, the difference in torque at the oncoming clutch between the state where it was slipping and the state where it has locked up at the end of the inertia phase is very large. Thus, the transmission output torque drops severely, causing heavy torque vibrations at the end of the gearshift. This behaviour was already observed in Figure 3.37, which showed an upshift from 1st to 2nd gear with conventional clutch-to-clutch control for dry friction with negative gradient. However, in Figure 3.37 only the torque vibrations at the end of the shift were visible and the rise in clutch torque was concealed beneath the torque "hump". Although, the change to a negative gradient in the friction coefficient does not influence the performance of clutch slip and engine speed control, it nevertheless heavily affects the performance of the gearshift controller in terms of shift quality. A remedy for this problem will be presented in Chapter 5.

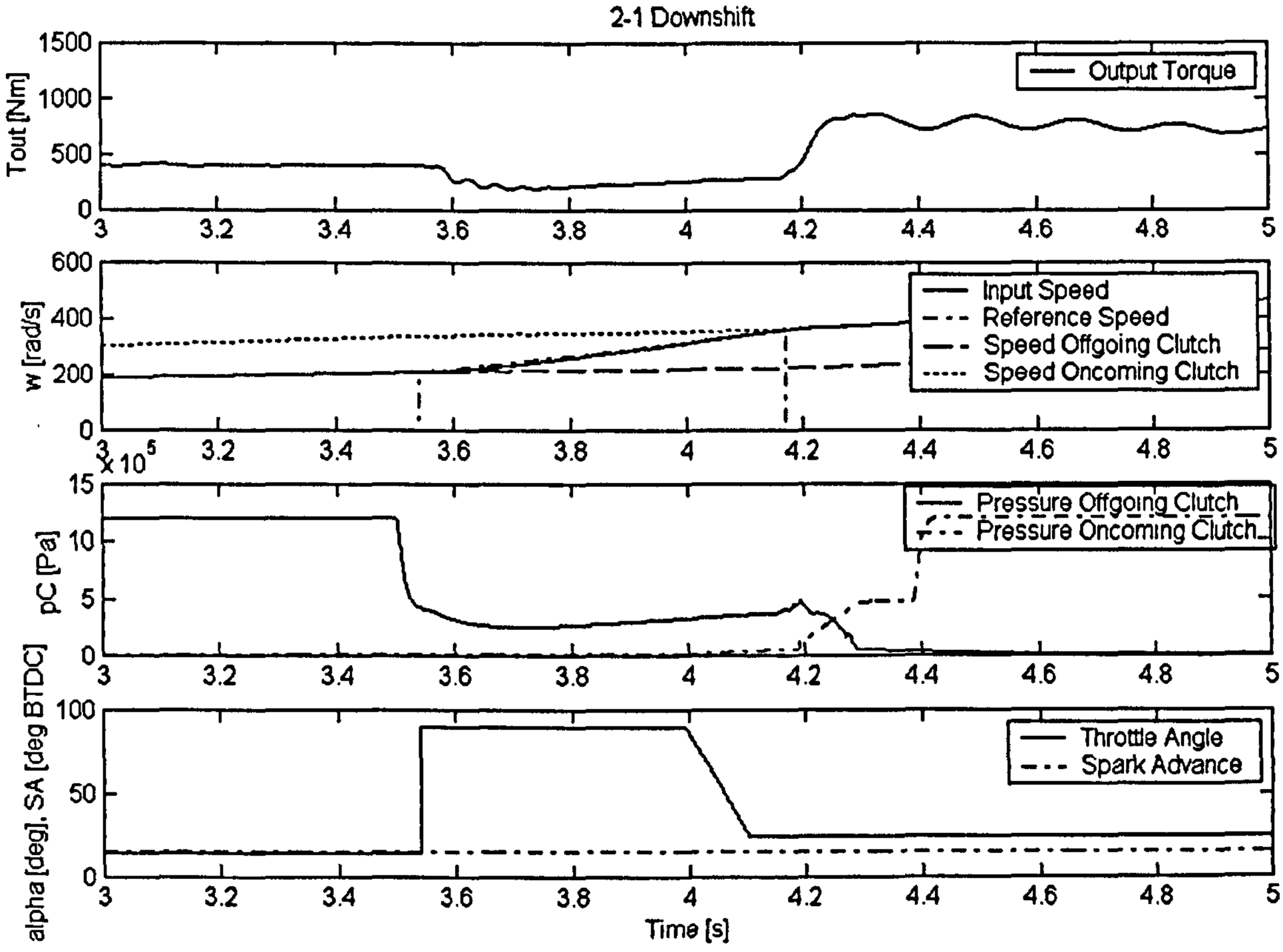

Figure 4.44 Simulation result: Downshift from 2nd to 1st gear from Figure 4.22, with wet-type friction with a negative gradient

The same analysis can be carried out for the downshift. Figure 4.44 shows the downshift (from 2nd to 1st gear) from Figure 4.22 only with the friction characteristic changed from a wet-type friction coefficient with a positive gradient to wet-type friction coefficient showing a negative gradient with slip speed.

Comparing Figure 4.22 with Figure 4.44 little difference can be noticed apart from slightly more pronounced torque vibrations subsequent to the gearshift. The lack of difference indicates that the performance of clutch slip controller and engine speed controller are not affected by the change in the friction gradient. Also the performance of the gearshift controller from a shift quality point of view remains unchanged as can be observed by the unaffected transmission output torque profile. This might come as a surprise at first sight because here also the slip speed at the (offgoing-) clutch is varied throughout the inertia phase. However, the clutch pressure is much lower as compared to the upshift and hence also the friction torque at the offgoing clutch. This explains that although the profile of the friction coefficient is different between the two compared downshifts, the actual difference in friction torque and hence the difference in the transmission output torque is much smaller.

4.5.3 Robustness to Sensor Noise

To check the robustness against a noise polluted measurement signal from speed sensors, a white noise was added to the signals of engine speed and speeds of both input shafts. The white noise (band-limited white noise with power level of 0.05, sample time of $5*10^{-4}$s) generated a random, Gauss-distributed signal that varied around the unpolluted signal with a maximum deviation of +/-20rad/s (roughly +/- 200rpm). The level of noise pollution was chosen arbitrarily but deliberately at a high level. This was necessary because no accurate information about measurement accuracy or the noise level that exists in a production speed sensor for automotive applications (often a hall-effect sensor or less often a tooth-type inductive sensor) could be obtained. Normally, repeatability and accuracy of speed sensors in production automatic transmissions is lower compared to engine speed sensors. It is believed that the level of the noise pollution chosen here represents a worst-case scenario.

Figure 4.45 depicts a simulation result for an upshift from 1st to 2nd gear and a downshift from 2nd to 1st gear with noise-polluted speed signals (see second graph from top in Figure 4.45 for speed signals). For reasons of space, the simulation results for upshift and downshift have been combined in one diagram. Analysing the simulation result in Figure 4.45, it can be seen that

both gearshifts are executed properly despite the noise in the speed signal. However, a couple of details reveal that the operation of the gearshift controller is negatively affected by the addition of sensor noise to the speed signal.

Turning to the upshift first, the transmission output torque trajectory indicates no negative influence of the sensor noise on the shift quality. The operation of the clutch slip control is also not influenced by the senor noise, producing an unimpaired transfer of engine torque in the torque phase. Even the tracking of the engine reference profile, although hidden somewhat beneath the noise in the graph, remains relatively unaffected. However, when looking at the engine speed controls (throttle angle and spark advance) it seems that these are jumping up and down "chaotically" (dashed circle in Figure 4.45) in the inertia phase. Although this does not seem to have a strong effect on this particular upshift, it indicates that the operations of the upshift controller is impaired and cannot be guaranteed to be fully functional for the whole operating range of the powertrain.

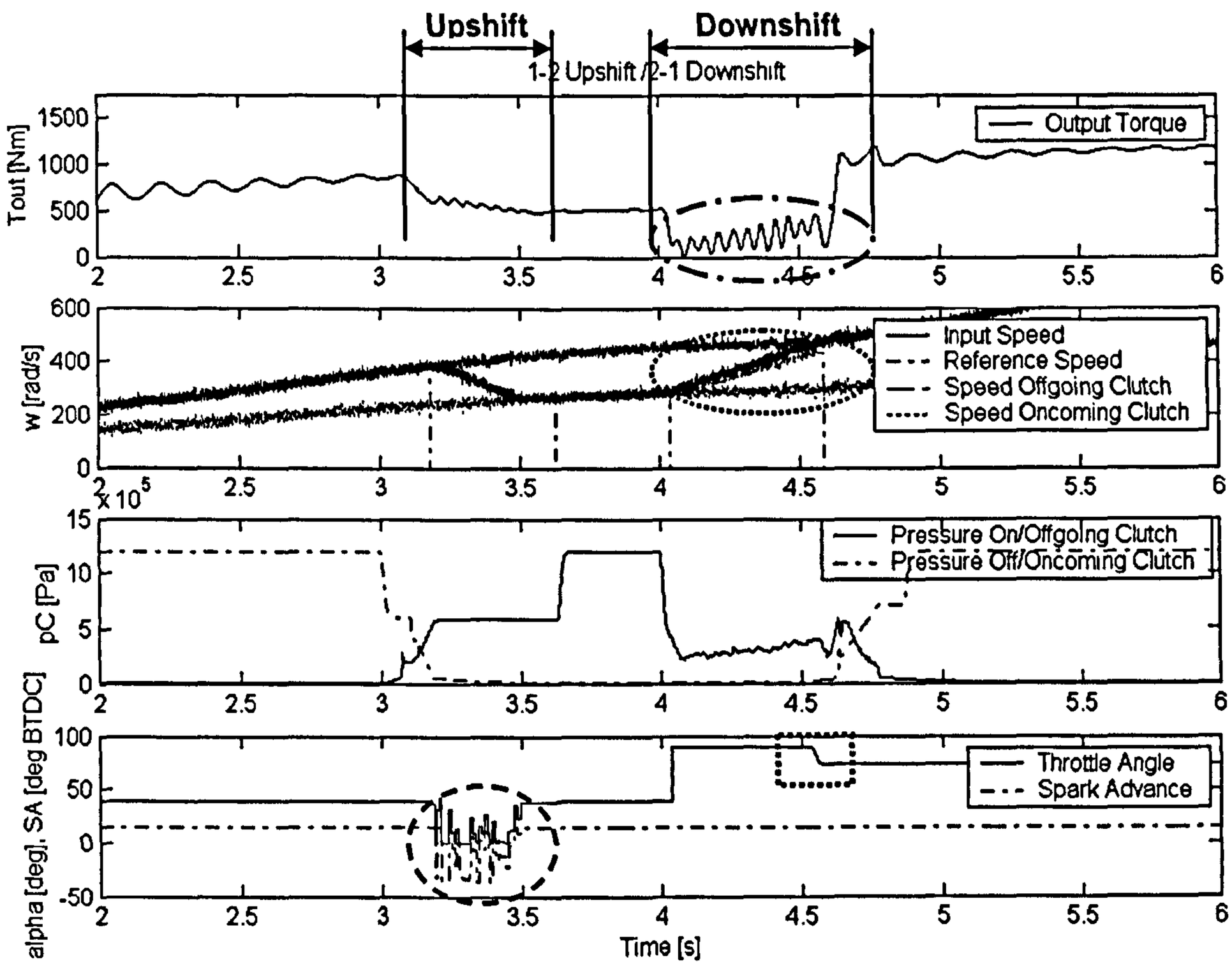

Figure 4.45 Simulation result: Upshift and downshift between 1st and 2nd gear, noise polluted speed signals (second graph from top)

The situation at the downshift is even more dangerous: the transmission output torque starts to oscillate in the inertia phase (dash-dotted circle in Figure 4.45) as a result of tiny ripples in the pressure profile at the offgoing clutch. The tracking of the engine reference speed profile is also heavily influenced showing an increasing steady state error (dotted circle). Also, the throttle angle cannot be decreased to its original value (dotted rectangle) due to poor tracking of the reference profile. However, the clutch slip controller seems to be unaffected by the noise in the speed signals, although the transmission output torque rises more rapidly in the torque phase as compared to the noise-free case (Figure 4.22 for example).

One obvious problem with sensor noise is that the reference speed trajectories (Equations (60) and (63)) used by the engine speed controller are constructed from information about the speed of the oncoming input shaft, which is also noise polluted. This means that the reference speed trajectory also shows traces of sensor noise, which clearly affects the performance of the engine speed controllers.

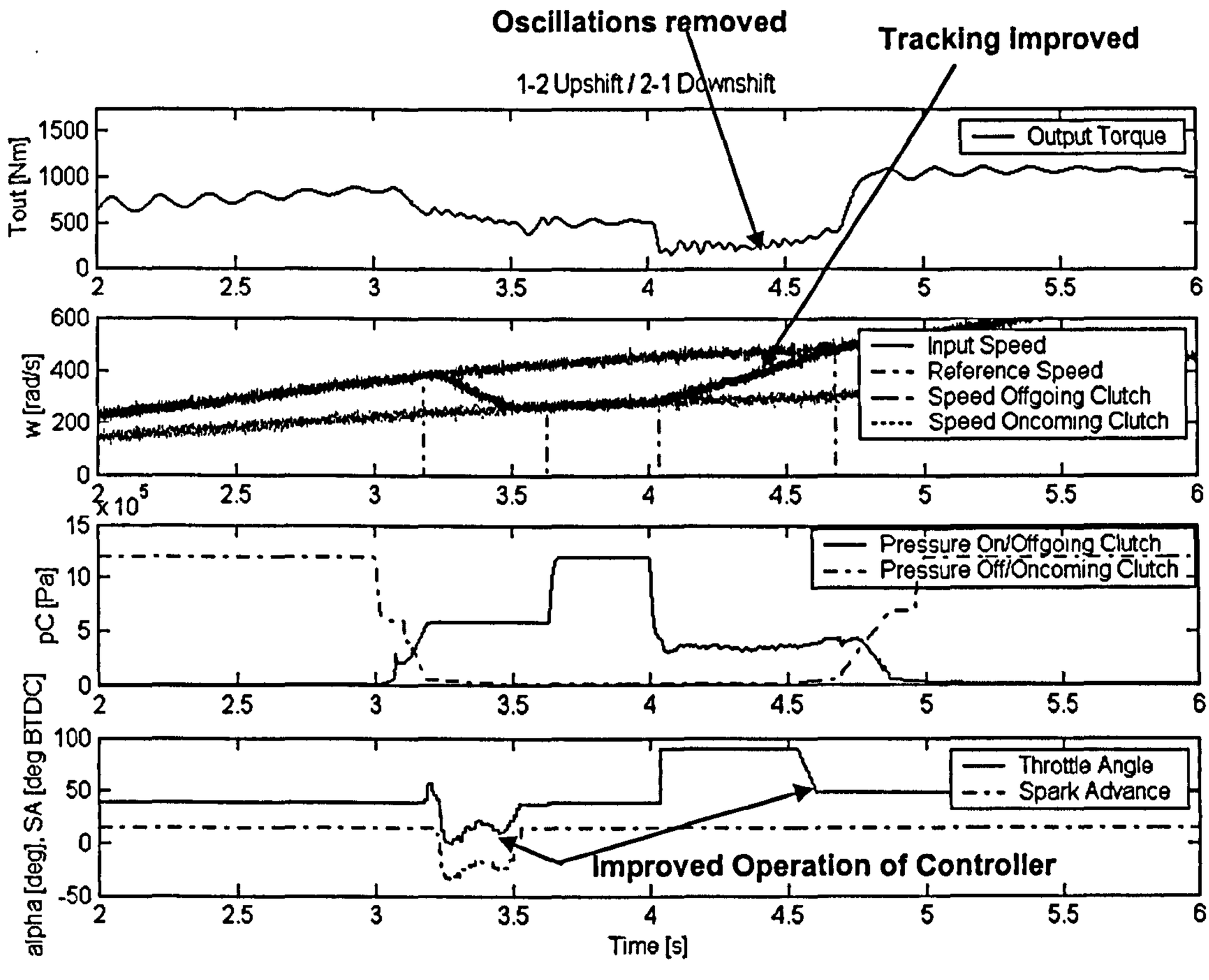

Figure 4.46 Simulation Result: Upshift and Downshift between 1st and 2nd gear, Filter applied to noise polluted speed signals

To eliminate all these problems filtering of the speed signals was employed. For the upshift it turned out that it is important to filter (lowpass 1st order Butterworth filter, corner frequency 60

rad/s) the speed of the oncoming input shaft in order to produce a noise-free engine speed reference trajectory. As a second measure, the engine speed (or transmission input speed) was also filtered by a low pass filter (1st order Butterworth, corner frequency 60 rad/s). The speed signals inputted to the clutch slip controller have not been filtered as the operation of that controller did not seem to be affected by the noise.

As measure for the downshift, a lowpass filter (again 1st order Butterworth, corner frequency 60 rad/s) was only applied to the speed signal of the oncoming clutch (input shaft). It turned out that filtering the engine speed in this case introduced too much response delay in the controller, which would have resulted to instability. However, in order to improve the tracking performance of the speed controller and to eliminate the torque vibrations, the rate of change of the error signal inputted to the derivative term of the PID speed controller was limited at both ends (slew rate limited to range from –5000 to 5000). Thus, the sensitivity of the critical derivative part to high frequency signal parts (noise) could be reduced and hence, the performance of the speed controller improved. Again, the speed signals inputted to the clutch slip controller have not been filtered.

The simulation from Figure 4.45 is repeated in Figure 4.46, only that here the above described filters and rate limiters are applied to the controllers. As can be seen from Figure 4.46 the "chaotic" up and down of the throttle angle and spark advance was eliminated on the upshift. Also, the tracking performance of the speed controller employed on the downshift could be radically improved. The oscillatory behaviour of the transmission output torque during the inertia phase of the downshift could be eliminated as well.

4.6 Conclusions

It was clearly demonstrated, based on simulation results, that by controlling clutch slip at the offgoing clutch the operation of a one-way (i.e. freewheeler- or overrunning-) clutch could be replicated to smoothly transfer engine torque. The creation of a negative torque at the offgoing clutch in the torque phase could thus be avoided in both the upshift and the downshift. As demonstrated, this helped to improve the shift quality in the torque phase over conventional clutch-to-clutch shift controls utilising open-loop clutch pressure manipulation.

It was further observed from the simulation results, that the creation of a negative torque at the offgoing clutch is in particular noticeable if the inertia phase of a power-on upshift is controlled via engine torque manipulation to remove the "torque hump".

In the inertia phase engine torque manipulation was employed in both upshift and downshift. The way throttle angle and spark advance and clutch pressure were manipulated by the integrated powertrain controller to control engine synchronisation in the inertia phase, presented a new control approach.

A further important observation was made on how the lock up of the oncoming clutch at the end of the gearshift affects shift quality. For upshifts it was found that through a fast increase of engine torque (through increase in spark advance) torque vibrations could be suppressed.

At the end of this chapter an extensive investigation into robustness of the gearshift controller in terms of shift quality and controller stability was undertaken. It was demonstrated that the proposed gearshift controller is in general robust to changes in the clutch friction coefficient, changes in the parameters of the powertrain (-model) and to sensor noise. Robustness problems could be handled by simply introducing low pass filters or rate limiter at the controller inputs.

However, following issues could not be resolved by the gearshift controller developed in Chapter 4:

- On upshifts it was noticed that changing the gradient of the friction coefficient from a positive one to a negative one lead to a drastic deterioration of the shift quality.
- On downshifts it was noticed that different downshifts with different shift parameters did have transmission output torque profiles in the torque phase, which differed in shape and thus also shift quality.

Chapter 5

Gearshift Controller for Twin Clutch Transmissions and Torque Control

In Chapter 4 the basic version of a novel gearshift controller was developed for gearshifts on twin clutch transmissions. At the end of the chapter it was demonstrated that this basic gearshift controller was robust to changes in the powertrain parameters and sensor noise.

In Chapter 5 an optional transmission output torque controller is developed that can be added to the basic gearshift controller described in Chapter 4. This torque controller enables integration of the gearshift controller in a torque control management scheme where powertrain components are controlled to provide certain wheel torque trajectories. How the torque controller can cope with the deficiencies of the basic gearshift controller listed at the end of Chapter 4 will be also demonstrated in Chapter 5.

The first section of this chapter (Section 5.1) explains the motivation for introducing the control of torque to the basic gearshift strategy from Chapter 4. In the second section (Section 5.2) of this chapter the torque controller is developed in full firstly, for power-on upshifts (Section 5.2.1) and then secondly for power-on downshifts (Section 5.2.2).

A detailed description of the structure of the torque controller is given in Section 5.3. The robustness of the torque controller is investigated in Section 5.4. The findings of Chapter 5 are summarised in Section 5.5.

5.1 Motivation for Control of Driveline Torque

5.1.1 General Aspects of Driveline Torque Control

Driveline torque control is the control of torque in the driveline or specifically at the output of the transmission by a manipulation of powertrain controls (-variables) such as hydraulic pressure at the clutch (or clutches) in an automatic transmission, or by manipulation of engine controls such as spark advance and throttle angle (SI-engine) or fuel injection (diesel engine).

The torque signal can be obtained through a torque sensor or through application of a mathematical observer, which provides an estimate of the torque value. The advantages and disadvantages of torque measurement versus mathematical observation have been discussed in Chapter 2. Torque sensors offer a more accurate and robust torque signal once they are calibrated properly, however, they introduce additional costs. Torque observation on the other hand is inexpensive to implement, however, its accuracy depends on the quality of the inverse model of the drive train used in the observer and the robustness of the observer to parameter variations. The control of driveline torque is sometimes also summarised under the term "torque coordination (or management) scheme".

In some applications it might be desired to control the wheel torque instead of the driveline torque, in particular if (controlled-) locking differentials or other torque distributing devices are employed. This "torque vectoring" technique often involves controlling the torque at each wheel separately to affect the traction properties or lateral dynamics of a vehicle. This specific form of torque controller will not be treated here.

Following is a list of some of the advantages a control of driveline torque can provide:

1. All powertain components can be controlled by a coordinated (integrated-) powertrain controller to provide a pre-defined driveline torque. This has the advantage that the driver's request for acceleration (propulsion power) can be directly controlled. The integrated powertrain controller can then select the optimum operating points or trajectories (low fuel consumption, etc.) and control the powertrain components accordingly.
2. Controlling the driveline torque provides a more direct influence on the traction at the wheels thus, avoiding a spinning of the wheels. In case of wheels spinning, the driveline torque can be reduced.
3. Because driveline torque is directly related to the longitudinal vehicle acceleration, transients in the operation of engine and transmission can be detected and compensated for by the torque controller to provide a jerk free operation of the vehicle. Transferred to the automatic transmission, this means, that by controlling the driveline torque, the shift quality can be directly influenced and hence improved.
4. Changes in the parameters of the powertrain (due to wear, change in the driving environment, faulty operation etc.) and their effect on the driving performance and feel can be compensated to some degree by the driveline torque controller. Again, for the automatic transmission this means, that any change in parameters on the transmission would likely result to a deterioration of shift quality. Control of driveline torque can

compensate for these changes by ensuring that the quality of the gearshift remains unaltered.

Only those aspects that are examined under point 3 and 4 are relevant to gearshifts on automatic transmissions and hence only those aspects of driveline torque control are considered here.

5.1.2 Benefits of Transmission Output Torque Control for the Control of Gearshifts

This section discusses the control of transmission output torque as a specific form of driveline torque control. This is often the preferred location of the torque sensor, since usually the powertrain controller cannot manipulate any drivetrain component downstream from the output of the transmission (assuming a driveline without a controlled differential).

In addition to being able to influence the characteristics and quality of the gearshift by selecting different torque trajectories for the torque controller, the torque controller can add robustness to the gearshift controller by guaranteeing an unaffected transmission output torque trajectory. In particular, Chapter 4 has shown that in some cases the proposed integrated powertrain controller for gearshifts produced less satisfactory results. Two key areas were identified:

- Problem 1: "change in clutch friction"
- Problem 2: "change in torque profile"

Problem 1("change in clutch friction"): The deterioration of shift quality on upshifts with changing clutch friction characteristics was illustrated in Figure 4.43 where the gradient of the friction coefficient (as a function of slip speed) at the oncoming clutch was changed from a positive value to a negative value. The change to a negative gradient had the effect of letting the friction torque increase at the oncoming clutch during the inertia phase (clutch pressure remained constant), thus producing a large difference in torque at the end of the inertia phase where the oncoming clutch changed its state from slipping to stiction. This drop in torque excited heavy torque vibrations in the driveline. From a shift quality point of view, this deterioration in shift quality has to be avoided. This situation is illustrated again in Figure 5.1, which compares the transmission output torque profiles of two upshifts from 1st to 2nd gear with different clutch friction gradients. The upper graph in Figure 5.1 shows the transmission output torque profile of Figure 4.13 (positive gradient) and the lower graph that of Figure 4.43 (negative gradient).

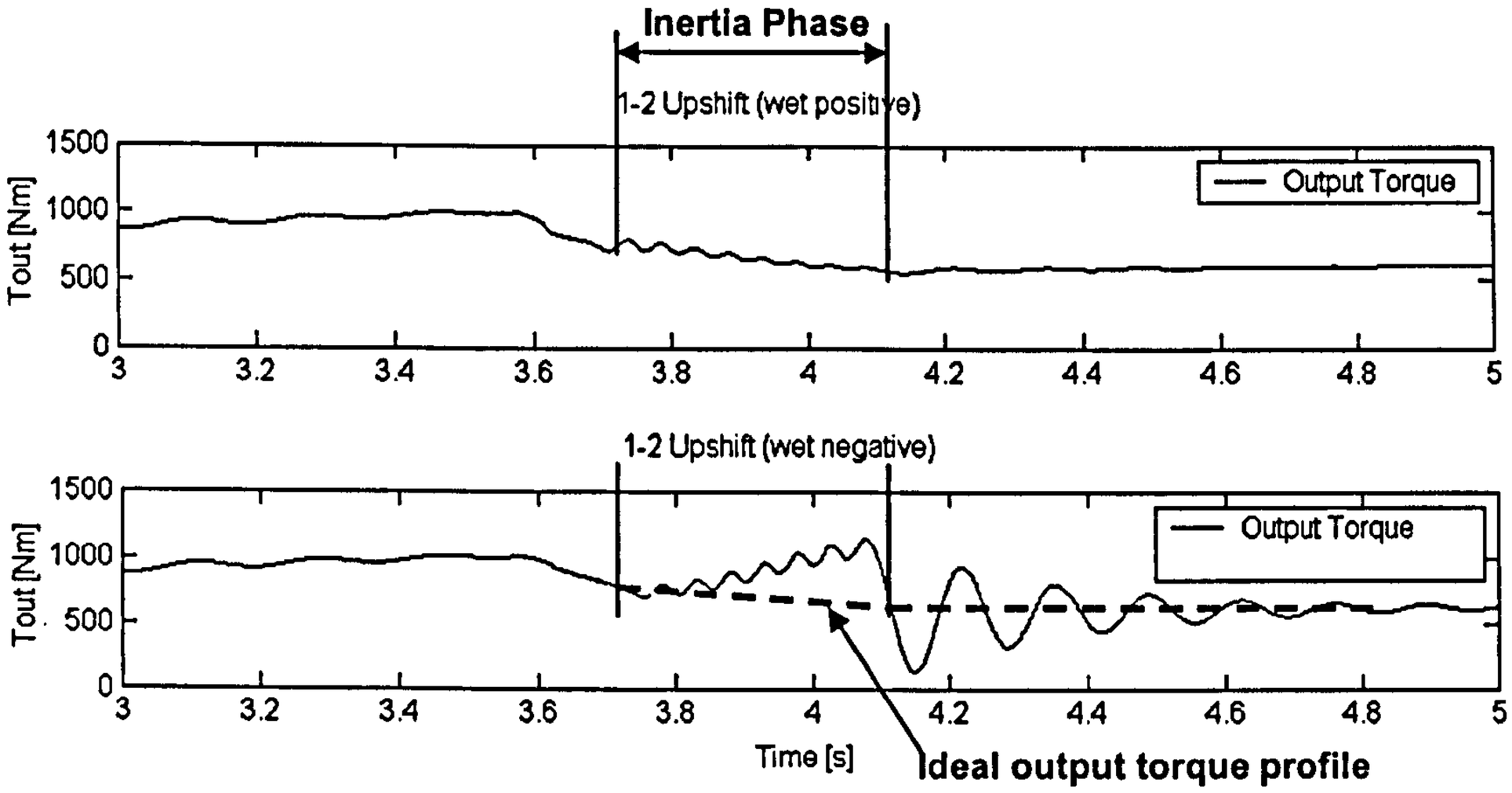

Figure 5.1 Problem 1: Upshift from 1st to 2nd gear (transmission output torque profiles of Figure 4.13 and Figure 4.43) with different clutch friction gradients

In both upshifts (Figure 4.13 and 4.43) the pressure at the oncoming clutch was kept constant in the inertia phase and the engine synchronisation was managed by manipulation of engine controls alone. However, the difference in the gradient of the friction coefficient with slip speed also implied that the friction torque at the oncoming clutch had to change differently when the slipping speed at the clutch was reduced to zero. To avoid any influence of the friction coefficient on the transmission output torque profile and hence, on the shift quality, the driveline or transmission output torque has to be controlled along a specified reference trajectory in the inertia phase. Such a reference trajectory is sketched in the lower graph of Figure 5.1 (dashed line) as an ideal torque profile.

Problem 2 ("change in torque profile"): In Chapter 4, it was observed that the shape of the transmission output torque profile in the torque phase of downshifts did change with varying operating conditions and for downshifts between different gears. Although, it was demonstrated that the clutch slip controller could reduce the vehicle jerk in the torque phase as compared to a conventional clutch-to-clutch shift controller, it is desirable to be able to select the transmission output torque trajectory in the torque phase independently of the operating conditions. Thus, a gentle transmission output trajectory would produce a longer shift with good shift quality (sketched as dashed line in the top graph of Figure 5.2) and a steep profile would produce a more sporty and faster shift resulting to increased vehicle jerk.

It was also noticed that, although the clutch slip controller worked well for different target gears, the shape and gradient of the transmission output torque profile did vary with a change in shift time or the gear ratios involved in the downshift. This situation is illustrated in Figure 5.2, which compares the transmission output torque profiles of the downshift from Figure 4.22 (from 2nd to 1st gear), the downshift from Figure 4.24 (from 2nd to 1st gear with reduced shift time) and the downshift from Figure 4.27 (from 4th to 3rd gear).

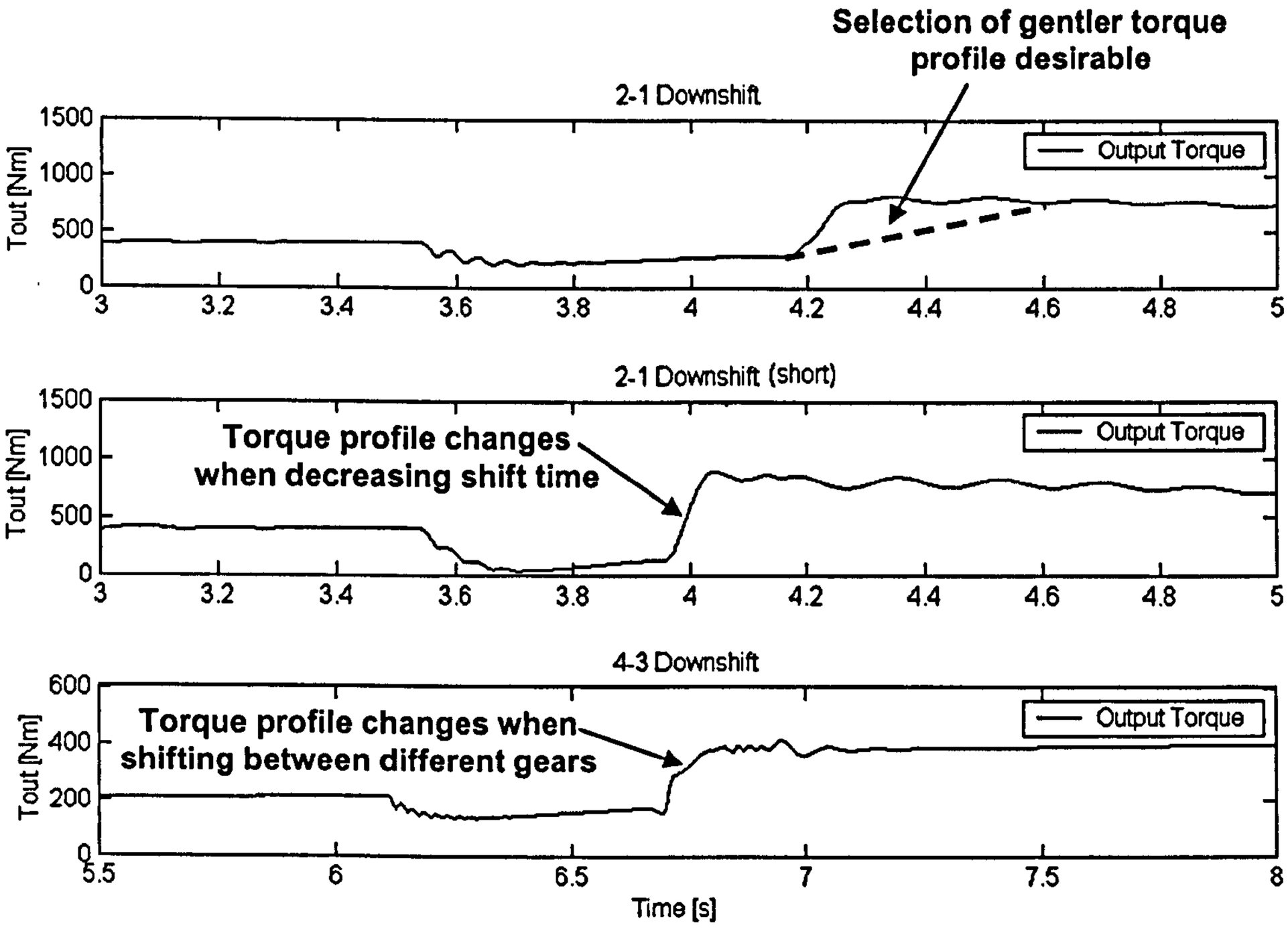

Figure 5.2 Problem 2: Change of transmission output torque profiles in a downshift; top graph: from 2nd to 1st gear (Figure 4.22), middle graph: the same downshift with shorter shift time (Figure 4.24), and bottom graph: from 4th to 3rd gear (Figure 4.27).

It can be seen that the transmission output torque profile takes different shapes in the three downshift cases depicted in Figure 5.2, confirming that the torque profile changes with changing operating conditions. To ensure that the torque profile and hence shift quality does not change with the involved gear ratios (bottom graph in Figure 5.2) or shift time (middle graph in Figure 5.2), the transmission output torque needs to be controlled to a specified reference trajectory.

5.2 Integration of the Control of Transmission Output Torque in the Gearshift Control Strategy

This section will explain in detail how the transmission output torque control scheme can be integrated in the gearshift control strategy developed in Chapter 4. It will be demonstrated, that the proposed transmission output torque control scheme can (together with the gearshift control strategy from Chapter 4) compensate for the problems described in Section 5.1. This will be only demonstrated for power-on gearshifts in this work. Power-off gearshifts take place at lower clutch pressures and have less variation in output torque, hence, above described problems do not significantly influence shift quality on power-off gearshifts.

5.2.1 Integrated Powertrain Controller for Power-on Upshifts including Torque Controller

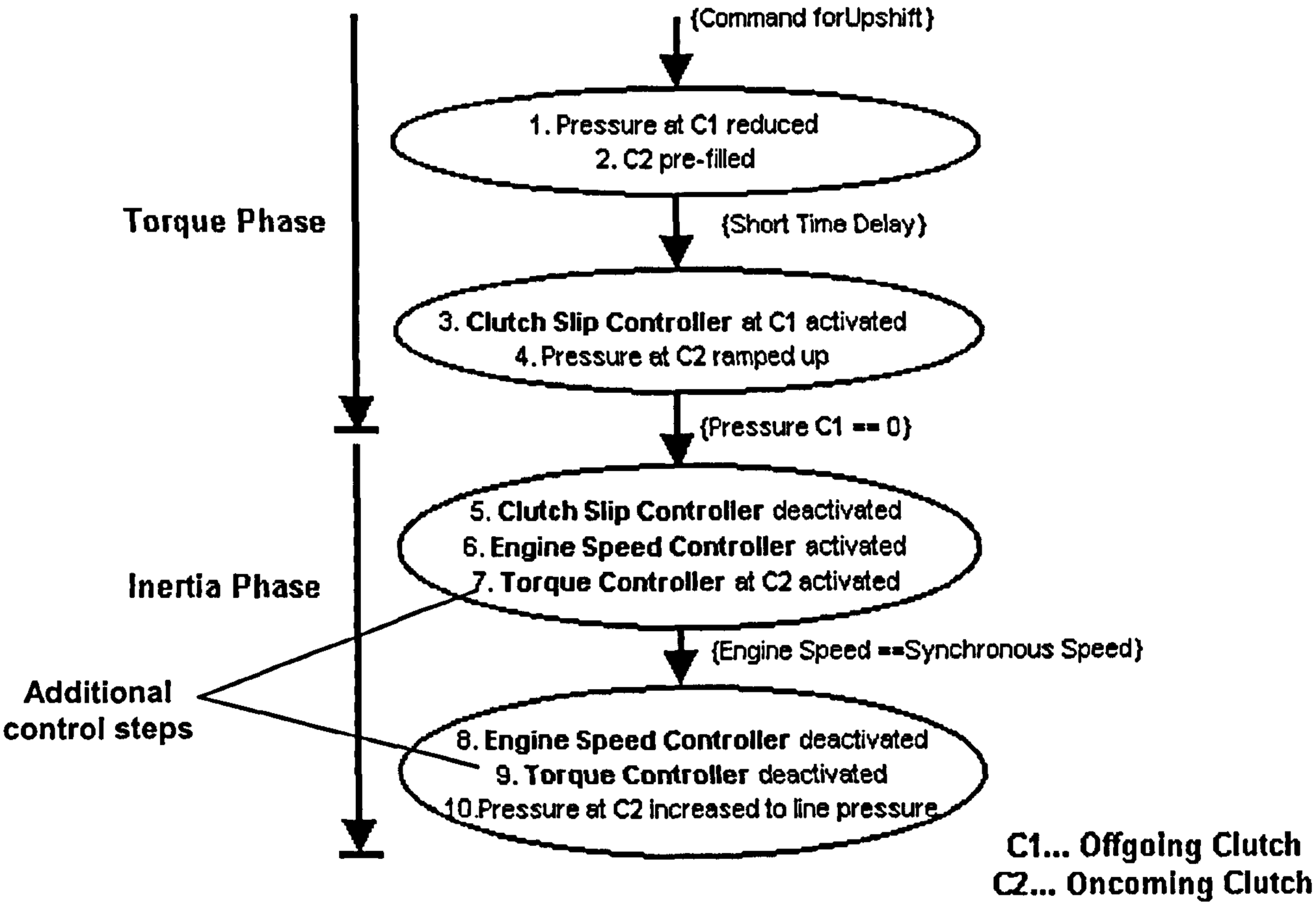

Figure 5.3 Control algorithm for proposed integrated powertrain controller for power-on upshifts (Figure 4.9) including control of transmission output torque (step 7 and 9)

As discussed in Section 5.1 (Problem 1 "change in clutch friction"), it is desirable to control transmission output torque in the inertia phase of a power-on upshift along a specified reference trajectory. The control strategy for power-on upshifts, developed in Chapter 4 (upshift control algorithm Figure 4.9), did not feature a variation of hydraulic pressure at the oncoming clutch during the inertia phase (engine synchronisation was controlled by manipulating engine controls). This means that a manipulation of pressure at the oncoming clutch would add an additional degree of freedom to the gearshift controller, which could be used for controlling the transmission output torque.

Figure 5.3 shows the control algorithm for power-on upshifts from Figure 4.9 extended by two control steps (step 7 and 9), in which the torque controller is activated. The torque controller operates by manipulating hydraulic pressure at the oncoming clutch ("C2" in Figure 5.3). Apart from these two additional steps the control algorithm remains unchanged.

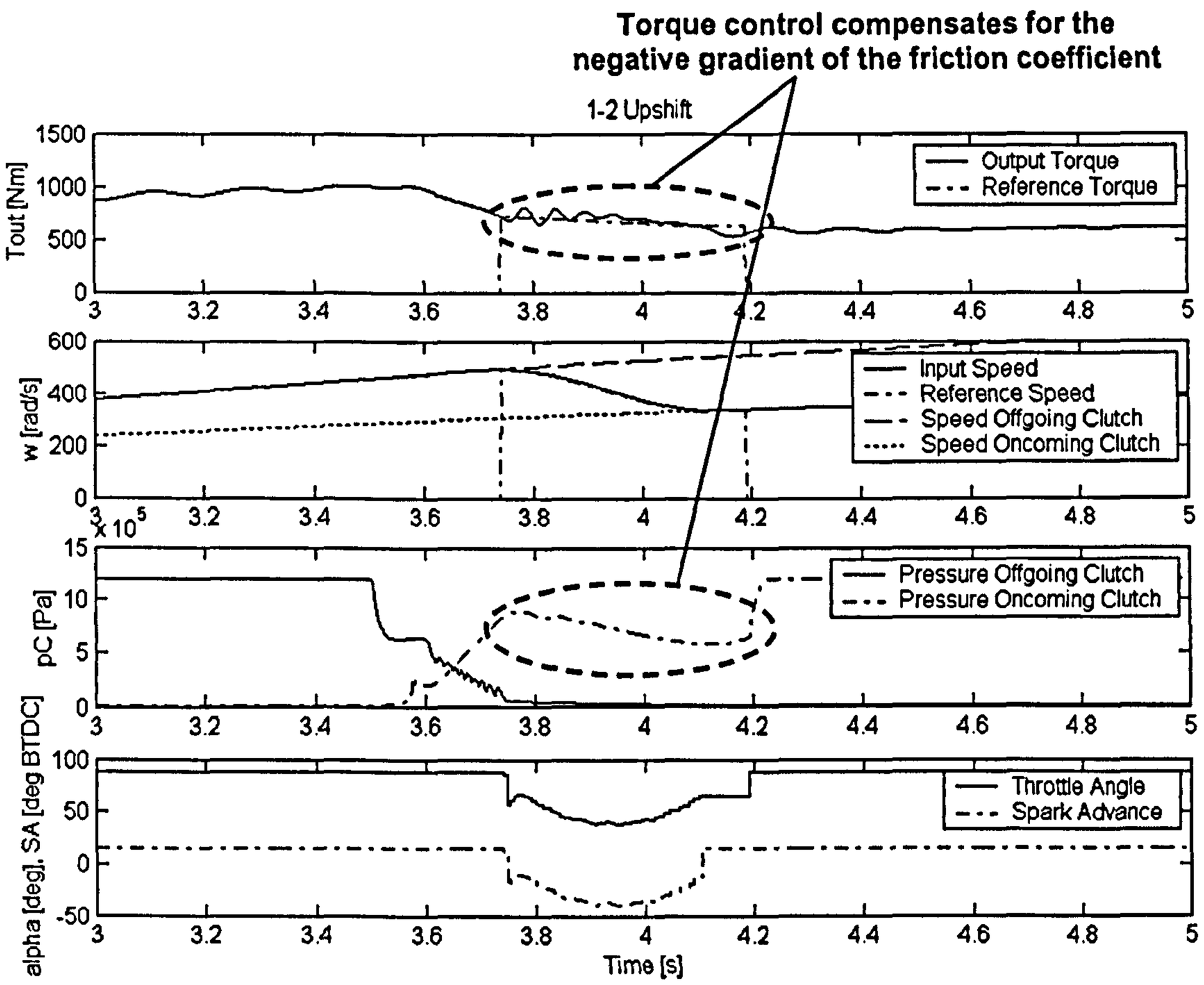

Figure 5.4 Simulation result: Proposed upshift controller plus torque controller, power-on upshift from 1st to 2nd gear (similar to Figure 4.43), wet friction, negative gradient

Figure 5.4 shows a simulation result of an upshift from 1st to 2nd gear similar to that in Figure 4.43 (friction coefficient with a negative gradient) but, in addition, in Figure 5.4 the torque

controller is active. The phase where the torque controller is active is indicated in the graphs showing hydraulic pressure and output torque (dashed circles in Figure 5.4). The reference torque trajectory selected for the upshift represented a linear decrease from a torque value sampled at the end of the torque phase to a torque level corresponding to the change in gear ratio at the end of the inertia phase (for the equation of the reference trajectory see equation (67)).

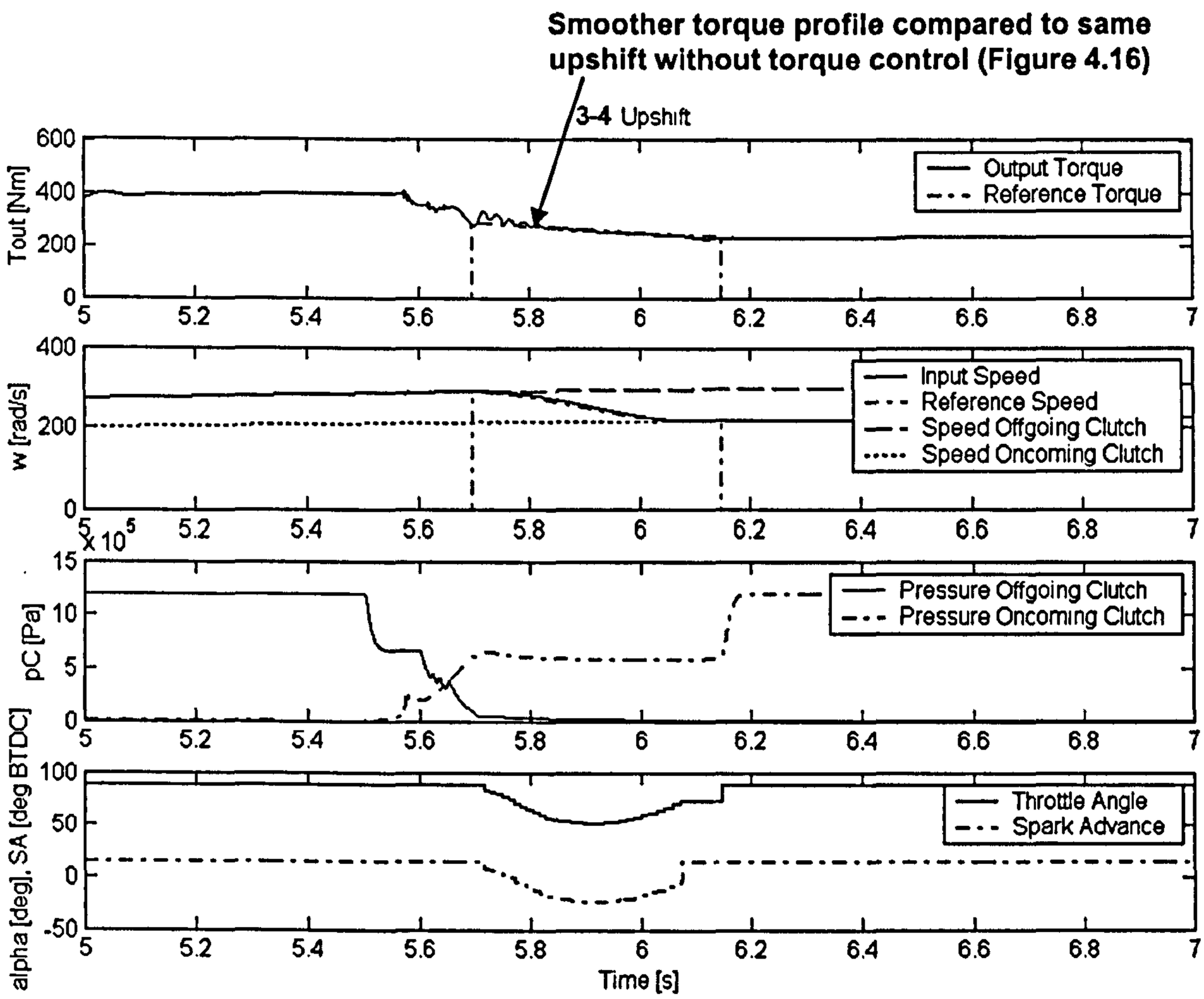

Figure 5.5 Simulation result: Proposed upshift controller plus torque controller, power-on upshift from 3rd to 4th gear, wet friction, positive gradient (similar to Figure 4.16)

From Figure 5.4 it can be seen that the torque controller does not affect the operation of the engine speed controller and that the tracking of the reference engine speed profile is still good. The tracking of the reference torque profile is good as well, showing only small oscillations at the beginning of the inertia phase, which have already been observed for the upshift without torque controller. The reason why the torque controller does not attempt to eliminate these vibrations is, that a low pass filter was added in front of the torque controller, which filtered exactly these vibrations for proper operation of the torque controller. The reason for employing this low pass filter will be explained in more detail in Section 5.3. It can be seen in Figure 5.4 that the torque controller successfully compensates for the negative gradient of the change in friction coefficient and that the transmission output torque trajectory does not change if the

torque controller is activated. The heavy torque oscillations from Figure 5.1could be eliminated and thus good shift quality could be maintained.

Figure 5.5, which depicts an upshift from 3rd to 4th gear, demonstrates that the torque controller improves the shift quality on other upshifts too. The tracking performances of both engine speed controller and transmission output torque controller are good in Figure 5.5. Comparing the simulation results for the upshift from 3rd to 4th gear without a torque controller (Figure 4.16) to the same upshift with a torque controller (Figure 5.5), shows that the torque profile in the latter case has become slightly smoother by introducing torque control indicating improved shift quality. This small improvement due to the introduction of the torque controller was observed, despite the fact that in both, Figure 5.5 and Figure 4.16, a friction coefficient with a positive gradient was employed.

5.2.2 Integrated Powertrain Controller for Power-on Downshifts including Torque Controller

In Section 5.1 (Problem 2 "change in torque profile") it was demonstrated that it would be beneficial for the shift quality, if the transmission output torque could be controlled in the torque phase of a power-on downshift. By controlling the transmission output torque along a specified reference trajectory, it is possible to select a gentler torque profile and to ensure this profile remains unchanged regardless of the gear to be shifted to. This ensures that the shift quality is unaffected by the gear ratios involved in the downshift and it enables to directly influence the vehicle acceleration profile (i.e. shift quality).

The control strategy for downshifts developed in Chapter 4, required that in the torque phase the clutch slip controller had to manipulate the pressure at the offgoing clutch and the pressure at the oncoming clutch had to be ramped up. The pressure ramp at the oncoming clutch was necessary in order to force the clutch slip controller to decrease pressure at the offgoing clutch and thus transfer engine torque. In order to implement the control of output torque without loosing the function of the clutch slip controller, the pressure manipulation at the oncoming clutch has to be split into two control actions. The first control action requires ramping up the pressure at the oncoming clutch; however, at a lower rate than before (without torque controller). This is necessary to force the clutch slip controller to gradually transfer engine torque. Then, the second control action comes from the closed-loop torque controller, which adds its contributions in the pressure manipulation to the pressure ramp of the first control

action. This procedure will become clearer when discussing the simulation results. Before doing that, the necessary modifications of the power-on downshift control algorithm from Chapter 4 will be explained.

Figure 5.6 shows the control algorithm for power-on downshifts from Figure 4.21 including the two additional steps (step 8 and step 11) necessary for activating the torque controller. The reference torque profile (Equation (68)) takes the form of a simple linear increase in torque with time, which starts at the transmission output torque value sampled at the beginning of the torque phase. The slope of the reference torque ramp can be selected according to the requirements. A gentle slope for increased shift quality and a steep slope for shorter sporty shifts. The reference torque ramp terminates when the pressure at the offgoing clutch has been decreased to zero by the clutch slip controller; i.e. engine torque has been transferred to the oncoming clutch in full.

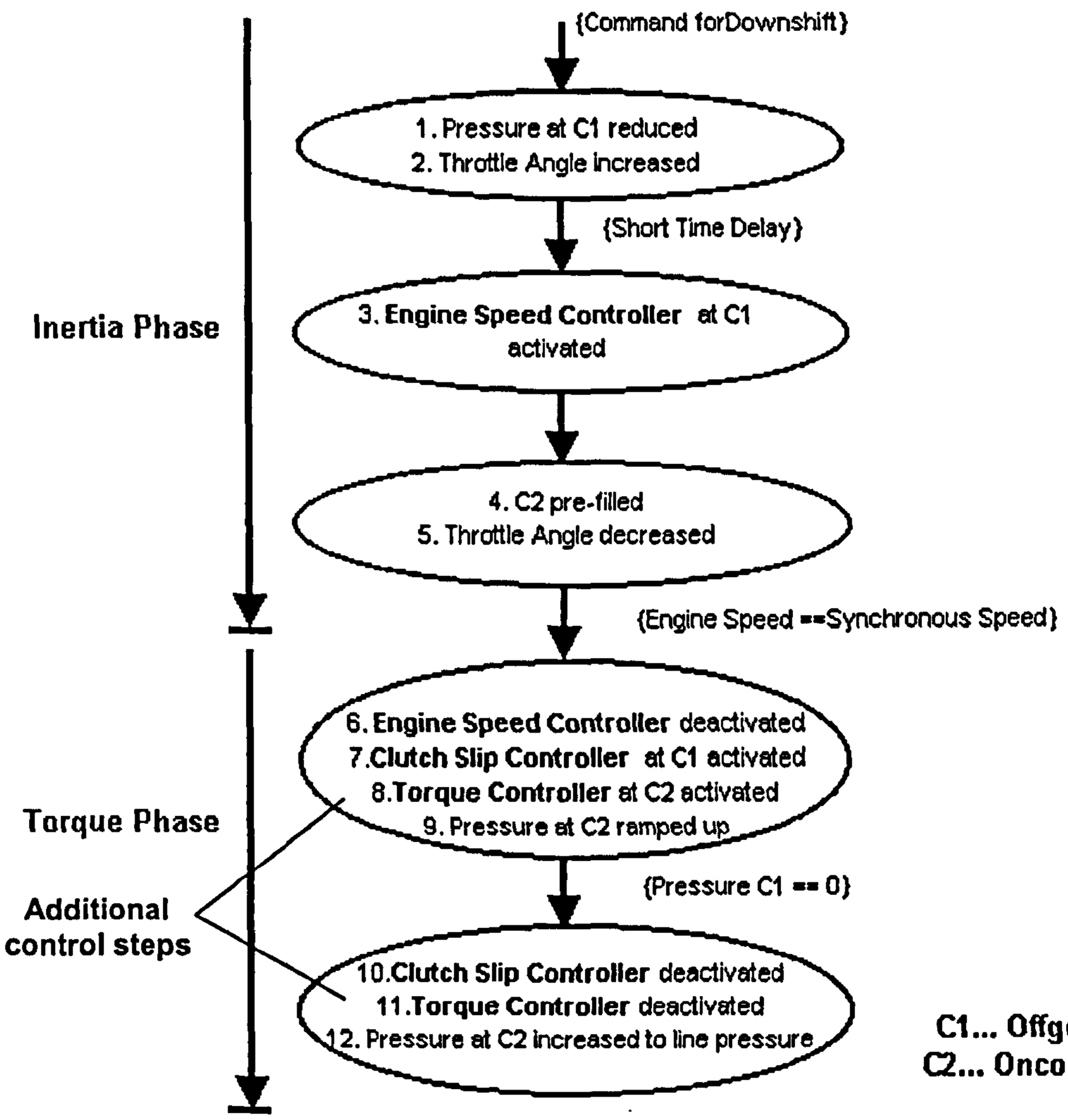

Figure 5.6 Control algorithm for proposed integrated powertrain controller for power-on down shifts (Figure 4.21) including control of transmission output torque (step 8 and step 11)

This dual control action allows a manipulation of the transmission output torque profile in the torque phase without interfering with the transfer of engine torque. Using the torque controller alone without employing a controller for the transfer of engine torque, would suffer from the problem that the transmission input torque changes over the duration of the gearshift, thus in the torque phase the transmission output torque does not simply change according to the change in the gear ratio, i.e. the exact target torque level is unknown. This makes it very difficult to construct a torque reference trajectory from information about the transmission output torque alone (further information about torque at one of the two clutch would be necessary).

Figure 5.7 shows a simulation result for the power-on downshift from 2nd to 1st gear from Figure 4.22, but with the difference that in Figure 5.7 the torque controller is active in the torque phase. The gearshift from Figure 5.7 is identical to that in Figure 4.22 up to the point where the engine runs synchronous with the target gear (left end of dashed circle).

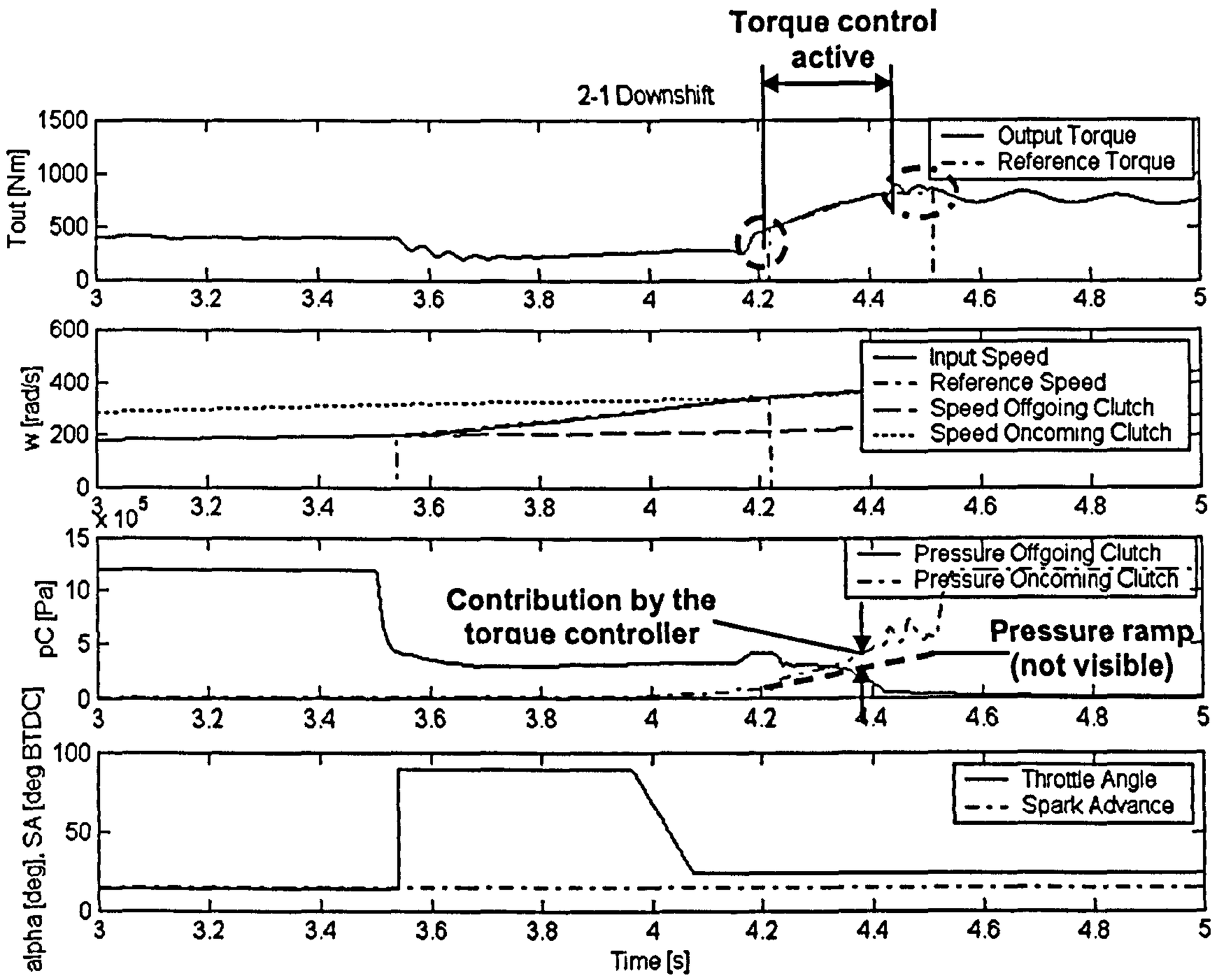

Figure 5.7 Simulation result: Proposed downshift controller plus torque controller, power-on downshift from 2nd to 1st gear from Figure 4.22 with control of torque

It was observed that for a smooth operation of the torque and clutch slip controller it is first necessary to ensure that the engine speed stays at the speed level of the target gear. This can be

achieved by keeping the engine speed controller active for a short period of time after the synchronous speed has been reached (dashed circle in Figure 5.7). After this extended period of operation of the engine speed controller, the torque phase can be entered where engine torque is transferred between the two clutches and transmission output torque is controlled. The pressure ramp at the oncoming clutch is indicated in Figure 5.7 by a dashed line. The additional pressure contribution by the torque controller is also shown. As can be seen in Figure 5.7 the tracking of the reference torque trajectory is good and the operation of the clutch slip controller is not negatively affected.

It was noticed that at the end of the reference torque ramp (i.e. end of torque phase), because the oncoming clutch is still slipping, a lock-up of the oncoming clutch through increase in clutch pressure caused torque vibrations. This problem was also due to the fact that at the point of lock-up the transmission output torque has to change abruptly from the ramp profile to the more horizontal profile. In order to reduce these torque vibrations the reference torque trajectory and hence also the torque control phase was extended by a short segment with the aim of keeping the transmission output torque to the level at the end of the reference torque ramp (dash dotted circle in Figure 5.7). During this extended control period the torque controller produced variations in the clutch pressure that lead to a lock-up of the oncoming clutch. Although these variations in the clutch pressure had spike-like character, it was nevertheless observed that the torque vibrations were reduced.

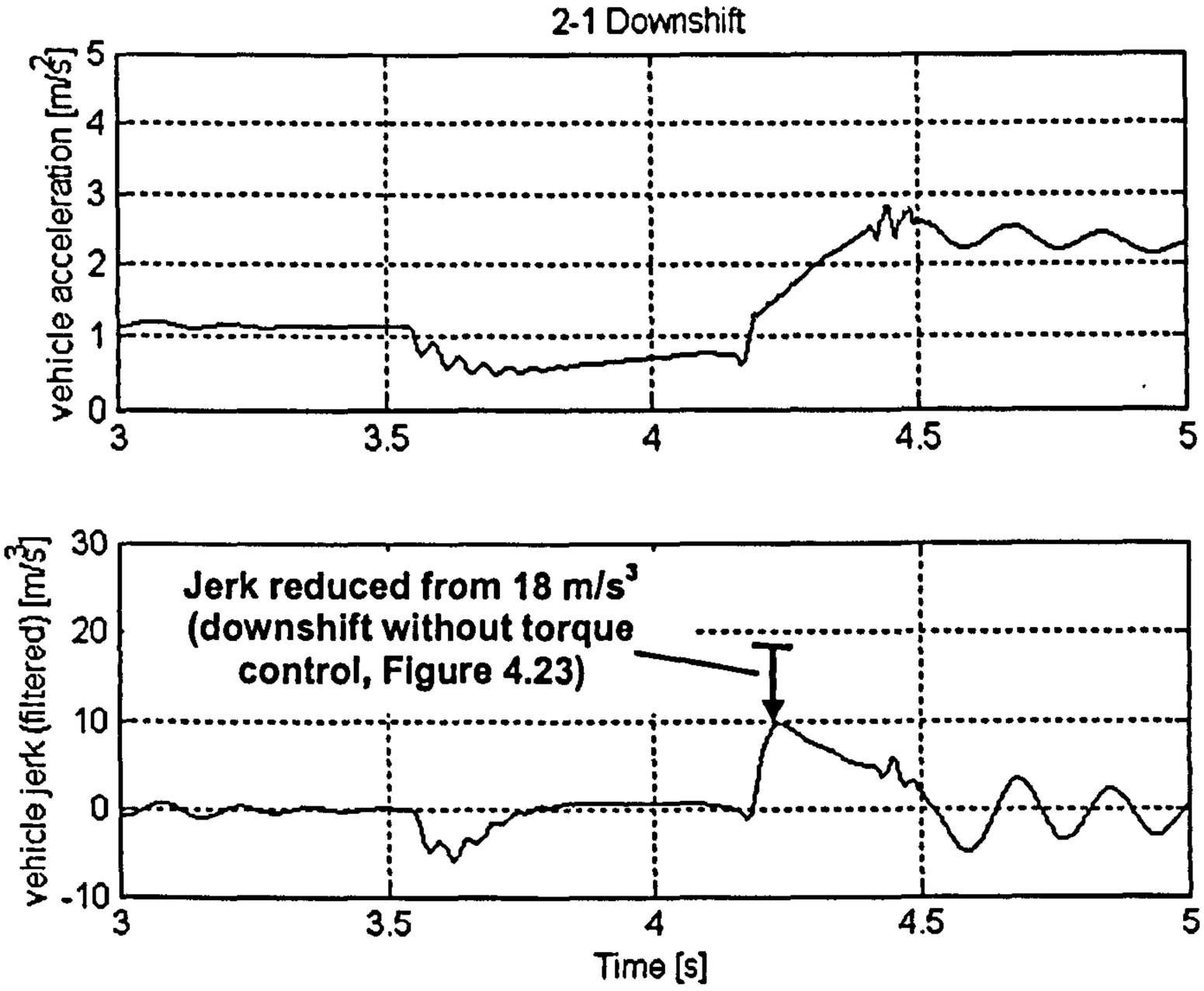

Figure 5.8 Vehicle acceleration and jerk for downshift from Figure 5.7

The downshift depicted in Figure 5.7 shows a much smoother torque trajectory as compared to the downshift without torque control (Figure 4.22). This is also reflected in its vehicle jerk profile (Figure 5.8). Comparing the vehicle jerk levels in Figure 5.8 to those for a gearshift without torque controller (Figure 4.23) shows that the level of vehicle jerk in the torque phase could be reduced from around 18 m/s^3 to 10 m/s^3 by introducing the torque controller. However, the torque vibrations at the end of the downshift are slightly increased, which can also be seen in the oscillatory vehicle jerk subsequent to the downshift.

So far it has been demonstrated that the torque controller enables to influence the shape of the torque trajectory in the torque phase of a downshift and thus allows the selection of a gentler profile for improved shift quality. However, in Figure 5.2 it was also demonstrated that the torque profile changed with changing parameters of the gearshift (e.g. shift time and gear ratios involved in the gearshift).

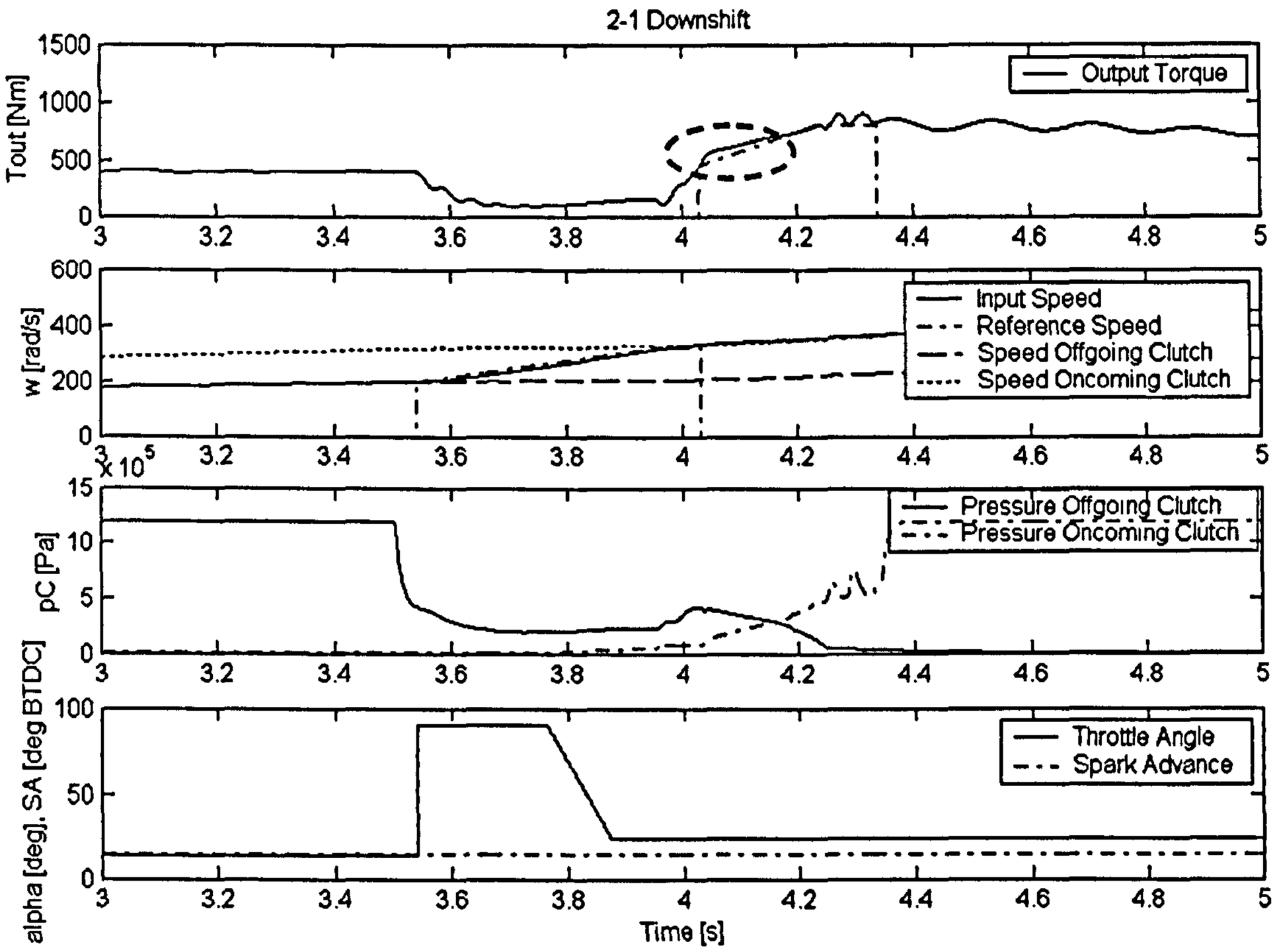

Figure 5.9 Simulation result: proposed downshift controller plus torque controller, power-on downshift from 2nd to 1st gear from Figure 5.7, with inertia phase reduced by 0.25 seconds

Figure 5.9 shows the downshift from Figure 5.7 with the inertia phase reduced by 0.25 seconds. Despite the shorter inertia phase the torque profiles of Figure 5.7 and Figure 5.9 look similar, which is attributable to the fact that the same reference torque trajectory has been employed for the two shifts. Hence, Figure 5.9 demonstrates that by adding torque control to the gearshift

control, the change in the torque profile in the torque phase due to a shorter inertia phase (see middle graph in Figure 5.2) is compensated for by the torque control, thus guaranteeing unaffected shift quality. The tracking performance in Figure 5.9 is not optimal at the beginning of the torque phase (dashed circle) but could be improved by a better tuning of the torque controller.

It remains to be demonstrated that the torque controller can also handle gearshifts between different gear ratios, without changes in the torque profiles. For this reason, Figure 5.10 shows a downshift from 4^{th} to 3^{rd} gear similar to that depicted in Figure 4.27. However, in Figure 5.10 the torque controller is active in the torque phase. This leads to a much smoother transmission output torque trajectory as compared to Figure 4.27 (or bottom graph in Figure 5.2). Since the change in torque in the torque phase is less pronounced in a gearshift from 4^{th} to 3^{rd} gear compared to a downshift from 2^{nd} to 1^{st}, a gentler torque profile had been selected for the downshift in Figure 5.10. The very low gradient of the reference torque profile in Figure 5.10 leads to a slowly changing transmission output torque profile, an indicator for very good shift quality. The tracking of the torque profile is generally good, only initially the torque profile does not settle immediately onto the reference trajectory.

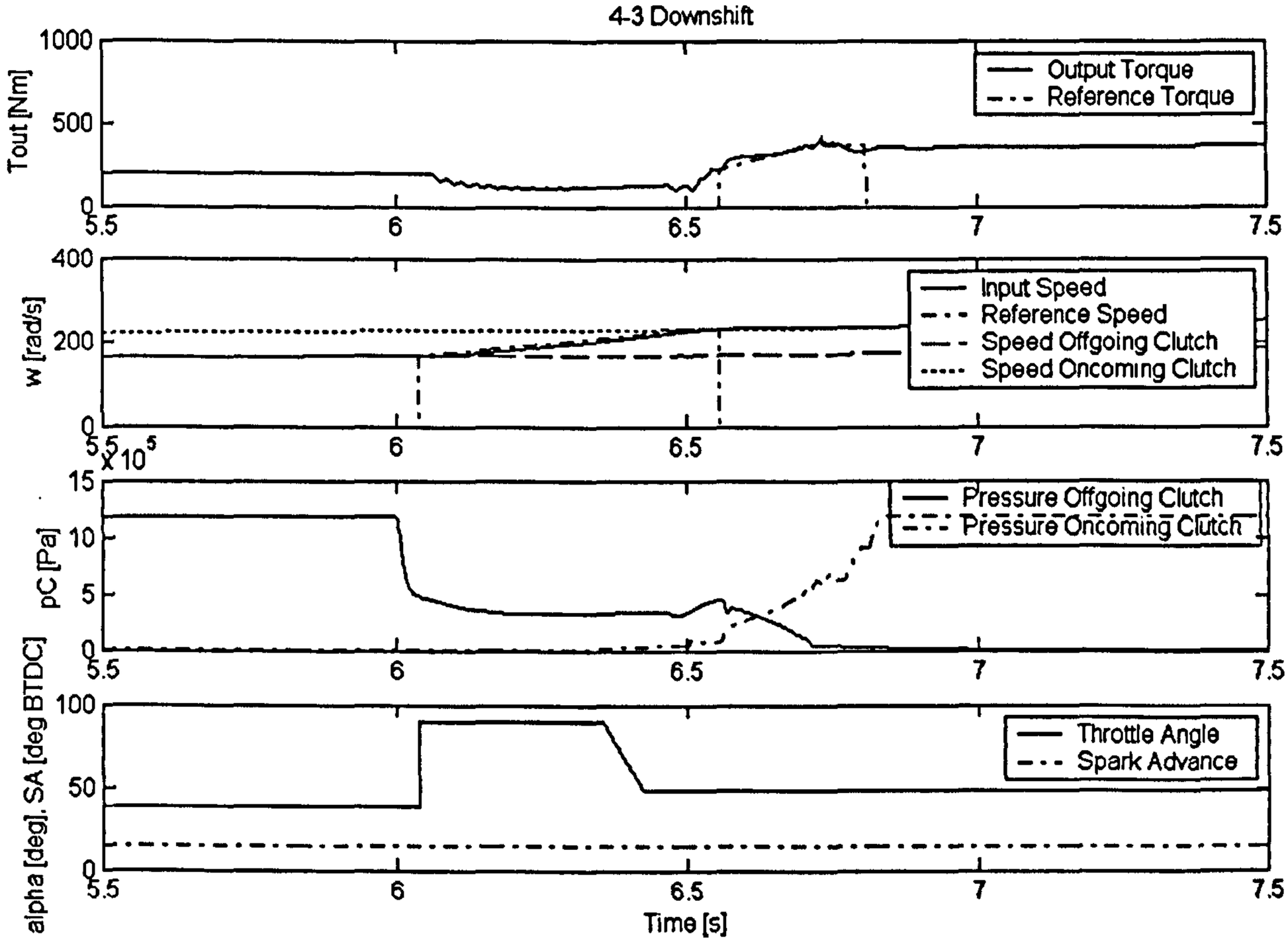

Figure 5.10 Simulation result: proposed downshift controller plus torque controller, power-on downshift from 4^{th} to 3^{rd} gear as in Figure 4.27 with control of torque

5.3 Structure of the Proposed Gearshift Controller including Torque Controller

The structure of the proposed integrated powertrain controller for gearshifts remains in principle the same as depicted in Figure 4.36 and is here only extended by adding the transmission output torque controller for both clutches. The structure (block diagram) of this gearshift controller extended by the torque controller is depicted in Figure 5.11. For reasons of clarity, the clutch slip and engine speed controllers were lumped into one block for each clutch in Figure 5.11 (Figure 4.36 depicts both controllers as separate blocks).

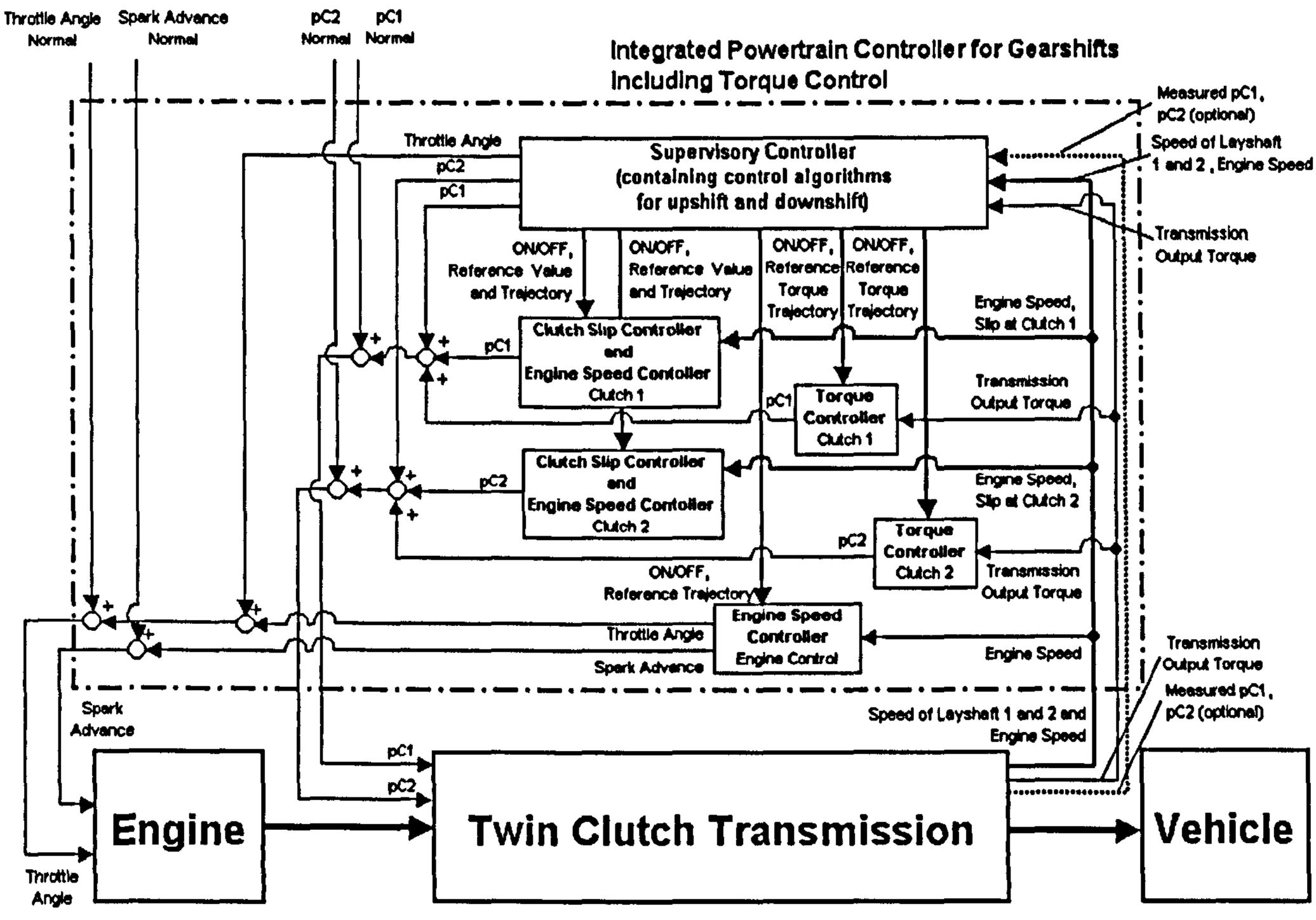

Figure 5.11 Structure of proposed integrated powertrain controller for gearshifts including torque controllers for both clutches

In Figure 5.11, the information about the transmission output torque is obtained at the output of the twin clutch transmission block. For the torque controller it was assumed that the transmission output torque is available as a measured signal. As explained, a mathematical observation of the torque signal is also possible, but the design of such an observer was not

undertaken in this work. It is assumed here that the transmission output torque is measured at the output shaft of the transmission. This transmission output torque signal is available at the inputs of the torque controllers at both clutches. The torque controllers output a clutch pressure (actually an input voltage to the solenoid valve) at either of the two clutches.

The supervisory controller (Top block in Figure 5.11) contains the control algorithms for upshift and downshift (Figure 5.3 and Figure 5.6) and activates the two torque controllers; it also generates the reference torque trajectories for the two torque controllers. For the generation of the reference torque trajectories the transmission output torque signal has to be available at the input of the supervisory controller. The clutch pressure signals (voltage signals) produced by the torque controllers are then added to the contributions of clutch slip and engine speed controllers. The total controller output is finally summed with the normal operating clutch pressure before being passed on to the solenoid valves.

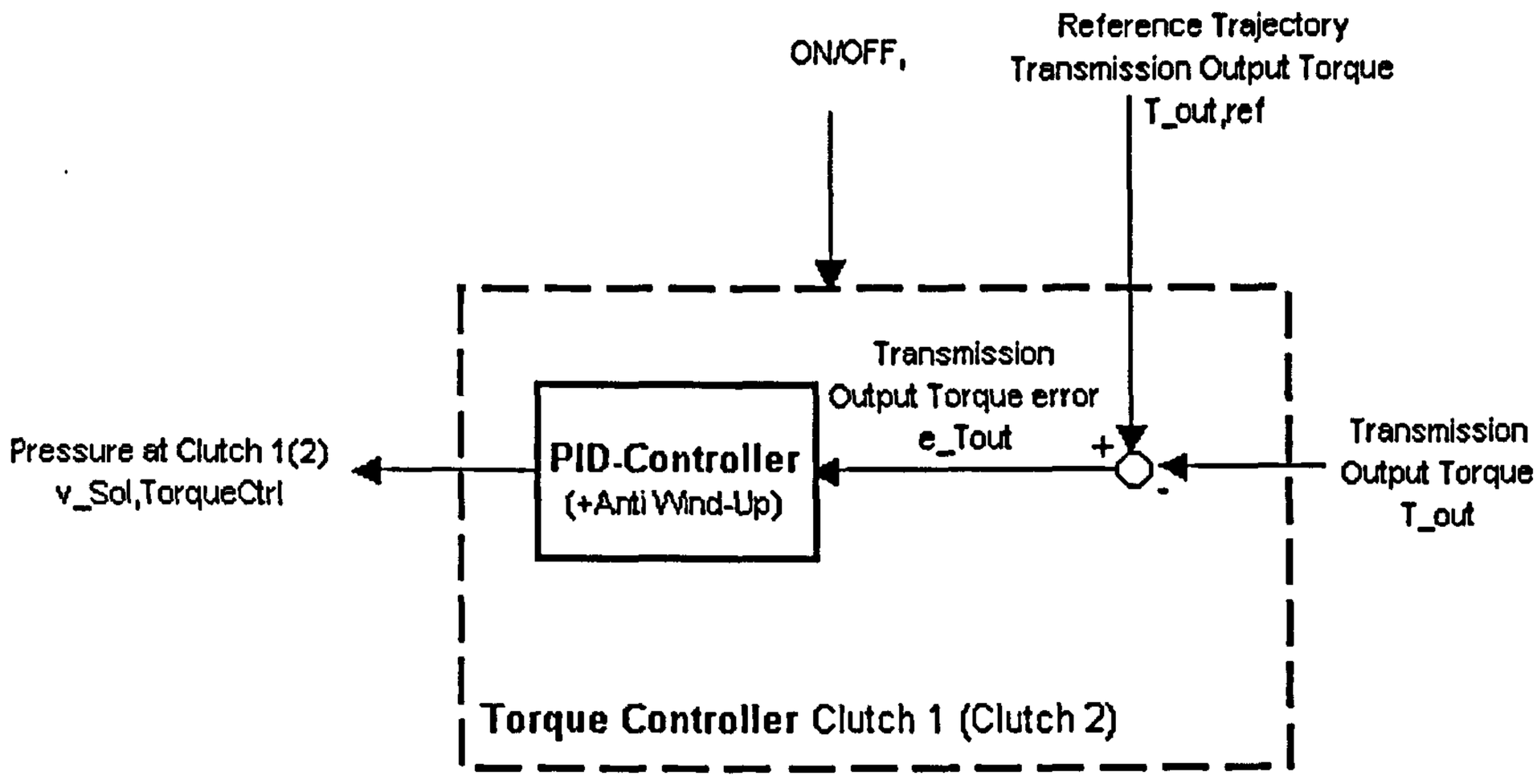

Figure 5.12 Detail of the torque controllers depicted in Figure 5.11

A more detailed block-diagram of the torque controller is provided in Figure 5.12. The error in transmission output torque (e_{Tout}) is calculated as difference of the measured transmission output torque (T_{out}) and the reference trajectory for transmission output torque ($T_{out,ref}$) according to equation (65). A PID controller produces a corrective output by applying equation (64) to the transmission output torque error. At the output, the torque controller produces a voltage signal that is inputted to the solenoid valve at the hydraulic clutch actuator ($v_{Sol,TorqueCtrl}$). The algorithm of the PID controller is given in equation (64) for the s-domain without sample and hold units (implemented as digital PID control algorithm in the simulation model).

$$v_{Sol,TorqueCtrl}(s) = (K_p + \frac{K_i}{s} + sK_d)e_{Tout}(s) \tag{64}$$

where:

$$e_{Tout} = T_{out,ref} - T_{out} \tag{65}$$

The measured transmission output torque used for the torque controller is actually the torque at the output gear of the differential according to equation (66). This is the transmission output torque that would be measured on a front wheel drive application as modelled here. The driveshaft torque (T_{drive}) can also be used for torque measurement. In practice, the difference between these two torque values will be very little. However, when comparing the results presented in this work to applications with rear wheel drive, it has to be kept in mind that the torque trajectories presented here do include the multiplication factor of the final drive, which essentially changes the scaling of the torque profiles.

$$T_{out} = (T_{kOut1} + T_{kOut2})i_f \eta_{Diff} \tag{66}$$

The reference trajectory for the torque controller on the upshift (Equation(67)) was selected to be a simple linear decrease from the torque value sampled at the beginning of the inertia phase ($T_{0,inertia}$) to a torque value at the end of the inertia phase that represents the change of transmission output torque over the whole upshift ($T_0 i_{high/low}$) according to the change in gear ratio. To determine this torque level at the end of the upshift the transmission output torque is sampled at the beginning of the shift (T_0) and then multiplied by the change in gear ratio (parameter $i_{high/low}$ in equation (67)). The parameter that controls the length of time of the reference trajectory ($t_{inertia}$) is the same as used by the engine speed controller. Hence, it can be ensured that the transmission output torque reference trajectory does indeed end at the appropriate torque level once the engine speed has reached the speed of the target gear.

In order to keep the torque controller operating properly even under circumstances of heavy torque vibrations at the transmission output, the torque value sampled at the beginning of the gearshift was actually a mean value. To obtain this mean value, the peaks of the torque signals had to be determined from the first time derivative (set to zero) of the torque signal (minimum or maximum were identified from the second time derivative). Then in the next step the mean value was determined to lie at half of the peak-to-peak distance. This value was held constant until a new mean value was calculated (following peak). The reference trajectory for transmission output torque controller as used in the power-on upshift controller is given in equation (67):

$$T_{out,ref} = (T_{0,inertia} - T_0 i_{high/low}) \frac{(t - t_{0,inertia})}{t_{inertia}} \tag{67}$$

The reference torque trajectory for the downshift (Equation (68) was also a of linear form, however, with an increasing gradient. The reference profile starts at a transmission output torque value sampled at the beginning of the torque phase of the downshift ($T_{0,torque}$ in equation (68)). From this torque value, the reference profile increases linearly with a gradient that can be selected accordingly (parameter Tgrad in equation (68)). The reference profile increases until the torque phase has been completed and the full amount of engine torque has been transferred to the oncoming clutch. From the end of the torque phase onwards the reference torque is simply held constant for a short period of time.

The reference torque trajectory in equation (68) does not contain the change in gear ratio, since the torque controller does not attempt to control the engine torque transfer directly (task of clutch slip controller), it simply determines the shape of the transmission output torque trajectory while engine torque is transferred between the two clutches. However, a steeper gradient in the reference trajectory naturally leads to a shorter, or in case of a gentler gradient to a longer, torque phase. The reference trajectory for transmission output torque controller as used in the power-on downshift controller is given in equation (68):

$$T_{out,ref} = T_{0,torque} + Tgrad(t - t_{0,torque}) \tag{68}$$

Three details are worthwhile noting for a successful integration of the torque controller in the gearshift controller:

- The torque controller applied to the power-on upshift controller was fitted with a lowpass filter at its input. The lowpass filter was of 3rd order Butterworth type and filtered the transmission output torque with a corner frequency of 60 rad/s. This measure was necessary because small high frequency torque vibrations at the beginning of the inertia phase caused the torque control loop to exhibit instability (clutch pressure and transmission output torque would become oscillatory with amplitudes increasing in size). These small vibrations are produced by a stick-slip transition of the clutch as a result of the deactivation of the clutch slip controller. Although, these small torque vibrations are harmless for shift quality because their amplitude is small and the frequency above that noticeable by the driver, they resulted in system instability when the torque controller was activated. Once the lowpass filter was fitted at the input of the torque controller, the system became stable with activated torque controller.

- In case of the power-on downshift controller, the output of the torque controller ($V_{Sol,TorqueCtrl}$) was limited at the lower end to allow only positive values. This measure was necessary in order to avoid a decrease of clutch pressure below the level of the underlying pressure ramp by the torque controller. By this measure it could be ensured that the torque controller did not affect the clutch slip controlled engine torque transfer.
- The controller gains of the PID torque controllers were different for upshift and downshift, which requires a PID controller where the controller gains can be switched between two sets.

5.4 Investigation into Robustness of the Transmission Output Torque Control

Similar to Chapter 4, the robustness of the transmission output torque controller applied to power-on upshift and downshift will be investigated for the following key sources of disturbances/variations:

- Change in parameters of the powertrain (-model)
- Change in the friction coefficient
- Disturbance due to sensor noise

5.4.1 Robustness to Parameter Changes

The variation of powertrain (-model) parameters was carried out in the same way as in Chapter 4 by varying the parameter values between the upper and lower limits given in Table 4.2. This section concentrates on the effects of the parameter variation on the torque controller. Following parameter variations were identified to have an influence on the performance of the torque controller:

- Damping in the driveline (weak effect)
- Stiffness of driveshafts (strong effect)

Interestingly, contrary to the findings in the robustness analysis for the engine speed controller (Chapter 4), reducing the damping rates in the driveline to the limits given in Table 4.2 did not have any significant influence on the torque controllers of upshift and downshift. However, it was noticed that an increase in damping (absolute damping rates) due to transmission drag did

deteriorate the tracking performance of the torque controller on the downshift. The torque controller on the upshift was unaffected by an increase in driveline damping.

However, the stiffness of the driveshafts was identified as the main influence on the performance of the torque controller. Increasing the driveshaft stiffness did not pose any problems at all. However, decreasing the driveshaft stiffness to the lower limits in Table 4.2 did produce instability (on the upshift). A similar situation was observed for a reduction in tyre stiffness. Interestingly, only the torque controller on the upshift seemed to be affected. The torque controller on the downshift was not affected at all (see Appendix B.2, Figure B.5 for a simulation result).

Figure 5.13 shows the upshift from 1st to 2nd gear from Figure 5.4 but with reduced driveshaft stiffness (k_{drive}=35000 Nm/rad). The instability of the torque controller as a result of the decreased driveshaft stiffness can be clearly seen in the profiles of clutch pressure, throttle angle, spark advance and transmission output torque.

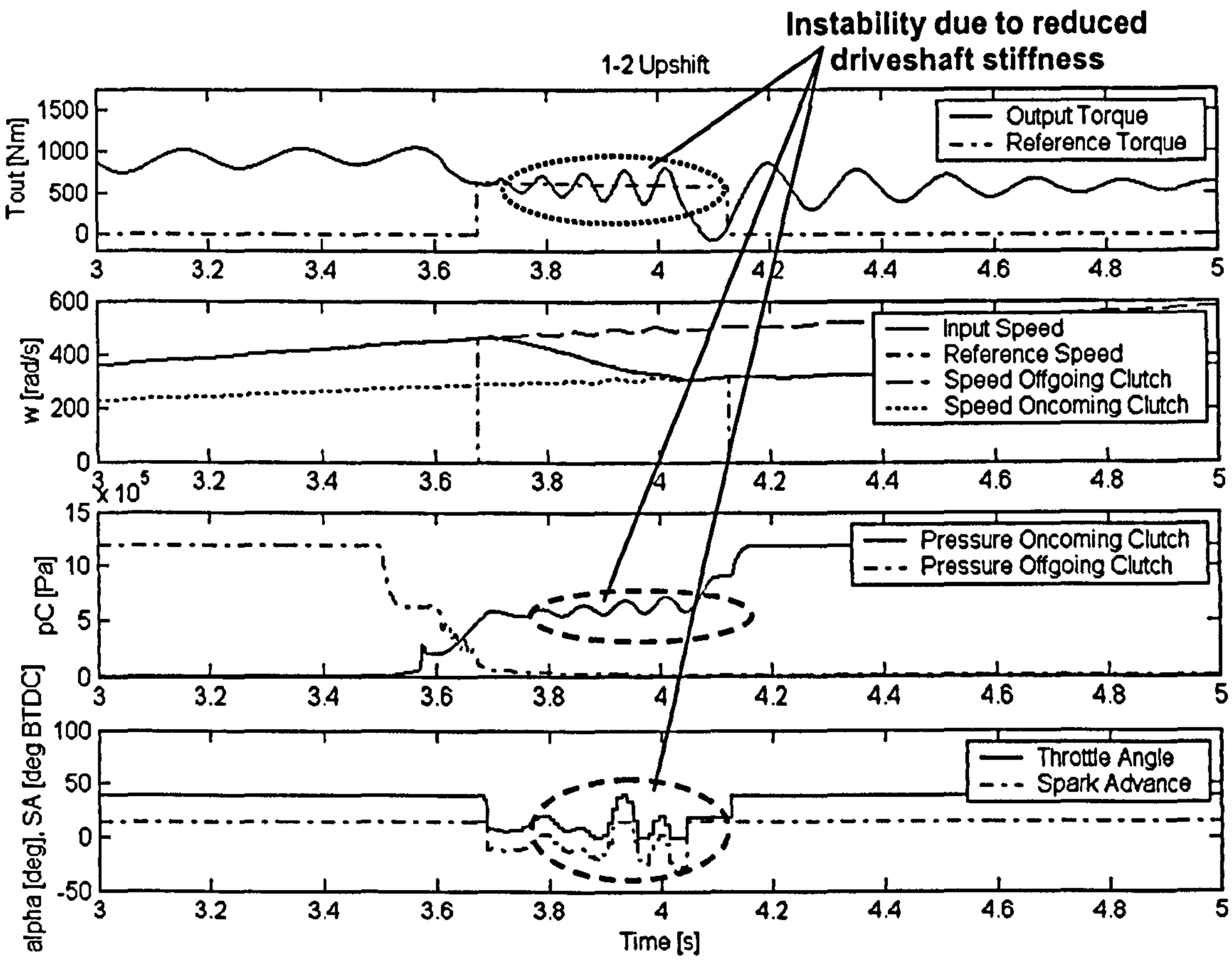

Figure 5.13 Simulation result: Proposed upshift control strategy plus torque controller, power-on upshift from 1st to 2nd gear from Figure 5.4, with reduced driveshaft stiffness (k_{drive}=35000 Nm/rad)

In Figure 5.13, the manipulated variables of the speed controller (throttle angle, spark advance) and of the torque controller (pressure at oncoming clutch) show unstable oscillatory behaviour with increasing amplitude (dashed circles in Figure 5.13). This results in torque vibrations (dotted circle in Figure 5.13) with increasing amplitude and a large drop in output torque at the end of the gearshift. This behaviour is clearly not only critical from a tracking performance point of view for speed and torque controller, but also for the shift quality on the whole and has to be avoided at all cost.

In the discussion of the robustness of the speed controller as used on upshifts (Chapter 4), it was observed that the stability problems could be solved by modifying the controller gains of the PID controllers that manipulate throttle angle and spark advance. Furthermore, it was remarked that reduced driveshaft stiffness showed the same stability problems as reduced driveline damping. Hence, in a first attempt to avoid the instability behaviour observed in Figure 5.13, the controller gains were modified in the same way as done in Chapter 4, Section 4.5.1. This first modification eliminated the oscillations in throttle and spark advance and the drop in output torque at the end of the shift became smaller. However, the instability of the torque controller could not be removed entirely.

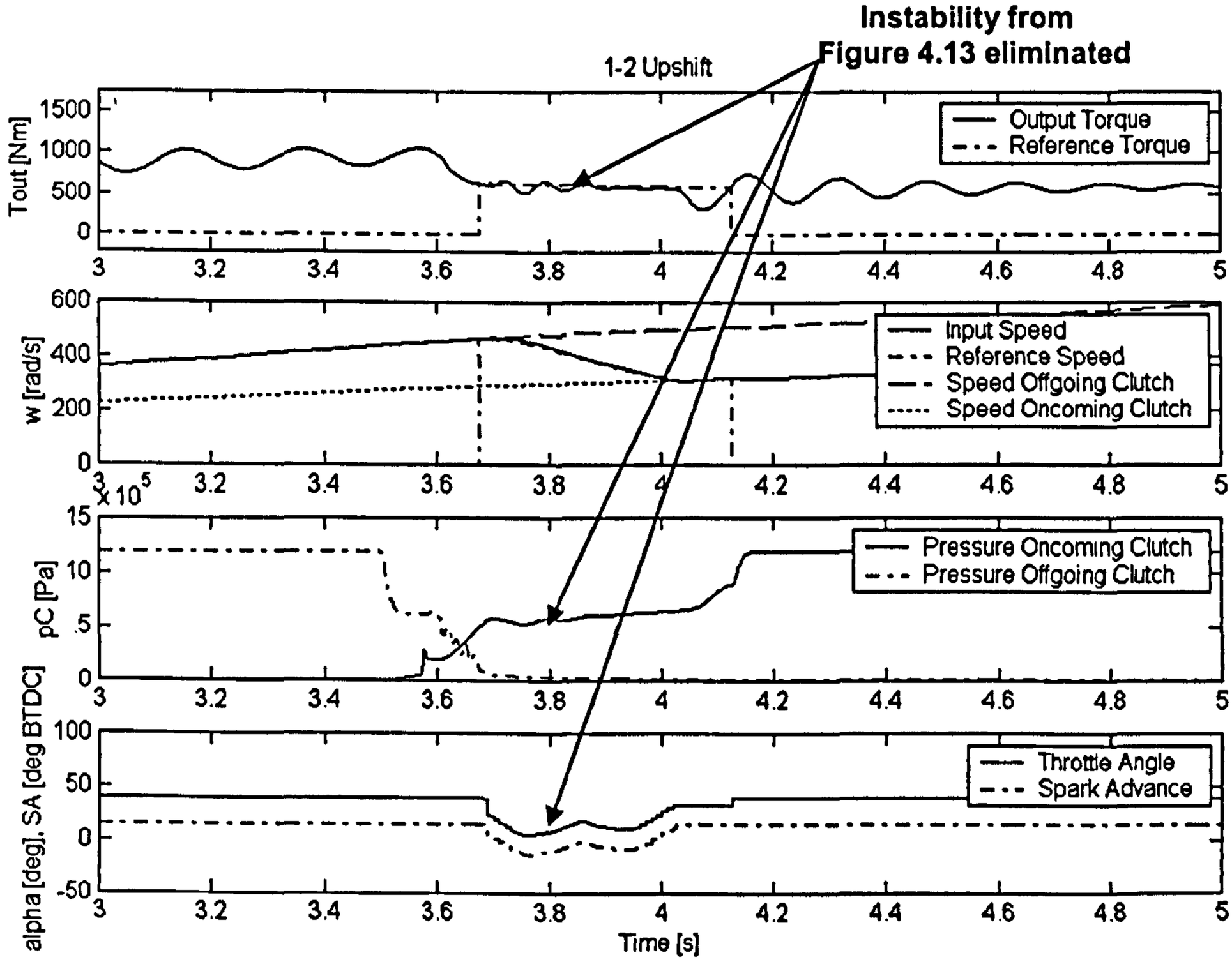

Figure 5.14 Simulation result: Upshift from Figure 5.13, with modified PID controller gains (engine speed controller) and modified corner frequency of low pass filter (torque controller)

Now, as was explained before, the low pass filter in front of the torque controller helped to produce a stable torque controller. With this fact in mind, it can be found that by reducing the corner frequency of this low pass filter from 60 rad/s to 50 rad/s, the torque controller becomes stable again despite the reduced driveshaft stiffness. These two measures are applied in Figure 5.14, which shows the upshift from Figure 5.13, with modified gains of the speed controller (From K_p= 4 to K_p= 2 for both PID of throttle angle and spark advance and from K_I= 8 to K_I= 4 for PID of throttle and from K_I= 9 to K_I= 5 for PID of spark advance) and with modified corner frequency (from 60 rad/s to 50rad/s) of the low pass filter at torque controller input. As can be seen from Figure 5.14, the unstable oscillations could be successfully removed from the manipulated variables (throttle and spark advance, pressure at oncoming clutch). As a consequence the torque vibrations were eliminated too, establishing good shift quality again (increased torque vibrations at the beginning and end of the shift are a product of the low driveshaft stiffness).

5.4.2 Robustness to Changes in the Friction Coefficient

It was found that a change in the clutch friction characteristic (from a positive gradient to a negative gradient) did not influence the stability of the torque controller either on an upshift or a downshift. The influence of the change in the clutch friction characteristics on the tracking performance of the torque controller or shift quality will be discussed briefly now.

On upshifts, a variation in the friction characteristics was one of the main motivations for developing the torque controller. It has been demonstrated that the torque controller on the upshift, works despite the change in the friction coefficient. Furthermore, it compensates for the influence of the changed friction coefficient on shift quality.

On downshifts, the shift quality was not affected at all. Also the tracking of the torque controller was not significantly affected. Only, at the beginning of the torque phase a small deviation from the reference profile could be observed, which can possibly be removed by better tuning of the PID torque controller (see Appendix B.2, Figure B.6 for a simulation result).

5.4.3 Robustness to Sensor Noise

To test the sensitivity of the torque controller to sensor noise a white noise signal (band-limited white noise with power level of 0.03, sample time of $5*10^{-4}$s) with amplitudes ranging from around –60 to 60 Nm was added to the transmission output torque signal before being fed back into the torque controller. The parameters of the noise signal were selected in order to produce a variation in amplitude that is roughly +/-10% of the nominal signal in the medium transmission output torque range (around 600 Nm). It is thought that this variation in amplitude in the noise signal represents a realistic figure for noise pollution existing in torque measurements.

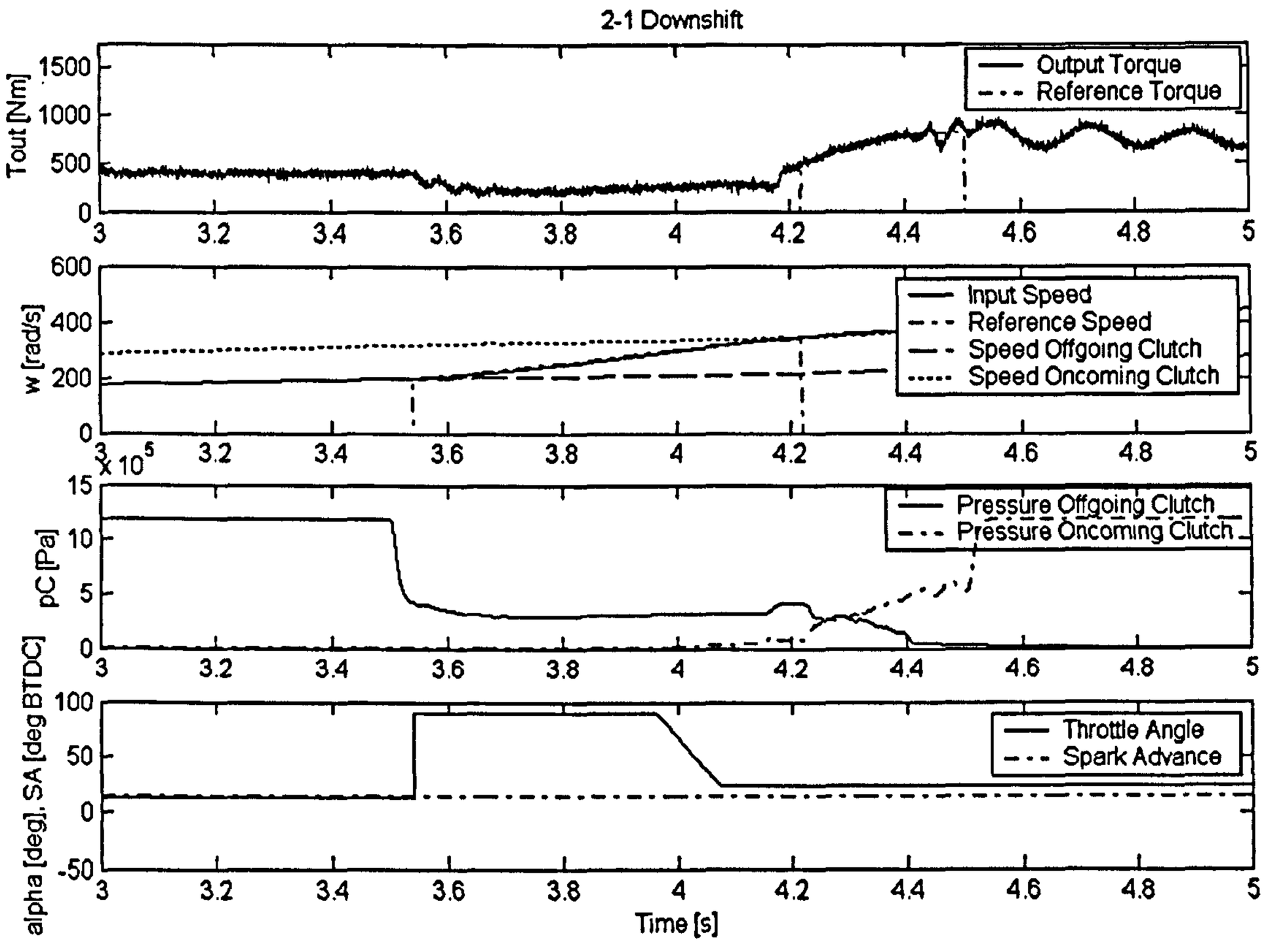

Figure 5.15 Simulation Result: Downshift from 2nd to 1st gear from Figure 5.7, with noise polluted transmission output torque signal (top graph) and rate limiting of the torque error signal

The tracking performance of the torque controller and the shift quality remained completely unaffected by the sensor noise on upshifts. The explanation for the robustness of the torque controller on the upshift is, that the low pass filter at the input of the PID torque controller effectively filters all high frequency signal portions including noise (a simulation result of an upshift with control of torque and senor noise is presented in the Appendix B.2, Figure B.7).

The situation at the downshift was completely different: Adding noise with the same specification as above to the measurement signal of transmission output torque rendered the torque controller completely inoperative. The reference torque trajectory was not tracked at all and also the torque phase was unnecessarily elongated.

Fortunately, the remedy for this problem was simple: Limiting the rate of change of the tracking error (slew rate of the signal was limited to-5000 to 5000), before inputting it to the PID torque controller, did reduce sensitivity of the derivative part of the PID controller to high frequency portions in the tracking error signal such as contributions coming from the noise. This measure effectively restored full operation of the torque controller on the downshift despite noise being present in the torque signal as can be seen in Figure 5.15. However, torque vibrations at the end of the torque phase seemed to be more pronounced compared to the case without sensor noise. This seems to be a problem of the torque controller that occurs while tracking the horizontal part of the reference trajectory and has to do with the lock-up of the clutch not being executed smoothly enough.

5.5 Conclusions

A unique feature of the gearshift controller developed in this thesis was the use of a transmission output torque controller on power-on upshifts and downshifts as an optional element.

In this chapter it was clearly demonstrated that the addition of a transmission output torque controller could improve the performance of the basic gearshift controller developed in Chapter 4, in terms of robustness to variations in the gearshift parameters and to changes in the clutch friction, to achieve better shift quality.

A specific novelty was the solution on how to integrate the transmission output controller in the control of to the torque phase of a downshift, where the engine torque transfer is managed by a control of clutch slip. This required a unique approach to enable an unaffected operation of the clutch slip controller, whilst clutch pressure is manipulated at the oncoming clutch by the torque controller.

Once more the robustness of the proposed controller, this time the torque controller, to changes in the friction coefficients and other powertrain parameters and sensor noise was investigated. It

was demonstrated that the torque controller is robust in terms of controller stability to the above mentioned parameter changes and disturbances. The unique ability of the torque controller to guarantee an unaffected shift quality despite changes in the friction coefficient and shift parameters could also be demonstrated clearly.

One problematic issue that has crystallised in the last two chapters was the lock up behaviour of the clutch at the end of the gearshift, in particular, on downshifts. On upshifts this problem was solved in this thesis by abruptly raising the spark advance at the point of lock up. For downshifts a similar solution (modulating spark at point of clutch lock up) is possible.

Chapter 6

Gearshift Controller for Twin Clutch Transmissions applied to Doubleshifts

In Chapter 4 and 5 the gearshift controller has been applied with or without a torque controller to single gearshifts (i.e. shifts such as from 1st to 2nd or from 3rd to 2nd gear etc.).

In this chapter the same control loops will be applied to doubleshifts (e.g. from 4th to 2nd gear) or other multiple gearshifts in the same transmission half (e.g. from 6th to 2nd gear). However, these double/multiple gearshifts will be accomplished as integrated or interlinked gearshifts, hence the driver notices only one gearshift event.

Chapter 6 starts with a review of the difficulties involved with gearshifts between gears in the same transmission half in Section 6.1.

In the subsequent section, Section 6.2 the new integrated controller for double/multiple gearshifts is developed, firstly, as a basic version, featuring closed-loop control of clutch slip and of engine speed (Section 6.2.1) and then secondly, as an extended version which includes the control of transmission output torque (Section 6.2.2). Each of these two subsections starts with (multiple-)downshifts as the more important case and then goes on to a brief treatment of (ultiple-) upshifts.

The chapter finishes with a conclusions section (Section 6.3).

6.1 Difficulties with Shifts between Gears on the same Transmission Half

As already explained (Chapters 4 and 5), gearshifts between odd and even gears (and vice versa) can be accomplished as simple clutch-to-clutch shifts on a twin clutch transmissions. This is in principle also true of gearshifts skipping gears, so called multiple gearshifts (sometimes also

called "direct" shifts), as long as the gearshift involves shifting to a gear located in the other half of the transmission (i.e. a gearshift between odd and even gears). This is one advantage of the twin clutch transmissions over planetary-type transmissions, where multiple gearshifts from e.g. 5^{th} to 2^{nd} gear can often not be accomplished as single clutch-to-clutch shifts. Whether multiple gearshifts (or only limited cases of multiple gearshifts) are possible on a planetary-type transmission depends on the mechanical layout (how planetary gearsets are connected with each other) and the hydraulic layout (often, the clutches and brakes have to be operated in a pre-determined order).

Coming back to twin clutch transmissions, the difficulties arise when shifting between gears located in the same half of the transmission. In such cases, multiple gearshifts cannot be accomplished as simple clutch-to-clutch shifts. A prominent form of such a multiple gearshift is the doubleshift (e.g. a gearshift from 4^{th} to 2^{nd} gear), which involves shifting between two even (or two odd) gears and skipping the odd (or even) gear in between. This form of multiple gearshift or doubleshift requires the change from the currently engaged gear to the target gear to take place on the same transmission half. This means, for a conventional twin clutch transmission design, a change of synchronisers on the same half of the transmission. A change of synchronisers, in particular the engagement of the synchroniser carrying the target gear, can only be executed if the according half of the twin clutch transmission is torque-free. This in turn means that the clutch in the transmission half of the current and the target gear, has to be disengaged during the doubleshift or multiple gearshift.

In this chapter only this form of multiple gearshift is discussed. To avoid confusion with other multiple gearshifts (executed as clutch-to-clutch shifts), the following text only uses the term doubleshift. However, the control techniques developed here for doubleshifts apply similarly for other multiple gearshifts within the same transmission half (e.g. from 6^{th} to 2^{nd} gear).

The obvious forms of controlling a doubleshift are:

1. <u>Doubleshifts with interruption in traction:</u> If the other clutch is not involved in the doubleshift, the simplest form of controlling a doubleshift would be similar to controlling gearshifts on an automated manual transmission. This form of control produces very fast doubleshifts. However, as with the automated manual transmission the doubleshift suffers from an interruption in the tractive force at the wheels, which is unacceptable for a twin clutch transmission, if powershift capability is to be retained.
2. <u>Doubleshift as consecutive gearshifts:</u> The second alternative is to split the doubleshift into single gearshifts that can be accomplished as clutch-to-clutch shifts. The advantage of this strategy is that the tractive force at the wheels stays above zero during the clutch-to-clutch

shifts. However, the necessary change of gear (i.e. synchronisers) between single clutch-to-clutch shift events takes a relatively long period of time, which means an increase in the overall shift time. A further disadvantage of this form of double-downshift is, that the acceleration of the engine is interrupted between the single downshifts, in order to change the synchronisers. This forces the engine speed to remain "constant" for a relatively long period of time. Also, the transmission output torque drops twice due to the fact that the engine has to be accelerated twice (in each single downshift). Because of these phenomena the driver is able to clearly distinguish two consecutive gearshift events instead of the desired single doubleshift event [Wagner 1994]. The long shift time of a such-controlled doubleshift is, in particular, disadvantageous for downshifts, where the driver often desires an instant response of the vehicle to accelerate.

To demonstrate these two forms of controlling doubleshifts, the following two simulation results show doubleshifts from 3rd to 1st gear. First executed as two single clutch-to-clutch shifts (Figure 6.1) and secondly, executed as single gearshift with interruption in traction (Figure 6.2).

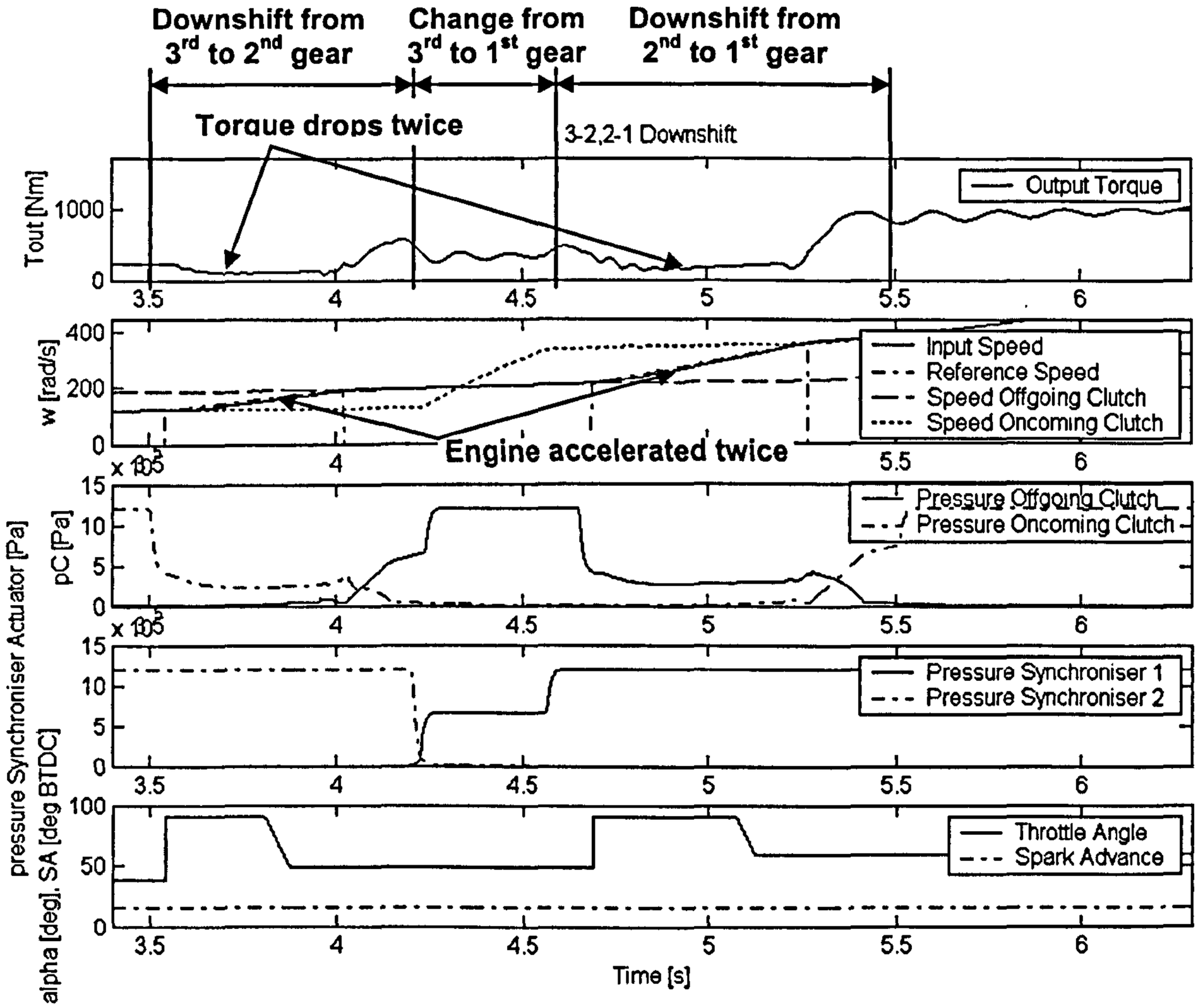

Figure 6.1 Simulation result: Doubleshift executed as two consecutive downshifts from 3rd to 2nd and further from 2nd to 1st gear.

The simulation results presented in this chapter were produced by using the extended model of the twin clutch transmission (see Chapter 3). The simulation diagrams are basically the same as used throughout Chapters 4 and 5, but are extended here by one additional graph (second graph from bottom) showing the actuation pressure at the (hydraulically actuated) synchronisers.

The doubleshift form 3rd to 1st gear in Figure 6.1 is accomplished as two single downshifts. It starts with a clutch-to-clutch shift from 3rd to 2nd gear. After the first downshift has been completed, a change of gears from 3rd to 1st gear takes place on the same transmission half. The change of gear involves as a first step, decreasing the pressure at the actuator of the synchroniser carrying the 3rd gear to zero (synchroniser 2 in Figure 6.1). As a second step, the 1st gear can be engaged, which involves increasing the pressure at the actuator of the synchroniser carrying the 1st gear (synchroniser 1 in Figure 6.1): Firstly, to a level required for the synchronisation within a certain time and secondly, to the line pressure (maximum pressure in the hydraulic actuation circuit) once synchronisation of the 1st gear is completed. The synchronisation of the target gear can be observed in the acceleration of the oncoming input shaft (denoted as oncoming clutch in Figure 6.1). After the target gear (1st gear) has been engaged a second clutch-to-clutch shift finally changes to 1st gear.

The following things can be observed in Figure 6.1:

- The overall shift time of the two consecutive downshifts amounts to around 2 seconds.
- An interruption in traction does not occur in the doubleshift in Figure 6.1 and the transmission output torque stays above zero level.
- The doubleshift in Figure 6.1 is clearly discernable by the driver as two single gearshifts because the output torque drops twice in each of the two inertia phases only to rise twice again in each of the subsequent torque phases. Also, the engine speed increases twice and remains almost "constant" in between. As explained, this shift feel is not desirable for doubleshifts.

Figure 6.2 shows the case where a doubleshift is executed with interruption in traction. The torque-transmitting clutch is disengaged for the time of synchronisation (dotted circle in Figure 6.2) and the transmission output torque drops to zero during that time (dashed circle in Figure 6.2). The change of gears (i.e. synchronisers) was accomplished in the same way as in the doubleshift of Figure 6.1 and therefore also takes the same amount of time as in the previous doubleshift case. At the end of the gear change when the synchronisation of the engine speed is completed the clutch is engaged again. The throttle angle was not reduced to zero for the time the clutch was disengaged.

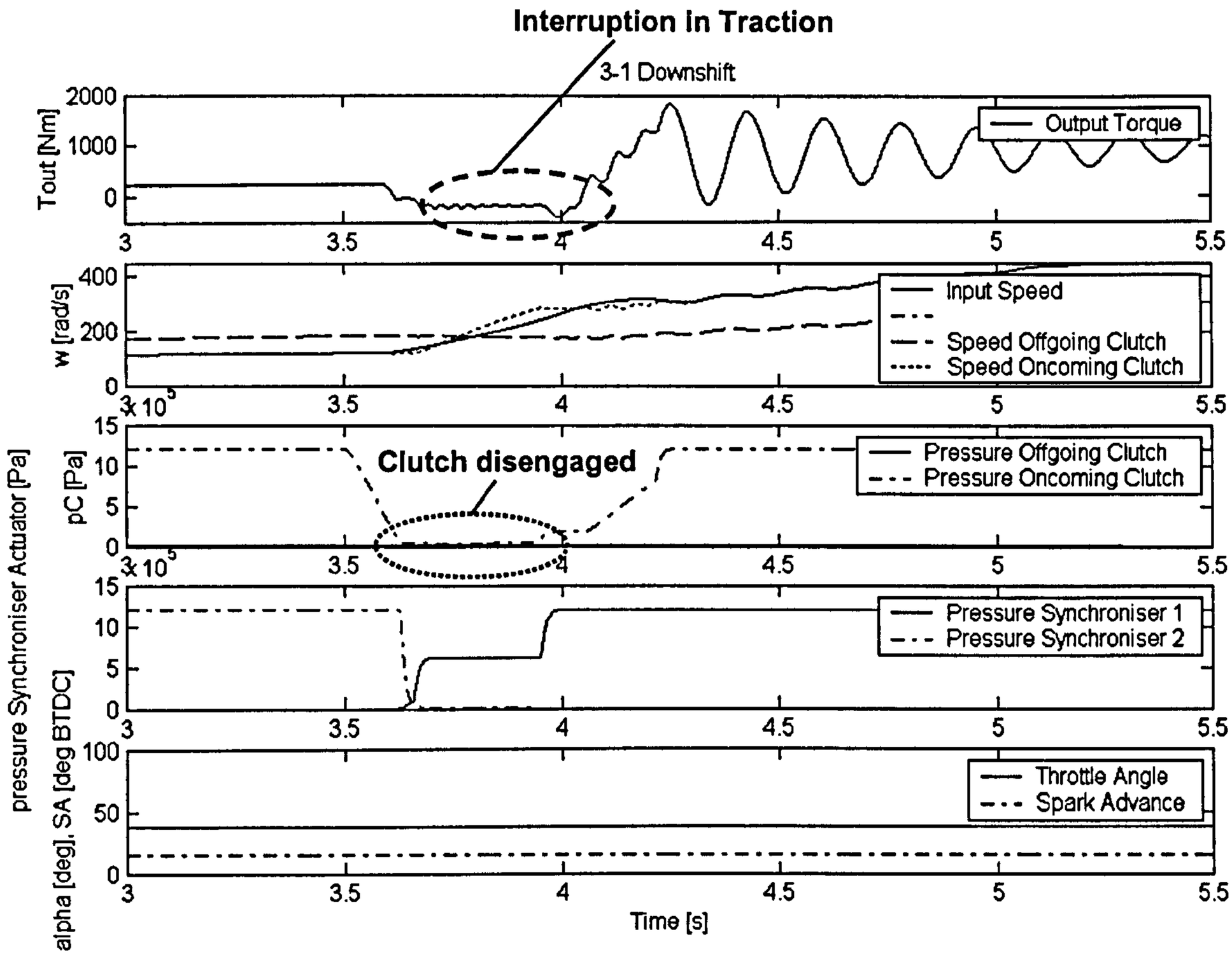

Figure 6.2 Simulation result: Doubleshift executed as single downshift from 3rd to 1st gear with interruption in traction.

Following things can be observed for the doubleshift in Figure 6.2:

- The doubleshift with interruption in traction produces a much faster shift of around 0.75 seconds.
- The driver senses the shift depicted in Figure 6.2 as a single gearshift event, feeling a continuous acceleration of the engine during the gearshift.
- The big disadvantage of the control method depicted in Figure 6.2 is the interruption in tractive force at the wheels (dashed circle in Figure 6.2), which produces an even negative transmission output torque due to the application of the synchroniser.
- A smooth re-application of the clutch also seems to be difficult to control, as can be seen from the transmission output torque profile in Figure 6.2, which shows heavy torque vibrations subsequent to the gearshift.

The above discussion has shown that it is desirable to find a more sophisticated control approach to doubleshifts on twin clutch transmissions in order to improve the shift quality of these special shifts. In particular, a solution for double-downshifts is important since the transmission is required to respond much faster in case of a power-on downshift (acceleration of

vehicle requested) than in case of an upshift. Also, the text concentrates on power-on doubleshifts as power-off double- or other power-off multiple gearshifts could be executed as gearshifts with interruption in traction (control case 1 from above) on twin clutch transmissions without any major drawbacks.

6.2 Proposed Control of Power-On Doubleshifts

In Chapter 2 it was mentioned that the problem of "double-downshifts" was discussed in [Wagner 1994], who proposed an alternative control strategy that does not result in either an interruption in tractive force or to two consecutive gearshifts. The idea is simple: during the phase where the torque-transmitting clutch is disengaged, for a change of gears (synchronisers), the second clutch carrying the gear ratio between the initial and the target gear is engaged partially (see Figure 2.6). This procedure ensures that the second clutch transmits at least part of the engine torque during the doubleshift. The other clutch can then be disengaged for a change of the synchronisers without resulting to an interruption in traction during the doubleshift.

The method described in [Wagner 1994] is preferred in this work over other approaches (see Chapter 2) because of the higher level of the tractive force during the doubleshift. This method will henceforth be denoted as "integrated doubleshift" in the text and was explained and sketched in Chapter 2 (Figure 2.6). However, the control strategy of [Wagner 1994] only used open-loop pressure ramps. In order to use the full potential of engine involvement and closed-loop control for the control of doubleshifts, in this work, the approach of [Wagner 1994] is extended by applying the control strategies developed in Chapters 4 and 5, thus providing improved robustness and shift quality.

The following section will develop this new integrated powertrain controller for "doubleshifts" in detail. Firstly, this will be explained for a basic version featuring an engine-assisted synchronisation of the engine and control of clutch slip. Secondly the basic control will be extended to incorporate torque control. Each section details the control strategies firstly, for downshifts and secondly, for upshifts. The control strategy is described in greater detail for a "double-downshift" due to the greater importance of these shifts in comparison to "double-upshifts", which are explained with less detail. Again, the simulation results shown in the following sections make use of the extended model of the twin clutch transmission (see Chapter 3).

6.2.1 Basic Control Strategy for "Integrated Doubleshifts"

Basic Control Strategy for "Integrated Double-Downshifts"

Figure 6.3 shows the principle of the control strategy for double-downshifts executed as "integrated double-downshifts". As mentioned before, the idea of partially engaging the second clutch during the change of gear was adopted here. This basic control principle will be extended here to incorporate the same control features (engine speed controller, clutch slip controller and torque controller), and thus attached advantages, as already introduced for single downshifts in Chapters 4 and 5.

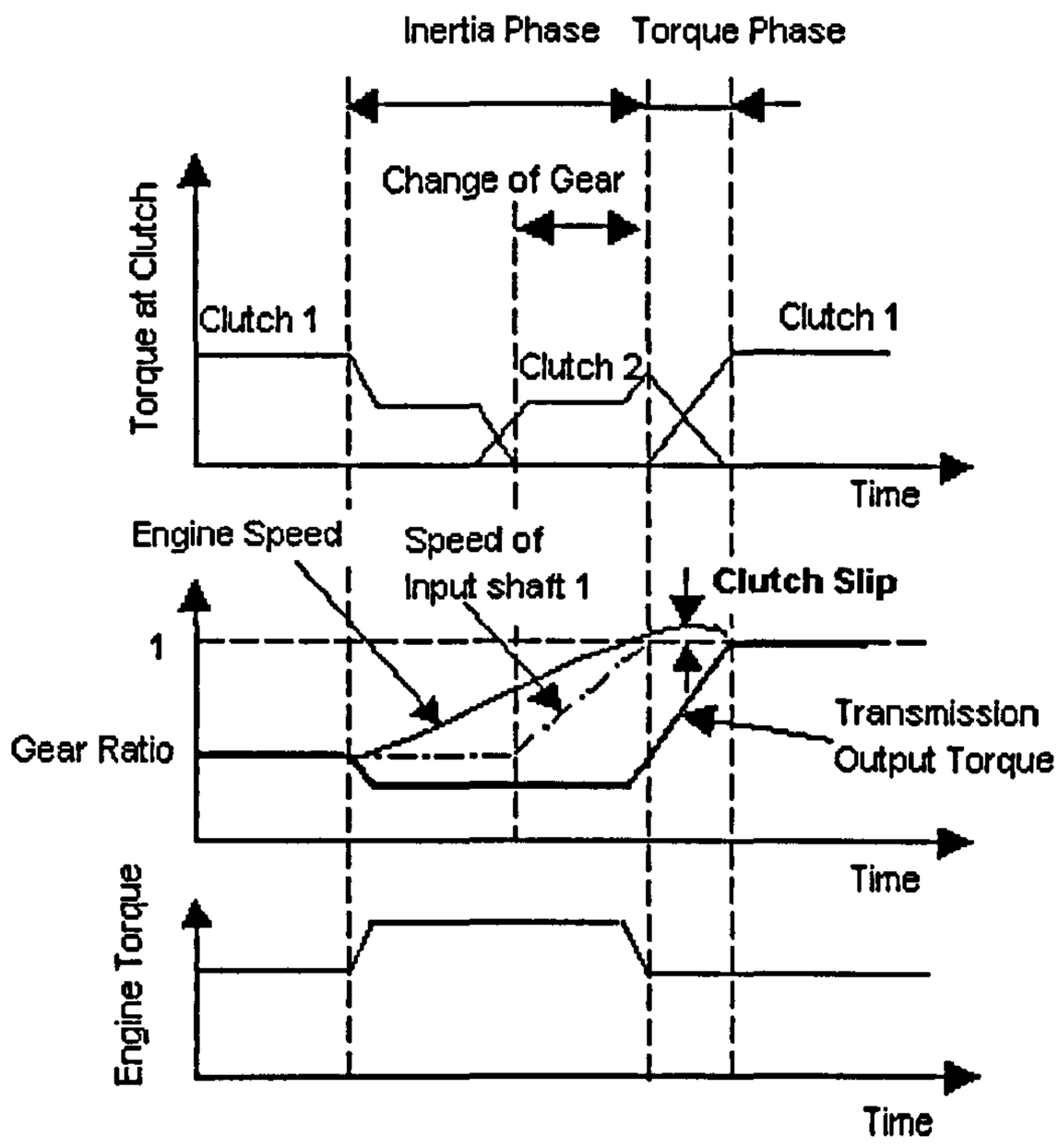

Figure 6.3 Principle of the control of integrated double-downshifts

Referring to Figure 6.3, the control of integrated double downshift works as follows:

At the beginning of the gearshift the pressure at the offgoing clutch (clutch 1 in Figure 6.3) is decreased in order to bring the offgoing clutch to slip. At the same time engine torque is raised to assist the engine acceleration. These two actions enable the engine to start its acceleration. The transmission output torque drops slightly because only part of the engine torque is transferred to the transmission output (the other part is used by the engine for its own acceleration). This so far is the same procedure as for normal downshifts. Now, when the engine speed has reached the speed level of the intermediate gear (gear carried by clutch 2 in Figure 6.3), clutch 1 is disengaged and clutch 2 is partially engaged. The reason for this partial

engagement of clutch 2 is to allow the engine to continue its acceleration. The transmission half of clutch 1 is now torque-free, enabling a change of gears. The engagement and synchronisation of the target gear leads to an acceleration of the according input shaft (input shaft 1 in Figure 6.3). Once the engine speed has reached the level of the target gear, clutch 2 is disengaged again and engine torque can be fully transferred to clutch 1. This transfer of engine torque is assisted by controlling clutch slip in the same way as described in Chapter 4. As a consequence of the transfer of engine torque to clutch 1 the transmission output torque rises according to the change in gear ratios in the same way as for single downshifts.

The underlying control algorithm for such an integrated double-downshift is depicted in Figure 6.4. The control algorithm remains unchanged from that for normal downshifts up until step 5. So far, this is the same procedure as for the control of normal downshifts developed in Chapter 4. The difference starts after step 5 (the control steps different from those of the normal downshift are also indicated in the simulation result depicted in Figure 6.5). Instead of commencing the torque phase and transferring engine torque in full when the engine has reached the speed level of the intermediate gear (next lower gear), engine torque is only partially transferred to the other clutch (Clutch 2 in Figure 6.4) as described above. This partial transfer of engine torque is controlled in an open-loop way by ramping the pressure at the offgoing clutch (Clutch 1 in Figure 6.4) down to zero in step 6 and ramping up the pressure at the other clutch (Clutch 2 in Figure 6.4) in step 7. The fact that an open-loop approach was sufficient for controlling the partial transfer of engine torque is demonstrated later on in this section.

Once the partial transfer of engine torque is completed (pressure at clutch 1 has become zero), the transmission half of clutch 1 is torque-free and is therefore ready for a change of gears. The closed-loop speed controller can be activated again in step 8, however, now manipulating the clutch that had provided the fill-in torque (clutch 2 in Figure 6.4) in this part of the inertia phase. In step 9 the synchroniser carrying the initial gear is disengaged (by reducing the actuator pressure to zero). Once the disengagement of the initial gear is confirmed, the engagement of the synchroniser carrying the target can be carried out. This happens in two steps: In step 10 the actuator pressure at the oncoming synchroniser is increased to a pre-specified level (pressure level controls synchronisation time and depends on the target gear). Once the synchronisation of the target gear is completed and the synchroniser has been engaged in full (dog clutch part engaged), the pressure at the actuator of the target gear can be increased to the full line pressure (step 11).

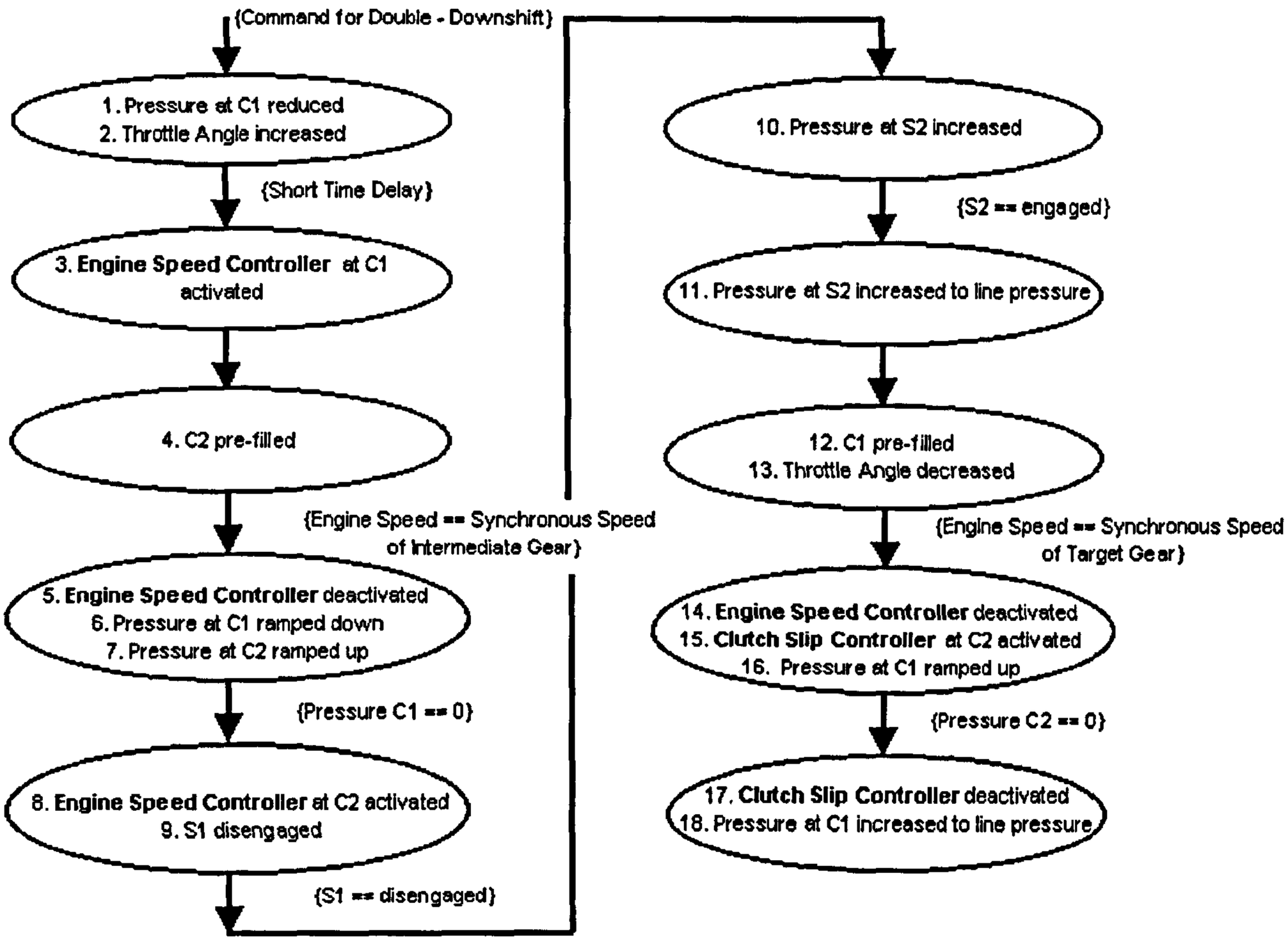

Figure 6.4 Algorithm for the control of integrated double-downshifts

Before the inertia phase is completed, the oncoming clutch (Clutch 1 in Figure 6.4) is prepared for the torque phase through pre-filling in step 12. Also, the throttle angle is reduced to its original value at this point (step 13). Once the engine speed has reached the synchronous speed of the target gear, the torque phase can be started where finally the full transfer of engine torque takes place. The torque phase is controlled in the same way as on normal downshifts in this work by employing a clutch slip controller (steps 14-16). Also, the final control steps (step 17 and 18) of the integrated double-downshift are similar to those on single downshifts. In addition, as demonstrated for single downshifts (Chapter 5), an output torque controller can be employed in the torque phase. This option is treated in Section 6.2.2. The control algorithm of Figure 6.4 makes use of the same controller layout and control loops used for single downshifts (Chapter 4, Figure 4.36).

Figure 6.5 shows the simulation result for a downshift from 3rd to 1st gear executed as "integrated double-downshift" according to the algorithm given in Figure 6.4. This gearshift,

although not the one that occurs most frequently in driving practice, involves the largest change in gear ratios and hence shows the effectiveness of the control strategy in terms of shift quality most clearly.

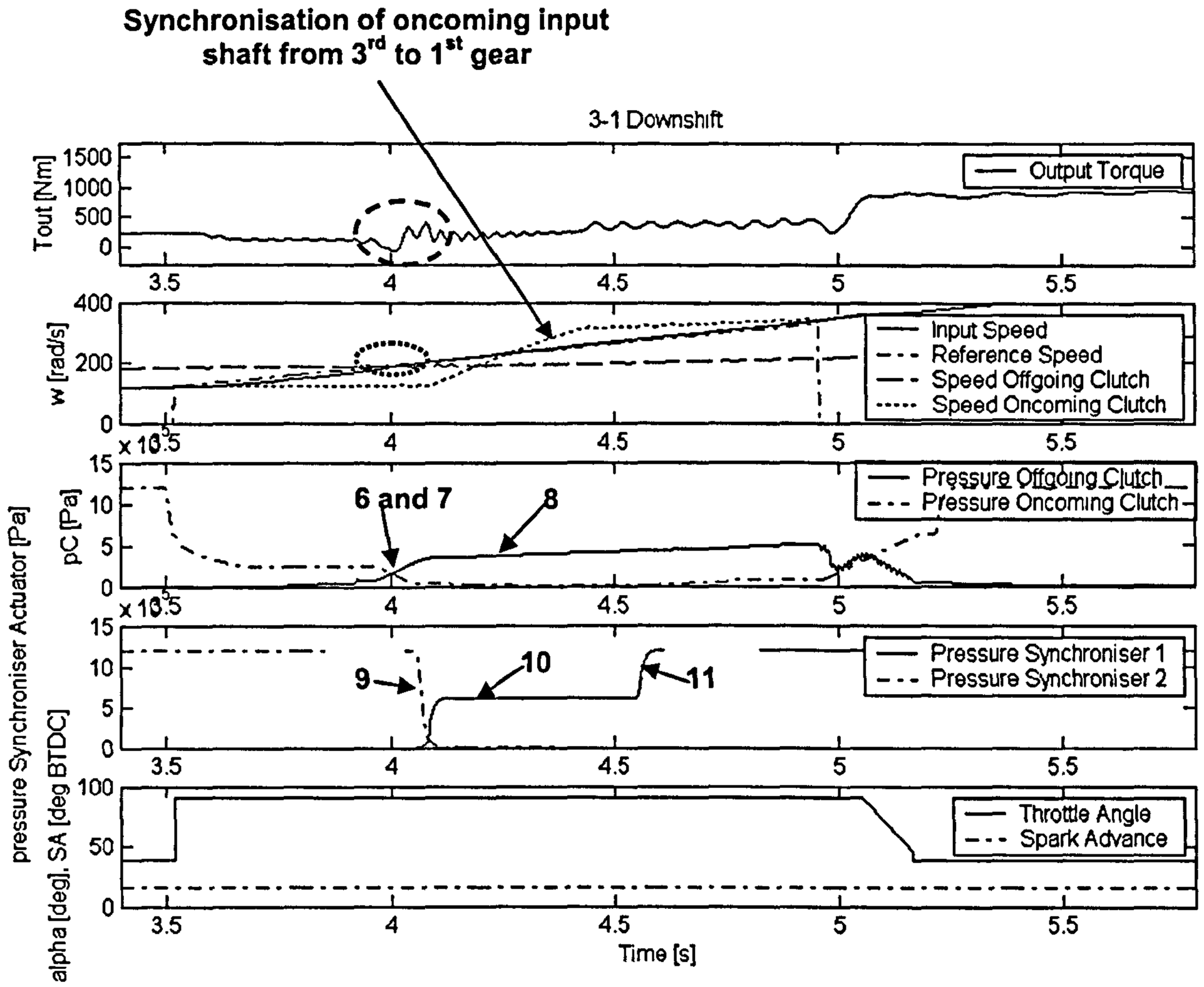

Figure 6.5 Simulation result: Integrated double-downshift from 3rd to 1st gear at a vehicle speed of around 20 km/h, (additional control steps of Figure 6.4 are indicated)

Figure 6.5 is built up in a similar as the graphs introduced in Chapters 4 and 5, showing the transmission output torque profile in the top graph, followed by graphs showing angular speeds at the clutches, hydraulic actuation pressure at both clutches and throttle angle and spark advance at the bottom. New in this figure is the graph above the bottom one, which depicts the pressure at the hydraulic actuators of the synchronisers. The gearshift in Figure 6.5 starts at 3.5 seconds where the pressure at the offgoing clutch (designated as oncoming clutch in Figure 6.5) is decreased and the engine starts to accelerate. In this first phase of the shift the engine speed is governed along a reference trajectory (simple linear increase in speed similar to reference trajectory for single downshift). At around 3.95 seconds (dotted circle in Figure 6.5) the engine speed has reached the speed of the clutch used for torque fill-in (designated as offgoing clutch in Figure 6.5), which is running with the speed of the intermediate gear (2nd gear). At this point

engine torque is partially transferred to the clutch used for torque fill-in. The engine uses the rest of the engine torque to continue its acceleration.

As explained, the partial transfer of engine torque is simply carried out by ramping down the pressure at the offgoing clutch and ramping up pressure at the clutch used for torque fill-in (steps 6 and 7 in Figure 6.5). The disadvantage of such an open-loop controlled engine torque transfer is that it produces small torque vibrations (dashed circle in Figure 6.5). This behaviour makes it clear that careful pressure calibration is necessary in that phase in order to keep these vibrations small. However, these torque vibrations are of course larger for the doubleshift in Figure 6.5 because of the large gear ratios involved (from 3rd to 1st gear). On doubleshifts between higher gears the torque vibrations due to the open-loop controlled partial torque transfer become much smaller (see e.g. Figure 6.7). In fact, the only justification for using open-loop control in this phase is, that only part of the engine torque is transferred and that any closed-loop control would make the whole control strategy more complex. The control of clutch slip, which works so well in the torque phase, is practically impossible to realise since the engine accelerates faster than the input shafts and thus clutch slip changes constantly. To control the clutch slip to a "constant" value during the phase of the partial engine torque transfer would mean halting the engine acceleration for this period of time. This would result in a heavy deceleration and subsequent strong acceleration of the engine with severely increased vehicle jerk and would be similar in shift feel to two consecutive downshifts.

At the point where the partial engine torque transfer is completed (pressure at the offgoing clutch has become zero), the transmission half of the offgoing clutch is torque-free and the change of gears can take place. Therefore, the pressure at the actuator of the synchroniser carrying the 3rd gear (synchroniser 2 in Figure 6.5) is reduced to zero (step 9 in Figure 6.5). Before the pressure at the oncoming synchroniser (synchroniser 1 in Figure 6.5) can be modulated, the actuator of this synchroniser needs to be pre-filled similarly to the procedure for clutch actuators. Due to the smaller size of the synchroniser actuators the filling process is much faster than that at the clutch. After pre-filling the actuator, the pressure at the actuator of the synchroniser of the 1st gear is increased (synchroniser 1 in Figure 6.5). The increase in pressure at the synchroniser (step 10 in Figure 6.5) produces a friction torque at the synchroniser, which accelerates the oncoming input shaft from the level of the 3rd gear to the level of the 1st gear (arrow in Figure 6.5). The energy for this acceleration is taken from the output of the transmission, which, as a consequence, leads to a drop in transmission output torque. This drop in output torque can be kept relatively small in size due to the long time that is available for the synchronisation of the target gear on a doubleshift (on single shifts the time for synchronisation can be much shorter, for a discussion of that problem see Chapter 7). Once the oncoming

synchroniser has engaged (dog-clutch like part has mechanically locked the synchroniser), the actuator pressure is raised to the line pressure (step 11 in Figure 6.5).

Throughout the whole period in which the synchronisers are changed and during the rest of the second part of the inertia phase, the engine speed is again controlled to track the speed reference profile (step 8 in Figure 6.5). At the point where the engine has reached the synchronous speed of the target gear (1^{st} gear in Figure 6.5), the inertia phase is completed and the control algorithm proceeds to the torque phase. The oncoming clutch is pre-filled at the end of the inertia phase in order to be prepared for a control action at the beginning of the torque phase. The torque phase is then controlled in the same way as on single downshifts, by activating a clutch slip controller that maintains a constant reference value for clutch slip. The fact that in Figure 6.5 the throttle angle is decreased in the torque phase instead of at the end of the inertia phase was found to be irrelevant to the shift quality or the dynamics of the downshift.

Despite the small torque fluctuations from the partial engine torque transfer, the double-downshift shown in Figure 6.5 still demonstrates that in general the transmission output torque stays above zero and therefore traction at the wheels is maintained. Furthermore, the engine speeds up continuously without halting for a moment. This, in particular, produces a shift feel that is similar to that of a single downshift. Consequently, the driver is not able to distinguish the integrated double-downshift from a single downshift apart from the increased shift time.

Also, the shift time was reduced from 2 seconds for a doubleshift carried out as two consecutive downshifts (Figure 6.1) to 1.7 seconds for the integrated double-downshift in Figure 6.5. That this shift time can be reduced even further to around 1.4 seconds is demonstrated in Figure 6.6, which shows the integrated double-downshift from Figure 6.5 with the inertia phase reduced by 0.3 seconds (steeper engine speed reference trajectory). This then represents a reduction in shift time of 0.6 seconds from the overall shift time of the case with two consecutive downshifts depicted in the Figure 6.1. From the torque profile of Figure 6.6 it can also be observed that the traction is maintained throughout the doubleshift despite the decreased shift time. To avoid too large a reduction in pressure by the speed controller and thus a loss of traction at the wheels, the output of this controller was limited at the lower end. This explains the slightly inferior tracking at the beginning of the downshift due to the steep engine speed reference trajectory.

Figure 6.7 shows an integrated double-downshift from 4^{th} to the 2^{nd} gear. This gearshift occurs more often in driving practice compared to a shift from 3^{rd} to 1^{st} gear. The control principle is the same as in the previously discussed integrated double-downshifts. The transmission output torque drops during the inertia phase to allow the engine to accelerate, but still stays slightly

above zero to avoid interruption in traction. A less steep reference speed trajectory would have allowed transmitting more engine torque via the clutch used for torque fill-in and thus the drop in transmission output torque would have been smaller.

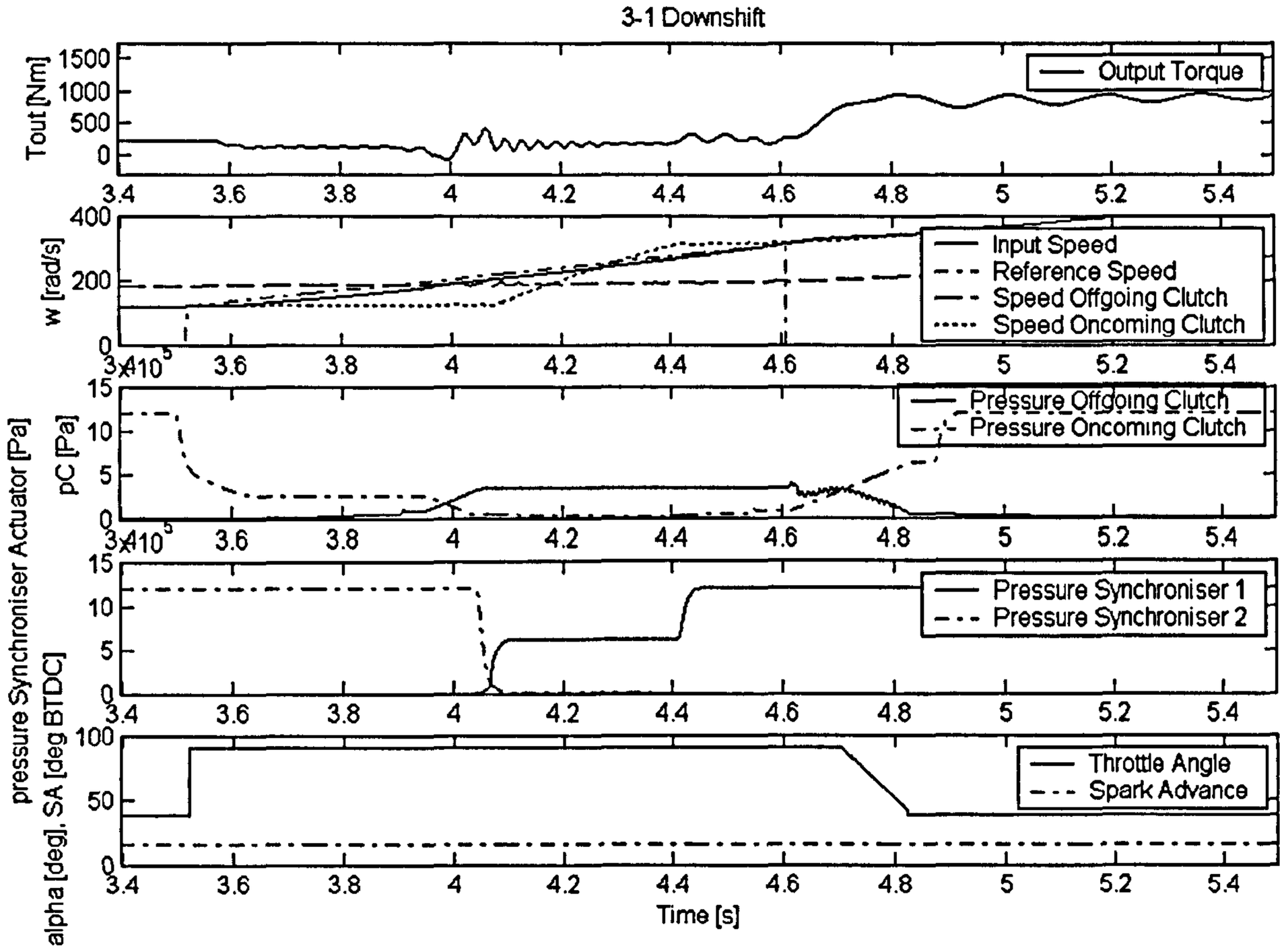

Figure 6.6 Simulation result: Integrated double-downshift from Figure 6.5 with inertia phase reduced by 0.3 seconds

The partial engine torque transfer to the clutch carrying the intermediate gear (3rd gear) in Figure 6.7 produces an abrupt increase in output torque although small in size. Shortly after this partial torque transfer, the output torque drops again due to the synchronisation of the target gear (2nd gear in Figure 6.7). The torque vibrations following the torque phase (as a result of clutch lock-up) seem to be more pronounced compared to the previously presented simulation results. However, this is largely due to the different scaling on the ordinate.

To demonstrate that the proposed integrated double-downshift control also works for multiple downshifts occurring within the same half of the transmission, a downshift from 6th to 2nd gear was simulated and is depicted in Figure 6.8. It has the same characteristic sequence of firstly, partially engaging the clutch used for torque fill-in and then secondly, transferring engine torque back to the oncoming clutch in the torque phase. The intermediate gear in Figure 6.8 was again as in the doubleshift of Figure 6.7, the 3rd gear. The reason for this is, that the change in speed

and torque between the initial gear (6th gear) and the intermediate gear (3rd gear) is roughly equal to the change in speed and torque from the intermediate gear to the target gear (2nd gear), hence the 3rd gear provides a much better choice than the 5th gear. Also, the 3rd gear naturally produces a larger transmission output torque than the 5th gear when the torque fill-in clutch is engaged.

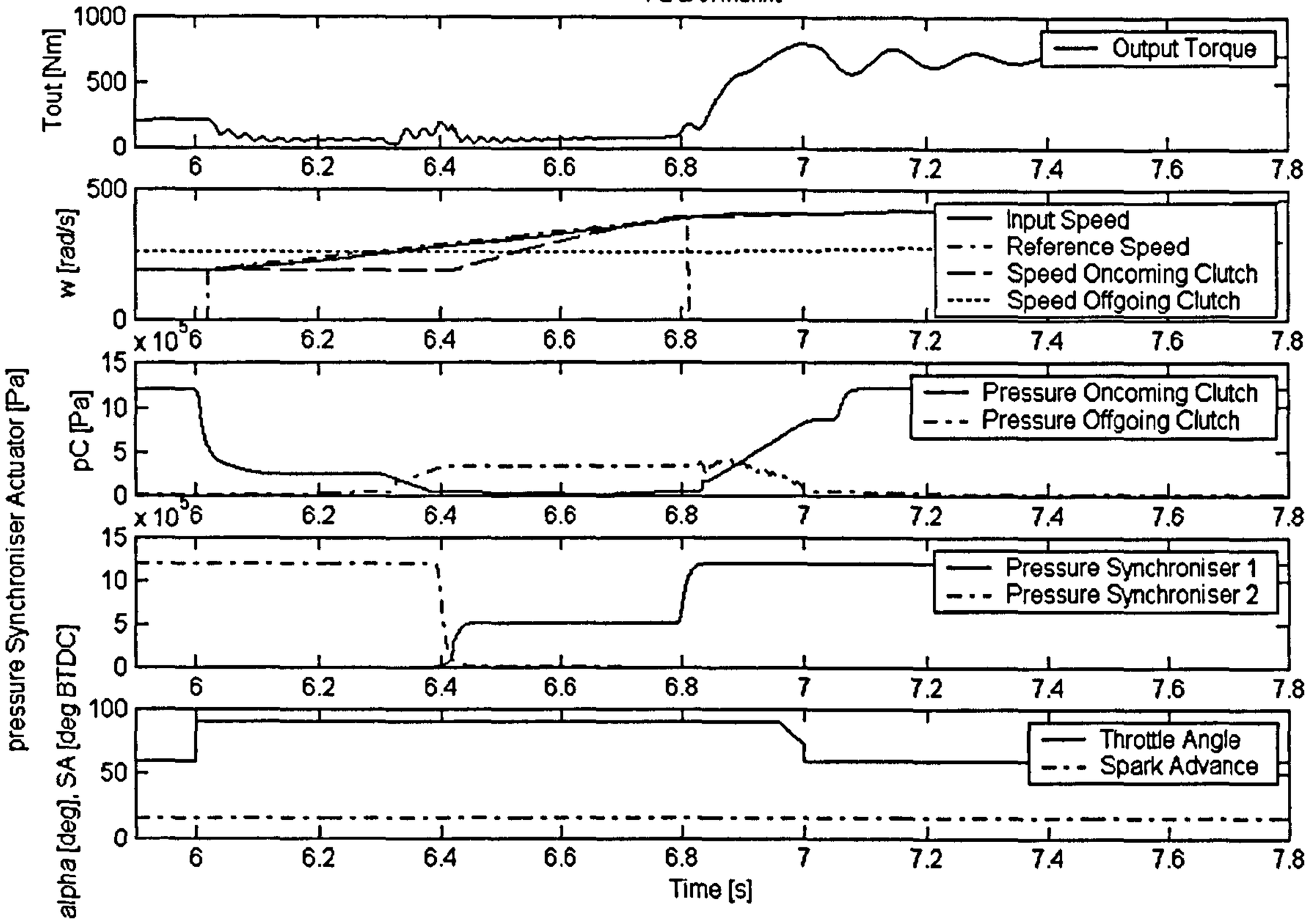

Figure 6.7 Simulation result: Integrated double-downshift from 4th to 2nd gear at a vehicle speed of around 40 km/h

The multiple downshift from 6th to 2nd gear (Figure 6.8) shows a smooth engine speed trajectory indicating a continuous acceleration of the engine throughout the two parts of the inertia phase. The transmission output torque stays above zero (although only barely in the first part of the inertia phase) indicating that traction is, in general, maintained throughout the multiple downshift. The overall shift time amounts to around 1.6 seconds, which is good for a multiple-downshift spanning such a wide range of gear ratios. However, the shift time is strongly related to the time the engine needs to accelerate to the speed of the target gear. More powerful engines would, with the same decrease in clutch pressure, provide faster acceleration and thus reduce shift time. One effect that also influences shift time is the synchronisation time of the target gear. A faster acceleration of the engine would also require a shorter synchronisation time for the target gear. This would in turn require (with conventional synchronisers), more torque being

transferred form the transmission output to the synchroniser and thus would result to decreased torque at the wheels.

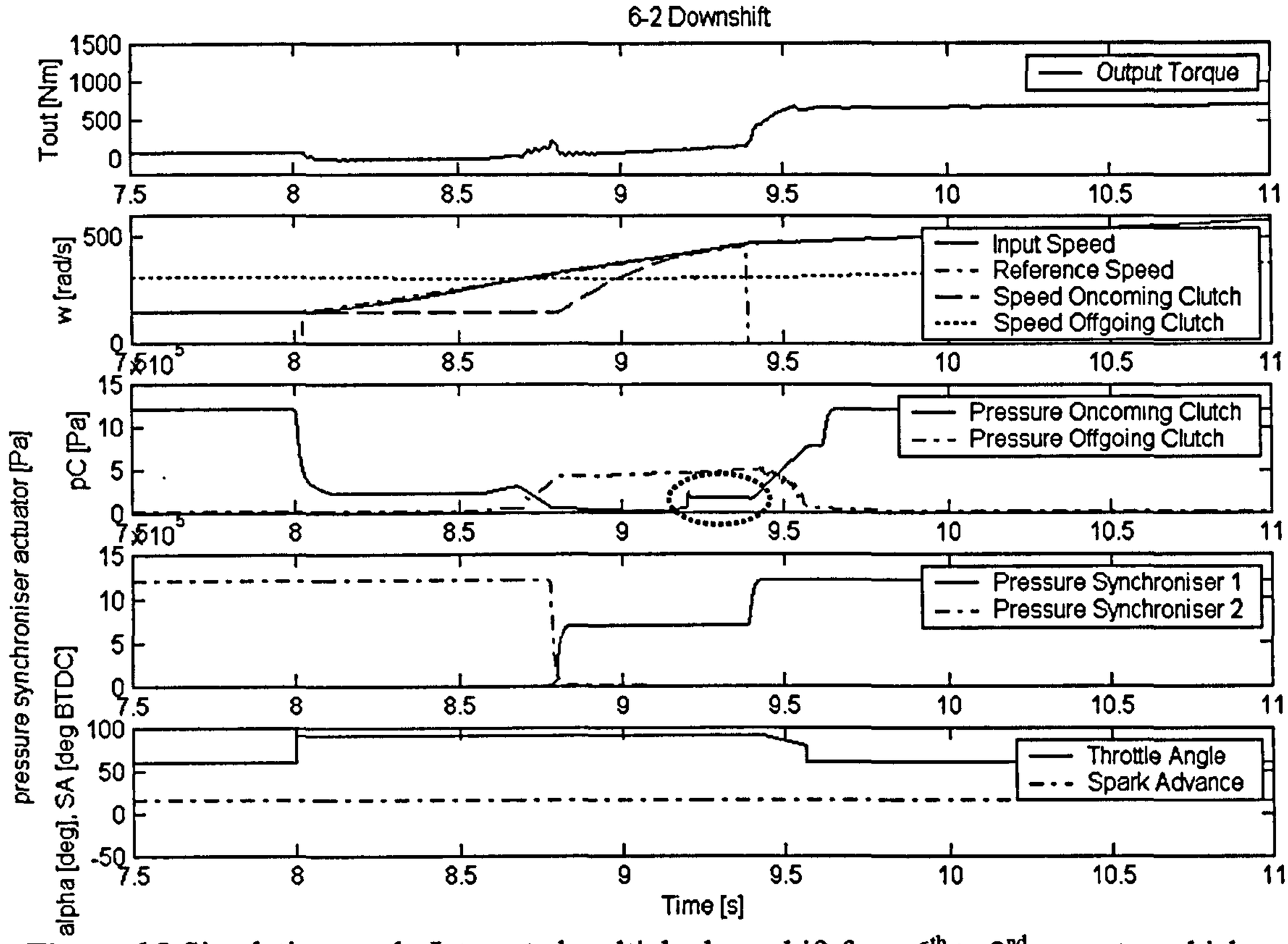

Figure 6.8 Simulation result: Integrated multiple-downshift from 6th to 2nd gear at a vehicle speed of around 50 km/h

One way out of this dilemma is to use the oncoming clutch to aid the synchroniser in synchronising the target gear. An early application of the oncoming clutch, before the start of the torque phase, results in an acceleration of the input shaft (carrying the target gear) to the engine speed. In a mild form this was already applied in Figure 6.8 (dotted circle) by pre-filling the oncoming clutch early and at a slightly increased pressure. The use of the oncoming clutch as an aid for synchronisation has the advantage that the energy necessary for synchronisation is taken from the engine instead of the transmission output. Also, the oncoming clutch only has to accelerate the nominal inertia of the input shaft (and connected gearwheels), whereas the synchronisers have to accelerate the nominal inertia multiplied by the square of the gear ratio.

Basic Control Strategy for "Integrated Double-Upshifts"

As mentioned before, double (or multiple) upshifts are rarely problematic regarding shift time. Upshifts and double- (or multiple) upshifts are usually (in automatic mode) not executed based

on a direct request by the driver. Downshifts, on the other hand, can be initiated by the driver through a "kick-down", even when the transmission is in automatic mode. This means, that in case of a downshift the driver requests a fast response of the vehicle (short shift time required), whereas in case of an upshift the driver has no such expectations. If a longer shift time is accepted on upshifts, a double-upshift (e.g. form 2nd to 4th gear) could also be executed as two consecutive upshifts with gentle engine speed trajectories in the inertia phases. The gentle engine speed trajectories would then ensure that the interruption in engine deceleration between the inertia phases (torque phase of second downshift) is less noticeable to the driver. However, if two consecutive upshifts are not acceptable, because of reasons of shift feel or increased shift time, then a double (or multiple) upshift can be executed based on the same principle as developed for double-downshifts (use of the second clutch for fill-in torque). This leads to the concept of an integrated double-uphift. Of course the control principle of integrated double-upshifts can also be applied to multiple-upshifts within the same half of the transmission (e.g. form 2nd to 6th gear), hence, the following description of integrated double-upshifts applies likewise to integrated multiple-upshifts skipping more than one gear.

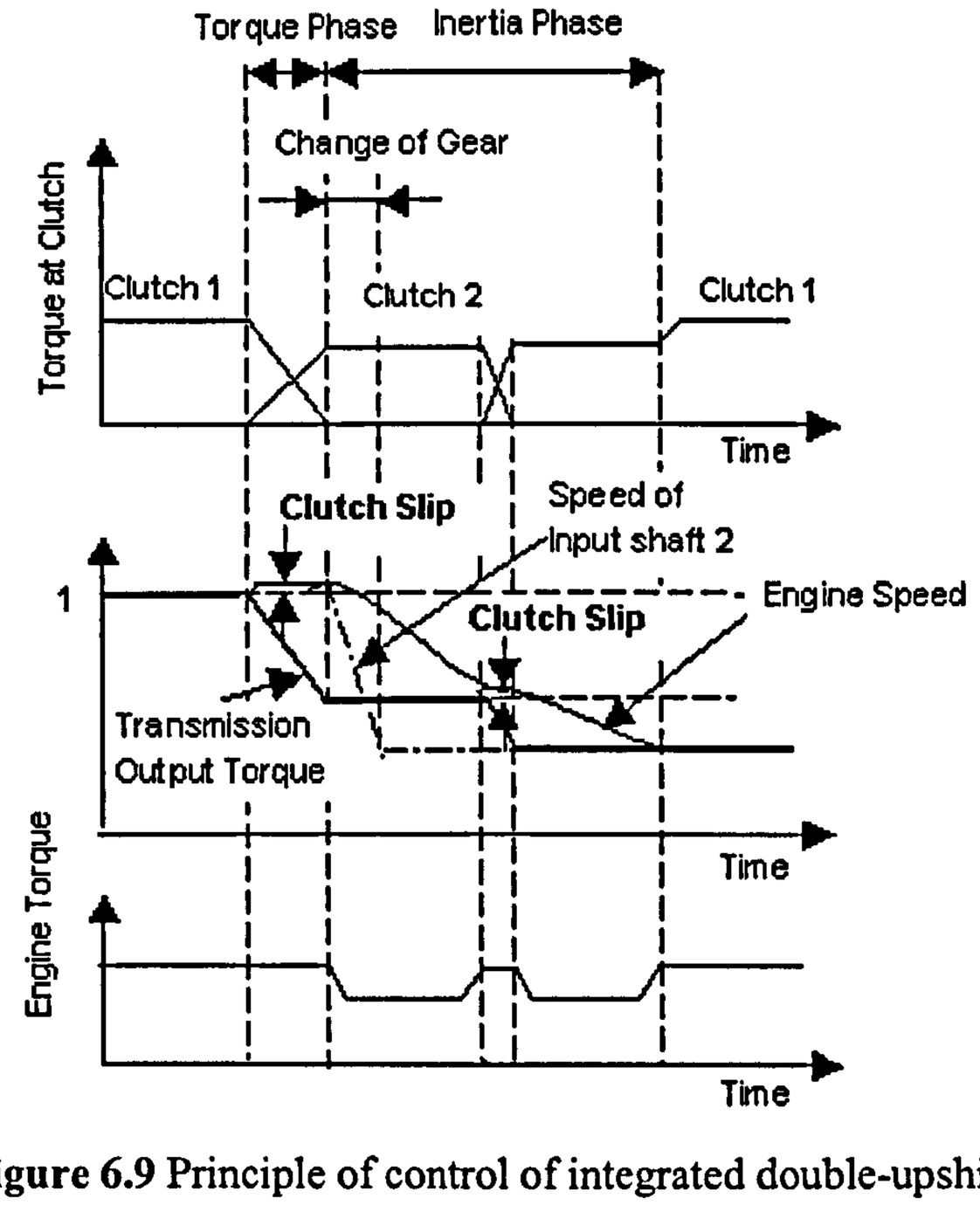

Figure 6.9 Principle of control of integrated double-upshifts

Figure 6.9 shows the principle of the integrated double-upshift control strategy. On first, sight the speed and output torque trajectories look like those of two consecutive upshifts. However, on closer inspection it can be seen that, although there are actually two torque phases and two inertia phases, the second torque phase is so short that the synchronisation of the engine is

barely interrupted. This ensures that the driver feels only one inertia phase (see Figure 6.9) with a smooth engine speed trajectory throughout the whole double-upshift. Also, the change of gears (and thus synchronisers) is accomplished in the first part of the inertia phase instead of in between two consecutive upshifts (reduces shift time). This will be clearer when discussing the simulation results.

The torque phase at the beginning of the double-upshift (see Figure 6.9) is controlled in the same way as that on a single upshift by activating the clutch slip control at the offgoing clutch (clutch 1 in Figure 6.9). The pressure at the clutch used for torque fill-in (clutch 2 in Figure 6.9) is ramped up for a full transfer of engine torque in the torque phase. After the torque phase has been completed the first part of the inertia phase starts where the engine speed controller is activated to let engine speed track a specified reference speed profile by manipulating throttle and spark advance (indicated in Figure 6.9 by the reduction in engine torque). Also taking place after the torque phase has been completed and the transmission half of clutch 1 has become torque-free, is the change of gear.

Once the engine has reached the speed level of the intermediate gear, engine torque is again transferred to the oncoming clutch (clutch 1 in Figure 6.9). This is accomplished by employing clutch slip controller at the clutch used for torque fill-in. This was necessary since, contrary to the double-downshift, the level of transmission output torque is much higher and an open-loop controlled transfer of engine torque would have, because of the difficulty in timing the clutch application, increased the risk of strong torque reactions at the transmission output. Once the second torque transfer has been completed, the engine speed controller continues to track the engine reference speed trajectory in this second part of the inertia phase. The PID controllers and the control loops are the same as those developed for single upshifts in Chapter 4 and Chapter 5.

Figure 6.10 shows the control algorithm behind the integrated double-upshift. Since the control steps are very similar to those of two consecutive upshifts, the following description focuses on those control steps, which are different for the integrated-double-upshift (These are also indicated in the simulation result depicted in Figure 6.11). Similar to single upshifts the control starts with a reduction in pressure at the offgoing clutch (clutch 1 in Figure 6.10) in step 1 to a level close to the point where the clutch starts to slip. The transition of the offgoing clutch to a slipping state and the control of the subsequent transfer of engine torque (Step 3 and 4) to the clutch used for torque fill-in, is accomplished in the same way as described for single upshifts in Chapter 4.

In the first part of the inertia phase (again similar to single upshifts) the engine speed is controlled through modulation of throttle angle and spark advance (step 6) and the pressure at the clutch used for torque fill-in (clutch 2 in Figure 6.10) is kept constant (step 7) throughout this phase. The change of gear in the torque-free half of the transmission can be performed as soon as the pressure at the offgoing clutch has become zero. Similar to double-downshifts, the synchroniser carrying the initial gear (Synchroniser S1 in Figure 6.10) is disengaged in step 8. When the disengagement of the synchroniser is confirmed, the pressure at the actuator of the synchroniser of the target gear (Synchroniser S2 in Figure 6.10) can be increased after a short filling phase (step 9). This pressure determines the speed of the synchronisation of the target gear. After the synchroniser has engaged (mechanically locked) the actuator pressure is raised to the line pressure (step 10). Throughout the second part of the inertia phase the engine speed controller is activated again (step 6).

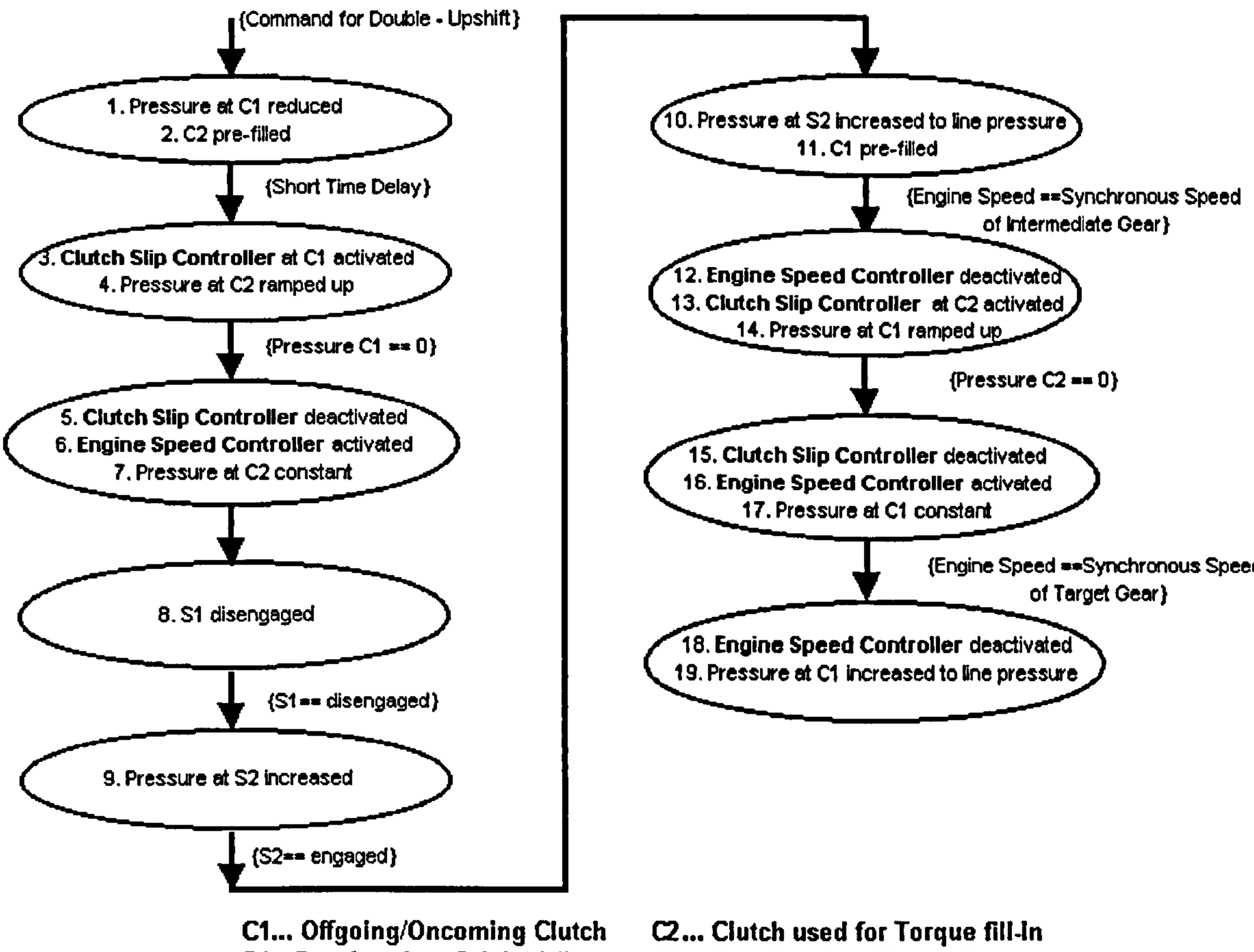

Figure 6.10 Algorithm for the control of integrated double-upshifts

Once the change of gear is completed and the engine speed has reached the level of the intermediate gear, the clutch used for torque fill-in can be disengaged and the oncoming clutch (clutch 1 in Figure 6.10) can be engaged again (step 13 and 14). This second torque phase is

controlled through control of clutch slip at the clutch used for torque fill-in for already explained reasons. After this second transfer of engine torque has taken place, the clutch slip controller is deactivated (step 15) and the inertia phase is continued by activating the engine speed controller again (step 16). The pressure at the oncoming clutch is kept constant throughout this second part of the inertia phase (step 17). Once the engine reaches the speed level of the target gear the inertia phase is completed, the engine speed controller is deactivated and the clutch pressure is raised to the line pressure (step 18 and 19). Similar, to the control of single upshifts an abrupt rise in spark advance at the point where the oncoming clutch locks-up seemed to suppress torque vibrations somewhat.

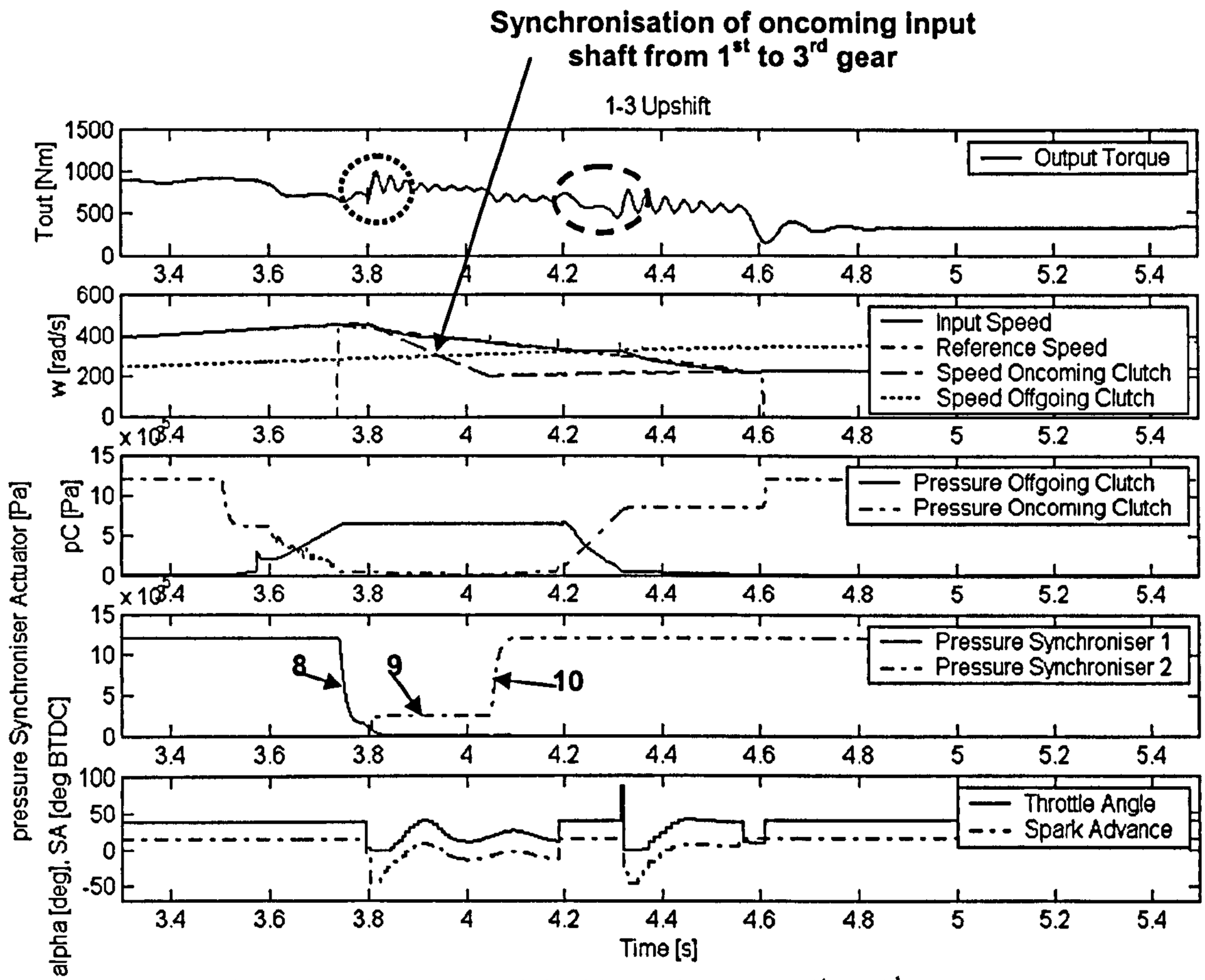

Figure 6.11 Simulation result: Integrated double-upshift from 1st to 3rd gear at a vehicle speed of around 30 km/h, (additional control steps of Figure 6.10 are indicated)

Figure 6.11 depicts a simulation result for an integrated double-upshift from 1st to 3rd gear executed according to the control algorithm depicted in Figure 6.10. The (first) torque phase of the double-upshift in Figure 6.11 looks essentially similar to that on single upshifts presented in Chapter 4, owing to the similarity of the control of the engine transfer via clutch slip controller. However, at the beginning of the first part of the inertia phase a short but small increase in transmission output torque can be observed (dotted circle in Figure 6.11), which comes from the

change of synchronisers, as becomes clear when inspecting the plots showing the synchroniser actuation pressure. This increase in transmission output torque is a direct result of synchronisation torque being transferred from the synchroniser to the transmission output in order to decelerate the input shaft for a synchronous run with the target gear. The problem of torque reactions at the transmission output due to engagement of (conventional) synchronisers is discussed in full in Chapter 7.

The tracking of the engine reference speed profile is in general acceptable, however, the manipulated variables (throttle angle and spark advance) show signs of oscillatory behaviour, which might indicate that the tuning of the PID speed controllers is not optimal (as discussed in Chapter 4). In the second torque phase where clutch slip is controlled at the clutch used for torque fill-in (offgoing clutch in Figure 6.11), the engine speed is kept near that of the input shaft of the intermediate gear (denoted as speed of the offgoing clutch in Figure 6.11) until the engine torque is transferred in full and the clutch slip controller can be switched off again. This interruption in engine deceleration (although only short in time) necessarily introduces some torque fluctuations as can be seen from the output torque profile (dashed circle in Figure 6.11). However, transferring engine torque without use of clutch slip controller in this second torque phase would have resulted to even larger torque vibrations. In the subsequent second part of the inertia phase the engine speed controller is activated again, the tracking of the engine speed reference trajectory is continued and the synchronisation of the engine with the target gear can be completed. Tracking of the speed reference trajectory in this part of the inertia phase is acceptable. In general, the short interruption in deceleration of the engine (during second torque phase) is thought to be less noticeable and thus the driver should experience the double-upshift as a single gearshift event, which was the objective behind the development of this control strategy.

6.2.2 Control Strategy for "Integrated Doubleshifts", including Control of Torque

Control Strategy for "Integrated Double-Downshifts" including Control of Torque

This section aims to demonstrate that the torque controller developed in Chapter 5 for single downshifts can also be advantageously applied to integrated double (or multiple) downshifts. In the last section (downshifts) it could be noticed, similarly to single downshifts, that the shape of

the torque profile in the torque phase varies for different double-downshifts. Similar to single downshifts, it is desired to guarantee a shift quality that can be influenced directly and that is unaffected by the gear ratios involved in the double (or multiple) downshift or by other shift parameters.

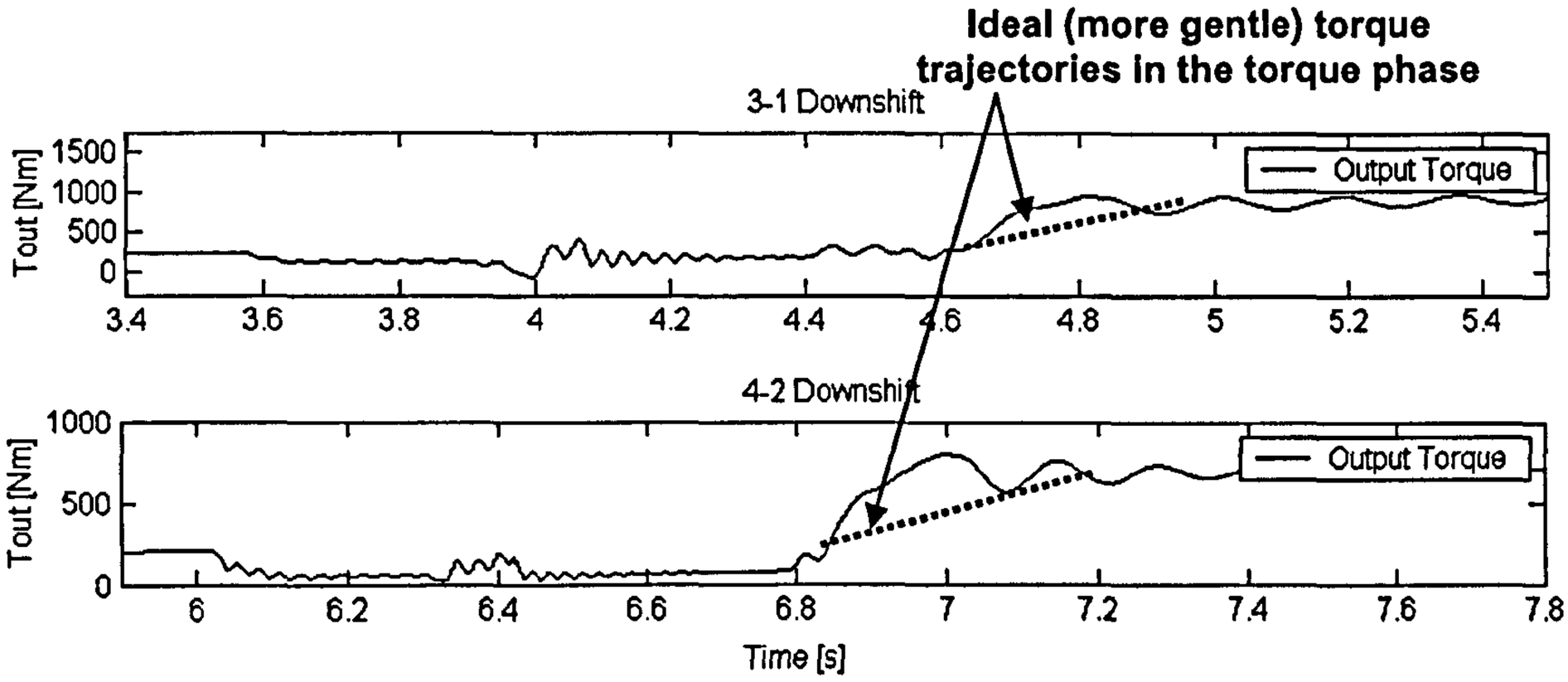

Figure 6.12 Transmission output torque trajectories of the doubleshifts from Figure 6.6 and 6.7 with ideal torque trajectory indicated

This is illustrated in Figure 6.12, which shows the transmission output torque trajectories of the doubleshifts from Figure 6.6 and 6.7. In Figure 6.12 the ideal torque trajectories in the torque phase are indicated as well (dotted lines). To accomplish these ideal (more gentle) torque profiles, transmission output torque has to be controlled along these specified trajectories.

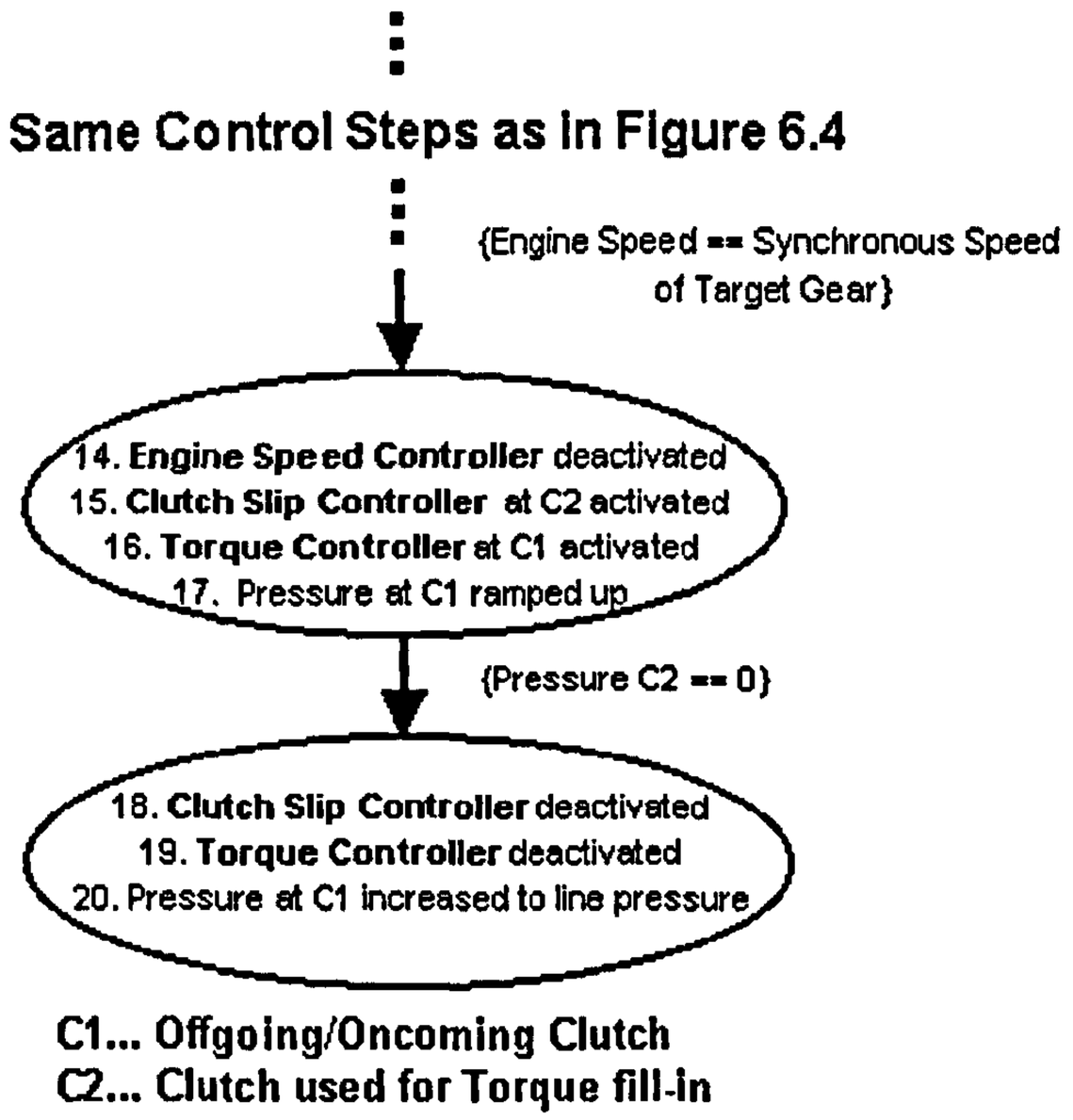

Figure 6.13 Extended control algorithm for integrated double-downshifts with torque control

To integrate the torque controller into the integrated double-downshift control strategy, the control algorithm for integrated double-downshifts (Figure 6.4) has to be modified in the same way as explained in Chapter 5. In particular, the control algorithm of Figure 6.4 has to be extended by including two additional control steps as illustrated in Figure 6.13.

Basically only steps 16 and 19 have been added, which activate the torque controller in the torque phase and deactivate the torque controller in the terminal phase of the double-downshift. The same dual control action, as described in Chapter 5, has to be performed at the oncoming clutch to allow full operation of the clutch slip controller in parallel with an activated torque controller. This, similarly to single downshifts, requires ramping up the pressure at the oncoming clutch with a lower rate as compared to the case without torque controller. The torque controller then adds its pressure contribution on top of this pressure ramp to allow a tracking of the reference torque profile. At the clutch used for torque fill-in, the pressure is manipulated by the clutch slip controller in the same way as for single downshifts.

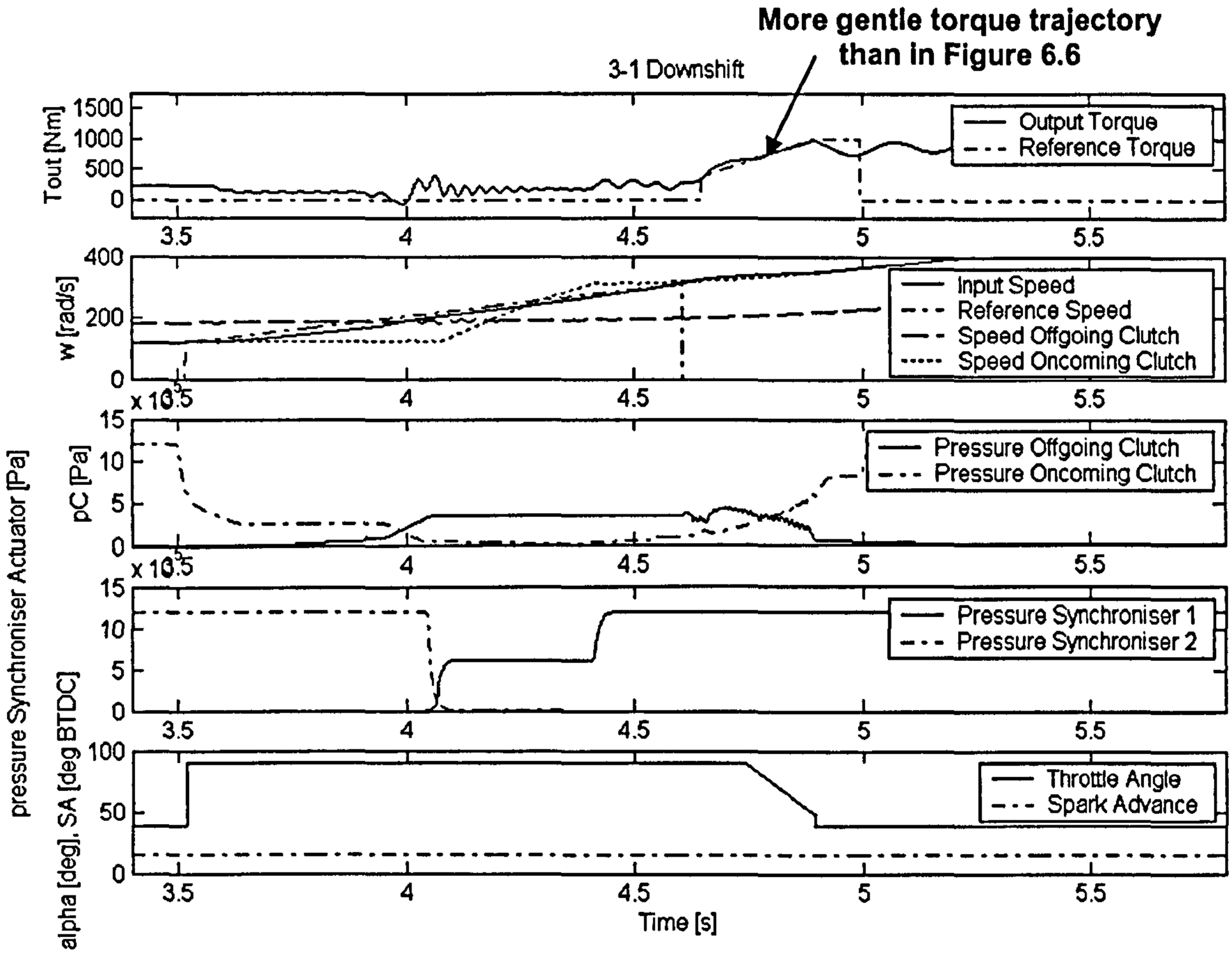

Figure 6.14 Simulation result: Integrated double-downshift from 3rd to 1st gear (Figure 6.6), with activated torque controller in the torque phase

Figure 6.14 shows the double-downshift from Figure 6.6, but this time with activated torque controller in the torque phase. The tracking performance of the torque controller is in general

good apart from a tiny initial deviation. A more gentle torque profile could be selected in the torque phase of the downshift Figure 6.14 (by introducing torque control), as compared to the doubleshift without torque control (Figure 6.6). The downside of employing a gentle torque profile is that the torque phase is increased in time. Hence it has to be decided between improved shift quality on one hand and short shift time on the other hand. At the point of clutch lock up, at the end of the torque phase torque, vibrations are visible again. These torque vibrations are a result of the lock up of the oncoming clutch and are more pronounced when shifting to low gears (e.g.1st gear in Figure 6.14).

Figure 6.15 shows a double-downshift from 4th to 2nd gear (from Figure 6.7) with activated torque controller and Figure 6.16 shows a multiple downshift from 6th to 2nd gear (from Figure 6.8) also with activated torque controller. Tracking performance of the torque controller is in both cases good and the torque controller enables to select very gentle torque profiles in the torque phase. This leads in both cases to an almost "flat" looking torque profile indicating very good shift quality.

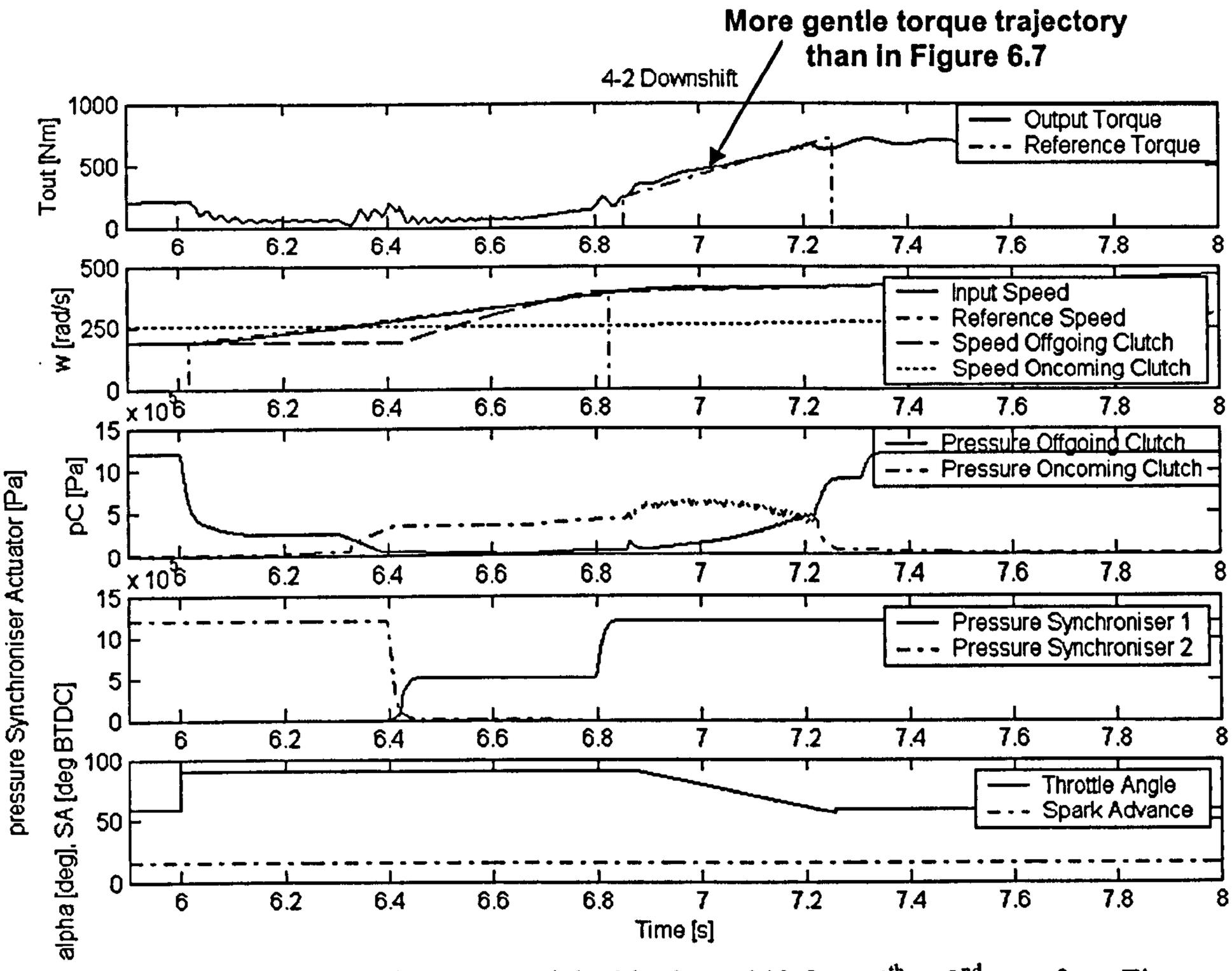

Figure 6.15 Simulation result: Integrated double-downshift from 4th to 2nd gear from Figure 6.7, however, with activated torque controller in the torque phase

However, because of this gentle torque profile the torque phase increases in time and thus also the total shift time. The gradients of the reference torque profiles used in Figure 6.14 and 6.15 are very close in value, although this is not immediately obvious because of the different scaling on the ordinate of the torque plots. The vibrations at the end of the torque phase are in both cases much smaller compared to the double-downshift from 3rd to 1st gear depicted in Figure 6.14.

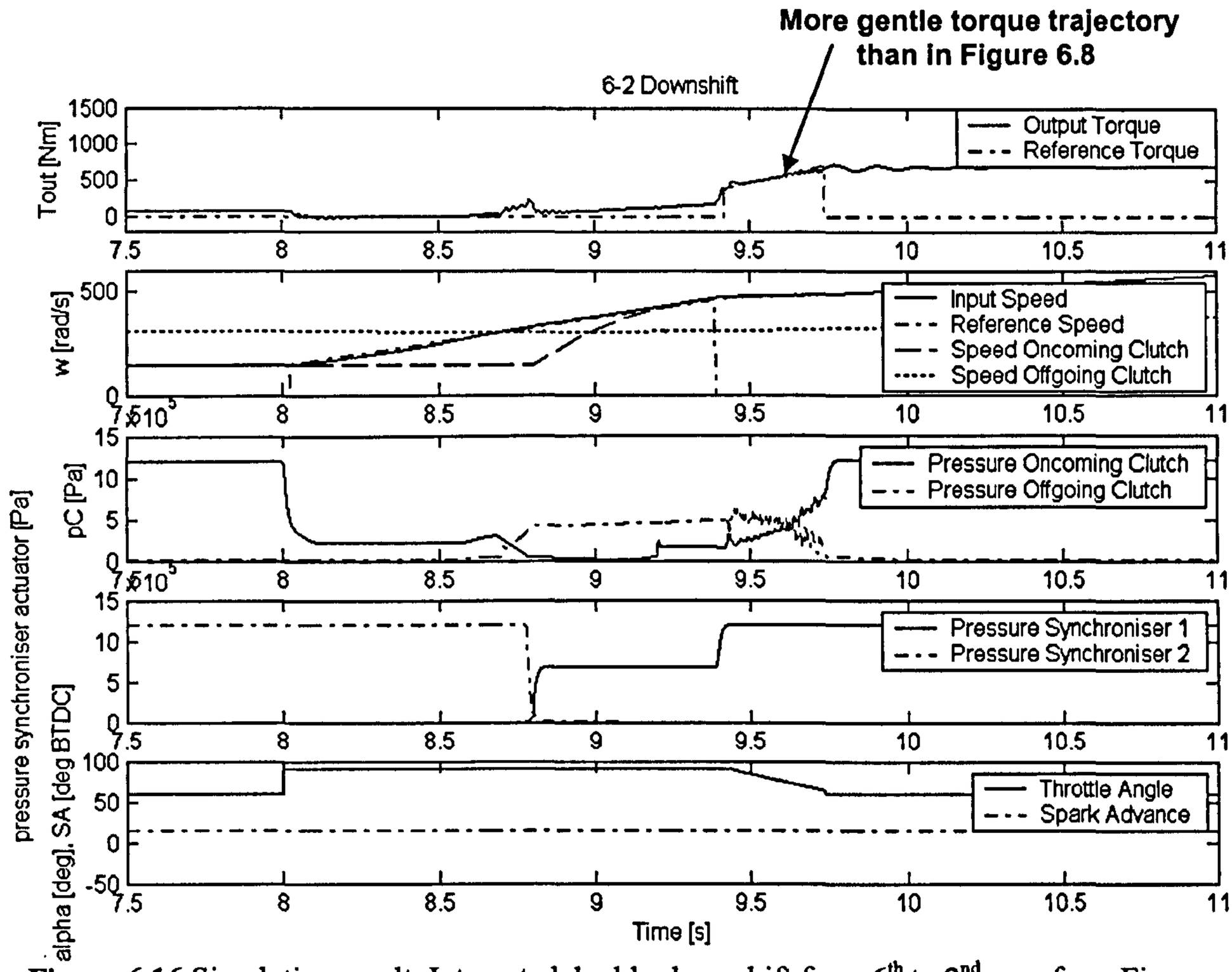

Figure 6.16 Simulation result: Integrated double-downshift from 6th to 2nd gear from Figure 6.8, however, with activated torque controller in the torque phase

Control Strategy for "Integrated Double-Upshifts" including Torque Control

In the section describing the control strategy for integrated double upshifts, it was noticed that the change of gears and the change of clutches in the second torque transfer did produce fluctuations in the transmission output torque trajectory (see Figure 6.11 dashed and dotted circles). For this reason, and for increased robustness in general, it seems appropriate to also introduce transmission output torque control to double/multiple upshifts. Figure 6.17, which depicts the torque profile of the double upshift of Figure 6.11, illustrates this situation and shows that if the transmission output torque could be controlled to track the indicated ideal (i.e.

reference) torque trajectory, the fluctuations in the transmission output torque should be greatly reduced and thus shift quality improved.

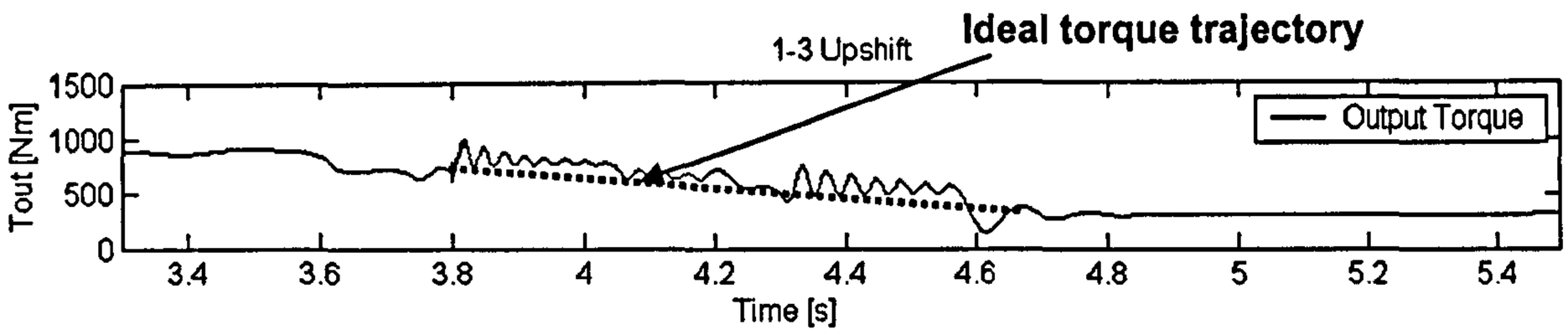

Figure 6.17 Transmission output torque trajectories of the doubleshift from Figure 6.11 with ideal torque trajectory indicated

To implement torque controller in the inertia phase(s) of the integrated double-upshift similarly to single upshifts, the control algorithm for integrated double-upshifts from Figure 6.10 must be modified accordingly.

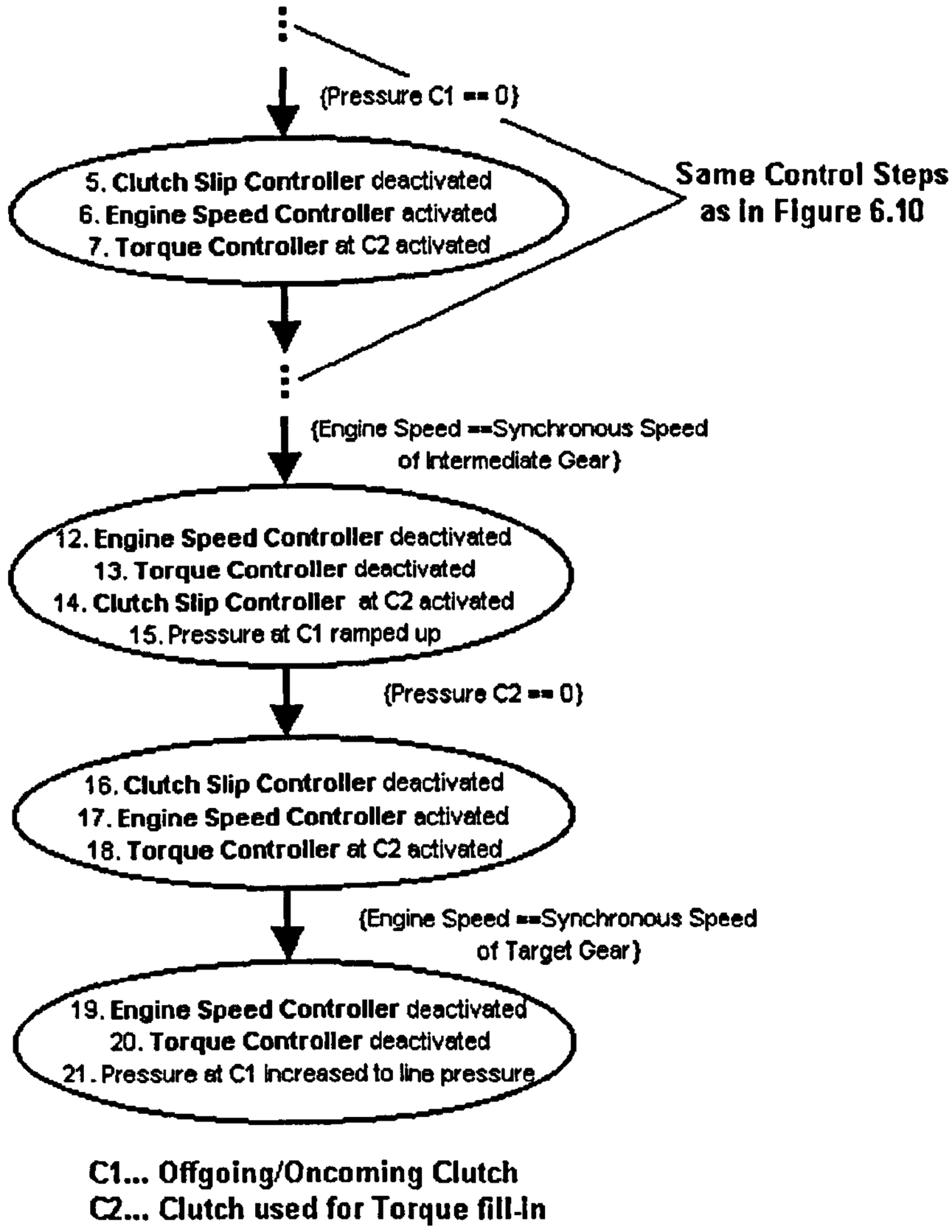

Figure 6.18 Extended control algorithm for integrated double-upshifts with torque controller

This can be accomplished in a simple way by letting the torque controller manipulate clutch pressure in the inertia phase, instead of leaving the clutch pressure constant. The modified

control algorithm for integrated double-upshifts with torque controller is depicted in Figure 6.18. In this algorithm the torque controller is switched off in the second torque phase to avoid increasing complexity. However, it should be, in principle, possible to implement torque controller in that phase in a similar way as explained for the torque controller applied to the torque phase of downshifts (dual control of clutch slip and output torque).

Figure 6.19 shows the double-upshift from Figure 6.11, but with activated torque controller in the inertia phase(s). Comparing Figure 6.19 to Figure 6.11 (or to Figure 6.17) clearly demonstrates that employing a torque controller produces a much smoother transmission output torque profile. Apart from this improvement, of course, also the robustness against changes in the friction coefficient is improved as already demonstrated for single upshifts (Chapter 5).

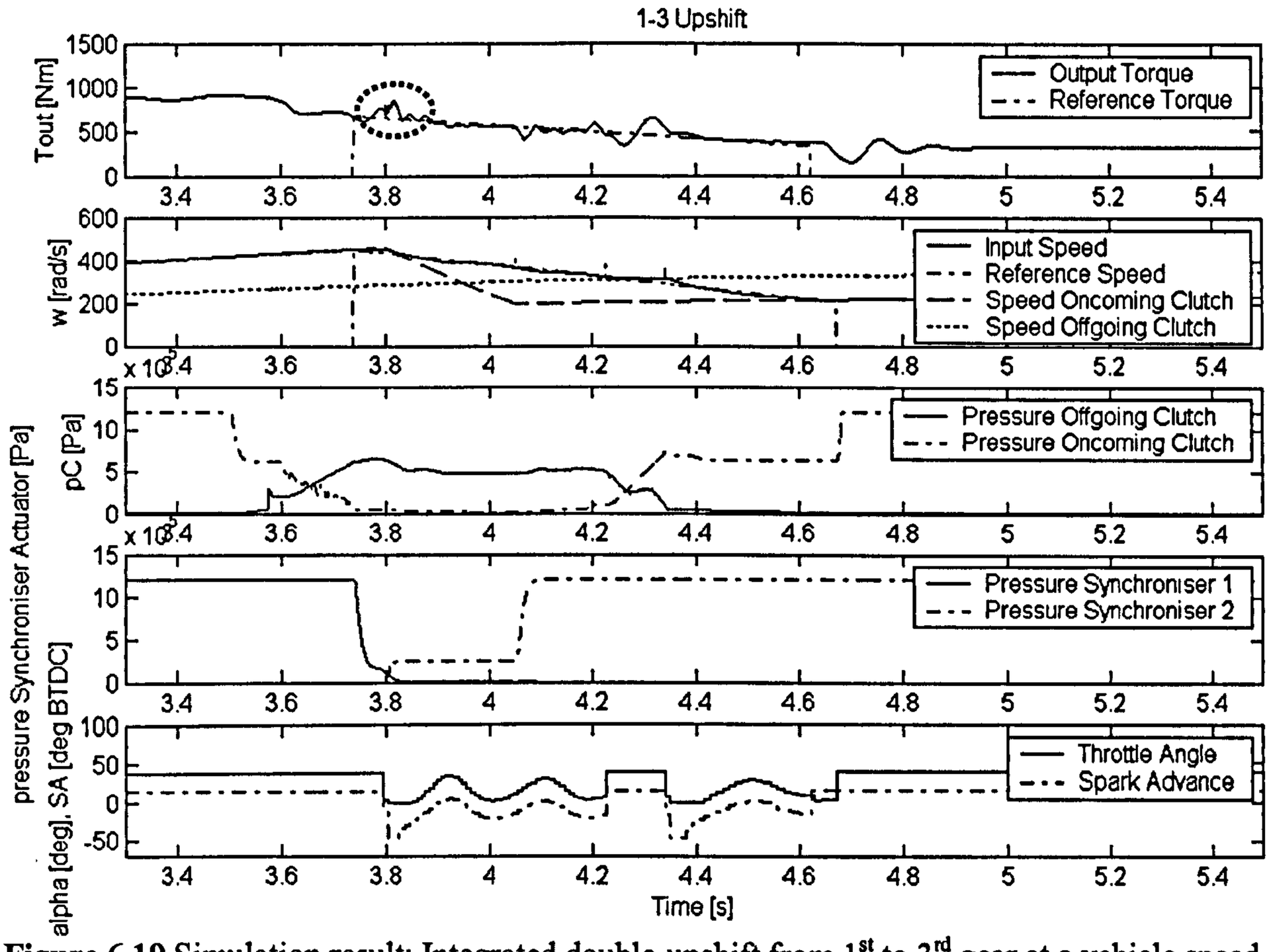

Figure 6.19 Simulation result: Integrated double-upshift from 1st to 3rd gear at a vehicle speed of around 30 km/h (Figure 6.11), including torque controller

However, at the beginning of the inertia phase, a short but small increase in transmission output torque can still be observed (dotted circle in Figure 6.19) which can be attributed to the synchronisation of the target gear. The torque controller reacts too sluggishly to remove this fluctuation. The sluggish reaction of the torque controller is a consequence of the low pass filter at the input of the torque controller. However, during the rest of the first part of the inertia phase the tracking of both torque and speed reference trajectories are good. Still, the engine speed

controller shows some oscillations in the manipulated variables as can be seen from the throttle and spark advance signals. Interestingly, this behaviour is worse with the torque controller active. However, it is believed that better tuning of the PID controller gains of the speed control can eliminate those oscillations (as was already demonstrated when discussing the robustness of this engine speed control for single gearshifts, see Section 4.5.1 and 5.4.1).

6.3 Conclusions

The principle of controlling double shifts developed in [Wagner 1994] was extended in this chapter to incorporate the control elements developed in Chapter 4 and 5 (i.e. clutch slip controller, engine speed controller through engine manipulation and torque controller) as an improvement in terms of shift quality over the open-loop control strategies presented in that paper.

It was demonstrated that the torque controller from Chapter 5 could be successfully applied to double/multiple shifts to improve shift quality even further. On double/multiple upshifts the torque controller could effectively compensate for the torque reactions due to the gear change. On double/multiple downshifts the torque controller could improve shift quality in the torque phase when a gentler reference torque profile was selected.

As an additional improvement for the proposed control strategy of multiple downshifts it was suggested that the change of gear and pre-selection of the target gear could be assisted by engaging the oncoming clutch early, thus decreasing the resulting torque reactions at the transmission output.

Chapter 7

Control of Gear Pre-Selection

Chapter 4,5 and 6 have dealt with one part of gearshifts on twin clutch transmissions: the control of clutch-to-clutch shifts. In Chapters 4 and 5 a control strategy for single clutch-to-clutch shifts was developed. These control concepts were then extended in Chapter 6 to be applicable to double/multiple clutch-to-clutch shifts.

The other part of a gearshift on twin clutch transmissions is the gear pre-selection, which is treated in this chapter. Section 7.1 gives an introduction to the devices and methods of gear synchronisation and discusses the suitability of these devices for a gear pre-selection on twin clutch transmissions. Section 7.2 then discusses in full the problems involved with using conventional synchronisers for the gear pre-selection.

Based on the findings of Section 7.2, a control strategy is proposed in Section 7.3 that attempts to compensate for the problems resulting from gear pre-selection with conventional synchronisers.

In Section 7.4 the robustness of the suggested compensating control strategy is investigated in detail. Finally, Section 7.5 summarising the findings of this chapter.

7.1 Introduction to Gear Pre-Selection

As explained before, a complete gear change on a twin clutch transmission consists of two main parts:

- A clutch-to-clutch shift involving a transfer of engine torque to the clutch carrying the target gear and a synchronisation of the engine to the speed of the target gear
- A pre-selection of a target gear on the torque-free half of the transmission

For the gear pre-selection two key issues can be identified:

1. The choice of the target gear to be pre-selected
2. The device, or method of synchronising (pre-selecting) the target gear

1) The choice of the target gear to be pre-selected: Questions such as which target gear has to be pre-selected and at what point in time the engagement of that gear should take place belong to the area of shift schedules. One example of such a shift schedule simply requires that on the torque-free half of the transmission a gear lower than the one currently engaged has to be pre-selected [Wagner 1994]. For example, if the 3rd gear is engaged on the half of the transmission, which is currently transmitting torque, then the gear pre-selection strategy requires the engagement (pre-selection) of the next lower gear i.e. the 2nd gear on the other (torque-free) half. This strategy has the advantage of always ensuring that the transmission is prepared to execute a clutch-to-clutch downshift (driver desires fast response of the vehicle) without first having to change the target gear.

A quick response of the transmission is mainly required when downshifting and is less important when upshifting. This circumstance is the motivation behind the above-described gear pre-selection strategy, which requires a pre-selection of the target gear prior to an upshift and subsequent to a downshift. The following example will make this clear: If for example, on the torque transmitting half of the transmission, the 3rd gear is currently engaged and on the other half the 2nd gear, then a clutch-to-clutch downshift from 3rd to 2nd gear can take place immediately. After the downshift has been completed, the initially torque-transmitting half is torque-free and a new target gear (1st gear) has to be selected on this half. This requires disengagement of the 3rd gear and engagement and synchronisation of the 1st gear in order to be prepared for a downshift from 2nd to 1st gear. However, if the next shift will be an upshift from 2nd to 3rd gear, the gear on the torque-free half of the transmission needs to be changed again from 1st gear to 3rd gear before commencing the clutch-to-clutch upshift.

2) The device, or method of synchronising (pre-selecting) the target gear: The question of which device (or form of control strategy) is used for synchronising (pre-selecting) the target gear is the second important consideration with gear pre-selection. It is only this part of the gear pre-selection that will be discussed in this chapter.

For automated manual transmissions, mainly the following three, synchronisation concepts (devices) are known:

1) Hydraulically (or electrically) actuated conventional synchronisers ("synchromesh"): The synchroniser consists of a synchronisation clutch (typically one or more conical friction surfaces) and a dog clutch-like part, which enables a mechanical locking of the synchroniser once the two halves of the synchroniser run with the same speed. The synchroniser can be actuated manually through a gear lever and linkage (manual transmission) or it can be actuated automatically through use of hydraulic or electric actuators. With conventional

synchronisers, the friction torque developed at the synchroniser during the synchronisation process is transferred to or from the wheels (or transmission output).

2) Synchronisation through control of engine torque: The engine is used for synchronisation while the clutch remains engaged all the time. In a first step, engine torque has to be reduced to zero and the currently engaged gear has to be disengaged. In a second step, engine torque is manipulated (and/or a brake is applied) for synchronisation (clutch remains engaged). After synchronous speed is reached, the synchroniser can be locked mechanically and full engine torque can be applied again at the end of the gearshift. This concept requires only the use of simple dog clutches instead of the more complicated synchronisers discussed under point 1.
3) Central synchronisation: Similar to 2) only that here the energy for synchronising the target gear (acceleration of input shaft) is taken from an "external" source (e.g. electric motor). If the synchronisation involves a deceleration of the input shaft, a brake (contained in the transmission housing) can be applied. This concept also requires only the use of simple dog clutches. The clutch has to be disengaged during the gearshift. The central snychronisation is sketched in Figure 7.1.

For a twin clutch transmission only concepts 1) and 3) are relevant since a decrease of engine torque to zero for the synchronisation would conflict with the concept of a powershift, which requires the maintenance of the power transfer to the wheels.

Concept 1) seems to be the method currently employed on twin clutch transmissions [Rudolph et.al. 2003] with the actuation of the synchroniser being hydraulic. This certainly makes sense if the actuation of the twin clutch is also hydraulic. However, if dry clutches were employed, use of hydraulic actuation would only add complexity and would decrease fuel economy (the oil pump in the transmission has to be driven by the engine at all times). The response of a hydraulic actuation seems to be much faster than that of an electric actuation (with current designs). The disadvantage of Concept 1), is that the synchronisation (gear pre-selection) produces strong torque reactions at the transmission output if not controlled properly.

In Concept 3) (see Figure 7.1) the energy for acceleration of gearwheels is provided by an electric motor (additional or modified battery required). The energy for recharging the battery that supplies this electric motor (denoted as "e-motor" in Figure 7.1) is taken from the engine; however, the recharging can be accomplished alongside normal operation of the powertrain without affecting the transmission output torque during the synchronisation of the target gear. Deceleration is achieved through an internal brake. Apart from these two elements only simple dog clutches are required at the gearwheels and a device that can couple either of the two input

shafts on each half of the transmission to the electric motor or brake. The big advantage of this concept is that gear synchronisations can be very fast without any major effect on the transmission output torque (because no energy is transferred from the output of the transmission). Furthermore, because of the nature of the twin clutch design the torque-transmitting clutch can remain engaged during the gear pre-selection, whereas on an automated manual transmission the clutch has to be disengaged (or engine torque has to be reduced to zero). The disadvantage is certainly the additional complexity and cost introduced by the central synchronisation.

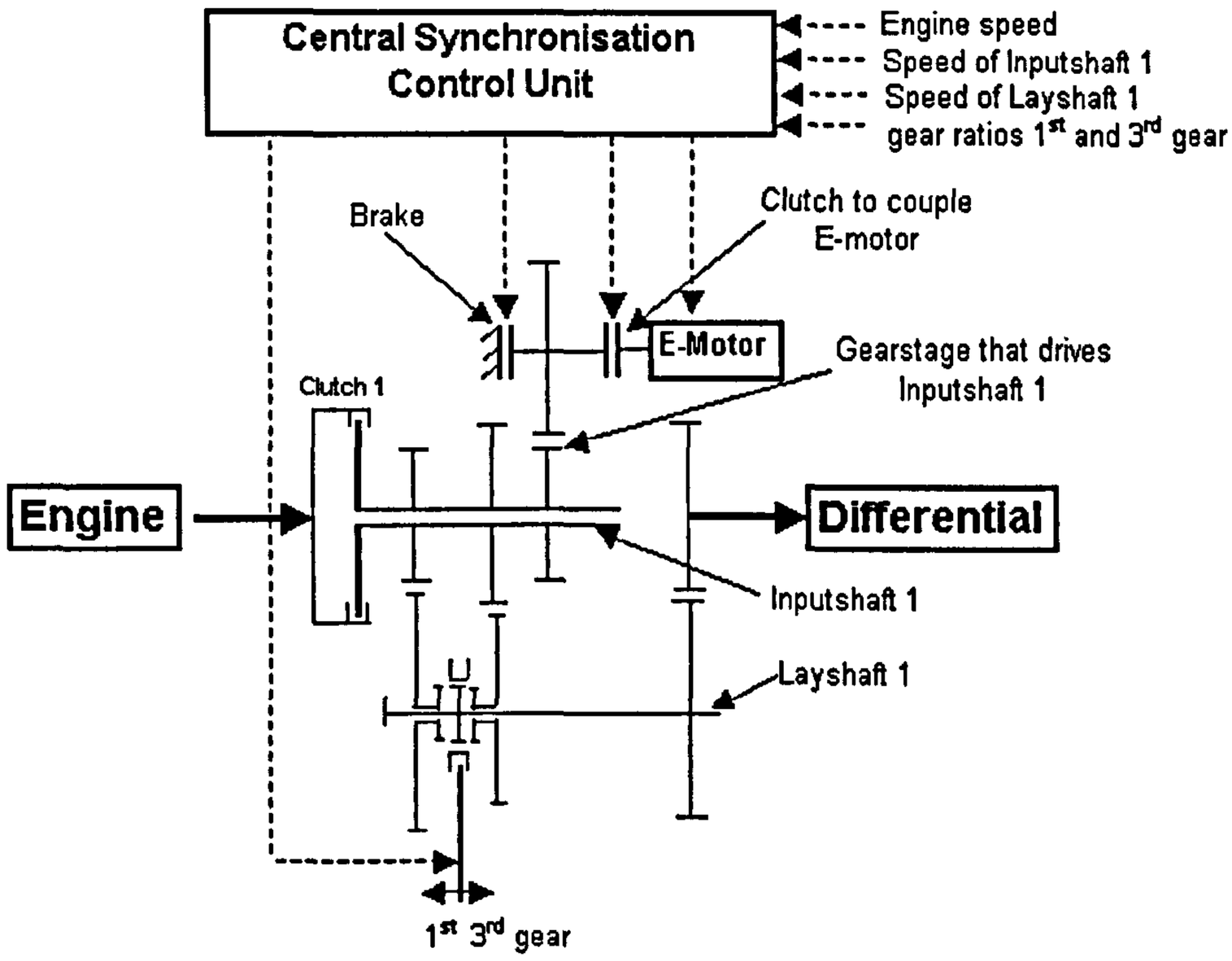

Figure 7.1 Principle of the central synchronisation (shown for transmission half 1 and for 1st and 3rd gear only)

Since the use of conventional hydraulically actuated synchronisers (concept 1) seems to represent the current status of twin clutch transmission design, only this concept will be investigated further in this chapter. It is assumed in the following discussions that the gear pre-selection is carried out according to the above-described method (pre-selection of next lower gear).

The next section will describe in detail the problems using conventional synchronisers. A remedy for these problems is proposed in the section thereafter. All simulation results presented in this chapter were produced using the extended transmission model (see Chapter 3), which enables simulation of synchroniser-to-synchroniser shifts.

7.2 Problems with Gear Pre-Selection utilising Conventional Synchronisers

7.2.1 General Comments on the Dynamics of Synchroniser Engagements

The equations modelling the dynamics of an engagement of a conventional synchroniser ("synchromesh" type) with conical friction contact and dog clutch-like part were given in Chapter 3. To gain better insight into the problem of gear pre-selection the essential equations of Chapter 3 are repeated here in a simplified form, which is thought to be sufficient for illustrating the basic dynamic processes underlying the engagement of a cone-type synchroniser.

The torque balance at the input shaft on the torque-free half of the transmission (according clutch is disengaged) where the gear pre-selection should take place is given (for transmission half 1), for a slipping synchroniser, in equation (21). Restating these equations with the simplification of neglecting the compliance of the input shafts and lumping the inertia of the output half of the clutch together with the inertia of the input shaft and the gear wheels into a single inertia reduced to the input of the synchroniser (Equation (70)) yields equation (69). As a further simplification, the drag torque (modelled in Chapter 3 as dampers "connected" to the "ground") and losses in mechanical efficiency are summed into a single term named torque loss (T_{Loss}). Equation (69), describes in a simple form the dynamics of the input shaft (and connected parts) during synchronisation.

The speed of the input shaft is represented by ω_{In} and has to be divided by the gear ratio of the gear to be engaged in order to produce the speed at the synchroniser input. The variable T_{syn} in equation (69) is the friction torque produced at the friction surface of the synchroniser (Equation (23)) and is a function of the clamp force at the friction contact and thus also of the hydraulic pressure at the actuator of the synchroniser. As can be seen from the equations of motion at the transmission output derived in Chapter 3 (Equations (22), (34) and (42)), the friction torque produced at the synchroniser (T_{syn}) directly (via compliance of output shaft and final drive ratio) influences the torque at the transmission output.

$$T_{Syn} = -J_{S,in}\frac{\dot{\omega}_{In}}{i_{1,\ldots,6}} - T_{Loss} \tag{69}$$

$$J_{S,in} = (J_{eff,In} + J_{C,out})i_{1,\ldots,6}^2 \tag{70}$$

Where: $T_{Loss}=f(\omega_{In})$, $T_{Syn}=f(p_S)$

Equipped with equation (69) and equation (70) and the fact that the torque at the synchroniser directly influences transmission output torque one can draw the following conclusions:

1. The sign of the rate of change of the input shaft speed depends on whether a higher or lower gear is pre-selected.
    - Pre-selection of a higher gear requires a deceleration of the input shaft thus $\dot{\omega}_{In} < 0$
    - Pre-selection of a lower gear requires an acceleration of the input shaft thus $\dot{\omega}_{In} > 0$
2. According to equation (70) the reduced inertia that has to be accelerated or decelerated (see conclusion 1 above) during the synchronisation of the target gear, depends on the gear ratio squared. This means that for lower gears the effective inertia as seen by the synchroniser becomes much larger than for higher gears. This in turn requires, for a certain specified rate of change of the input shaft speed (synchronisation time), an according larger friction torque (actuation pressure) for low gears and an according smaller friction torque for high gears.
3. For the assumption that the torque loss is smaller than both the friction torque at the synchroniser and the inertial torque, analysing equation (69) yields to the following important conclusions about how the transmission output torque changes during the synchronisation process:
    - Pre-selection of a higher gear ($\dot{\omega}_{In} < 0$): $T_{syn}>0$, which leads to an increase in transmission output torque ($T_{out} \uparrow$)
    - Pre-selection of a lower gear ($\dot{\omega}_{In} > 0$): $T_{syn}<0$, which leads to a decrease in transmission output torque ($T_{out} \downarrow$)
4. According to equation (69) the torque loss has different effects on the synchronisation process:
    - Pre-selection of a higher gear ($\dot{\omega}_{In} < 0$): for a given $\dot{\omega}_{In}$ the torque loss decreases the necessary friction torque at the synchroniser T_{Syn} and thus also the necessary actuation pressure decreases.
    - Pre-selection of a lower gear ($\dot{\omega}_{In} > 0$): for a given $\dot{\omega}_{In}$ the torque loss increases the necessary friction torque at the synchroniser T_{Syn} thus also the necessary actuation pressure increases.

Due to the dependency of the torque loss on the input shaft speed, the above effects become larger with increasing input shaft speeds (i.e. pre-selection of lower gears).

5. For short synchronisation times (high actuation pressures) in the range of up to around 0.3 seconds (this limit was found for the transmission modelled here and has to be understood as a band of values rather than a single exact value) the necessary friction torque at the synchroniser becomes much larger than the torque loss ($T_{syn}>>T_{Loss}$) thus the contribution of the torque loss and its dependency on the speed of the input shaft becomes less noticeable. By additionally assuming that the actuation pressure and the friction coefficient stay constant (i.e. T_{Syn}= const.) during the synchronisation process, the rate of change of the input shaft speed will stay constant ($\dot{\omega}_{In} = const.$) as well (see equation (69)). As a result the input shaft speed changes linearly with time during the synchronisation. For longer synchronisation times (>0.3 seconds) as for example encountered on double-downshifts in Chapter 6, the necessary actuation pressure and thus friction torque becomes smaller and the dependency of the torque loss on the input shaft speed cannot be neglected anymore. This leads to the consequence that the rate of change of the input shaft does not stay constant ($\dot{\omega}_{In} \neq const.$) during the synchronisation. This phenomenon could be observed in some simulation results for double-downshifts (see Chapter 6) where the synchronisation times were in the range of 0.5 seconds and where it could be observed that the trajectory of the input shaft speed did not follow a linear trajectory with time anymore. Of course, these findings are valid only when considering the same gear (e.g. naturally, lower gears require in general a larger actuation pressure than higher gears, because of the larger effective inertia).

With these general findings, the problems of gear pre-selection can now be discussed separately for upshifts and downshifts based on simulation results.

7.2.2 Gear Pre-Selection on Upshifts

As explained in Section 7.1, the gearshift on a twin clutch transmission consists of two main parts, the change of a (target-) gear on the torque-free half of the transmission (gear pre-selection) and the actual clutch-to-clutch shift where engine torque is transferred from the offgoing clutch to the oncoming clutch (torque phase) and engine speed is synchronised to the level of the target gear (inertia phase). Whether the pre-selection of the target gear occurs before or after the clutch-to-clutch shift (preparing the transmission for a next gearshift) depends on the pre-selection strategy and whether an upshift or downshift is considered. As explained before, the gear pre-selection strategy adopted in this work is that of always selecting as target gear a gear lower than the currently engaged one.

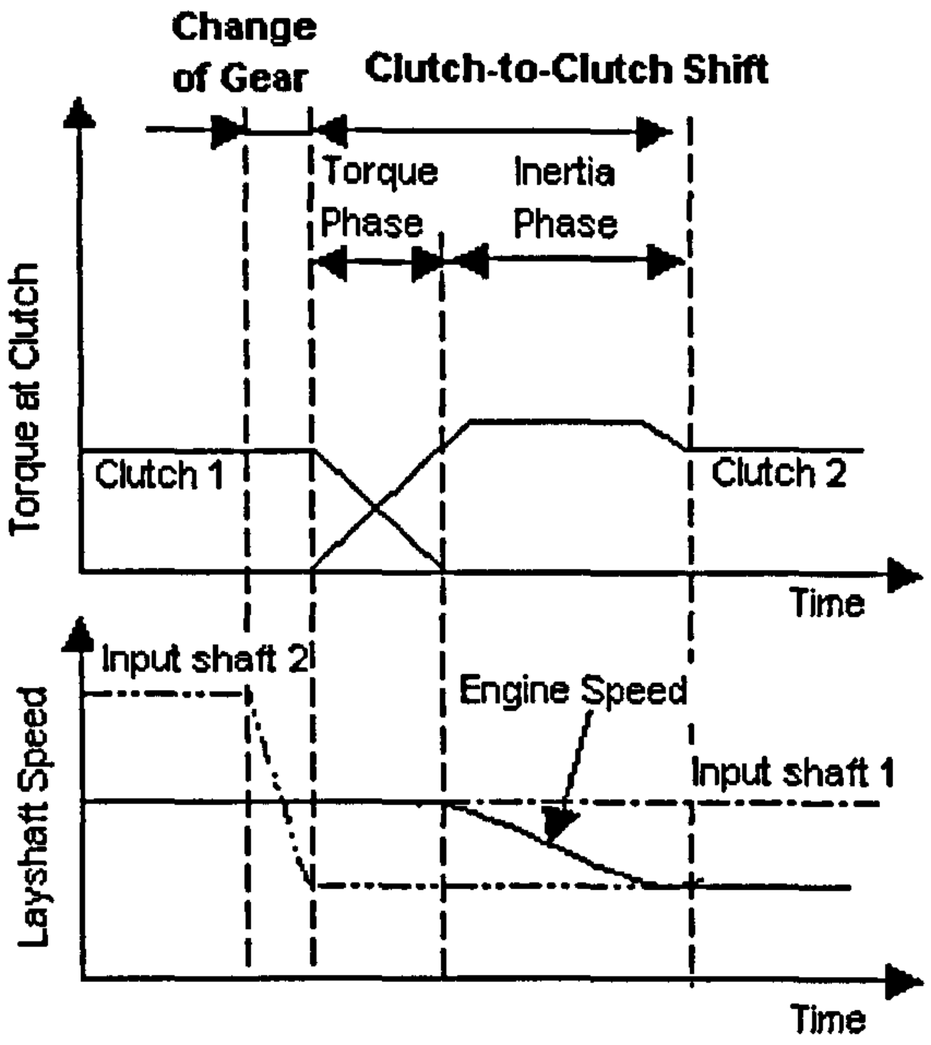

Figure 7.2 Schematic of a power-on upshift on a twin clutch transmission, incorporating a change of gear on the torque-free half of the transmission (gear pre-selection) and a (conventional-) clutch-to-clutch shift.

For an upshift this requires changing (it is assumed that on both transmission halves a gear is engaged at all times) from a gear lower to a gear higher than the currently engaged gear before commencing the clutch-to-clutch shift. A schematic of such an upshift that illustrates the whole shifting procedure including a clutch-to-clutch shift and change of gear is depicted in Figure 7.2. Figure 7.2 shows that, indeed, before commencing the clutch-to-clutch shift, the half of the transmission carrying the target gear (torque-free half) is prepared for the clutch-to-clutch shift by changing gears (i.e. the target gear) beforehand. Changing from a lower gear to a higher gear means that the input shaft on the torque-free half of the transmission (input shaft 2 in Figure 7.2) has to be decelerated to the speed level of the target gear. Such a complete upshift (clutch-to-clutch shift part as developed in Chapters 4 and 5) was simulated for a power-on upshift from 2^{nd} to 3^{rd} gear and is depicted in Figure 7.3.

The timing of the application of the synchronisers involved in the gear pre-selection can be seen from the actuation pressure profiles at the two synchronisers, which are depicted in the fourth graph from top in Figure 7.3. The disengagement of 1^{st} gear is accomplished by decreasing the actuation pressure to zero (dotted circle in Figure 7.3) at the according synchroniser (synchroniser 1 in Figure 7.3). The engagement of the 3^{rd} gear (target gear) first involves a synchronisation of the according input shaft (and connected gear wheels) to the speed level of the target gear (upper arrow in Figure 7.3 pointing at speed of oncoming clutch).

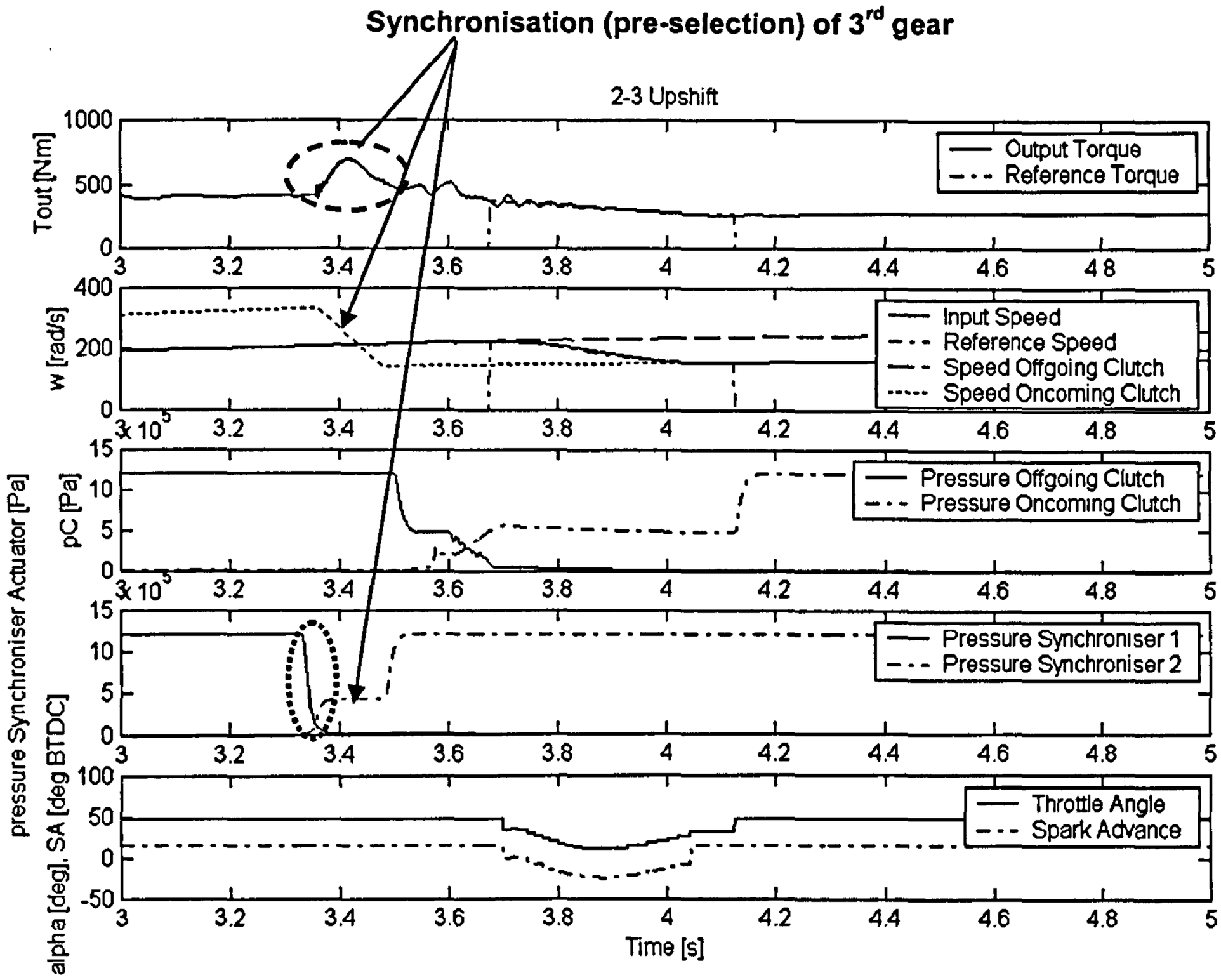

Figure 7.3 Simulation result: Power-on upshift from 2nd to 3rd gear with change of gear (1st disengaged and 3rd engaged) prior to the clutch-to-clutch shift.

The synchronisation of the input shaft can be accomplished by increasing pressure at the synchroniser of the target gear (lower arrow in Figure 7.3 pointing at pressure of synchroniser 2). For a given target gear the pressure level at the oncoming synchroniser determines the speed of the synchronisation. The time selected for synchronising the target gear in Figure 7.3 was 0.12 seconds (fast synchronisation). After the input shaft has reached synchronous speed the synchroniser of the target gear can be locked mechanically by engaging the dog clutch-like part of the synchroniser. After the synchroniser has locked up the actuation pressure can be increased to the line pressure.

The synchronisation of the target gear requires a deceleration of the input shaft. The speed trajectory of the input shaft has the form of a linear decrease with time during the synchronisation (see upper arrow in Figure 7.3), which was to be expected given the short synchronisation time (for an explanation see Section 7.2.1). The deceleration of the input shaft transfers synchronising (friction-) torque from the synchroniser to the output shaft of the transmission (explained in Section 7.2.1) and results to an increase ("hump") in the output

torque profile (dashed circle in Figure 7.3) prior to the clutch-to-clutch shift. This "hump" becomes more extreme as the time available for synchronisation decreases. The size of this torque "hump" also depends on the target gear to be synchronised and is larger for lower gears (larger gear ratios) because of the fact that the effective inertia at the synchroniser input increases with the gear ratio squared (see Equation (70).

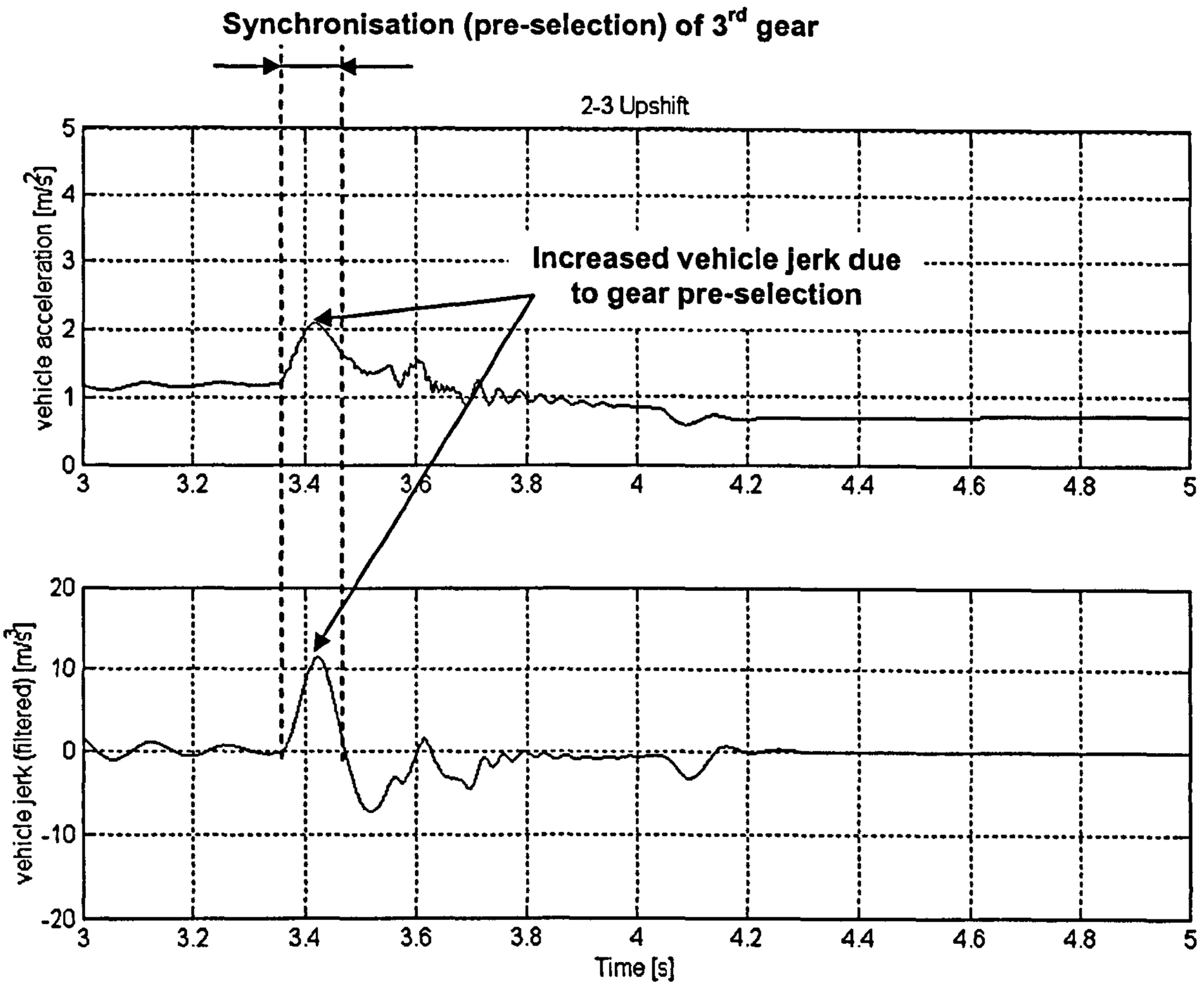

Figure 7.4 Vehicle acceleration and jerk for the upshift form Figure 7.3

The effect of the torque "hump" on the vehicle jerk is illustrated in Figure 7.4, which shows increased vehicle jerk (see arrows in Figure 7.4) in the phase of gear pre-selection and thus reveals the negative influence of the gear pre-selection (with conventional synchronisers) on the gearshift quality. Increasing the synchronisation time in the upshift depicted in Figure 7.3 would naturally lead to a decrease of the torque "hump". However, in practice, this is often not desired since it would lead to an increase in total shift time. This means that either a compromise must be made between shift comfort and fast synchronisation or an alternative synchronisation mechanism has to be employed (e.g. central synchronisation). A third alternative for power-on upshifts is proposed in Section 7.3.

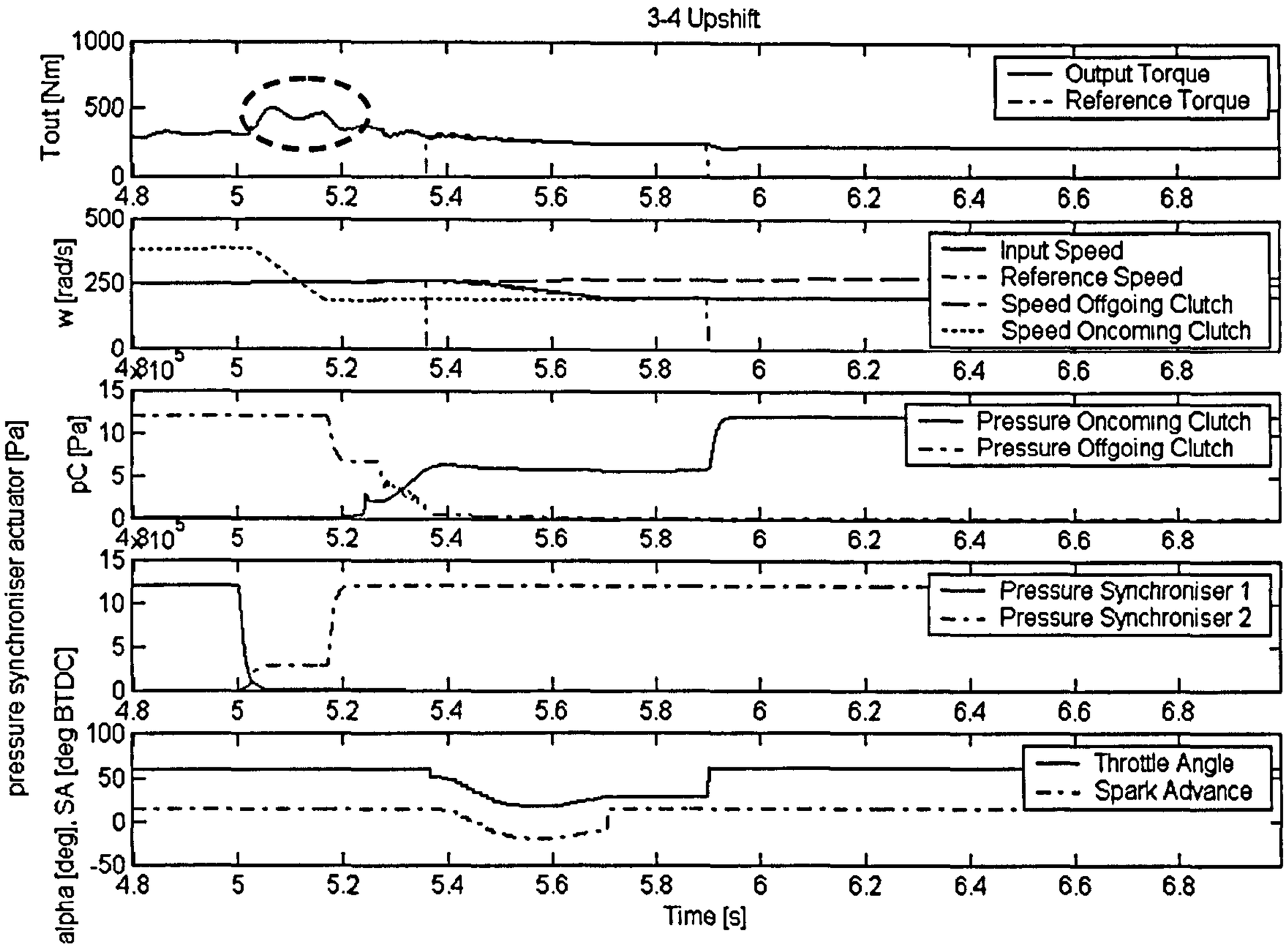

Figure 7.5 Simulation result: Power-on upshift from 3rd to 4th gear with change of gear (2nd disengaged and 4th engaged) prior to the clutch-to-clutch shift.

Although, as explained, the torque "hump" decreases in size for higher target gears, the problem does not vanish entirely. This is illustrated for a power-on upshift from 3rd to 4th gear in Figure 7.5. The synchronisation time for this shift is around 0.13 seconds and the torque "hump" is marked by a dashed circle in Figure 7.5.

Figure 7.6 shows a power-off upshift from 2nd to 3rd gear. Although, the time for synchronising the target gear in Figure 7.6 is in the same range (around 0.12 seconds) as that of the power-on upshift from Figure 7.3, the torque "hump" is less extreme compared to the power-on upshift (vehicle jerk reaches only 6 m/s^3 on the power-off upshift in Figure 7.6). The reason for this is that the actuation pressure at the synchroniser can be selected to be lower compared to power-on shifts. This is, because the speed trajectories are in general descending (vehicle slows down) instead of ascending (power-on shift); therefore, the effective change of the slope of the input shaft speed during the synchronisation (energy required for synchronisation) is smaller compared to the power-on shift case. Also, a power-off upshift is in most cases not critical in terms of total shift time, thus, the time available for synchronising the target gear can be increased and hence the torque "hump" decreased. For these reasons, power-off upshifts will not

be considered henceforth and the discussion about remedies for gear pre-selection (see Section 7.3) focuses on power-on upshifts.

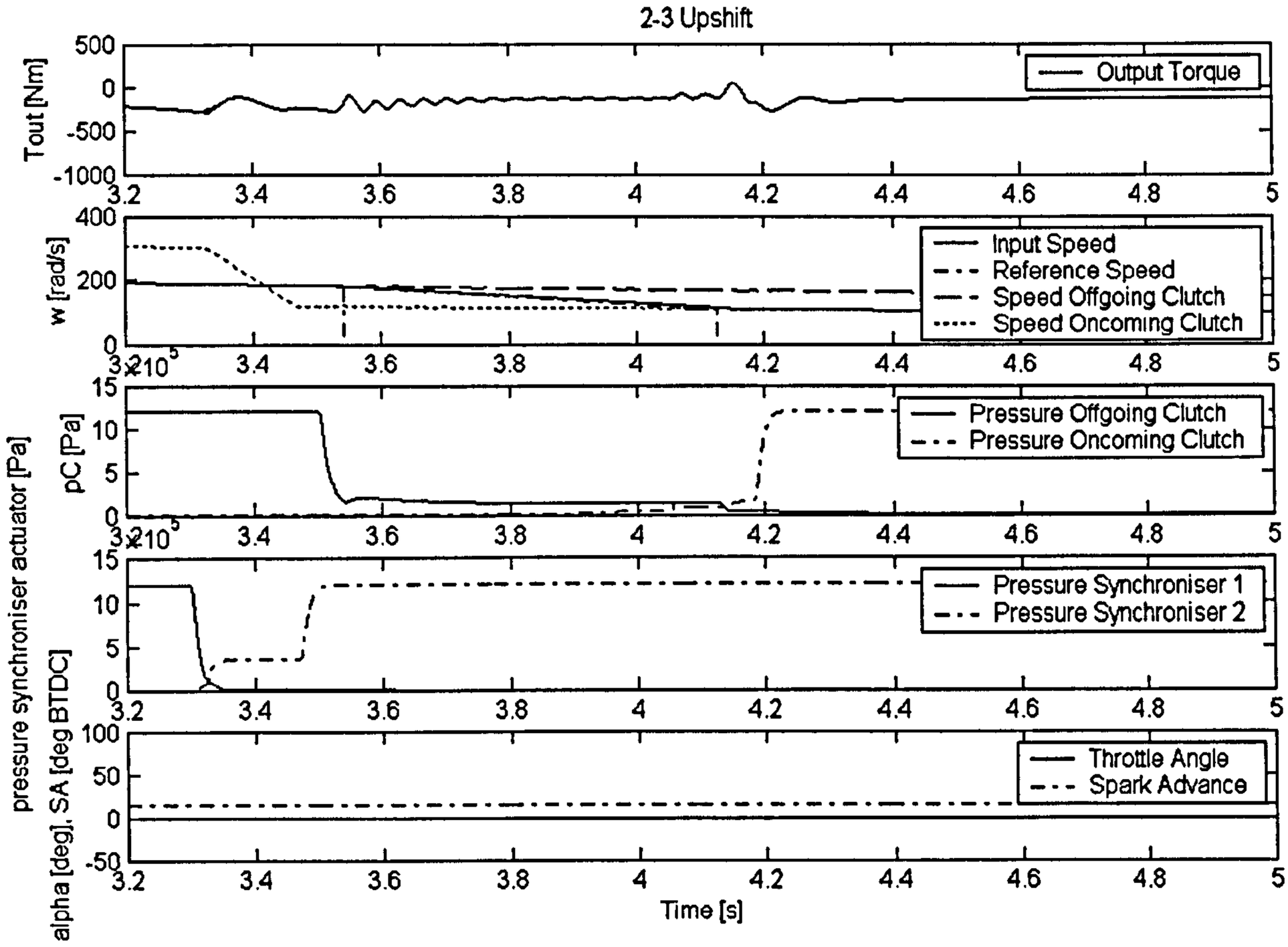

Figure 7.6 Simulation result: Power-off upshift from 2nd to 3rd gear with change of gear (1st disengaged and 2nd engaged) prior to the clutch-to-clutch shift.

7.2.3 Gear Pre-Selection on Downshifts

The gear pre-selection strategy described in Section 7.1 requires, on a downshift, a change of the target gear on the torque-free half of the transmission subsequent to the clutch-to-clutch shift. The schematic of a complete (power-on) downshift on a twin clutch transmission incorporating a clutch-to-clutch shift and a change of target gear is depicted in Figure 7.7.

As illustrated in Figure 7.7 the gear pre-selection (denoted as change of gear in Figure 7.7) requires changing the target gear from a gear higher to a gear lower (larger gear ratio) than the currently engaged one. This means that the input shaft (input shaft 2 in Figure 7.7) on the torque-free half of the transmission needs to be accelerated to the speed of the target gear.

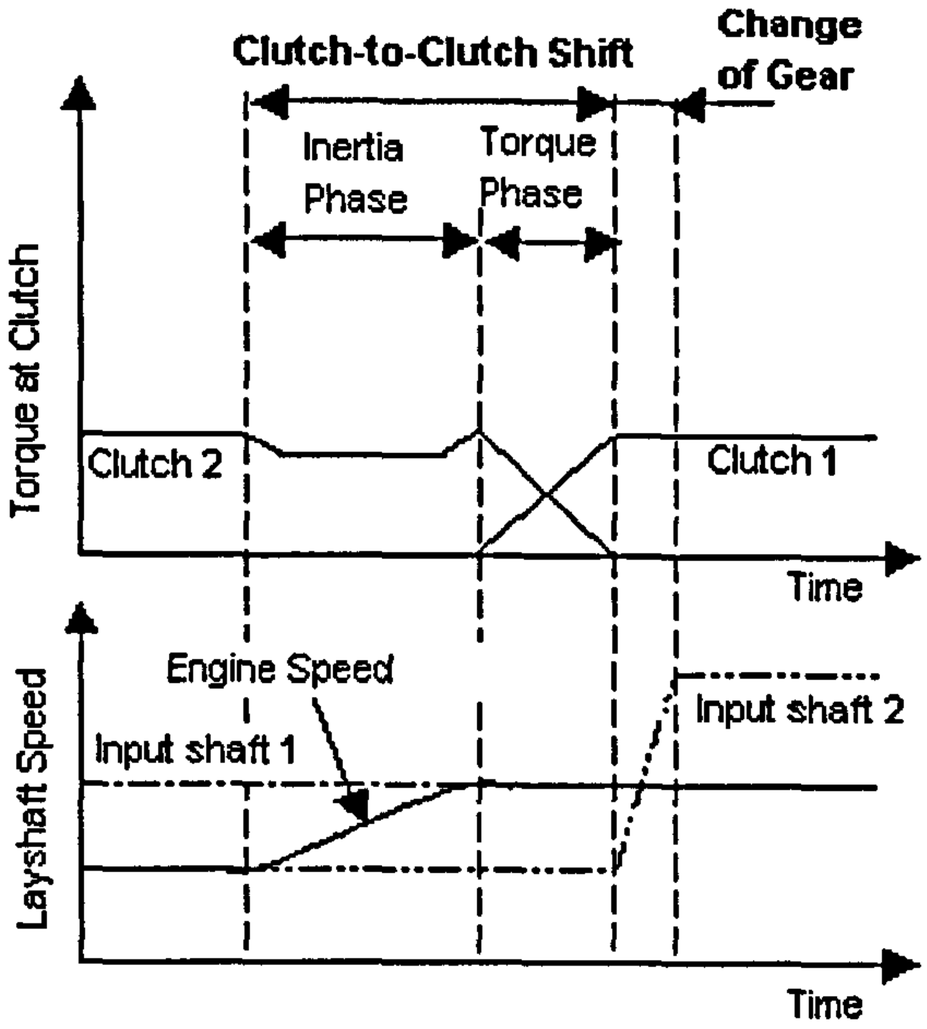

Figure 7.7 Schematic of a power-on downshift on a twin clutch transmission, incorporating a change of gear on the torque-free half of the transmission (gear pre-selection) and a (conventional-) clutch-to-clutch shift.

Figure 7.8 depicts the simulation result for a power-on downshift from 3rd to 2nd gear, where subsequent to the clutch-to-clutch shift (carried out according to the downshift control strategy developed in Chapters 4 and 5), the target gear is changed from 3rd to 1st gear. This requires the disengagement of the 3rd gear by decreasing the actuation pressure at the according synchroniser to zero (pressure synchroniser 2 in Figure 7.8) and can be immediately commenced after the torque phase of the clutch-to-clutch shift has been completed. After the disengagement of the 3rd gear has been accomplished, the actuation pressure at the oncoming synchroniser can be increased to the level necessary for synchronisation (lower arrow in Figure 7.8 pointing at pressure at synchroniser 1). As a consequence of this increase in actuation pressure at the synchroniser the input shaft on the torque free half of the transmission is accelerated to the speed level of the target gear (upper arrow in Figure 7.8 pointing at the speed of offgoing clutch). The energy (synchronising friction torque) required for the acceleration of the input shaft during the synchronisation process is transferred from the transmission output (and thus from the wheels) to the synchroniser. This causes the transmission output torque to drop during the gear pre-selection (dashed circle in Figure 7.8).

Again, as with upshifts the actuation pressure at the oncoming synchroniser determines, for a given target gear, the time of the synchronisation process. Thus, the pressure at the synchroniser also determines the size of the drop in transmission output torque. The more time is available (lower actuation pressure) for the synchronisation of the target gear, the smaller is the drop in

torque during gear pre-selection. In Figure 7.8, the synchronisation was again accomplished in a relatively short period of time (around 0.12 seconds).

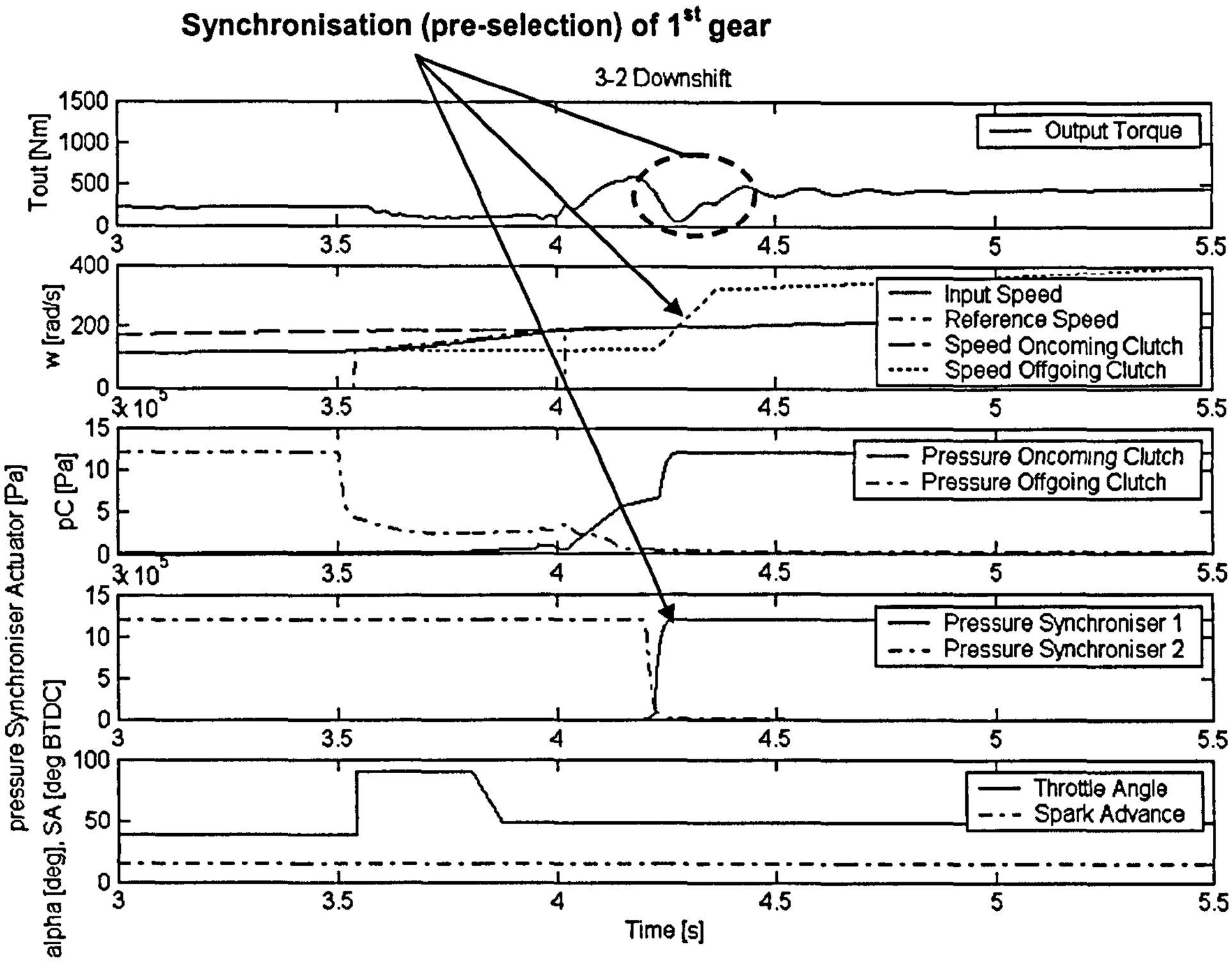

Figure 7.8 Simulation result: Power-on downshift from 3rd to 2nd gear with change of gear (3rd disengaged and 1st engaged) subsequent to the clutch-to-clutch shift.

Increasing this synchronisation time in the gearshift in Figure 7.8 would have naturally smoothed the drop in output torque, but on the other hand, would have increased the total shift time. Similar to upshifts, in practice it is often not desired to increase time for synchronising the target gear and hence also the total shift time on a downshift. Again, either a compromise between shift comfort and fast synchronisation must be made or alternative ways of synchronisation have to be used (e.g. central synchronisation). In Section 7.3 a way of improving shift quality on power-on downshifts by smoothing the effects of the gear pre-selection is proposed.

How the drop in transmission output torque (due to gear pre-selection) in the downshift in Figure 7.8 (dashed circle in Figure 7.8) influences the vehicle jerk can be seen in Figure 7.9, which shows that the gear pre-selection leads to a negative peak in vehicle jerk of around -20 m/s^3 (see arrows in Figure 7.9).

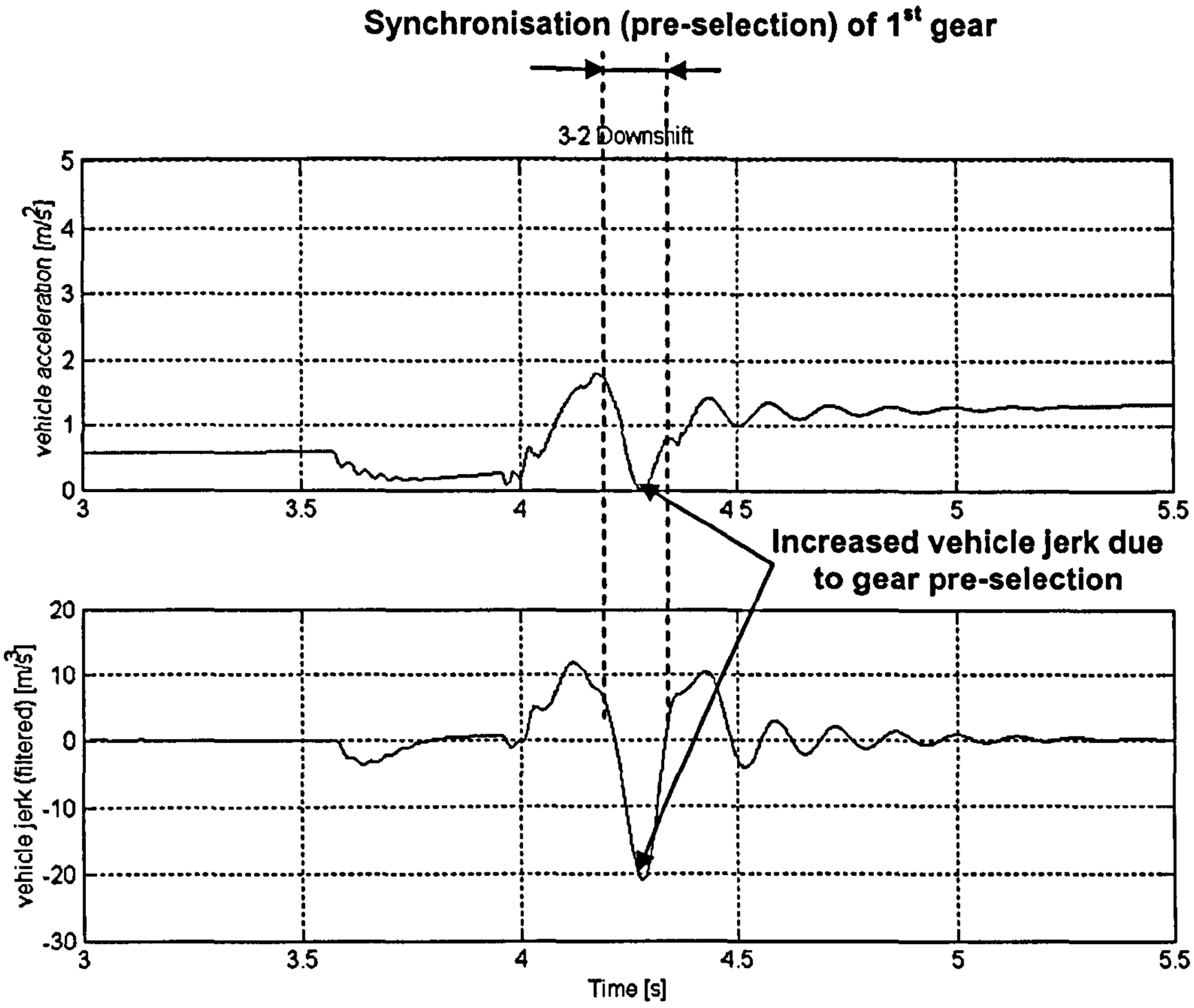

Figure 7.9 Vehicle acceleration and jerk for the downshift from Figure 7.8

Although, as explained, the drop in transmission output torque during gear pre-selection on downshifts decreases in size for the synchronisation of higher target gears, a drop in transmission output torque can still be distinguished clearly for downshifts between higher gears. This situation is illustrated for a power-on downshift from 4th to 3rd gear in Figure 7.10. The dashed circle in the transmission output torque profile Figure 7.10 marks the torque drop due to the gear pre-selection. The torque drop (change relative to the level of output torque right before gear pre-selection takes place) is smaller as compared to the one of the downshift from 3rd to 2nd gear depicted in Figure 7.8. Also the vehicle jerk is smaller: -12 m/s^3, for the 4-3 downshift from Figure 7.10 (vehicle jerk profile not shown) and -20 m/s^3, for the 3-2 downshift from Figure 7.8.

Figure 7.11 shows a power-off downshift from 3rd to 2nd gear. Although, the time for synchronising the target gear is in the same range (also 0.12 seconds) as that of the power-on downshift from Figure 7.8, the drop in torque is less extreme compared to the power-on downshift (vehicle jerk reaches only -14 m/s^3 on power-off downshift). The reason for this is that, despite the power-off shift having the same synchronisation time as the power-on shift, the actuation pressure at the synchroniser was smaller in the power-off shift (Figure 7.11) compared

to the power-on shift (Figure 7.8). The lower actuation pressure was possible, because the level of the input shaft speed prior to the gear pre-selection and hence also the total change in speed during the gear-pre-selection was smaller in the power-off shift.

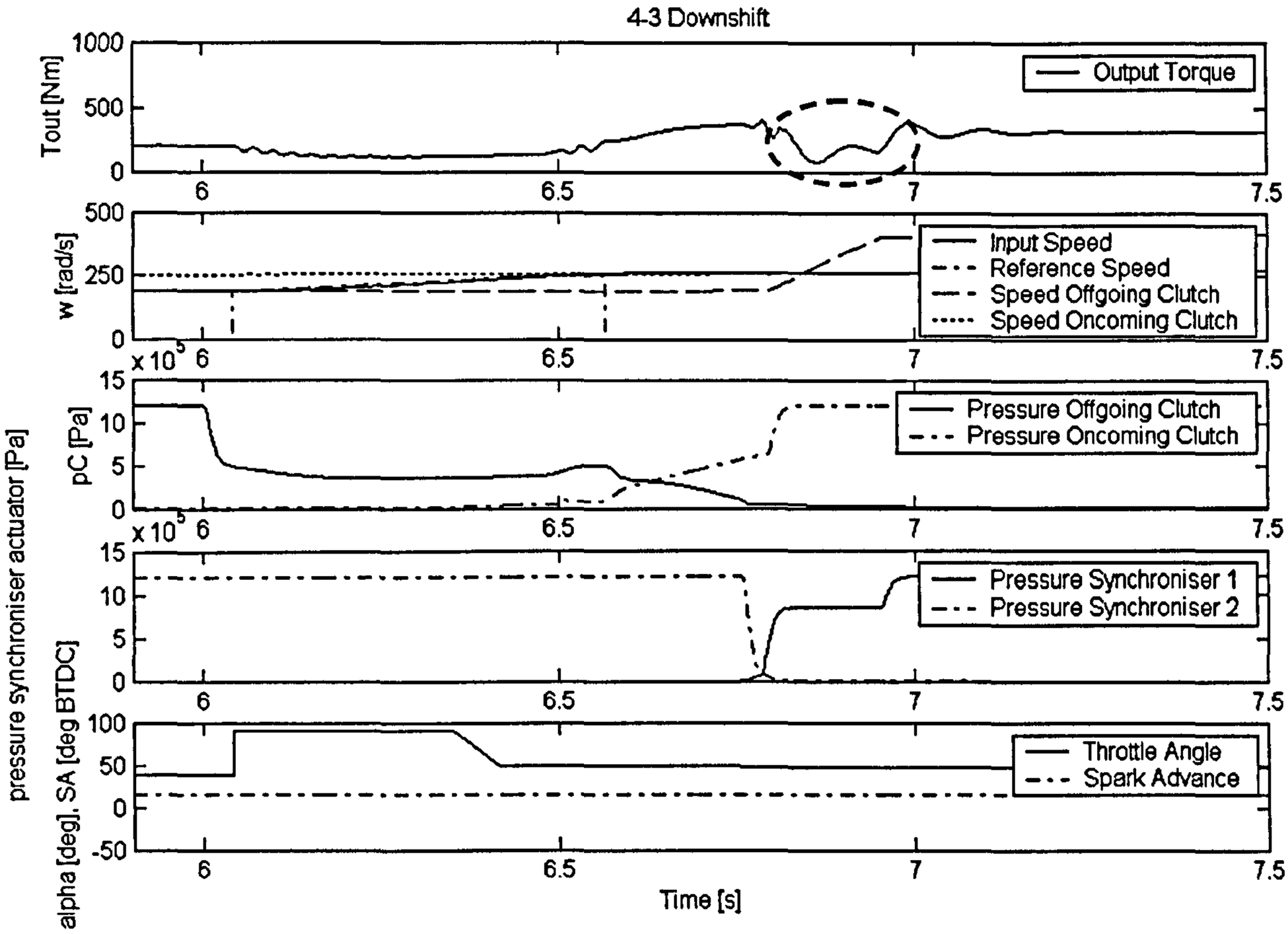

Figure 7.10 Simulation result: Power-on downshift from 4th to 3rd gear with change of gear (4th disengaged and 2nd engaged) subsequent to the clutch-to-clutch shift.

Also, power-off downshifts are usually not time critical, thus longer synchronisation times could be selected, which would decrease the size of the torque drop. The only case where power-off downshifts are critical concerning shift time is when shifting down through several gears under heavy braking. However, braking of the vehicle anyway leads to increased negative wheel torque (transmission output torque) and the effect of gear pre-selection is thus believed to be less noticeable when shifting down under heavy braking. Alternatively, if the influences of gear pre-selection are not acceptable for cases where consecutive power-off downshifts have to take place within a short period of time, the power-off downshift can be accomplished as an integrated double-downshift or the downshift is not executed at all until the vehicle is accelerated again. However, the second strategy means that still the appropriate target gear needs to be pre-selected based on the vehicle speed; only the actual clutch-to-clutch shift can be postponed until when the vehicle is accelerated again.

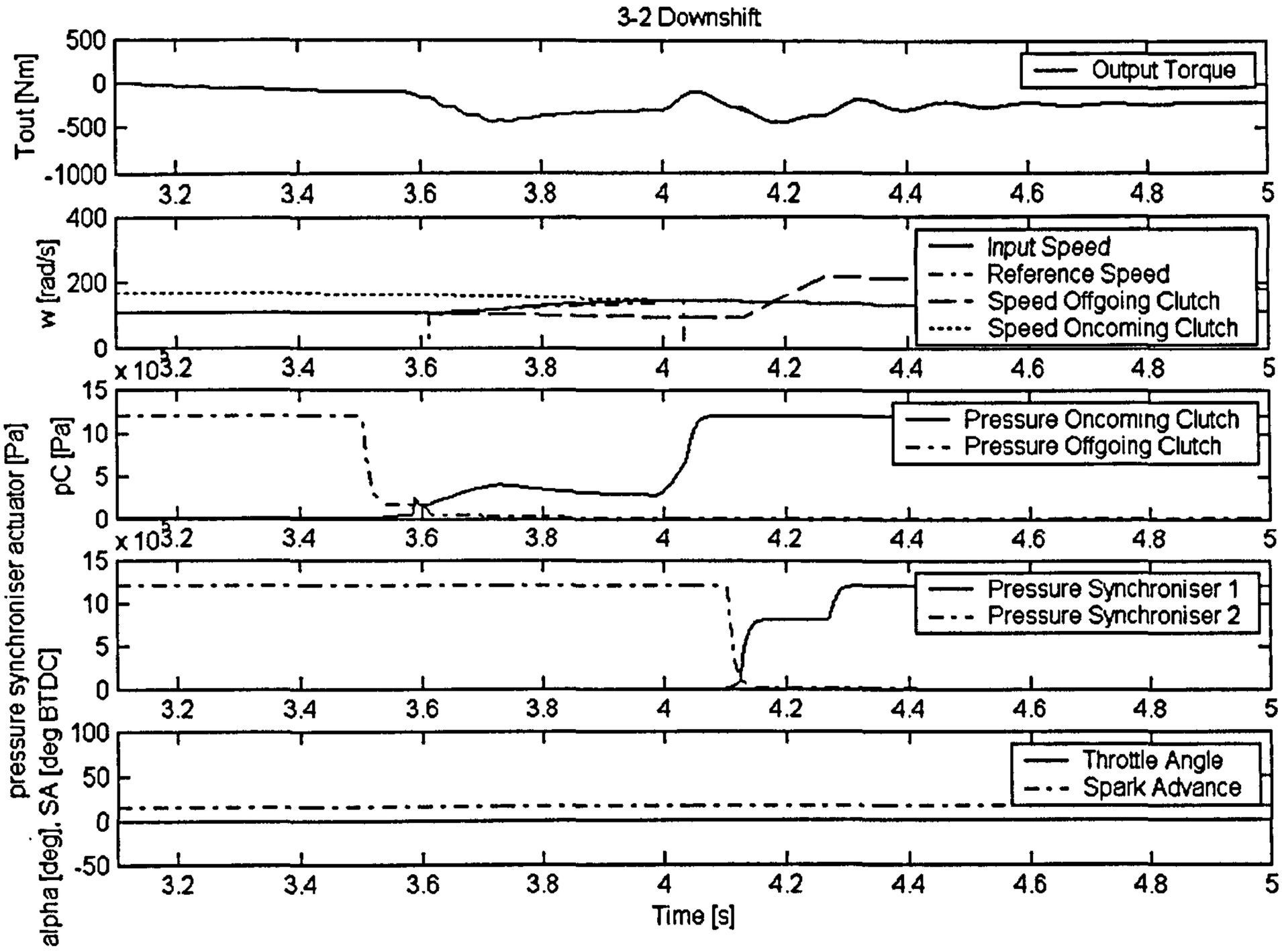

Figure 7.11 Simulation result: Power-off downshift from 3rd to 2nd gear with a change of gear (3rd disengaged and 1st engaged) subsequent to the clutch-to-clutch shift.

The discussion has shown that the only time-critical case of a power-off downshift is when the vehicle is braking heavily, which can be solved by one of the above-described approaches. All other cases of power-off downshifts are not time-critical hence time for gear pre-selection can be increased. For these reasons it is less important to improve the gear pre-selection on power-off downshifts, hence the following discussion (see Section 7.3) concentrates on finding a way of improving the gear pre-selection on power-on downshifts.

7.3 Ways of Improving the Gear Pre-Selection

7.3.1 Compensating Control strategy for the Gear Pre-Selection on Power-On Upshifts

In Section 7.2.2 it was found, that the pre-selection of a higher gear on power-on upshifts leads to a torque "hump" prior to the actual clutch-to-clutch shift. It was furthermore found, that this is due to friction torque produced at the synchroniser, which is used to decelerate the input shaft

and which is transferred to the transmission output where it leads to an increase in transmission output torque.

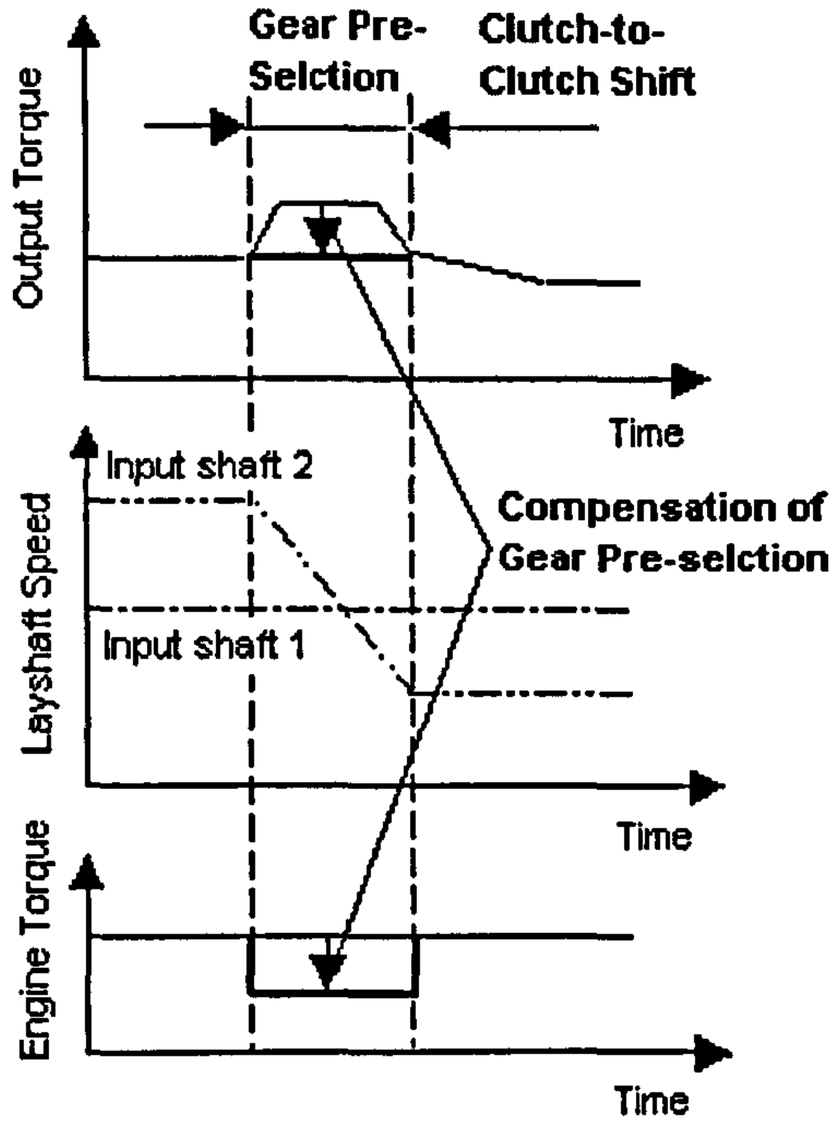

Figure 7.12 Schematic of compensating the torque "hump" resulting from the gear pre-selection on upshifts by engine torque reduction

Now, if it would be possible to decrease engine torque for the time of the gear pre-selection by exactly the same amount as is produced at the synchroniser (considering the multiplications by the gear ratios in between), it should be possible to compensate for the torque "hump" produced by the gear pre-selection. This simple form of control strategy with the aim of compensating the effect of the gear pre-selection is illustrated in Figure 7.12.

For the aim of compensating the effects of the gear pre-selection, a simple open-loop control strategy will be developed here that accomplishes exactly the compensation sketched in Figure 7.12. This open-loop control strategy works with a manipulation of engine torque (modulation of spark advance) and is thus simple, relatively robust and is well suited as add-on solution for production twin clutch designs, which feature conventional synchronisers. The open-loop control algorithm can be simply implemented by any engine controller, which accepts a torque reduction request from the transmission controller. In this work, since utilising a SI-engine, also the translation of a request for engine torque reduction (torque signal) to that of a request for a change in spark advance is developed in detail.

To derive the amount of reduction in engine torque required for the gear pre-selection, information about two variables could be used:

1. The necessary synchronising torque, which depends on the inertial torque and the torque loss (Equation (69))
2. The (actual-) friction torque at the synchroniser as a function of friction coefficient, actuation pressure and dimensions of the friction contact at the synchroniser according to equation (71).

The first variable, the necessary synchronising torque, could be inferred from the knowledge of the effective inertia of the parts to be synchronised, together with the rate of change of the input shaft speed (linear trajectory assumed for short synchronisation). The difficulties arise with the torque loss, which is not exactly known and depends on the input shaft speed. Although, it was found that the torque loss can be small in comparison to the inertial torque, the lack of knowledge about this contribution has lead to inaccurate values for engine torque reduction and the control strategy did not compensate the effects of the gear pre-selection satisfactorily.

Hence, the second variable the (actual-) friction torque at the synchroniser was used to determine the necessary reduction in engine torque. This variable provided a much more accurate information about the increase in transmission output torque during the gear pre-selection. The friction torque produced at the synchroniser when slipping is given in a simplified form by the following relationship (one friction contact (cone) assumed):

$$T_{Syn} = \mathrm{sgn}(\omega_{In} - \omega_{Out}) \frac{R_m}{\sin\alpha} \mu_k (p_S A_p - F_{spring}) \tag{71}$$

with: $F_{Spring}=k_R\, x_{pstroke}$

Equation (71) is simply a generalisation of equation (23) (half 1 of the transmission) with the relationship between the clamp force (F_N) and the actuation pressure (p_S) simplified to the static equilibrium at the piston at the end of its idle stroke (friction surfaces are in contact) and neglecting the effects of piston damping and the mass of the piston. This is justified because, for the development of the algorithm of the compensating control strategy, the only state of the synchroniser that is relevant is where the synchroniser is slipping and the actuator piston motion is negligible.

With the following assumptions:

- The dimensions of the synchroniser (R_m,α) and actuator (A_p)are known
- The force of the piston return spring (when actuator piston is in equilibrium at the end of its stroke) is known and constant (F_{spring}=const.)

- The friction coefficient is known and stays constant during the synchronisation (μ_k=const.)

the friction torque at the synchroniser can be written in the form given by equation (72). The "sign" function in equation (71) produces a positive sign for synchronisations to higher gears (upshifts) since the speed at the input stays above that at the output during synchronisation.

$$T_{Syn} = (C_1 p_S - C_2) \tag{72}$$

with constants C_1 and C_2:

$$C_1 = \frac{R_m}{\sin\alpha}\mu_k A_p \tag{73}$$

$$C_2 = \frac{R_m}{\sin\alpha}\mu_k F_{spring} \tag{74}$$

The actual actuation pressure at the synchroniser (p_S) can be easily inferred from the voltage signal produced by the transmission controller, if the relationship between voltage signal and actual pressure at the synchroniser is known. In practice, the actuation pressure stays constant during the synchronisation and the actuation pressure is only varied in crude steps for which the relationship between input voltage and actual actuation pressure could be easily established. Alternatively, if the synchroniser actuators are fitted with pressure sensors the information can be obtained directly.

Once the value of the friction torque at the synchroniser is calculated according equation (72), the necessary change (reduction) in engine torque can be simply calculated according to equation (76). In equation (76) it is assumed that the synchronisers are located at the output shafts (transmission design according to Figure 3.7) and that the change in the transmission output torque due to the gear pre-selection (ΔT_{out}) can be thus calculated by multiplying the synchronising torque by the final drive ratio according to equation (75). Working back from the transmission output to the engine along the torque-transmitting path, the gear ratio of the final drive cancels out and only the gear ratio of the currently engaged gear needs to be considered (Equation (76):

$$\Delta T_{out} = T_{Syn} i_f \tag{75}$$

$$\Delta T_e = \frac{\Delta T_{out}}{i_g i_f} = \frac{1}{i_g} T_{Syn} = \frac{1}{i_g}(C_1 p_S - C_2) \tag{76}$$

The block diagram of the control strategy that compensates the effects of the gear pre-selection on power-on upshifts is illustrated in Figure 7.13. Input to the block, where the necessary

amount of reduction in engine torque is calculated, is the actuation pressure at the synchroniser. Figure 7.13 indicates the above-discussed choice of deriving the actuator pressure from the input voltage signal or by sensor measurement.

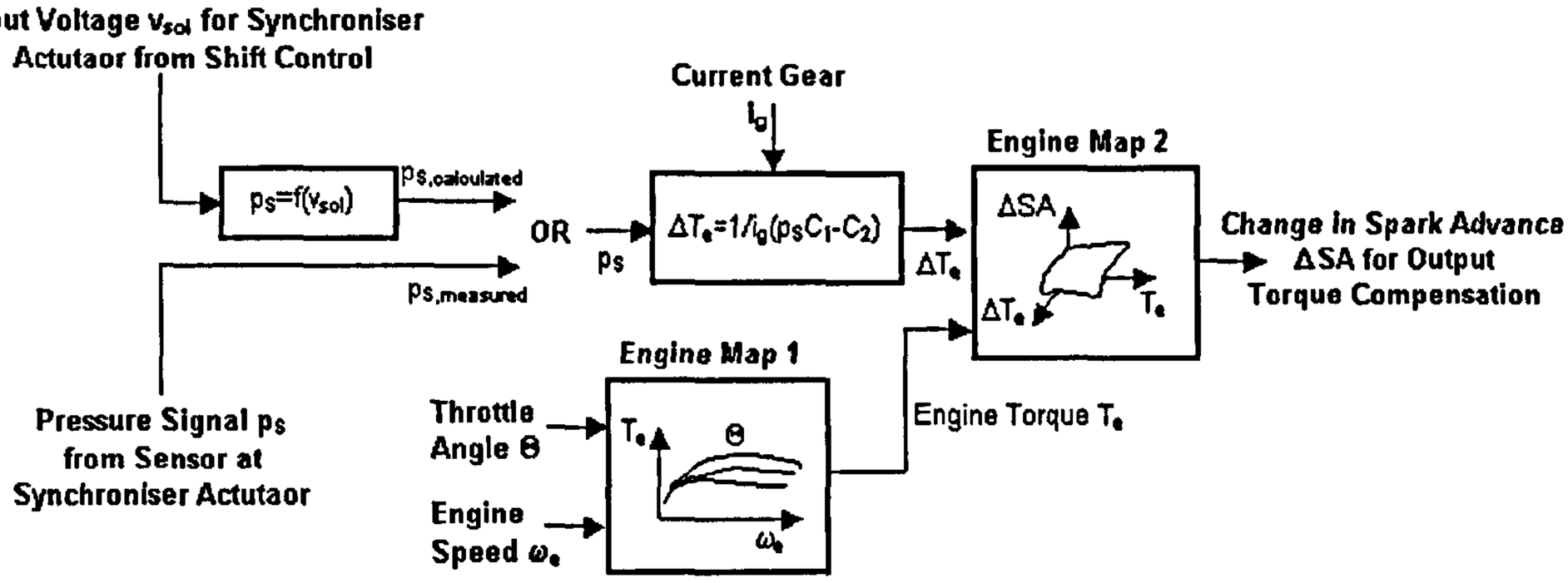

Figure 7.13 Scheme of control strategy compensating the torque "hump" of the gear pre-section, applied to a SI-engine.

The engine torque reduction is calculated according to equation (76) depending on the actuation pressure and the current gear. The value calculated for the engine torque reduction is inputted to an engine map (Engine map 2 in Figure 7.13, is the same engine map as depicted in Figure. 3.6) together with the value of the current engine torque, to derive the change in spark advance necessary for compensating the torque "hump". This three-dimensional engine map was necessary because a change in spark advance usually has different consequences on the change in engine torque at different operating points (values of engine torque). The value of the current engine torque can be obtained from the engine map depicted in Figure 3.5 (Engine map 1 in Figure 7.13) as a function of engine speed and throttle angle.

The "torque hump compensating control strategy" sketched in Figure 7.13 can be naturally also applied to diesel engines, with the only difference that the value calculated for engine torque reduction (ΔT_e) is inputted to engine maps, which produce at their outputs a necessary change in fuel amount (or timing of fuel injection) instead of a value for spark advance.

To demonstrate the effectiveness of the proposed compensating control strategy the simulation results presented in Section 7.2.2 (power-on upshifts with gear pre-selection) are repeated here with the compensating control strategy active. Starting with Figure 7.14, which shows the same power-on upshift from 2^{nd} to 3^{rd} gear as depicted in Figure 7.3 (pre-selection in Figure 7.14

starts 0.1 seconds earlier), only in Figure 7.14 the control strategy compensating the torque "hump" is active. As can be clearly seen in Figure 7.14 the control strategy compensates successfully for the torque "hump" coming from the synchronisation of the target gear by decreasing the spark advance accordingly (dash-dotted circles in Figure 7.14). The control strategy produces a very smooth transmission output torque trajectory showing no traces of the gear pre-selection.

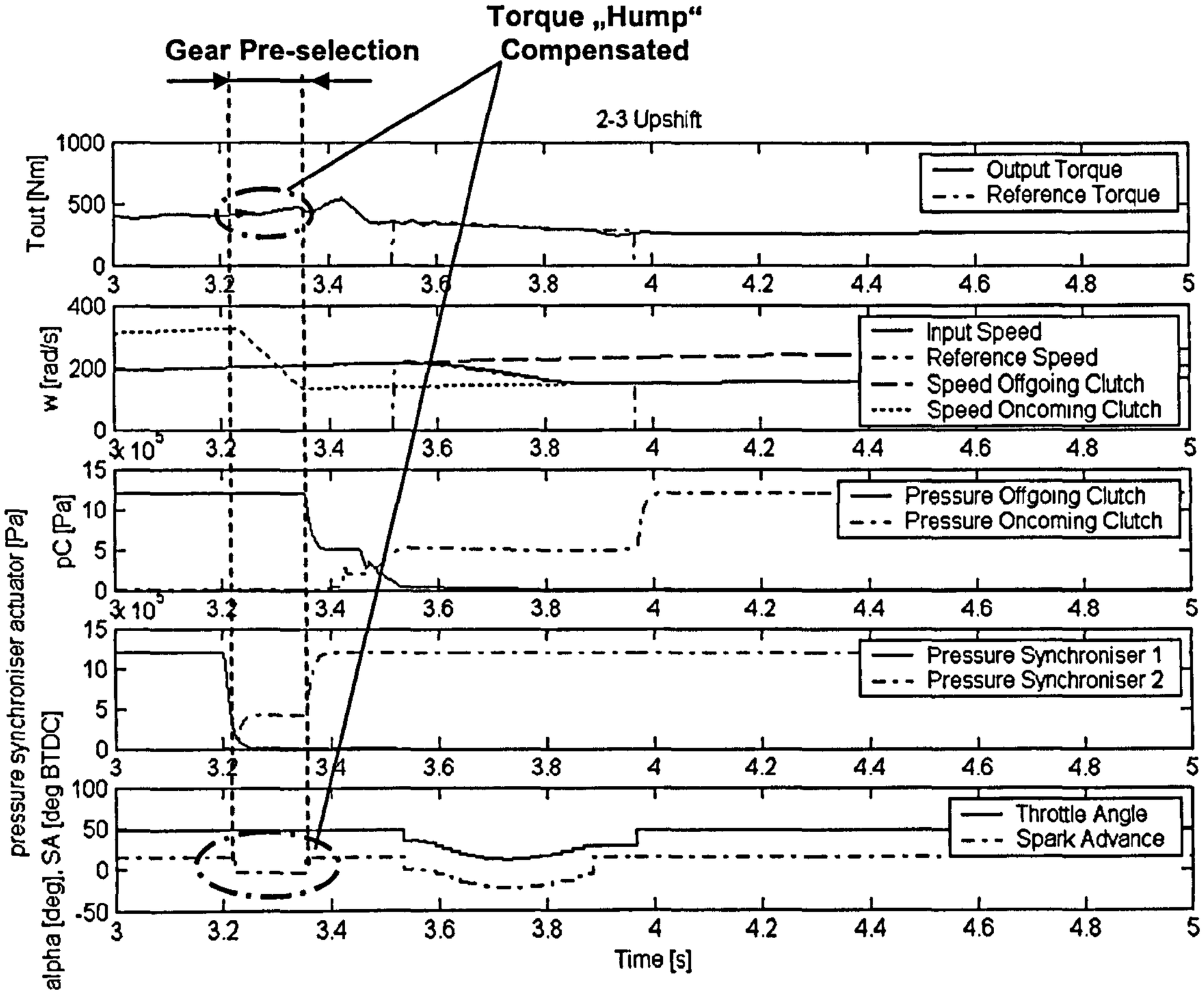

Figure 7.14 Simulation result: Power-on upshift from 2nd to 3rd gear similar to Figure 7.3, with compensating control strategy active during gear pre-selection.

This is also revealed when looking at the vehicle jerk of the gearshift of Figure 7.14, which is depicted in Figure 7.15. Contrary to the same gear shift without compensating control strategy, which showed jerk levels of above 10 m/s^3 (Figure 7.4), the vehicle jerk profile of the gearshift with compensating control strategy (Figure 7.15) shows no sign of increased vehicle jerk during the gear pre-selection (dash-dotted circles in Figure 7.15).

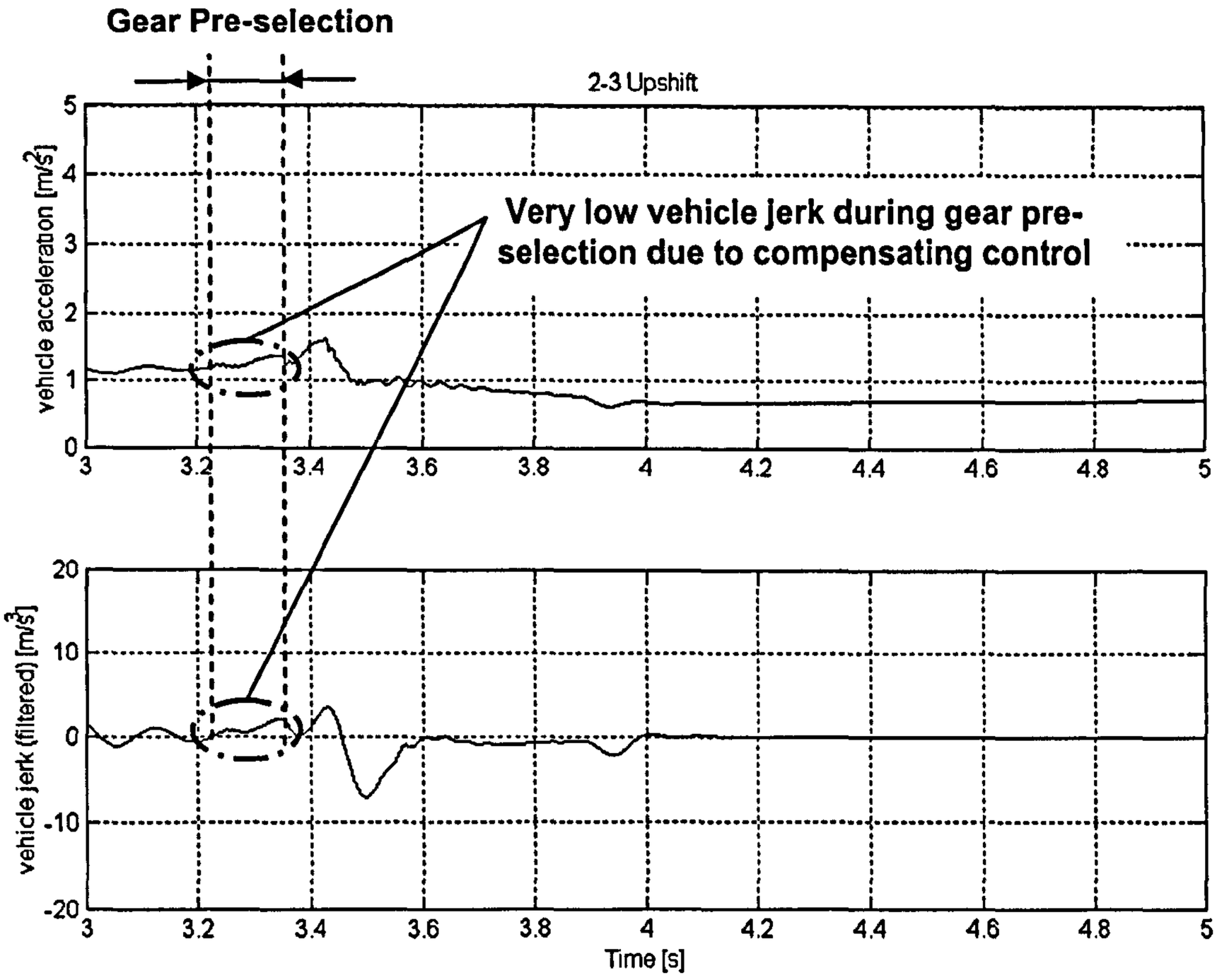

Figure 7.15 Vehicle acceleration and jerk for the upshift form Figure 7.14

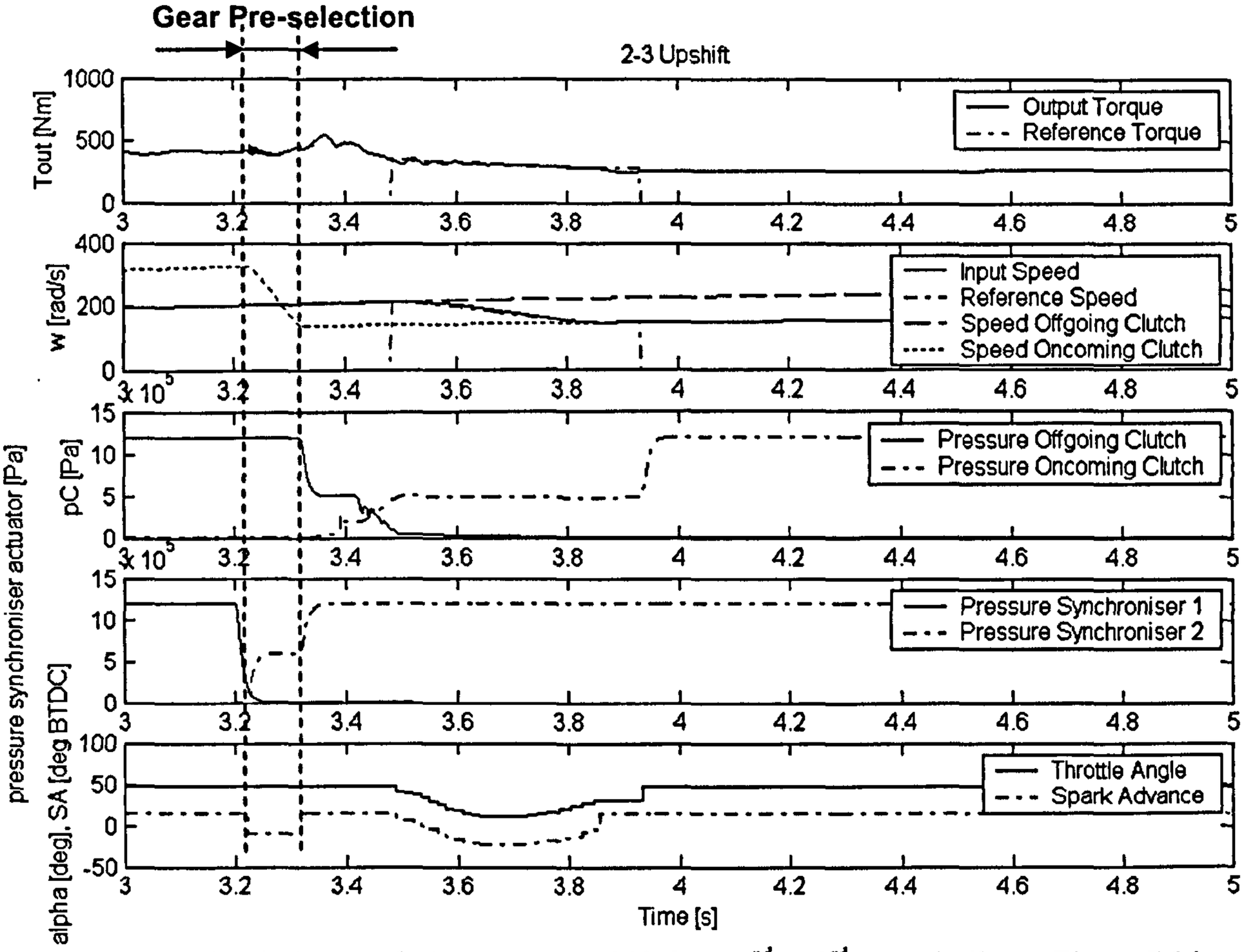

Figure 7.16 Simulation result: Power-on upshift from 2nd to 3rd gear similar to Figure 7.14, with even shorter synchronisation time (0.09 seconds)

The fact that the proposed compensating control strategy for gear pre-selections on power-on upshifts works successfully for even shorter synchronisations times, where the torque "hump" naturally has to become larger is demonstrated in Figure 7.16, which shows a similar shift to Figure 7.14, only that the synchronisation time is reduced to 0.09 seconds. Again, the transmission output torque trajectory looks smooth during the period of time of the gear pre-selection.

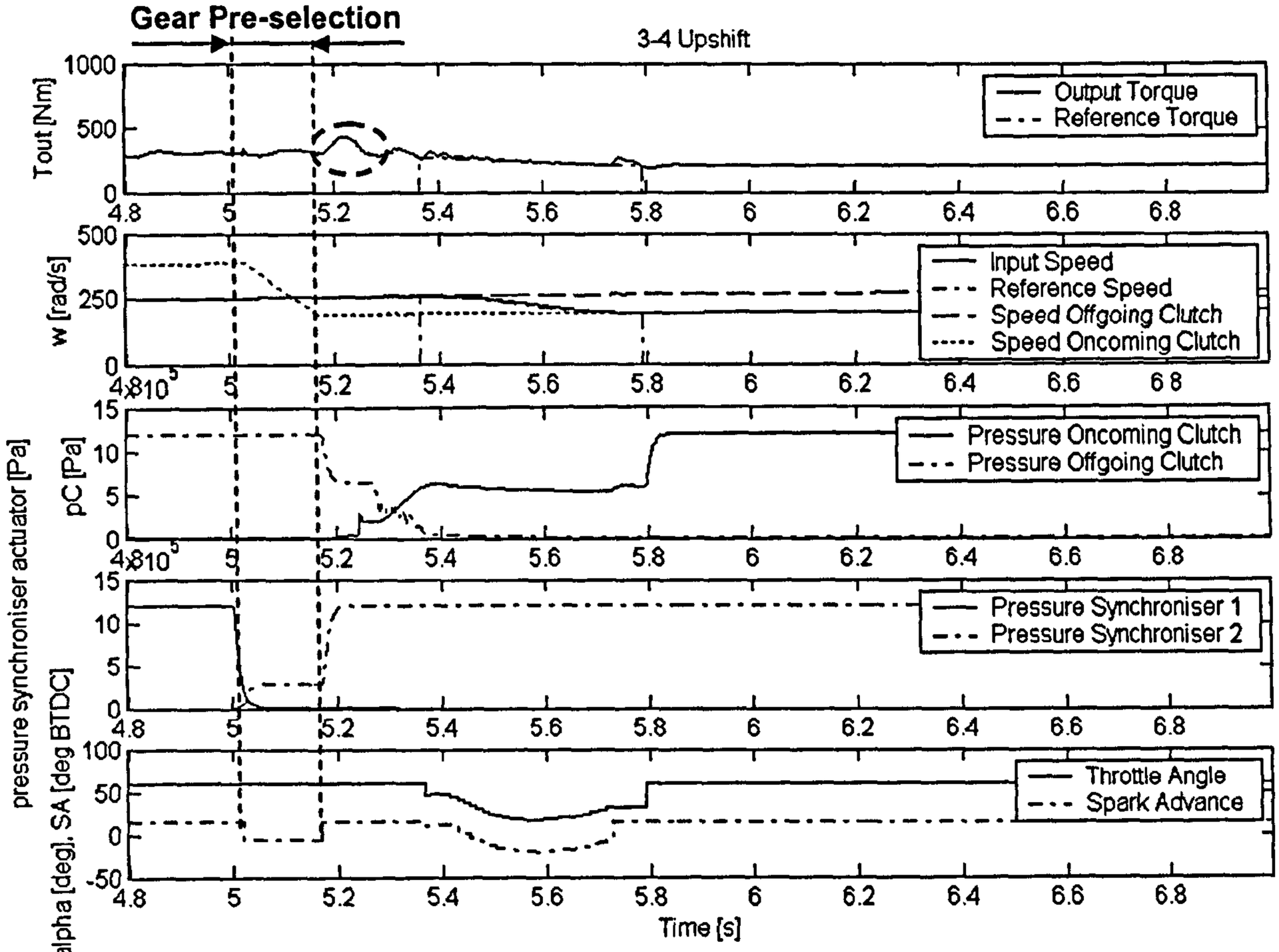

Figure 7.17 Simulation result: Power-on upshift from 3rd to 4th gear from Figure 7.5, with compensating control strategy active during gear pre-selection.

In Figure 7.17 the upshift from 3rd to 4th gear from Figure 7.5 is depicted with activated compensating control strategy. Again, the torque "hump" from the gear pre-selection is compensated effectively. Only shortly after the gear pre-selection is completed, at the beginning of the torque phase (dashed circle in Figure 7.17), the transmission output torque profile shows a small torque "hump". This small increase in transmission torque is probably due to the abrupt increase in spark advance to the original level at the end of the control phase. A dynamic loading of the drivetrain when the spark advance is abruptly raised could be responsible for the small torque increase observed in Figure 7.17. However, also the torque "hump" due to gear pre-selection becomes smaller the higher the pre-selected gear is due to the smaller effective inertia, so that this effect might not be a problem in practice. Alternatively, the reapplication of

the spark advance could be accomplished in the form of a ramp and thus the increase in engine torque would be less abrupt.

7.3.2 Compensating Control strategy for the Gear Pre-Selection on Power-On Downshifts

As explained, the gear pre-selection on a downshift requires the synchronisation of a lower gear as target gear and thus involves an acceleration of the according input shaft subsequent to the clutch-to-clutch shift. As discussed in Section 7.2.3, with conventional hydraulically actuated synchronisers, this input shaft acceleration necessitates that energy (torque) is transferred from the transmission output (i.e. driven wheels) to the synchroniser. The result of this transfer of synchronising torque is that the transmission output torque drops during gear pre-selection.

To compensate for this drop in transmission output torque, the engine torque would have to be increased during synchronisation (pre-selection) of the target gear. The only possible way of doing this is by increasing the throttle angle (or fuel amount on a diesel engine). However, such an increase in throttle angle provides only a very slow way of increasing engine torque and is thus not well suited to the short synchronisation times involved in a gear pre-selection. This means that (at least on a SI-engine) there is no direct way of compensating for the drop in transmission output torque due to gear pre-selection comparable to the concept developed in Section 7.3.1 for upshifts.

However, results from several simulations of downshifts with gear pre-selection have shown, that a dynamic loading of the drivetrain through a sudden increase in spark advance could be used to provide a small amount of fill-in torque. In order to use the dynamic effect of abruptly increasing the spark advance, the spark advance, naturally, has to be decreased beforehand. This decrease in spark advance, if applied early in the torque phase of the downshift, can be also used to reduce the increase in transmission output torque at the end of the clutch-to-clutch shift. An optimised profile for the reduction in spark advance can thus be used to smooth the transmission output torque profile, in both the torque phase and the phase where the gear pre-selection takes place. The principle of this "smoothing control strategy" is sketched in Figure 7.18 and relies solely on modulation of the spark advance.

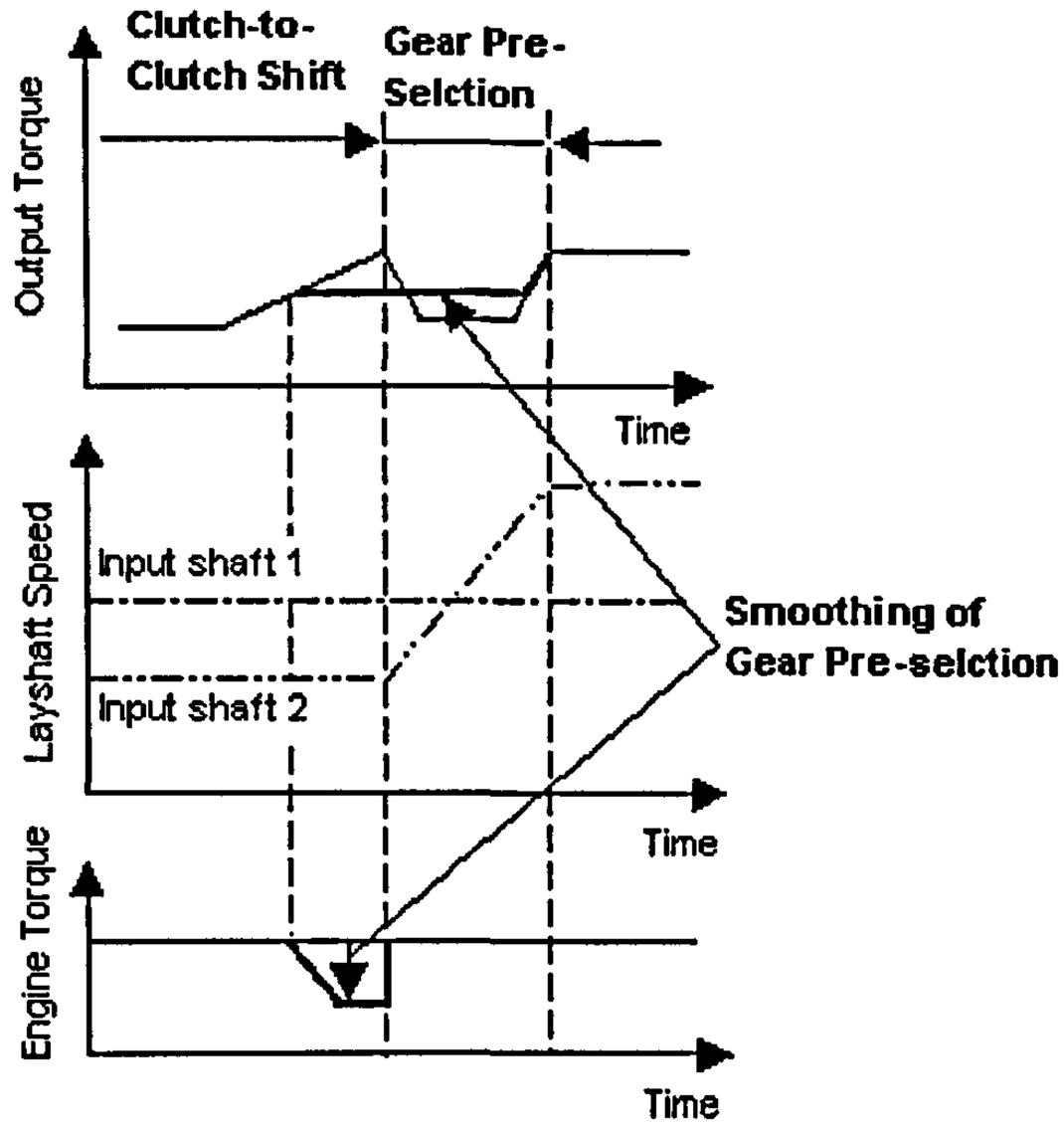

Figure 7.18 Schematic of "smoothing control strategy" by engine torque modulation and dynamic loading of the drivetrain to reduce the torque drop coming from the gear pre-selection

The "smoothing control strategy" depicted in Figure 7.18 has more the character of a qualitative solution rather than the more exact solution of the compensating control strategy introduced for power-on upshifts. Still, the proposed "smoothing control strategy", is able to improve shift quality on downshifts with gear pre-selection considerably. The concept sketched in Figure 7.18 is furthermore easy to implement since it only involves a simple request for reduction in spark advance from the transmission control unit. It is thus also well suited as an add-on solution for existing production engine/transmission control units.

The "smoothing control strategy" was applied here only to power-on downshifts, which do not make use of control of torque in the torque phase. However, it is in principle also applicable to downshifts employing a torque controller as described in Chapter 5.

To demonstrate the effectiveness of the above described solution, the proposed "smoothing control strategy" was applied first to the downshift from 3rd to 2nd gear with gear pre-selection depicted in Figure 7.8. The simulation result of the downshift with "smoothing control strategy" is depicted in Figure 7.19. The phase where the "smoothing control strategy" is applied is indicated in Figure 7.19, together with the amount of reduction in spark advance (dashed circle). The profile of the transmission output torque has become smoother during gear pre-selection when applying the "smoothing control strategy" and the drop in torque has become less severe as compared to the original downshift (Figure 7.8).

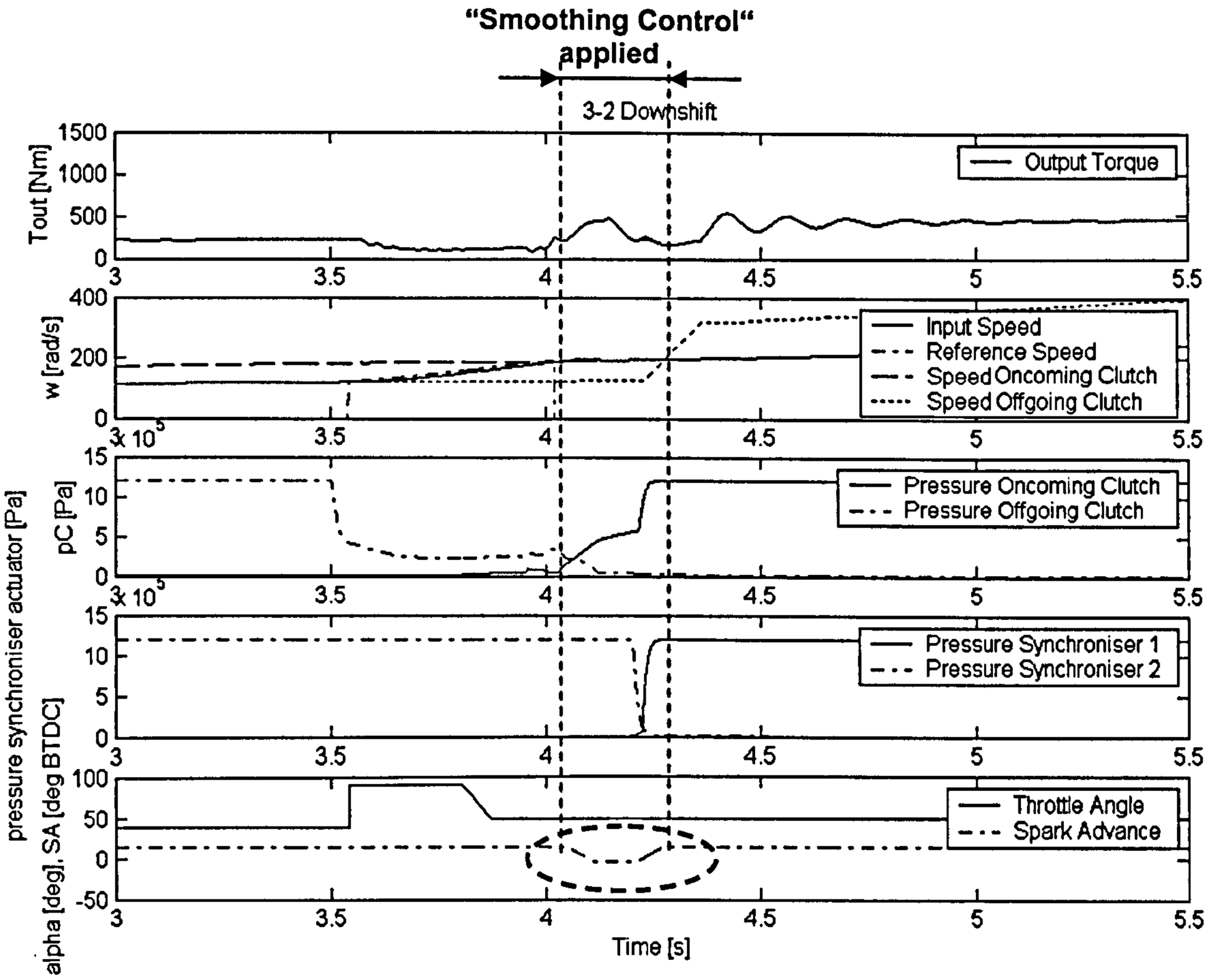

Figure 7.19 Simulation result: Power-on downshift from 3rd to 2nd from Figure 7.8, with "smoothing control strategy" applied.

The thus improved shift quality is also manifested in a much reduced vehicle jerk during the gear pre-selection. The vehicle jerk for the downshift of Figure 7.19 is depicted in Figure 7.20 and reveals that the maximum vehicle jerk in the phase of gear pre-selection is reduced from around -20 m/s^3 (Figure 7.9) to around -10 m/s^3 (see arrow in Figure 7.20) if the "smoothing control strategy" was applied. The vehicle jerk remains still quite high during the gear pre-selection having two other peaks (with positive values) in the area of $10m/s^3$. These values decrease for downshifts (and gear pre-selections) between higher gears. The peak in vehicle jerk at the end of the gear pre-selection (dashed circle in Figure 7.20) could be, in principle, also decreased by reducing spark advance for a short moment. However, this has not been investigated further here for reasons of time.

A further point that can be observed in Figure 7.19 is that the profile of the reduction in spark advance (dashed circle in Figure 7.19) looks different from the one sketched in Figure 7.18 (principle of the "smoothing control strategy"). In particular, the re-application of the spark advance is accomplished by using a ramp profile in Figure 7.19 as opposed to the abrupt increase sketched in Figure 7.18. It was observed that for the downshift in Figure 7.19 an abrupt

increase of the spark advance has lead to overshoot in the torque profile and thus slightly inferior shift quality. The amount of reduction of spark advance was also optimised to a value of around –30 deg BTDC.

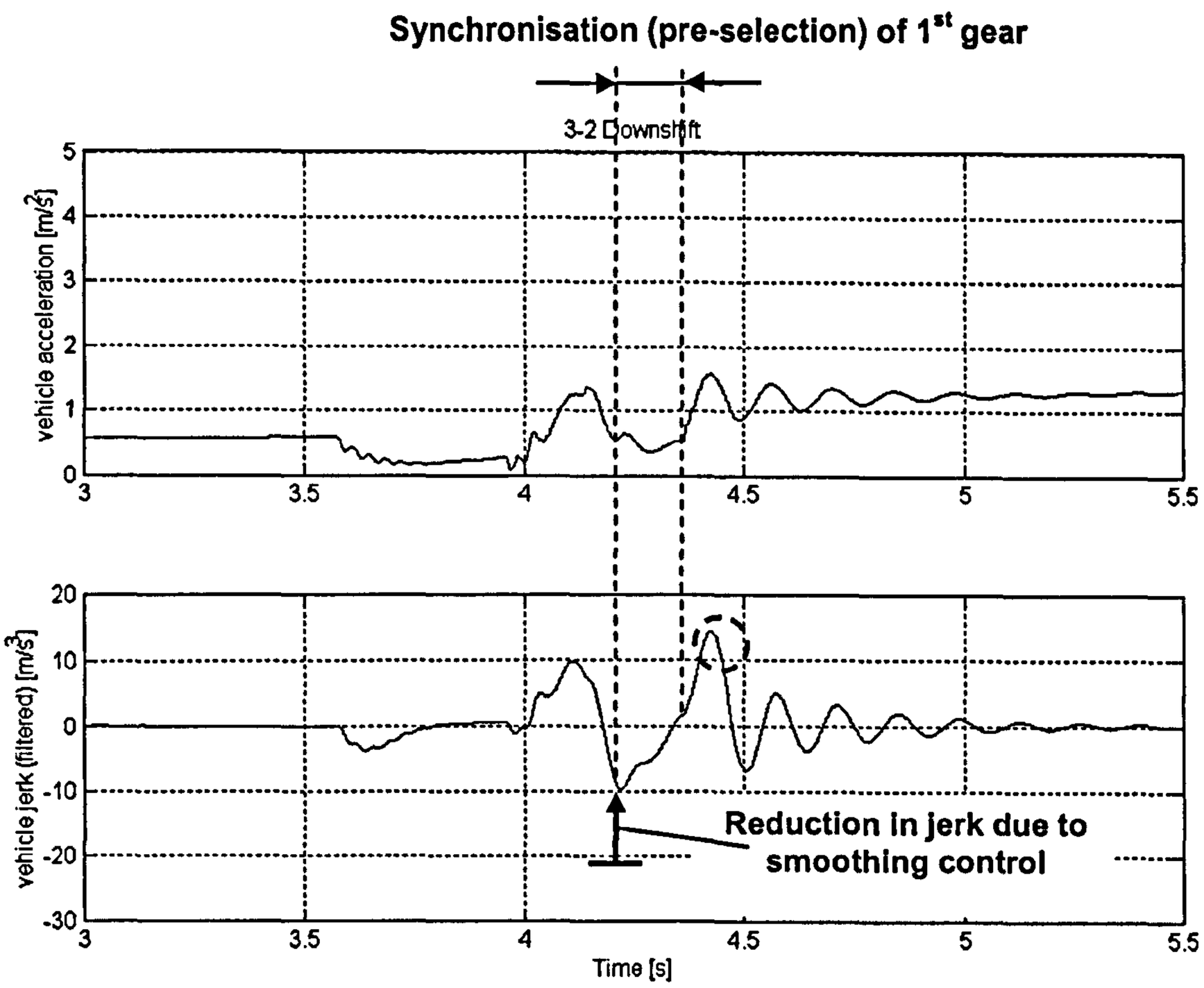

Figure 7.20 Vehicle acceleration and jerk for the downshift form Figure 7.19

That the smoothing control strategy also works for downshifts in the higher gear range, is demonstrated in Figure 7.21, which shows the downshift from 4th to 3rd gear from Figure 7.10 with activated "smoothing control strategy". Comparing the torque profiles of the 4-3 downshift with (Figure 7.21) and without (Figure 7.10) "smoothing control strategy", clearly shows that activating the proposed control strategy produces a much smoother transmission output torque profile and hence also better shift quality. The shape of the spark advance modulation in the 4-3 downshift of Figure 7.21 (dashed circle in Figure 7.21) looks like the one sketched in Figure 7.18 (principle of smoothing control strategy) and shows an abrupt increase (re-application) in spark advance at the end of the control phase. However, the amount of spark reduction was, at a value of around –30 deg BTDC, the same as in the 3-2 downshift from Figure 7.19.

The jerk levels for the downshift from 4th to 3rd gear could be reduced to a value of around 5 m/s^3 by applying the "smoothing control strategy" during gear pre-selection. However, as observed in the jerk profile of the downshift from 3rd to 2nd gear in Figure 7.19, the jerk at the end of the gear pre-selection (see dashed circle in Figure 7.20) also had a value of around 10

m/s^3 for the downshift from 4th to 3rd gear. Applying a reduction in spark advance for a second time could, as already hinted, help to decrease vehicle jerk in that area.

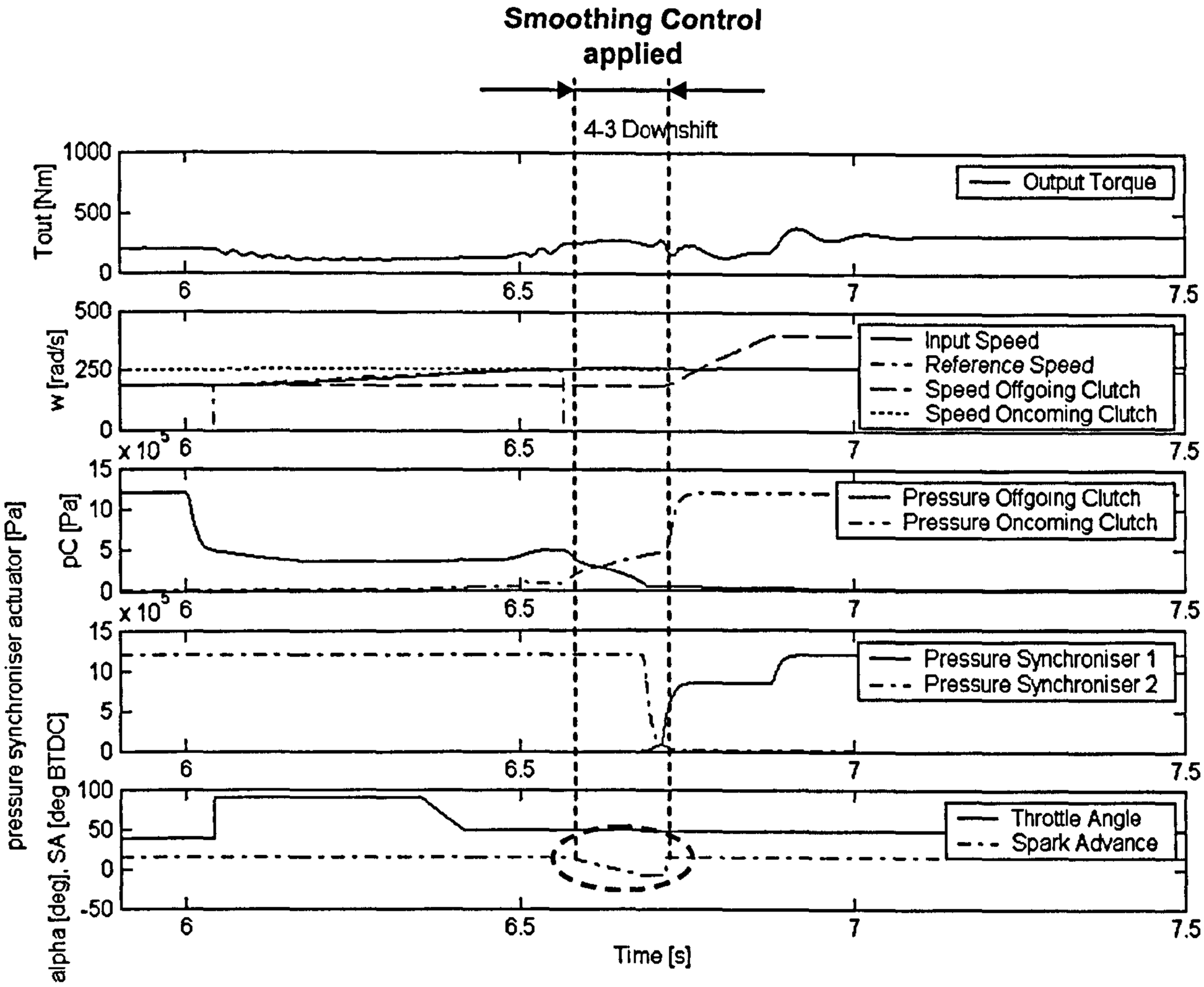

Figure 7.21 Simulation result: Power-on downshift from 4th to 3rd from Figure 7.10, with "smoothing control strategy" applied.

It was demonstrated that the effect of a dynamic loading of the drivetrain by a sudden increase in spark advance could, indeed, be used to help smoothing the transmission output torque profile during gear pre-selection. However, as could be observed in the presented simulation results of the two different downshifts, the profile of the reduction in spark advance differed for the two shifts. This indicates that it is necessary to optimise and calibrate the spark advance reduction profile for different shifts, which is a small disadvantage. However, the easy implementation of the proposed "smoothing control strategy" is definitely an advantage.

7.4 Robustness of the Control Strategies Compensating for the Gear Pre-Selection

Similar to the investigation into the robustness of the clutch-to-clutch shift control strategy developed in Chapters 4 and 5, the robustness of the two compensating control strategies proposed, in the last section (Section 7.3), for gear pre-selections on upshifts and downshifts, shall be investigated here. The stability of these control strategies with varying parameters or sensor noise is not an issue, since they are of open-loop type. Only a change in performance (shift quality) with variations in powertrain parameters due to modelling errors or variation in the engine/transmission characteristics shall be investigated here. Therefore, the robustness investigation for the compensating control strategies for gear pre-selection will only deal with a variation in the powertrain (model-) parameters and, specifically, a variation in the friction coefficient at the synchroniser. An investigation into the robustness against senor noise is of minor importance to an open-loop control strategy concept and will be therefore omitted here.

7.4.1 Robustness to Parameter Variations

The investigation into robustness of the compensating control strategies developed in Section 7.3 to parameter variations is carried out in much the same way as in Chapters 4 and 5. Also, the range of variation used for the robustness analysis here is the same as in Chapters 4 and 5 (see Table 4.2). A variation of the following parameters was assumed to be of relevance to an investigation into the robustness of the compensating control strategies:

- Engine inertia
- Reduced inertia of transmission half 1(2)
- Damping in the transmission, driveshafts and tyres
- Stiffness of driveshafts

The effects of these parameter variations on the performance of the compensating control strategies will be discussed separately for upshifts and downshifts.

Upshift:

The compensating control strategy was not affected by a change in the engine inertia to either the lower or the upper limit given in Table 4.2. Also, a change in the effective inertia in each half of the transmission to either the lower or the upper value (Table 4.2) did not seem to

deteriorate the performance of the control strategy. Furthermore, changes in drivetrain damping and driveshaft stiffness did not influence the performance of the compensating control strategy either.

These observations show that the proposed compensating control strategy can be considered as robust to changes, within reasonable limits, in the above listed parameters. The reason for this robustness, is that a change in these parameters does not directly affect the calculation of the amount of engine torque reduction as carried out by the compensating control strategy, only the synchronisation time (i.e. slope of input shaft speed trajectory) and the dynamics of the powertrain changes.

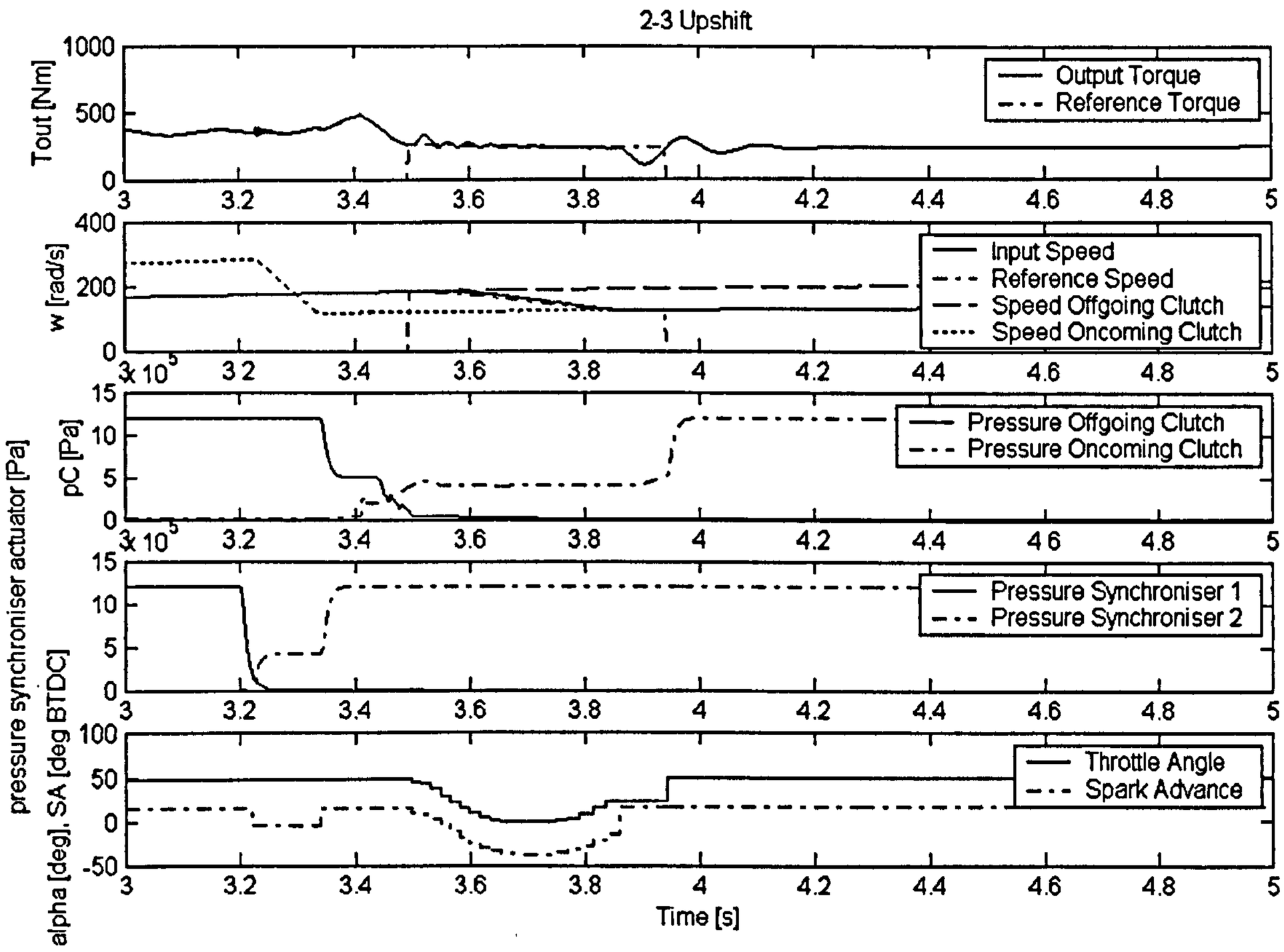

Figure 7.22 Simulation result: Power-on upshift from 2nd to 3rd gear with compensating control strategy from Figure 7.14, with engine inertia increased to 0.25 kgm^2.

An example of the results of the parameter variation is given in Figure 7.22, which shows the upshift from Figure 7.14 with activated compensating control strategy for increased engine inertia of 0.25 kgm^2 (normal value is 0.15 kgm^2). As can be observed the torque "hump" of the gear pre-selection is effectively compensated despite the larger engine inertia and thus slowed response of the engine to changes in the spark advance.

Downshift:

Since the "smoothing control strategy" developed for gear pre-selections on downshifts relies to a great extent on highly dynamic effects such as the loading and unloading of the drivetrain with engine torque, it is to be expected that changes in inertia, stiffness and damping parameters of the drivetrain ought to have a strong influence on the performance of the "smoothing control strategy". Again the above listed parameters were varied within the parameter ranges given in Table 4.2.

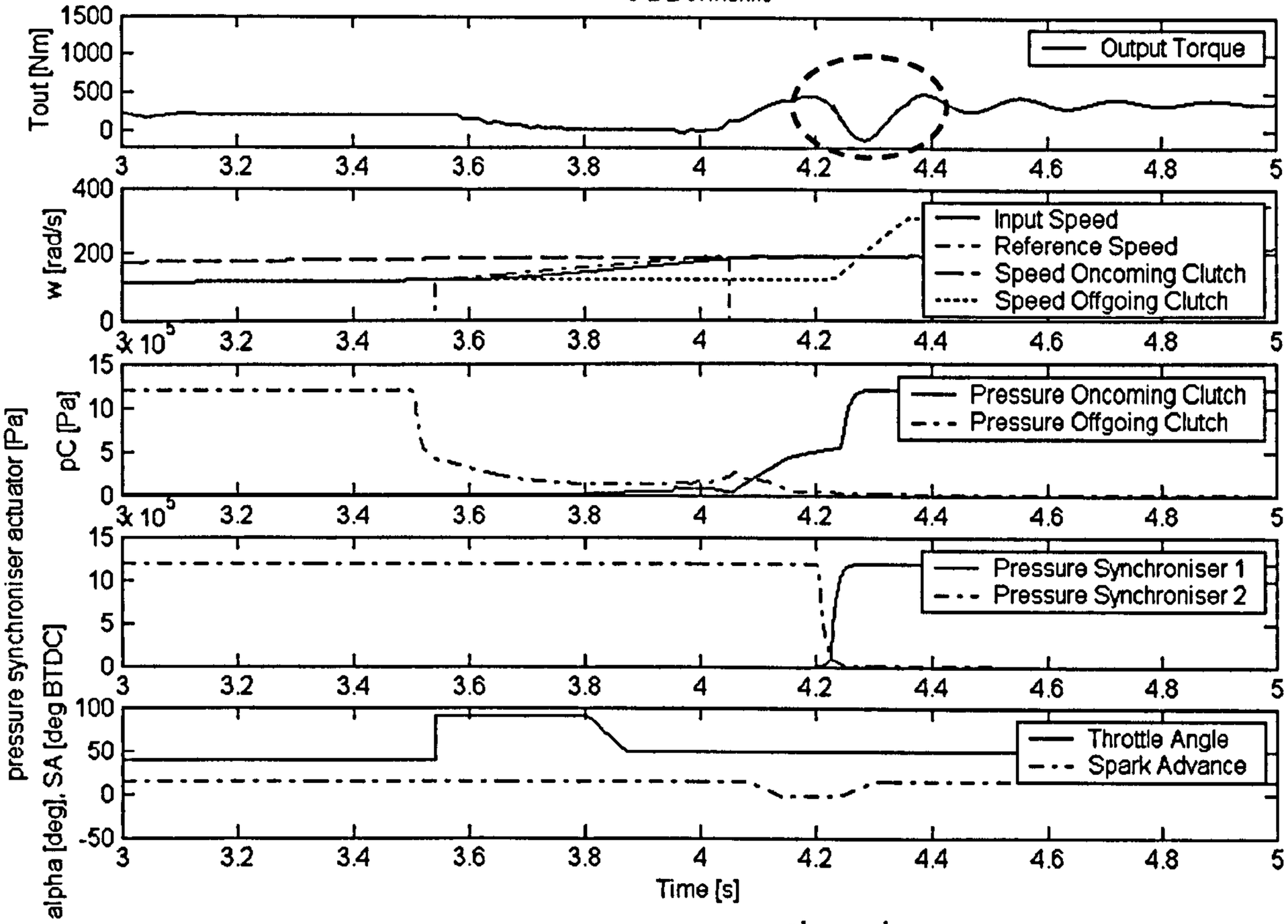

Figure 7.23 Simulation result: Power-on downshift from 3rd to 2nd gear with smoothing control strategy from Figure 7.19, with engine inertia increased to 0.25 kgm^2

A change in the stiffness of the driveshaft has lead to an even smoother transmission output torque profile in case of a decrease in stiffness. However, a change in driveshaft stiffness resulted to a slightly harsher profile in case of an increase in stiffness, as would have been expected. Still, the basic operation of the "smoothing control strategy", in reducing the torque drop (caused by the gear pre-selection) and in decreasing vehicle jerk, was still maintained, despite the variation in driveshaft stiffness. A similar behaviour was observed when changing the damping in the drivetrain. A variation in the effective inertia in the transmission halves (to the limits given in Table 4.2) did also not have any significant effect on the functioning of the "smoothing control strategy". These observations lead to the important conclusion that the

"smoothing control strategy" remains operational, although with slightly inferior performance, under a wide range of parameter variations.

Only when changing the engine inertia the performance of the "smoothing control strategy" was influenced. In particular, an increase in engine inertia resulted to a large drop (dashed circle in Figure 7.23) in transmission output torque as if the "smoothing control strategy" did not operate at all. This case is depicted in Figure 7.23, which shows the same downshift as in Figure 7.19, but with the inertia of the engine increased from 0.15 kgm^2 to 0.25 kgm^2.

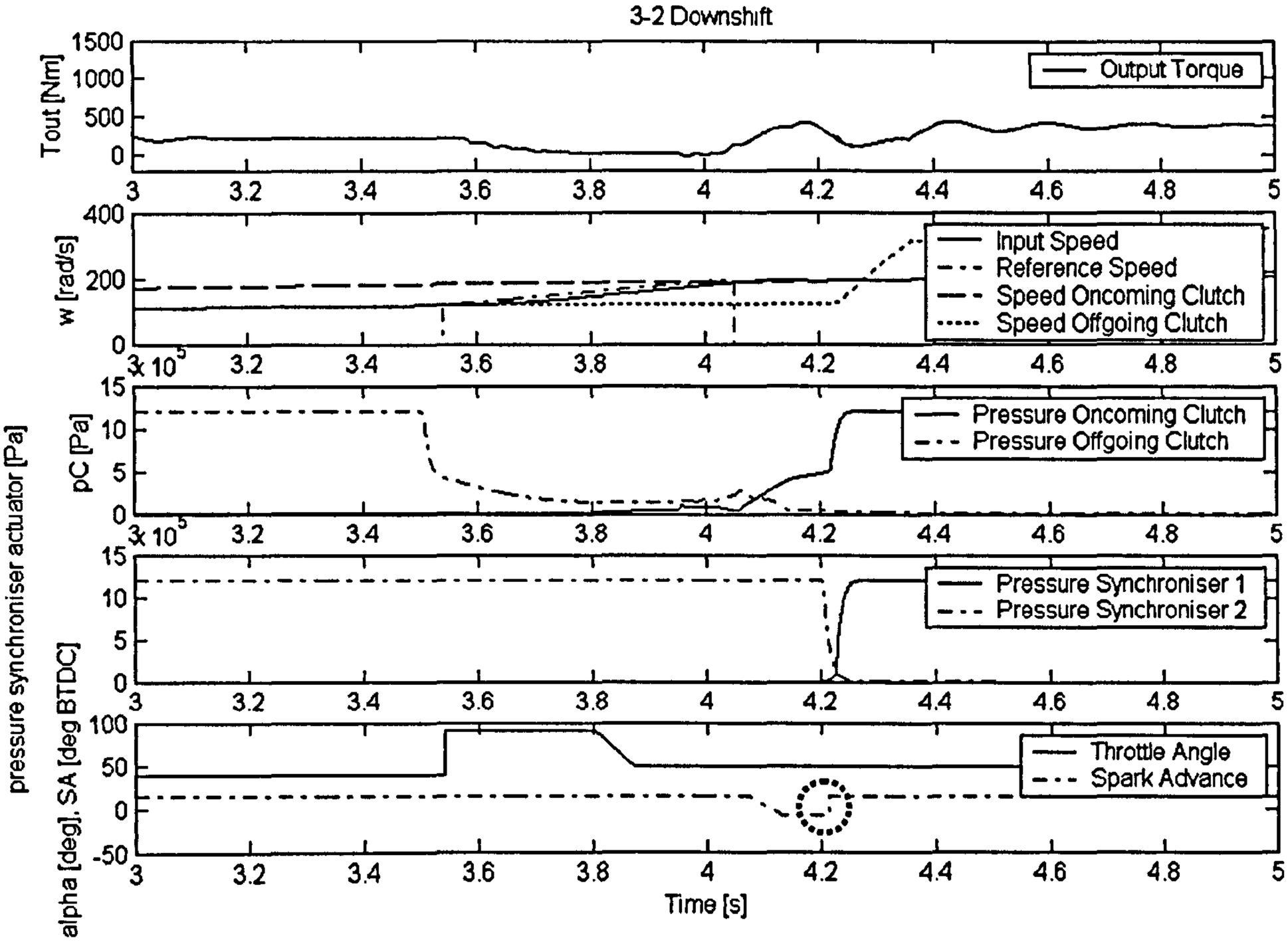

Figure 7.24 Simulation result: Power-on downshift from Figure 7.23 with engine inertia increased to 0.25 kgm^2, different profile for re-application of spark advance.

This lack of robustness of the "smoothing control strategy", with increased engine inertia, is fortunately resolved easily by altering the profile of the modulation (reduction) of spark advance. This is demonstrated in Figure 7.24, which shows the same downshift as in Figure 7.23, but with a slightly modified profile of the spark advance modulation during gear pre-selection. In particular, the drop in spark advance during gear pre-selection is larger as compared to Figure 7.23 and, very importantly, the re-application of the spark advance is abrupt (see dotted circle in Figure 7.24). This shows that by experimenting with different spark

advance modulation profiles the drop in transmission output torque due to gear pre-selection can still be effectively reduced, regardless of the choice of parameters in the powertrain.

7.4.2 Robustness to Changes in the Friction Coefficient at the Synchroniser

The robustness of the compensating control strategies developed in Section 7.3 to changes in the friction coefficient at the synchroniser shall be investigated in this subsection. In particular, a variation around the nominal value of the friction coefficient at the synchroniser (μ_s=0.12 and μ_k=0.1) as used in the powertrain model developed in Chapter 3 will be investigated.

Upshift:

An increase in the friction coefficient at the synchroniser above the nominal value (μ_s=0.12 and μ_k=0.1) results to increased synchronising torque (if actuation pressure remains unaltered). Since the control algorithm still uses the nominal value internally, the calculated value of the reduction in engine torque is too low to compensate for the increased synchronising torque as a result of the increased actual friction coefficient. Similar is true for a decrease in the friction coefficient at the synchroniser, which, because undetected by the compensating control strategy, leads to a calculated value of the reduction in engine torque that is too large.

To compensate for the error made in calculating the necessary engine torque reduction due to a change in the actual friction coefficient, a variation in the friction coefficient at the synchroniser could be detected by monitoring the slope of the input shaft speed. To implement such a speed monitoring in practice, it can be assumed that the input shaft speed changes linearly with time during a short synchronisation process (see discussion in Section 7.2.1). Thus, only a rough sampling of the rate of change of the input shaft speed at some point in time during the synchronisation process would be necessary.

Entering equation (69) in (71) and writing the resulting equation for two different friction coefficients and two different rates of change of input shaft speeds and assuming that all other variables and parameters remain unchanged, shows that when subtracting the resulting two equations the torque loss cancels out. This leads to the following simple relationship given in equation (77):

$$\Delta\mu_k = C_3 \Delta\dot{\omega}_{in} \tag{77}$$

with:

$$C_3 = -\frac{J_{S,in}\sin\alpha}{i_{1,\ldots,6}R_m(p_S A_p - F_{spring})} \tag{78}$$

Since the actuation pressure at the synchroniser (p_S) is varied in practice only in crude steps, it should be possible to establish a look up table where the constants C_3 are stored as a function of the gear ratio of the selected target gear and the actuation pressure. If a change in the rate of change of the input shaft speed is detected for a given pair of target gear and actuation pressure the change in friction coefficient could be calculated according to equation (77) with the appropriate C_3. Of course, to detect a change in the rate of change of the input shaft speed, the value under normal operation needs to be established first. This can be done by an initial calibration of the compensating control strategy.

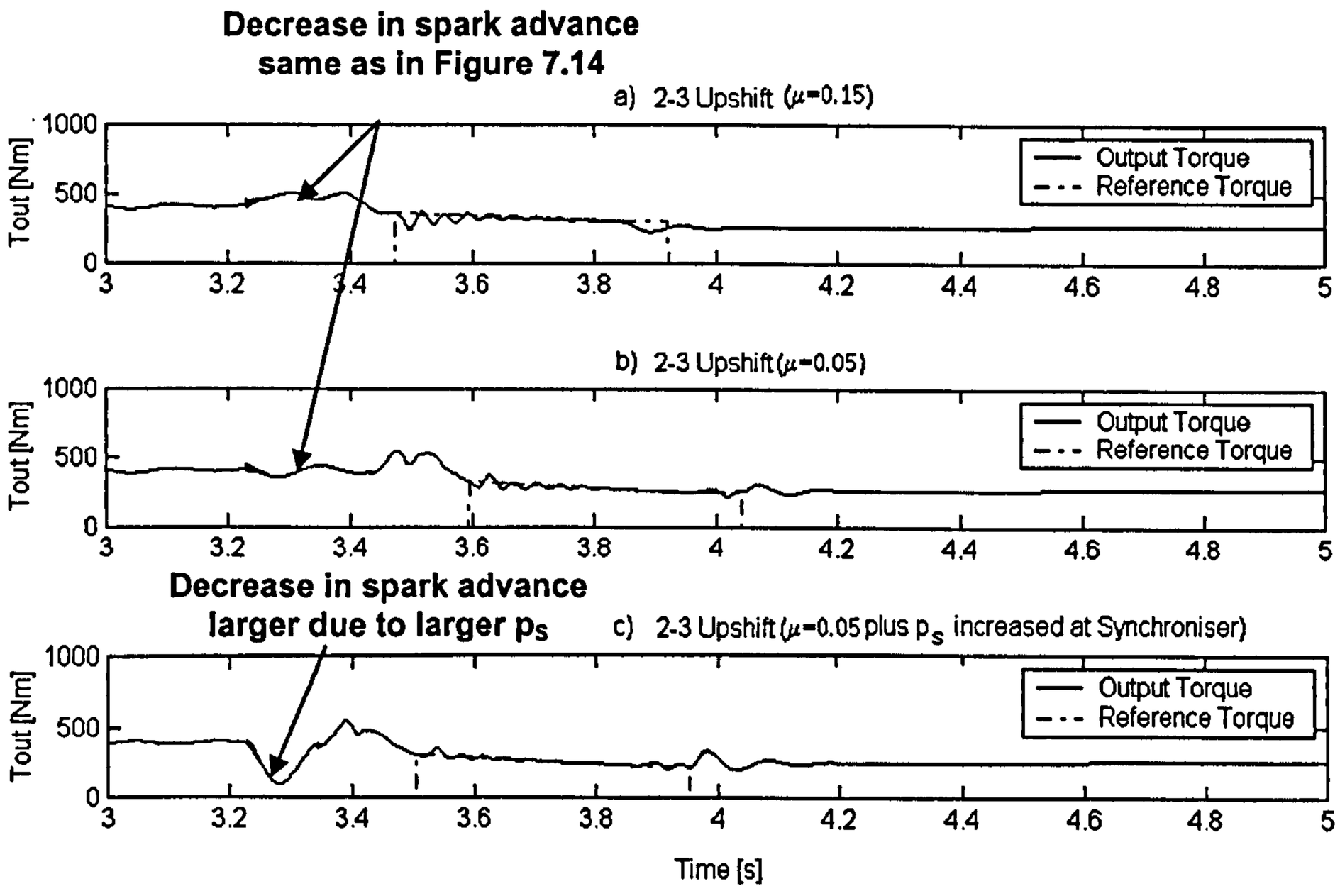

Figure 7.25 Simulation result: Power-on upshift from 2nd to 3rd gear with compensating control strategy from Figure 7.14; the actual kinetic friction coefficient at the synchroniser is changed from 0.1 to a) 0.15, b) 0.05, c) 0.05 + compensation by increased actuation pressure

Figure 7.25 shows transmission output trajectories of gearshifts from 2nd to 3rd gear with compensating control strategy active (similar to Figure 7.14); however, in Figure 7.25a) the friction coefficient at the synchroniser was increased from 0.1 (nominal value) to 0.15, in Figure 7.25b) the friction coefficient was decreased to 0.05 and in Figure 7.25c) the friction coefficient

was decreased to 0.05 plus the decrease in friction coefficient was compensate by an increase in actuation pressure to achieve the same synchronisation time as in Figure 7.14. The compensating control strategy applied in Figure 7.25 still uses the nominal friction coefficient (μ_k=0.1) internally; only the actual friction coefficient at the synchroniser was varied in Figure 7.25.

In the first two cases (Figure 7.25 a) and b)) the change in the friction coefficient at the synchroniser leads to a different synchronising torque hence also synchronising time (the actuation pressure remains unchanged). This means that, because the control strategy still uses the nominal value for the friction coefficient (μ_k= 0.1) internally, the calculation of the value for engine torque reduction and hence spark advance produces either a value that is too large or too small. Interestingly, the effect of the error in the calculated value for engine torque reduction on the transmission output torque profile seems to be quite small. The transmission output torque rises a bit in Figure 7.25a) (reduction in spark advance too small) and drops a bit in Figure 7.25b) (reduction in spark advance too large).

However, in Figure 7.25c) the additional increase in actuation pressure (to compensate for the lower friction coefficient) seems to amplify the consequence of the discrepancy between the actual friction coefficient and the one used by the control algorithm. The large drop in transmission output torque that can be observed in Figure 7.25c) (see arrow in Figure 7.25c)) can be attributed to the high actuation pressure in combination with the change in friction coefficient at the synchroniser.

These findings show that it is desirable to have some form of adaptability for the friction coefficient used by the compensating control strategy. Such an adaptive algorithm was sketched in equation (77). For the case depicted in Figure 7.25c), this means as a first step the change in the rate of change of the input shaft speed from Figure 7.13 (nominal friction coefficient) needs to be detected (around $\Delta d\omega_{in}/dt$ =710). For the current values of actuation pressure at the synchroniser (also used internally by the compensating control strategy) and gear ratio the constant C_3 can be calculated according equation (78). The two thus derived values ($\Delta d\omega_{in}/dt$ and C_3) can then be entered in equation (77) to yield the change in the friction coefficient (in case of Figure 7.25c): $\Delta\mu_k$=-0.061). The friction coefficient used by the control algorithm has to be modified accordingly. In case of Figure 7.25c) to μ_k=0.039, which is slightly lower than actual the actual μ_k=0.05 at the synchroniser. As this example has shown the corrected value of the friction coefficient might deviate from the actual value at the synchroniser (due to errors in

the values of $\Delta d\omega_{in}/dt$ and C_3), still the corrected value provides a better match as compared to the original value used by the control algorithm.

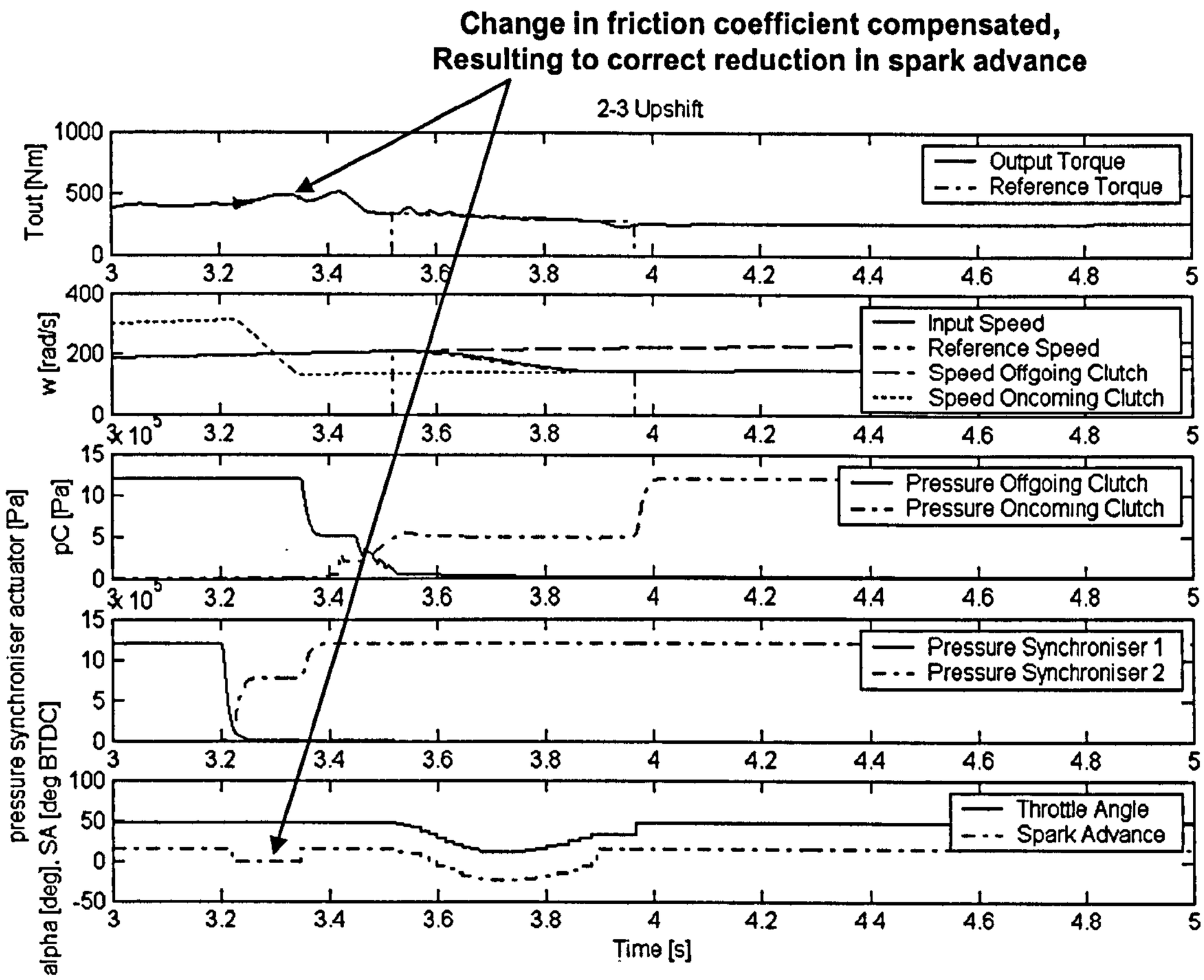

Figure 7.26 Simulation result: Power-on upshift from Figure 7.25 c) with monitoring of rate of change of input shaft speed and adaptation of friction coefficient.

Figure 7.26 shows the gearshift from Figure 7.25c), now with the control algorithm using the corrected value for the friction coefficient in (μ_k=0.039). It can be seen that although the corrected value deviates slightly from the actual value at the synchroniser, it still leads to a much better value for the reduction in spark advance thus avoiding the large drop in transmission output torque that was observed in Figure 7.25c).

Downshift:

Since the "smoothing control strategy" does not rely on an information about the friction coefficient, it itself is unaffected by a change in the friction coefficient at the synchroniser. However, an increase in the friction coefficient at the synchroniser above the nominal value has the consequence that the synchronising torque increases (if actuation pressure remains constant at the same time), the synchronisation time becomes shorter and the drop in transmission output

torque, that has to be compensated by the "smoothing control strategy", increases. For the downshift case studied in Figure 7.19, this means that the "smoothing control strategy" cannot fully compensate for effects of this thus increased synchronising torque.

A decrease in the friction coefficient below the nominal value leads to a smaller synchronising torque (if actuation pressure remains constant) and thus a longer gear pre-selection process. The drop in transmission output torque becomes smaller and the smoothing control strategy can achieve even better results.

This brief consideration shows that the smoothing control strategy works fine up to a certain synchronising torque (independent of the friction coefficient) and is not able to compensate for larger synchronising torques. For a variation in the friction coefficient at the synchroniser this means that large friction coefficients might need to be compensated by smaller actuation pressures if the synchronising torques become very large. Otherwise, the proposed smoothing control strategy becomes ineffective and a deterioration of shift quality has to be accepted.

7.5 Conclusions

In this chapter the problems of pre-selecting a gear on a twin clutch transmission with conventional synchronisers have been treated in much detail. Following from the problems identified for these gear pre-selections, novel "compensating control strategies" were developed in this chapter, to compensate for the problematic torque reactions at the transmission output that are associated with fast engagements of synchronisers.

The compensating control strategy proposed for gear pre-selections on power-on upshifts, was able to exactly compensate the torque reactions at the transmission output coming from the engagement (pre-selection) of the target gear. In the case of the power-on downshift the transmission output torque profile could be smoothed effectively to reduce vehicle jerk and thus increase shift quality. Both control strategies made use of a modulation of the engine spark advance. It was demonstrated that both compensating control strategies were sufficiently robust to variations in powertrain parameters (including friction coefficient).

The aim of this chapter and the suggested control strategies was to improve shift quality for a gear selection with conventional synchronisers. However, it was clearly pointed out that the fundamental disadvantage of using conventional synchronisers, namely the transfer of synchronising torque to the transmission output, could not be removed. To remove the

problematic transfer of synchronising torque to the transmission output entirely, either alternative synchronisation devices have to be found, or alternative gearshift strategies that synchronise the target gear during the gearshift and make use of the main clutches for this synchronisation have to be developed.

Chapter 8
Conclusions

This chapter discusses the contributions of this work to the control of gearshifts on twin clutch transmissions and examines at the end of this chapter scope for future research activities.

Conclusions of the thesis:

A mathematical model of a powertrain with a twin clutch transmission was developed in, what is believed, unprecedented detail. As an extension to existing transmission models for controller development, the dynamic model of the twin clutch transmission developed in this thesis allowed modelling of different friction characteristics by including a friction coefficient as a function of the differential speed across the clutch. This provided an important result so far not discussed in the literature in that consequence, namely, that only the dependency ("gradient") of the friction coefficient on slip speed is of relevance to the development of a gearshift controller and not the absolute value of the friction coefficient [Goetz, M. Levesley, M.C. Crolla, D.A. 2003 (Proc. Intern. Conf. on Modern Practice in Stress and Vibrations Analysis)].

Also, the internals of the twin clutch transmission were modelled in more detail (e.g. synchronisers, stiffness of shafts inside the transmission) as compared to existing transmission models used for controller development. In particular, the development and use of comprehensive models of the synchronisers (dynamics of the friction contact and the actuation) has introduced an unprecedented level of detail to the analysis of gearshifts that incorporate synchroniser-to-synchroniser shifts. Thus, gear pre-selections in gearshifts on twin clutch transmissions could be simulated and investigated in detail for the first time, which provided a solid basis for the development of an improved and realistic control strategy for the gear pre-selection.

In order to have a sufficiently accurate but simple model of the hydraulic actuation of synchronisers and clutches that can also be easily integrated in the powertrain model, a new phenomenological model of the hydraulic actuation was developed. By including this simplistic hydraulic actuation model in the transmission model and adding a comprehensive model of the engine, the dynamics (especially delays) of all actuators in the powertrain that are of importance to the development of a gearshift controller could be thus captured.

Based on this detailed powertrain model, the problems of gearshifts on twin clutch transmissions could be identified and a comprehensive and pragmatic gearshift controller could be developed that overcomes the shortcomings of existing clutch-to-clutch controllers.

It was, for the first time, clearly demonstrated (based on simulation results) that a clutch slip controller effectively mimics the operation of a one-way (i.e. freewheeler- or overrunning-) clutch [Goetz, M. Levesley, M.C. Crolla, D.A. 2003 (VDI-paper) and 2004] and is thus indispensable for clutch-to-clutch shifts on a twin clutch transmission, if the creation of a negative torque at the offgoing clutch and thus a harsh change in transmission output torque is to be avoided. A new finding was also, that the creation of a negative torque at the offgoing clutch on a power-on upshift, if not suppressed properly, can negate the improvements that an engine assisted engine speed synchronisation brings in terms of shift quality at the point of transition from torque to inertia phase.

A unique gearshift strategy was developed in this work that combines engine manipulation for a synchronisation of the engine and the control of clutch slip. The advantage of this (engine-) integrated powertrain control approach over non-integrated control concepts in terms of shift quality was clearly demonstrated in this work [Goetz, M. Levesley, M.C. Crolla, D.A. 2003 (VDI-paper) and 2004]. In particular, the specific use of throttle angle and spark advance on a SI-engine for the control of engine synchronisation on upshifts and downshifts was developed in detail. In addition, a deeper insight into the dynamics of clutch lock up was gained in this thesis and a novel form of controlling this event (on upshifts) through a quick rise in engine torque (modulation of spark advance) was proposed.

As an extension to existing clutch-to-clutch control strategies, the control of transmission output torque on power-on upshifts and downshifts, was introduced as an optional feature. For the first time it was clearly demonstrated what improvements a control of transmission output torque, could bring to the control of gearshifts, in terms of robustness to variations in the gearshift parameters and changes in the clutch friction coefficient [Goetz, M. Levesley, M.C. Crolla, D.A. 2003 (VDI paper)]. The application of the control of transmission output torque to the torque phase of a downshift, in particular in combination with a control of clutch slip [Goetz, M. Levesley, M.C. Crolla, D.A. 2004], represented an original control concept. This "dual" control strategy in the torque phase required a novel approach to enable a manipulation of the pressure at the oncoming clutch for a robust control of transmission output torque, whilst ensuring an unaffected operation of the clutch slip controller at the offgoing clutch. The benefits of this "dual" control strategy were, the ability to control the transmission output torque along a

specified reference trajectory, whilst at the same time ensuring a correct control of the transfer of engine torque.

In addition to the development of the above-described gearshift controller, a full investigation and account of the robustness of the gearshift controller in terms of shift quality and controller stability was undertaken in an unprecedented depth. It was demonstrated that the proposed gearshift controller is robust to changes in the clutch friction coefficient, changes in the parameters of the powertrain (-model) and to sensor noise coming from speed or torque sensors.

The ideas of controlling double shifts developed in [Wagner 1994] have been extended in this thesis, to incorporate control of clutch slip, the control of engine speed through engine manipulation and, as a novelty, optional control of transmission output torque [Goetz, M. Levesley, M.C. Crolla, D.A. 2005? (under review)]. It was demonstrated that the inclusion of these closed-loop control strategies could improve robustness and shift quality of double/multiple gearshifts.

The problems involved with a gear pre-selection on a twin clutch transmissions, in particular as occurring in conjunction with the use of conventional (hydraulically actuated) synchronisers, have not been treated in the literature so far and were discussed in detail in this thesis for the first time [Goetz, M. Levesley, M.C. Crolla, D.A. 2005? (under review)].

In order to compensate for the problematic torque reactions at the transmission output associated with fast engagements of synchronisers (as required for powershifts on twin clutch transmissions), a novel control strategy was developed in this work. In the case of a power-on upshift the proposed control strategy was able to compensate for the torque reactions exactly, in the case of a power-on downshift the transmission output torque profile could be smoothed successfully. Both "compensating" control strategies rely on a modulation of spark advance and showed sufficient robustness to variations in powertrain parameters.

Scope for future research activities:

- It was found that a lock up of the oncoming clutch at the end of the gearshift, in particular on downshifts, was often accompanied by torque vibrations. This is due to the difference in friction torque when the clutch transits from a state of slipping to a state of stiction. This problem could not be solved by the torque control. A successful remedy, found in this thesis for upshifts, was to abruptly raise the spark advance at the point where the clutch locks up. A similar strategy could be applied to downshifts. However, a deeper investigation into this

issue might identify whether the clutch lock up at the end of the gearshift is really a problem for shift quality and how it can be removed effectively.

- It was demonstrated, that by employing the "compensating" control strategies proposed in this thesis for gear pre-selections, the shift quality could be improved on power-on gearshifts. However, the principle disadvantage of the transfer of synchronising torque to the transmission output could not be eliminated. In order to remove this key disadvantage of synchroniser engagements and their associated torque reactions, either an alternative device for synchronisation has to be found or alternative gearshift strategies have to be devised where the main clutches are also used for a synchronisation of the target gear.

References

Abdel-Halim,N.A. Barton,D.C. Crolla,D.A. Selim,A.M. (2000) Performance of multicone synchronizers for manual transmissions, **IMechE Journal of Automobile Engineering,** 214 Part D, pp 55-65

Albers,A. Götze,T. Eibler,G. (2003) Gangablösung und Rekuperation mit umschaltbaren Freiläufen durch Drehzahlüberrollung im Parallelstranggetriebe, **VDI-Berichte,** 1786, pp 339-362

Bai,S. Moses,R.L. Schanz,T. Gorman,M.J. (2002) Development of a New Clutch-to-Clutch Shift Control Technology, **SAE Technical paper,** 2002-01-1252

Beckley,J. Kalinin,V. Lee,M. Voliansky,K. (2002) Non-Contact Torque Sensors based on SAW Resonators , **2002 IEEE International Frequency Control Symposium and PDA Exhibition,** pp 202-213

Bruni,S. Cheli,F. Resta,F. (1997) On the Identification in Time Domain of the Parameters of a Tyre Model for the Study of In-Plane Dynamics, **Vehicle System Dynamics Supplement, 27,** pp 136-150

Centea,D., Rahnejat,H. Menday,M.T.(1999) The Influence of the interface coefficient of friction upon the propensity to judder in automotive clutches, **IMechE 1999 Proc. Instn Mech Engrs Journal of Automobile Engineering,** 213 Part D, pp 245-257

Centea,D. Rahnejat,H. Menday,M.T. (2001) Non-linear multi-body dynamic analysis for the study of clutch torsional vibrations (judder), **Applied Mathematical Modelling,** 25, pp177-192

Cho,B.H. Jung,G.H. Hur,J.W. Lee,K.I. (1999) Modelling of Proportional Control Solenoid Valve for Automatic Transmission Using System Identification Theory, **SAE Technical Paper,** 1999-01-1061, pp 291-297

Cho,D. Hedrick,J.K (1989) Automotive Powertrain Modeling for Control, **ASME J. of Dynamic Systems, Measurement and Control,** 114 (4), pp 568-576

Ciesla,C.R. Jenninigs,M.J. (1995) A Modular Approach to Powertrain Modeling and Shift Quality Analysis, **SAE Technical paper,** 950419, pp 139-147

Crossley,P.R. Cook,J.A. (1991) A nonlinear Engine Model for Drivetrain System Development, **IEE Conference Publication,** 2 (332), pp 921-925

Daimler Chrysler AG (2001), Verfahren zum Schalten eines Doppelkupplungsgetriebes, **Patent DE 199 39 334 A1**

Daimler Chrysler AG (2000), Doppelkupplungs-Mehrganggetriebe, **Patent DE 199 37 716 C1**

Ercole,G. Mattiazzo,G. Mauro,S. Velardocchia,M. Amisano,F. (1999) Co-Operating Clutch and Engine Control for Servoactuated Shifting Through Fuzzy Supervisor, **SAE Technical Paper,** 1999-01-0746, pp 1-9

Flegl,H. Stelter,N. Szodfridt,I. Wuest,R. (1982) Porsche Double Clutch Transmission (PDK) - An Alternative Transmission Concept, **XIX International FISITA Congress Proceedings,** 2

Flegl,H. Wuest,R. Stelter,N. Szodfridt,I. (1987) Das Porsche- Doppelkupplungs (PDK-) Getriebe, **ATZ Automobiltechnische Zeitschrift,** 89 (9), pp 439-452

Förster, J. (1991) **Automatische Fahrzeuggetriebe,** Springer Verlag

Franke,R. (1999) Das Automatische Doppelkupplungsgetriebe für sechs oder acht lastfrei, ohne Antriebsunterbrechung und ohne Verspannung schaltbare Gänge, **ATZ Automobiltechnische Zeitschrift,** 101 (5), pp 350-357

Fredriksson,J. Egardt,B. (2000) Nonlinear Control applied to Gearshifting in Automated Manual Transmissions, **Proc. of the IEEE Conference on Decision and Control v1 (2000) Sydney, Australia Dec.,** pp 444-449

Furukawa,H. Hagiwara,K. Fujita,M. Uchida,K. (1994) Robust Control of an Automatic Transmission System for Passenger Vehicles, **Proc. Of the Third IEEE Conference on Control Applications,** pp 397-402

Gaillard,C.L. Singh,R.(2000), Dynamic analysis of automotive clutch dampers, **Applied Acoustics,** 60, pp 399-424

Gebert,J. Kücükay,F. (1997) Schaltkomfort als neue Regelgroesse bei PKW-Automatikgetrieben, **Symposium Steuerungssysteme fuer den Antriebstrang von Kraftfahrzeugen TU Berlin ISS fahrzeugtechnik** , pp 2-14,

Geering,H.P. Schmid,A. (1995) Optimal geregelte Schaltvorgaenge eines Automatik-Getriebes, **VDI Berichte,** Nr. 1175, pp 241-263

Gillespie,T. (1992) **Fundamentals of Vehicle Dynamics,** Society of Automotive Engineers, Warrendale, PA

Goetz,M. Levesley,M.C. Crolla,D.A. (2003) Dynamic Modelling of a Twin Clutch Transmission for Controller Design, **Proceedings of the 5th International Conference on Modern Practice in Stress and Vibrations Analysis, Glasgow, Scotland, 9-11- September 2003, Material Science Forum,** Vols 440-441, pp 253-260

Goetz,M. Levesley,M.C. Crolla,D.A. (2003) A Gearshift Controller for Twin Clutch Transmissions, **VDI-Berichte,** Nr. 1786, pp 381-400

Goetz,M. Levesley,M.C. Crolla,D.A. (2004) Integrated Powertrain Control of Gearshifts on Twin Clutch Transmissions, **SAE Technical paper,** 2004-01-1637

Goetz,M. Levesley,M.C. Crolla,D.A. (2005?) Dynamics and Control of Gearshifts on Twin Clutch Transmissions, **IMechE 2005? Proc. Instn Mech Engrs Journal of Automobile Engineering,** Part D – currently under review

Großpietsch,W. Sudau,J. (2000) Doppelkupplung für lastschaltbare Getriebe - ein altes Schaltelement mit neuer Zukunft ?,**VDI Berichte,** 1565, pp 259-273

HaessigJr.,D.A. Friedland,B. (1991) On the Modelling and Simulation of Friction, **Journal of Dynamic Systems, Measurement and Control,** vol 113, pp 354-362

Hahn,J.O. Hur,J.W. Cho,Y.M. Lee,K.I. (2001) Robust Observer-Based Monitoring of a Hydraulic Actuator in a Vehicle Power Transmission Control System, **Proceedings of the 40th IEEE/ Conference on Decision and Control, Orlando, Florida, USA,** pp 522-528

Haj-Fraj,A. Pfeiffer,F. (2000) Optimization of Gear Shift Operations in Automatic Transmissions, **International Workshop on Advanced Motion Control, AMC (2000)** pp 469-473

Haj-Fraj,A. Pfeiffer,F. (2001) Optimal control of gear shift operations in automatic transmissions, **Journal of the Franklin Institute** 338, pp 371-390

Haj-Fraj,A. Pfeiffer,F. (2002) A model based approach for the optimization of gearshifting in automatic transmissions, **Int. J. of Vehicle Design,** Vol. 28, Nos. 1/2/3, pp 171-188

Hendricks,E. (1997) Engine Modeling for Control Applications: A critical survey, **Meccanica,** 32, pp 387-396

Höhn,B.R. Pflaum,H. Mosbach,C. (2003) Methodik zur Beurteilung des Schmierstoff-einflusses auf das Reibschwingverhalten nasslaufender Kupplungen, **VDI-Berichte,** 1786, pp 455-468

Hojo,Y. Iwatsuki,K. Oba,H. Ishikawa,K. (1992) Toyota Five-Speed Automatic Transmission with Application of Modern Control Theory, **SAE Technical Paper,** 920610, pp 25-36

Holgerson,M. Lundberg, J. (1999) Engagement behaviour of a paper-based wet clutch Part1: influence of drive torque, **IMechE Journal of Automobile Engineering,** 213 Part D, pp 341-348

Holgerson,M. Lundberg,J. (1999) Engagement behaviour of a paper-based wet clutch Part2: influence of temperature, IMechE **Journal of Automobile Engineering,** 213 Part D, pp 449-455

Hong,K-S. Yang,K-J. Lee,K-I. (1999) Object-Oriented Modeling for Gasoline Engine and Automatic Transmission Systems, **Computer Applications in Engineering Education,** 7 (2), pp107-119

Ibamoto,M. Uchida,M. Kuroiwa,H. Minowa,T. Sato,K. (1997) Transitional control of gear shift using estimation methods of drive torque without a turbine speed sensor, **JSAE Review,** 18, pp 71-73

Jiang,J. Ulbrich,H. (2001), Derivation of coefficient of friction at high sliding speeds from energy conservation over the frictional interface, **Wear,** 247, pp 66-75

Jacobson,B. (2000) Outline of a new control concept for power shifting of fixed step ratio automotive transmissions, **IMechE 2001 Proc Instn Mech Engrs Journal of Automobilr Engineering,** 215 PartD, pp 613-624

Kégresse (1939) Zahnräderwechselgetriebe für Kraftfahrzeuge, **Patent DE 894 204**

Kim,Y.H. Yang,J. Lee,J.M. (1994) A Study on the Transient Characteristics of Automatic Transmission with Detailed Dynamic Modeling, **SAE Technical Paper,** 941014,pp 173-182

Klages,B. Woermann,R. Theurkauf,H. (1997) An Improved Real Time Model of a Planetary Gear Train, **SAE Technical Paper,** 970970, pp 113-120

Kwon,B. Kim,H. (2000) Dynamic Analysis of Shift Quality for Clutch-to-Clutch Controlled Automatic Transmission, **KSME International Journal,** 14 (12), pp 1348-1357

Löffler,J. (2000) Optimierungsverfahren zur adaptiven Steuerung von Fahrzeugantrieben, **PhD Universität Stuttgart**

Lorenz,K. Hofmann,R. Hoennebeck,K. (1988) Interactive Engine and Transmission Control, **International Congress on Transportation Electronics, Convergence 88,** pp 25-31

Meinhard,R. Berger,R. (2003) Doppelkupplungen für die Automatgetriebe von morgen, **VDI-Berichte,** 1786, pp 319-337

Minowa,T. Kimura,H. Ishii,J. Morinaga,S. Shiraishi,T. Ozaki,N. (1994) Smooth Gear Shift Control System Using Estimated Torque, **SAE Technical paper,** 941013, pp 165-171

Minowa,T. Kurata,K. Kuroiwa,H. Ibamoto,M. Shida,M. (1996) Smooth Torque Control System Using Differential Value of Shaft Speed, **SAE Technical paper,** 960431,pp 107-113

Minowa,T. Ochi,T. Kuroiwa,H. Liu K-Z. (1999) Smooth Gear Shift Control Technology for Clutch-to-Clutch Shifting, **SAE Technical paper,** 1999-01-1054, pp 1-6

Mitschke,M. (1972) **Dynamik der Kraftfahrzeuge,** Springer Verlag

Moskwa,J.J. Hedrick,J.K. (1990) Nonlinear Algorithms for Automotive Engine Control, **IEEE Control Systems Magazine,** 10 (3), pp 88-93

Moskwa,J.J. Hedrick,J.K. (1992) Modeling and validation of automotive engines for control algorithm development, **Transaction of ASME J. of Dynamic System, Measurement and Control,** 114, pp 228-285

Moskwa,J.J. (1993) Sliding Mode Control of Automotive Engines, **Journal of Dynamic Systems, Measurement and Control,** 115, pp 687-693

Moskwa,J.J. Pan,C.H. (1995) Engine Load Torque Estimation using Nonlinear Observers, **Proceedings of the 34th Conference on Decision & Control, New Orleans,** pp 3397-3402

Moskwa,J.J. Munns,S.A. Zachary,J.R. (1997) The Development of Vehicular Powertrain System Modeling methodologies: Philosophy and Implementation, **SAE Technical paper,** 971089, pp 1-9

Narumi,N. Suzuki,H. Sakakiyama,R. (1990) Trends of Powertrain Control, **Proc. of the International Congress on Transportation Electronics,** pp 313-323

Naruse,T. Nakashima,Y. Murayama,Y. Akiyoshi,Y. Kurachi,T. (1993) A study on Evaluation Method and Improvement of Shift Quality of Automatic Transmission, **SAE Technical paper** 930673, pp 93-97

Ogata,K. (1997) **Modern Control Engineering,** Prentice Hall International Inc.

O'Neil,A. Harrison,A. (2000) Robotized powershift AMTs, **Ricardo International Conference 2000,** pp 217-230

OpdeBeck,P. Stelter,N. Bofinger,B. (1983) Elektronische Regelung eines Doppel-kupplungsgetriebes, **VDI-Berichte,** Nr. 466, pp101-108

Pan,C.H. Moskwa, J.J. (1995) Dynamic Modeling and Simulation of the Ford AOD Automobile Transmission, **SAE Technical paper,** 950899, 153 –162

Pankiewicz,E. Schuller,J. (2002) Equations of motion for one-dimensional structure variable multibody systems in mechatronic real time applications, **Int. Journal of Vehicle Design,** vol 28, Nos. 1/2/3; pp 68-83

Petterson,M. Nielsen,L. (2000) Gear Shifting by Engine Control, **IEEE Transactions on Control Systems Technology,** 8 (3), pp 495-507

Pfeiffer,F. Glocker,C. (2000) **Multibody Dynamics with Unilateral Contacts,** Springer Wien New York

Powell,B.K. Bailey,K.E. Cikanek S.R. (1998) Dynamic Modeling and Control of Hybrid Electric Vehicle Powertrain Systems, **IEEE Control Systems Magazine,** 18 (5), pp 17-33

Quinn,S. Lyons,V. (1998) Drivetrain System Design in Simulink® and Stateflow™, **AVEC 98,** pp 147-152

Rabeih,E.M.A. Crolla,D.A. (1996) Intelligent control of clutch judder and shunt phenomena in vehicle drivelines, **Int. Journal of Vehicle Design,** 17 (3), pp 318-332

Rinderknecht,S. Rühle;G. Seufert,M. Nageleisen,F. (2002) Automated Manual Transmission (AMT) of second generation with extremely reduced shift times, **www.getrag.de/publikationen**

Rudolph,F. Steinberg,I. Günter,F. (2003) Die Doppelkupplung des Direktschaltgetriebes DSG® der Volkswagen AG, **VDI-Berichte,** 1786, pp 401-411

Ruser,H. Tröltzsch,U. Horn,M. (2002) Low-cost magnetic torque sensor principle, **Sensors 2002, Proceedings of IEEE,** Vol. 2, pp 901-904

Sanada,K. Kitagawa,A. (1998) A study of two-degree-of-freedom control of rotating speed in an automatic transmission, considering modeling errors of a hydraulic system, **Control Engineering Practice,** 6, pp 1125-1132

Sawamura,K. Saito,Y. Kuroda,S. Katoh,A. (1998) Development of an integrated powertrain control system with an electronically controlled throttle, **JSAE Review,** 19, pp 39-48

Schmid,A. (1994) **Optimale Regelung für Systeme mit variabler Struktur,** Eidgenoessische Technische Hochschule Zürich, PhD, 1994

Schreiber,U. Schindler,J (2001) Simulation kompletter KFZ-Antriebstränge, **ATZ Automobiltechnische Zeitschrift,** 103 (6), pp 532-539

Schwab,L. (1994) Development of a Shift Quality Metric for an Automatic Transmission, **SAE Technical paper,** 941009, pp 139-144

Schwab,M. (1990) Electronically-Controlled Transmission Systems- Current Position and Future Developments, **SAE Technical paper,** 901156, pp 335-342

Scott,W. Suntiwattana,P. (1995) Effect of oil additives on the performance of a wet friction clutch material, **Wear,** 181-183, pp 850-855

Shin,B.K. Hahn,J.O. Lee,K.I. (2000) Development of Shift Control Algorithm Using Estimated Turbine Torque, **SAE Technical paper,** 2000-01-1150, pp1-7

Song,J.-B. Byun,K.-S. (1999) Throttle Actuator Control System for Vehicle Traction Control, **Mechatronics,** 9, pp 477-495

Szadkowski,A. (1991) Shiftability and Shift Quality Issues in Clutch-Transmission Systems, **SAE Technical Paper,** 912697, pp 618-628

Szadkowski,A. McNerney, G.J. (1993) Engineering Method for Rating Shift Quality, **SAE Technical Paper,** 932996, pp 842-847

The Math Works (1998) **Using Simulink and Stateflow in Automotive Applications,** Natick, MA, 1998

Turner,J.D. (1988) Development of a rotating-shaft torque sensor for automotive applications, **IEE Proceedings,** Part D, Vol. 135, No. 5, pp 334-338

Vaughan,N.D. Gamble,J.B. (1996) The Modelling and Simulation of a Proportional Solenoid Valve, **Journal of Dynamic Systems, Measurement and Control,** Vol. 118, No.1, pp 120-125

Veehof,D.A. (1996) **Simulation Doppelkupplungsgetriebe,** Studienarbeit

Volkswagen AG (1998) Verfahren zum Schalten eines Doppelkupplungsgetriebes und Doppelkupplungsgetriebe mit Synchronisiereinrichtung, **Patent DE 196 31 983 C1**

Volkswagen AG (1998) , Verfahren zum Schalten eines Doppelkupplungsgetriebes und Doppelkupplungsgetriebe, **Patent DE 197 11 820 A1**

Wagner,G. (1994) Doppelschaltungen bei Doppelkupplungsgetrieben,**VDI-Berichte,** Nr. 1170, pp 119-135

Wang,Y. Kraska,M. Ortmann,W. (2001) Dynamic Modeling of a Variable Force Solenoid and a Clutch for Hydraulic Control in Vehicle Transmission Systems, **Proceedings of the American Control Conference, Arlington, 2001,** pp 1789-1793

Watechagit,S. Srinivasan,K. (2003) Modeling and Simulation of a Shift hydraulic System for a Stepped Automatic Transmission, **SAE Technical Paper,** 2003-01-0314

Webster,H. (1981) A Fully Automatic Vehicle Transmission Using a Lay shaft Type Gearbox, **SAE Technical Paper,** 810104,

Weeks,R.W. Moskwa,J.J. (1995) Automotive Engine Modeling for Real-Time Control using MATLAB/SIMULINK, **SAE Technical paper,** 950417, pp 123-137

Wheals,J. Harrison,A. Turner,W. Behrenroth,J. (2001) Integrated Powertrain Control Applied to AMT Designs for Improved Shift Quality, Efficiency and other Characteristics Using Novel Hardware and Sensors, **VDI-Berichte,** 1610, pp 379-416

Wheals,J.C. Crewe,C. Ramsbottom,M. Rook,S. Westby,M. (2002) Automated Manual Transmissions- A European Survey and Proposed Quality Shift Metrics, **SAE Technical Paper,** 2002-01-0929

Willumeit,H.-P. Park,B.Y. (1998) **Modelle und Modellierungsverfahren in der Fahrzeugdynamik**, B.G. Teubner Stuttgart Leibzig

Wouters,M. (1991) A New Method to Calculate Energy Dissipation and Temperature Distribution in Multidisc Clutches in Powershift Transmissions, **SAE Technical Paper,** 911882, pp 387-394

www.raybestos.de/english/produkte/kupplungen/material.html

Yang,Y. Lam,R. C. Fujii,T. (1998) Prediction of Torque Response During the Engagement of Wet Friction Clutch, **SAE Technical paper,** 981097,pp 233-242

Yang,Y. Lam,R.C. (1998) Theoretical and experimental studies on the interface phenomena during the engagement of automatic transmission clutch, **Tribology Letters,** 5, pp 57-67

Yi,K. Shin,B.-K. Lee,K.-I. (2000) Estimation of Turbine Torque of Automatic Transmissions Using Nonlinear Observers, **Transactions of ASME 122 June 2000 Dynamic Systems and Control,** pp 276-283

Yoon,A. Khargonekar,P. Hebbale,K. (1999) Randomized Algorithms for Open-Loop Control of Clutch-to-Clutch Transmissions, **ASME Journal of Dynamic Systems, Measurement and Control,**121,pp 508-517

Zegelaar,P.W.A. Pacejka,H.B. (1997) Dynamic Tyre Responses to Brake Torque Variations, **Vehicle System Dynamics Supplement,** 27, pp 65-79

Zheng,Q. Srinivasan,K. Rizzoni,G. (1998) Dynamic Modeling and Characterization of Transmission Response for Controller Design, **SAE Technical paper,** 981094,pp 193-203

Zheng,Q. Srinivasan,K. Rizzoni,G. (1999) Transmission shift controller design based on a dynamic model of transmission response, **Control Engineering Practice** 7, pp 1007-1014

Zhong,Z. Xiang,C. Zheng,M. (1999) Drivetrain Modeling and Model Analysis for Real-Time Application, **Proc. of the IEEE International Vehicle Electronics Conference (IVEC '99),** pp 298-304

Appendix

A.1 Equations of the Engine Torque Production Model (taken from [Crossley and Cook 1991])

Throttle Body

The assumption for the throttle body model is that the flow of air through it is a one-dimensional steady compressible flow of ideal gas.

$$\dot{m}_{ai} = f(\theta)g(p_m) \tag{A.1}$$

With:

$$f(\theta) = 2.821 - 0.05231\theta + 0.10299\theta^2 - 0.00063\theta^3 \tag{A.2}$$

$$g(p_m) = 1, p_m \le \frac{p_0}{2} \tag{A.3a}$$

$$g(p_m) = \frac{2}{p_0}\sqrt{p_m p_0 - p_m^2}, p_m > \frac{p_0}{2} \tag{A.3b}$$

Intake Manifold Dynamics

$$\dot{p}_m = \frac{RT}{V_m}(\dot{m}_{ai} - \dot{m}_{ao}) \tag{A.4}$$

$$\dot{m}_{ao} = -0.366 + 0.08979\omega_e p_m - 0.0337\omega_e p_m^2 + 0.0001\omega_e^2 p_m \tag{A.5}$$

To determine the total mass rate that is pumped into the cylinder (m_a), equations A.1- A.5 have to be solved iteratively and the mass flow rate out of the intake manifold has to be integrated over each intake stroke event (180° of crankshaft rotation).

Compression Stroke

To account for the compression of the air/fuel mixture after the intake stroke, the combustion and therefore the torque production is delayed by 180° of crankshaft rotation.

Engine Torque Generation

$$T_{ind} = -181.3 + 379.36m_a + 21.91\frac{A}{F} - 0.85\left(\frac{A}{F}\right)^2 + 0.26\sigma - 0.0028\sigma^2 + \\ + 0.027\omega_e - 0.000107\omega_e^2 + 0.00048\omega_e\sigma + 2.55\sigma m_a - 0.05\sigma^2 m_a \quad \text{(A.6)}$$

A.2 Equations of Motion of Transmission Half 2

Clutch 2

Clutch 2 in a state of slipping:

Torque balance at mass inertia $J_{C2,in}$

$$J_{C2,in}\dot{\omega}_{c2} = T_{k12} - T_{C2} - c_{C2,in}\omega_{c2} \quad \text{(A.7)}$$

Torque balance at mass inertia $J_{C2,out}$

$$J_{C2,out}\dot{\omega}_{c2o} = T_{C2} - T_{kIn2} - c_{C2,out}\omega_{c2o} \quad \text{(A.8)}$$

$$T_{C2} = \mathrm{sgn}(\omega_{c2} - \omega_{c2o})R_m F_{N2}\mu_k z \quad \text{(A.9)}$$

Clutch 2 in the "engaged" state

$$\omega_{c2} = \omega_{c2o} = \omega \quad \text{(A.10)}$$

$$(J_{C2,in} + J_{C2,out})\dot{\omega} = T_{k12} - T_{kIn2} - (c_{C2,in} + c_{C2,out})\omega \quad \text{(A.11)}$$

$$T_{C2,engaged} = \frac{J_{C2,out}(T_{k12} - c_{C2,in}\omega) + J_{C2,in}(T_{kIn2} + c_{C2,out}\omega)}{J_{C2,in} + J_{C2,out}} \quad \text{(A.12)}$$

The conditions for transition can be stated for clutch 2 in the same way as for clutch 1

- *Clutch 2 engaged*:

IF $\{-\mu_s R_m F_{N2} z \le T_{C2,engaged} \le \mu_s R_m F_{N2} z\}$ AND $\{\omega_{c2} = \omega_{c2o}\}$ THEN {Clutch Engaged}

(Or stated differently: (A.13)

IF $\{|T_{C2,engaged}| \le \mu_s R_m F_{N2} z\}$ AND $\{\omega_{c2} = \omega_{c2o}\}$ THEN {Clutch Engaged})

- *Clutch 2 slipping:*

IF $\{|T_{C2,engaged}| > \mu_s R_m F_{N2} z\}$ THEN {Clutch Slipping} (A.14)

Inputshaft 2

$$T_{kIn2} = k_{In2}(\varphi_{c2o} - \varphi_{In2}) + c_{In2}(\omega_{c2o} - \omega_{In2}) \quad \text{(A.15)}$$

k_{In2} = f(gear=2,4,6), c_{In2} = f(gear=2,4,6)

Transmission Half 2: Gearing and Synchroniser of 2nd, 4th and 6th Gear

$$J_{eff,In2} = J_{gear7} + J_{gear9} + J_{gear11} + J_{gear8}\left(\frac{1}{i_2}\right)^2 + J_{gear10}\left(\frac{1}{i_4}\right)^2 + J_{gear12}\left(\frac{1}{i_6}\right)^2 \quad \text{(A.16)}$$

$$J_{S2,in} = J_{eff,In2} \cdot i_{2,4,6}^2 \quad \text{(A.17)}$$

$$i_{2,4,6} = \frac{\omega_{In2}}{\omega_{gear8,10,12}} \quad \text{(A.18)}$$

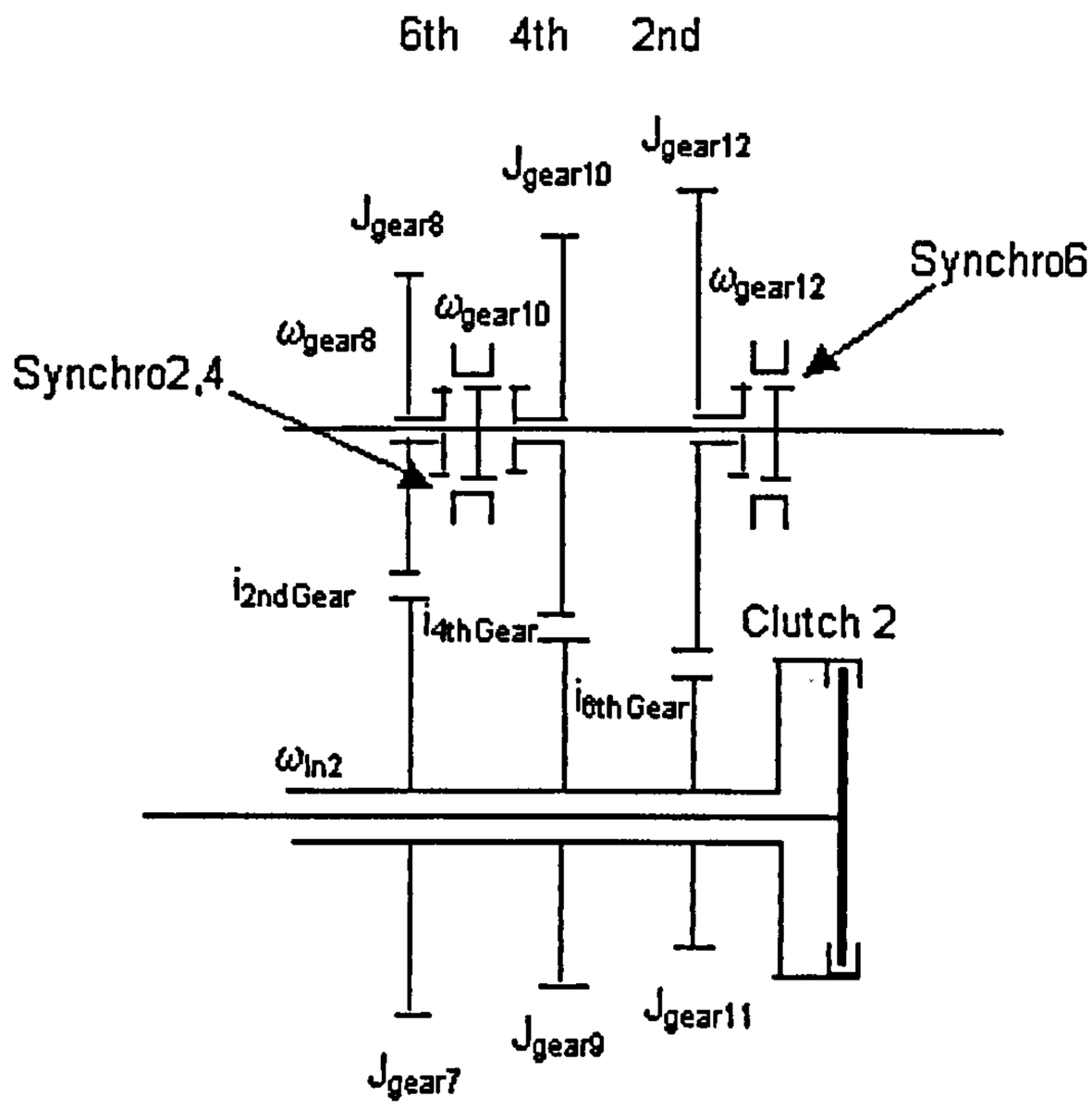

Figure A.1 Half 2 of the twin clutch transmission depicted in Figure 3.7

Synchroniser in state of slipping:

$$J_{S2,in}\frac{\dot{\omega}_{In2}}{i_{2,4,6}} = T_{kIn2}i_{2,4,6}\eta_{gearbox2} - T_{Syn2} - c_{S2,in}\frac{\omega_{In2}}{i_{2,4,6}} \quad \text{(A.19)}$$

$$J_{S2,out}\dot{\omega}_{Out2} = T_{Syn2} - T_{kOut2} - c_{S2,out}\omega_{Out2} \quad \text{(A.20)}$$

$$T_{Syn2} = \text{sgn}(\omega_{In2} - \omega_{Out2})\frac{R_m}{\sin\alpha}F_{N,S2,4,6}\mu_k z \quad \text{(A.21)}$$

Synchroniser in the "engaged" state:

$$\frac{\omega_{In2}}{i_{2,4,6}} = \omega_{Out2} = \omega \quad \text{(A.22)}$$

$$(J_{S2,in} + J_{S2,out})\dot{\omega} = T_{kIn2} i_{2,4,6} \eta_{gearbox2} - T_{kOut2} - (c_{S2,in} + c_{S2,out})\omega \quad \text{(A.23)}$$

$$T_{S2,engaged} = \frac{J_{S2,out}(T_{kIn2} i_{2,4,6} \eta_{gearbox2} - c_{S2,in}\omega) + J_{S2,in}(T_{kOut2} + c_{S2,out}\omega)}{J_{S2,in} + J_{S2,out}} \quad \text{(A.24)}$$

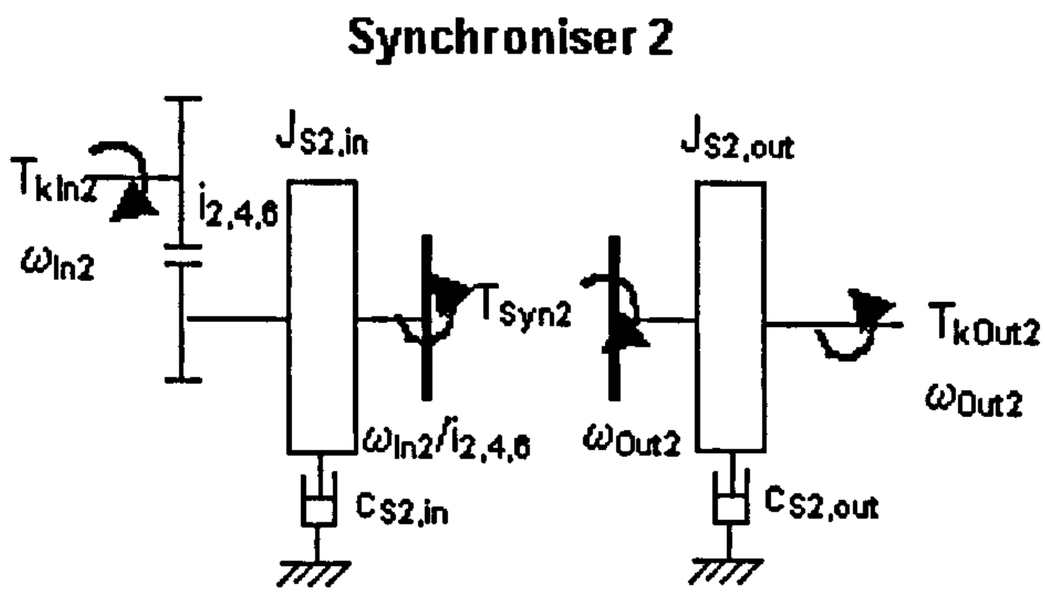

Figure A.2 Free-body diagram of the synchroniser 2 in the "slipping" state

Conditions for transitions between states of the synchroniser 2:

- *Engaged:*

  Transition from state "Slipping":

$$\text{IF } \{|T_{S2,engaged}| \le \mu_s \frac{R_m}{\sin\alpha} F_{N,S2,4,6} z\} \text{ AND } \{\frac{\omega_{In2}}{i_{2,4,6}} = \omega_{Out2}\}$$

$$\text{THEN } \{\text{Synchroniser Engaged}\} \quad \text{(A.25)}$$

  Transition from state "Mechanically Locked":

$$\text{IF } \{x_s < x_{s,\max}\} \text{ THEN } \{\text{Synchroniser Engaged}\} \quad \text{(A.26)}$$

- *Slipping:*

  Transition from state "Engaged":

$$\text{IF } \{|T_{S2,engaged}| > \mu_s \frac{R_m}{\sin\alpha} F_{N,S2,4,6} z\} \text{ THEN } \{\text{Synchroniser Slipping}\} \quad \text{(A.27)}$$

  Transition from state "Mechanically Locked":

$$\text{IF } \{|T_{S2,engaged}| > \mu_s \frac{R_m}{\sin\alpha} F_{N,S2,4,6} z\} \text{ AND } \{x_s < x_{s,\max}\}$$

$$\text{THEN } \{\text{Synchroniser Slipping}\} \quad \text{(A.28)}$$

- *Mechanically Locked:*

  Transition from state "Engaged":

$$\text{IF } \{x_s \ge x_{s,\max}\} \text{ THEN } \{\text{Synchroniser Mechanically Locked}\} \quad \text{(A.29)}$$

  Transition from state "Slipping":

$$\text{IF } \{\left|T_{S2,engaged}\right| \le \mu_s \frac{R_m}{\sin\alpha} F_{N,S2,4,6} z\} \text{ AND } \{\frac{\omega_{In2}}{i_{2,4,6}} = \omega_{Out2}\}$$

$$\text{AND } \{x_s \ge x_{s,\max}\} \text{ THEN } \{\text{Synchroniser Engaged}\} \quad \text{(A.30)}$$

Layshaft 2

$$T_{kOut2} = k_{Out2}(\varphi_{Out2} - \varphi_{Diff}) + c_{Out2}(\omega_{Out2} - \omega_{Diff}) \quad \text{(A.31)}$$

k_{Out2} = f(gear=2,4,6), c_{Out1} = f(gear=2,4,6)

A.3 Equations of Motion of the Nonlinear Solenoid Valve and Actuator Model

Model of Proportional Solenoid Valve

Solenoid Dynamics:

$$\dot{\phi} = \frac{v_{Sol} - iR_{wind}}{N} \quad \text{(A.32)}$$

$$MMF = MMF_{air} + MMF_{steel} \quad \text{(A.33)}$$

$$MMF_{air} = H_{air} L_{gap} = \frac{B}{\mu_0} L_{gap} \quad \text{(A.34)}$$

$$MMF_{steel} = H_{steel} L_{steel} \quad \text{(A.35)}$$

$$H_{steel} = f(B),\ L_{gap} = f(x_v) \quad \text{(A.36)}$$

$$B = \frac{\phi}{A_{air}} \quad \text{(A.37)}$$

$$i = \frac{MMF}{N} \quad \text{(A.38)}$$

Solenoid force:

$$F_{Sol} = \frac{B^2 A_{air}}{2\mu_0} \quad \text{(A.39)}$$

Equation of motion of the armature/spool assembly:

$$m_v \ddot{x}_v + c_v \dot{x}_v + k_v x_v = F_{Sol} - p_C A_v \quad \text{(A.40)}$$

Hydraulic flow forces that are created at the valve ports due to a change in the direction of the oil flow are not considered here. The term that incorporates the pressure at the right hand side of equation (A.40) is due to the pressure feedback on the proportional pressure-reducing valve and is missing on a proportional directional valve.

The net oil flow at the control port (and into clutch cylinder):

$$Q_{control} = Q_{sup\,ply} - Q_{exhaust} - Q_{feedback} \tag{A.41}$$

$$Q_{supply} = 0 \qquad 0 \le x_v \le x_1 \tag{A.42}$$

$$Q_{sup\,ply} = C_D A_{sup\,ply}\,\mathrm{sgn}(p_{sup\,ply} - p_C)\sqrt{\frac{2\left|p_{sup\,ply} - p_C\right|}{\rho_{oil}}} \qquad x_1 < x_v \le x_{max}$$

$$Q_{exhaust} = C_D A_{exhaust}\sqrt{\frac{2p_C}{\rho_{oil}}} \qquad 0 \le x_v < x_2 \tag{A.43}$$

$$Q_{exhaust} = 0 \qquad x_2 \le x_v \le x_{max}$$

$$A_{sup\,ply} = \frac{A_{max\,sup\,ply}(x_{sup\,ply} - x_{max} + x_v)}{x_{sup\,ply}} \tag{A.44}$$

$$A_{exhaust} = \frac{A_{max\,exhaust}(x_{exhaust} - x_v)}{x_{exhaust}} \tag{A.45}$$

$$A_{max\,sup\,ply(exhaust)} = d_{spool}\pi x_{sup\,ply(exhaust)} \tag{A.46}$$

$$Q_{feedback} = A_v\dot{x}_v + \frac{V_{v,0} + A_v x_v}{\beta}\dot{p}_C \tag{A.47}$$

Model of the Hydraulic Actuator Flow Dynamics:

$$\dot{p}_C = \frac{\beta}{x_p A_p}\left(Q_{control} - \dot{x}_p A_p\right) \tag{A.48}$$

A.4 List of Parameter Values of the Powertrain Model

The parameters of the powertrain model were either calculated from given or estimated dimensions of the components or where this was not possible, reasonable values were taken from the literature. To get an idea about the dimensions of the components in a twin clutch transmission, the scaled sketch of a twin clutch transmission [O'Neil and Harrison 2000] was taken as a starting point. From these dimensions, the stiffness of the shafts, the inertia of the internal parts and the dimensions of clutch and synchroniser were determined. The damping rates of the shafts in the drivetrain model were estimated by using eigen-frequencies of a comparable drivetrain found in the literature [Willumeit and Park 1998].

$A_{air} = 5.02 \cdot 10^{-5}\ m^2$

$A_{front} = 1.5\ m^2$

$A_{maxsupply} = 2.83 \cdot 10^{-5}\ m^2$

$A_{maxexhaust} = 2.83 \cdot 10^{-5}\ m^2$

$A_p = 5 \cdot 10^{-3}\ m^2$ (clutch), $3 \cdot 10^{-3}\ m^2$ (synchroniser)

$A_v = 1 \cdot 10^{-5}\ m^2$

A/F= 14.6

$c_{C1,2,in} = 0.01, 0.01$ Nms/rad

$c_{C1,2,out} = 0.01, 0.01$ Nms/rad

$c_D = 0.3$

$c_{Diff} = 0.01$Nms/rad

$c_{drive} = 12$ Nms/rad

$c_{In1} = 2$ (1^{st} gear), 1.5 (3^{rd} gear), 1.3 (5^{th} gear) Nms/rad

$c_{In2} = 5$ (2^{nd} gear), 2.5 (4^{th} gear),1.5 (6^{th} gear) Nms/rad

$c_{out1} = 2$ (1^{st} gear), 2 (3^{rd} gear),0.9 (5^{th} gear) Nms/rad

$c_{out2} = 0.5$ (2^{nd} gear), 0.5 (4^{th} gear),0.75 (6^{th} gear) Nms/rad

$c_p = 10$ Ns/m (clutch, synchroniser)

$c_{S1,2,in} = 0.01, 0.01$Nms/rad

$c_{S1,2,out} = 0.01, 0.01$Nms/rad

$c_{TD} = 15$ Nms/rad

$c_{tyre} = 40$ Nms/rad

$c_v = 20$ Ns/m

$c_{12} = 0.3$ Nms/rad

$C_D = 0.62$

$d_{spool} = 6 \cdot 10^{-3}\ m$

f_R= 0.015

g= 9.81 m/s^2

i_{Acc}= 1.5

i_f= 4.5

$i_{1,3,5}$=3.7 (1st gear), 1.5 (3rd gear), 0.85 (5th gear)

$i_{2,4,6}$=2.3 (2ndgear),1.1 (4th gear), 0.7 (6th gear)

J_{Acc}= 0.002 kgm^2

$J_{C1,2,in}$= 0.0016, 0.004 kgm^2

$J_{C1,2,out}$= 0.001, 0.001 kgm^2

J_e= 0.15 kgm^2

J_{Diff}= 0.13 kgm^2

$J_{gear1,2,3,4,5,6}$= 0.001, 0.0018, 0.001, 0.001, 0.001, 0.0015 kgm^2

$J_{gear7,8,9,10,11,12}$= 0.001, 0.001, 0.001, 0.0016, 0.001, 0.0012 kgm^2

$J_{rot,non\text{-}driven}$=0.9 kgm^2

$J_{S1,2\ out}$= 0.0015, 0.0015 kgm^2

J_{Wheel}= 0.9 kgm^2

k_{drive}= 55000 Nm/rad

k_{CP}= 1·10^7 N/m

k_{In1}= 130000 (1st gear), 100000 (3rd gear), 80000 (5th gear) Nm/rad

k_{In2}= 620000(2nd gear), 310000 (4th gear), 210000 (6th gear) Nm/rad

k_{out1}=390000(1st gear), 390000 (3rd gear), 165000 (5th gear) Nm/rad

k_{out2}= 120000(2nd gear), 120000 (4th gear), 165000 (6th gear) Nm/rad

k_R=1·10^5 N/m (clutch, synchroniser)

k_{TD}= 820,40,30,640 Nm/rad (stage 1,2,3,4)

k_{tyre}= 220000 Nm/rad

k_v= 7000 N/m

k_{12}= 8500 Nm/rad

K_d= clutch slip: 2.5·10^3 (upshift), 0.5·10^3 (downshift); torque: 10 (upshift), 50 (downshift)

K_i= clutch slip: 0.5·10^6 (upshift, downshift); torque: 1.2·10^4 (upshift), 5000 (downshift)

K_p= clutch slip: 0.6·10^5 (upshift), 0.3·10^5 (downshift); torque: 200 (upshift), 5000 (downshift)

K_d= 0.1 (engine speed, throttle), 0.1 (engine speed, spark), 50 (engine speed, clutch pressure)

K_i= 8 (engine speed, throttle), 9 (engine speed, spark), 1·10^4 (engine speed, clutch pressure)

K_p= 4 (engine speed, throttle), 4 (engine speed, spark), 1·10^4 (engine speed, clutch pressure)

K_1= 2.06·10^5 Pa/V (clutch, synchroniser)

K_2= 4·10^6 (clutch, synchroniser)

L_{steel} = 0.1 m

m_p= 0.5 kg (clutch), 0.2 kg (synchroniser)

m_v= 0.04 kg

$m_{vehicle}$= 1000 kg

N= 1100

p_{supply}= $12 \cdot 10^5$ Pa

p_0= $1.1 \cdot 10^5$ Pa (used in engine model: $1.6 \cdot 10^5$ Pa)

r_{tyre}= 0.3 m

RT/V_m= 0.41328 $(s^2m)^{-1}$

R_i= 0.04 m (clutch), 0.028 m (synchroniser)

R_o= 0.06 m (clutch), 0.031 m (synchroniser)

R_{wind}= 2 Ω

T_{Acc}= 15 Nm

V_{offset}= 4.2 V

$V_{v,0}$= $5 \cdot 10^{-8}$ m^3

$x_{exhaust}$= $1.5 \cdot 10^{-3}$ m

x_{max}= $3 \cdot 10^{-3}$ m

$x_{pstroke}$= $2.5 \cdot 10^{-3}$ m (clutch, synchroniser)

$x_{s,max}$= $2.5 \cdot 10^{-3}$ m

x_{supply}=$1.5 \cdot 10^{-3}$ m

x_1= $1.5 \cdot 10^{-3}$ m

x_2= $1.5 \cdot 10^{-3}$ m

z= 4 (wet clutch), 2 (dry clutch), 1 (synchroniser)

α= 7 deg

β= $7 \cdot 10^8$ Pa

ζ_1 = 0.93 and ζ_3= 0.75 (clutch, synchroniser)

η_{Acc}= 0.98

η_{Diff}= 0.96

$\eta_{gearbox1}$= 0.99

$\eta_{gearbox2}$= 0.99

$\mu_k$at wet clutch, negative gradient: A=0.15, B=-0.003, C=$1 \cdot 10^{-5}$, D=$-5 \cdot 10^{-6}$, E=$3.4 \cdot 10^{-7}$, F=$-5 \cdot 10^{-9}$

$\mu_k$at wet clutch, positive gradient: A=0.12, B=0.002, C=$-1 \cdot 10^{-5}$, D=$5 \cdot 10^{-6}$, E=$-3.4 \cdot 10^{-7}$, F=$5 \cdot 10^{-9}$

μ_k at dry clutch, negative gradient: A=0.4, B=-0.005, C=$3 \cdot 10^{-4}$, D=$-1 \cdot 10^{-5}$, E=0, F=0

μ_k at dry clutch, positive gradient: A=0.4, B=0.005, C=$-3 \cdot 10^{-4}$, D=$8 \cdot 10^{-6}$, E=0, F=0

μ_k= 0.1 (Synchroniser)

μ_s= 0.16 (wet clutch, negative gradient)

μ_s= 0.13 (wet clutch, positive gradient)

μ_s= 0.45 (dry clutch, negative gradient)

μ_s= 0.45 (dry clutch, positive gradient)

μ_s= 0.12 (Synchroniser)

μ_0= $1.2566 \cdot 10^{-6}$ H/m

ρ_{air}= 1.2 kg/m^3

ρ_{oil}= 830 kg/m^3

$\Delta\varphi_{1,2}$=0.35, - 0.17 rad

$\Delta\omega_{ref}$= 5 rad/s

ω_1=20 Hz ω_3 = 80 Hz and α_2= $5 \cdot 10^{-3}$

B.1 Supplementary Simulation Results for Chapter 4, Section 4.5

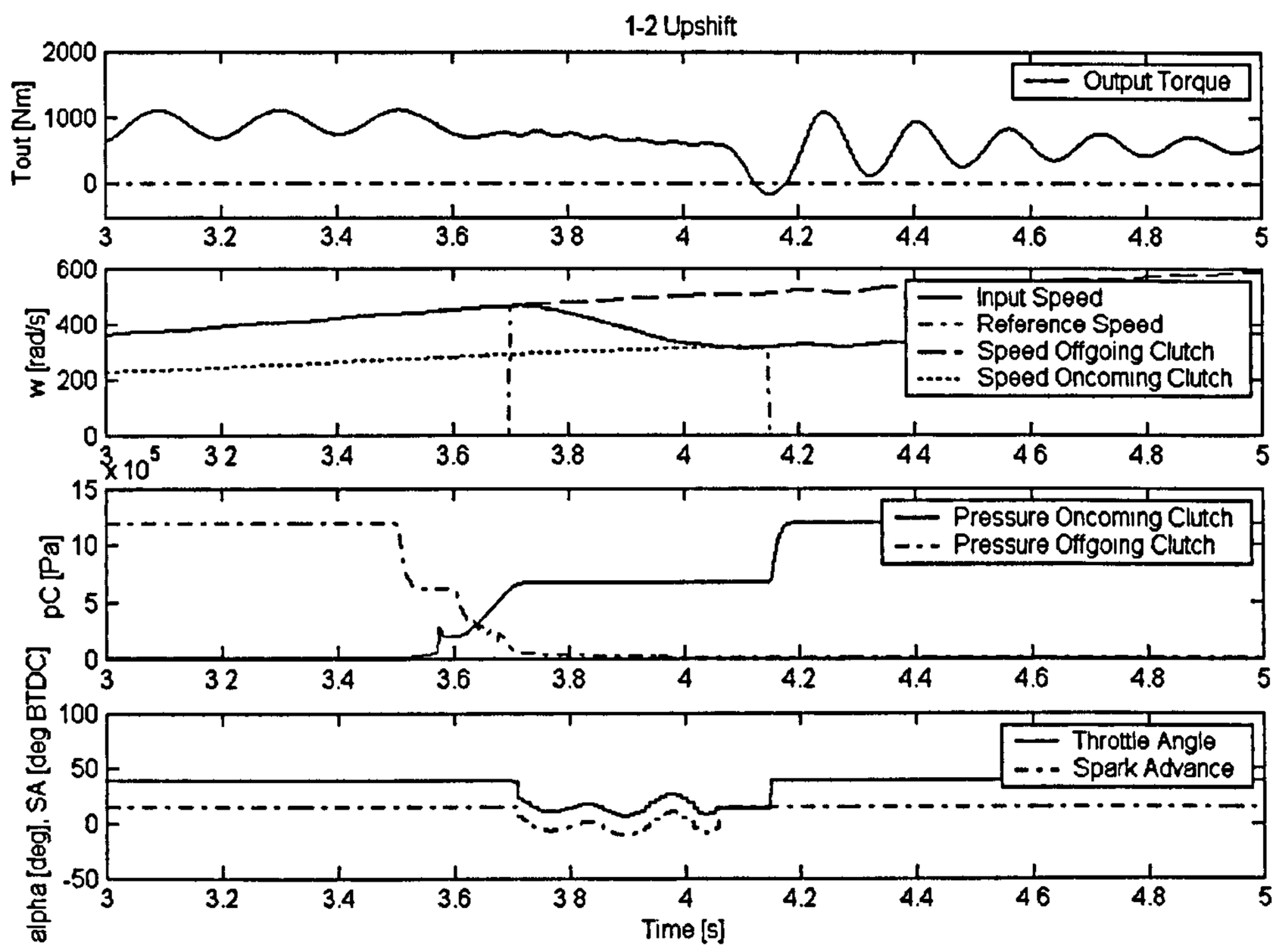

Figure B.1 Simulation result: Upshift from 1st to 2nd gear, reduced driveshaft stiffness

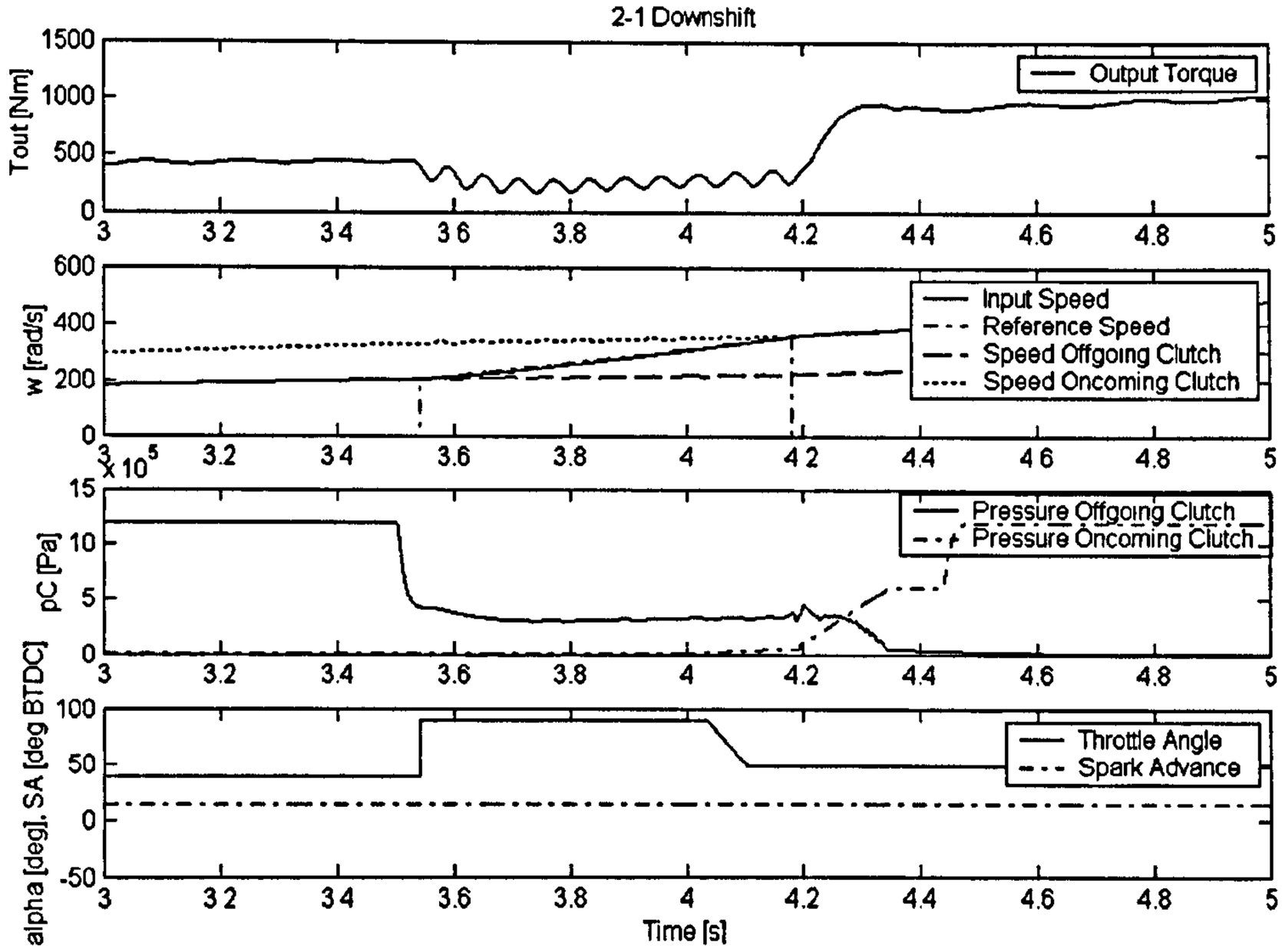

Figure B.2 Simulation result: Downshift from 2nd to 1st gear, reduced driveshaft stiffness

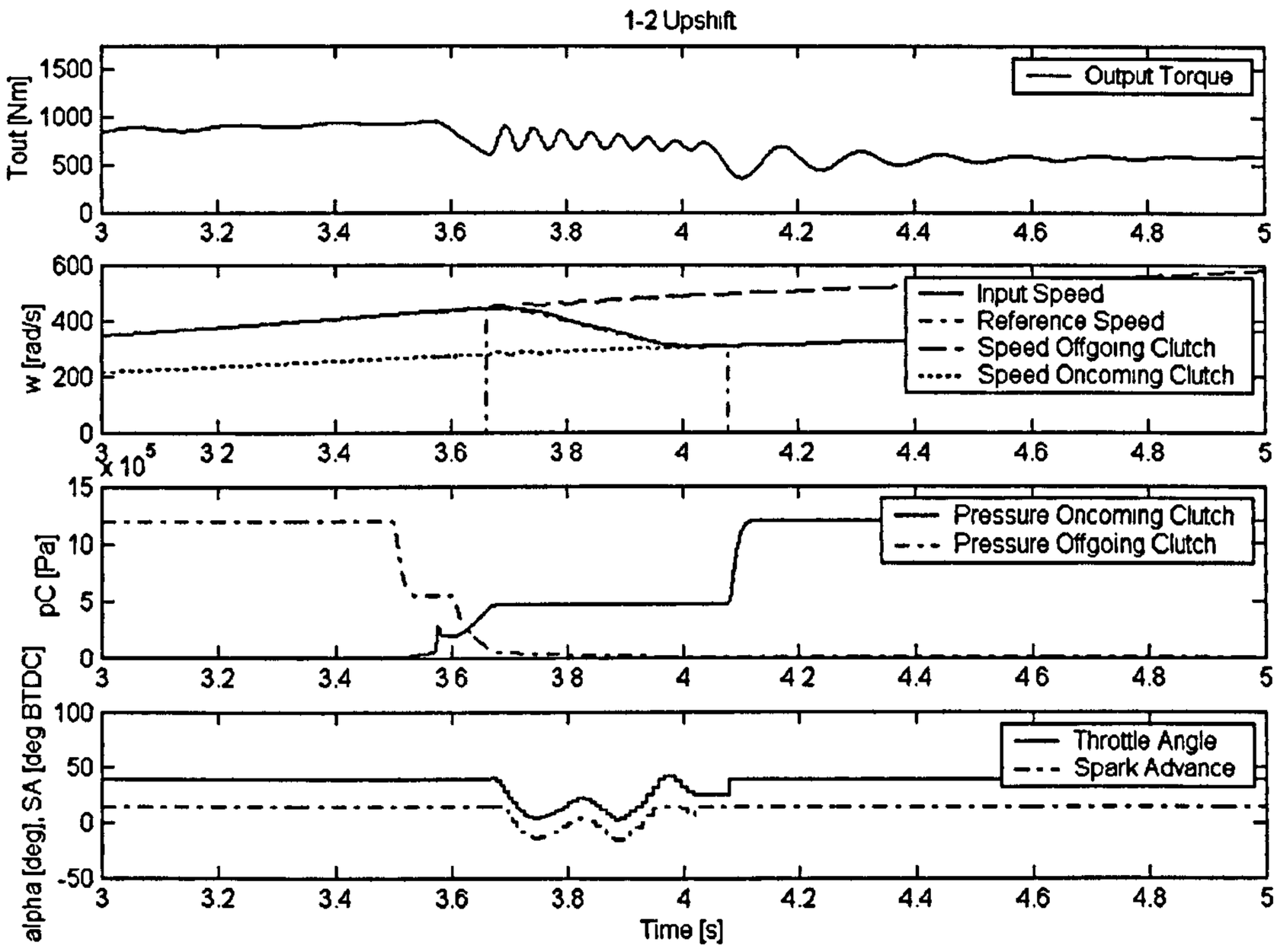

Figure B.3 Simulation result: Upshift from 1st to 2nd gear, with dry-type friction with a positive gradient

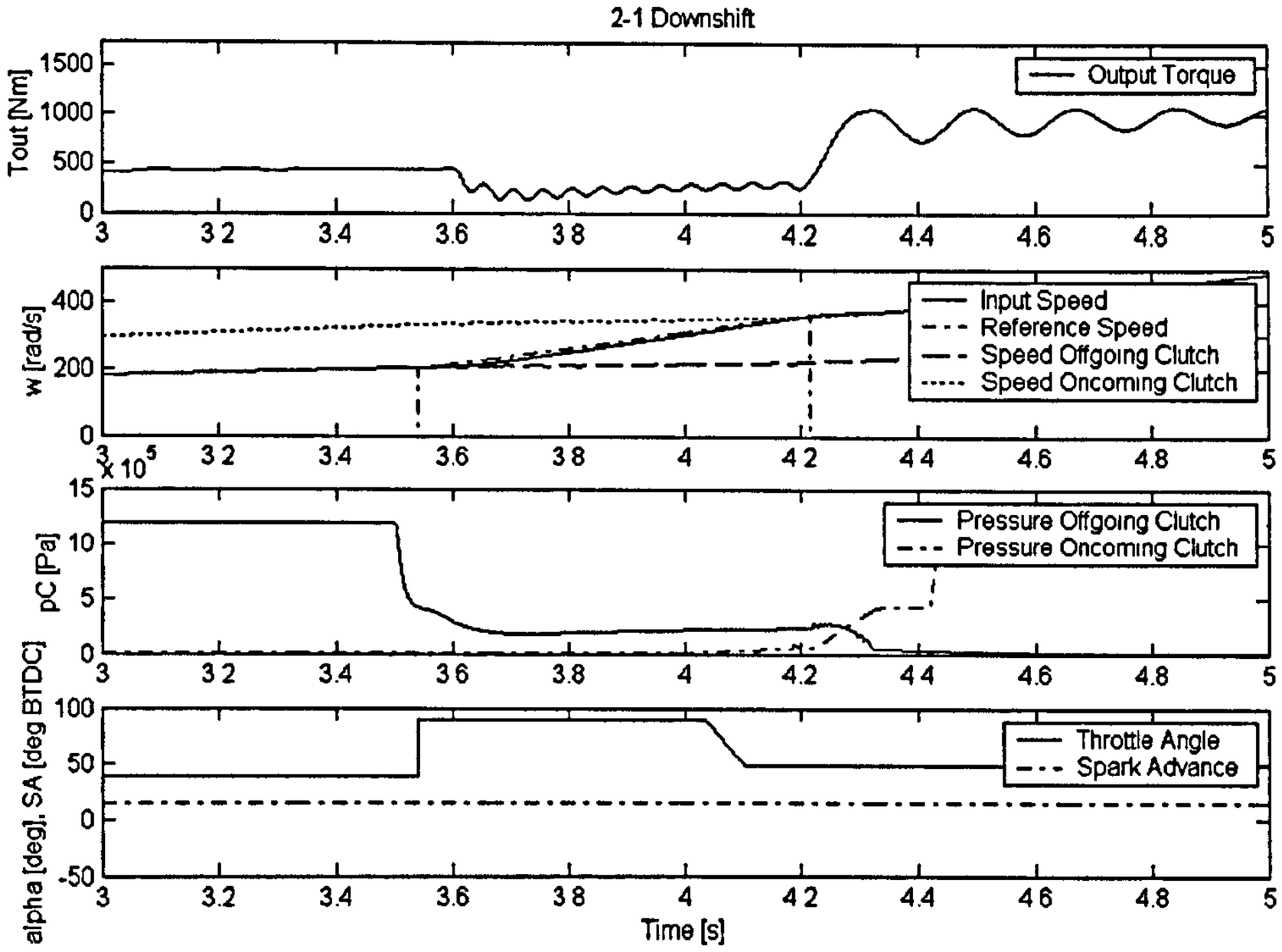

Figure B.4 Simulation result: Downshift from 2nd to 1st gear, with dry-type friction with a positive gradient

B.2 Supplementary Simulation Results for Chapter 5, Section 5.3

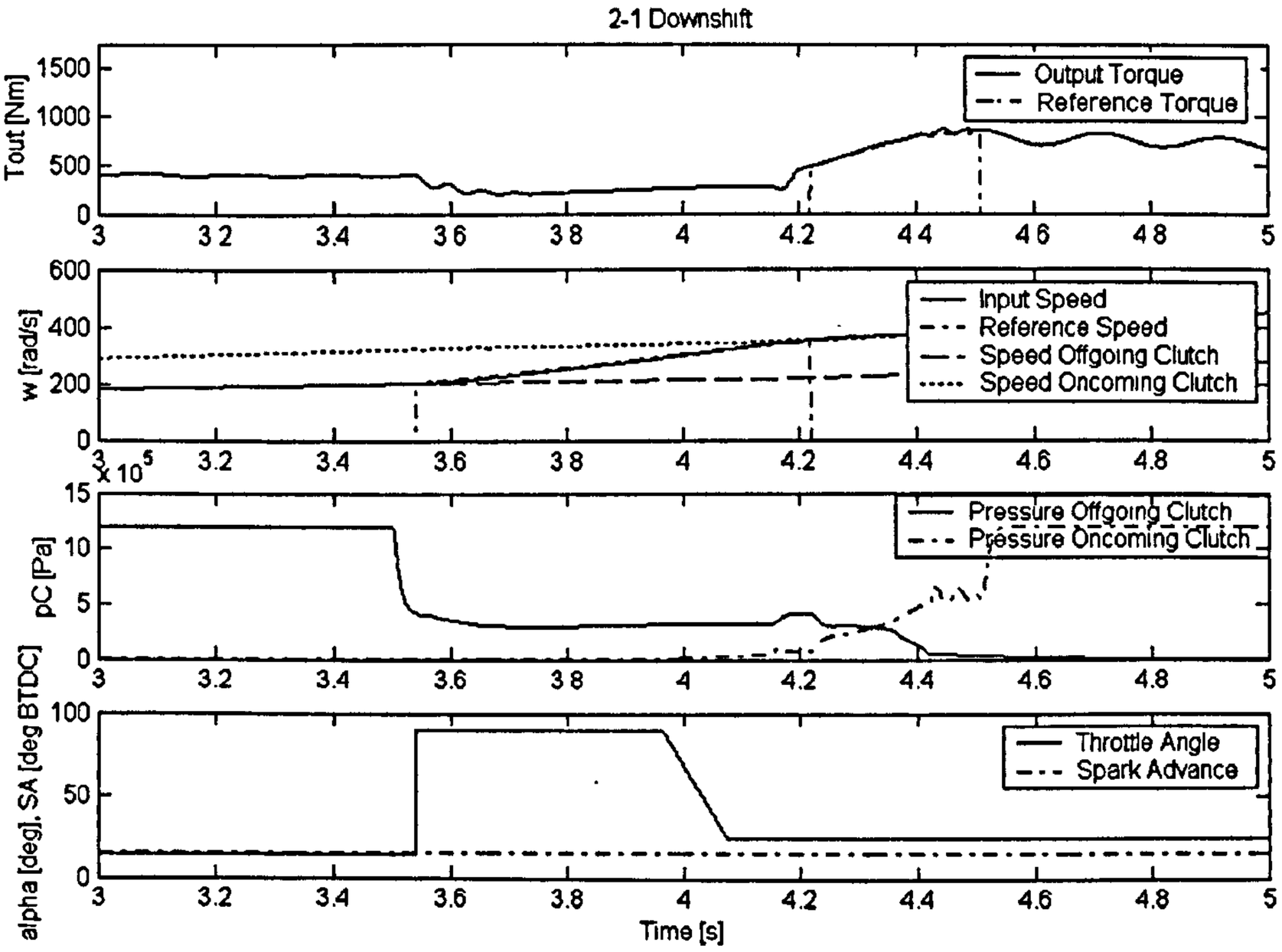

Figure B.5 Simulation result: Downshift from 2nd to 1st gear plus torque control, with reduced driveshaft stiffness (k_{drive}=35000 Nm/rad)

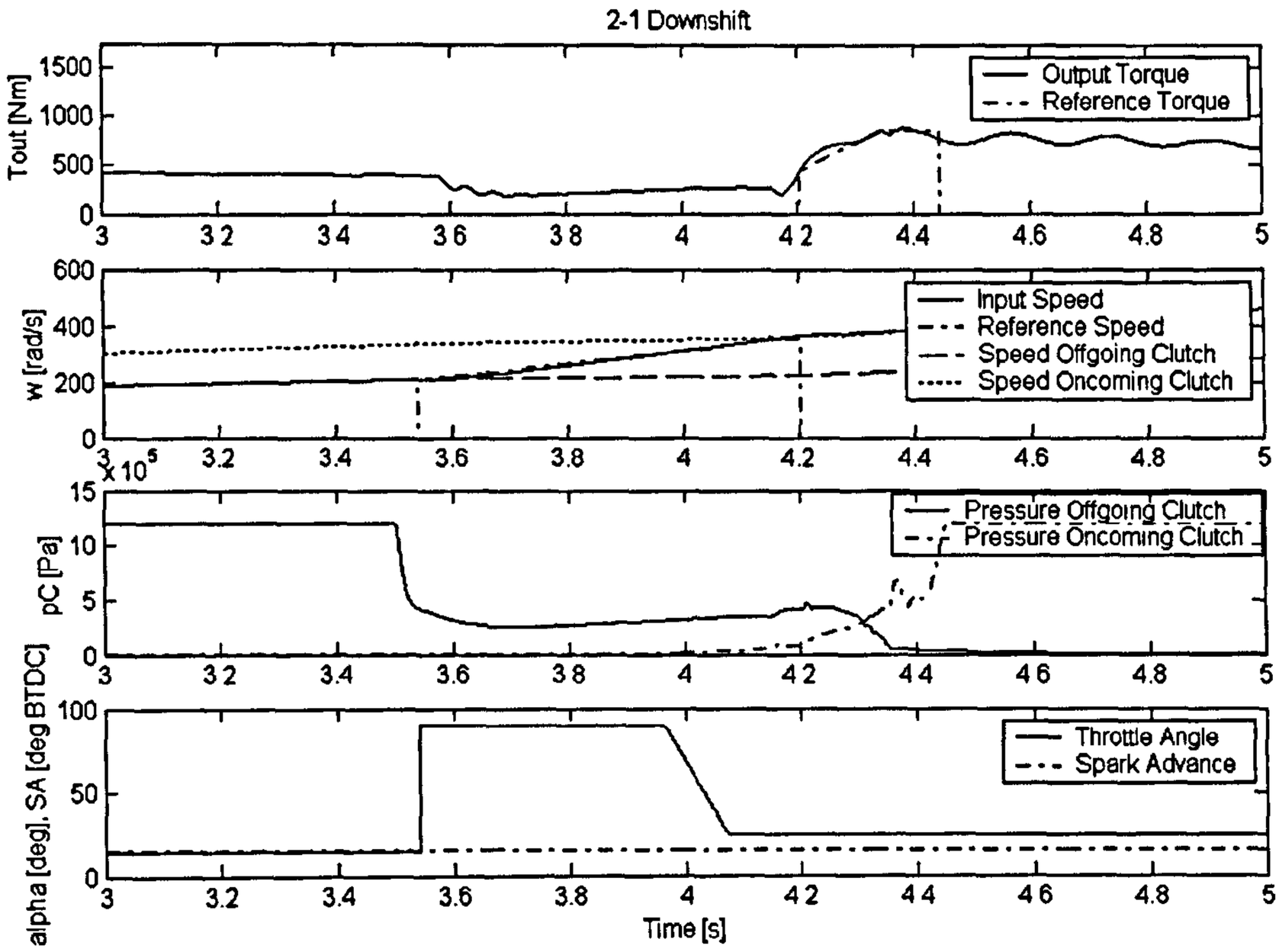

Figure B.6 Simulation result: Downshift from 2nd to 1st gear plus torque control, with wet friction, negative gradient

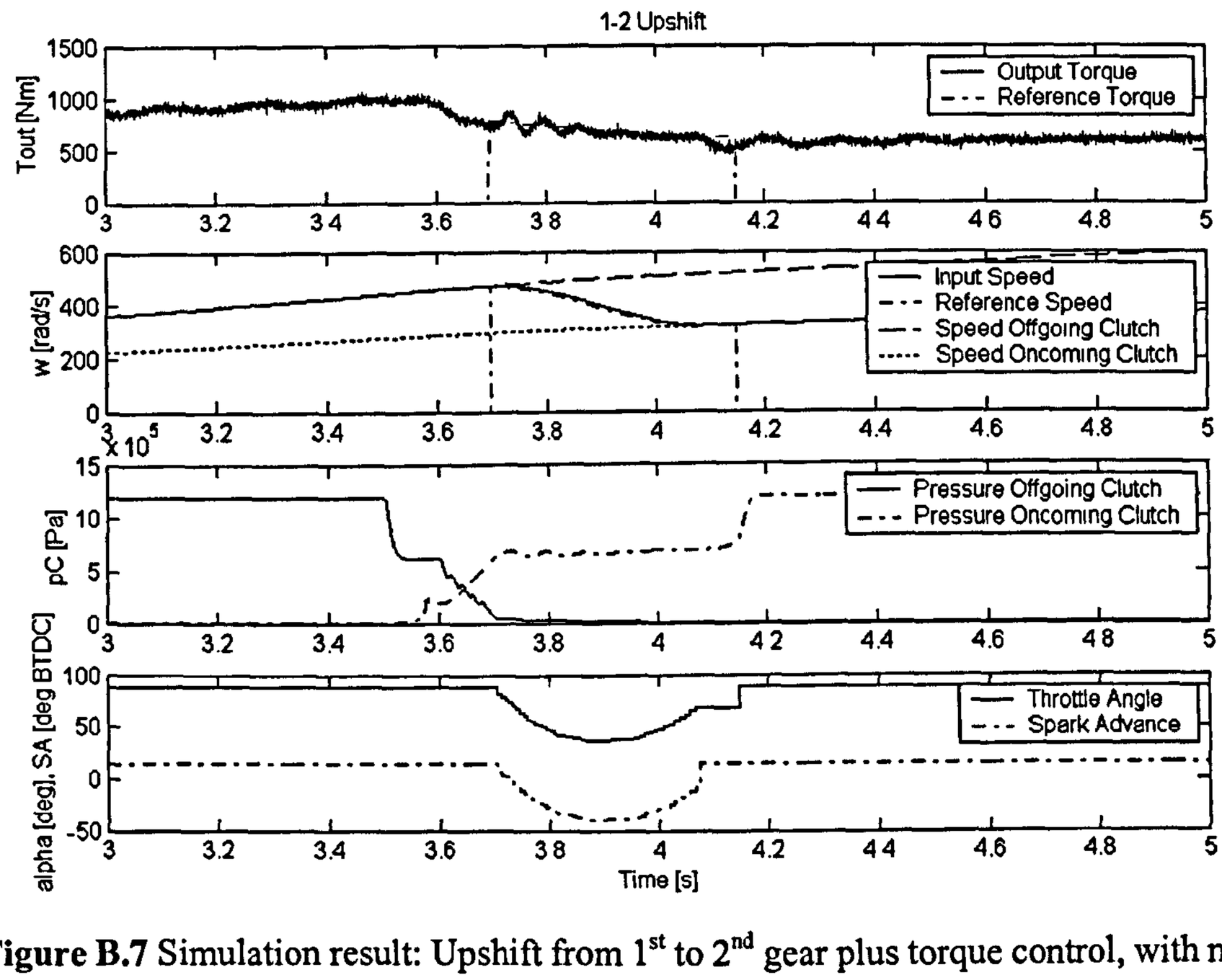

Figure B.7 Simulation result: Upshift from 1st to 2nd gear plus torque control, with noise polluted transmission output torque signal